STRONTIUM ISOTOPE GEOCHEMISTRY

AND POTASSIUM-ARGON STUDIES

ON VOLCANIC ROCKS FROM

THE CAMEROON LINE, WEST AFRICA

Hugh Mirams Dunlop

Ph.D. Thesis

University of Edinburgh

April 1983

EX DIST. UNIV. EDINBURGEN.

DECLARATION

I declare that this thesis is entirely my own work and has not been submitted for a degree at any other university.

Hugh M. Dunlop

ABSTRACT

The Cameroon line is a chain of Tertiary - Recent transitional to strongly alkaline volcanoes extending for 1600Km from the Atlantic island of Pagalu to the northern part of the Cameroon Republic. North of the Oku Massif the line splits into two branches. One runs northwards into N.E.Nigeria while the other runs eastwards through the Tchabal Mbabo and Ngaoundéré Plateaux of eastern Cameroon. Eleven volcanic centres have been investigated: four islands in the Gulf of Guinea; six volcanoes in Cameroon; and the Biu Plateau in Nigeria.

The geology of these volcanoes is reviewed and new K-Ar and Rb-Sr age determinations are presented from Principe, São Tomé, Etinde, Manengouba, Bambouto, Oku, Mandara, and Biu. Volcanism has been continuous from 66Ma ago up to the present day. Activity began with central volcanoes on the continental sector composed mainly of oversaturated salic rocks and voluminous continental basaltic rocks have only been erupted in the last 10Ma. The oldest dated volcanism on the oceanic sector occurred 31Ma ago and most of the island lavas are basaltic with lesser quantities of evolved phonolites and trachytes. There is no marked age trend along the chain and recent activity is evident in most centres.

87Sr/86Sr ratios of nephelinites, basanites, basalts and hawaiites from the oceanic sector (0.7028-0.7037) fall within the range observed from most other islands in the central-south Atlantic Ocean and demonstrate the lack of involvement with seawater - altered lithosphere. An almost identical Sr isotopic (0.7029-0.7038) and chemical spectrum exists for the uncontaminated mafic rocks from the continental centres. In particular the relatively primitive, ultramafic xenolith bearing Biu Plateau basalts show very similar, fine scale isotopic heterogeneities to those recorded in mafic lavas from the Gulf of

Guinea islands. These inhomogeneities consistently correlate with degree of alkalinity whereby alkaline lavas have lower 87Sr/86Sr ratios relative to more transitional basalts. These data illustrate that all these volcanoes, on both sides of the continental margin, share the same heterogeneous mantle source region common to many terrestrial anorogenic volcanic fields and oceanic islands. Magmas are considered to have been generated by a thermal anomaly/hotzone in the lower mantle which had previously given rise to the Benue trough. Liquids subsequently migrate to the surface undergoing diffusive zone refining and mixing with the overlying depleted MORB reservoir.

A few basalts and intermediates from several of the Cameroon volcanoes have slightly elevated initial 87Sr/86Sr ratios (0.7039-0.7047) and are shown to reflect small degrees of crustal contamination superimposed on mantle derived heterogeneities. The major element chemistry of these lavas indicate that such contamination is not necessarily restricted to selective Sr migration from the crust. Phonolites and trachytes from the islands of São Tomé and Principe are cogenetic with their mafic counterparts although very small levels of interaction with oceanic sediment during fractionation is reflected in the initial 87Sr/86Sr ratios of some evolved rocks from São Tomé. On the continental sector peralkaline trachytes, rhyolites and ignimbrites have all undergone varying degrees of crustal contamination with the most salic rocks representing 80-90% crustal melts. Where crustal interaction has not occurred during fractionation, liquids evolve to uncontaminated phonolites by identical processes to those giving rise to the oceanic sector fractionates. The sample population is sufficiently large to conclude that the initial 87Sr/86Sr ratios of uncontaminated within-plate basalts from this region are very unlikely to be higher than 0.7037-0.7038 or lower than 0.7027.

ACKNOWLEDGEMENTS

I wish to express my thanks to the heads of departments and staff at: the Grant Institute of Geology, Edinburgh University; the S.U.R.R.C., East Kilbride; the Department of Earth Sciences, Open University; and the Centre de Recherches sur la Synthèse et Chimie des Minéraux, C.N.R.S./B.R.G.M.,Orléans for making this thesis possible. I am grateful to N.E.R.C. for funding and to the Nigerian Geological Survey for providing logistical support for fieldwork in Nigeria and Cameroon.

In addition I would like to mention the following people to whom I am indebted:

Dr. Godfrey Fitton for suggesting this research project, for access to a vast amount of major and trace element data, for continual advice, guidance and encouragement, and for reading drafts, often at very short notice.

Carolyn Hirst for advice on the parts of this thesis concerning Manengouba and for access to unpublished data.

At East Kilbride: Dr. Mitch MacIntyre and Tom McMenamin for considerable assistance during K-Ar work; Drs. Otto Van Breemen and Alex Halliday for discussions and advice on Rb-Sr methods; John Hutchinson for making high precision Sr isotope analysis possible on the temperamental AEI MS12; Julian Joceyln for help on sample preparation; Dr. Hugh de Souza and Al Moyes for lively discussions in the S.U.R.R.C. postgraduate room.

Dr. Z. Johan and Dr. Chris Neary for understanding and encouragement, and for substantial assistance in the production of this thesis.

Mrs. Dianne Howes for efficiently typing this work and for putting up with long-distance communication;and Mme. Humbert for making corrections.

Dr. Chris Hawkesworth for the isotope facilities at the Open University;Pascal Oustrière (B.R.G.M.) for computing, valuable discussions on the Ngaoundéré plateau and for access to unpublished K-Ar data.

My parents for their constant encouragement and interest; and finally, Elisabeth for typing the figure legends and for her patience and moral support.

TABLE OF CONTENTS

	Page
Chapter 1 INTRODUCTION	1
1.1 Geological Framework of the Cameroon Line Volcanoes	1
1.2 Statement of Problem and Aims	6
Chapter 2 PRINCIPLES AND METHODOLOGY OF THE ISOTOPE TECHNIQUES EMPLOYED	13
2.1 Theory of Rb-Sr Geochronology and Isotope Geochemistry	13
2.2 The K-Ar Method of Dating	19
Chapter 3 GEOLOGY AND AGE OF VOLCANISM OF THE CAMEROON LINE	26
3.1 Oceanic Sector	26
3.1.1 Principe	26
3.1.2 São Tomé	33
3.1.3 Bioko (formerly Fernando Poo)	39
3.1.4 Pagalu (formerly Annobon)	43
3.2 Continental Sector	46
3.2.1 Mt. Cameroon	46
3.2.2 Etinde	51
3.2.3 Manengouba	52
3.2.4 Bambouto Mountains	56
3.2.5 Oku Massif	60
3.2.6 Mandara Mountains	63
3.2.7 Biu Plateau	67
3.2.8 Ngaoundéré and Tchabal Mbabo Plateaux	72
3.3 Palaeocene - Eocene Continental Igneous Complexes	73
3.3.1 Kirawa	75
3.3.2 Intrusive Ring Complexes	75
3.4 Discussion	78

		Page
Chapter 4	GEOCHEMISTRY OF THE OCEAN ISLANDS	84
4.1	Principe	84
	4.1.1 Geochemistry	84
	4.1.2 Strontium Isotope Studies	88
4.2	São Tomé	105
	4.2.1 Geochemistry	105
	4.2.2 Strontium Isotope Studies	108
4.3	Bioko and Pagalu	122
	4.3.1 Bioko	123
	4.3.2 Pagalu	129
4.4	Discussion of Mafic Rocks from Islands in the Gulf of Guinea	136
Chapter 5	GEOCHEMISTRY OF VOLCANIC ROCKS FROM CAMEROON	154
5.1	South Cameroon	154
	5.1.1 Mt. Cameroon	154
	5.1.2 Etinde	172
	5.1.3 Manengouba	195
5.2	North Cameroon	202
	5.2.1 Bambouto and Oku	202
	5.2.2 Mandara Mountains	216
	5.2.3 Discussion on the Genesis of the Bambouto, Oku and Mandara Salic Rocks	224
5.3	Strontium Isotope Data from the Tertiary Ring Complexes	229
5.4	Summary of the Sr - Isotope Data on the Mafic Volcanic Rocks from Cameroon	232
Chapter 6	GEOCHEMISTRY OF VOLCANIC ROCKS FROM N.E. NIGERIA	237
6.1	Major and Trace Element Geochemistry	237
6.2	Strontium Isotope Results and Discussion	250

		Page
Chapter 7	PETROGENESIS OF THE CAMEROON LINE VOLCANOES	262
7.1	Anorogenic Intraplate Volcanism on the Oceanic and Continental Sectors of the Cameroon Line	262
7.2	Inferences Concerning the Chemical and Isotopic Structure of the Sub-Oceanic and Sub-Continental mantle	270
7.3	Tectonic Models Concerning the Origin of the Cameroon Line and its Association with the Neighbouring Benue Trough	276
Appendix A	ANALYTICAL TECHNIQUES	280
A1	Rb-Sr Techniques	280
	A1.1 Sample Preparation	280
	A1.2 Chemical Procedures	281
	A1.3 Analytical Blanks	282
	A1.4 Mass - Spectrometry	282
	A1.5 Data Treatment	284
	A1.6 Replicate and Standard Analyses	288
A2	K-Ar Techniques	288
A3	X-Ray Fluorescence Methods	291
Appendix B	WHOLE - ROCK X-RAY FLUORESCENCE ANALYSES	296
Appendix C	CLASSIFICATION SCHEME EMPLOYED	305
Appendix D	LIST OF SAMPLES STUDIED	306
Appendix E	ARTICLE BY DUNLOP AND FITTON (1979)	316
ABBREVIATIONS		317
REFERENCES		318

LIST OF FIGURES

		page
1.1	Map showing the Cameroon line Tertiary-Recent volcanoes	2
1.2	Cenozoic volcanism and structural units of Africa	3
1.3	Islands in the central-south Atlantic Ocean	5
1.4	Review of strontium isotope data in volcanic rocks	9
2.1	The branching decay scheme of ^{40}K	21
2.2	Explanation of K-Ar isotope ratio plot	25
3.1.1	Geological and sample location map of Principe	27
3.1.2	Schematic section through Principe	28
3.1.3	Geological and sample location map of São Tomé	34
3.1.4	Location of Bioko on the West African continental shelf	40
3.1.5	Geology and palaeomagnetic sampling sites of Bioko	41
3.1.6	Geology and palaeomagnetic sampling sites of Pagalu	44
3.2.1	Geology and sample location map of S. Cameroon	47
3.2.2	Geology and sample location map of the Biu plateau (Nigeria) and Mandara (Cameroon)	64
3.3.1	Location of lower Tertiary igneous complexes	74
3.3.2	Rb-Sr isochron diagram of Kirawa rhyolites	76
3.3.3	Summary of age data from the Cameroon line	82
4.1.1	Major element variation in the Principe volcanic rocks	85
4.1.2	Lanthanum-yttrium variation in Principe lavas	85
4.1.3	Differentiation Index plotted against degree of silica over- and under- saturation for the Principe lavas	87
4.1.4	Zirconium and strontium variation in Principe lavas	89
4.1.5	Rb-Sr plot of the Principe lavas	92
4.1.6	Differentiation Index versus Sr for Principe rocks	93
4.1.7	Initial Sr isotope ratios plotted against La/Y for the basic volcanic rocks of Principe	94
4.1.8	Rb-Sr isochron diagram for the Principe data	94

page

4.1.9 Iron oxidation ratio plotted against initial strontium isotope ratios in Principe rocks 98

4.1.10 Initial strontium isotope ratios plotted against Sr contents in Principe rocks 99

4.1.11 Initial strontium isotope ratios plotted against SiO_2 in Principe rocks 101

4.1.12 Initial strontium isotope ratios plotted against Rb contents in Principe rocks 102

4.2.1 Differentiation Index plotted against degree of silica over- and under- saturation for São Tomé volcanic rocks 106

4.2.2 Major element variation in São Tomé volcanic rocks 107

4.2.3 Rb-Sr plot of São Tomé volcanic volcanic rocks 111

4.2.4 Strontium isotope ratio plot of data on the São Tomé basic rocks 113

4.2.5 Initial strontium isotope ratios versus Sr contents in São Tomé volcanic rocks 115

4.2.6 Rb-Sr isochron diagram of São Tomé fractionated lavas 116

4.2.7 Initial strontium isotope ratios versus SiO_2 contents in São Tomé rocks 118

4.3.1 Differentiation Index plotted against degree of silica over- and under- saturation for Bioko volcanic rocks 124

4.3.2 Strontium isotope ratio plot of Bioko volcanic rocks 128

4.3.3 Differentiation Index plotted against degree of silica over- and under- saturation for Pagalu volcanic rocks 131

4.3.4 Strontium isotope ratio plot of Pagalu volcanic rocks 134

4.4.1 Rb-Sr plot of the oceanic islands in the Gulf of Guinea 138

4.4.2 Normalized trace element diagram for the oceanic islands in the Gulf of Guinea 139

4.4.3 Frequency histogram of Sr isotope data from Principe, São Tomé, Bioko and Pagalu 141

4.4.4 Initial strontium isotope ratios plotted against degree of silica over- and under- saturation for lavas with more than 4%MgO on islands in the Gulf of Guinea 144

4.4.5 Initial Sr isotope ratios plotted against Rb/Sr ratios for all oceanic islands and MORB 148

4.4.6 Initial Sr isotope data from islands in the Atlantic Ocean and MORB 151

		page
4.4.7	Initial strontium isotope ratios of oceanic islands plotted against $K_2O/(K_2O+Na_2O)$	152
5.1.1	Differentiation Index plotted against degree of silica over- and under- saturation for the S.Cameroon volcanoes	155
5.1.2	Major element variation in rocks from the continental sector of the Cameroon line	157
5.1.3	Na_2O+K_2O plotted against SiO_2 for the continental sector volcanic rocks	160
5.1.4	Trace element variation in rocks from the continental sector	161
5.1.5	Cr plotted against Zr for the S.Cameroon volcanoes	165
5.1.6	Normalized trace element abundances in the continental sector volcanic rocks	166
5.1.7	Rb versus Sr diagram for the S.Cameroon volcanoes	169
5.1.8	Strontium isotope ratio diagram for mafic rocks from S.Cameroon	170
5.1.9	Initial strontium isotope ratios plotted against SiO_2 contents in mafic lavas from Etinde, Mt.Cameroon and Manengouba	173
5.1.10	Initial strontium isotope ratios plotted against Sr contents in mafic rocks from Cameroon and N.E.Nigeria	174
5.1.11	K_2O versus Ce diagram for Mt.Cameroon and Etinde lavas	180
5.1.12	P_2O_5 plotted against Ce for Mt.Cameroon and Etinde lavas	182
5.1.13	Ce plotted against La and Nd for Etinde and the remainder of the Cameroon line	184
5.2.1	Differentiation Index plotted against degree of silica over- and under- saturation for Bambouto and Oku	203
5.2.2	Rb-Sr diagram for the N.Cameroon volcanoes	205
5.2.3	Strontium isotope ratio diagram of mafic rocks from Bambouto, Oku and Mandara	208
5.2.4	Initial strontium isotope ratios versus Sr contents for fractionated rocks from Bambouto, Oku and Mandara	211
5.2.5	Rb-Sr isochron diagrams of Bambouto trachytes and rhyolites	215
5.2.6	Rb-Sr isochron diagrams of Oku trachytes, rhyolites and ignimbrites	218
5.2.7	Differentiation Index plotted against degree of silica over- and under- saturation for Mandara volcanic rocks	220

		page
5.2.8	Normative quartz and feldspar compositions of Mandara trachytes and rhyolites plotted in the quartz-feldspar ternary system	222
5.2.9	Rb-Sr isochron diagrams of Mandara trachytes and rhyolites	226
5.2.10	Initial strontium ratios versus SiO_2 contents for Bambouto volcanic rocks and crustal xenoliths	228
5.4.1	Frequency histogram of Sr isotope data on basic lavas from the Cameroon volcanoes	233
5.4.2	Initial strontium isotope ratios plotted against degree of silica over- and under- saturation for basic lavas from the Cameroon volcanoes	235
6.1.1	Differentiation Index plotted against degree of silica over- and under- saturation for lavas from the Biu, Song and Longuda plateaux	238
6.1.2	Na_2O+K_2O plotted against SiO_2 for lavas from the Biu, Song and Longuda plateaux	240
6.1.3	Major element variation in lavas from the Biu and and Song plateaux	241
6.1.4	Trace element variation in lavas from the Biu and Song plateaux	244
6.1.5	A-F-M diagram of the Biu and Song lavas compared to the remainder of the Cameroon line	246
6.1.6	Cr plotted against Zr for the Biu and Song lavas	248
6.1.7	P_2O_5-Ce and Zr-Nb correlation diagrams of the Biu and Song lavas	251
6.1.8	Ti-Zr-Y discrimination diagram for the Biu and Song lavas	252
6.2.1	Frequency histogram of Sr isotope data from Biu and Song compared to basic rocks from the Gulf of Guinea islands and from Cameroon	254
6.2.2	Rb-Sr plot of Biu and Song lavas	255
6.2.3	Strontium isotope ratio plot of Biu and Song lavas	256
6.2.4	Initial strontium isotope ratios plotted against degree of silica over- and under- saturation for the Biu and Song lavas	258
6.2.5	Lanthanum-yttrium variation in Biu and Song lavas	259

		Page
7.1.1	Alkali-silica diagram for the Cameroon line volcanic rocks	263
7.1.2	Normalized trace element diagram for the Cameroon line mafic rocks	264
7.1.3	Histogram of initial 87Sr/86Sr ratios in mafic rocks from the Cameroon line volcanoes	266
7.1.4	Histogram of initial 87Sr/86Sr ratios in intermediate and evolved rocks from the Cameroon line volcanoes	269

LIST OF TABLES

		Page
3.1.1	K-Ar Data from Principe	31
3.1.2	K-Ar Data from São Tomé	37
3.1.3	K-Ar Data from Other Sources from São Tomé	38
3.1.4	K-Ar Data from Pagalu	46
3.2.1	K-Ar Dates of the Cameroon Volcanoes from Other Sources	50
3.2.2	K-Ar Data from Etinde	52
3.2.3	K-Ar Data from Manengouba	55
3.2.4	K-Ar Data from Bambouto	59
3.2.5	K-Ar Data from Oku	62
3.2.6	K-Ar Data from the Mandara Mountains	66
3.2.7	K-Ar Data from the Biu Plateau from Other Sources	69
3.2.8	K-Ar Data from the Biu Plateau	69
3.3.1	Rb-Sr Isotope Dilution Analyses of the Kirawa Rhyolite	77
3.3.2	Rb-Sr Ages of Intrusions	79
3.3.3	K-Ar Ages of Intrusions	80
3.4.1	Chronology of the Cameroon Line	83
4.1.1	Rb, Sr and 87Sr/86Sr Data from Principe	91
4.1.2	Principe Regressions	96
4.2.1	Rb, Sr and 87Sr/86Sr Data from São Tomé	109
4.2.2	São Tomé Regression Data - Fractionated Rocks	116
4.3.1	Recalculated CIPW Norms of Bioko Chemical Analyses	125
4.3.2	Geochemical and 87Sr/86Sr Data from Bioko	127
4.3.3	Recalculated CIPW Norms of Pagalu Lava Samples	132
4.3.4	Geochemical and 87Sr/86Sr Data from Pagalu	135
4.4.1	Mean Selected Element Abundances and Ratios in Lavas from the Oceanic Islands	142
4.4.2	Mean Elemental Ratios and 87Sr/86Sr Ratios of Mafic Rocks Selected from the Oceanic Islands for Isotopic Analysis	142

		Page
5.1.1	Mean Element Abundances and Ratios of Lava Samples from Cameroon	167
5.1.2	87Sr/86Sr Data from Mt. Cameroon	171
5.1.3	Enrichments of Some Incompatible Elements in Etinde Lavas	178
5.1.4	87Sr/86Sr Data from Etinde	186
5.1.5	87Sr/86Sr Data from Manengouba	199
5.1.6	Mean 87Sr/86Sr Ratios from the Manengouba Volcanoes	200
5.2.1	87Sr/86Sr Data of Mafic Rocks from Bambouto	206
5.2.2	87Sr/86Sr Data of Mafic Rocks from Oku	207
5.2.3	87Sr/86Sr Data of Contaminated Mafic and Intermediate Volcanic Rocks from Cameroon, and Granulite Xenoliths	209
5.2.4	87Sr/86Sr Data of Fractionated Rocks from Bambouto	214
5.2.5	87Sr/86Sr Data of Intermediate and Fractionated Rocks from Oku	217
5.2.6	Strontium Isotope Data of Mafic Rocks from Mandara	223
5.2.7	Strontium Isotope Data of Trachytes and Rhyolites from Mandara	225
5.3.1	Published Initial Strontium Isotope Data from the Tertiary Ring Complexes	230
6.1.1	Mean Element Abundances and Ratios from the Biu and Song Plateaux Lavas	249
6.2.1	Strontium Isotope Data from N.E. Nigeria	253
6.2.2	Strontium Isotope Dilution Data of Megacrysts in Biu Lavas	260
7.1.1	Mean Initial 87Sr/86Sr Ratios of ne and hy Norm Lavas from Principe, São Tomé and Biu	268
7.2.1	Mean Initial Strontium Isotope Ratios From the Cameroon Line Volcanoes	271
7.2.2	Mean Initial Strontium Isotope Ratios of Atlantic Ocean Islands and West African Volcanic Fields	272
A1	Replicate 87Sr/86Sr Analyses	286
A2	Duplicate Rb-Sr Isotope Dilution Analyses	287
A3	Replicate Flame Photmetric Potassium Analyses Compared with XRF Data	290

		Page
A4	U.S.G.S. Standards - Duplicate XRF Analyses	294
A5	Comparison of Edinburgh XRF and S.U.R.R.C. Isotope Dilution Rb and Sr Analyses	295
B1	XRF Analyses of Biu Plateau Lavas	297
B2	XRF Analyses of Volcanic Rocks from the Mandara Mountains	300
B3	Biu Plateau CIPW Norms	302
B4	Mandara Mountains CIPW Norms	304

CHAPTER 1

INTRODUCTION

1.1 Geological Framework of the Cameroon Line Volcanoes

The Cameroon line is a chain of Tertiary to Recent, transitional to strongly alkaline intraplate volcanoes. The line extends from the S. Atlantic island of Pagalu (formerly named Annobon), through the islands of São Tomé, Principe and Bioko (formerly Fernando-Poo) and onto the continental centres of Etinde, Mt. Cameroon, Manengouba, Bambouto and the Oku Massif. North of Oku the chain splits into two branches. One branch trends northwards to the Biu Plateau in N.E. Nigeria while the other trends eastwards through the Tchabal Mbabo Plateau to the Ngaoundéré Plateau of E. Cameroon (Figure 1.1). The oceanic islands rise above the abyssal plain, with the exception of Bioko which rests on the West African continental shelf.

The continental volcanoes are situated on intercratonic Pan-African granite-gneiss (~600 Ma, Lasserre, 1967; Grant, 1970) between the N.W. African and Congo cratons (Figure 1.2). Mt. Cameroon and the Biu Plateau also partially cut through Cretaceous sediments (Figures 3.2.1 and 3.2.2). Some of the volcanoes have fissures or dykes with long axes parallel to the trend of the Cameroon line (overall N.E.-S.W., in Biu N-S, in Ngaoundéré N.W.-S.E.)

Volcanic activity of the centres mentioned above dates back to about 35 Ma (Gouhier et al., 1974; Dunlop and Fitton, 1979; this study, Chapter 3) and shows no consistent migration with time. Signs of recent activity in the form of small scoria cones, are present at most of these magmatic centres. Earlier, Palaeogene

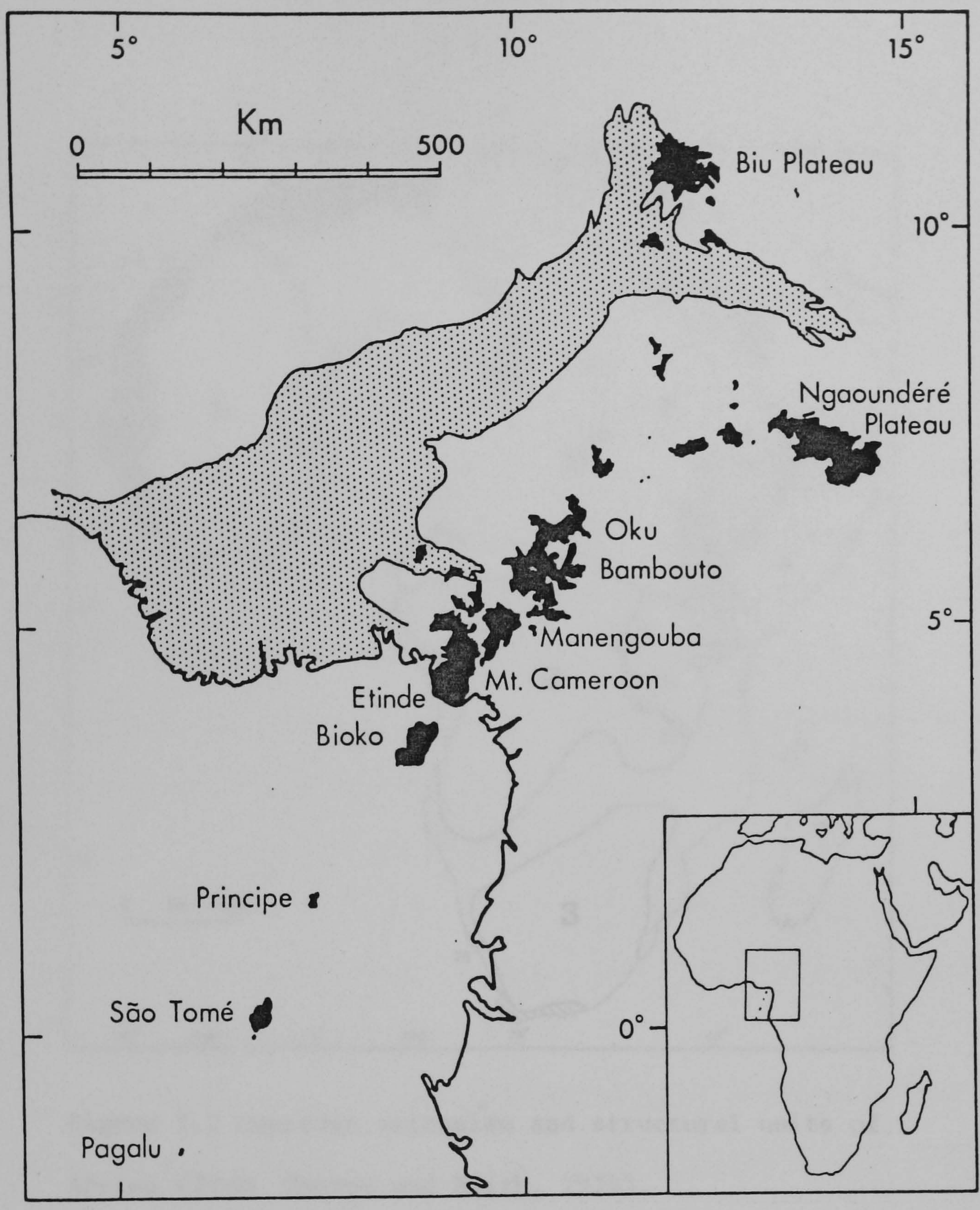


Figure 1.1 Map showing the Cameroon line Tertiary-Recent volcanoes (black) and the limits of the neighbouring Benue trough Cretaceous sediments (stippled area).

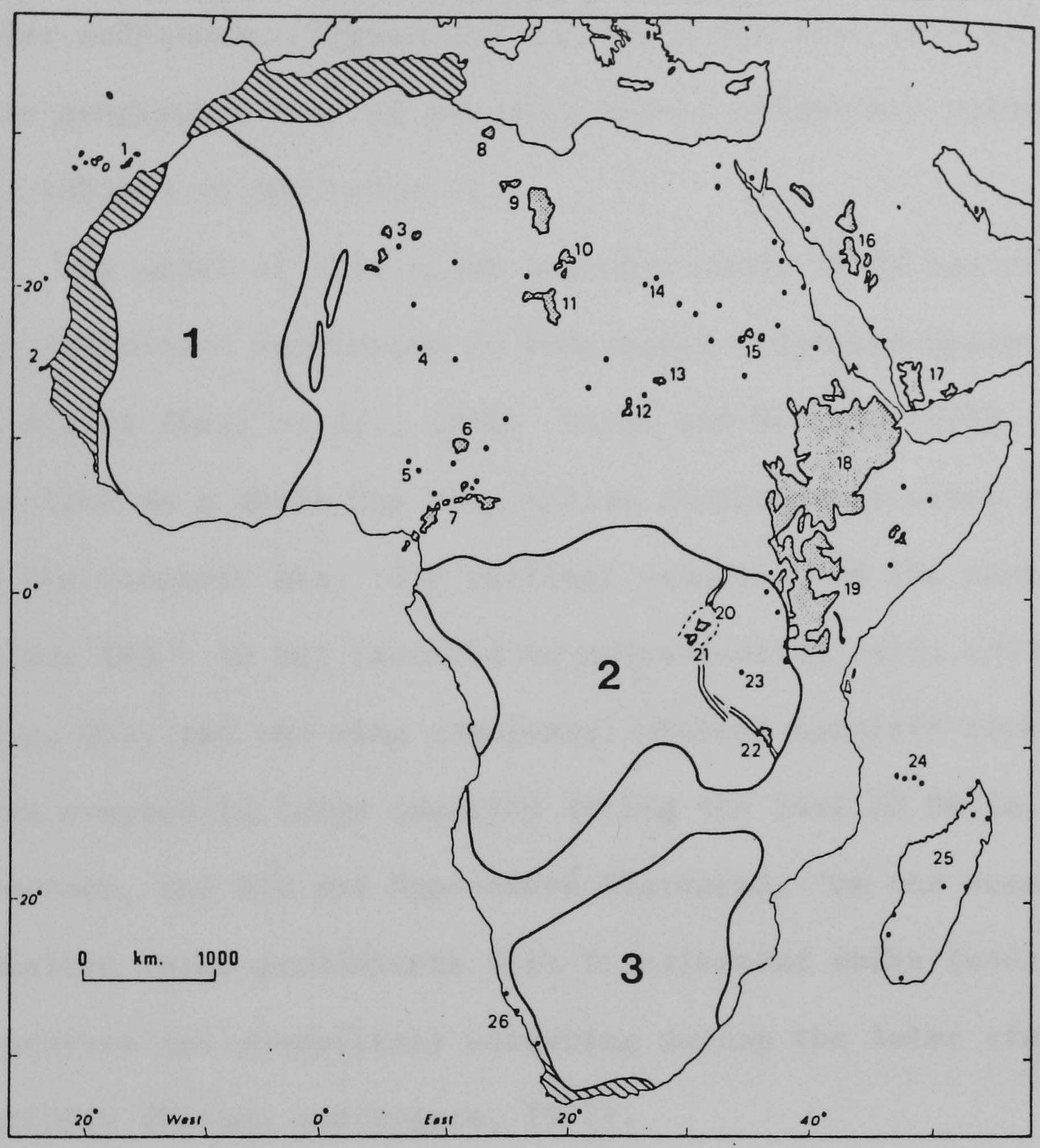


Figure 1.2 Cenozoic volcanism and structural units of Africa (from Thorpe and Smith, 1974).

Extensive Cenozoic volcanic fields are shown stippled and smaller areas of Cenozoic volcanism are shown as single dots. Individual volcanic areas are as follows : 1=Canary Islands; 2=Dakar; 3=Hoggar; 4=Aïr; 5=Jos; 6=Biu; 7=Cameroon Line; 8=Tripolitania; 9=J. Haruj; 10=Eghei; 11=Tibesti; 12=J. Marra; 13=Meidob; 14=J. Uweinat; 15=Bayuda; 16=West Arabia; 17=South Arabia and Aden; 18=Ethiopa; 19=East African (Kenya) Rift with 20=Birunga; 21=Kivu; 22=Rungwe; 23=Igwisi Hills; 24=Comores; 25=Madagascar; 26=Southwest Africa. The dashed line encloses the Pan-African "thermal node" of Clifford (1967) and the thin lines outline the trend of the Western Rift. Cratons are shown in outline as follows: 1=Northwest African Craton; 2=Congo Craton; 3=Kalahari Craton. The diagonally lined areas have been affected by post-Pan-African orogenies and volcanics associated with these young fold belts are not shown.

igneous activity associated with the Cameroon line occurred with the emplacement of anorogenic syenite-granite ring complexes between 30 and 65 Ma (Catagrel et al., 1978; Lasserre, 1978; Jacquemin, 1981 ; Jacquemin et al., 1982) having minor remnants of mainly acidic volcanism. This phase clearly represents the eroded remnants of older volcanoes. Figure 3.3.1 illustrates that they fall in the same geographic zone as the more recent voluminous volcanics forming the subject of this thesis.

The onset of this major activity about 35 Ma ago coincides with the postulated initiation of widespread Oligocene-Recent volcanism in Africa (Gass et al., 1978; Burke and Wilson, 1976). However, the line as a whole has been active continuously since the beginning of the Cenozoic Era. The earliest volcanism on the continental sector (65 - 10 Ma) resulted in oversaturated salic central volcanoes (e.g. Oku, and the ring complexes) whereas basaltic rocks have only been erupted in large quantity during the last 10 Ma (e.g. Mt. Cameroon, and Biu and Ngaoundéré Plateaux). On the oceanic islands basaltic rocks predominate with fractionated rocks (undersaturated trachytes and phonolites) occurring during the later stages of activity (Fitton and Hughes, 1977).

Volcanism has been accompanied by broad regional uplift of the Pre-Cambrian basement in excess of 1000 m (Burke et al., 1972; Black and Girod, 1970; Le Bas, 1971) but there is no evidence for rift faulting as has been postulated in the adjacent Benue trough (Cratchley and Jones, 1965; Ajakaiye and Burke, 1973; Adighije, 1979). Other associated magmatism in this sector of the African Plate includes the Jos Plateau (N. Nigeria) granite intrusives and associated volcanics and further north, the centres of Aïr, Hoggar and Tibesti (Figure 1.2).

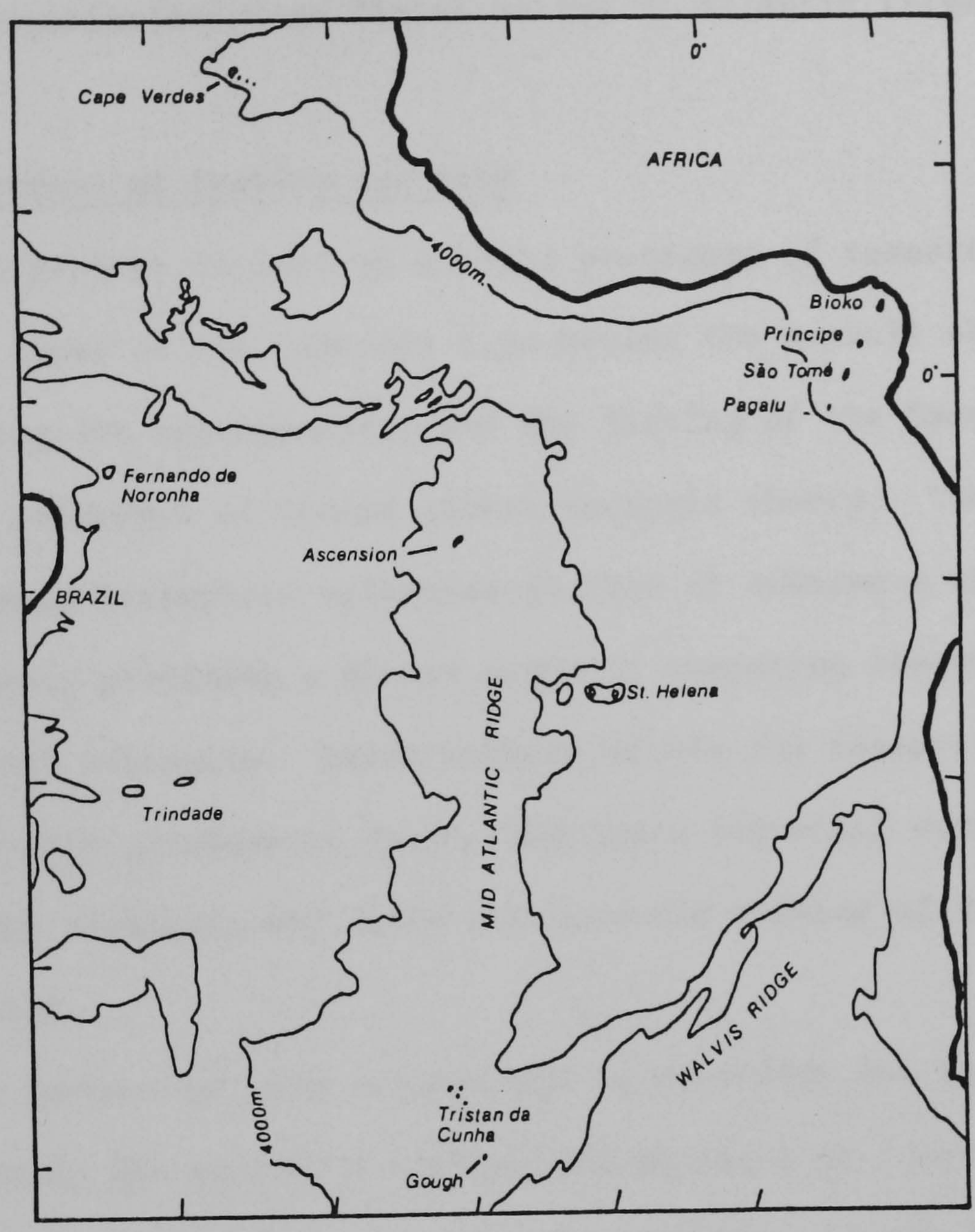


Figure 1.3 Islands in the Central-south Atlantic Ocean.

This figure also illustrates the concentration and restriction of African volcanism to the intercratonic, mainly Pan-African belts (Thorpe and Smith, 1974). On the oceanic sector, the Cameroon line is possibly associated with the islands of St. Helena (African Plate) and/or Ascension (American Plate) in the S. Atlantic (Figure 1.3).

1.2 Statement of Problem and Aims

This project is part of a large programme of research on the volcanic rocks of the Cameroon line having the overall objectives of determining its petrogenesis, and the fitting of the Cameroon line into the framework of modern global tectonic theory. The province is unique among intraplate volcanoes in that it crosses a continental margin hence providing a direct means of comparing oceanic and continental volcanism. Other workers within the research group are involved with geochemical (major and trace elements) work, electron-microprobe analysis, and field and tectonic studies of various sections of the line.

The purpose of this project was to determine the age of volcanism and to study the strontium isotope geochemistry of representative material from the Cameroon line; with the intention of helping to elucidate the overall genesis, the relationship with the adjacent Benue trough and other areas of igneous activity in West Africa and the S. Atlantic. In particular, a comprehensive high precision $^{87}Sr/^{86}Sr$ ratio study was envisaged since the strontium isotopic composition of igneous rocks provides a basis for discussion, both of the origin of magmas and of the mantle evolution of strontium through time. Rb-Sr work on representative samples allows studies of: (a) broad changes in $^{87}Sr/^{86}Sr$ ratios along the line; (b) intravolcanic centre variations in

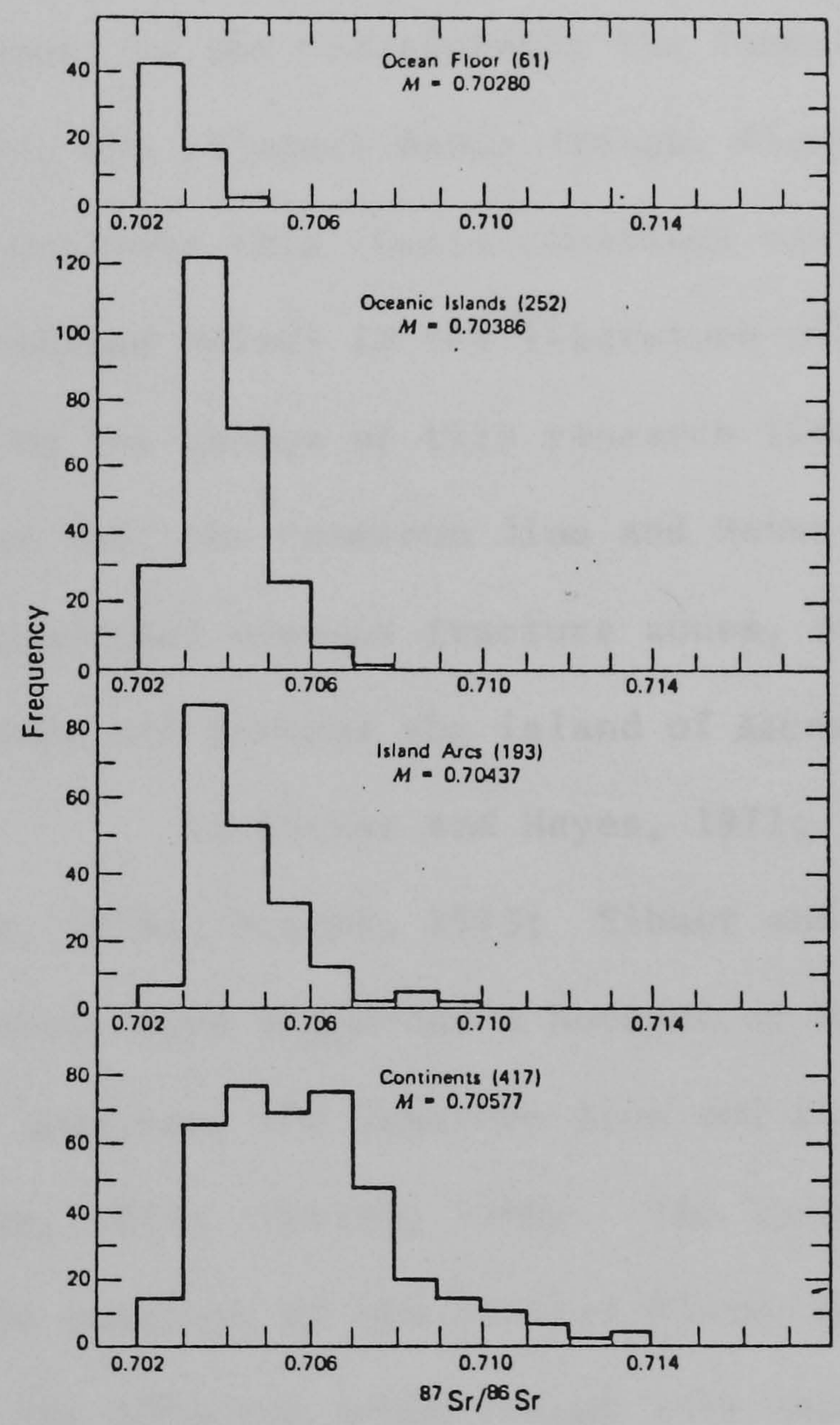
$^{87}Sr/^{86}Sr$ ratios; (c) comparisons with existing models and data from other oceanic islands and continental volcanics; (d) discussion of contamination, magma mixing and mantle genesis mechanisms to account for the patternsof variation seen in strontium isotopes and in major and trace element data.

Further (c) and (d), it was intended to investigate the relationship between continental and oceanic volcanic centres, their source regions and to ascertain the degree (if any) of interaction between magma and continental crust or altered oceanic lithosphere. The Cameroon line could be thought of in terms of three individual sectors: the three islands (Principe, São Tomé and Pagalu) rising from the abyssal plain; Bioko, the island on the continental shelf; and the continental sector situated between two Archaean cratons on Pan-African (~600 Ma) basement (Figures 1.2 and 3.1.4). Hence this area of volcanic activity (1600 km long) provides a unique opportunity to study and compare associated, but chemically varied (from olivine tholeiite to melilite-nephelinite) within plate continental and oceanic magmatism. The continental sector is underlain by a substantially thicker lithosphere than is the oceanic sector (Pollack and Chapman, 1977) and the broadly similar chemistry of the volcanics from both sectors enables one to study closely the overprinting effects of the more radiogenic, continental lithosphere.

It has been observed for some time that continental volcanics exhibit highly variable trace element and Sr-isotope characteristics ranging from similar features to MORB as in the Tertiary basalts from Baffin Bay (O'Nions and Clarke, 1972) to $^{87}Sr/^{86}Sr$ ratios far in excess of fresh oceanic island basalts (Faure and Hurley, 1963; Bell and Powell, 1969; Powell and Bell, 1974; Faure et

al., 1974; Vollmer, 1975, 1976, 1977; Cox et al., 1976; Carter et al., 1978). The mean $^{87}Sr/^{86}Sr$ of oceanic island basalts is 0.70386 whereas that of continental basalts is 0.70577 (Faure, 1977). However, although one commonly sees low continental values (Pankhurst, 1977) overlapping the oceanic island field, the oceanic sector (Figure 1.4) does not approach the $^{87}Sr/^{86}Sr$ maximum of the continental array. Whilst these differences are often attributed to various contamination processes (e.g. Green and Ringwood, 1967; Bell and Powell, 1969; Ewart and Stipp, 1968 ; Faure et al., 1974; Thompson et al, 1982) some authors have recently accounted for trace element and Sr and Nd isotope variations (De Paolo and Wasserburg, 1976a, 1976b, 1979; Wasserburg and De Paolo, 1979; De Paolo, 1978; Carter et al., 1978; Sun and Hanson, 1976; Leeman, 1975, 1977, 1982; Menzies, 1978; Basu and Tatsumoto, 1980; Menzies and Murthy, 1980a; Kornprobst et al., 1981) to chemical differences existing between the suboceanic and subcontinental mantle. On the other hand some researchers have produced and discussed convincing geochemical and isotope evidence to show the existence of similarities between suboceanic and subcontinental mantle and volcanics (e.g. Schwarzer and Rogers, 1974; Beswick, 1978; Pankhurst, 1977; Frey et al., 1978; Carter et al., 1979; Basu and Tatsumoto, 1980; Allègre et al., 1981, 1982; Loubet, 1981; Anderson, 1982; Bell et al., 1982). In addition it has been suggested (Bailey, 1974, 1977; Le Bas, 1971; Thorpe and Smith, 1974; Lloyd and Bailey, 1975; Duda and Schminke, 1978; Gass et al., 1978) that the lithospheric structural fabric, thermal state, composition and thickness controls the site of initial crustal swelling and subsequently the character of continental magmatism. This would imply that the continental lithosphere would impose characteristics on the magmatism not incorporated in the oceanic volcanics and one might therefore expect to observe

A



B

Figure 1.4 $^{87}Sr/^{86}Sr$ volcanic data as reviewed by Faure and Powell (1972, figure A) and Faure (1977, figure B).

geochemical and isotopic differences between the oceanic and continental sectors of the Cameroon line volcanoes. If, however, crustal swelling or doming was an effect rather than the cause of mid-plate magmatism, as would be the case if fixed, sub-lithospheric hotspots or zones under a stationery plate controlled the site of igneous activity (Wilson, 1963; Morgan, 1971, 1972; Schilling, 1973; Anderson, 1975; Burke and Wilson, 1976), the geochemistry and isotopes would reflect the signature of their mantle source regions especially if crustal magma residence times were minimal.

With respect to the relationship the Cameroon line bears to the South Atlantic, the adjacent Benue trough, Nigerian magmatism and the African continent this thesis considers various conflicting proposals (outlined below) in the literature with new results obtained during the course of this research (Chapter 7). It has been suggested that the Cameroon line and Benue trough are intimately related to equatorial oceanic fracture zones, pre-existing continental lineaments and perhaps the island of Ascension (Hedberg, 1968; Burke, 1969; Le Pichon and Hayes, 1971; Gorini and Bryan, 1976; Wright, 1976a; Mascle, 1975; Sibuet and Mascle, 1978). Other researchers have suggested a hotspot or hotzone link between the Nigerian granites, the Cameroon line and the island of St. Helena (Morgan, 1972; Fitton, 1980). The latter, together with an appropriate movement of the African Plate, may account for the relationship the adjacent Benue trough (the failed arm of a r-r-r triple junction, Burke et al., 1971; Burke and Wilson, 1976) bears to th Cameroon line (Fitton, 1980). Alternatively, Freeth (1978a, 1978b, 1979) explained the magmatism in West Africa and the Gulf of Guinea in terms of membrane stresses (as described by Oxburgh and Turcotte, 1974) generated by the movement of the African Plate over a non-spherical earth, giving rise to tectonic activity (doming and

rifting) invoked as initiating volcanism.

A programme of combined K-Ar and Rb-Sr isotope data acquisition was therefore proposed (Nd analysis was not available) to attempt to resolve some of these controversies. K-Ar ages were considered necessary for the interpretation of initial $^{87}Sr/^{86}Sr$ ratios (especially on fractionated rocks) as well as establishing the history of volcanism. Also, ages of the oceanic islands afford critical evidence on the evolution of the Atlantic Ocean.

Principal methods employed were: high precision $^{87}Sr/^{86}Sr$ isotope geochemistry; Rb-Sr isotope dilution analyses; ^{36}Ar-^{40}Ar dating studies and K flame photometry; and major and trace element determinations by X-ray fluorescence (at Edinburgh University) of samples not previously analysed by other workers.

Rocks analysed were collected from the islands of Principe and São Tomé in 1974 and from South-Central Cameroon in 1975 by J.G. Fitton and D.J. Hughes. Samples from the Biu Plateau (N. Nigeria) and the Mandara Mountains (N. Cameroon) were collected in 1977-1978 by the author, J.G. Fitton and D.J. Hughes. Palaeomagnetic core samples analysed were collected by J.D.A. Piper and the late A. Richardson from the islands of Bioko and Pagalu. At the time of data acquisition at S.U.R.R.C., East Kilbride no samples were available from the eastern branch of the Cameroon line, the Ngaoundéré Plateau.

Chapter 2 gives a review of the isotope methodology employed and Chapters 3-6 describe the geology, age data, isotopes and geochemistry of the various volcanic centres forming the Cameroon line. Chapter 7 is a synthesis of this data and discusses the problems set out above.

Some of the results of the research group have already been published: Dunlop and Fitton (1979, a copy of which appears in the appendix); Fitton and Hughes (1977); Fitton (1980); Fitton and Hughes (1981); Dunlop and Fitton (1981).

CHAPTER 2

PRINCIPLES AND METHODOLOGY OF THE ISOTOPIC TECHNIQUES EMPLOYED

2.1 The Theory of Rb-Sr Geochronology and Isotope Geochemistry

Rubidium has two naturally occurring isotopes $^{85}_{37}Rb$ and $^{87}_{37}Rb$ whose isotopic abundances are 72.1654 and 27.8346 respectively (Catanzaro et al., 1969). ^{87}Rb is radioactive and decays to the stable nuclide ^{87}Sr by negative β particle emission. The associated decay energy is only 0.275 MeV and this has made accurate determination of the halflife and the decay constant (λ) difficult. Along with most other isotope laboratories, the S.U.R.R.C. has now adopted the λ value of 1.42×10^{-11} yr^{-1}. (Davis et al., 1977; Steiger and Jager, 1977). This almost unanimous agreement (a result of the 1976 I.U.G.S. Subcommission on Geochronology meeting, held in Australia, to adopt a new standard set of decay constants and isotopic abundances) means direct comparisons of results from different laboratories are now possible.

Strontium has four naturally occurring stable isotopes: $^{88}_{38}Sr$, $^{87}_{38}Sr$, $^{86}_{38}Sr$, and $^{84}_{38}Sr$. Their respective isotopic abundances are 82.53%, 7.04%, 9.87%, and 0.56%. The nuclide ^{87}Sr is the only isotope produced by radioactive decay of another nuclide and thus ^{88}Sr, ^{86}Sr and ^{84}Sr are assumed to remain constant through time. Geological processes do not produce any fractionation of strontium isotopes that can be detected with existing analytical techniques.

The total ^{87}Sr in a rock or mineral is composed of ^{87}Sr present at the time of the rock's formation plus the ^{87}Sr radiogenic component produced since that time by the decay of ^{87}Rb. The precise isotopic composition of strontium therefore depends on the age and

Rb/Sr ratio of the rock or mineral in question. This may be expressed in the following relation:

$$^{87}Sr/^{86}Sr_{present} = {}^{87}Sr/^{86}Sr_{0} + {}^{87}Rb/^{86}Sr_{present}\ e^{\lambda t} - 1$$

where t is time since closure of the isotopic system and λ is the decay constant. The ^{87}Sr isotopic parameters are ratioed against ^{86}Sr since in mass-spectrometry (see Appendix A1) relative values are always determined. This is the equation of a straight line (isochron) where the intercept gives the initial $^{87}Sr/^{86}Sr$ ratio and the slope ($e^{\lambda t} - 1$) is proportional to the age. A plot of $^{87}Rb/^{86}Sr$ versus $^{87}Sr/^{86}Sr$ (measured) for a series of contemporaneous rock samples should then yield a straight line indicating isotopic equilibrium. A suite of volcanic rocks will have the same initial $^{87}Sr/^{86}Sr$ ratios if they are comagmatic and when the rocks have remained closed to rubidium and strontium since crystallization.

Rubidium is a group IA alkali metal and has an ionic radius (1.48Å) sufficiently similar to that of potassium (1.33Å) to allow Rb to substitute for K in all K - bearing phases. Strontium is a Group IIA alkaline earth and has an ionic radius (1.13Å) slightly larger than that of calcium (0.99Å) which it can replace in many phases. Thus it occurs in Ca-bearing minerals such as plagioclase and apatite. During magmatic crystallization, strontium tends to be concentrated in early-formed calcic plagioclase while rubidium remains in the liquid phase. As a result the Rb/Sr ratio of the residual magma will increase with differentiation. Thus evolved rocks tend to have progressively higher Rb/Sr ratios and consequently will, in time, develop elevated $^{87}Sr/^{86}Sr$ ratios in relation to their mafic counterparts. In the case of this study evolved rocks occur in most of the volcanic centres under consideration and these plot on iso-

chrons indicating the approximate age of volcanism.

Apart from giving information concerning the age of a mineral or rock, Rb-Sr isotopic methods can give important information to geochemical and petrological studies with the diagnostic 'tracer' ratio of initial $^{87}Sr/^{86}Sr$. The best insight into the present day strontium isotopic composition of the earth's mantle has come from measurement of $^{87}Sr/^{86}Sr$ ratios of young oceanic basaltic rocks. These rocks are rich in strontium (frequently >1000 p.p.m.) and are not therefore very easily affected by any natural contamination caused by assimilation of strontium from sources in the earth's crust. Also, the young lavas which erupt on oceanic islands presumably have issued through earlier volcanics and thus assimilation of wall-rocks should not significantly alter the $^{87}Sr/^{86}Sr$ values. Rubidium and strontium in general tend to behave as incompatible elements and are therefore removed at the source by small degrees of partial melting.

Variations in $^{87}Sr/^{86}Sr$ ratios probably represent primary features and are not likely to be due to isotopic fractionation since such fractionation is unlikely to occur in isotopes as heavy as those of strontium (where the mass difference is very slight compared to, say, oxygen isotopes). Even if ^{87}Sr and ^{86}Sr were partitioned differentially between phenocrysts and liquid (O'Hara, 1977) such resultant fractionation would be removed by laboratory procedures employed for correcting mass-spectrometer fractionation.

Basalts from oceanic regions show a restricted range in $(^{87}Sr/^{86}Sr)_0$ values ranging from 0.702 to 0.706 (Faure, 1977). In particular, samples from the ocean floors fall within a very small range of 0.7025 to 0.7035 (with the majority falling between 0.7023-0.7027) whilst oceanic islands are far more variable (Hofmann and Hart, 1978, figure 1). The pattern is one of distinct groupings of

basalts from the different environments in terms of isotopic compositions. Strontium isotopic compositions have been used to set constraints on the origin and composition of the source material of volcanic rocks (e.g. Gast et al., 1964; Hedge and Peterman, 1970; O'Nions et al., 1976; Sun and Hanson, 1975a). Variations in $^{87}Sr/^{86}Sr$ ratios in oceanic basalts were initially ascribed to disequilibrium partial melting of a homogeneous mantle (Graham and Ringwood, 1971; O'Nions and Pankhurst, 1974; Flower et al., 1975; O'Hara et al., 1975; James, 1975; Beswick, 1976, 1978; Beswick and Carmichael, 1977, 1978). However it is now more generally thought to be due to equilibrium partial melting of a heterogeneous mantle (e.g. Cox et al., 1976; Brooks et al., 1976a; Hanson, 1977; Hofmann and Hart, 1978; Dunlop and Fitton, 1979; Sun, 1980).

Volcanics from continental regions show a much larger range in initial values from 0.703 to higher than 0.710. Thus Faure (1977), (Figure 1.4) suggested that there are systematic differences in the average $^{87}Sr/^{86}Sr$ ratios of volcanics from different environments and also that real variations exist within volcanic rocks in each of four categories: oceanic basin; ocean island; island arc; and continent. High values of $(^{87}Sr/^{86}Sr)_0$ from continental volcanic rocks may be due to various contamination mechanisms with high Rb/Sr continental crust such as: assimilation (Faure et al., 1974; Thompson et al., 1982); wall-rock interactions (Green and Ringwood, 1967; De Paolo, 1981); selective ^{87}Sr migration and isotopic re-equilibrium; or elevation of $^{87}Sr/^{86}Sr$ ratios during protracted fractionation (e.g. McCarthy and Cawthorn, 1980). These processes are most likely for material erupted in continents having passed through a large thickness of silicic crust but may also apply to oceanic islands where magmas may be contaminated by sediments derived from nearby continents or by assimilation of volcanics which have had previous interaction with seawater or meteoric

water (such as pillow lavas) as has been proposed by O'Hara (1977) and Grant et al., (1976). Alternatively, higher isotopic ratios from continental regions may not be due to crustal contamination but rather inherited directly from the subcontinental mantle which may possess anomalous strontium compositions (Brooks et al., 1976b). On the other hand, these elevated ratios may be due to recent enrichment events such as mantle metasomatism (Menzies and Murthy, 1978; 1980a; 1980b; 1980c; Wass and Rogers, 1980) or alternatively to long-lived heterogeneities established 1600-2000 Ma ago (Brooks et al, 1976b; De Paolo and Wasserburg, 1976a; 1976b; Tatsumoto, 1978; Bell et al., 1982).

Published studies of initial strontium ratio variations in igneous rocks have frequently shown up significant positive correlations of initial $^{87}Sr/^{86}Sr$ ratios with Rb/Sr (Bell and Powell, 1969; Dickinson et al., 1969; Cox et al, 1976; Brooks et al; 1976a; 1976b; Carter and Norry, 1976; Duncan and Compston, 1976; Hawkesworth and Vollmer, 1979; Dunlop and Fitton, 1979; Calvez and Lippolt, 1980). Such correlations have been variously called pseudo-isochrons, mantle isochrons, erupted isochrons and errorchrons. These correlations have been taken to indicate chemical, mantle heterogeneities (Brooks et al., 1976a; 1976b; 1976c; Duncan and Compston, 1976; Brooks and Hart, 1978; Pankhurst, 1977) which have existed for millions of years as indicated by "ages" derived from these correlations being in gross excess of true eruption ages. Such correlations are not always regarded as the result of mixing of two or more end-members since plotting initial strontium ratios against the definitive parameters of Sr (p.p.m.) or 1/Sr (Faure, 1977) do not give the desired patterns of hyperbolas and straight lines respectively.

Geochemists are now satisfied that $^{87}Sr/^{86}Sr$ ratio variations in the mantle are not random features since strontium and neodymium isotopic variations in many young basalts are strongly correlated (De Paolo and Wasserburg, 1977; 1979; De Paolo, 1979; O'Nions et al., 1977). Prior to this discovery the possibility existed that $(^{87}Sr/^{86}Sr)_0$ ratio variations were random and not representing systematic differences in age or chemistry between reservoirs, which could be understood in terms of relatively simple petrogenetic processes, since lead isotopic data often bears no simple relationship to strontium systematics. However, one simple relationship does exist: the Rb-Sr mantle isochron for tholeiites is nearly identical in age (1.6 ± 0.2 Ga) to ages (secondary isochrons) of oceanic rocks based on the isotopic composition of Pb (1.8 ± 0.1 Ga, Brooks et al., 1976a; Tatsumoto, 1978). In addition Zindler et al., (1982) have shown that Nd-Sr-Pb isotope ratios from ocean islands and MORB describe a plane in 5 dimensions illustrating the coherence of Nd-Sr-Pb isotope systematics in the present day suboceanic mantle.

Variations in initial $^{87}Sr/^{86}Sr$ ratios of volcanics from both oceanic and continental regions have been accounted for by a large variety of mechanisms and models by various workers and are described and discussed in chapters 4 - 7 . To evaluate and employ these methods and theories the whole-rock analysis of basalts and associated evolved volcanics were performed on carefully selected (free of alteration) samples from centres of the Cameroon line which encompasses two of the four basic isotopic environments; oceanic island and continental in what appears to be one magmatic system. For this study to be a contribution to petrogenesis, $^{87}Sr/^{86}Sr$ data of high precision (by the unspiked method) is required along with

rubidium and strontium concentrations determined by either isotope dilution mass-spectrometry or X-ray fluorescence spectrometry. In addition major and trace element data is required to enable the full study of the $^{87}Sr/^{86}Sr$ relations in these suites. Appendix A1 and A3 give details of the Rb-Sr and X.R.F. analytical techniques employed respectively.

2.2 The K-Ar Method of Dating

Potassium has three naturally occurring isotopes ^{39}K, ^{40}K and ^{41}K in the proportions 93.08%, 0.0119%, and 6.91% respectively (Nier, 1950). The decay of ^{40}K to stable ^{40}Ar occurs by electron capture and by positron emission. Figure 2.1 illustrates the branching decay scheme of ^{40}K. The growth of radiogenic ^{40}Ar and ^{40}Ca in a system closed to potassium, calcium and argon is expressed by:

$$^{40}Ar^* + {}^{40}Ca^* = {}^{40}K\,(e^{\lambda t} - 1) \qquad \text{equation 2.2.1}$$

where λ = total of $\lambda\beta$ (decay constant of ^{40}K to ^{40}Ca) plus

λe (decay constant of ^{40}K to ^{40}Ar)

* = radiogenic isotope

Values used are $\lambda\beta = 4.962 \times 10^{-10}\,yr^{-1}$, and $\lambda e = 0.581 \times 10^{-10}\,yr.^{-1}$ (Wetherill, 1966; Beckinsale and Gale, 1969; Steiger and Jager, 1977).

The growth of radiogenic $^{40}Ar^*$ in the rock may be expressed as:

$$^{40}Ar^* = \frac{\lambda e}{\lambda}\,{}^{40}K(e^{\lambda t} - 1) \qquad \text{equation 2.2.2}$$

which may be solved for age (t):

$$t = \frac{1}{\lambda} \ln \left[{}^{40}Ar^*/{}^{40}K\left(\frac{\lambda}{\lambda e}\right) + 1\right] \qquad \text{equation 2.2.3}$$

^{40}K is calculated from the potassium content (in weight percent) determined by flame photometry and $^{40}Ar^*$ is calculated from the isotopic mass-spectrometric analysis of argon in the sample where the ^{36}Ar, ^{38}Ar, and ^{40}Ar peak heights are determined. The amount of $^{40}Ar^*$

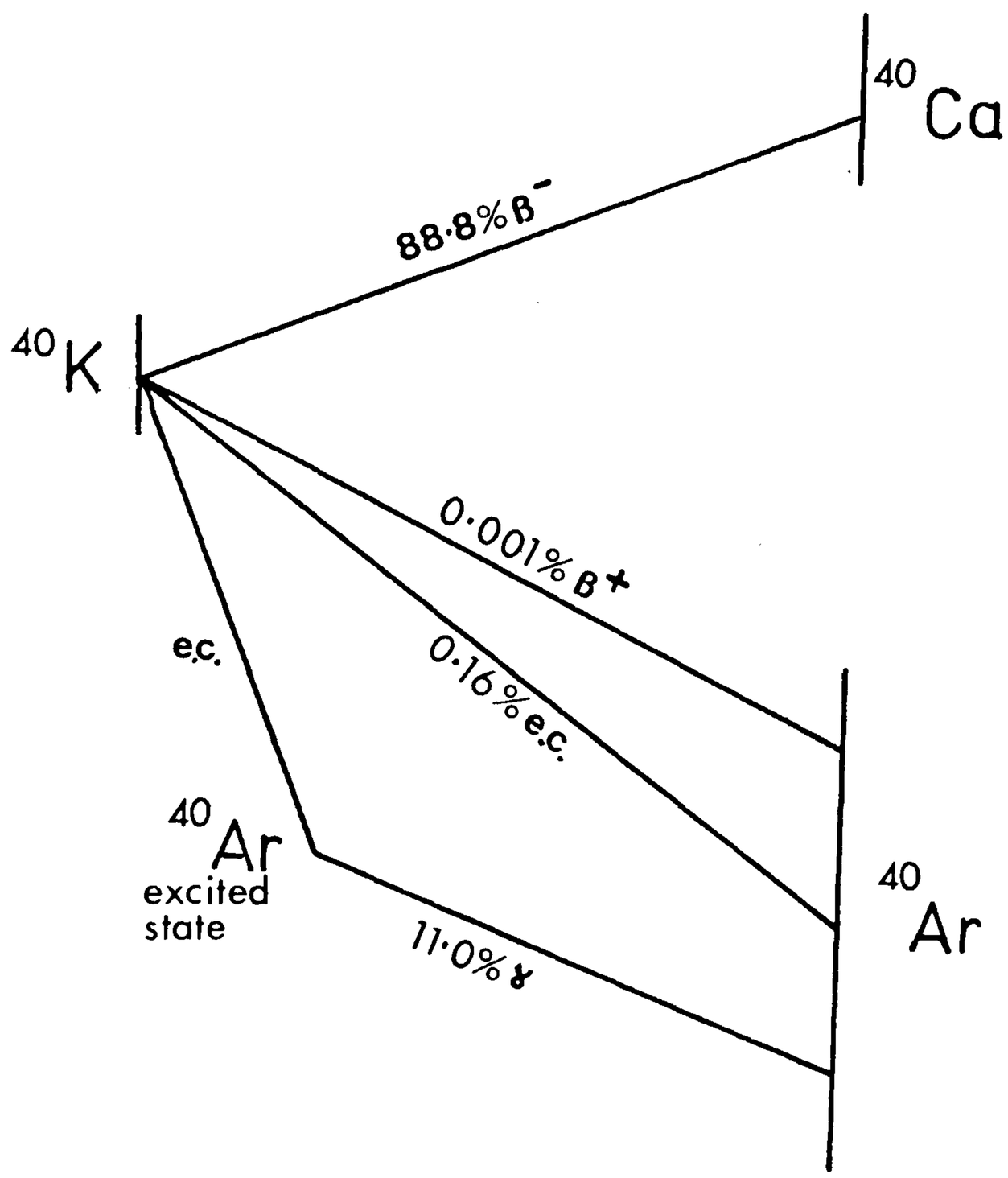


Figure 2.1 The branching decay scheme of ^{40}K.

e.c. = electron capture.

present is computed by subtracting the ^{40}Ar contribution of any atmospheric contamination from the total ^{40}Ar measured by monitoring ^{36}Ar, since the relative proportions of atmospheric argon isotopes are known ($^{40}Ar/^{36}Ar$ atmos. = 295.5), and thus the equation below is employed for calculating the radiogenic component of ^{40}Ar:

$$^{40}Ar^* = {}^{40}Ar_{total} - 295.5 \times {}^{36}Ar \qquad \text{equation 2.2.4}$$

Analytical techniques are given in detail in Appendix A2.

The age of a sample calculated from equation 2.2.3 is its age of formation if the following conditions hold (Faure, 1977); (a), there has been no loss of radiogenic $^{40}Ar^*$ prior to analysis; (b), the rock became closed to ^{40}Ar soon after formation; (c), no excess ^{40}Ar was incorporated into the rock at any time; and (d), the rock has been closed to potassium since formation. The calculation also assumes that any nonradiogenic argon present has the composition of modern atmospheric argon.

The precision of the method depends on the errors associated with the potassium and $^{40}Ar^*$ determinations. Potassium determinations are precise to $\pm$ 1.5%; however, the $^{40}Ar^*$ measurement is largely dependant on the proportion of the atmospheric contribution to the total ^{40}Ar which tends to be high (rarely less than 30%) in rocks analysed in this study. This results in errors in the ages of up to 8% at the 95% confidence level on samples up to approximately 6 Ma old. The error falls to 3% or lower with samples having ages of 20-35 Ma (Mt. Bambouto, Oku Massif, and the Mandara Mts.)

Whole-rock determinations were made in this study since the rocks were too fine grained for the separation of potassium minerals suitable for dating. This technique has given reliable age data to many workers including: Baker and Francis (1978); Dalrymple and Lanphere (1969); Dalrymple et al. (1975, 1977); Burke et al. (1969); McDougall and Schminke (1977); Webb and McDougall (1967). For whole-rock K-Ar

dating the material should be free of chemical weathering and alteration; fine grained and homogeneous; and free of xenoliths, fluid inclusions, amygdales, glass, secondary minerals, and of minerals containing excess argon.

Dalrymple and Lanphere (1969) pointed out that in general K-Ar whole-rock dating of material showing any alteration should be avoided. In particular, the potassium bearing phases should be unaltered. In basalts the critical phases are therefore the feldspars and the groundmass, which are the last phases to crystallize (Mankinen and Dalrymple, 1972). In alteration, potassium is one of the most mobile of elements (Wood et al., 1976) and thus any alteration, such as feldspar kaolinization and sericitization and glass devitrification will affect the argon content of the mineral. Consequently the apparent age will be affected in direct proportion to the amount of potassium the altered phase contains with respect to the whole-rock (Mankinen and Dalrymple, 1972). Minor alteration of olivine and pyroxene is acceptable since they usually contain negligible potassium compared to the total rock. The argon retention characteristics of glass are not well known, but it has been shown that K-Ar determinations on glassy rocks tend to be lower than their true age (Armstrong and Besançon, 1970; Armstrong et al., 1975). Thus in this study, samples bearing glass were not analysed, and as much of the material comprising the Cameroon line is holocrystalline this presented no difficulties in the selection of representative samples. However, the analysis of alteration free material was not always possible (e.g. the Mandara Mts., Chapter 3). Webb and McDougall (1967) obtained reliable dates from quite altered basalts, which compare well with their data from sanidine separates from the same suite.

De Souza (1974) has also obtained reliable ages of basalts from Carboniferous volcanics which appear to have lost little or no argon despite considerable groundmass alteration. De Souza (1979) devised a sequence of degree of alteration and deduced that the maximum degree of alteration showing little or no argon loss was where the olivine was completely altered, feldspars were sericitized along cracks and chloritic mesostasis was present. In this thesis only samples analysed from the Bambouto Mts., Oku Massif, and the Mandara Mts. showed any alteration. These analyses were carefully considered in the light of Rb-Sr isochron age indications.

No samples were analysed which contained xenoliths, megacrysts or amygdales since they are all possible carriers of minerals holding excess argon (Fisher, 1971; this study, chapter 3) which has been derived by outgassing of older potassium minerals in the crust and mantle. The presence of excess ^{40}Ar increases the measured age.

Correct sample preparation for argon isotopic analysis is important to ensure minimum atmospheric argon contamination. Air argon contamination occurs from three principal sources: the sample, the copper foil encapsulating the sample, and the gas extraction system. It is important to reduce air argon contamination to a minimum since atmospheric argon severely masks the small radiogenic $^{40}Ar^*$ component in young volcanics. Gilletti (1974) makes the point that reporting K-Ar ages is no longer a complete process unless the analysis particle size is also given. Keeling and Naughton (1974) studied the amount of air argon uptake during crushing. It was noted that atmospheric argon was acquired in significant quantities and was difficult to remove by baking only when the analysis particle size fell below

63 μm and went higher than 4 mm. The size fractions used in this study were -1.4 mm +20mesh (+750 μm) and -20mesh (-750 μm) +30mesh (+500 μm); and they coincided with the area of minimum air argon contents on Keeling and Naughton's (1974) Figure 1. In addition, crushing removes a large proportion of the loosely held argon within the sample; and reduces errors arising from any sample heterogeneity. Thus it is important to strike an optimum balance, with respect to analysis grain size, to reduce atmospheric argon contamination to a minimum.

Atmospheric argon is removed by baking the samples and the extraction system (the molybdenum crucible having previously been outgassed, following Charlton and Mussett (1973), to 120°C overnight. Hayatsu and Carmichael (1977) observed that atmospheric argon contamination increases with sample storage time after crushing and becomes progressively more difficult to remove by baking. Samples were analysed as soon as possible after crushing; the maximum interval being four weeks.

The study of K-Ar isochrons of $^{40}Ar/^{36}Ar$ versus $^{40}K/^{36}Ar$ has in many instances (e.g.: Fitch et al., 1976; Hayatsu and Carmichael, 1970; Shafiqullah and Damon, 1974) given more precise age dates than the conventional method described above. However, this is the case only when atmospheric contamination is very low (less than 5%). Although much effort was made to reduce air argon contamination, it rarely fell below 30% and as a consequence any straight lines forming on the plot of $^{40}Ar/^{36}Ar$ versus $^{40}K/^{36}Ar$ would merely be mixing lines between the pure sample and air argon composition (Baksi, 1973). This effect of atmospheric argon is shown diagramatically in figure 2.2a and in practice for the Principe Younger Lava Series and phonolites in figure 2.2b.

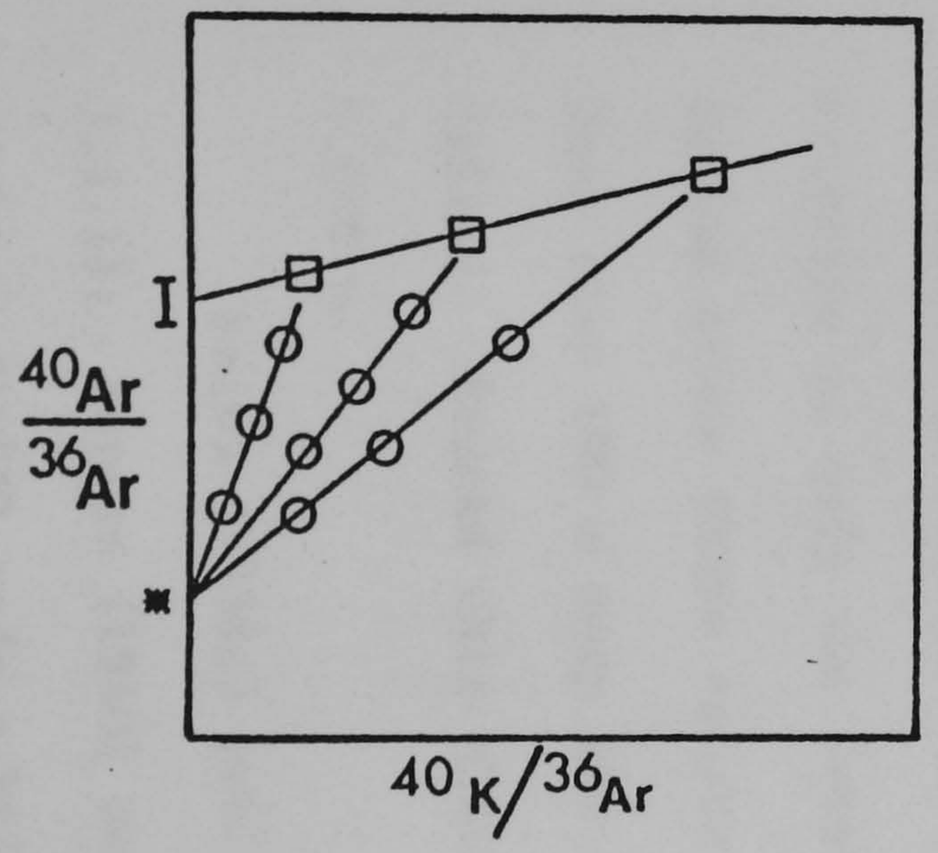


Fig. 2.2a (left) Samples (squares) will define true ages and initial ratios (I) only when they are free of air argon contamination. If air argon is present replicate analyses (circles) will fall on mixing lines between pure sample and atmos. argon composition (*).

Fig. 2.2b (below) Results of replicate analyses from Principe showing a mixing relationship on an argon isochron plot.

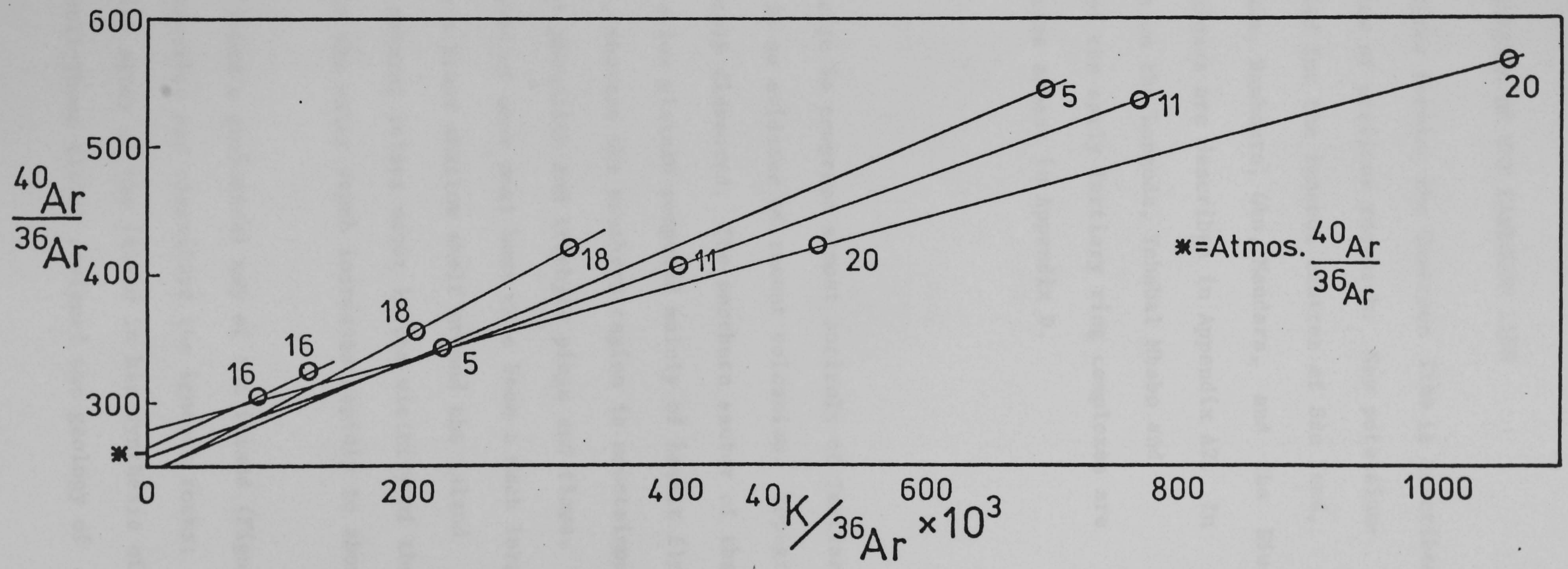


Figure 2.2 Explanation of K-Ar isotope ratio diagrams.

CHAPTER 3

GEOLOGY AND AGE OF VOLCANISM OF THE CAMEROON LINE

The geology of the centres forming the Cameroon line is described and integrated with a review of previous research. New potassium-argon age data are presented for the igneous centres of São Tomé, Principe, Etinde, Manengouba, Bambouto, Oku, Mandara, and the Biu Plateau. Analytical techniques are described in Appendix A2. In addition pre-existing data on the Longuda, Tchabal Mbabo and Ngaoundére plateaux, and of the early Tertiary ring complexes are discussed. Sample localities appear in Appendix D.

3.1 Oceanic Sector

3.1.1 Principe

The island of Principe is composed almost entirely of Tertiary volcanic rocks and there is no evidence of recent volcanism. Topographically the island is severely dissected. The northern sector of the island takes the form of a low plateau composed mainly of basalt flows (Figures 3.1.1 and 3.1.2), whereas the southern region is mountainous and elevated consisting of phonolite and trachyte plugs and flows. Principe is only the remnant of what must have once been a much larger island since there exists a broad shallow shelf around the island less than 100 m deep and several islets occur in the vicinity of the island. Beyond this shelf the water depth increases rapidly to about 4,000 m.

Neiva (1956a) published a geological map of the island (Figure 3.1.1); Barros (1960) described and classified the igneous rocks; Hedberg (1968) made a brief study of the island in his synthesis of the Cameroon Line; Mitchell-Thome (1970) reviewed the geology of

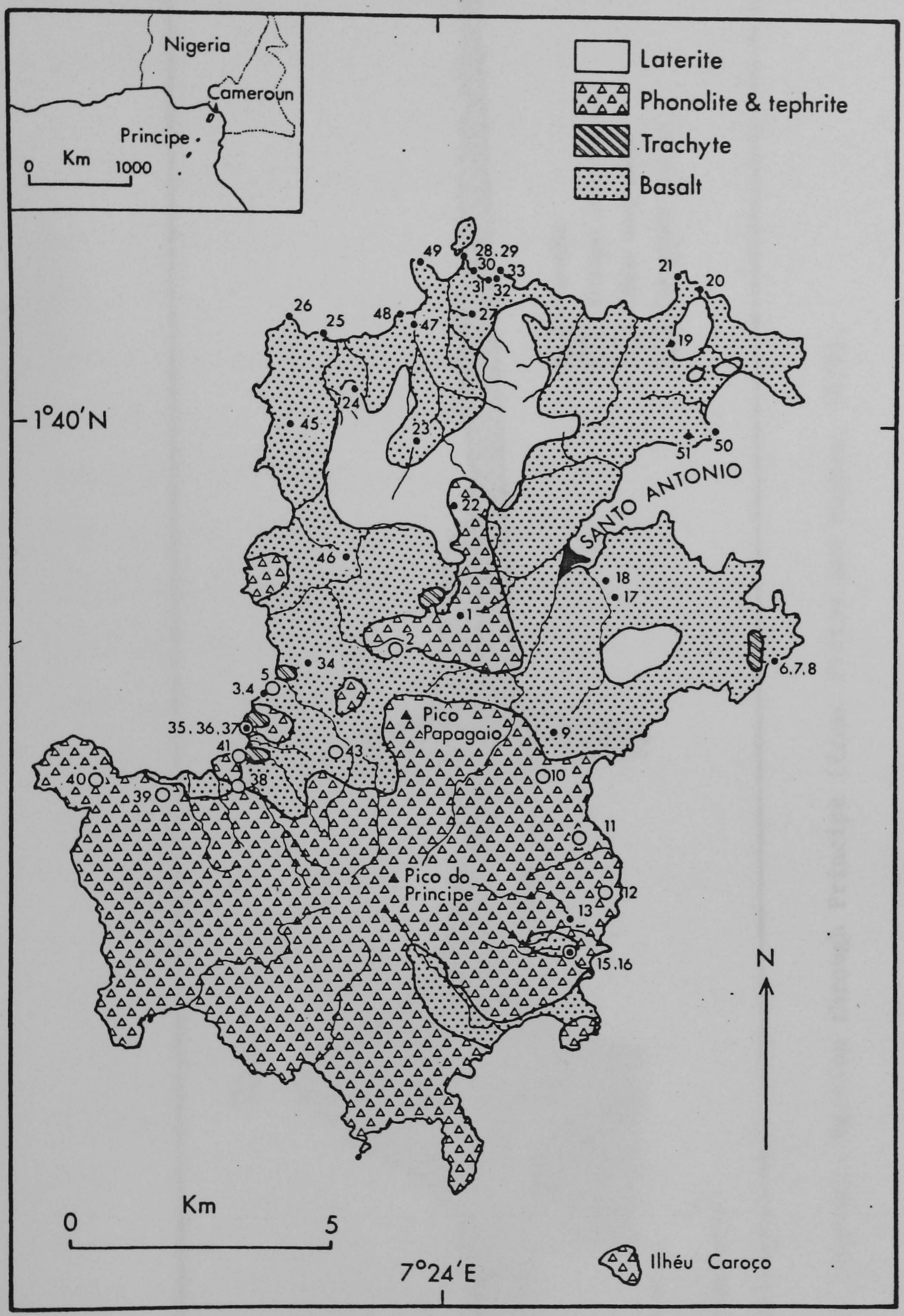


Figure 3.1.1 Geology and sample location map of Principe (Fitton and Hughes, 1977; after Neiva 1956a).

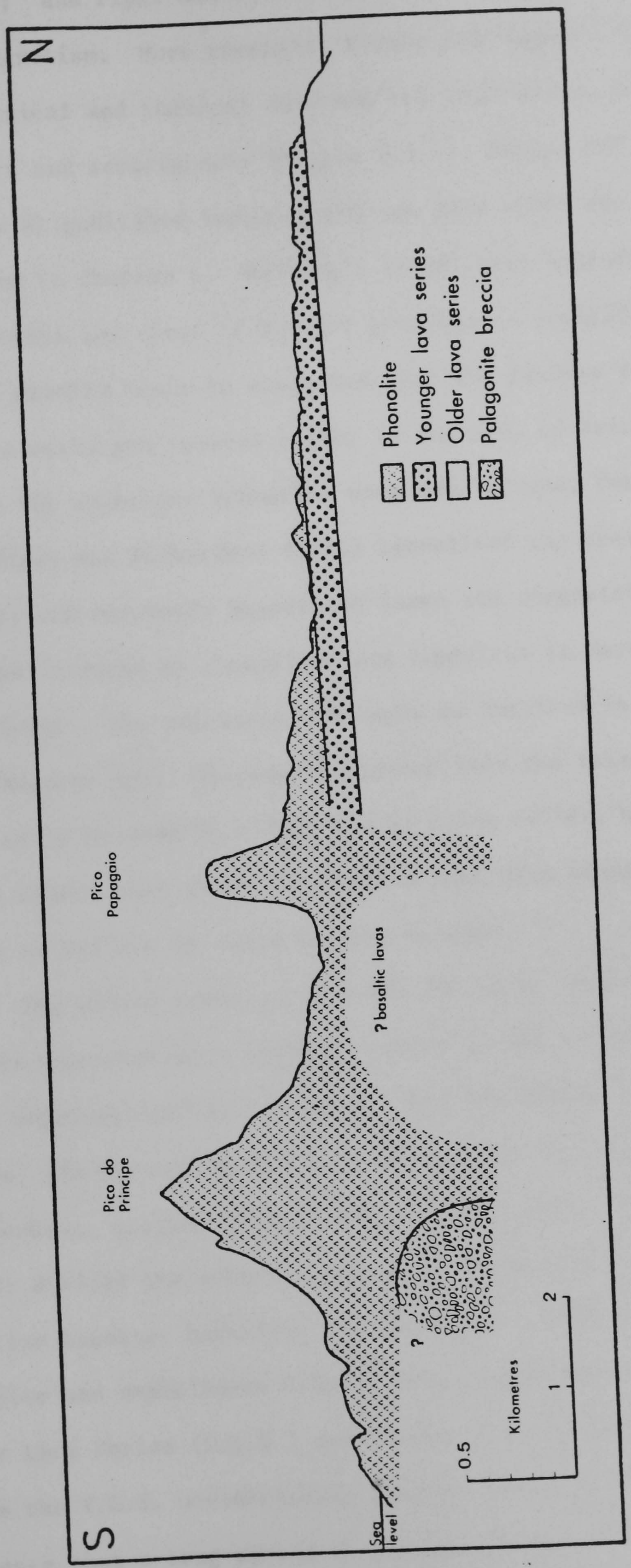


Figure 3.1.2 Schematic section through Principe (from Fitton and Hughes, 1977).

Principe; and Piper and Richardson (1972) examined the island's palaeomagnetism. More recently, Fitton and Hughes (1977) published mineralogical and chemical data and new information regarding the structure and stratigraphy (Figure 3.1.2). Dunlop and Fitton (1979, Appendix E) published isotopic and age data which are presented below and in Chapter 4. Hedberg's (1968) work included gravity measurements and since it was not possible to identify any well-defined gravity highs he suggested that the feeders for the island's volcanic rocks are located either in the S.W. of Principe or beneath the extensive submarine wave-cut terrace, further to the S.W. Piper and Richardson (1972) identified the presence of both normally and reversely magnetised lavas and suggested that the lava pile was intruded by phonolites and tephrites in more than one phase of activity. The palaeomagnetic pole so obtained is probably of Lower Miocene age. Miocene limestones from the island have been reported by Mendelsohn (1942) and Da Silva (1958), however Hedberg (1968) showed that these limestone blocks were probably brought from Lisbon as ballast by early trading vessels.

The oldest rocks on Principe are small inliers of palagonite breccia representing a submarine phase in the evolution of the island. These breccias contain blocks of fresh tholeiitic basalt, in which augite, olivine and plagioclase phenocrysts are set in a matrix of plagioclase, augite, titanomagnetite and glass. Fitton and Hughes (1977) divided the subaerial basaltic lavas into a series of mildly alkaline basalts, hawaiites and dykes and a series of strongly alkaline basanite and nephelinite flows. They termed these two units the Older Lava Series (O.L.S.) and Younger Lava Series (Y.L.S.) respectively since the Y.L.S. unconformably overlies the O.L.S. and field evidence suggests that a long period of erosion separated the eruption of the two units. All rocks comprising the O.L.S. contain phenocrysts of titanaugite, only the most evolved hawaiites are olivine free, and

phenocrysts of plagioclase and titanomagnetite occur in all but the most basic basalts. The matrix of all these rocks is made up of plagioclase, augite and titanomagnetite. The Y.L.S. comprises strongly olivine and titanaugite-phyric basanites, aphyric basanites and olivine nephelinites. The groundmass of the basanites is composed of titanaugite, olivine, plagioclase, alkali feldspar, nepheline, titanomagnetite and apatite. The matrix of the olivine nephelinites consists of titanaugite, olivine, titanomagnetite and nepheline. The Y.L.S. flows are generally fresher than the O.L.S. lavas and are not seen to be intruded by dykes. The pre-Y.L.S. topography of Principe must have been very subdued as the base of this series occurs at about the same height above the present sea level wherever it is observed. Phonolite lavas overlie the basic lavas of the Y.L.S. and the lava pile is intruded, in the southern part of Principe, by plugs ranging in composition from tristanite to phonolite. These evolved rocks form two suites: the volumetrically rare tristanite to trachy-phonolite suite and the phonolite suite. The trachyphonolite-tristanite suite rocks contain phenocrysts of alkali feldspar with lesser aegirine-augite, hornblende, sphene and titanomagnetite phenocrysts set in a groundmass of mainly sanidine microcrysts with minor plagioclase and aegirine-augite. The phonolites contain sanidine, nepheline and aegirine-augite phenocrysts and sometimes sodalite and hornblende phenocrysts occur.

Nine samples, free of glass, secondary minerals and visible alteration in thin section were selected for K-Ar age studies. (The location of these samples is marked on Figure 3.1.1) Analytical techniques are given in Appendix A. The K-Ar age data (Table 3.1.1) of representative samples from all the volcanic units exposed on Principe establish the history of volcanism and also assist in the

TABLE 3.1.1

K-Ar Data from Principe

Sample No.	Rock Type	K (%)	$^{40}Ar^*/^{40}Ar_T$	$^{40}Ar^*$ (x 10^{-6} scc/g)	Age (Ma)
Lava from palagonite breccia					
P15	Tholeiite	0.445	0.166	0.537	30.79±2.3
			0.194	0.530	30.37±1.9
Older Lava Series					
P25	Hawaiite	1.175	0.687	0.873	19.01±0.44
			0.474	0.884	19.25±0.56
P28	Basalt	1.085	0.570	0.983	23.15±0.60
			0.389	1.021	24.05±0.81
Younger Lava Series					
P18	Nephelinite	1.340	0.251	0.296	5.68±0.28
			0.181	0.288	5.52±0.37
P20	Basanite	1.875	0.377	0.258	3.54±0.12
			0.251	0.254	3.48±0.17
Phonolites					
P5	Phonolite	4.270	0.447	0.903	5.43±0.16
			0.346	0.863	5.22±0.19
P11	Phonolite	5.120	0.459	1.113	5.60±0.16
			0.310	1.067	5.37±0.22
Tristanite-trachyphonolite suite					
P12	Tristanite	3.535	0.430	0.672	4.88±0.15
			0.411	0.675	4.91±0.16
P16	Trachyphonolite	4.020	0.153	1.057	6.96±0.55
			0.108	1.049	6.91±0.80

λ_e: $0.581 \times 10^{-10} y^{-1}$ $\quad$ $\lambda\beta$: $4.962 \times 10^{-10} y^{-1}$

$^{40}Ar^*$: Radiogenic ^{40}Ar $\quad$ $^{40}Ar_T$: Total ^{40}Ar

interpretation of the measured $^{87}Sr/^{86}Sr$ ratios, particularly of the evolved rocks. A block of tholeiitic basalt within an inlier of basal palagonite breccia gives a mean age of 30.6 ± 2.1 Ma and probably represents the period of initial submarine activity on the island.

The data presented here substantiate Fitton and Hughes' (1977) division of the subaerial volcanic rocks into two lava series. The O.L.S. is of Lower Miocene age since a hawaiite and a basalt give ages of 19 ± 0.5 Ma and 23.6 ± 0.7 Ma respectively. These results give a mean of 21.4 Ma ± 1.6 Ma (2σ about the mean) for the age of the O.L.S. Hedberg (1968) reported a single K-Ar date of 24 Ma from the same lava series, and Piper and Richardson (1972) suggest that palaeomagnetic evidence indicates a Lower Miocene age. That a long period of erosion separates the O.L.S. from the Y.L.S. basanites and nephelinites is supported by K-Ar age data. A nephelinite and a basanite of the Y.L.S. gave ages of 5.60 ± 0.32 Ma and 3.51 ± 0.15 Ma respectively, indicating a gap of between 13.5 Ma and 20 Ma between the two series.

K-Ar data on two phonolite samples gave ages of 5.32 ± 0.18 Ma and 5.48 ± 0.19 Ma. The phonolite suite of evolved rocks therefore falls within the Pliocene eruption period of the Y.L.S. This is further substantiated because Rb-Sr isotope data of the Y.L.S. and the phonolite suite from an isochron (Chapter 4, Figure 4.1.8) having an age of 5.9 ± 0.3 Ma. Two samples from the tristanite-trachyphonolite suite also fall in this eruption period since they have ages of 4.89 ± 0.15 Ma and 6.93 ± 0.68 Ma. However, the latter age for trachyphonolite P16 may be incorrect since it would imply that P16 should have an unreasonably low initial $^{87}Sr/^{86}Sr$ ratio of 0.70143 whereas an age of 6.0 Ma would give a more acceptable initial ratio of 0.70271 (Table 4.1.3). K-Ar data from this sample (Table 3.1.1) indicate the presence of a large proportion of atmos-

pheric argon in this sample (77%) compared to other analyses, accounting for the large error associated with this age and thus less confidence may be placed on the K-Ar data from trachyphonolite P16.

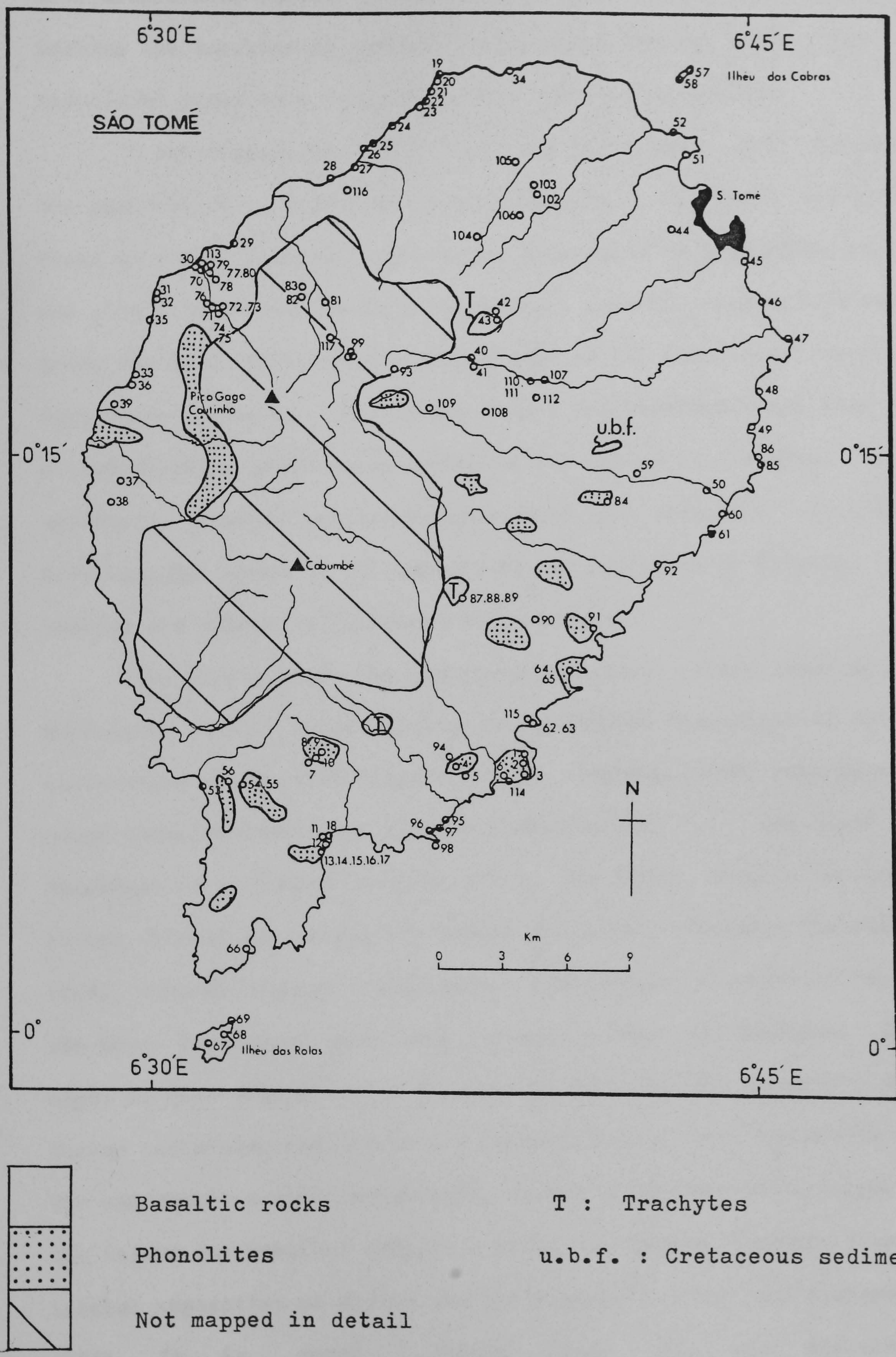
In conclusion, the volcanism on the island of Principe dates back to at least 31 Ma, followed by the two main subaerial eruption periods in Lower Miocene and Pliocene times. For strontium initial ratio calculations (Chapter 4) ages of the 31 Ma, 21 Ma, and 6 Ma have been assigned to the tholeiite P15, the Older Lava Series, and Younger Lava Series plus evolved rocks respectively.

3.1.2 São Tomé Island

São Tomé rises from the abyssal plain at a depth of over 6,000 m to an elevation of 2,024 m above sea level. Volcanic rocks predominate on the island and it is largely built up of mildly alkaline basalts. Lesser volumes of basanites, ankaramites, intermediates (tephrites, trachybasalts, benmoreites), evolved rocks (phonolites, trachytes, trachyphonolites), and high level cumulates are present. The centre of the island is a very rugged and heavily eroded volcanic complex intruded by phonolite and tephrite domes. This area is largely inaccessible and has not so far been mapped (Figure 3.1.3). The bulk of the northeast and southern parts of the island are covered by young basalt flows and a number of recent basalt scoria cones are found in the northeastern and southern sectors of the island and also on Ilhéu das Rolas.

Aspects of the geology and petrology have been discussed by Neiva (1954a, b, 1956b), Assunção (1956, 1957), Neiva and Albuquerque (1962) and Hedberg (1968). The most recent geological map published (Figure 3.1.3) is that of Neiva (1956b). A summary of the geology (as described by the above authors) was given by Mitchell-Thomé (1970). Hedberg (1968) noted the existence of two pronounced gravity highs in

Figure 3.1.3 Geology and sample location map of São Tomé (after Neiva, 1956b).



the N.N.E. and S.W. parts of the island separated by a gravity low stretching across the centre of the island, encompassing the younger, more mountainous region. These gravity highs were interpreted as marking the location of central feeder pipes for the lavas. The associated peaks have long since been levelled by erosion.

A palaeomagnetic study (Piper and Richardson, 1972) illustrates the presence of at least two polarity epochs in São Tomé. Along the N. coast an older, normally magnetised, succession of palagonite tuffs and pillow lavas are overlain by younger, reversed, subaerial lavas. Along the east and northeast coasts most of the lava units sampled have normal polarity. Fitton and Hughes (unpublished data) have made a comprehensive geochemical survey of the island's volcanics. No systematic chemical variations were noted with respect of volcanic stratigraphy, which is in contrast to the volcanics of Principe. Their results are discussed in detail in Chapter 4.

The oldest rocks are quartzose sandstones, first reported by Mendelsohn (1942), which outcrop in the Ubabudo Plantation in the east-centre of São Tomé (Figure 3.1.3). Hedberg (1968) subsequently named these sediments the Ubabudo Formation (U.B.F.). The total thickness is estimated as being 275 m. The lower, massive section is barren of fossils, except for poorly preserved radiolaria (Teixeira, 1949), however Hedberg (1968) made a lithological correlation with the Lower Cretaceous sandstones present in Gabon and Cameroon. The upper section consists of a sequence of fine grained sandstones and shales containing radiolaria and foraminifera of Late Cretaceous age. The sandstones contain metamorphic mineral fragments which suggest the island may possibly contain a micro continental fragment from the initial separation of Africa and South America (Piper and Richardson, 1972). It is more likely that they were derived from the mainland and then uplifted

as a block. Grunau et al (1975) published details of a seismic profile running across the submarine extension of São Tomé and noted the existence of a sedimentary wedge on the north-east flank, thought to be of Late Cretaceous age.

Seven samples, free of alteration, were selected for whole-rock K-Ar radiometric age determinations (Table 3.1.2). Analytical techniques employed are given in Appendix A and the sample locations are marked on Figure 3.1.3. Two hypersthene normative basalts gave ages of 6.40 ± 0.17 Ma (dyke) and 0.51 ± 0.06 Ma (flow), whilst an olivine basanite lava from the northeast of the island is 2.53 ± 0.10 Ma old. This supports the observation (Fitton and Hughes, unpublished data) that no stratigraphic correlation with chemical character exists on Sao Tome. Five basalts analysed by Hedberg (1968) range in age from recent to 2.5 Ma (Table 3.1.3). Macedo et al (1977) noted a range in phonolitic and basaltic eruptions over the period 1.5-1.1 Ma. It may therefore be concluded that São Tomé surface mafic rocks were erupted over a continuous period from Uppermost Pliocene to Recent times. This is supported by the rugged topography, the immature nature of the surrounding submarine shelf and the presence of numerous recent cinder cones. In a seismic section across the São Tomé submarine pedestal Grunau et al (1975) observed that the sedimentary sequence is strongly disturbed, suggesting repeated volcanic activity from the Late Cretaceous to Recent times.

A mildly nepheline normative trachyte (ST43) from Pico São Tomé northeast of Pico Gago Coutinho gave an age of 1.32 ± 0.08 Ma and a phonolite (ST90) from the southeast gives 3.26 ± 0.09 Ma. Six evolved phonolites, trachyphonolites, and trachytes (including ST90) plot on a rubidium-strontium isochron of 3.93 ± 0.51 Ma (Figure 4.2.6). These are of a similar age to two dates of 3.5 Ma and 4.0 Ma from

TABLE 3.1.2

K-Ar Data from São Tomé

Sample No.	Rock Type	K (Wt.%)	$^{40}Ar^*/^{40}Ar_T$	$^{40}Ar^*$ (x 10^{-6} $sccg^{-1}$)	Age (Ma)
Hypersthene Normative Lavas					
ST60	Basalt	0.785	0.111	0.016	0.51 ± 0.06
ST96	Basalt	2.310	0.640	0.576	6.37 ± 0.15
			0.420	0.580	6.42 ± 0.20
Nepheline Normative Lavas					
ST44	Basanite	1.315	0.397	0.134	2.66 ± 0.09
			0.304	0.121	2.39 ± 0.10
Trachytes and Phonolites					
ST43	Trachyte	3.820	0.207	0.200	1.35 ± 0.08
			0.227	0.191	1.29 ± 0.07
ST84	Trachyte	4.670	0.802	1.393	7.64 ± 0.16
			0.822	1.379	7.56 ± 0.16
ST90	Phonolite	4.803	0.536	0.617	3.30 ± 0.09
			0.584	0.601	3.22 ± 0.08
Quartz Normative Trachyte					
ST57	Trachyte	3.750	0.387	1.939	13.25 ± 0.45
			0.350	1.885	12.88 ± 0.47

λ_e: $0.581 \times 10^{-10} y^{-1}$ $\lambda\beta$: $4.962 \times 10^{-10} y^{-1}$

$^{40}Ar^*$: Radiogenic ^{40}Ar $^{40}Ar_T$: Total ^{40}Ar

TABLE 3.1.3

K-Ar Data from Other Sources of São Tomé

Rock	Age	Reference
Phonolitic and basaltic eruptions in period:	1.5-1.1 Ma	Macedo et al. 1977
Albitised trachyte qz in mode	15.7 ± 0.8	Grunau et al. 1975
Phonolites in south:		
Pico San Pedro	3.5 Ma	Hedberg, 1968
Mt. Sinai	4.0 Ma	
Basalt overlying U.B.F.	2.5 Ma	"
Basalt, airport	0.1 Ma	"
Base of flat topped cinder cone, N. coast	0.35 Ma	"
Rio Manuel George Bridge, Basalt	0.2 Ma	"
Abade coulee basalt	Recent	"

Pico São Pedro and Mt. Sinai, respectively, in the southern sector of the island (Hedberg, 1968). A nepheline normative trachyte (ST84) overlying the Ubabudo Formation Cretaceous sandstones gives a K-Ar age of 7.60 Ma ± 0.16 Ma and while it is almost identical geochemically to ST43 (Chapter 4, Figure 4.2.1) it is therefore considerably older. K-Ar analyses on a strongly quartz normative trachyte from Ilhéu das Cabras gave an age of 13.07 ± 0.46 Ma. Grunau et al (1975) reported an albitised trachyte, described as containing modal quartz, having an age of 15.7 Ma ± 0.8 Ma (Table 3.1.3); however they omitted to describe the sample location.

The majority of the volcanism on São Tomé is considered to be of Upper Pliocene to Recent in age but there is evidence of earlier eruptive activity in Lower Miocene-Upper Miocene times resulting in the accumulation of evolved rocks. Piper and Richardson (1972) concluded by saying their collection belongs entirely to the last few million years, although basement rocks may be older. The pole positions from São Tomé were derived from material of Lower Miocene or younger in age. For strontium isotope ratio considerations, all the mafic rocks analysed are assumed to be too young to warrant the necessity for any age corrections. With the exception of the quartz trachytes and ST43 and ST84 the age assumed for the evolved rocks is 4 Ma.

3.1.3 Bioko (Formerly Fernando Póo)

Bioko is the largest of the four islands in the Gulf of Guinea and is situated on the continental rise, 50 km from the mainland (Figure 3.1.4). The northeastern side lies on the shelf and the southwestern sector is situated near the foot of the continental rise. The island (Figure 3.1.5) is a complex of three volcanoes: Santa Isabel in the north; and two peaks, San Carlos and Pico Biao, in the south.

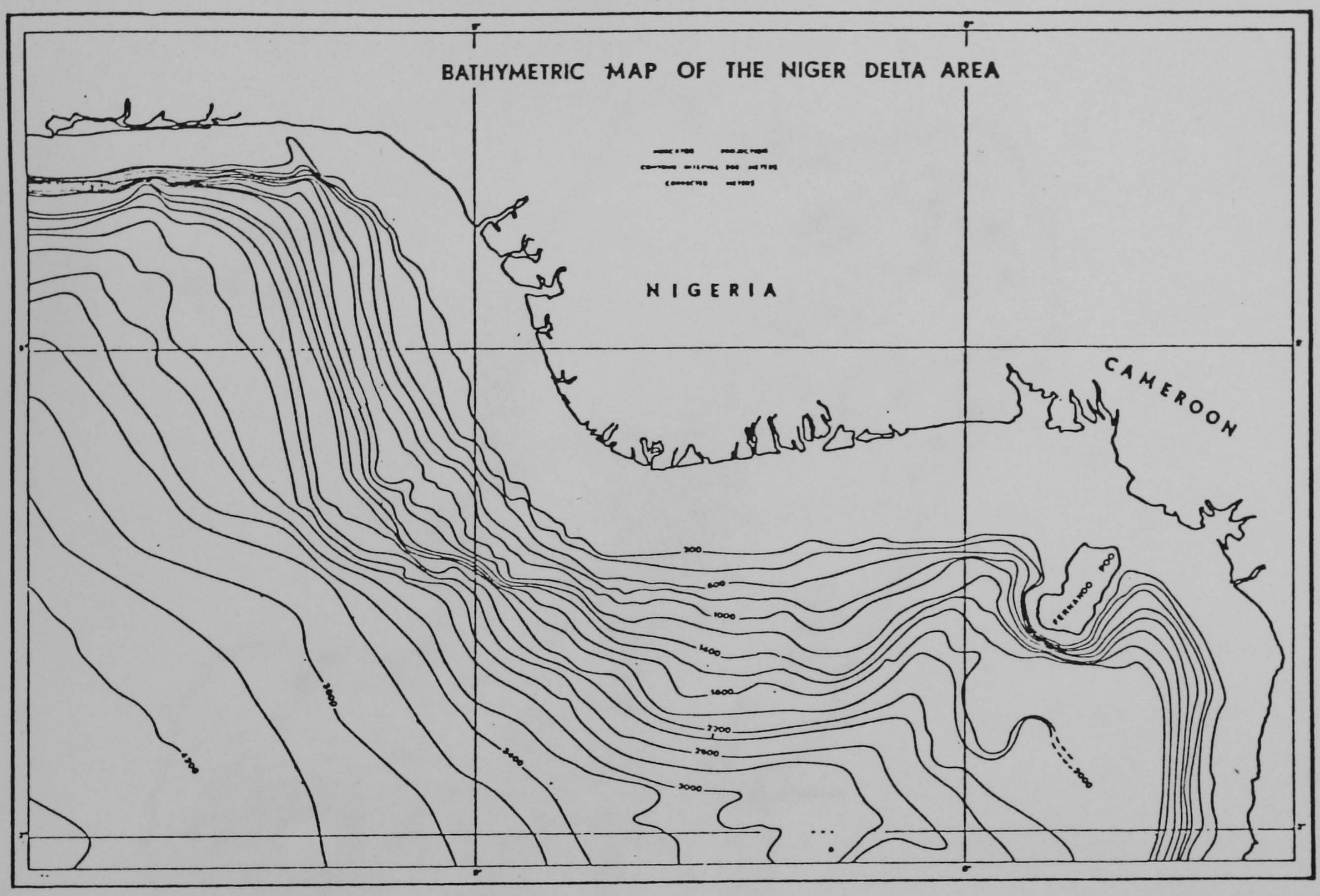


Figure 3.1.4 Location of the island of Bioko (formerly Fernando Poo) on the West African Shelf (from Mascle, 1975).

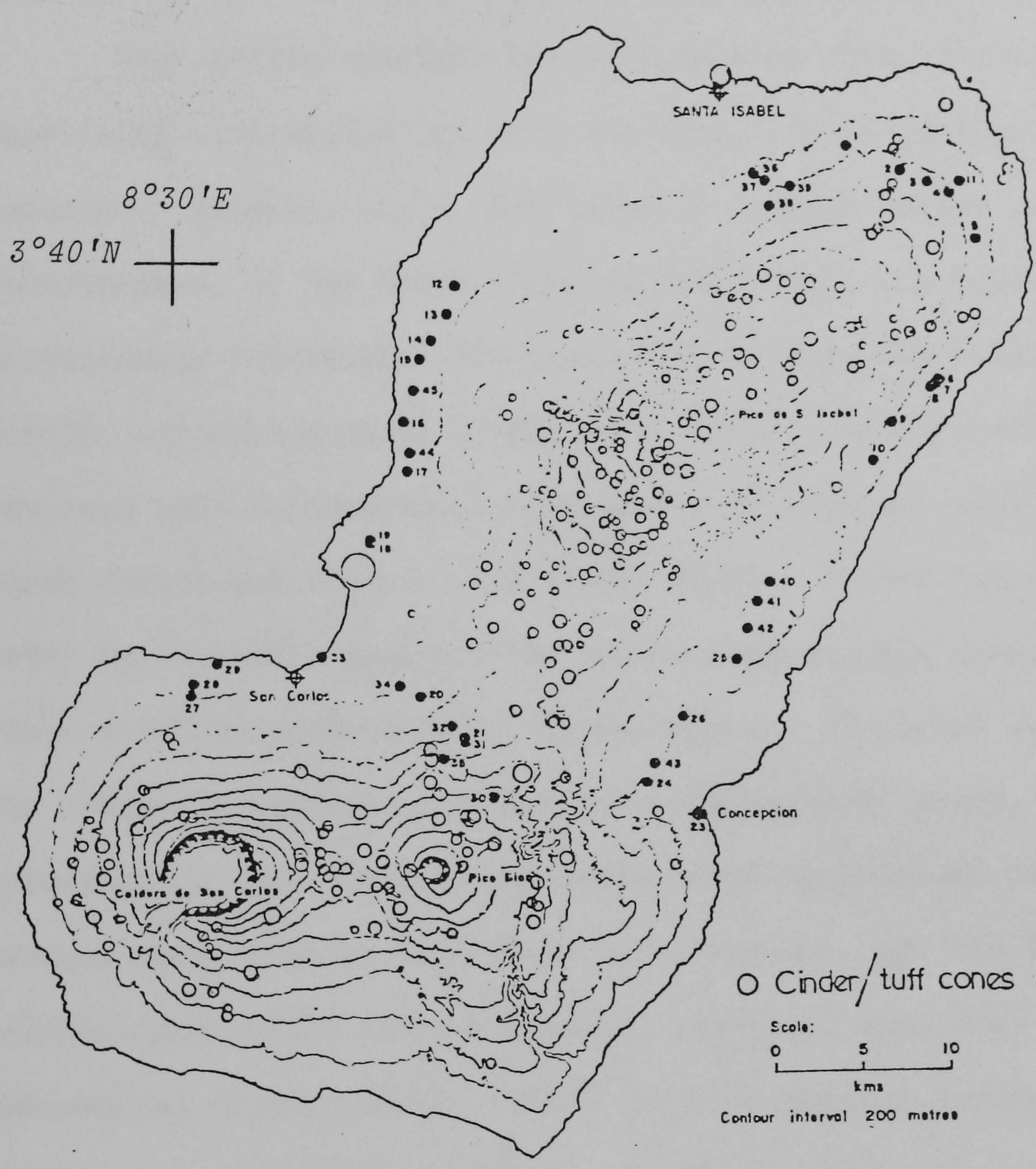


Figure 3.1.5 Geology and paleomagnetic sampling sites on the island of Bioko (from Piper and Richardson, 1972).

Santa Isabel is a well shaped cone whilst the other two summits are volcanic calderas. The three volcanoes are covered with numerous small cinder cones and explosion craters. The flanks of the volcanoes are deeply dissected by precipitous ravines radiating away from the summits and there is only a very narrow shelf surrounding the island. The last recorded eruption took place in 1898.

Very little research has been made of Bioko which is surprising considering its size and proximity to the Cameroon mainland. However, since this formerly Spanish island gained independence, it has become impossible to visit the island. Brief petrographic information has been given by Schüster (1887), Boese (1912), and Fuster-Casas (1950, 1954, 1956). Mitchell-Thomé (1970) reviewed this information and presented 16 chemical analyses of Boese (1912) and Fuster-Casas (1950, 1954). Fitton (pers. comm. 1982) has recently analysed the palaeomagnetic core samples of Piper and Richardson (1972). These data are discussed in Chapter 4. The island is composed entirely of young basaltic rocks, associated pyroclastics, agglomerates and tuffs, with an apparent absence of any evolved rocks such as phonolites or trachytes. All the flows are transitional alkali olivine basalts, picrites, oceanites and ankaramites (Fuster-Casas, 1956). Olivine basalts predominate and they have a remarkable constancy of mineral composition consisting of olivine, diopsidic or titaniferous augite, plagioclase, titanomagnetite and ilmenite (Fuster-Casas 1950, 1954). From a gravity survey, Hedberg (1968) observed that all three volcanic peaks have associated gravity highs: Santa Isabel +117.5 mgal; Pico Biao +151.7 mgal; and San Carlos +136.1 mgal. These highs probably mark the location of the central feeder pipes for the lavas. However, the two southern centres have substantially higher anomalies than Santa Isabel even though they

do not reach the altitude (3,008 m) of Santa Isabel.

Hedberg (1968) suggested, on the basis of Bioko's youthful topography and bathymetry, that the volcanics are probably no older than early or even middle Pliocene age. He presented one K-Ar age of 1.1 Ma for a basanite from Santa Isabel which supports the above age estimate.

Piper and Richardson (1972) in a palaeomagnetic survey noted that nearly all the lavas are normally magnetised since the flows are clearly very young (they show lesser degrees of laterisation than do the volcanics of Principe, São Tomé and Pagalu). They conclude that virtually the whole volcanic edifice has grown in Bruhnes epoch time and is therefore younger than 0.7 Ma. This is nearly consistent with Hedberg's age date and indicates that lava accumulation must have been very rapid.

3.1.4 Pagalu (Formerly Annobon)

The small island of Pagalu represents the southwestern limit of the Cameroon Line, being situated 700 km from Cameroon and 150 km southwest of São Tomé. Pagalu is surrounded on all sides by a relatively narrow shelf generally less than 1 km wide and has an immature topography, particularly in the south where there are deep ravines and wave cut scarps. It is the eroded top of a stratovolcano 5,000 m high and like Fernando Póo, consists entirely of Tertiary-Recent volcanic rocks. The lava pile is largely composed of basaltic flows and pyroclastics which are cut by innumerable basic dykes (Figure 3.1.6). A basaltic crater, Quivéo, occupies the central part of the island and the last lava from this focus flowed through the northwestern rim of the caldera. Seismic profiles (Gorini and Bryan, 1976) indicate that the island was built entirely on oceanic crust.

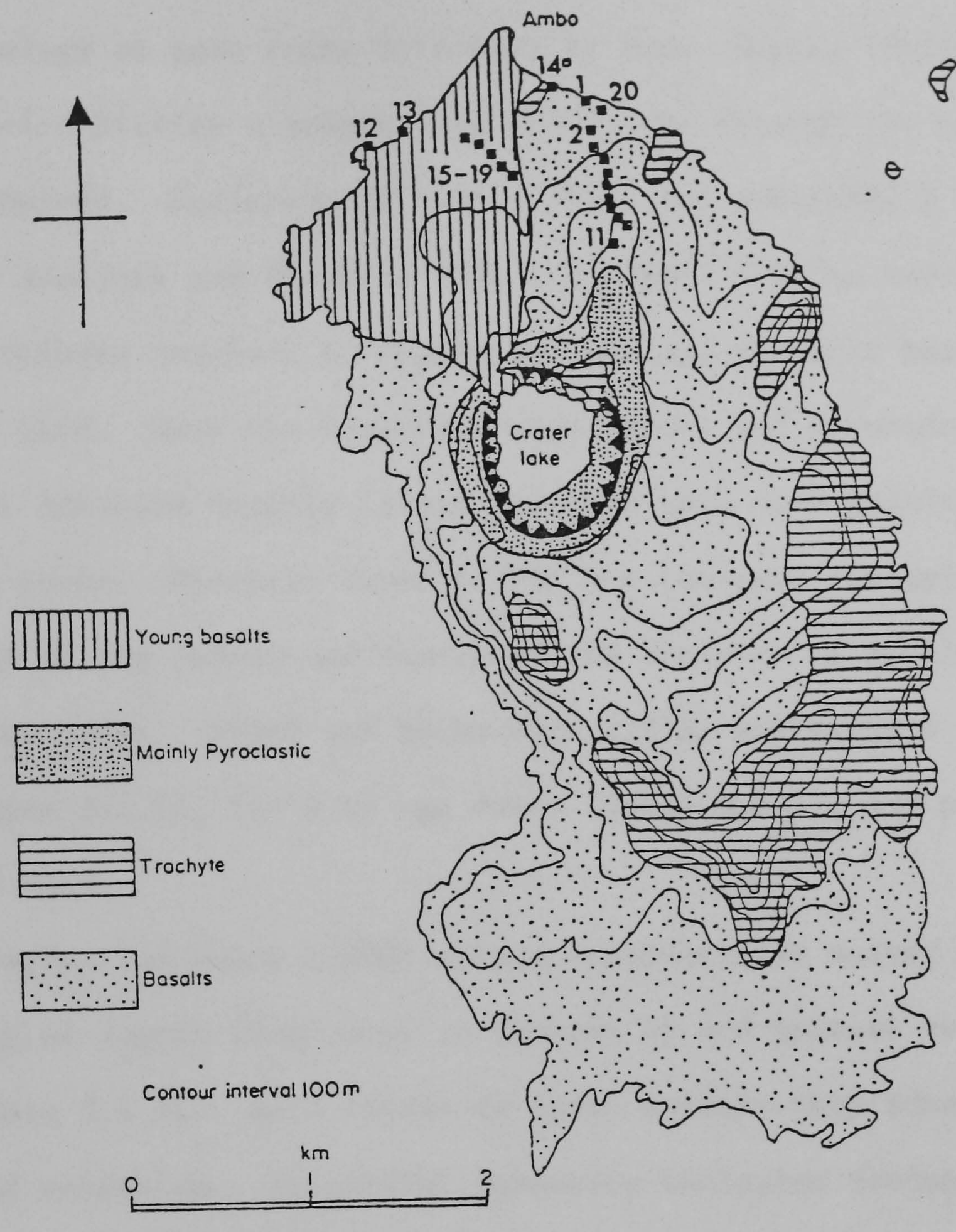


Figure 3.1.6 Geology and paleomagnetic sampling sites on the island of Pagalu (formerly Annobon) in the Gulf of Guinea (from Piper and Richardson, 1972).

Very little research has been done on Pagalu, due to its inaccessibility. Schulze (1913) presented a topographic map and made a brief mention of the island's geology. Tyrrell (1934) described the petrology of some rocks collected by Capt. Barns, including an intrusive biotite trachyte plug which cuts through the northern wall of Quivéo. Fuster-Casas (1950, 1954) has published a few chemical analyses and observed that the alkali olivine basalts (often rich in olivine nodules) of Pagalu are perhaps the most basic of the Cameroon Line. Only the Canaries, Cape Verdes and Fernando de Noronha in the S. Atlantic oceanic island province have more primitive basaltic rocks. Mitchell-Thomé (1970) has reviewed the geology and geography of the island and discussed the analyses of Schulze, Tyrrell, and Fuster-Casas. Piper and Richardson (1972) published a geological map (Figure 3.1.6), two K-Ar age dates (Table 3.1.4), and palaeomagnetic data.

Cornen and Maury (1980) give a comprehensive survey of the petrology of Pagalu (discussed in Chapter 4) and present two K-Ar ages (Table 3.1.4). As a result of their studies they identify four phases of volcanism. Initially, submarine volcanism produced palagonite breccia (outcropping in the E. and W. coastal cliffs) cut by basanitic and ankaramitic dykes. No radiometric age data are available for this first phase of activity. Secondly, the effusion of basanite lavas, which cover most of the island. The oldest flow has given a K-Ar age of 18.4 Ma (Piper and Richardson, 1972). Numerous dykes intersect and feed this pile; one of which is 5.35 Ma old (Cornen and Maury, 1980). The third phase consisted of the emplacement of tristanitic and oversaturated trachytic plugs. A sample of tristanite gave an age of 3.9 Ma (Cornen and Maury, 1980). The final activity manifested itself as ankaramitic basanite flows (young

basalts on Figure 3.1.6) from which Piper and Richardson (1972) obtained an age of 2.6 Ma.

The volcanics on Pagalu are therefore of similar age to those of São Tomé and Principe; apparent initial activity being slightly older than volcanic rocks on São Tomé and younger than Principe. Like Principe, Pagalu shows an erosional gap between periods of volcanicity. For initial strontium isotope ratio studies (Chapter 4) an age of 18.4 Ma was assumed for the older volcanic succession and no age correction is necessary for the younger lavas.

Table 3.1.4

K-Ar age data from Pagalu

Sample	K_2O (Wt.%)	$^{40}Ar^*$ %	Age (Ma)		Reference
Basal Lava			19.2) 17.5)	18.4	Piper and Richardson, 1972
Young Lava (N. coast)			2.8) 2.4)	2.6	Piper and Richardson, 1972
Dyke	1.3	39 40	5.3) 5.4)	5.35±0.25	Cornen and Maury, 1980
Tristanite	4.97	71.2 70	3.75) 4.0)	3.93±0.2	Cornen and Maury, 1980

3.2 Continental Sector Volcanoes

3.2.1 Mt. Cameroon

Mount Cameroon is one of the world's largest volcanoes and rises from below sea level to an altitude of 4,070 metres (Figure 3.2.1). The mountain is ellipsoidal in outline, measuring approximately 50 km by 35 km, with the larger axis trending northeast-southwest. It is the only volcano on the Cameroon line which is still active - 13 eruptions have been reported since 1800 (Guillaume, 1966). New activity has been

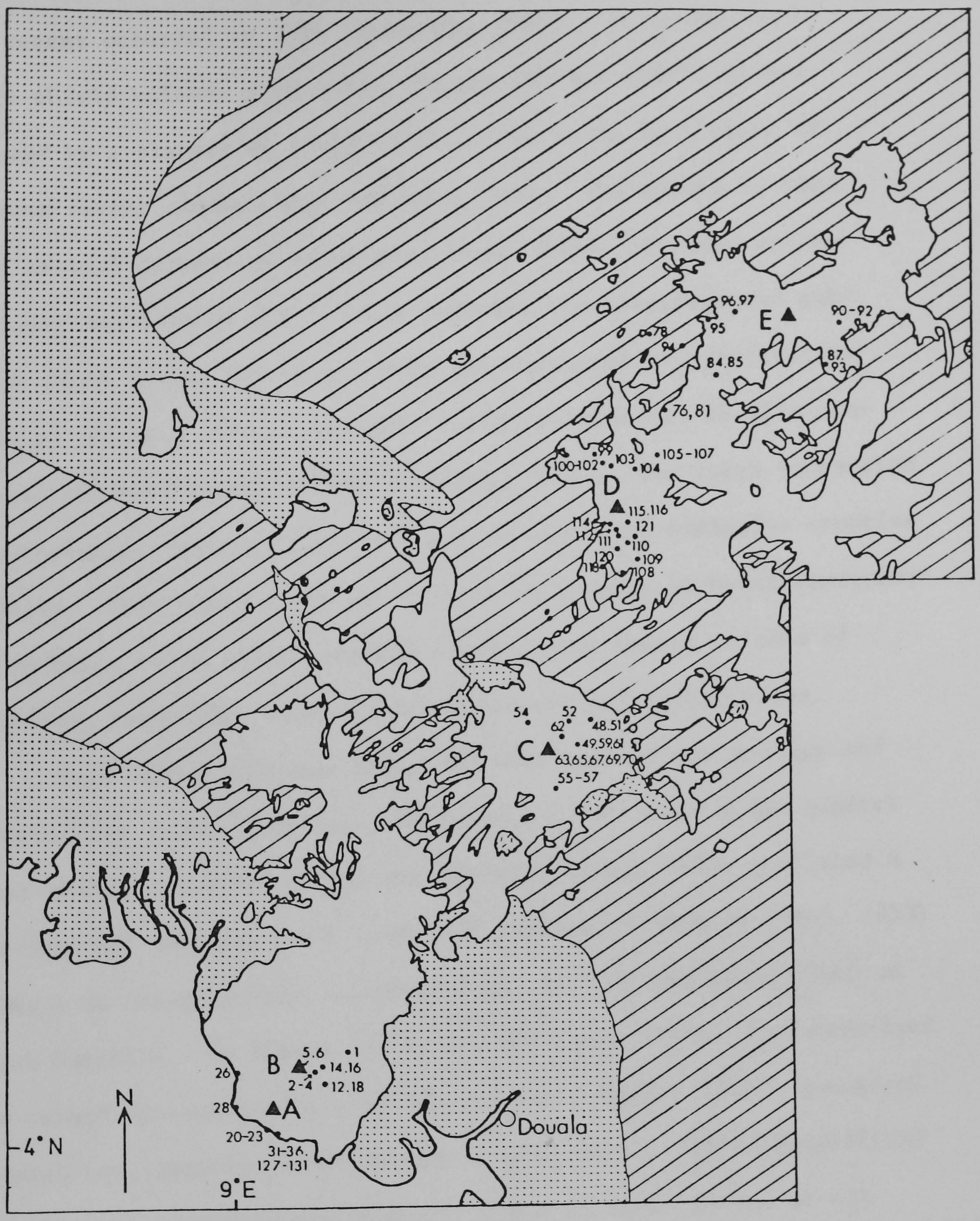


Figure 3.2.1 Sample location and geological map (after Dessauvagie, 1975) of south and central Cameroon. Symbols as for figure 3.2.2, and where [ ] = lower Tertiary granites

A = Etinde

B = Mt. Cameroon

C = Manengouba

D = Bambouto

E = Oku

observed at the time of writing (October, 1982) and before that the most recent occurred in 1959 (Jennings, 1959). It is an alkali basalt shield volcano with steep, deeply incised middle slopes followed by a plateau at 2,000-3,000 metres which is covered by numerous recent cinder cones and lava flows. The summit is made up of several craters of varying ages and states of preservation. The lower sections of the volcano comprise hyloclastites and sub-marine flows whilst the upper parts are dominated by pyroclastics (Gouhier et al., 1974). Volcanic tuffs, ashbeds and basalts constitute the most recent strata (Hedberg, 1968). The large proportion of pyroclastic material indicates a high degree of explosive eruptive activity. Only mafic rocks are seen to be present on Mount Cameroon; the majority being alkali olivine basalts with lesser volumes of hawaiites, basanites, nephelinitic basanites and nephelinites.

Very little previous study has been made of the geology and geochemistry of Mt. Cameroon. Guillemain (1909) made a few general observations and Mesch (1916) and Jérémine (1941, 1943) published a few chemical analyses which have been reviewed in Gèze's (1943, 1953) studies on the geography, geomorphology, geology and petrography of Mount Cameroon. De Swardt (1954) and Guillaume (1966) have described the recent igneous activity of the volcano. Dumort (1967) presented several more chemical analyses and Gouhier et al. (1974) established the alkaline nature of the basaltic rocks in their review of all available geochemical data. Piper and Richardson (1972) have made a brief palaeomagnetic survey of the massif, and the most recent geological map is that of Dessauvagie (1975). J.G. Fitton and D.J. Hughes visited Mount Cameroon in 1975, collected 23 samples, and have determined major and trace element concentrations on these samples. Their results are discussed in Chapter 5 in con-

junction with the strontium isotope studies carried out on the same samples by the author.

The timing of initial volcanism of Mount Cameroon was formerly thought to be of Upper Cretaceous age (Gèze, 1943) since Guillemain (1909) had reported the existence of volcanic tuffs interstratified with marine sediments. Geze (1943) therefore concluded that the bulk of the volcanic material belonged to his "Inferior Black Series" basalts. The "Middle White Series" (trachytes, phonolites, and ignimbrites of other localities) was considered to be absent, as on the island of Bioko, although it could have been covered up by the "Upper Black Series" which comprises the recently erupted material. However, Vincent (1971) dated several basaltic flows by K-Ar techniques which indicated a Pliocene-Quaternary age. This is consistent with the palaeomagnetic studies of Piper and Richardson (1972). All sites measured by these authors were normally magnetised and they believed that the entire edifice was constructed in Brunhes epoch times (the base of which is equivalent to 0.7 Ma). Hedberg (1968) concluded from a combined study of field relations, heavy mineral analyses of nearby sediments and radiometric dating, thatthe age of initial extrusion was no older than Mid-Miocene and no younger than Early Pliocene. The absence of augite and olivine from Lower Miocene marine sediments located at the base of Mount Cameroon strongly suggested a more recent origin of the volcano than Burdigalian. The oldest age Hedberg (1968) presents is 9 Ma (Table 3.2.1) for a sample of basalt in Miocene-Pliocene shale from a core taken at 2,420 metres below sea level between Fernando Póo and Mount Cameroon. He quotes an age of 4.7 ± 0.8 Ma for a basaltic dyke and two younger ages from Tiko Scarp flows of 0.8 ± 0.3 Ma and 0.5 ± 0.3 Ma. The last two samples were originally thought to be intercalated with Upper Cretaceous

TABLE 3.2.1

K-Ar Age Dates of Cameroon from Other Sources

Sample	Rock Type	K_2O (Wt.%)	% $^{40}Ar^*$	Age (Ma)	Reference	Equivalent Sample (This Study)
NK, Manengouba	Hawaiite	1.41	18.5	1.55 ± 0.1	1	
BA3, Bamenda	Basanite	1.98	52.3	5.8 ± 0.2	1	
BA1, Bambouto	Trachyte	4.55	64.0	15.9 ± 1.0	1	
BA5, Bambouto	Trachyte	3.77	54.4	22.7 ± 1.0	1	C107
Etinde	Nephelinite			0.34 ± 0.06	4	
Mandara	Basalt			27.4 ± 0.5	2	
Mandara	Trachyte			29.6 ± 0.6	2	
Tchabal Mbabo	Basalt			37.2 ± 0.2	4	
NG15, Ngaoundere	Basalt	0.82	17.6) 12.1)	7.02 ± 0.2	1	
NG8, Ngaoundere	Trachyte	5.44	82	7.9 ± 0.2	1	
NG4, Ngaoundere	Trachyte	4.85	35.6	9.8 ± 0.2	1	
JA, Oku	Basalt	1.80	69.9) 77.7)	21.0 ± 2	1	C93
Mount Cameroon						
Tiko Scarp Flow	Basalt			0.8 ± 0.3	3	
Dyke	Basalt			0.5 ± 0.3	3	
Core, 2420 m below s.l. between Mt. Cameroon and Bioko				9	3	

References:
1: Gouhier et. al., 1974
2: Vincent and Armstrong, 1973
3: Hedberg, 1968
4: Armstrong (unpublished)

sediments. Thus it is likely that volcanism was initiated no earlier than Upper Miocene times whilst the bulk of extrusion occurred much more recently in mid-Pliocene to present times. All the samples collected by Fitton and Hughes were considered too young to warrant K-Ar geochronological studies and accurate age control was not required for interpretation of the $^{87}Sr/^{86}Sr$ ratios (Chapter 5) of these relatively unfractionated samples.

3.2.2 Etinde

Etinde, or Little Mount Cameroon, is a dissected cone-shaped volcano located to the south-south-west of Mount Cameroon (Figure 3.2.1), between Victoria and the main summit, and rises to a height of 1,715 metres. Esch (1901) was the first to describe and sample Etinde. Gèze (1943, 1953), Dumort (1967) and Gouhier et al (1974) discussed the analyses Esch (1901) presented and established the extreme alkaline nature of this centre. Tilley (1953) analysed two samples from the Cambridge University Harker collection and described the nepheline phenocrysts, concluding them to be a potassic orthorhombic feldspathoid phase as suggested by Esch (1901). Fitton and Hughes collected 20 samples from accessible parts of the volcano (most of Etinde is shrouded in dense tropical rain forest) and their chemical analyses (Fitton, pers. comm.) show that the lavas range in composition from melanephelinitic through leucite-melilite-hauyne -bearing nephelinites to leuconephelinites. The rocks are feldspar-free throughout their entire range. Etinde is the type locality of Etindite (Lacroix, 1923) which is a term, now obselete, corresponding to a leucite nephelinite. The chemical character of the lavas is quite distinct from that of nearby Mount Cameroon (the geochemistry is discussed in Chapter 5) and from that of the closest island, Bioko.

EDINBURGH UNIV. LIBRARY

Etinde is considered by Gèze (1943) and Fitton (pers. comm. 1979) to be the oldest volcano in the Mount Cameroon area, on the basis of its advanced stage of dissection and field relations. However, it still retains the original volcanic cone-shape and cannot therefore be much older than Pliocene, if even as old. There has been no geochronologi studies published on Etinde prior to this study although Marechal (1977) mentioned one unpublished nephelinite K-Ar age of 0.34 ± 0.06 Ma (analysed by R.L. Armstrong). One K-Ar age determination carried out by the author (Table 3.2.2) gave an age of 0.07 ± 0.2 Ma. However, the large error associated with this determination (due to the large atmospheric ^{40}Ar component present in the sample) implies that it may only be concluded confidently that this sample is less than approximately 0.5 Ma old. This suggests Etinde is probably not as old as has previously been suggested but closely predates the voluminous recent activity of Mount Cameroon.

Table 3.2.2

K-Ar Data from Etinde

Sample	Rock Type	K% (Wt.%)	$^{40}Ar^*/^{40}Ar_T$	$^{40}Ar^*$ ($sccg^{-1}$)	Age (Ma)
C36	Leuconephelinite	5.13	0.07	1.512×10^{-8}	0.082 ± 0.3
			0.07	1.260×10^{-8}	0.065 ± 0.1

λ_e: 0.581×10^{-10} y^{-1} $\quad$ λ_β : 4.962×10^{-10} y^{-1}

$^{40}Ar^*$: Radiogenic ^{40}Ar $\quad$ $^{40}Ar_T$: Total ^{40}Ar

3.2.3 Manengouba Mountains

The Manengouba volcanoes are situated 120 km northwest of Mount Cameroon (Figure 3.2.1) on a plateau of Cambrian-Precambrian granite and gneiss basement. The entire complex is approximately 25 km in diameter and is made up of two calderas. The older caldera (Elengoum),

which is 2,336 m high, is deeply dissected and has an extensive vegetation cover. This volcano consists mainly of trachyte flows and pyroclastic deposits. To the west of Elengoum lies Eboga caldera, which is virtually unweathered and has a well defined crater rim. The caldera is 6 km in diameter and reaches an altitude of 2,420 m. Within and around this younger caldera are numerous recent cones and small explosion craters (two of which form small lakes within Eboga caldera) and those on the crater floor form a northeast-southwest lineation, parallel to the overall trend of the Cameroon Line. Basalt and mugearite lava flows have breached Eboga crater and in places overlie the Elengoum volcanics.

Geochemical analysis of 25 samples (Fitton, unpublished data), mainly taken from Eboga caldera, showed the volcanics to be transitional in character with a continuous range of composition from basalt to trachyte with a preponderance of intermediate rock types. Within the Eboga caldera the complete range is present whereas only basalts are observed on the lower slopes of Eboga (C. Hirst, pers. comm., 1980). Most of the basaltic rocks are porphyritic containing phenocrysts of olivine, clinopyroxene and plagioclase. The intermediate and evolved rocks frequently contain hornblende in addition to feldspar and pyroxene phenocrysts.

Gèze (1943, 1953) was the first to study Manengouba and described its physical features and attempted to fit the various components of volcanism into his three-fold classification of Cameroon volcanic rocks. Jérémine (1943) described the petrography and Dumort (1967) in presenting nine geochemical analyses established the chemical nature of these rocks. Tchoua (1974) made a more recent petrographic and geochemical study of Manengouba. The chemistry is presently being studied in detail by Fitton and Hirst and their results are discussed

in Chapter 5. Piper and Richardson (1972) paid little attention to the complex but they did establish that all six samples they collected were normally magnetised.

Gouhier et al (1974) presented one K-Ar age date of 1.55 Ma (Table 3.2.1) for a hawaiite from the periphery of Manengouba. Four samples from Fitton and Hughes' collection were dated employing K-Ar methods by the author (Table 3.2.3). C52 is a basanite taken from a flow on the lower, northern slope (Figure 3.2.1) of Eboga and gave an age of 0.40 ± 0.04 Ma. Basalt C55 and trachybasalt C57 were sampled from the older volcano, Elengoum, and gave ages of 0.94 ± 0.06 Ma and 0.60 ± 0.35 Ma respectively. When considered in association with knowledge of the field relations (Fitton, and Hirst, pers. comm.) these determinations put age constraints on the formation of this complex. All of the Elengoum volcanics are probably older than 0.5 Ma with initial activity taking place prior to 1.55 Ma (this assumes that Gouhier et al., 1974 sample came from Elengoum). Eboga must be younger, but it is likely to be closely related in time to Elengoum since one of the last eruptions of lava from this volcano is 0.40 Ma old. However, there is abundant evidence that Eboga has been active up until recent times, in the form of cones and explosion craters subsequent to caldera collapse. Hirst (pers. comm., 1982) has completed K-Ar studies of Manengouba, establishing that Eboga is probably younger than 0.8 Ma with the caldera collapse occurring 0.3 Ma ago. A quartz-normative trachyte dome (C54) has an age of 11.8 ± 0.24 Ma, indicating a period of earlier volcanic activity on the Manengouba Massif. However, this sample (12 km northwest of Eboga caldera) is considered not to relate to the activity associated with the development of either Elengoum or Eboga volcanoes. It is concluded that it is impossible to relate Gèze's (1943) three-fold

TABLE 3.2.3

K-Ar Data from Manengouba

Sample No.	Rock Type	K (%)	$^{40}Ar^*/^{40}Ar_T$	$^{40}Ar^*$ ($\times 10^{-6}$ sccg^{-1})	Age (Ma)	Mean (Ma)
Lava from Eboga Volcano						
C52	Basanite	2.125	0.119	0.033	0.40±0.04	
Lavas from Elengoum Volcano						
C55	Basalt	1.250	0.190	0.045	0.94±0.06	
C57	Trachybasalt	1.680	0.029	0.031	0.48±0.29	0.60
			0.029	0.044	0.71±0.42	
Dome from Northwestern Manengouba						
C54	Quartz-Trachyte	4.520	0.955	1.966	11.15±0.22	11.8
			0.935	2.203	12.49±0.25	

λ_e : $0.581 \times 10^{-10} y^{-1}$ $\quad$ λ_β : $4.962 \times 10^{-10} y^{-1}$

$^{40}Ar^*$: Radiogenic ^{40}Ar $\quad$ $^{40}Ar_T$: Total ^{40}Ar

episodic history of volcanism; that of a "Lower Black Series" of basalt followed by a "Middle White Series" of trachytes and finally an "Upper Black Series" of basalt, since trachyte rocks appear interstratified with basaltic material. Even the trachytic rocks of Elengoum do not approach the much older age of similar rocks from Bambouto, Oku or the Mandara Mountains (Sections 3.2.4 to 3.2.8) which Gèze (1943) equated to his "Middle Series."

3.2.4 Bambouto Mountains

The Bambouto Mountains are situated 190 km northeast of Mount Cameroon (Figure 3.2.1) and consist of an area of volcanics covering 50 km from southwest to northeast and having a breadth varying between 25 and 50 km. The volcanics reach a maximum altitude of 2,740 m, being 1,000 - 2,000 m above the granite-gneiss basement. The massif represents the extensively eroded remnant of a hawaiian type shield volcano with 3 collapsed calderas (Tchoua, 1972, 1974), extensive trachytic extrusives (up to 800 m thick) and plugs. The upper slopes are steeper than those lower down the volcano and reach up to 15^{o}. This is due to viscous trachyte eruptions. Fitton and Hughes collected 27 samples from this region, including a representative stratigraphic collection from the southern side of the complex. Their geochemical analyses show (unpublished data, pers. comm.) the mafic rocks to be mostly ne-normative olivine-plagioclase-clinopyroxene phyric basalts (Figure 5.1). The evolved rocks consist principally of quartz normative trachytes and rhyolites which contain phenocrysts of feldspar, amphibole and quartz, and sometimes aenigmatite. Lesser amounts of nepheline normative trachytes and phonolites are also present. There appears to be a complete absence of intermediate rocks (see Chapter 5 for discussion on geochemistry).

Previous research on the volcanism of Bambouto has been made by Gèze (1943, 1953), Jérémine (1943), Dumort (1967), Tchoua (1972, 1973, 1974) and Gouhier et al. (1974). All these publications are limited to brief general descriptions, petrography and a few geochemical analyses. Piper and Richardson (1972) briefly mention Bambouto in their palaeomagnetic study of the Cameroon Line and note that the samples they analysed are all normally magnetised. However, they do not discuss the age of the complex. Gèze (1943, 1953) equates the basic rocks to his "Lower Black Series" and the extensive trachytes and phonolites to his "Middle White Series". However, Tchoua (1972, 1973, 1974), postulates a more complex history of volcanism consisting of early trachyte and ignimbrites followed by basalts and finally a suite of trachytes and phonolites. Tchoua (1973, 1974) reports the presence of widespread ignimbrites containing inclusions of basement, trachyte and lignite. He notes an absence of basaltic inclusions. The lignite inclusions are thought by Tchoua to be equivalent to the Lignite Group of Nigeria; which is of Lower Eocene/Miocene age. Tchoua observed that the ignimbritic sheets rest on the basement and described them as being older than the basaltic extrusives and assigned a Lower Tertiary age to these basal volcanics. Neither Gouhier et al. (1974) nor Fitton and Hughes (pers. comm.) have observed ignimbrites in the vicinity of the Bambouto Mountains and it is more likely that rocks Tchoua (1972, 1973, 1974) termed ignimbrites are in fact trachytes or rhyolites. Gouhier et al. (1974) pointed out that field observations of Eno and Ossch (1974) invalidate Tchoua's postulated history since ignimbritic cliffs top the "Middle White Series" in Bamenda. The scheme of Tchoua (1973) is not necessarily invalidated since Bamenda is near the Oku massif and interfingering of flows must have occurred.

Conventional K-Ar ages were determined on four samples from Bambouto (Table 3.2.4) and further age information is given from rubidium-strontium isotopic studies (Chapter 5). The observed K-Ar ages for evolved rocks range from 22.72 ± 1.41 Ma (C107, trachyte) through 18.51 ± 0.38 Ma (C100, rhyolite) to 15.83 ± 0.39 Ma (C111, trachyte). This data fits the field relations, since the more recent flows, including C111, occur near the summit whereas those at the periphery of the massif are older. These ages are consistent with two previously reported dates (Samples BA5 and BA1) obtained by Gouhier et al. (1974). Quartz trachyte (BA5) was sampled close to C107 in the vicinity of the Santas caldera and is 22.7 ± 1.0 Ma old (Table 3.2.1). This age agrees very well with that of C107 and it is concluded that this caldera is the oldest of the three. Quartz trachyte (BA1) is from the "external flank" of Mount Bambouto and its age of 15.9 ± 1 Ma is equivalent to that obtained from C111, although the exact locality of BA1 was not stated by Gouhier et al. (1974).

The six point trachyte isochron (Figure 5 .2.5) gave an age of 16.6 ±0.4 Ma. Although there is geological scatter associated with this isochron (MSWD = 5.0), the samples were taken from the whole area and represent a mean age.

It may therefore be concluded that the bulk of the trachyte activity occurred in the period between 23 Ma and 16 Ma. One aphyric basalt (C108) taken from a point 20 km south of the summit (Figure 3.2.1) gave a K-Ar age of 14.9 ± 0.35 Ma (Table 3.2.4) and one analysis of a basanite (Gouhier et al., 1974; sample BA3) from 22 km north of the summit is 5.8 ± 0.2 Ma old. It would therefore appear likely that the basic rocks are substantially younger than the evolved lavas and domes. This conflicts with the observations of Gèze (1943, 1953) and Gouhier et al (1974). However, Tchoua's (1972, 1973) scheme included basalts post-dating early trachytes and "ignimbrites". In common with other volcanic centres in Cameroon,

TABLE 3.2.4

Bambouto K-Ar Data

Sample No.	Rock Type	K (%)	$^{40}Ar^*/^{40}Ar_T$	$^{40}Ar^*$ ($\times 10^{-6}$ sccg^{-1})	Age (Ma)
C100	Rhyolite	3.436	0.937	2.501	18.71 ± 0.38
			0.881	2.458	18.31 ± 0.38
C107	Trachyte	3.905	0.217	3.356	22.00 ± 1.24
			0.183	3.582	23.44 ± 1.58
C111	Trachyte	4.185	0.695	2.671	16.40 ± 0.38
			0.554	2.494	15.26 ± 0.40
C108	Basalt (aphyric)	1.693	0.802	0.940	14.33 ± 0.31
			0.520	0.916	13.84 ± 0.38

λ_e: $0.581 \times 10^{-10} y^{-1}$ λ_β : $4.962 \times 10^{-10} y^{-1}$

$^{40}Ar^*$: Radiogenic ^{40}Ar $^{40}Ar_T$: Total ^{40}Ar

it may be concluded that Gèze's classification of these rocks into just two groups the "Lower Black Series" and the "Middle White Series" is not applicable. Bambouto is one of only two volcanic areas under study here, in Cameroon, which do not exhibit any signs of recent volcanism. The other such centre is the Mandara Mountains.

3.2.5 Oku Massif

The Oku Massif is located 270 km northeast of Mount Cameroon and 80 km northeast of the Bambouto Mountains (Figure 3.2.1). This region represents the furthest centre inland of an almost continuous chain of volcanism stretching northeast for 300 km from Etinde (Figure 1.1). The Oku extrusive rocks cover an area which is approximately 85 km across with volcanics distributed on all sides of the summit, Mt. Oku (3,011 m above sea level). According to Perrone (1969), up to 500 m of basalts and intermediate volcanics occur, together with pelean domes and needles of trachyte and rhyolite. There is also an abundance of tuffs and rhyolitic ignimbrites. The final volcanism is represented by numerous small craters (some of which now contain lakes) rich in pyroclastics and poor in basalt flows.

Apart from Perrone (1969) the only other published work on the area is that of Gouhier et al. (1974), who presented several chemical analyses and one K-Ar age date (see below). Fitton and Hughes collected and subsequently geochemically analysed 24 samples, mainly from the lower slopes of the mountain. The mafic rocks are transitional in character, being moderately alkaline and both nepheline and hypersthene normative types are present. Phenocrysts of olivine, clinopyroxene and plagioclase occur in the basalts and hawaiites, whilst magnetite is also present as a significant phenocryst phase

in some hawaiites. All the evolved rocks in the Oku region are silica saturated or oversaturated as there is an absence of undersaturated trachytes or phonolites. The geochemical data of Fitton and Hughes is discussed in Chapter 5.

Three samples from the collection of Fitton and Hughes were selected for whole-rock K-Ar age analysis (Table 3.2.5). C85 is from a columnar jointed rhyolitic lava located about 28 km southwest of Mount Oku (Figure 3.2.1) and gave an age of 22.23 ± 0.45 Ma. With an initial ratio of 0.705 this sample would have an Rb-Sr age of 23.44 Ma (Chapter 5). C95 is a rhyolitic ignimbrite situated 23 km west of Mount Oku and is 23.19 ± 0.50 Ma old. Assuming an initial ratio at 0.705 it would have a Rb-Sr age of 23.69 Ma. A six point rubidium-strontium isochron (Figure 5.2.6) consisting of four ignimbrites, and two rhyolites gave an age of 24.1 ± 1.30 Ma (this includes C85 and C95). Although there is large inherent geological scatter (MSWD = 63.3) in this isochron it gives a good estimation of the mean age of the evolved rocks of the region because of the extremely fractionated nature of these samples, as expressed by their high Rb/Sr ratios. Thus it appears that most, if not all, of the evolved volcanism occurred in Lower Miocene times.

A hawaiite (C91), located 19 km east of Mount Oku gave a K-Ar age of 17.51 ± 0.40 Ma and Gouhier et al (1974) obtained an age of 21 ± 2 Ma (Table 3.2.1) on an hawaiite (sample JA) collected about 20 km southeast of Mount Oku. This sample of Gouhier et al. (1974) is equivalent to basalt C93 of Fitton and Hughes' collection which overlies an ignimbrite (C87) having an Rb-Sr age of 24.53 Ma, assuming an initial ratio of 0.705. This age therefore represents the basal value for mafic rocks at this locality and indicates the

TABLE 3.2.5

Oku K-Ar Data

Sample	Rock	K (%)	$^{40}Ar^*/^{40}Ar_T$	$^{40}Ar^*$ (10^{-6} sccg^{-1})	Age (Ma ± 1σ)
C85	Rhyolite	3.745	0.952	3.290	22.13 ± 0.44
			0.950	3.320	22.33 ± 0.45
C95	Rhyolitic Ignimbrite	4.350	0.841	3.987	23.32 ± 0.49
			0.799	3.906	23.05 ± 0.50
C91	Hawaiite	1.660	0.680	1.109	17.21 ± 0.40
			0.750	1.145	17.71 ± 0.39

λ_e : $0.581 \times 10^{-10} y^{-1}$

λ_β : $4.962 \times 10^{-10} y^{-1}$

$^{40}Ar^*$: Radiogenic ^{40}Ar

$^{40}Ar_T$: Total ^{40}Ar

existence of a gap of at least 3 Ma between the evolved rocks and the overlying mafic extrusives. However, as mentioned above, rhyolite C85 from the southwest of Mount Oku is only 1.2 Ma older than the hawaiite dated by Gouhier et al. (1974) and it is likely that the mafic rocks began erupting shortly after the end of evolved rock eruption and emplacement. Much more recent eruptive activity, perhaps only several hundred thousand years old, is evident in the form of pyroclastics and small explosion pits.

The volcanic history may be summed up in the sequence: initial eruptions and dome emplacement of trachyte, rhyolite and rhyolitic ignimbrite in the period 24 to 22 Ma; followed by the extensive eruption of basic and intermediate lavas (from 21 Ma to 17 Ma) after a short gap of perhaps 1 Ma; there then appeared to be a hiatus of volcanic activity from about 17 Ma until recent times when small scale pyroclastic eruptions occurred. The K-Ar data has provided age information critical for the interpretation of the strontium isotope ratios, since small variations in age produce large differences in initial $^{87}Sr/^{86}Sr$ ratios (Chapter 5) in these samples.

3.2.6 Mandara Mountains

The Mandara Mountains are located on the Nigeria-Cameroon border, 850 km northeast of Mount Cameroon and 325 km south of Lake Chad (Figures 1.1 and 3.2.2). This area has been previously referred to by various authors as Mokolo, Kapsiki, Roumsiki and Rhumsiki. Most of the region lies at an altitude greater than 1,000 m and consists of granite-gneiss Precambrian-Cambrian basement terrain cut by numerous trachyte and rhyolite plugs, and overlain

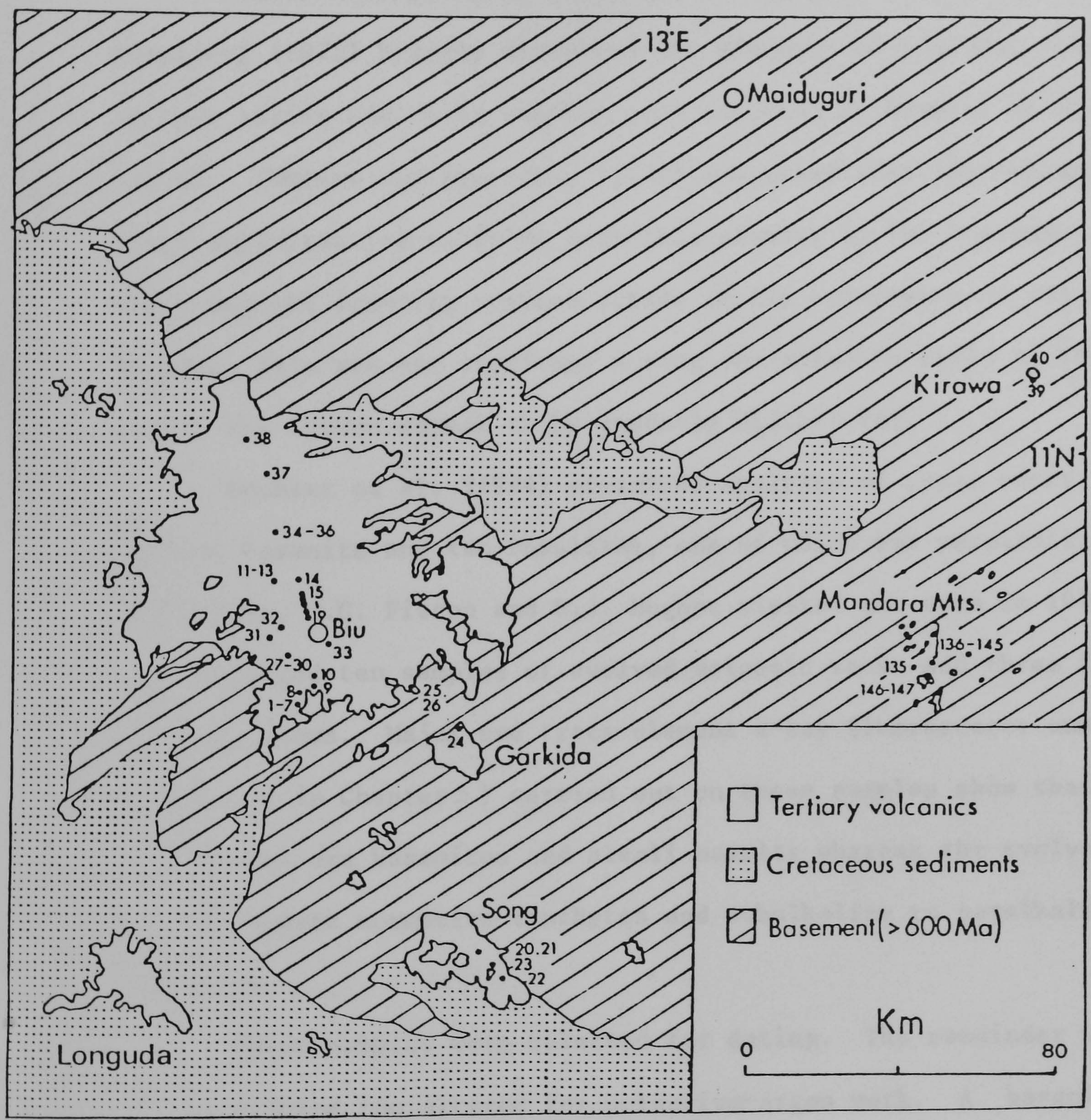


Figure 3.2.2 Sample location and geological map of the Biu Plateau (Nigeria) and the Mandara Mountains (Cameroon), after Dessauvagie (1975).

by less common basaltic flows. Most of the plugs have been deeply eroded to form spectacular spines, some of which rise 100 m above the surrounding topography whilst the remainder have crumbled, leaving jagged remnants.

Dresch (1952), Dumort and Perrone (1966) and Vincent and Armstrong (1973) briefly discussed the presence of volcanic rocks in this region and their studies were reviewed by Gouhier et al. (1974). Vincent and Armstrong (1973) suggested that the volcanic plugs exploited pre-existing weaknesses/faults in the basement and these authors identify various trends in the occurrence of the spines. However, this was not confirmed during the author's visit to the area; the spines appear to be randomly distributed.

Gouhier et al. (1974) presented analyses of three rocks; an olivine basanite and two rhyolites, one of which was peralkaline. The author, J.G. Fitton and D.J. Hughes visited the area in 1978 and collected ten samples of evolved volcanic rocks and three from basaltic flows. Major and trace-element x-ray fluorescence analyses (discussed in Chapter 5) carried out on these samples show that the mafic rocks are basanites and alkali basalts whereas the evolved rocks are all quartz normative trachytes and subalkaline to peralkaline rhyolites.

Three samples were selected for dating. The remainder were all considered too altered for potassium-argon work. A basanite (C146) and an alkali basalt (C147) sampled from Kila (8 km southeast of Roumsiki village) gave ages of 33.21 ± 1.33 Ma and 30.41 ± 0.69 Ma respectively (Table 3.2.6). Vincent and Armstrong (1973) reported an age of 27.4 ± 0.5 Ma (Table 3.2.1) for a basalt described as being southeast of Roumsiki and is likely to be situated on the same basaltic

TABLE 3.2.6

Mandara Mts. K-Ar Data

Sample	Rock	K% (Wt%)	$^{40}Ar^*/^{40}Ar_T$	$^{40}Ar^*$ ($\times 10^6$ sccg^{-1})	Age (Ma ± 1σ)
C145	Trachyte	4.425	0.182	5.906	34.00 ± 2.27
			0.178	6.365	36.62 ± 2.51
C146	Basanite	0.834	0.307	1.062	32.46 ± 1.33
			0.323	1.111	33.95 ± 1.33
C147	Basalt	1.305	0.732	1.574	30.75 ± 0.69
			0.709	1.538	30.06 ± 0.69

λ_e : $0.581 \times 10^{-10} y^{-1}$

λ_β : $4.962 \times 10^{-10} y^{-1}$

$^{40}Ar^*$: Radiogenic ^{40}Ar

$^{40}Ar_T$: Total ^{40}Ar

plateau as C146 and C147 (Figure 3.2.2). One trachyte (C145) from Omtemalé spine, situated 12 km north-north-west of Roumsiki village, was analysed by the author and gave an age of 35.31 Ma. Vincent and Armstrong (1973) presented an age of 29.6 ± 0.6 Ma for a trachyte located somewhere north of Roumsiki village. Rhyolite C144 from Aiguille Mchirgui spine, 12 km north-north-west of Roumsiki village would have an approximate Rb-Sr age of 29 ± 0.5 Ma, assuming an initial strontium ratio of between 0.709 and 0.716 (Chapter 5) and six rhyolites have an approximate age (as indicated by Rb-Sr isochron studies) of 32 Ma. Three trachytes plot about the rhyolite Rb-Sr isochron with much scatter and since there is no way of estimating an initial $^{87}Sr/^{86}Sr$ ratio with any confidence, it is difficult to assign an age to them. However, trachyte C145 must be older than 30 Ma and ages in the region between 35-40 Ma may be calculated using initial strontium ratios between 0.713 and 0.715.

Thus the rhyolites and basalts erupted in the period 33 to 27 Ma whilst the trachytes are probably no younger than 30 Ma old and at least one trachyte plug (C145) was emplaced prior to 35 Ma. With the exception of Kirawa and perhaps Tchabal Mbabo these rocks represent the oldest volcanism recorded in the Cameroon Line, and the activity is restricted to Upper Oligocene to Lowermost Miocene times. There is no evidence of recent activity, as has been recorded elsewhere in the Cameroon Line.

3.2.7 Biu Plateau

The Biu Plateau is located 160 km west of the Mandara Mountains and 800 km north-north-east of Mount Cameroon in Northern Nigeria (Figures 1.1 and 3.2.2) and consists of 5,000 km^2 of alkali basaltic

lavas attaining a maximum thickness of 250 m (du Preez, 1949). The flows are surmounted by youthful scoria and cinder cones composed of basaltic agglomerate, ash and tuffs. These cones trend in a NNW-SSE direction and have well defined craters with breached rims through which have flowed small volumes of lava (Wright, 1976). The Biu lavas are situated on the northeastern margin of the Benue Trough, overlying Precambrian basement and in the northern part, Cretaceous marine and deltaic sediments.

Falconer (1911) made the first significant geological contribution and there was no subsequent interest in the area until the mid 1960's when Carter et al. (1963) published their survey of the western part of the volcanic plateau and presented two chemical analyses from Biu and two from the Longuda plateau, which lies 90 km southwest of Biu (Figure 3.2.2). Prior to the author's research the Carter et al. (1963) analyses were the only ones published from the Biu Plateau. Black and Girod (1970) made brief mention of the volcanism in their synthesis of West African Tertiary igneous activity. Wright (1968, 1970) made petrographical studies of megacrysts present within the lavas and mentioned Biu in his review (Wright, 1976) of the volcanic rocks of Nigeria. Dessauvagie (1975) has published the most up-to-date map of Nigeria. Grant et al. (1972a) made a potassium-argon and rubidium-strontium isotopic study of volcanic rocks in Northern Nigeria and presented five K-Ar ages (Table 3.2.7) for Biu Plateau lavas.

In 1978 the author, J.G. Fitton and D.J. Hughes collected 31 samples of lava from the Biu Plateau, four from Song (located 90 km south of Biu), and six suites of ultramafic nodules and megacrysts. Chemical analyses performed on these rocks (Chapter 6) indicate that all of the lava samples from Song and all but five from Biu are alkali

TABLE 3.2.7

K-Ar Data from the Biu Plateau
obtained by Grant et al. (1972a)

Sample	Equivalent (This Study)	Rock	(Wt%)K	$^{40}Ar^*$ (10^{-6} sccg^{-1})	$^{40}Ar^*/^{40}Ar_T$	Age (Ma)
DF1	N24	Basalt	1.23	0.069	0.239	1.4 ± 0.1
DF8	N30	Basalt	1.20	0.223	0.385	4.7 ± 0.1
DB29	N38	Ol. Basanite	1.19	0.019	0.023	< 0.8
DB34	N8	Alkali Olivine Basalt	1.08	0.217	0.229	5.0 ± 0.2
15B1	N33	Basalt	1.40	0.162	0.198	2.9 ± 0.1

TABLE 3.2.8

K-Ar Data
(This Study)

Sample	Rock	K (Wt%)	$^{40}Ar^*$ (10^{-6} sccg^{-1})	$^{40}Ar^*/^{40}Ar_T$	Age (± 1σ)
N2	Basalt	1.062	0.215	0.194	5.20 ± 0.33
			0.221	0.196	5.35 ± 0.32
N38	Basanite	1.185	0.039	0.119	0.84 ± 0.09
N12F	Feldspar	0.815	0.390	0.029	12.28 ± 7.29
N30F	Feldspar	0.921	0.167	0.040	4.67 ± 1.74
			0.159	0.046	4.43 ± 1.38

λ_e : $0.581 \times 10^{-10} y^{-1}$

λ_β : $4.962 \times 10^{-10} y^{-1}$

$^{40}Ar^*$: Radiogenic ^{40}Ar

$^{40}Ar_T$: Total ^{40}Ar

Basalts with the remaining Biu samples consisting of four basanites and one hawaiite. No evolved rocks were present and the whole suite appears to be a uniform series of transitional alkali basalts ranging in normative character from 9% ne to 16.5% hy. Wright (1976) observed that thin flows cover wide areas and although no central source vents or fissures have been observed, Carter et al. (1963) and Black and Girod (1970) inferred eruption from central volcanoes of the Hawaiian or Strombolian type.

Four samples were selected for K-Ar age studies to supplement and compare with five already published by Grant et al (1972a). An olivine basalt (N2) from the southern limit of the Biu Plateau (Figure 3.2.2) gave an age of 5.28 ± 0.33 Ma (Table 3.2.8). This almost certainly dates the initial volcanic activity at this site since it overlies a flow (N1) resting on basement granite-gneiss. Grant et al. (1972a) obtained an age of 5.0 ± 0.2 Ma (Table 3.2.7) for a basalt sampled from near the top of the same basal series (same locality as basalt N8). These two ages therefore indicate that this initial period of eruptive activity in the southern part of the plateau was of the order of 300,000 years in duration. Although these data were determined in independent laboratories, they were analysed by the same methods, on the same type of mass-spectrometer and, as can be seen below, the two sources of data are directly comparable where samples from the same locality have been analysed.

A basanite from the northern margin of the Biu Plateau (N38) gave an age of 0.84 ± 0.09 Ma and Grant et al (1972a) quoted an age of <0.8 Ma for a sample from the same flow. An anothoclase megacryst (N30) from Lake Tila crater gave an age of 4.55 ± 1.56 Ma and Grant et al. (1972a) obtained an age of 4.70 ± 0.10 Ma for the basaltic host rock. This suggests that the feldspar megacrysts are in equili-

brium with their host, at least with respect to K-Ar and Sr isotope ratios (Chapter 6). However, another anorthoclase megacryst (N12) from Meringa cone gave an anomalous age of 12.28 ± 7.29 Ma. This cone cannot be more than 1 Ma old since it is very well preserved and retains its original topography. The large error associated with this determination is an indication of the very low radiogenic ^{40}Ar content (less than 3%). Fisher (1971) observed an anomalous age of 95 Ma for a plagioclase phenocryst enclosed within an alkaline basaltic plug within the Benue Trough (Dadin Kowa, situated 110 km southwest of Biu), generally agreed to be less than 10 Ma old (Wright, 1972; Fisher, 1971; Grant et al., 1972a, b). Grant et al. (1972a) analysed the host basalt and obtained a similarly anomalous age of 86 Ma. Fisher (1971) attributes this elevated age to the presence of excess radiogenic argon and Grant et al. (1972b) point out that these megacrysts may be either cognate (as suggested by Wright, 1972) or may have a crustal origin and there is no way of resolving this problem from Fisher's (1971) data alone. In the case of N12, it appears to be in isotopic equilibrium with its host rock in that they have the same $^{87}Sr/^{86}Sr$ ratios (Chapter 6) and it is concluded that no significance may be attached to the K-Ar age.

Grant et al. (1972a) published two further analyses (Table 3.2.7): a basalt flow from near the township of Biu (from the same lava flow as N33) in the plateau centre gave 2.9 ± 0.1 Ma; and a basalt lava from the Hawal River bed, 4 km southwest of Garkida (equivalent to N24), with enclosed pebbles of basement quartz and potassium feldspar gave an age of 1.4 ± 0.1 Ma. Activity has therefore been continuous on the Biu Plateau from before 5.3 Ma through to younger than 800,000 years ago.

Volcanic activity probably occurred prior to the observed date of 5.28 Ma on basal flow N2 since feeder dykes or fissures were not observed. Activity in the form of explosion craters and cinder cones containing abundant ultramafic nodules has occurred within the last million years although there is no historical record of volcanism in the area.

The smaller plateaux of Longuda and Song, each of which cover an approximate area of 250 km^2, are probably directly comparable to the Biu volcanism in age although there has been no K-Ar ages determined from these regions. Like the Biu Plateau, they are devoid of evolved rocks and take the same form of thin, extensive basaltic flows overlain by cinder cones. Four chemical analyses of lava samples from Song (Chapter 6) indicate a very similar chemical nature to the rocks of Biu. Likewise, the only two analyses of lavas from the Longuda Plateau (Carter et al., 1963) show that the chemistry of these basalts is similar to those from the Biu and Song Plateaux.

3.2.8 Ngaoundére and Tchabal Mbabo Plateaux

The only significant part of the Cameroon line which has not been studied in this research is the Ngaoundére volcanic plateau lying 400 km to the northeast of Mt. Oku (Figure 1.1) on the uplifted region of Adamaoua. The first significant study of the area was made by Sarcia and Sarcia (1952) who discussed the geology and tectonics of Adamaoua. On the geological map published by Dessauvagie (1975), these volcanics occupy an area of 14,000 km^2 and within this area there is a region of recent volcanism having cinder cones. Gouhier et al. (1974) published 12 chemical analyses and observed that all the mafic rocks are moderately to strongly alkaline basalts, basanites

and ankaramites. Evolved rocks consist of quartz and alkalic trachytes and phonolites. J.G. Fitton and D.J. Hughes visited the plateau in 1980 and their preliminary results (J.G.F., pers. comm.) support the observations of Gouhier et al. (1974).

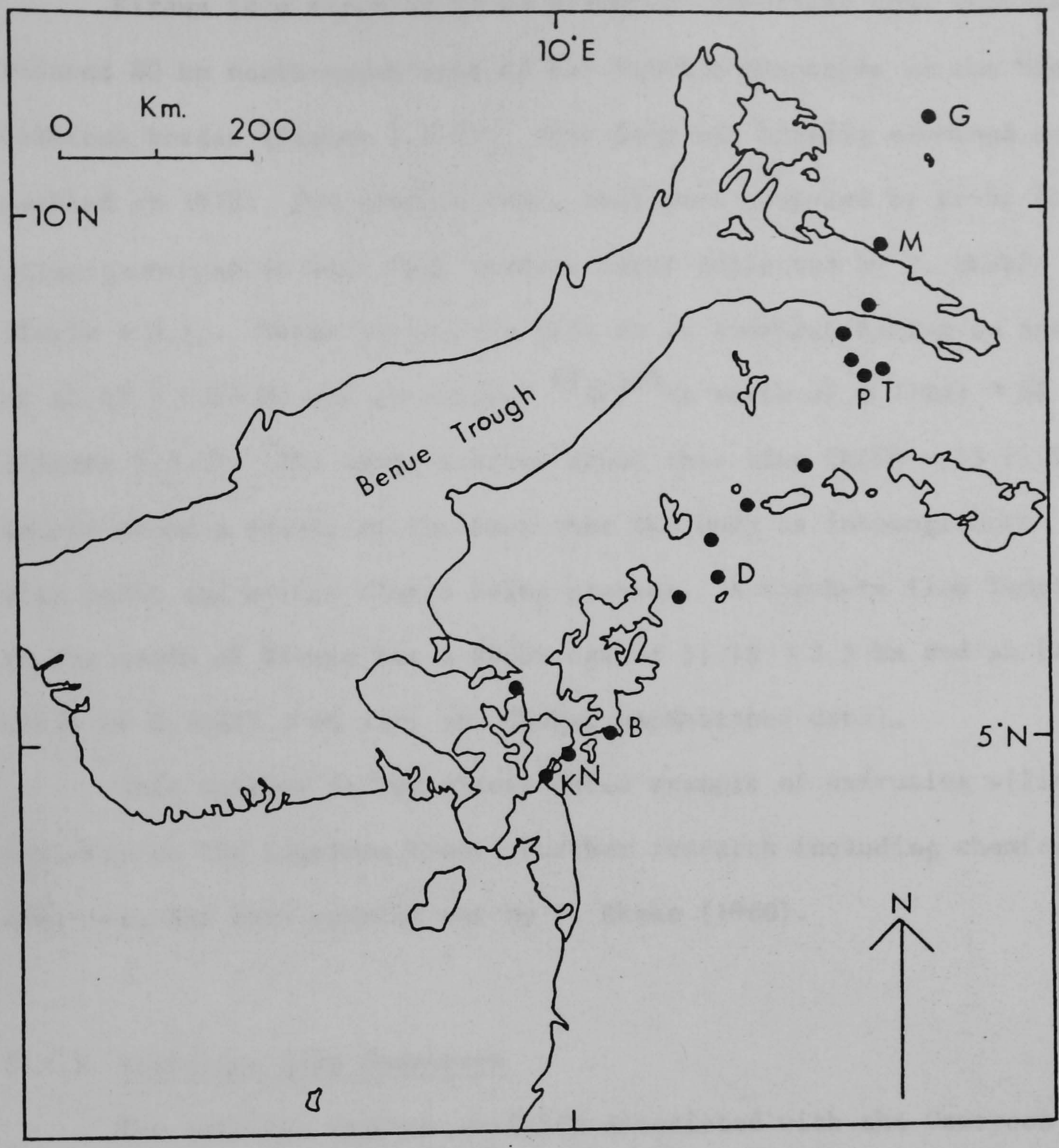
Gouhier et al. (1974) presented 3 potassium-argon age dates (Table 3.2.1) of 7 ± 0.2 Ma (basalt), 7.9 ± 0.2 Ma (trachyte) and 9.8 ± 0.2 Ma (trachyte). In addition Oustrière and Baubron (pers. comm. 1982) obtained a range of dates from 8.2 to 9.9 Ma for 4 basalts. Thus volcanism appears to range from 10 Ma through to very recent times although there is no record of historical activity.

In contrast however, a basalt situated on the Tchabal Mbabo volcanic field gave a Lower Oligocene K-Ar age of 37.2 Ma ± 0.2 Ma (Armstrong and Vincent unpublished data, described by Marechal, 1977). Tchabal Mbabo is situated on the Adamoua uplifted massif 100 km due west of the western edge of the Ngaoundéré Plateau and 160 km N.E. of Mt. Oku at the beginning of the eastern bifurcation of the Cameroon Line. This is the oldest date of any of the large extrusive centres either in Cameroon or from the islands in the Gulf of Guinea. Unfortunately no samples were available to confirm this data.

3.3 Palaeocene-Eocene Continental Igneous Complexes

In addition to voluminous extrusive volcanics, the Cameroon line includes numerous, small ring complexes of granite, syenite, gabbro, trachyte and rhyolite (Figure 3.3.1). With the exception of Kirawa, these centres were not studied since quite substantial research is being carried out (K-Ar and Rb-Sr isotope studies) by research workers at Clermont Ferrand and Nancy. A brief review of the age data they have published appears in Section 3.3.2 and of the Sr isotopic data in Chapter 5.

Figure 3.3.1 Lower Tertiary igneous intrusive complexes



G Golda Zuelva

M Mboutou

T Tchégui

P Poli

D Mayo Darle and Mba Namboe

B Bana

N Nlonako

K Koupé

3.3.1 Kirawa

Kirawa is a circular (3 km diameter) rhyolitic dome complex located 80 km north-north-east of the Mandara Mountains on the Nigeria-Cameroon border (Figure 3.2.2). This body was briefly examined and sampled in 1978. Two samples (N39, N40) were analysed by Rb-Sr isotope dilution methods as were four samples later collected by P. Okeke (Table 3.3.1). These six points plot on an isochron having an age of 45.45 ± 1.65 Ma and an initial $^{87}Sr/^{86}Sr$ ratio of 0.71243 ± 88 (2σ) (Figure 3.3.2). The large scatter about this line (MSWD = 53.7) is likely to be a result of the fact that the body is inhomogeneous with mafic and acidic clumps being present. A trachyte flow immediately to the south of Kirawa has a Rb/Sr age of 51.18 ± 2.5 Ma and an initial ratio of 0.70412 ± 80 (2σ) (P. Okeke, unpublished data).

This complex is the oldest dated example of extrusive silicic activity on the Cameroon Line. Further research including chemical analyses, has been carried out by P. Okeke (1980).

3.3.2 Intrusive Ring Complexes

The earliest igneous activity associated with the Cameroon line was the emplacement of anorogenic ring complexes between 30 and 66 Ma ago (Lasserre, 1966, 1978; Cantagrel et al., 1978; Jacquemin et al., 1982). These complexes consist of granite and syenite with lesser volumes of gabbro, trachyte and rhyolite. There are 40 such complexes occurring continually along the Cameroon line from Mount Koupé in Southern Cameroon, 30 km south of Mt. Manengouba, to Golda Zuelva, 40 km north of the Mandara Mountains (Figure 3.3.1). However none are present on any of the Gulf of Guinea islands nor are any known in the vicinity of the Biu Plateau.

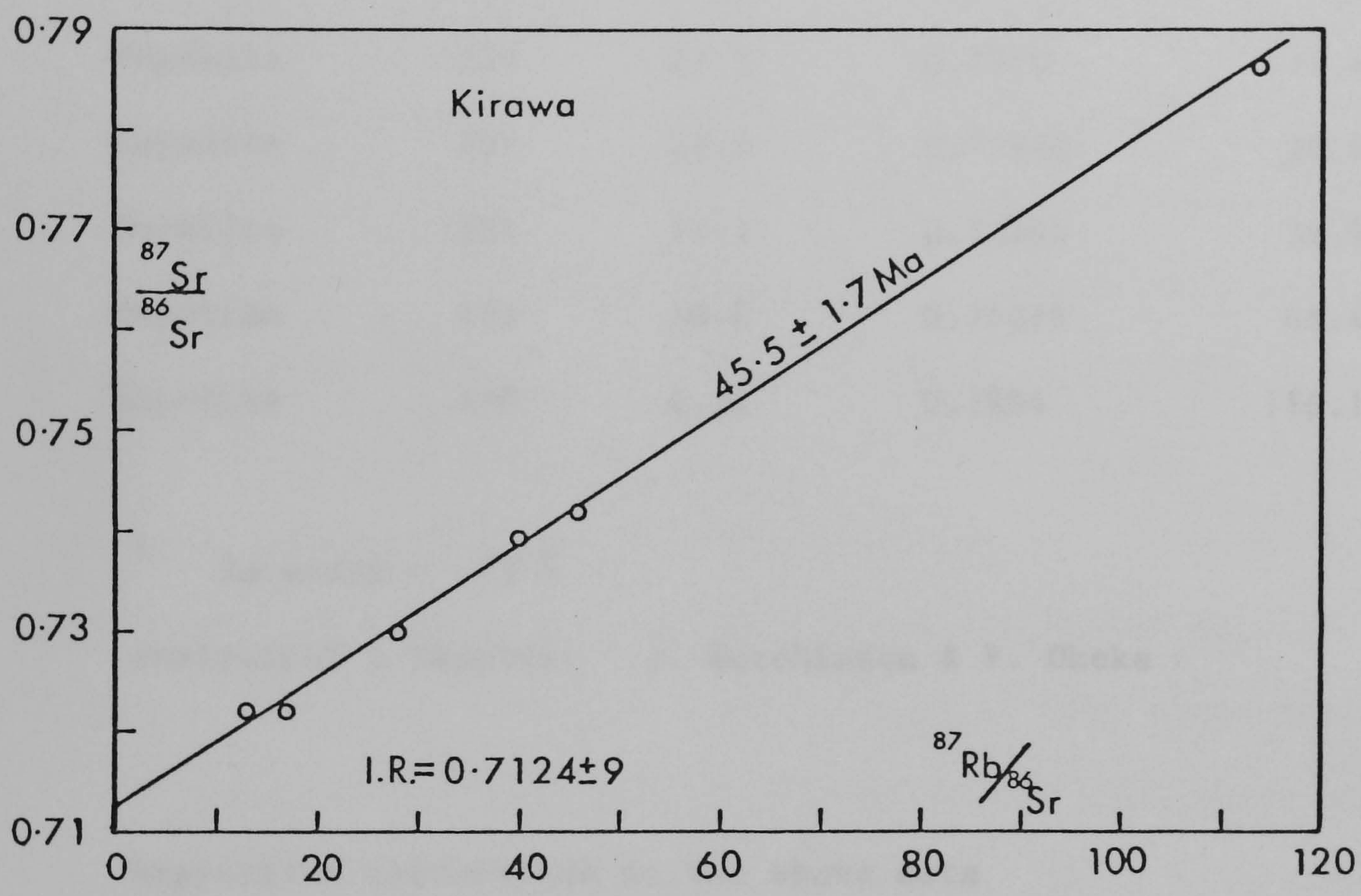


Figure 3.3.2 Whole rock Rb-Sr isochron diagram of Kirawa rhyolites. Data from this study and Okeke (1980).

TABLE 3.3.1

Rb-Sr Isotope Dilution Analyses of Kirawa

Sample	Rock Type	Rb	Sr	$^{87}Sr/^{86}Sr$[1]	$^{87}Rb/^{86}Sr$
L154	Rhyolite	175	40.2	0.72206	12.613
N40	Rhyolite	129	22.5	0.7219	16.605
L140	Rhyolite	131	13.5	0.72972	28.090
L146	Rhyolite	154	11.2	0.73894	39.936
L145	Rhyolite	173	10.8	0.74219	46.408
N39	Rhyolite	170	4.34	0.7864	114.14

[1] 2σ error = .03 %

analysts of L Samples: J. Hutchinson & P. Okeke

Regression calculation on the above data

Age = 45.45 ± 1.65 Ma (1σ)

Intercept = 0.71243 ± 88 (2σ)

MSWD = 53.7

Lasserre (1978) made a Rb-Sr geochronological study of 8 of these centres and observed ages ranging from 30 Ma to 63.3 Ma (Table 3.3.2). However, the ages quoted for Bana, Mboutou and Golda Zuelva are based on two point isochrons and very little confidence may be placed on them. Cantagrel et al. (1978) made a more comprehensive K-Ar age survey of 6 of the 8 centres Lasserre (1978) studied (Table 3.3.3) and their data show that two ring complexes (Golda Zuelva and Tchegui; Figures 3.3.1 and 3.3.3) have two or more phases of intrusive activity. At Golda Zuelva two phases of granitic emplacement (at 66.6 and 55.6 Ma) were followed by trachyandesite dykes about 38 Ma ago. In Tchégui, gabbro was emplaced between approximately 48 and 56 Ma (mean = 51 Ma), followed by the major syenite body between 37 and 33 Ma (mean = 34.9 Ma). Jacquemin et al. (1982) confirmed the older Golda Zuelva age described above by reporting a 7 point Rb-Sr isochron having an age of 66 ± 3 Ma (MSWD = 13.8). These ring complexes are likely to be the eroded remnants of early Tertiary-Uppermost Cretaceous volcanoes since small volumes of rhyolite and trachyte extrusives have been found associated with these intrusions.

There are no linear age trends associated with these complexes although the oldest recorded activity (Figure 3.3.3) is located at the northeastern extremity of the chain at Golda Zuelva (66 Ma). Intrusive activity in the period 30-38 Ma is recorded in most of the centres with the exception of Koupé, Mayo Darle and Mboutou. This shows that the line was active over much of its length during this period.

3.4 Discussion

In summary, extrusive activity along the Cameroon line has been radiometrically dated as occurring from the present (1959, 1982) continuously back to 37 Ma. The emplacement of the Kirawa rhyolite

TABLE 3.3.2

Rb-Sr Ages of Intrusions

Centre	Type	Age (Ma)	No. of Points	Reference
Poli	Granite	39.2 ± 2	8	1
Tchégui	Syenite, gabbro, trachyte	43 ± 6	10	1
Mayo Darlé) Mba Namboé)	Granite	63.3 ± 1.3	6	1
Nlonako	Syenite, microgabbro, granite	43.3 ± 0.3	6	1
Koupé	Syenite, gabbro, granite	46.4 ± 1	5	1
Bana	Granite	30	2	1
Mboutou	Granite	60	2	1
Golda Zuelva	Gabbro, granite, hawaiite, rhyolite	39.6	2	1
Golda Zuelva	Gabbro, granite, hawaiite, rhyolite	66 ± 3	7	2

References: 1 : Lasserre, 1978

2 : Jacquemin et al, 1982

TABLE 3.3.3

K-Ar Ages of Intrusions
from Cantagrel et al. (1978)

Rock Type		K (Wt%)	$^{40}Ar^*/^{40}Ar_T$	Age (Ma)	
Golda Zuelva					
KF	Granite	9.43	0.730	66.7 ± 2)	66.6
WR	Granite	3.66	0.625	66.5 ± 2)	
KF	Granite	9.00	0.853	55.6 ± 2	
WR	Trachyandesite (dyke)	3.81	0.880	38.2 ± 2	
Mboutou					
KF	Granite	6.40	0.928	56.5 ± 2	
Poli					
KF	Granite	7.23	0.659	31 ± 1	
Tchégui					
B	Syenite	6.66	0.438	37.3 ± 1)	
WR	Syenite	3.61	0.629	34 ± 1)	
WR	Syenite	4.19	0.689	37 ± 1)	34.9
WR	Syenite	3.23	0.636	33 ± 1)	
WR	Syenite	3.11	0.754	33 ± 1)	
WR	Gabbro	0.62	0.534	48 ± 1)	
WR	Gabbro	0.62	0.421	49 ± 2)	51.0
B	Gabbro	6.65	0.702	56 ± 2)	
Mayo Darle et Mba Namboe					
KF	Granite	6.49	0.801	49.5 ± 1)	49
KF	Granite	6.88	0.693	48.5 ± 2)	
Nlonako					
WR	Syenite	2.78	0.872	45 ± 1	
WR	Microgabbro	0.198	0.303	43 ± 2	
WR	Granite	4.01	0.966	35 ± 1	

WR: Whole rock

KF: Potassium feldspar

B: Biotite

dome occurred in the period 45-51 Ma and intrusive rocks span the period 30-66 Ma. These intrusive ring complexes often have remnants of volcanic rocks and probably represent the eroded cores of still older volcanoes. Isotopic and geochemical studies of Golda Zuelva (Jacquemin et al., 1982) show that the complexes and their extrusive remnants are cogenetic. Igneous activity has therefore been continuous from earliest Tertiary times until the present day.

There is not a linear age pattern along the chain since recent volcanism is observed at most extrusive centres with the exception of Principe Island, Mount Bambouto and the Mandara Mountains. Figure 3.3.3 shows the volcanic centres arranged geographically from Pagalu (bottom of Figure) in the southwest to Mandara (top of Figure) in the northeast. In this Figure, Mt. Cameroon through Mount Manengouba, Mount Bambouto and the Oku Massif, to Mandara apparently show a sequential increase in the age of oldest volcanism. This trend continues to Kirawa and the oldest recorded intrusive activity (Golda Zuelva) occurs at the northern extremity of the chain (Figures 3.3.1 and 3.3.3). However, the northern and eastern extremities, the extensive Biu and Ngaoundére Plateaux, show much younger recorded initial activity of 5 Ma and the Tchabal Mbabo plateau (situated in the centre of the continental sector) is apparently at least 37 Ma old (Armstrong and Vincent, unpublished data.) Hence it is concluded that this trend must be fortuitous. In addition, no linear trends have been recorded either in the continental intrusive rocks of Lasserre (1978) and Cantagrel et al. (1978) nor from rocks within the oceanic sector.

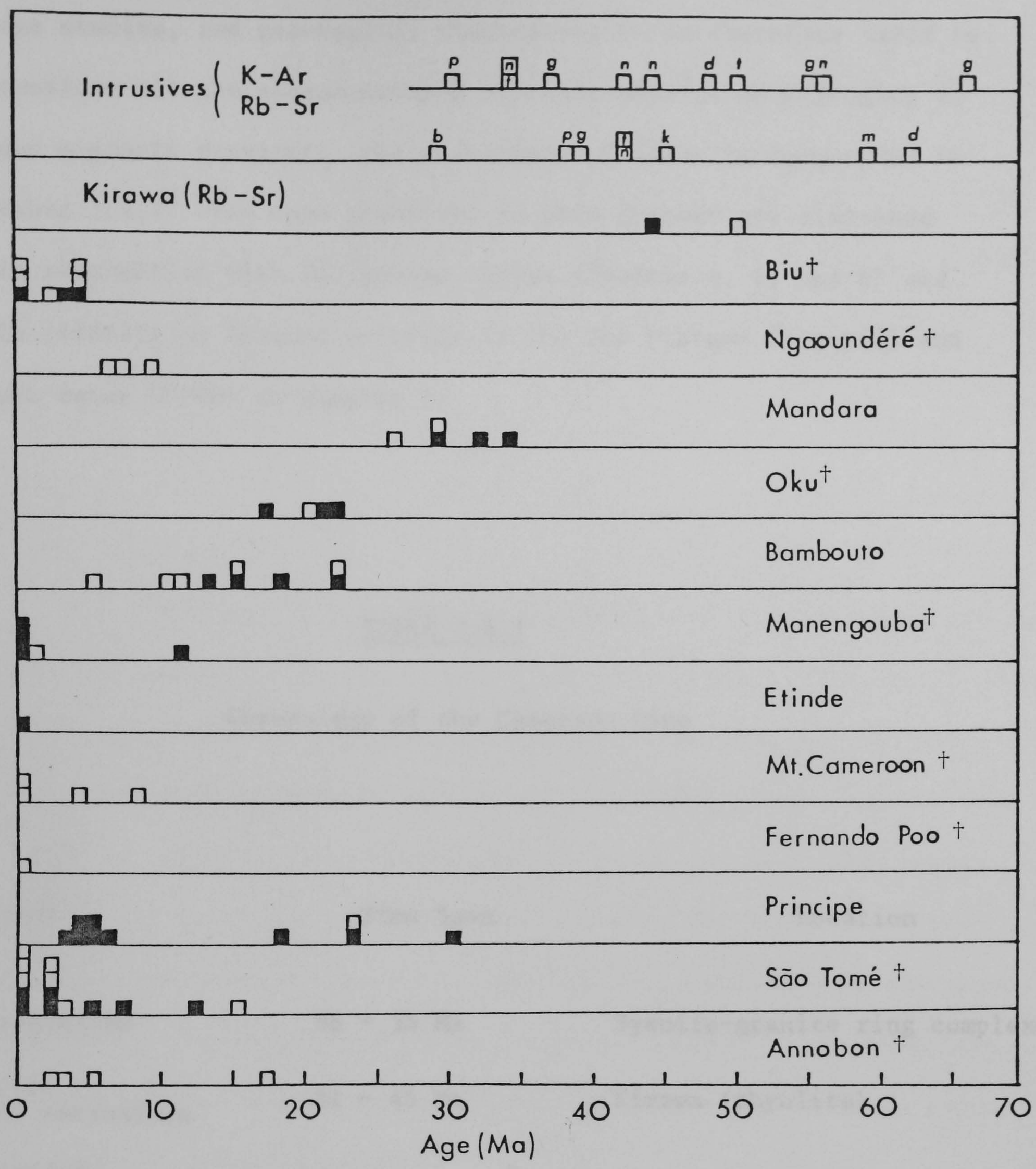


Figure 3.3.3 Summary histogram of age data from the Cameroon line. The data from Annobon to Biu were determined by K-Ar methods and ages of the intrusive complexes were determined as shown (■= this study; □ = data in the literature, as cited in text). Annobon and Fernando Poo have recently been renamed Pagalu and Bioko respectively. Symbols for the Lower Tertiary intrusives are as in Figure 3.3.1 . Recent activity in the form of cinder cones is also evident in most of the volcanic centres (†).

On the basis of geographical location, K-Ar and Rb-Sr age studies, and geochemical characters, it is therefore valid to consider all the aforementioned volcanic centres as belonging to one magmatic province; the chronology of which is summarized in Table 3.4.1. The data presented in this Chapter are discussed in conjunction with Sr isotope ratios (Chapter 4, 5, and 6) and in relation to igneous activity in the Jos Plateau (Nigeria) and the Benue trough in Chapter 7.

TABLE 3.4.1

Chronology of the Cameroon Line

Event	Time Span	Location
Earliest magmatism	66 - 35 Ma	Syenite-granite ring complexes
Oldest dated continental extrusives	51 - 45 Ma	Kirawa (rhyolite)
Oldest recorded oceanic extrusives	31 Ma	Principe (olivine tholeiite)
Predominantly salic central volcanoes	66 - 14 Ma	Ring complexes, Oku, Bambouto
Major continental basalt eruptions (mainly fissure type)	10 Ma - present	Mt. Cameroon, Etinde, Manengouba, Biu, Ngaoundéré
Major oceanic sector activity - mainly basaltic with late-stage evolved rocks	24 Ma - Recent	Principe-São Tomé, Pagalu, Bioko
Final stage cinder cones and basaltic flows	Recent	São Tomé, Bioko, Pagalu, Mt. Cameroon, Manengouba, Oku, Ngaoundére, Biu, Tchabal Mbabo

CHAPTER 4

GEOCHEMISTRY OF THE OCEANIC ISLANDS

Strontium isotope data of the islands of Principe, São Tomé, Pagalu and Bioko are presented and discussed with geochemical data collected by other workers. Analytical techniques are given in Appendices A1 and A3. Sample locations appear in Appendix D and are marked on the geology maps in Chapter 3.

4.1 Principe

A study was made of the petrochemistry of the island of Principe by Fitton and Hughes (1977) and a summary of their findings is given in Section 4.1.1. The geology of Principe is described in Chapter 3. Appendix C gives details of the classification scheme used in this thesis. Isotopic data determined by the writer have been interpreted in Section 4.1.2 in conjunction with the major and trace element analyses and normative compositions published by the above authors. These interpretations, together with K-Ar age data have been published by Dunlop and Fitton (1979). A copy of this paper appears in Appendix E.

4.1.1 Geochemistry

The oldest rocks are small inliers of palagonite breccias which may represent a submarine phase in the island's evolution. These breccias contain blocks of fresh olivine tholeiite (P15) which gave a K-Ar age (this study, Chapter 3) of 30.6 Ma. This basalt is hypersthene normative and is deficient in alkalies compared with the other mafic rocks of Principe (Figure 4.1.1). Its analysis would

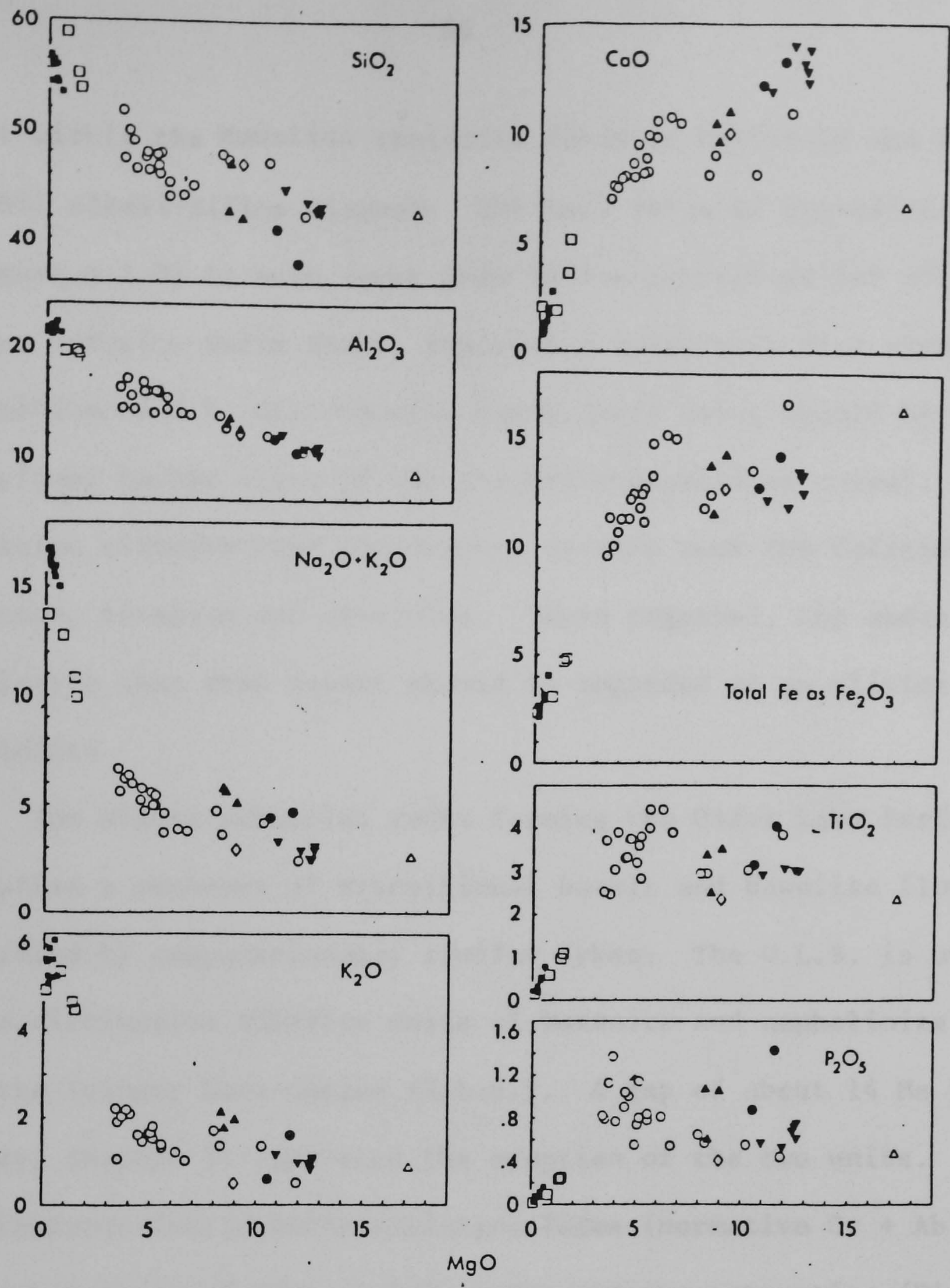


Figure 4.1.1 Major element variation (wt%) in the volcanic rocks of Principe. Symbols as in figure 4.1.3. From Fitton and Hughes (1977).

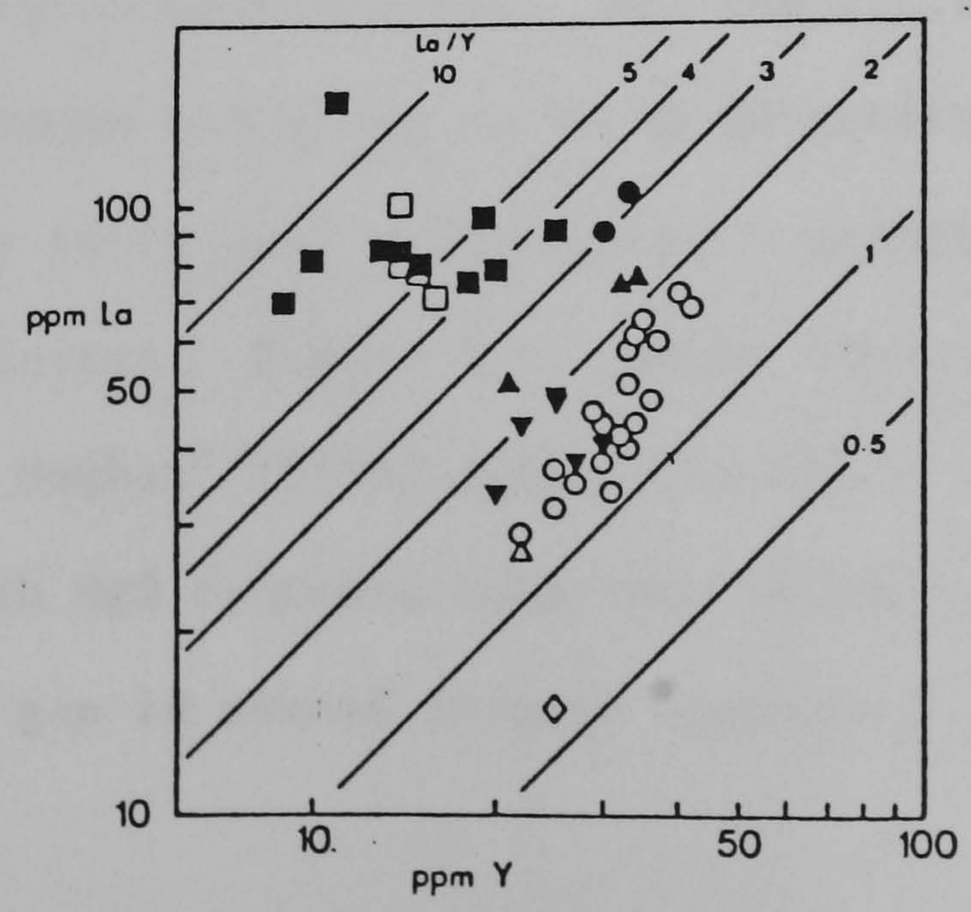


Figure 4.1.2 Lanthanum-yttrium variation in the same rocks. From Fitton and Hughes (1977).

plot within the Hawaiian tholeiite field of MacDonald and Katsura's (1964) alkali-silica diagram. The La/Y ratio of tholeiite P15 (Figure 4.1.2) is much lower than ratios determined for all the other Principe mafic rocks, implying a relatively flat chondrite-normalised R.E.E. distribution curve (La/Y ratio should be proportional to the slope of the chondrite-normalized curve). In addition clinopyroxene phenocrysts of this rock are deficient in calcium, titanium and aluminium. Taken together, the above data indicates that this basalt should be regarded as an olivine tholeiite.

The oldest subaerial rocks forming the Older Lava Series (O.L.S.) comprise a sequence of transitional basalt and hawaiite flows intruded by compositionally similar dykes. The O.L.S. is overlain by a distinctive alkaline suite of basanite and nephelinite flows of the Younger Lava Series (Y.L.S.). A gap of about 14 Ma (this study, Chapter 3) separated the eruption of the two units. A plot of Thornton-Tuttle Differentiation Index (normative Or + Ab + Ne + Qz + La) versus degree of SiO_2 under and oversaturation (Figure 4.1.3) illustrates the chemical range and normative character of the two mafic series. The O.L.S. lavas lie close to the critical plane of silica undersaturation. All the Y.L.S. rocks lie to the left of this plane and go up to 14.5% normative nepheline. This series belongs to Le Bas' (1978) group 1 association of alkali basalt-nephelinites. Figure 4.1.1 shows the major element variation of Fitton and Hughes' (1977) data. The O.L.S. samples fall into two groups with MgO contents less than 7% and greater than 8%. This compositional gap is common in most anorogenic volcano suites

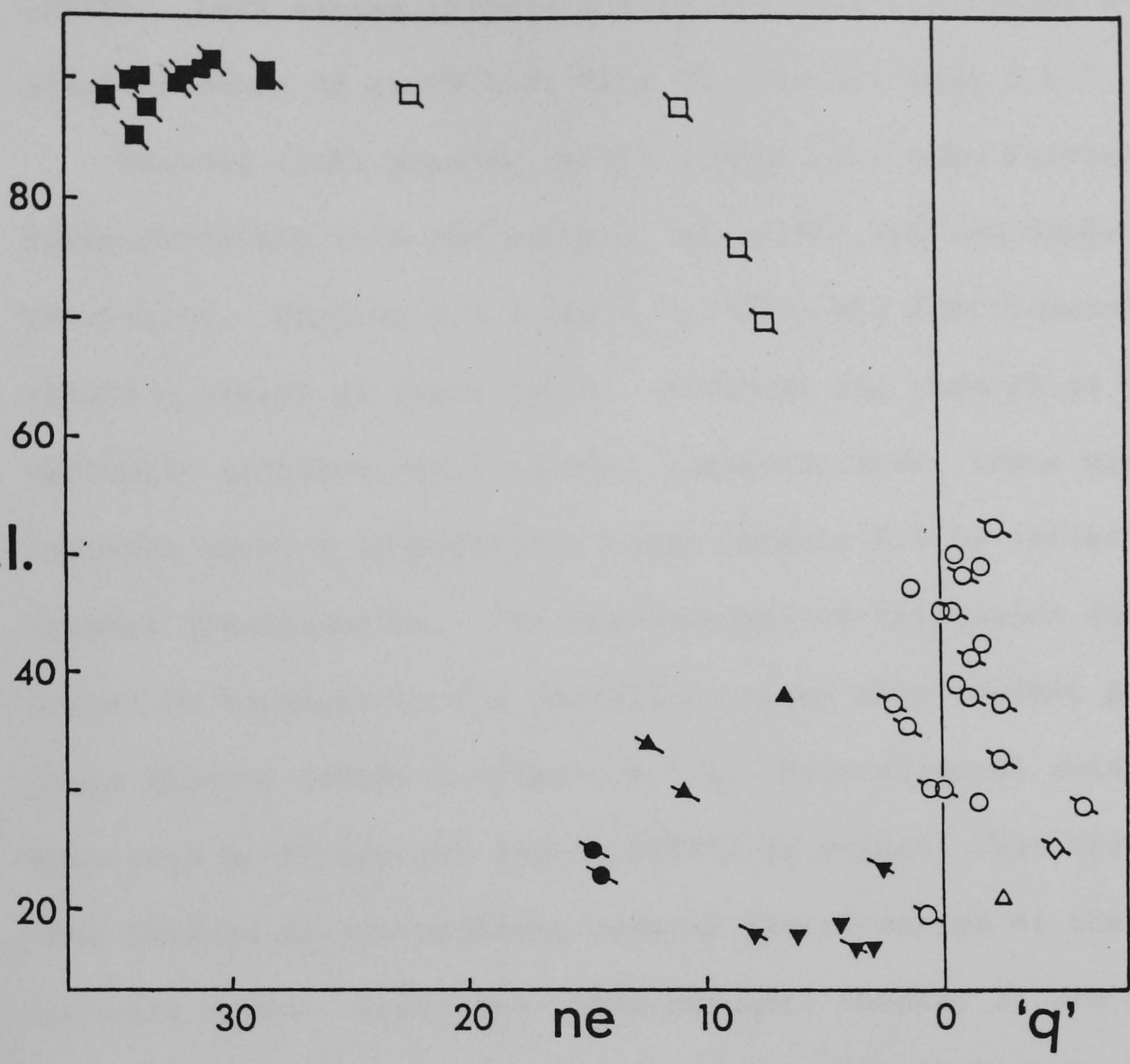


Figure 4.1.3 Thornton-Tuttle Differentiation Index (D.I.) plotted against degree of silica over- and under- saturation for the Principe volcanic rocks (from Fitton and Hughes, 1977).

ne weight % normative nepheline
'q' weight % SiO_2 equivalent to normative hypersthene
○ lavas and dykes of the older lava series
△ olivine dolerite (P4)
◇ basalt from palagonite breccia (P15)
▲ basanites of the younger lava series
▼ highly porphyritic basanites of the younger lava series
● olivine nephelinites of the younger lava series
□ tristanite-trachyphonolite suite
■ phonolites
\ analysed for strontium isotope ratios

worldwide and is equivalent to the basalt-hawaiite gap of Thompson (1972). La/Y ratios (Figure 4.1.2) are markedly higher in the alkaline rocks of the Y.L.S. than the transitional O.L.S. rocks.

Evolved rocks present on the island have been identified as being divisible into two suites: phonolite and trachyphonolite to tristanite. Figures 4.1.1 and 4.1.3 show the fractionated and alkaline nature of these rocks. Although the phonolites have virtually constant major element concentrations, trace element contents cover a considerable range (Figure 4.1.4) reflecting crystal fractionation. The trachyphonolite-tristanite suite cannot be parental to the phonolites since they exhibit parallel trace element trends on Figure 4.1.4. Mineralogical evidence had been used by Fitton and Hughes (1977) to suggest that the phonolites were derived by low-pressure crystal fractionation of the Y.L.S. basanite magma. K-Ar ages (this project, Chapter 3) are consistant with this derivation. Fitton and Hughes showed that the tristanite-trachyphonolite suite magmas could not have been comagmatic (see above) with the phonolites and that they would appear to have been derived from a separate, less undersaturated parent. They suggested that this suite could have been derived by the relatively high-pressure fractional crystallization of the O.L.S. magma. However, since K-Ar age dates on this suite all fall within the Pliocene (this study, Chapter 3) period and not the Lower Miocene of the O.L.S., any direct genetic link between the two would apparently be ruled out.

4.1.2 Strontium Isotope Studies

Unspiked, high precision $^{87}Sr/^{86}Sr$ ratios were determined on representative specimens from all the rock types mentioned above and

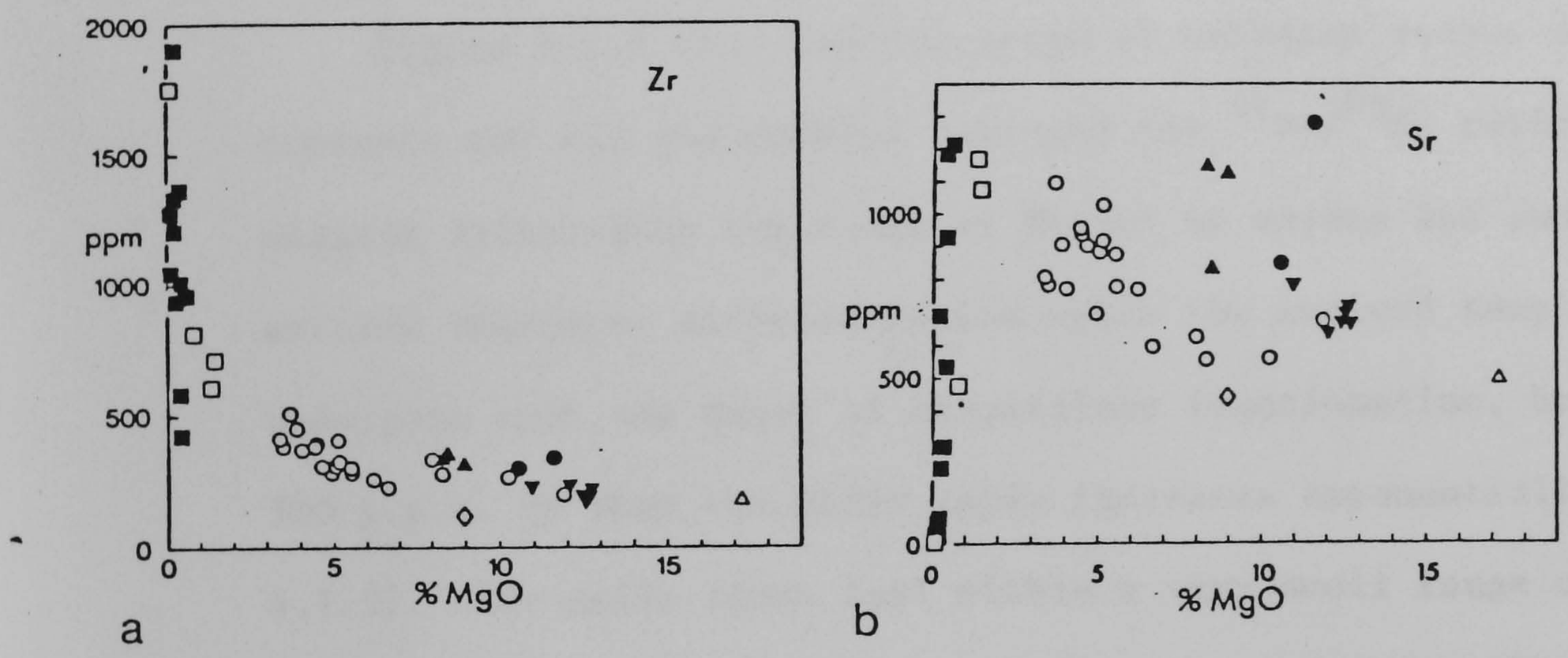


Figure 4.1.4 a and b. Variation of (a) zirconium and (b) strontium in the Principe rocks. Symbols as in figure 4.1.3. From Fitton and Hughes (1977).

the results are listed in Table 4.1.1. Some of the evolved samples were also analysed by isotope dilution and rubidium and strontium concentrations were later determined for all the samples by x-ray fluorescence spectrometry. Rb/Sr ratios have been calculated using the X.R.F. data (see Appendix A3 for a discussion on the relative merits of the two determinative methods). Initial ratios have been calculated using ages determined by the K-Ar dating (Chapter 3) of 31 Ma (ol.thol.), 21 Ma (O.L.S.) and 6 Ma (Y.L.S. and fractionated rocks).

Figure 4.1.5 is a log-log graph of rubidium versus strontium contents for all the samples analysed for $^{87}Sr/^{86}Sr$ ratios. This diagram illustrates the range of Rb and Sr values and shows the extreme degree of differentiation which the evolved samples have undergone with the onset of plagioclase fractionation, below about 500 p.p.m. Sr when the Rb/Sr ratio increases exponentially (Figure 4.1.5). The mafic rocks fall within a very small range of Rb/Sr ratios of between 0.08 and 0.07. Figure 4.1.6 shows the relation of Sr concentration to degree of fractionation as expressed by differentiation index.

It is clear from Figures 4.1.5, 4.1.6 and 4.1.7 that the single tholeiite sample, P15, is depleted in strontium and in La/Y ratio compared to the other mafic rocks. However, it has an initial strontium ratio of 0.70342 which places it within the strontium isotope ratio spectrum of the O.L.S. (see below). Only one sample of olivine tholeiite was available for analysis and while it was taken from a fresh basalt block containing very little glass (J.G. Fitton, pers. comm.), it is enveloped in a palagonite breccia which may have had some interaction with seawater. Seawater

Table 4.1.1

Rb, Sr and $^{87}Sr/^{86}Sr$ data from Principe

Sample no.	Rock type	*K*–Ar age (Ma)	Rb (ppm)	Sr (ppm)	$^{87}Sr/^{86}Sr$ ($\pm 2\sigma \times 10^5$)	$(^{87}Sr/^{86}Sr)_0$[a]
Lava from palagonite breccia						
*P*15	tholeiite	30.6	13.4	443	0.70344 ± 12 0.70348 ± 12	0.70342
Older Lava Series						
*P*3	hawaiite		13.3	712	0.70330 ± 12	0.70328
*P*6	hawaiite		17.5	936	0.70320 ± 12	0.70318
*P*8	hawaiite		23.1	792	0.70321 ± 8	0.70318
*P*21	hawaiite		20.3	596	0.70322 ± 9	0.70319
*P*25	hawaiite	19.1	29.2	871	0.70323 ± 8	0.70320
*P*26	hawaiite		27.9	919	0.70317 ± 6	0.70314
*P*27	hawaiite		24.8	896	0.70315 ± 8	0.70313
*P*28	basalt	23.6	27.8	567	0.70336 ± 10	0.70332
*P*29	hawaiite		45.4	772	0.70355 ± 11	0.70350
*P*31	basalt		37.5	620	0.70373 ± 12	0.70368
*P*32	basalt		29.2	553	0.70343 ± 8	0.70338
*P*33	hawaiite		36.2	943	0.70320 ± 6	0.70316
*P*50	basalt		5.7	708	0.70302 ± 8	0.70301
Younger Lava Series						
*P*17	basanite		29.6	762	0.70279 ± 9	0.70278
*P*18	nephelinite	5.60	38.8	1,295	0.70335 ± 8	0.70334
*P*19	basanite		41.2	1,158	0.70290 ± 10	0.70289
*P*20	basanite	3.51	40.4	1,180	0.70294 ± 10 0.70294 ± 10	0.70293
*P*34	nephelinite		59.5	844	0.70297 ± 8	0.70296
*P*45	basanite		19.5	676	0.70290 ± 9	0.70289
*P*51	basanite		23.0	660′	0.70299 ± 12 0.70298 ± 5 0.70302 ± 6	0.70299
Phonolites						
*P*2	phonolite		243	39.6	0.70433 ± 6	0.70282
*P*5	phonolite	5.32	392	84.5	0.70411 ± 11	0.70296
*P*11	phonolite	5.48	133	955	0.70310 ± 5	0.70307
*P*22	phonolite		177	1,230	0.70298 ± 6	0.70294
*P*35	phonolite		296	295	0.70310 ± 12 0.70307 ± 7	0.70283
*P*38	phonolite		192	1,205	0.70311 ± 7	0.70307
*P*39	phonolite		272	78.8	0.70391 ± 3	0.70306
*P*40	phonolite		218	236	0.70322 ± 6	0.70299
Tristanite-trachyphonolite suite						
*P*12	tristanite	4.89	181	1,117	0.70334 ± 10 0.70325 ± 4	0.70326
*P*13	tristanite		187	1,192	0.70302 ± 7 0.70297 ± 7	0.70295
*P*16	trachyphonolite	6.93	315	9.37[b]	0.71102 ± 30 0.71099 ± 10	0.70271
*P*41	trachyte		175	481	0.70311 ± 8	0.70302

[a] Initial $^{87}Sr/^{86}Sr$ ratio calculated assuming the following ages: palagonite breccia, 31 Ma; OLS, 21 Ma; YLS and evolved samples, 6 Ma

[b] Determined by isotope dilution (XRF gave 8.6 ppm)

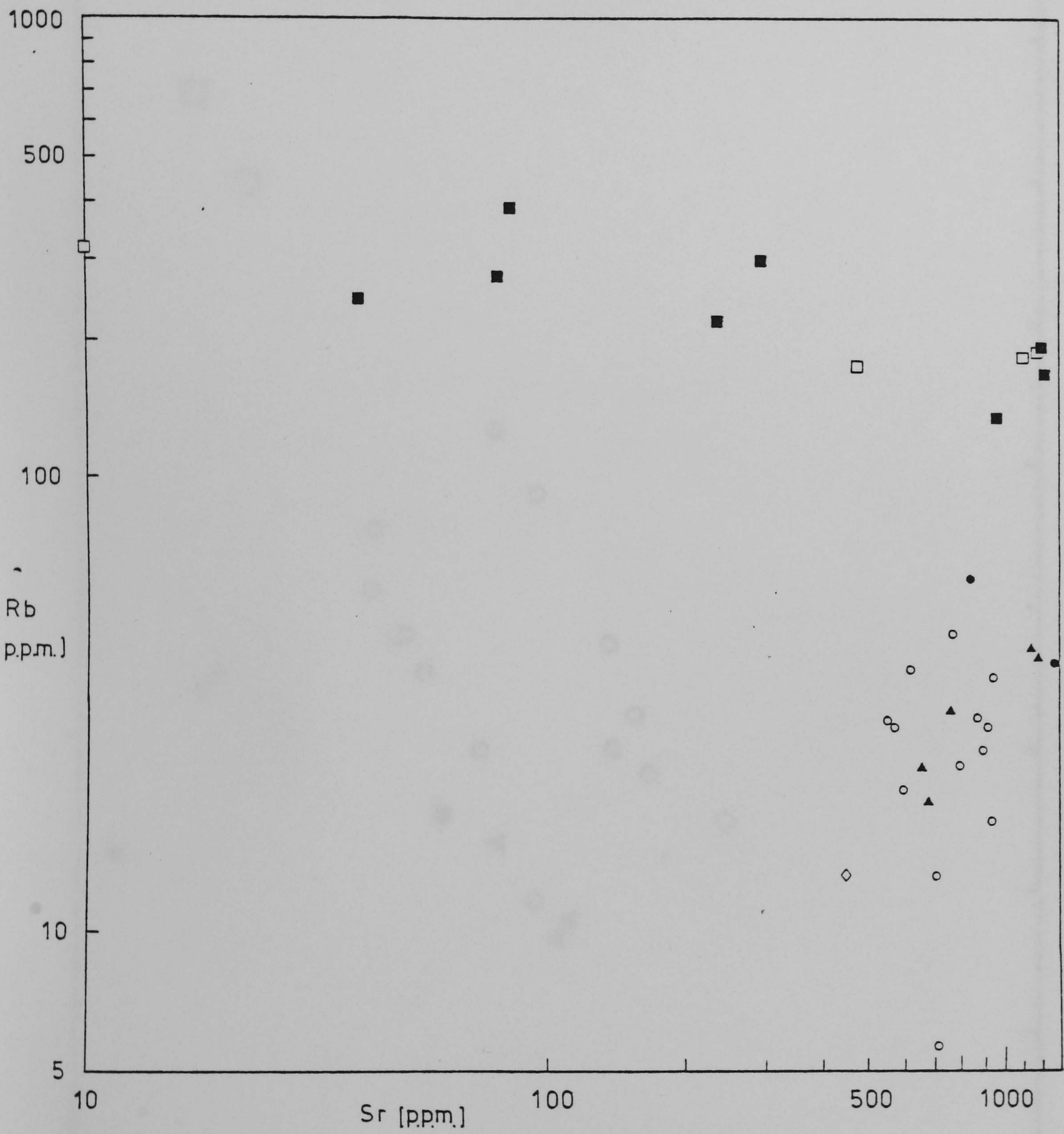


Figure 4.1.5 Rb-Sr plot of Principe rocks.

Symbols as in figure 4.1.8.

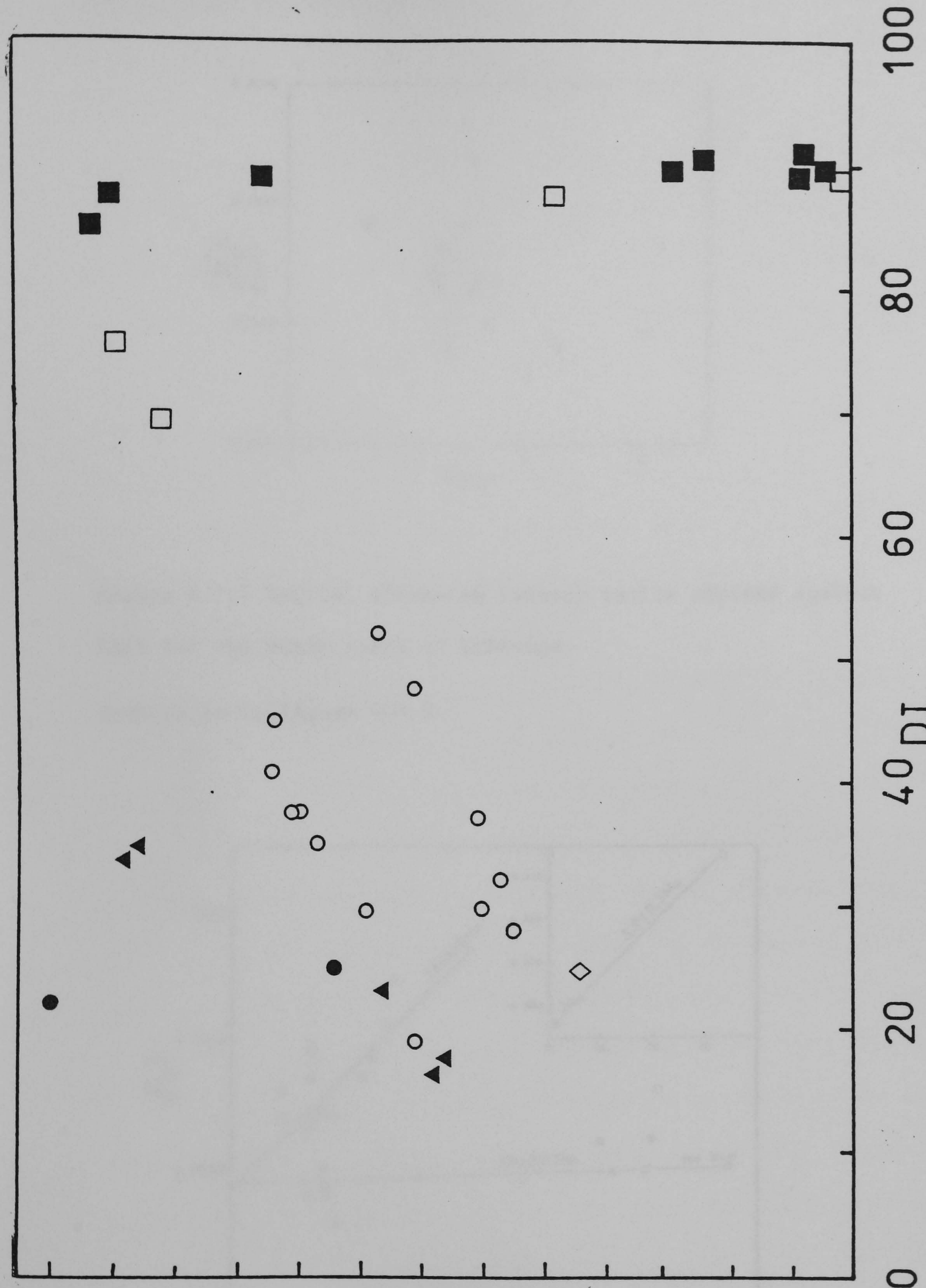


Figure 4.1.6 Sr contents plotted against Differentiation Index (DI).
Symbols as in figure 4.1.8.

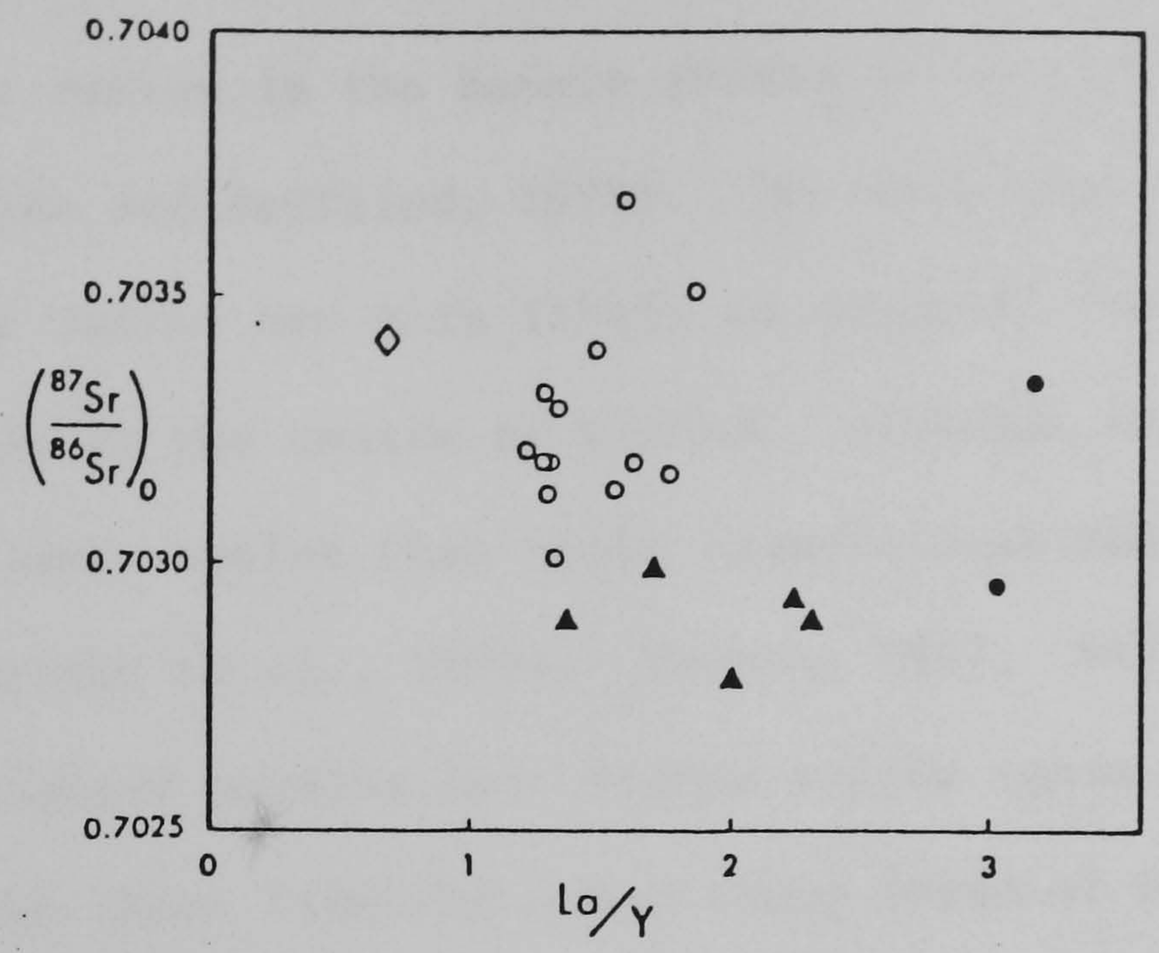


Figure 4.1.7 Initial strontium isotope ratios plotted against La/Y for the basic rocks of Principe.

Symbols as in figure 4.1.8.

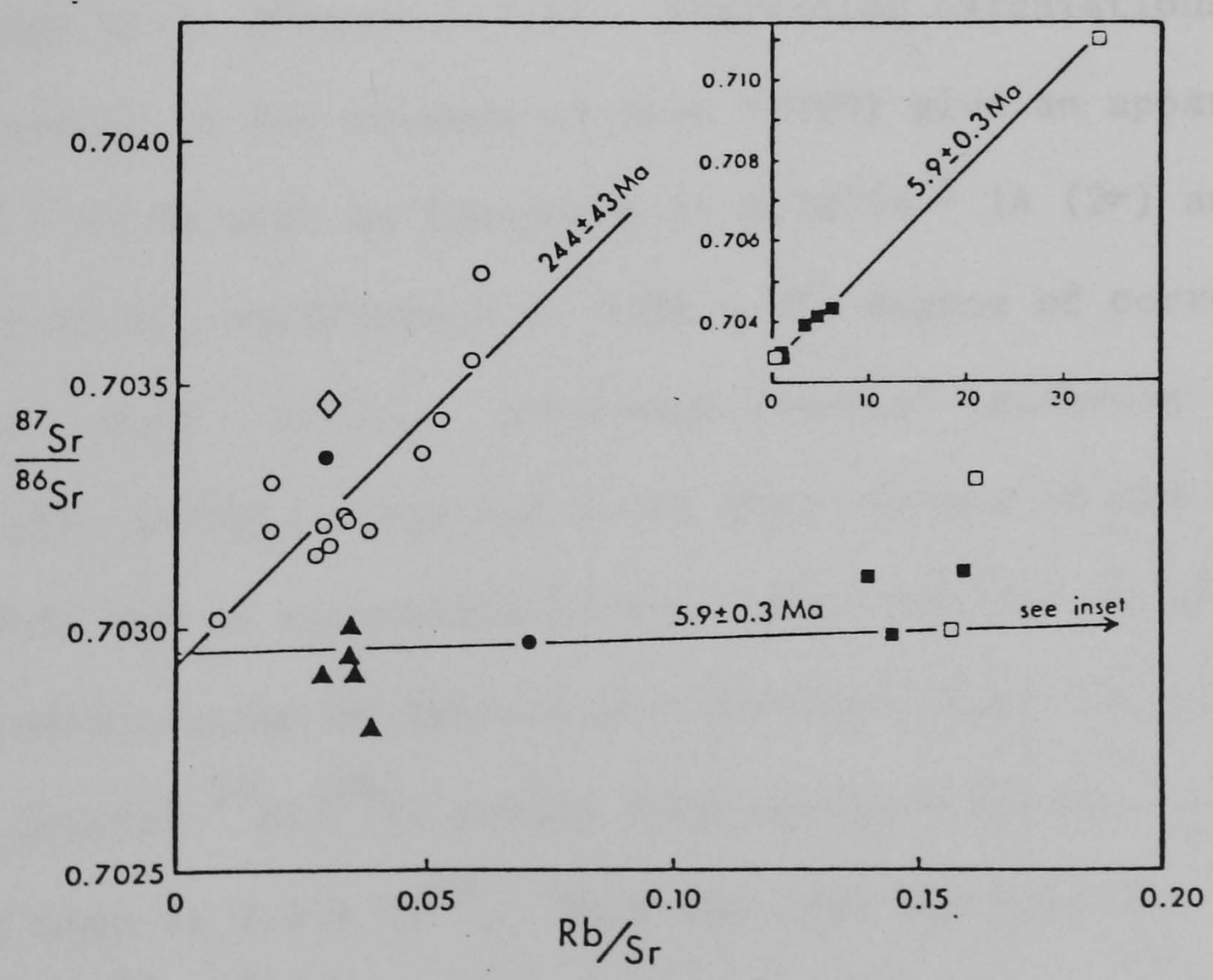


Figure 4.1.8 Rb-Sr whole-rock isochron diagram for the volcanic rocks of Principe. Symbols as in figure 4.1.3 except for the YLS basanites which are all grouped under ▲ here. The 5.9 Ma isochron has been calculated using the YLS and phonolite data (excluding P18); the tristanite-trachyphonolite suite samples were not included in the regression calculation. The 244 Ma isochron is derived from the OLS data only.

has an $^{87}Sr/^{86}Sr$ ratio of about 0.709 (Spooner, 1976) and any seawater-basalt interaction is going to result in elevated $^{87}Sr/^{86}Sr$ ratios in the basalt (Dasch et al.,1973; Hart et al., 1974 and Menzies and Seyfried, 1979). However, such changes in primary $^{87}Sr/^{86}Sr$ ratios are more likely to occur at the margins of pillow lavas than at the centre of blocks. Although most tholeiites tend to have lower ratios than their transitional and alkaline counterparts (Brooks et al., 1976a; Hanson, 1977; Hofmann and Hart, 1978) oceanic island basalts have higher values (mean of 0.70386; Faure, 1977) than those from the ocean floor (mean of 0.70280; Faure, 1977). Thus in the case of P15 it is concluded that the observed $^{87}Sr/^{86}Sr$ ratio is probably a primary, unaltered value, but any further conclusions can only be tentative.

The transitional basalt-hawaiite O.L.S. vary in measured $^{87}Sr/^{86}Sr$ from 0.70302 to 0.70373 (13 samples, Table 4.1.1). This series shows a positive correlation of measured $^{87}Sr/^{86}Sr$ ratios versus Rb/Sr (Figure 4.1.8). Regression calculations (Table 4.1.2) according to the methods of York (1969) give an apparent "age" of 244 ± 43 Ma with an intercept of 0.70293 ± 14 (2σ) and a Pearson correlation coefficient of 0.86. The degree of correlation compares well with other, published "mantle" isochrons (e.g. Brooks et al., 1976a). This age is in gross excess of the eruption age (19-24 Ma) as determined by K-Ar chronological studies (Chapter 3).

A consideration of Table 4.1.1 indicates that the maximum deviation of initial $^{87}Sr/^{86}Sr$ ratios from measured values is 5×10^{-5} and the mean is 3.2×10^{-5}. Thus the true age has very little effect on the $^{87}Sr/^{86}Sr$ isotope ratios.

TABLE 4.1.2

Principe Regressions

Suite	No. Samples	Age ($Ma \pm 1\sigma$)	Intercept ($\pm 2\sigma \times 10^5$)	MSWD	Pearson Corrln. Coefft.
O.L.S. basalts, Hawaiites	13	244 ± 43	0.70293 ± 14	4.05	0.86
Y.L.S. and Phonolites	14	5.87 ± 0.32	0.70295 ± 6	3.72	0.98
Y.L.S., phonolites and tristanites-trachyphonolites	18	5.80 ± 0.20	0.70297 ± 6	5.19	

That the correlation of $^{87}Sr/^{86}Sr$ with Rb/Sr (Figure 4.1.8) of the O.L.S. is a function of processes operating in the source region is indicated by several considerations. Firstly, no visible signs of hydrothermal alteration or secondary minerals are apparent in thin section and there is no correlation of $^{87}Sr/^{86}Sr$ with iron oxidation ratio (Figure 4.1.9) to suggest possible groundwater or seawater effects. Secondly, the fact that the Pb isotope regression line for oceanic basalts (Sun and Hanson, 1975a; Leeman, 1977) is distinctly different from the regression line for oceanic sediment and seawater argues against the involvement of seawater in the evolution of oceanic island subaerial magmas as suggested by O'Hara (1977). Thirdly, these variations are unlikely to be due to linear isotopic fractionation since all such isotopic fractionation is corrected for by normalising to a standard $^{88}Sr/^{86}Sr$ value (Chapter 2, Section 2.1). Any non-linear fractionation of heavy isotopes such as strontium (where the mass difference is very slight) which may occur will be insignificant. Fourthly, there is no observed correlation between $^{87}Sr/^{86}Sr$ and Sr (Figure 4.1.10) in the Principe samples, thereby ruling out contamination by material with substantially higher or lower ratios than the lavas. Finally the incompatible behaviour of Sr in the O.L.S. magmas (Figure 4.1.4, after Fitton and Hughes, 1977) suggests that the variation in Rb/Sr is due to differences in the mantle source rather than to plagioclase fraction-ation. The correlation observed in the O.L.S. samples is therefore considered primary and may represent a mantle isochron; the age of which may pertain to some relict mantle event. The significance of this correlation was discussed by Dunlop And Fitton (1979, Appendix E) and will be considered further in Sections 4.4 and 7.2 .

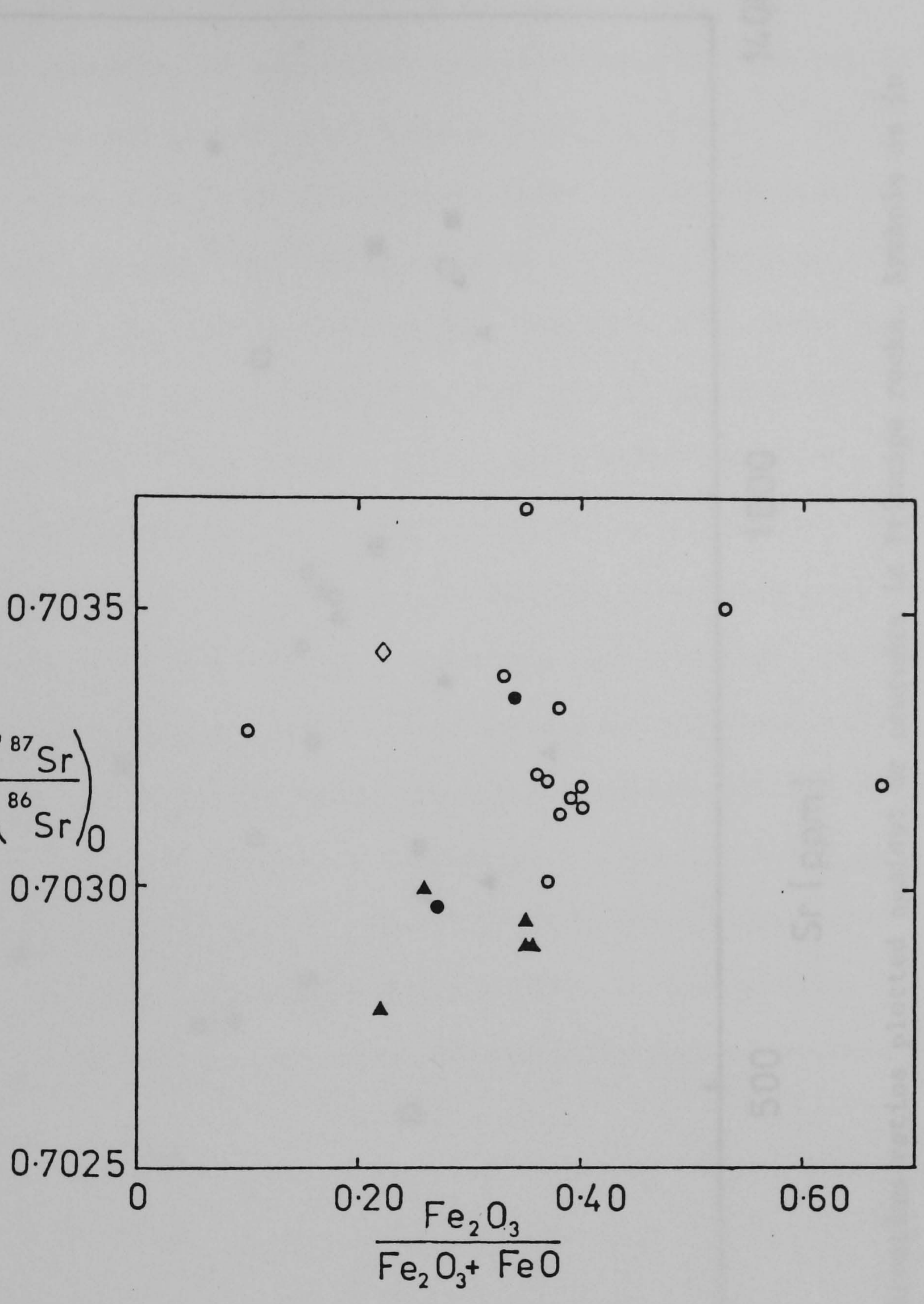


Figure 4.1.9 Initial strontium ratios plotted against iron oxidation ratios in Principe rocks. Symbols as in figure 4.1.8.

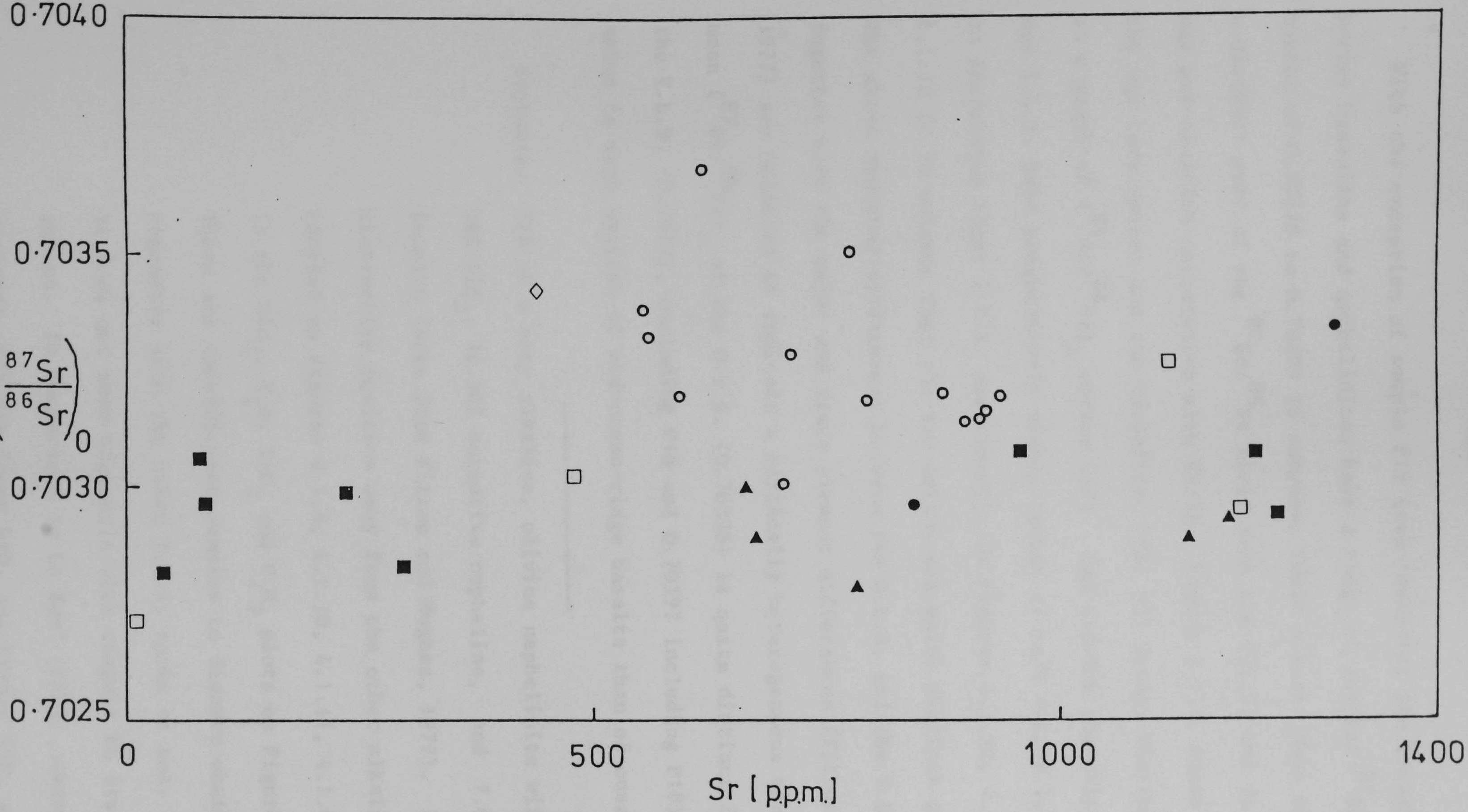


Figure 4.1.10 Initial strontium ratios plotted against Sr contents in Principe rocks. Symbols as in figure 4.1.8.

With the exception of sample P18 (see footnote) the Younger Lava Series basanites and nephelinites have a range of initial $^{87}Sr/^{86}Sr$ ratios of 0.70278 to 0.70299 (6 samples, Table 4.1.1) thus occupying a distinct part of the $^{87}Sr/^{86}Sr$ field from the O.L.S. and do not show any pre-eruption correlation with Rb/Sr. Figure 4.1.7. shows that the two lava series and the tholeiite, P15, all occupy distinct regions on a graph of $(^{87}Sr/^{86}Sr)_o$ versus La/Y. The olivine tholeiite, O.L.S. and Y.L.S. have progressively higher values of La/Y (which is equivalent to increasing light R.E.E. enrichment). In Figures 4.1.10, 4.1.11 and 4.1.12 it is evident that the two series are quite distinct geochemically. The above observed differences between the O.L.S. and the Y.L.S., together with the major and trace element differences (Fitton and Hughes, 1977) are believed to indicate a vertically heterogeneous mantle. The mean $(^{87}Sr/^{86}Sr)_o$ of the O.L.S. (0.70326) is quite distinct from that of the Y.L.S. (0.70291, excluding P18 and 0.70297 including P18). The Y.L.S. value is more typical of mid-ocean-ridge basalts than of oceanic island

---

Footnote: P18 is a very alkaline, olivine nephelinite with less than 38% SiO_2, 14.46% normative nepheline, and 7.69% normative leucite (data from Fitton and Hughes, 1977). It plots in a distinctive position away from the other alkaline Y.L.S. samples on Figures 4.1.8, 4.1.10, 4.1.11, 4.1.6, 4.1.4 and in the SiO_2, K_2O, TiO_2 and P_2O_5 plots on Figure 4.1.1. There are insufficient samples to discern whether P18 is cogenetic with the other Y.L.S. rocks or not. Certainly it does not seem cogenetic with respect to its $^{87}Sr/^{86}Sr$ ratios. In comparison to Le Bas' (1978) average of 81 analyses, P18 has lower SiO_2 and higher TiO_2 and P_2O_5 contents than those listed in his group 1 association.

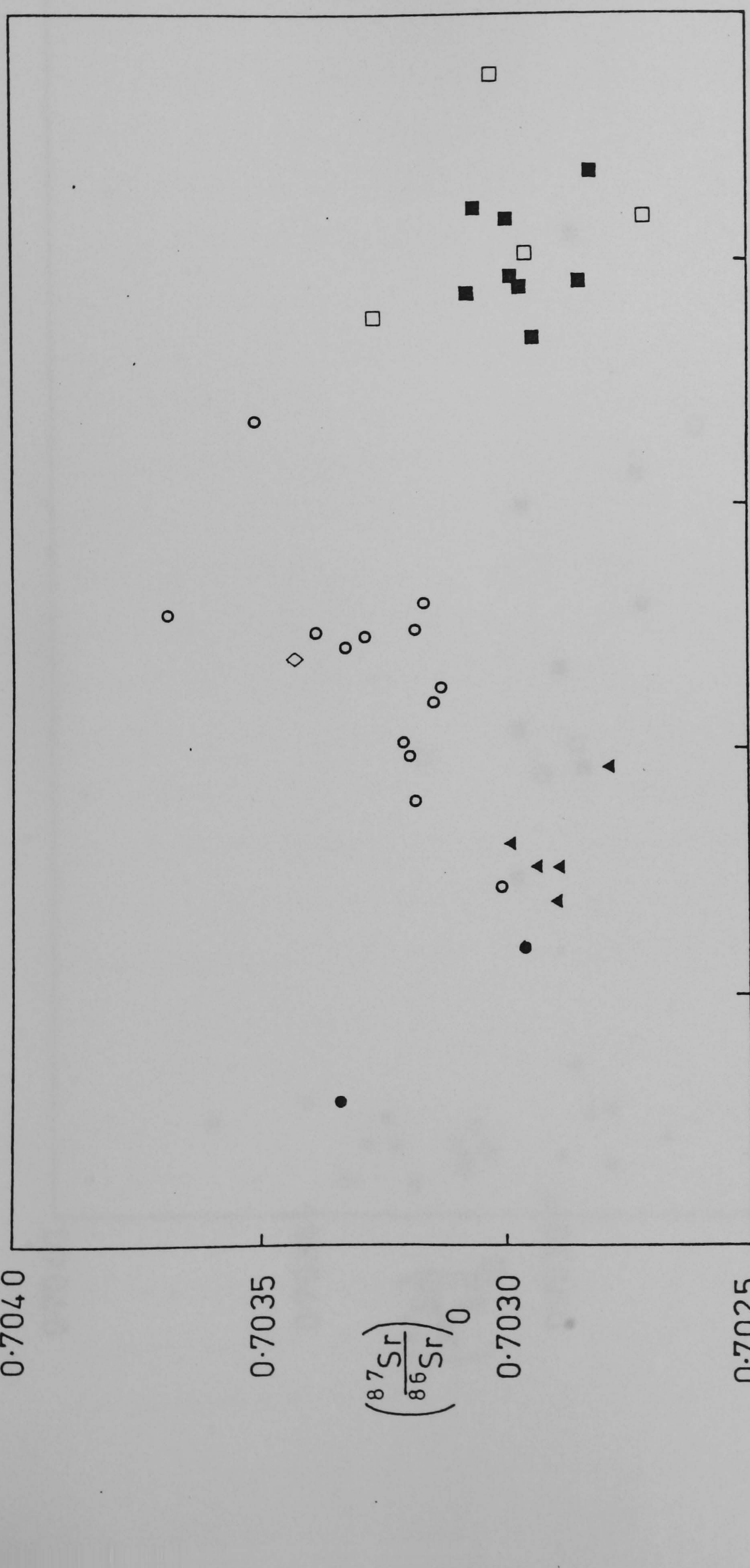


Figure 4.1.11 Initial strontium ratios plotted against SiO_2 contents in Principe rocks. Symbols as in figure 4.1.8.

Figure 4.1.12 Initial strontium ratios plotted against Rb contents in the Principe rocks.

Symbols as in figure 4.1.8.

alkaline rocks (Faure, 1977). Large-scale phase fractionation (O'Hara et al., 1975) is not likely to account for these differences. If there was a residue of clinopyroxene after partial melting then his mechanism implies that ^{86}Sr would be preferentially retained until higher degrees of melting occurred, thus giving rise to higher $^{87}Sr/^{86}Sr$ ratios for lavas derived by smaller degrees of partial melting. This is not the case on Principe where basanites and nephelinites (presumably derived by lower degrees of partial melting) give distinctly lower ratios than one would expect if this mechanism were to apply.

The Y.L.S. plot on a true age isochron (Figure 4.1.8) together with the phonolite flows and plugs. Analysed phonolites have a range of measured $^{87}Sr/^{86}Sr$ of 0.70433 to 0.70298 (8 samples, Table 4.1.1) and Rb/Sr ratios vary from 6.14 to 0.139. This Y.L.S.-phonolite isochron gave an age of 5.9 $\pm$ 0.3 Ma (Table 4.1.2) with an initial ratio of 0.70295 $\pm$ 6 (Pearson Correlation Coefficient = 0.98) which agrees well with K-Ar chronology (Chapter 3) and supports the conclusion of Fitton and Hughes (1977), based on major and trace element geochemical data, that the Y.L.S. magmas were parental to the phonolites. A comparison of data in Table 4.1.1 show that the initial ratios of the Y.L.S. and the phonolite suite are virtually identical indicating that it is fair to conclude that they are comagmatic.

Samples from the tristanite-trachyphonolite-trachyte suite plot close to the Y.L.S.-phonolite isochron and its extrapolation (Figure 4.1.8 and inset) although data from these samples were not included in the regression calculation discussed above. If they were included the resultant age and intercept would be 5.8 $\pm$ 0.1 Ma and 0.70297 $\pm$ 6. However, geochemical data (Fitton and Hughes, 1977) illustrates that the tristanite-trachyphonolite cannot lie on the same liquid line of

descent as the phonolites since they show parallel trends in Figures 4.1.4, 4.1.6 and parallel pyroxene trends in pyroxene diagrams (Fitton and Hughes, 1977, Figures 7, 8 and 9). It is suggested here, based on the similarity of K-Ar ages (Chapter 3) and apparent strontium isotopic equilibrium, that the two evolved suites had a common parent. It is possible, but unlikely, that the tristanite-trachyte-trachyphonolite suite originally evolved from the O.L.S. magma, at some elevated pressure, and then subsequently suffered remobilisation (to account for ages equivalent to the Y.L.S.). However initial $^{87}Sr/^{86}Sr$ ratios fall within the narrow limits of the phonolite suite (Figures 4.1.10, 4.1.11 and 4.1.12) and more scatter would be likely if isotopic re-equilibration had occurred. Also, widescale assimilation and mixing would be necessary for this to occur since the suites are relatively similar geochemically. There is no evidence of such widescale assimilation in hand specimen or thin section. In addition there are no correlations of Rb, Sr or SiO_2 with $(^{87}Sr/^{86}Sr)_o$ to suggest isotopic rehomogenisation occurring between the two suites. Instead they all plot as horizontal lines. Figure 4.1.11 shows that the evolved rocks have the same $(^{87}Sr/^{86}Sr)_o$ ratio characteristics as the basanites and nephelinites (excluding P18) and are quite distinct from those of the O.L.S.

When the isotopic evidence presented here is considered together with existing geochemical data it is likely that <u>both</u> the phonolite and trachyphonolite-tristanite suites on Principe evolved from the Y.L.S. basanitic magma. This would be possible under different P-T conditions. Alternatively the tristanite-trachyphonolite evolved suite could have fractionated from a basic magma, not represented by the samples collected, which had a common mantle source with the Younger Lava Series.

4.2 São Tomé

A geochemical investigation of the volcanic rocks of São Tomé is being made by J.G. Fitton and D.J. Hughes. As a result the writer has access to unpublished major and trace element analyses determined by the above workers. A summary of the geology of São Tomé is presented in Chapter 3. Included here under São Tomé are the islets of Rolas and Cabras.

4.2.1 Geochemistry

Basaltic lavas predominate throughout the island of São Tomé and the islet of Rolas. Besides these mafic lavas smaller quantities of trachyte flows and intrusive plugs of phonolite, trachyphonolite and trachyte also occur. In addition smaller inliers of Cretaceous sandstone are present in the N.E. part of the island (Figure 3.1.3). The mafic lavas vary in chemical composition from transitional, hypersthene normative basalts and hawaiites to strongly alkaline nephelinites, leucite basanites and tephrites (Figure 4.2.1). Unlike Principe there is no evidence of magmatic variation correlating with volcanic stratigraphy and there is a complete range of rock types present. The most recent lava flows show the whole range of normative compositions. Geochemically, all the volcanic rocks on São Tomé appear to belong to one cogenetic series. Figure 4.2.2 shows variations of major elements with respect to MgO contents (J.G. Fitton, unpublished data) and it is evident that chemical variation throughout the series may be accounted for by a simple, low pressure fractionation sequence. This is surprising since the mafic rocks involved vary from 13% normative nepheline to 4% normative hypersthene. The chemical variation can be accounted for by a magma differentiation sequence involving

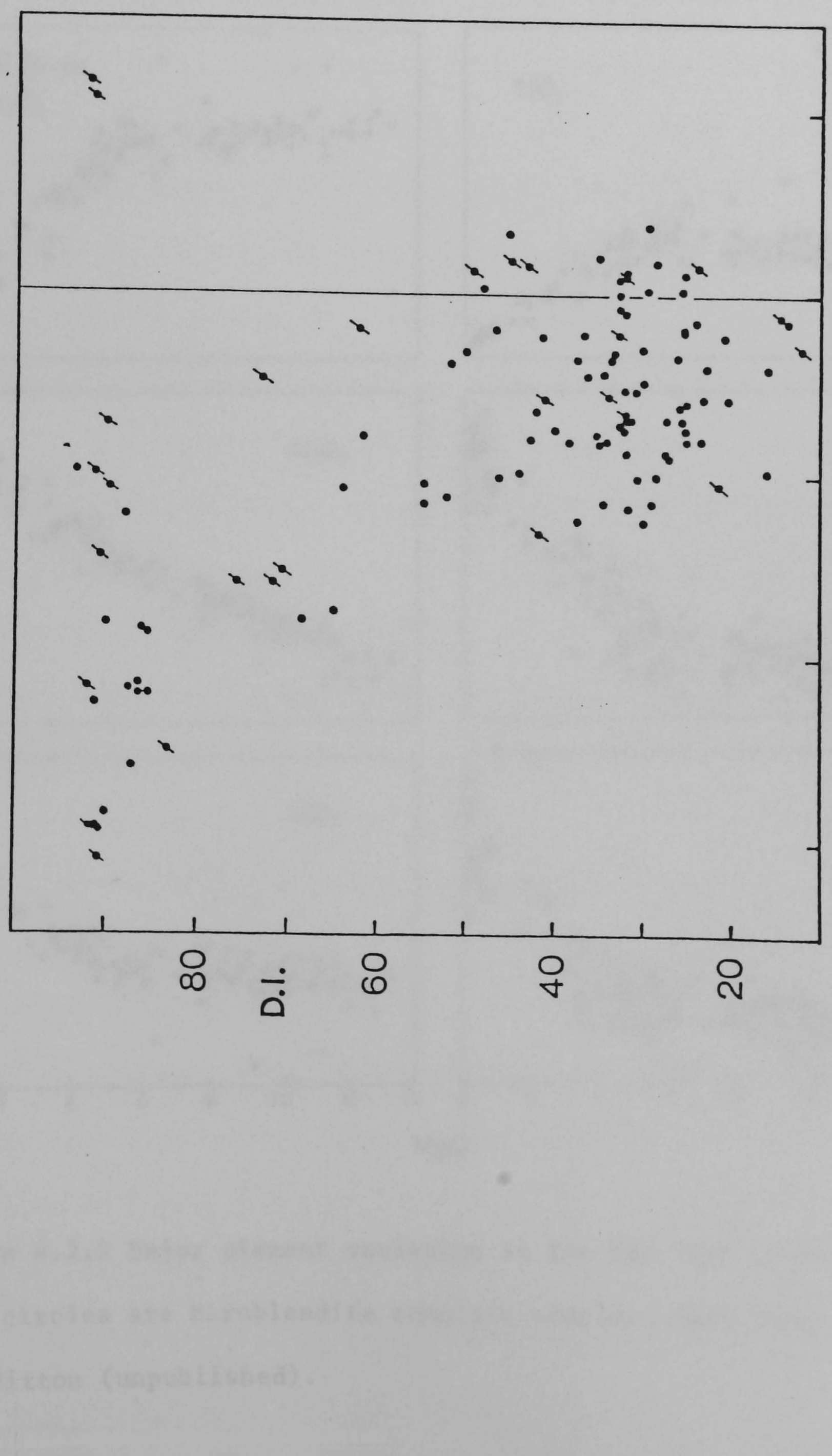


Figure 4.2.1 DifferentiationIndex plotted against degree of silica over- and under-saturation for the São Tomé volcanic rocks. Chemical data from J.G.Fitton(unpublished). / : analysed for $^{87}Sr/^{86}Sr$ ratios.

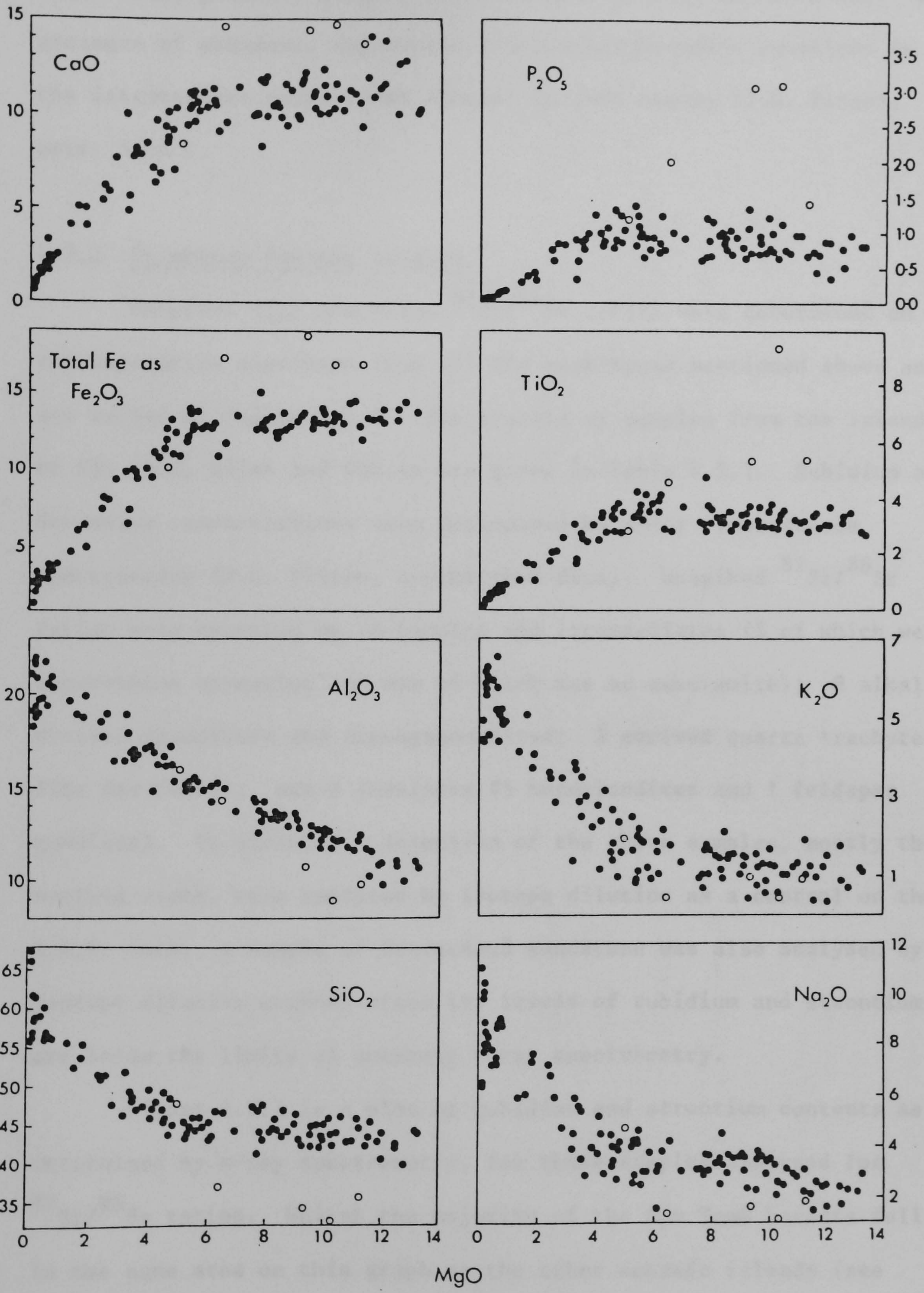


Figure 4.2.2 Major element variation in the São Tomé volcanic rocks. Open circles are hornblendite cumulate nodules. Data from J.G.Fitton (unpublished).

olivine and clinopyroxene precipitation followed by clinopyroxene, hornblende, possibly plagioclase and minor apatite and iron ore. The presence of abundant, apparently cognate hornblendite xenoliths in the intermediate rocks lends support to this theory (J.G. Fitton, pers. comm.).

4.2.2 Strontium Isotope Studies

Unspiked high precision $^{87}Sr/^{86}Sr$ ratios were determined on representative specimens from all the rock-types mentioned above and are marked on Figure 4.2.1. The results of samples from the islands of São Tomé, Rolas and Cabras are given in Table 4.2.1. Rubidium and Strontium concentrations were determined by x-ray fluorescence spectrometry (J.G. Fitton, unpublished data). Unspiked $^{87}Sr/^{86}Sr$ ratios were measured on 18 basalts and intermediates (5 of which were hypersthene normative and one of which was an ankaramite); 8 alkaline evolved phonolites and trachyphonolites; 2 evolved quartz trachytes from Ilha das Cabras; and 6 cumulates (5 hornblendites and 1 feldspar cumulate). In addition a selection of the above samples, mostly the evolved rocks, were analysed by isotope dilution as a control on the X.R.F. data. A sample of Cretaceous sandstone was also analysed by isotope dilution methods since its levels of rubidium and strontium are below the limits of accurate x-ray spectrometry.

Figure 4.2.3 is a plot of rubidium and strontium contents as determined by x-ray spectrometry, for those samples analysed for $^{87}Sr/^{86}Sr$ ratios. Whilst the majority of the São Tomé basalts fall in the same area on this graph as the other oceanic islands (see compilation Figure 4.4.1 of all 4 islands) of the Cameroon Line, two samples (ST12 and ST16) have notably higher Sr contents (1,528 and 1,967 ppm respectively). These rocks, which are as unaltered as the

TABLE 4.2.1

Rb, Sr and $^{87}Sr/^{86}Sr$ Data from São Tomé

Sample No	Rock Type	K-Ar Age (Ma)	Rb (ppm)	Sr (ppm)	$^{87}Sr/^{86}Sr$ ($\pm 2\sigma \times 10^5$)	$^{87}Rb/^{86}Sr$	$(^{87}Sr/^{86}Sr)_o$ [b]
Mafic Lavas							
ST5	Basalt (hy)		20, 16.0[a]	974, 985[a]	0.70360 ± 8	0.0594	0.70360
ST13	Basalt (ne)		18, 16.5[a]	1,181, 1,188[a]	0.70309 ± 10	0.0441	0.70309
ST19	Basanite		60	1,113	0.70289 ± 7	0.1560	0.70288
ST44	Basanite	2.53	40	1,087	0.70331 ± 8	0.1065	0.70330
ST60	Basalt (hy)	0.50	12	711	0.70320 ± 9	0.0488	0.70320
ST69	Basanite		35	954	0.70311 ± 7	0.1062	0.70310
ST92	Basalt (hy)		18	734	0.70307 ± 6	0.0710	0.70307
ST96	Hawaiite (dyke, hy)	6.40	62	1,056	0.70349 ± 5	0.1699	0.70348
ST98	Hawaiite		149	6,121	0.70338 ± 6	0.0704	0.70338
ST107	Hawaiite		62	1,102	0.70305 ± 9	0.1628	0.70304
ST109	Basanite		29	824	0.70299 ± 3	0.1018	0.70299
ST115	Ankaramite		36	425	0.70346 ± 5	0.2451	0.70345
Intermediate Lavas							
ST12	Phonolitic tephrite	126	1,528		0.70334 ± 8	0.2386	0.70333
ST16	Mugearite	100	1,967		0.70346 ± 10	0.1471	0.70345
ST35	Benmoreite	94	892		0.70309 ± 5	0.3049	0.70308
ST100	Benmoreite	139	1,204		0.70315 ± 7	0.3341	0.70313
ST110	Phonolitic tephrite	114	1,128		0.70296 ± 9	0.2924	0.70299
					0.70306 ± 8		
ST117	Phonolitic tephrite	102	1,183		0.70305 ± 6	0.2495	0.70304
Cumulate Nodules							
ST13A	Hornblendite	10	616		0.70343 ± 13	0.0470	0.70343
					0.70343 ± 8		
ST14	Hornblendite	10	1,360		0.70334 ± 10	0.0213	0.70334
ST16A	Hornblendite	13	783		0.70334 ± 7	0.0480	0.70334
ST80	Hornblendite	19	1,055		0.70339 ± 12	0.0521	0.70339
ST117A	Hornblendite	42	1,292		0.70347 ± 8	0.0941	0.70347
ST117B	Feldspar	108	351		0.70291 ± 6	0.8904	0.70286

a: Isotope dilution analyses

b: Calculated using an age of 4 Ma

c: Calculated using K-Ar ages

TABLE 4.2.1 (Continued)

Sample No	Rock Type	K-Ar Age (Ma)	Rb (ppm)	Sr (ppm)	$^{87}Sr/^{86}Sr$ ($\pm 2\sigma \times 10^5$)	$^{87}Rb/^{86}Sr$	$(^{87}Sr/^{86}Sr)_o$ [b]
Evolved Rocks							
ST3	Phonolite		160(157)[a]	221(221)[a]	0.70332 ± 8	2.0950	0.70320
					0.70333 ± 8		
ST10	Phonolite		223	116	0.70339 ± 10	5.8662	0.70306
ST39	Phonolite		178(170)[a]	248(243)[a]	0.70329 ± 5	2.0769	0.70314
					0.70324 ± 12		
ST43	Trachyte	1.32	129	463	0.70302 ± 6	0.8062	0.70301[c]
ST54	Phonolite		213	468	0.70332 ± 5	1.3170	0.70325
ST56	Phonolite		164(157)[a]	1,387(1,383)[a]	0.70328 ± 5	0.3422	0.70326
ST84	Trachyphonolite	7.60	200(192)[a]	19(16.6)[a]	0.70805 ± 9	33.411 [a]	0.70444[c]
					0.70804 ± 6		
ST90	Phonolite	3.26	239(231)[a]	36(33.4)[a]	0.70435 ± 3	20.016 [a]	0.70321
ST57	Qz-trachyte	13.07	124(120)[a]	231(226)[a]	0.70386 ± 8	1.5533	0.7036 [c]
					0.70400 ± 7		
ST58	Qz-trachyte		124(119)[a]	225(219)[a]	0.70386 ± 10	1.5947	0.70366[c]
					0.70291 ± 6		
Cretaceous Sediment							
UBF	Sandstone		2.38[a]	7.63[a]	0.70857 ± 6	0.9044[a]	0.70761 - 0.70697 (75 Ma) (125 Ma)

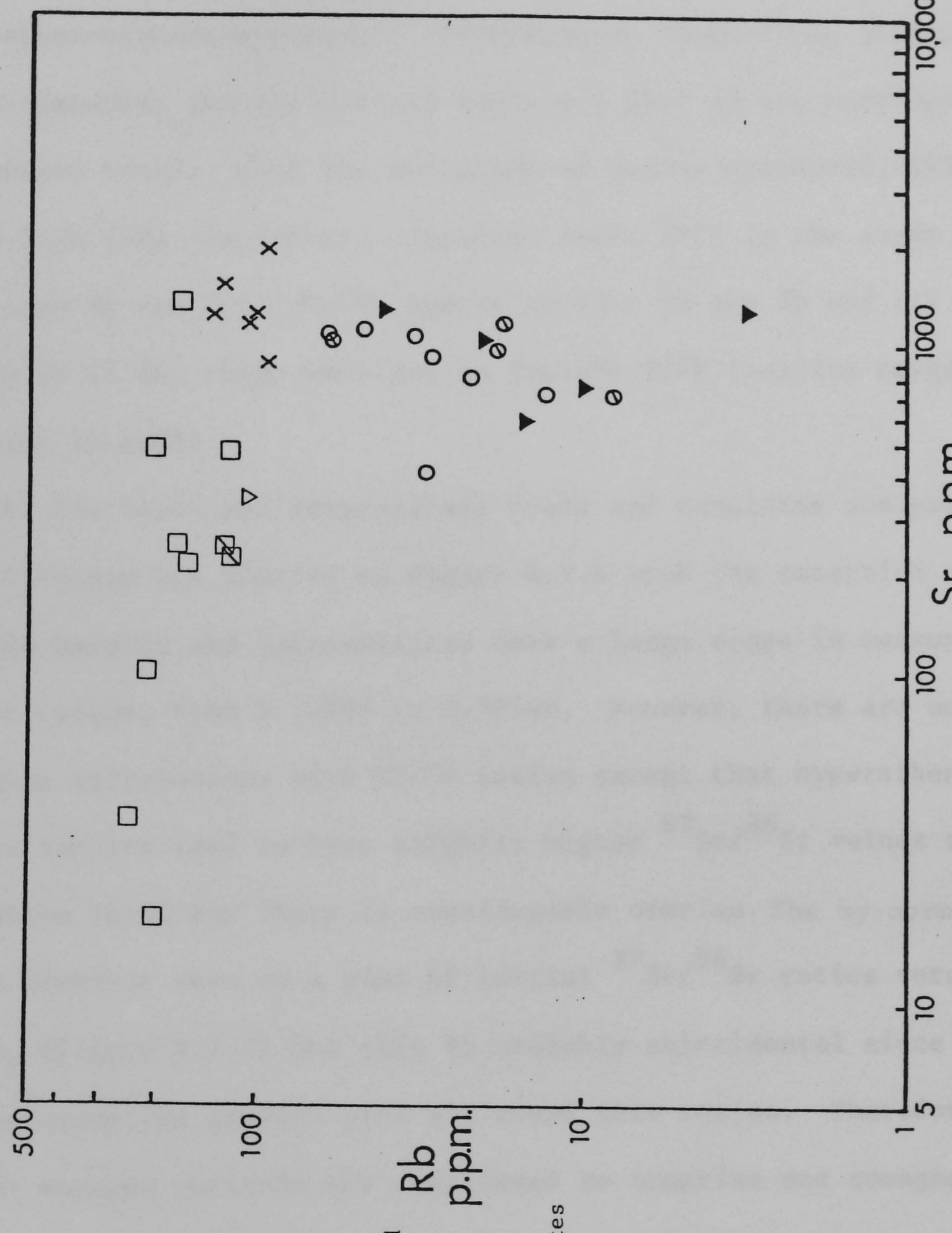


Figure 4.2.3 Rb-Sr plot of São Tomé volcanic rocks

other samples, do not show any strontium rich phase present in thin section. It must therefore be contained within the groundmass. Figure 4.2.3 also shows that Sao Tome possesses rocks with a complete range of Rb/Sr ratios and there is no intermediate gap. The hypersthene- and nepheline-normative basalts, intermediates (tephrites, benmoreites and trachybasalts) and the evolved rocks all plot on one continuous fractionation trend; with the exception of quartz trachytes, ST57 and ST58 from Ilha das Cabras. Basaltic rocks fall in the range of 12 - 149 ppm Rb and 711 - 6,121 ppm Sr or 12 - 62 ppm Rb and 711 - 1,181 ppm Sr if the range were not to include ST98 (zeolite amygdales are present in ST98).

All the basic and intermediate rocks and cumulates analysed for $^{87}Sr/^{86}Sr$ ratios are plotted on Figure 4.2.4 with the exception of ST98. The basalts and intermediates have a large range in measured $^{87}Sr/^{86}Sr$ ratios, from 0.70289 to 0.70360. However, there are no discernable correlations with Rb/Sr ratios except that hypersthene normative samples tend to have slightly higher $^{87}Sr/^{86}Sr$ values than ne normative lavas but there is considerable overlap. The hy-norm samples occupy a distinct area on a plot of initial $^{87}Sr/^{86}Sr$ ratios versus Wt.% SiO_2 (Figure 4.2.7) but this is probably coincidental since nepheline normative samples plot all round this region. Therefore, all the mafic samples analysed are considered to comprise one comagmatic suite. This agrees with the major element geochemical evidence for relating all the rocks on São Tomé (with the exception of the quartz trachytes from Ilheu das Cabras) by a low-pressure fractionation sequence. The comagmatic nature of São Tomé rocks is further supported by the K-Ar age data (Chapter 3) which do not show any systematic

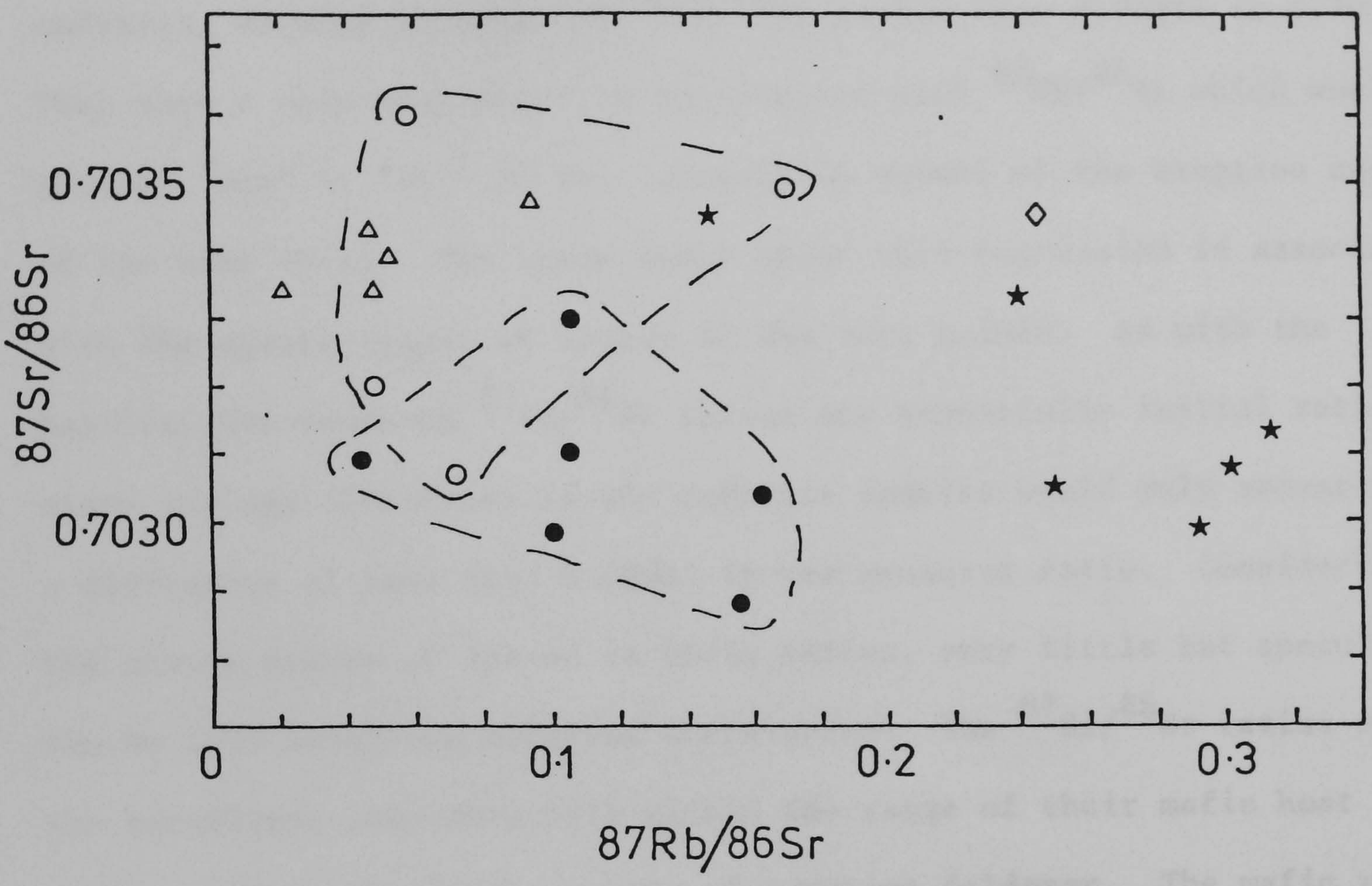


Figure 4.2.4 Strontium isotope ratio plot of São Tomé basic-intermediate lavas.

○ hypersthene-normative basalts
● nepheline-normative basalts and basanites
◇ ankaramite.
★ intermediate lavas
△ hornblendite nodules

differences between the hypersthene and nepheline normative rocks. On the same diagram are shown (Figure 4.2.4) the five hornblendite cumulates (ST13A, ST14, ST16A, ST80 and ST117A). The hornblendites plot on the upper left-hand of the area covered by basalts and intermediates, varying in measured $^{87}Sr/^{86}Sr$ ratios from 0.70334 to 0.70347. They show a very weak positive correlation with $^{87}Rb/^{86}Sr$ which would give an "age" of 111 $\pm$ 52 Ma; grossly in excess of the eruption age of the host rocks. The large error about this regression is associated with the minute degree of spread of the data points. As with the basalts, the measured $^{87}Sr/^{86}Sr$ ratios are essentially initial ratios since any age correction in the cumulate samples would only amount to a difference of less than 0.00001 in the measured ratio. Considering the minute degree of spread in Rb/Sr ratios, very little but speculation can be said about the observed correlation. The $^{87}Sr/^{86}Sr$ ratios of the hornblende cumulates fall within the range of their mafic host rocks, as does the single sample of cumulate feldspar. The mafic rocks and cumulates may therefore be considered cognate, which together with a horizontal trend in Figure 4.2.5 further strengthens the theory that the whole mafic suite is linked by low pressure fractionation.

Evolved rocks (excluding two quartz trachytes, ST57 and ST58) have a range in measured $^{87}Sr/^{86}Sr$ ratios of 0.70302 to 0.70805 (8 samples) with a corresponding range of $^{87}Rb/^{86}Sr$ values of 0.348 to 33.411 (Table 4.2.1). $^{87}Rb/^{86}Sr$ ratios have been calculated from X.R.F. data in all but the most evolved samples which were analysed by isotope dilution methods. Six of these samples plot on an isochron having an age of 3.9 $\pm$ 0.5 Ma (Figure 4.2.6 and Table 4.2.2). This age is consistent with the K-Ar age of 3.26 Ma (see Chapter 3) of one of the

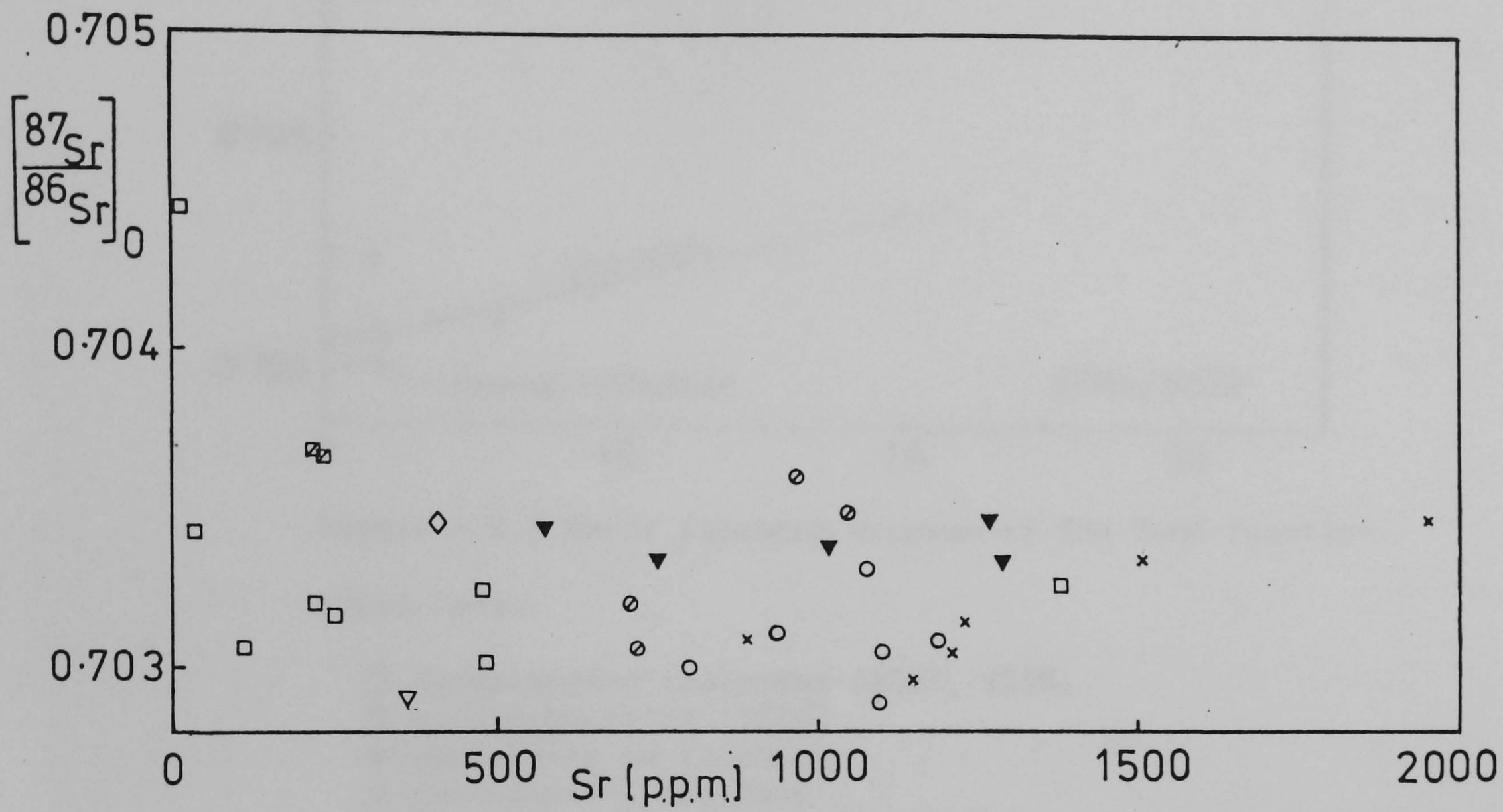


Figure 4.2.5 Initial strontium isotope ratios plotted against Sr contents in São Tomé volcanic rocks. Symbols as for figure 4.2.3 and where ◇ = ankaramite

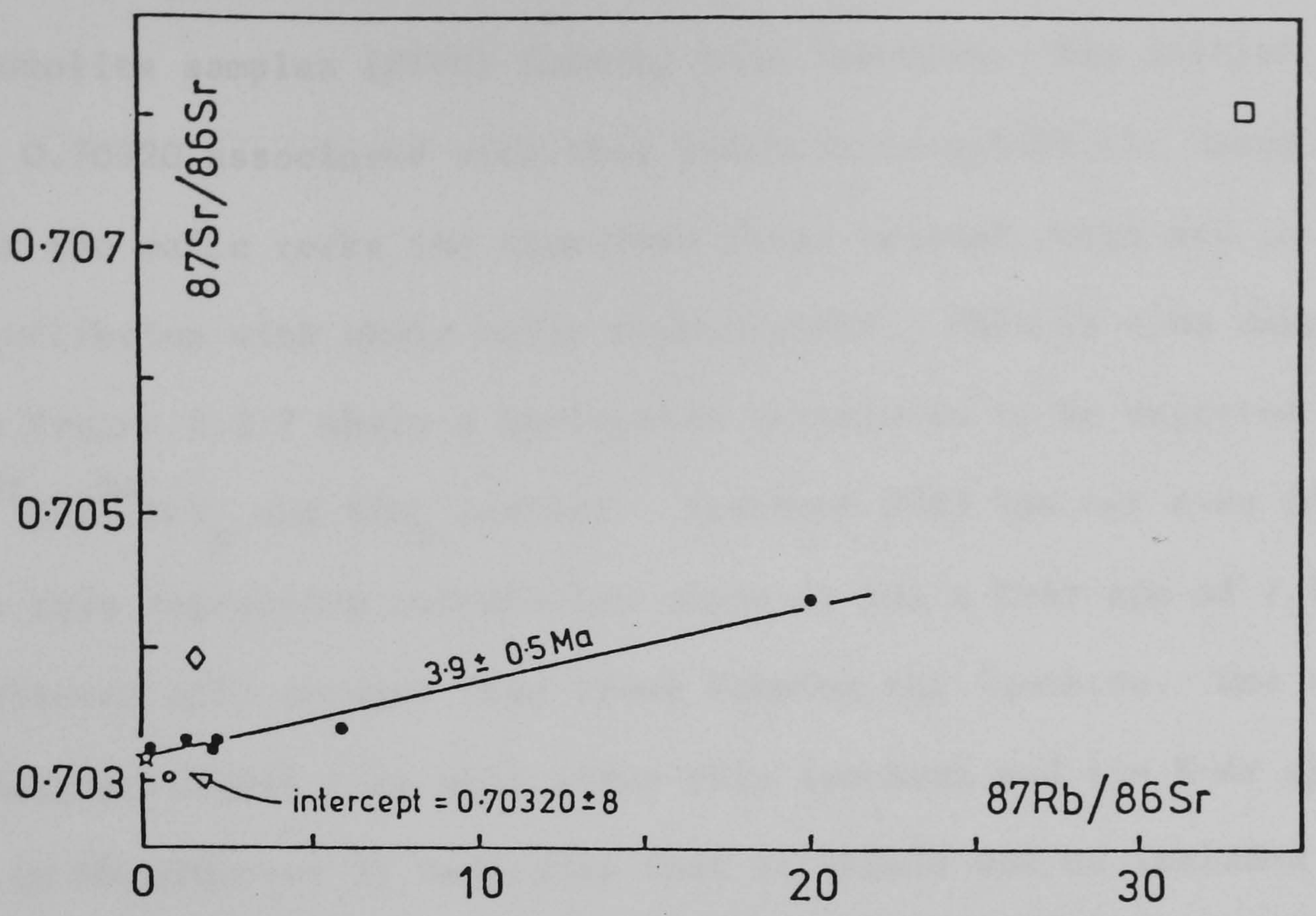


Figure 4.2.6 Rb-Sr isochron diagram of São Tomé fractionated lavas.

◇ Qz-normative trachytes (ST57, ST58)
□ trachyphonolite (ST84)
● phonolites on isochron
○ ne-normative trachyte
✡ average of Sao Tome mafic rocks

TABLE 4.2.2

São Tomé Regression Data - Fractionated Rocks

Slope:	5.585×10^{-5}	Intercept:	0.70320 ± 8 (2σ)
Age:	3.93 ± 0.51 Ma	MSWD:	0.50

No. Samples: 6 (ST3, ST10, ST39, ST54, ST56, ST90)

phonolite samples (ST90) forming this isochron. The initial ratio of 0.70320 associated with this isochron is within the range observed for the mafic rocks and therefore these evolved rocks are in isotopic equilibrium with their mafic counterparts. This is also displayed in Figure 4.2.7 where a horizontal pattern is to be expected between $(^{87}Sr/^{86}Sr)_o$ and SiO_2 content. Trachyte ST43 has not been included in this regression calculation since it has a K-Ar age of 1.32 Ma; substantially younger than those forming the isochron. One trachyte analysed (ST84) lies well above this isochron and its K-Ar age of 7.60 Ma (Chapter 3) indicates that it should not be included in the above regression calculation. However, when the age of 7.60 Ma is used to calculate an initial $^{87}Sr/^{86}Sr$ ratio, it is apparent that the $(^{87}Sr/^{86}Sr)_o$ ratio of 0.70444 is not compatible with the other evolved samples forming the isochron or with ST43. It would need to be 10.3 Ma old to bring the initial ratio within the same field as that of the other evolved samples. However, the figure of 10 Ma is well outside the limits of error on the K-Ar age, which has a relatively high (81%) percentage of radiogenic ^{40}Ar compared to other age determinations on rocks from Sao Tome (see Chapter 3). Prolonged fractionation alone could not generate the value of 0.70444 from an uncontaminated value since it would require an unreasonably long magma chamber residence period of about 3 Ma.

A possible explanation of this anomalous ratio is that isotopic re-equilibration with material rich in radiogenic ^{87}Sr has occurred. Such effects will be most apparent on those rocks having relatively low strontium contents. ST84 has 16.6 ppm Sr which is substantially lower than all the other evolved samples discussed earlier (Figure

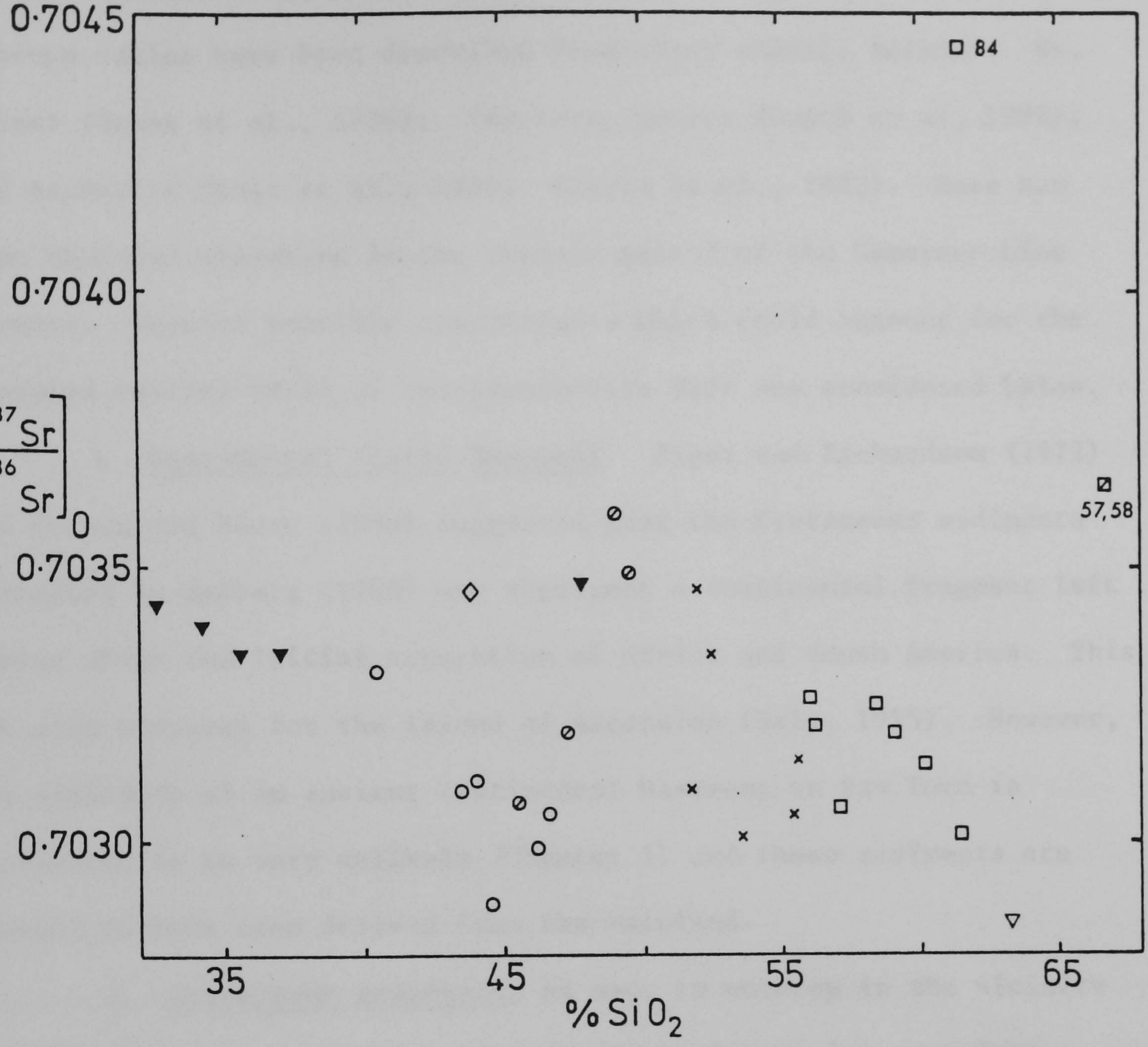


Figure 4.2.7 Initial strontium isotope ratios versus SiO_2 contents in São Tomé volcanic rocks. Symbols as in figure 4.2.3

4.2.5). Similar highly fractionated rocks having disturbed strontium isotope ratios have been described from other oceanic islands: St. Helena (Grant et al., 1976); Terciera, Azores (Dupré et al, 1982); and Ascension (Gast et al., 1964; Harris et al., 1982). None has been observed elsewhere in the oceanic sector of the Cameroon Line however. Several possible contaminants which could account for the elevated initial ratio of trachyphonolite ST84 are considered below.

1. Continental Sialic Basement Piper and Richardson (1972) and Cornen and Maury (1980) suggested that the Cretaceous sediments described by Hedberg (1968) may represent a continental fragment left behind after the initial separation of Africa and South America. This was also proposed for the island of Ascension (Daly, 1925). However, the existence of an ancient continental basement on Sao Tome is considered to be very unlikely (Chapter 3) and these sediments are thought to have been derived from the mainland.

2. Cretaceous sediments, as seen to outcrop in the vicinity of ST84 (Figure 3.1.3): By using the following mixing equation (Moorbath et al., 1981)

$$f = S_B(a_B - a_H) \Big/ S_c(a_H - a_c) + S_B(a_B - a_H)$$

where: f is the fraction of hybrid H contributed by contaminant c,

B refers to the uncontaminated end member,

S is the strontium concentration expressed as ^{86}Sr (in ppm),

a is the $^{87}Sr/^{86}Sr$ ratio at the time of contamination.

it is found that some 46% of the Cretaceous sediment (UBF), which has a very low Sr content (Table 4.2.1), would be required to change the $^{87}Sr/^{86}Sr$ ratio from 0.70320 (uncontaminated value, derived from the

mean of São Tomé basalts) to 0.70444 if the assimilation occurred after magmatic fractionation. Even larger amounts would be necessary if contamination of the basaltic magma (with 968 ppm Sr, São Tomé basalt average) occurred before fractionation (98% UBF required), or at some intermediate stage in the magmatic evolution (e.g. 100 ppm Sr would necessitate 84% contamination). Any one of these 3 percentages of UBF assimilation is untenable because major changes in the trachyphonolite's geochemistry and petrographic evidence of such assimilation would be apparent. The geochemistry of this sample may be entirely accounted for by extreme low pressure fractionation of the mafic and intermediate volcanics occurring on Sao Tome.

3. Seawater or seawater contaminated basalts Seawater, which has an $^{87}Sr/^{86}Sr$ ratio of 0.7091 (present day value, Peterman et al., 1970; Veizer and Compston, 1974) and a Sr content of 8 ppm (Turekian, 1964; Faure et al., 1967) is hence very similar to the UBF sandstone discussed above. Equally hugh proportions of seawater would therefore be required to disturb the strontium isotopic composition of ST84. If such a process occurred with the required extreme water/rock ratios a change would be recorded in the Pb isotopes of the sample since Pb isotopic ratios in seawater are distinct from those of uncontaminated magmatic rocks (Sun and Hanson, 1975a; Leeman, 1977). Although such data are unavailable for São Tomé, $^{208}Pb/^{204}Pb$, $^{207}Pb/^{204}Pb$ and $^{206}Pb/^{204}Pb$ ratios in similar trachytes (geochemically and with similar strontium isotope ratios) from Ascension do not show disturbed values (Gast et al., 1964; Harris et al., 1982) and it is concluded that seawater contamination alone is very unlikely to produce the observed data. By the same argument, assimilation of seawater-contaminated lavas in the volcanic pile (as suggested by O'Hara, 1980; O'Hara and Matthews,

1981) is untenable (as discussed in 4.1.1).

4. Oceanic sediments With respect of the remaining possible contaminant, no data on the isotopic composition or Sr content of such sediments near São Tomé are available. However, Turekian (1964) analysed 87 Atlantic Ocean sediments which have an average of 1,316 ppm Sr and Dasch (1969) reported such sediments near Ascension as having an $^{87}Sr/^{86}Sr$ ratio of 0.7213. By employing the equation above, 0.09% oceanic sediment assimilation by silicic magma would account for the elevated value of ST84. Such a low percentage of contaminant would not affect the magma's geochemistry and as discussed by Harris et al., (1982) would be unlikely to change the Pb isotopic composition. If however, contamination occurred before fractionation, then 5.1% of oceanic sediment would be required which would result in a change of the Pb isotopic composition from an assumed uncontaminated $^{206}Pb/^{204}Pb$ value of 19.53 and Pb content of 7.2 ppm ($^{206}Pb/^{204}Pb$ typical of oceanic basalts, e.g. Sun, 1980; and of Manengouba, C. Hirst, unpublished data; Pb content = São Tomé basalt mean) to a $^{206}Pb/^{204}Pb$ ratio of 19.24 and Pb content of 19 ppm (concentration present in ST84). For the purpose of this calculation a $^{206}Pb/^{204}Pb$ ratio of 18.8 (Stacey and Kramers, 1975; Sun, 1980) and a Pb concentration of 100 ppm (Harris et al, 1982) has been assumed for the oceanic sediment. By the same approach 0.09% contamination of the silicic magma would give a hybrid $^{206}Pb/^{204}Pb$ value of 19.526, virtually identical to the uncontaminated value.

Two quartz-normative trachytes, from Ilha das Cabras (Figure 3.1.3), also plot outwith the isochron in Figure 4.2.6. The initial ratio for these rocks is 0.70365, based on K-Ar age determinations

giving a mean of 13.07 Ma (Chapter 3). Geochemically, ST57 and ST58 are quite distinct from the nepheline-normative evolved rocks. Figure 4.2.1 shows their contrasting character by plotting to the right of the critical plane of undersaturation and illustrates that they cannot be related by low pressure fractionation to the mafic rocks from São Tomé. These rocks are also Rb and Sr poor (Figure 4.2.3 and Table 4.2.1), and SiO_2 enriched (Figure 4.2.7) compared to the other evolved rocks. If a process similar to that proposed above for ST84 occurred then some 0.43% of oceanic sediment would be required to elevate the $^{87}Sr/^{86}Sr$ ratio of the silicic magma from 0.70320 to 0.70365.

It is concluded that contamination of the already fractionated silicic magmas occurred with a material containing elevated $^{87}Sr/^{86}Sr$ ratios and high Sr contents. The most likely contaminant is considered to be oceanic sediment although isotopic re-equilibration may well be aided by the hydrothermal flux of seawater. The observation that only a few of the evolved rocks have elevated $^{87}Sr/^{86}Sr$ ratios would imply that the postulated isotopic re-equilibration process was of a localized nature. $\delta^{18}O$ analyses of the fractionated rocks from São Tomé would give further important information since the $\delta^{18}O$ of pelagic sediments (+19 to + 25‰ , Savin and Epstein, 1970) would give rise to hybrids with elevated $\delta^{18}O$ ratios relative to the uncontaminated magma ($\delta^{18}O$ = 5.4 to 6.3‰ , Sheppard, 1981) and would also indicate whether meteoric waters played a part in the geochemical history of these rocks (as suggested for St. Helena by Grant et al., 1976).

4.3 Bioko and Pagalu

The only samples available for analysis were cores collected by Piper and Richardson (1972) for palaeomagnetic studies. Most of

these are rather altered. However five were selected for Rb-Sr isotopic analysis from both Bioko and Pagalu on the basis of freshness in thin section (kindly made available by M.J. Norry). Sample numbers follow those of Piper and Richardson (1972). Analyses were performed on a V.G. Micromass MM30B mass-spectrometer at East Kilbride. Direct comparison with data received from the AEI MS12 is possible since values for the standard NBS 987 obtained from both instruments are identical within error limits (Appendix A1).

A summary of what little is known about these islands is given in Chapter 3. Since 1968 they have been inaccessible due to dictatorial regimes and further sample collection was therefore impossible. However the recent publication of Cornen and Maury (1980) indicates this is no longer the case, at least for Pagalu

4.3.1 Bioko

The rocks on Bioko are olivine basalts and hawaiites, often approaching picrites, oceanites or ankaramites in composition (Fuster Casas, 1956). 16 basalt analyses of Boese (1912), Fuster Casas (1950, 1954); Mitchell-Thomé (1970) illustrates that MgO content varies from 5.53 to 18.50 weight percent. From these analyses (to be found in Mitchell-Thomé, 1970, p.153) it is apparent that the volcanics on Bioko vary from moderately alkaline to quite strongly hypersthene normative in character. Normative calculations (assuming an iron oxidation ratio of 0.3, Table 4.3.1) illustrate that they vary continuously from 7.1% nepheline-normative to 21.2% hypersthene-normative. Figure 4.3.1 illustrates their chemical character as expressed by normative Ne and 'q' versus differentiation index. The samples display a large spread about the critical plane of undersaturation but with only a small variation in D.I. from 18 to 45. J.G. Fitton (pers. comm., 1982) has

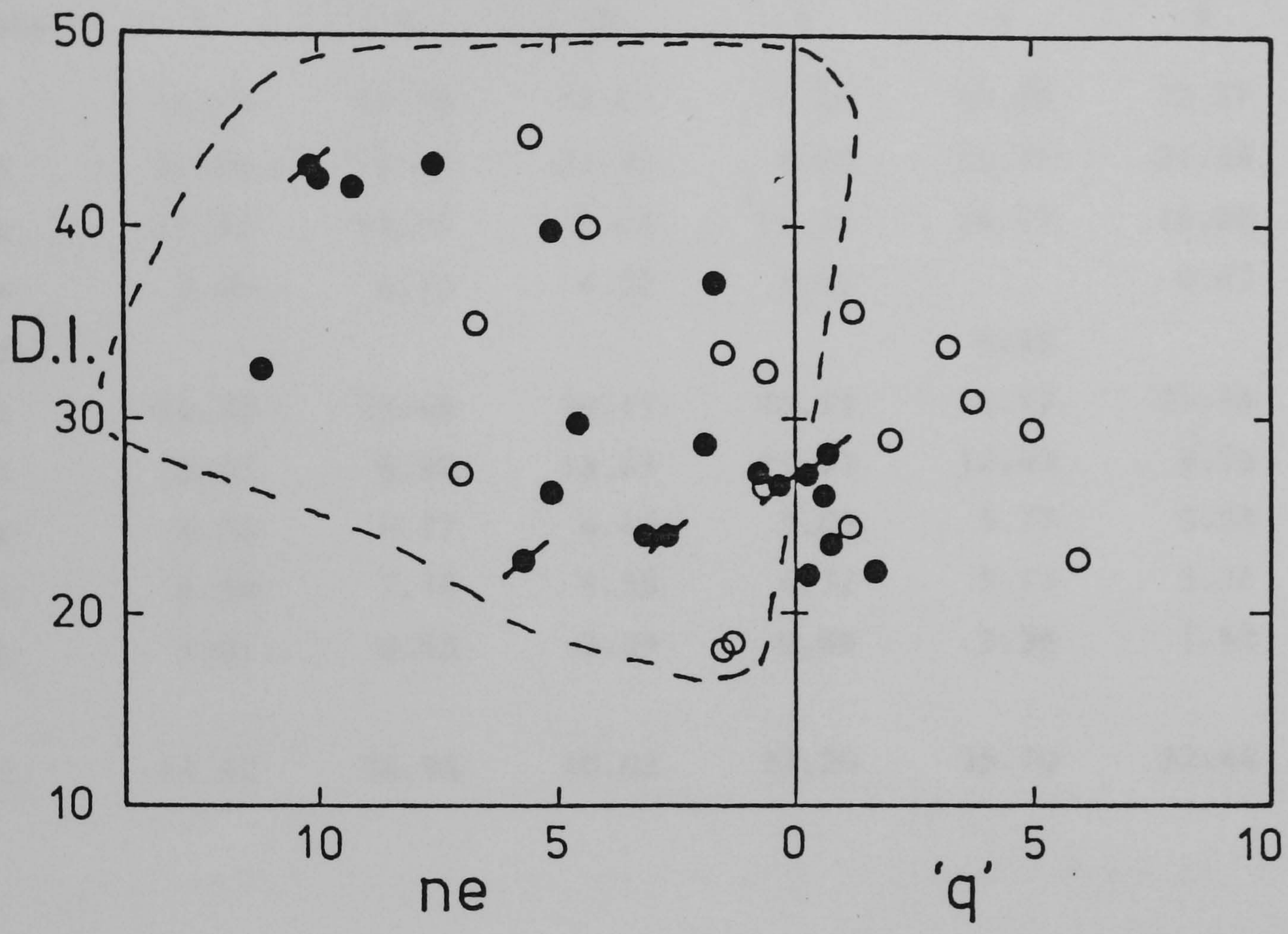


Figure 4.3.1 Differentiation index plotted against degree of silica over- and under-saturation for Bioko volcanic rocks

○ Analyses from Boese (1912) and Fuster Casas (1950,1954)

● Analyses of Piper and Richardson's (1972) cores (analyst: J.G. Fitton).

Core samples analysed for $^{87}Sr/^{86}Sr$ ratios

Field of Mt Cameroon lavas

TABLE 4.3.1

Recalculated C.I.P.W. Norms of Fernando Poo Chemical Analyses

(after the data of Boese, 1912; Fuster Casas, 1950, 1954; described in Mitchell Thome, 1970).

Sample	1	2	3	4	5	6
or	16.53	11.32	12.45	11.26	10.99	10.27
ab	22.60	16.87	23.25	8.93	24.71	21.55
an	12.57	14.34	8.05	16.21	14.99	16.08
ne	5.49	6.75	4.32	7.01		0.62
hy					4.48	
di	14.53	29.44	20.11	31.59	18.12	29.46
ol	12.42	6.92	15.43	14.93	12.40	9.55
mt	6.35	6.77	6.46	5.06	5.77	5.53
il	6.50	7.18	6.55	4.32	5.17	5.31
ap	3.01	0.45	3.39	0.69	3.36	1.62
D.I.	44.62	34.94	40.02	27.20	35.70	32.44

Sample	7	8	9	10	11	12	13	14	15	16
or	14.38	9.09	6.10	4.86	8.67	6.56	8.14	6.82	4.65	9.82
ab	17.56	24.67	24.84	24.02	13.99	17.85	17.68	9.99	13.91	19.62
an	17.02	12.81	14.20	18.11	24.22	15.48	17.09	11.35	10.00	23.03
ne	1.50						0.67	1.49		
hy		11.45	13.61	7.03	21.21	3.87			4.29	18.10
di	22.49	13.25	20.63	18.71	12.93	28.07	27.44	38.40	28.31	16.64
ol	14.65	14.06	7.80	16.01	6.09	17.02	17.02	21.28	27.58	0.64
mt	5.84	6.20	5.98	5.62	6.64	5.67	5.20	5.29	5.57	5.29
il	4.79	5.83	4.68	4.34	5.71	4.93	6.24	4.38	4.35	5.59
ap	1.77	2.64	2.16	1.31	0.54	0.55	0.51	1.00	1.34	1.26
D.I.	33.44	33.77	30.93	28.88	22.66	24.41	26.49	18.29	18.56	29.44

Norms recalculated on basis of $Fe_2O_3/(FeO + Fe_2O_3) = 0.3$

Abbreviations as for Table B3

recently analysed the Piper and Richardson (1972) palaeomagnetic core samples for major and trace element concentrations by X.R.F. spectrometry. These samples cover essentially the same range of compositions (Figure 4.3.1) as those described above but with an inclination to being more undersaturated. Unlike the other oceanic islands in the Gulf of Guinea, fractionated rocks are unknown on Bioko. It's age is probably no older than early-mid Pliocene (see Chapter 3) and numerous recent cinder cones occur on the island (Figure 3.1.5). This figure shows the location of samples with respect to the position of the three volcanoes. Pico de Santa Isabel is a well-shaped volcanic cone and the two calderas in the south straddle the continental rise.

Five samples have been analysed by precise Sr isotope dilution methods (Table 4.3.2); three from Pico de Santa Isabel and two from Pico Baio. The basalts and hawaiite range in measured $^{87}Sr/^{86}Sr$ from 0.70292 to 0.70337 and have a mean value of 0.70322 (0.70330 if FP38 is omitted). Rb and Sr contents are typical of oceanic island alkali basalts, plotting in a similar position to Principe, São Tomé and Pagalu (Figure 4.4.1). Figure 4.3.2 shows the spread of the $^{87}Sr/^{86}Sr$ data relative to that of $^{87}Rb/^{86}Sr$. The strontium isotope ratios may be considered initial since the island is no older than early Pliocene (Chapter 3; Hedberg, 1968) and because $^{87}Rb/^{86}Sr$ ratios are low. This diagram illustrates that 4 of the Bioko samples fall within a horizontal field having a restricted range of $^{87}Sr/^{86}Sr$ ratios from 0.70324 to 0.70337 which is virtually identical to that of nearby Mt. Cameroon. However, the fifth sample (FP38) analysed gave a Sr isotopic composition of 0.70292, 4×10^{-4} lower than the other basalts. This difference is much larger than the 2σ analytical

TABLE 4.3.2

Geochemical and $^{87}Sr/^{86}Sr$ data from Bioko (Fernando Poo)

Sample	Rock Type	Rb[a] (ppm)	Sr[a] (ppm)	$^{87}Sr/^{86}Sr$ ($\pm 2\sigma \times 10^5$)	$^{87}Rb/^{86}Sr$	MgO[a] (Wt %)	D.I.	ne or hy norm Wt %
FP 1	Basalt	27	728	0.70329 ± 3	0.1073	8.06	29	2.2 hy
FP23	Basalt	24	681	0.70324 ± 6	0.1020	6.29	25	2.7 ne
FP32	Hawaiite	61	1,195	0.70337 ± 3	0.1477	4.26	43	10.0 ne
FP38	Basalt	23	642	0.70292 ± 7	0.1037	10.85	26	0.7 ne
FP44	Basalt	33	815	0.70328 ± 7	0.1172	10.80	24	5.7 ne

a: Analyst: J.G. Fitton

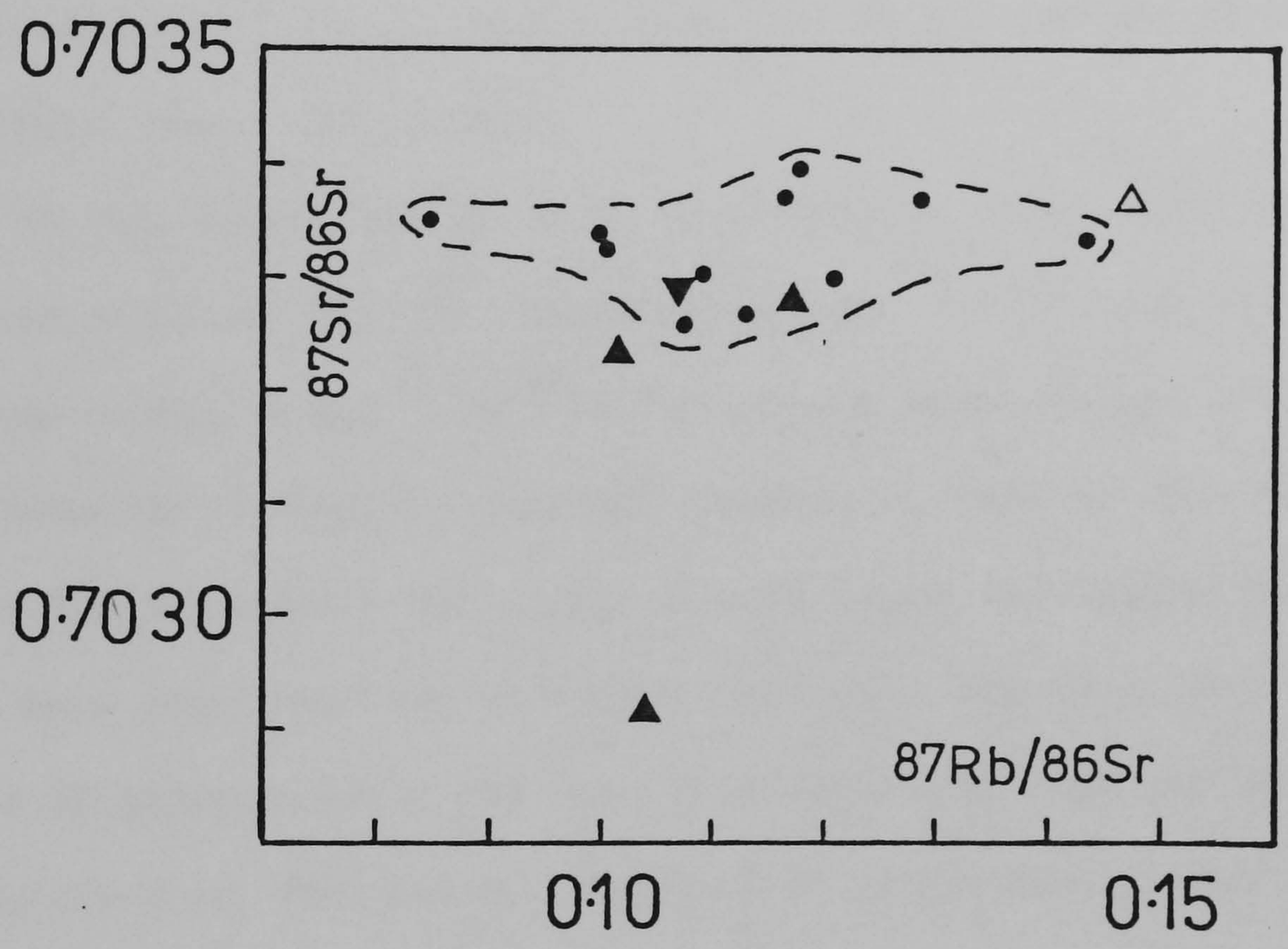


Figure 4.3.2 Strontium isotope ratio plot of Bioko volcanic rocks

▲ ne-normative basalts

▼ hy-normative basalts

△ hawaiite

● Mt-Cameroon

precision of $\pm$ 5 x 10^{-5}. Only the Principe Y.L.S. in the oceanic sector of the Cameroon Line shows such low values. Unlike the Principe Y.L.S. this sample is geochemically indistinguishable from the other Bioko samples (J.G. Fitton, unpublished data) and has similar Rb and Sr contents. MgO (Table 4.3.2) is somewhat higher than the Bioko average (8.53%, 23 samples) but this is most likely to be a result of cumulus olivine enrichment. FP38 was sampled from the northern volcano (Santa Isabel) but then so were FP1 and FP44 which are isotopically identical to those samples from one of the two southern volcanoes (Pico Biao; FP23, FP32).

It is concluded that overall, although the Bioko lavas are slightly less alkaline than Mt. Cameroon (Figure 4.3.1) they probably have the same source since $^{87}Sr/^{86}Sr$ ratios are very similar (although Bioko has lower Sr contents). Further support to this is that they both show a similar restricted range of rock types (no highly fractionated rocks have been recorded on either volcano), and that they have been active at approximately the same time (the last reported Bioko eruption occurred in 1898 and Mt. Cameroon is currently active) with the larger volcano, Mt. Cameroon being slightly older. FP38 may indicate that the mantle is isotopically heterogeneous but more comprehensive studies (sampling, geological mapping and geochemical analyses) are necessary before further discussion can be made.

4.3.2 Pagalu

The island of Pagalu represents the top of a strato-volcano built of pyroclastics, basanites and alkali olivine basalts, often containing peridotite nodules (Piper and Richardson, 1972; Cornen and Maury, 1980). Basalts from this island are perhaps the most

basic of the trend (Fuster Casas, 1954) with the common occurrence of picritic basalt, oceanite, limburgite and ankaramite. Four mafic rocks analysed by Tyrrell (1934) and Fuster Casas (1954) and five analysed by Cornen and Maury (1980) have MgO contents ranging from 11.22 to 16.52 weight percent. The first four samples mentioned above come from the same area as those collected by Piper and Richardson (1972), being from near San Antonio. The five mafic lavas analysed by Cornen and Maury (op. cit.) are basanites. Norms calculated by the author on these nine analyses (Figure 4.3.3, Table 4.3.3) indicate their strong alkaline nature with normative ne varying from 5.6 to 11.7%. This figure also illustrates the pronounced Daly gap between a D.I. of 35 and 70. The normative compositions of a potassic "hawaiite", a tristanite (benmoreite) and three quartz-trachytes from Cornen and Maury (op. cit.) were also calculated (Table 4.3.3) and plotted on Figure 4.3.3. The sample they termed a hawaiite is a basalt in most currently employed classification schemes, including that employed in this thesis (Appendix C). The basic lavas are similar to those of Principe but the evolved rocks are quartz-normative trachytes instead of phonolites and are distinctly potassic with K_2O/Na_2O ratios close to unity. These trachytes contain phlogopite and amphibole, and Cornen and Maury (op. cit.) account for their production by intense kaersutitic amphibole fractionation (such amphibole is present in the "hawaiite" and tristanite). The total observed variations in chemistry are compatible with olivine and clinopyroxene fractionation followed by clinopyroxene, amphibole, Fe-Ti oxides and apatite, followed by K-feldspar. These investigations suggested fractionation occurred under conditions of high water pressure (1-3 Kb H_2O) and high $f O_2$ (based on magnetite-ilmenite geothermometry and the presence of andesine-oligoclase feldspars).

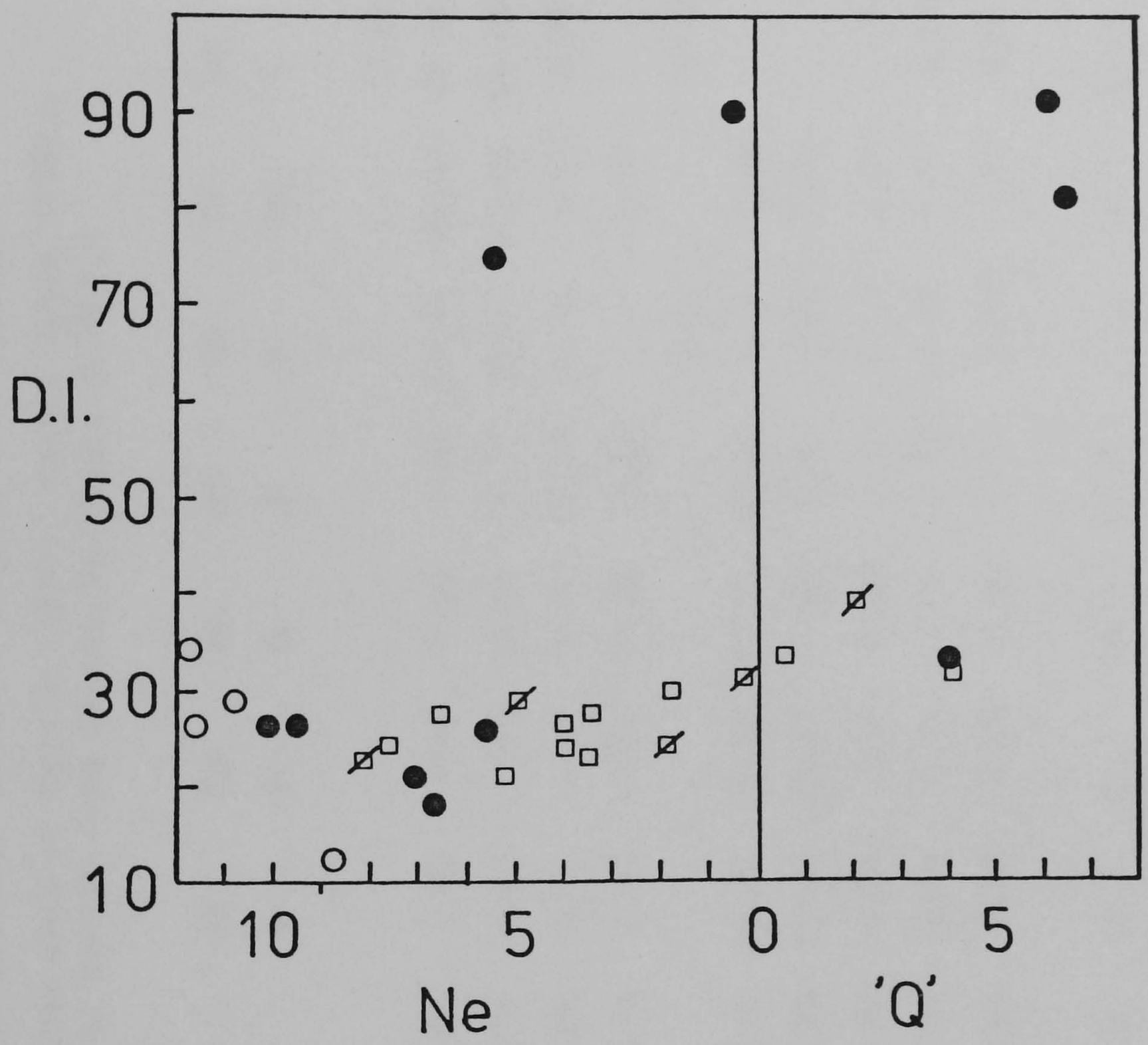


Figure 4.3.3 Differentiation index plotted against degree of silica over- and under-saturation for Pagalu volcanic rocks

○ Analysed by Tyrell (1934) and Fuster Casas (1954)

● Analysed by Cornen and Maury (1980)

□ Analyses of Piper and Richardson's (1972) cores (analyst : J.G. Fitton)

⊠ Core samples analysed for $^{87}Sr/^{86}Sr$ ratios

TABLE 4.3.3

Recalculated C.I.P.W. Norms of Pagalu Lava Samples

(Samples 1 to 4 from data of Tyrell (1934), Fuster Casas (1954);
Samples A1 to A10 from Cornen and Maury (1980).)

	1	2	3	4	A1	A2	A3	A4	A5	A6	A7	A8	A9	A10
	P	P	O	O	B	B	B	B	B	H	Bn	T	T	T
qz												5.51		5.77
or	9.47	9.71	10.88	6.28	8.04	7.68	7.98	7.80	7.21	12.35	29.37	29.07	35.04	33.98
ab	2.23	3.97	4.48	1.13	2.79	6.65	7.01	8.74	13.11	20.73	40.16	46.62	54.38	50.94
an	12.21	7.19	7.69	22.36	8.86	15.71	8.68	13.78	15.75	21.66	6.18	9.95	2.42	
ne	11.54	10.69	11.76	8.57	6.74	7.03	10.69	9.48	5.59		5.29		0.43	
hy										14.23		3.72		1.56
di	30.59	35.83	36.05	17.88	40.14	28.66	25.92	27.95	26.21	13.57	8.48		4.14	
ol	21.08	19.86	15.07	29.20	20.79	19.05	25.91	17.54	17.01	1.22	2.51		0.59	
mt	5.76	6.12	6.64	5.75	4.83	5.34	5.51	5.44	5.21	5.15	2.56	1.34	1.60	0.94
il	6.34	6.24	7.03	7.11	4.88	6.04	5.34	5.34	5.28	7.39	2.77	1.46	1.35	0.82
ap	0.79	0.41	0.41	1.70	1.44	1.83	2.20	2.46	1.72	1.95	1.27	0.32	0.37	0.86
co														3.04
D.I.	23.2	24.4	27.1	16.0	17.6	21.4	25.7	26.0	25.9	33.1	74.8	81.2	89.4	90.7

Calculated on the basis $Fe_2O_3/(Fe_2O_3 + FeO) = 0.3$

P: Picritic basalt; O: Oceanite; B: Basanite; H: Hawaiite; Bn: Benmoreite; T: Trachyte

n.b: These are names employed by original investigators

Abbreviations as for Table B3

Recently, J.G. Fitton (pers. comm. 1982) has completed X.R.F. analysis of 16 palaeomagnetic cores sampled by Piper and Richardson (1972). These data are distinctly comparable to those of Cornen and Maury (op. cit.) and are also plotted on Figure 4.3.3.

The oldest explosed volcanics have been dated at 18.4 Ma and the most recent flow on the N.W. coast at 2.6 Ma (both dates from Piper and Richardson, 1972). Three samples from the Piper and Richardson collection (AN3, AN8, AN20) were analysed for $^{87}Sr/^{86}Sr$ ratios from the older volcanic succession, and two (AN12, AN13) from the most recent lava flows. Figure 3.1.6 shows the sample locations in relation to the geology and Figure 4.3.3 indicates that the samples selected for isotopic analysis cover the chemical spectrum of the mafic rocks. Rb-Sr concentrations (Figure 4.4.1, Table 4.3.4) have a restricted range of 709-841 ppm Sr and 24-43 ppm Rb. Initial $^{87}Sr/^{86}Sr$ ratios vary from 0.70335 to 0.70358 for the older basalts and from 0.70316 to 0.70330 for the younger lavas (corrected to 18.4 Ma) (Table 4.3.4). The mean of all values is 0.70335 $\pm$ 30 (2σ about the mean). Figure 4.3.4 shows that the spread of these data against $^{87}Rb/^{86}Sr$ does not demonstrate the existence of any correlation. The field occupied by the Mt. Cameroon samples is also indicated for comparison. Thus overall the 5 points fall within the range of the other volcanoes. However, the two samples falling outwith the field defined by the Mt. Cameroon samples are chemically distinct from each other and from the 3 remaining samples in that the basalt having the highest $^{87}Sr/^{86}Sr$ ratio (AN8, 0.70358) is the only strongly hypersthene normative sample (6.8%) and the rock with the lowest ratio (AN13,

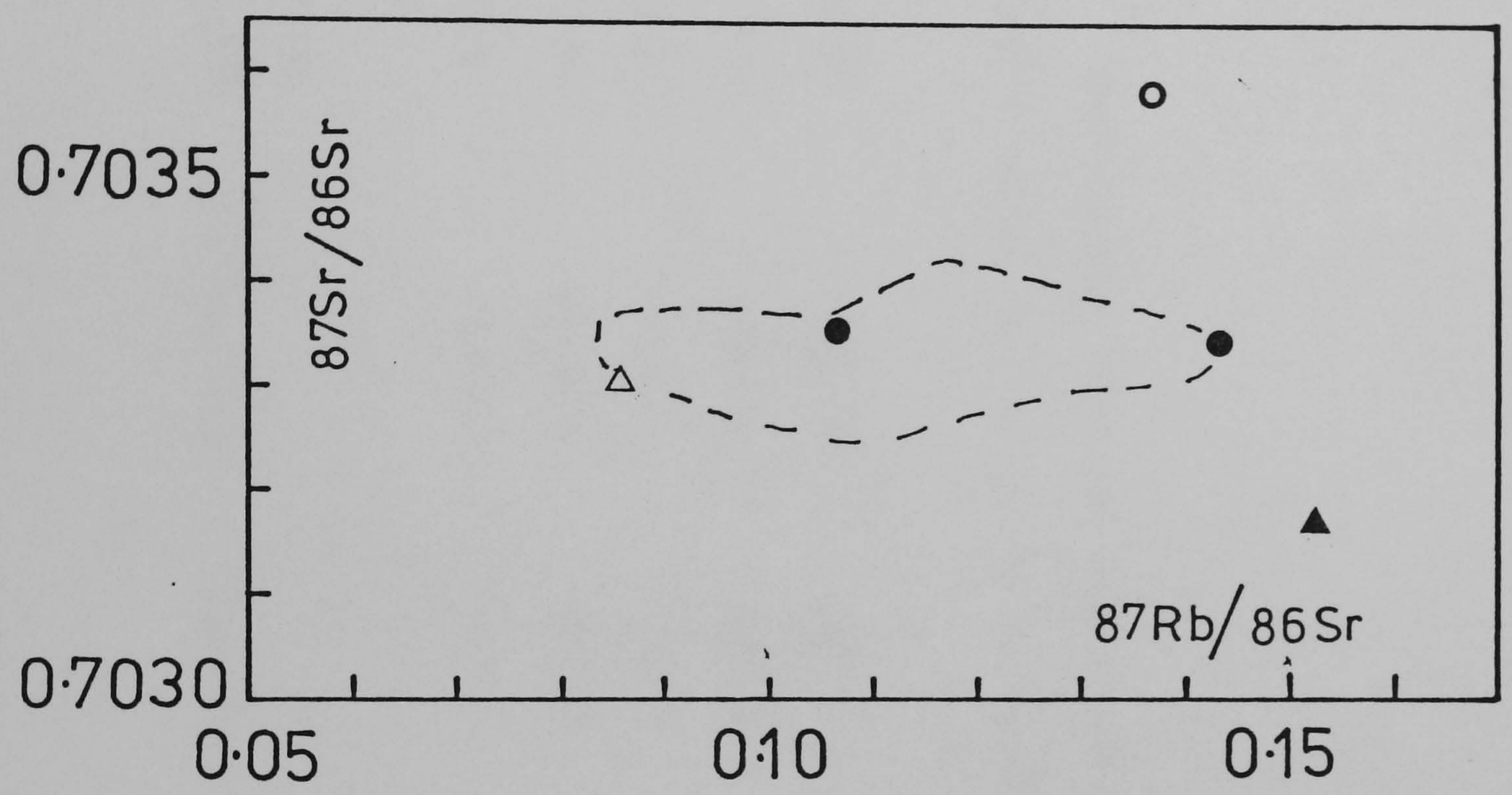


Figure 4.3.4 Strontium isotope ratio plot of Pagalu volcanic rocks

△ younger lava basalt

▲ younger lava basanite

● older lava ne-normative basalt

○ older lava hy-normative basalt

<⁻⁻> field of Mt. Cameroon

TABLE 4.3.4

Geochemical and $^{87}Sr/^{86}Sr$ Data from Pagalu (Annobon)

Sample	Rock Type	Rb^b (ppm)	Sr^b (ppm)	$^{87}Sr/^{86}Sr$ ($\pm 2\sigma \times 10^5$)	$^{87}Rb/^{86}Sr$	$(^{87}Sr/^{86}Sr)_o$ [a]	MgO^b (Wt %)	D.I.	Norm. (Wt %)
AN 3	Basalt	35	709	0.70337 ± 5	0.1428	0.70334	8.48	31	0.5 ne
AN 8	Basalt	36	760	0.70362 ± 4	0.1371	0.70358	4.55	39	6.8 hy
AN12	Basalt	24	814	0.70330 ± 6	0.0853	0.70330	12.85	24	1.9 ne
AN13	Basanite	43	816	0.70316 ± 4	0.1525	0.70316	14.81	23	8.2 ne
AN20	Basalt	31	841	0.70338 ± 4	0.1066	0.70335	10.63	27	5.2 ne

a: Initial ratios for AN3, AN8, AN20, calculated assuming an age of 18.4 Ma (Piper and Richardson, 1972). AN12, AN13 measured ratios are considered initial since they are from recent flows.

b: Analyst: J.G. Fitton

0.70316) is a much more alkaline basanite (8.2% ne normative). This is a very similar pattern to that observed on Principe (Dunlop and Fitton, 1979) where the more alkaline rocks have consistently lower $^{87}Sr/^{86}Sr$ ratios.

Because of their very primitive nature (the mean Mg number of the core samples is 66), the presence of ultramafic nodules, and mantle D values in amphibole ($\delta D = -75‰$ vs. S.M.O.W., S.M.F. Sheppard, unpublished data), these lavas are very likely to reflect the isotopic characteristics of their source. Hence it may be concluded that the upper mantle in this region is isotopically heterogeneous, having a variation of at least 0.0001 in the $^{87}Sr/^{86}Sr$ ratio.

4.4 Discussion of Mafic Rocks from Islands in the Gulf of Guinea

Collectively, the islands of Principe, São Tomé, Pagalu and Bioko comprise the Gulf of Guinea oceanic island province. São Tomé, Principe and Pagalu all rise from the oceanic abyssal plain whilst Bioko lies on the edge of the African continental shelf. They broadly make up one suite of alkaline to transitional basalts, similar to those of other islands in the S. Atlantic Ocean. However, significant inter and intra-island geochemical differences exist. Principe is the only member of the province to have two distinguishable lava series. São Tomé lavas cover the complete silica spectrum (Figure 4.2.1) whereas Principe has a distinct gap between D.I. 55 and 65 (Figure 4.1.3). Unlike the other islands, evolved rocks have not been reported from Bioko (Figure 4.3.1). From analyses of the few samples available (Tyrrell, 1934; Fuster-Casas, 1954; Cornen and Maury, 1980; J.G. Fitton, unpublished data) from Pagalu it is apparent that these are the

most basic lavas in the oceanic sector, having undergone very little fractionation.

On the basis of Rb-Sr concentrations it is evident that the fractionation of the volcanic rocks from all four islands is controlled by the same form of igneous processes. Figure 4.4.1 shows that basaltic lavas from São Tomé, Principe, Pagalu and Bioko all plot in the same field, Only São Tomé intermediate rocks occupy the gap between basalts and evolved rocks. Rubidium and strontium analyses of evolved rocks are from São Tomé and Principe only as none is available from Pagalu.

Patterns of selected mean incompatible element concentrations (Rb, Ba, Th, K, Nb, La, Ce, Sr, Nd, P, Zr, Ti, Y) normalized to the composition of primitive undepleted mantle (following Sun et al., 1979; Sun, 1980) of the oceanic sector mafic rocks (>4% MgO) are depicted on Figure 4.4.2. This diagram shows the Nb enrichment typical of within plate basalts (Pearce and Norry, 1979), the overall 10-50x enrichment with respect of N type MORB and the close similarity between the four islands. The Gulf of Guinea islands are slightly enriched (particularly Rb, LREE and Sr) relative to the oceanic alkali basalt average (Sun, 1980). If basalts with >8% MgO had been averaged instead of those with >4% MgO then the same degree of enrichment would still be observed and incompatible element ratios remain unchanged. The olivine tholeiite from Principe (P15) is depleted with respect to the rest of the oceanic sector but it retains the same pattern and has similar incompatible element ratios (e.g. K/Rb = 306, Zr/Nb = 5.2) and hence cannot be explained by generation from a source similar to that which produces N type MORB (depleted in incompatible elements, high K/Rb and Zr/Nb ratios).

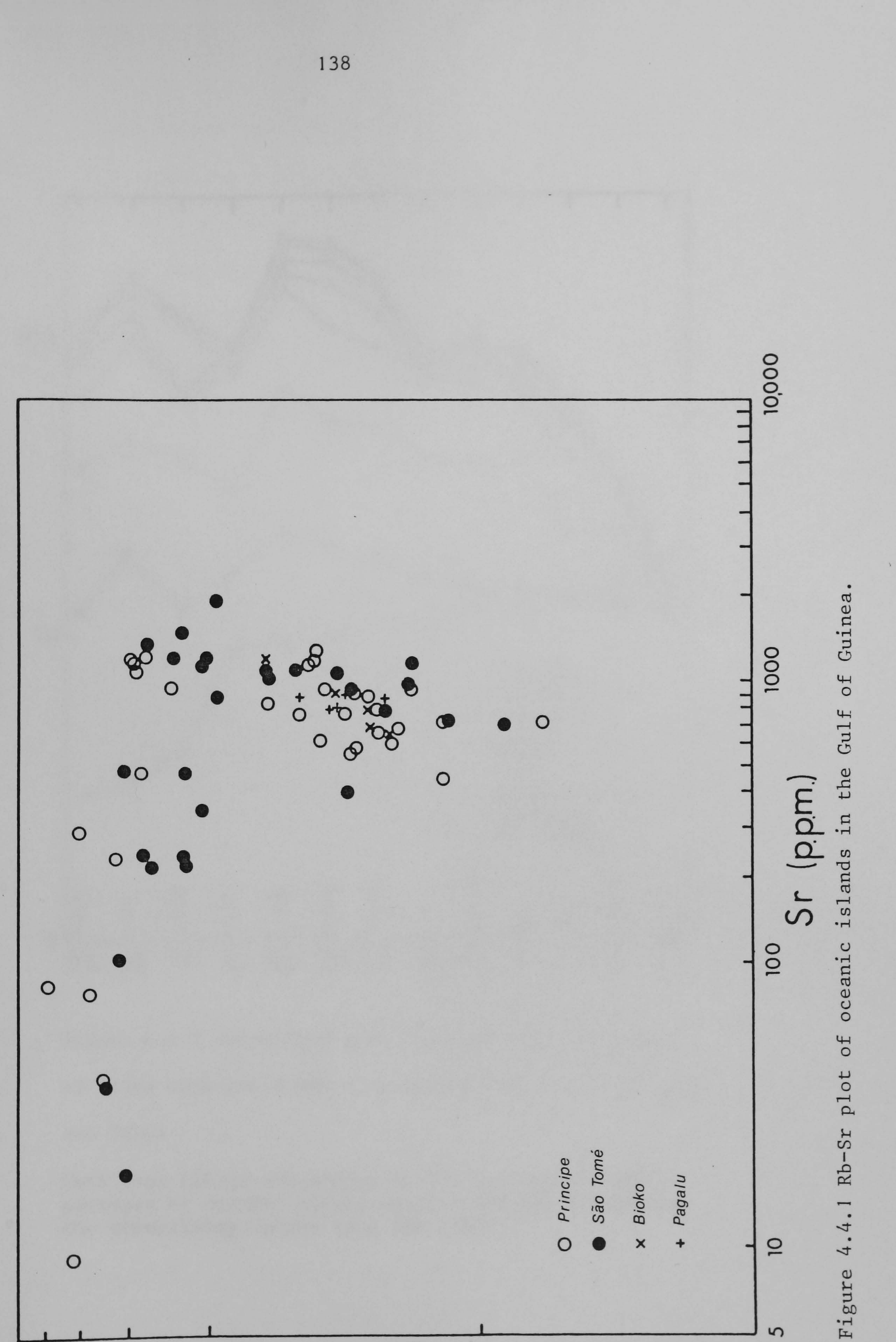


Figure 4.4.1 Rb-Sr plot of oceanic islands in the Gulf of Guinea.

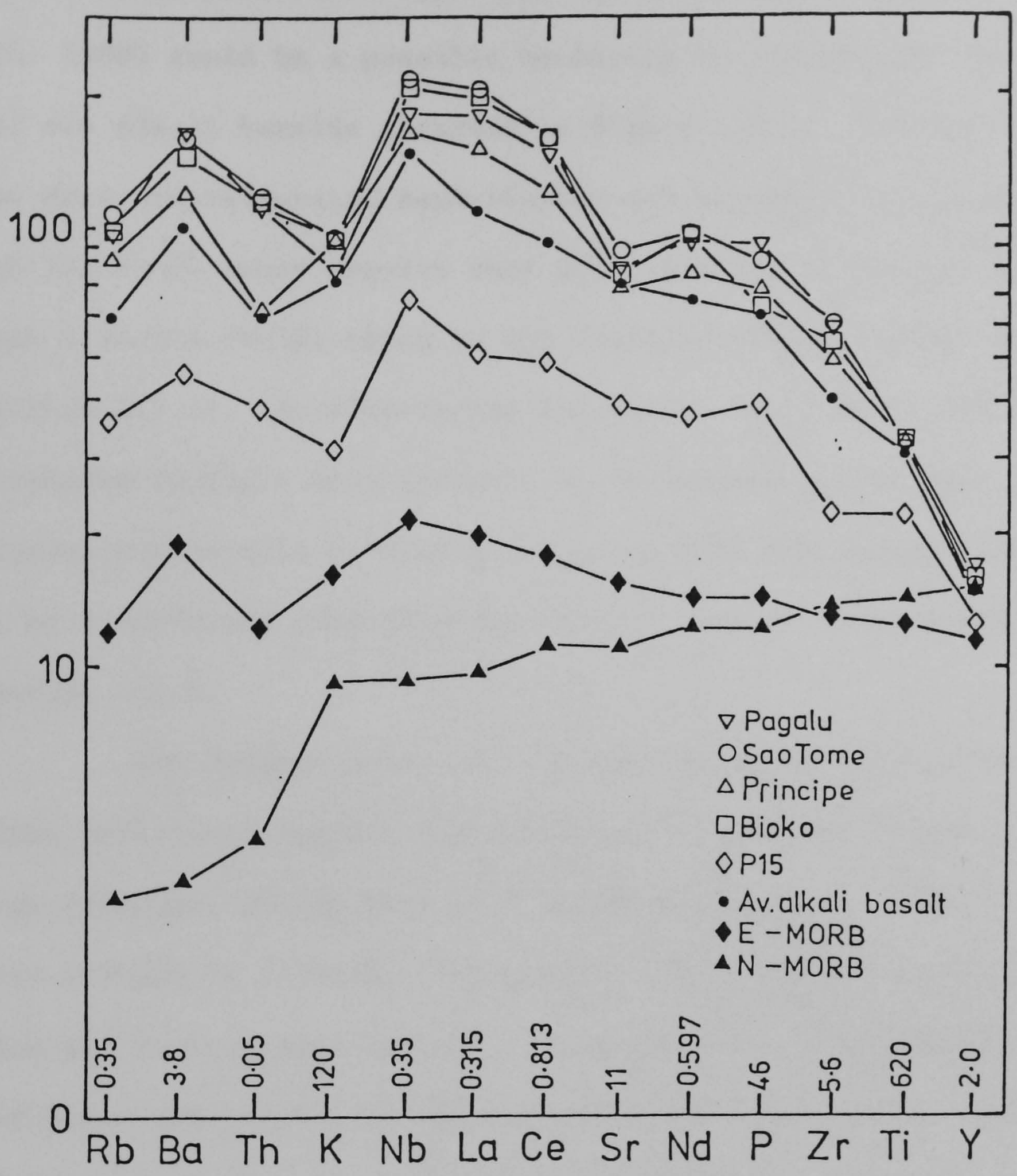


Figure 4.4.2 Normalized mean trace element abundances of lavas with >4 % MgO from Pagalu, São Tomé, Principe and Bioko.

Data from Fitton and Hughes (1977, and unpublished); averages of oceanic alkali basalt, N-MORB, E-MORB and the normalizing values from Sun (1980).

Small variations in the degree of partial melting of plume source which produces E type MORB (White and Schilling , 1978; Sun, 1980) could be a possible mechanism to account for the patterns of P15 and alkali basalts observed in Figure 4.4.2. However, to generate the more undersaturated nephelinites and basanites (Principe Y.L.S., and São Tomé) would require very small degrees of partial melting of such a source (≪5%) which is not feasible (Yoder, 1976; this work, Section 5.1.2). An alternative hypothesis, more in accord with the strontium isotopic data (below), is derivation either from a heterogeneous mantle more or less enriched in LREE and incompatible elements, or by a diffusive zone refining process similar to that described in Section 5.1.2.

The initial strontium isotope ratios of Pagalu, Sao Tome, and Bioko mafic-intermediate rocks all fall within the larger range of values from Principe, giving rise to a continuous range of $^{87}Sr/^{86}Sr$ ratios from 0.70278 to 0.70368. Figure 4.4.3 illustrates the spread of data from the four oceanic islands. Although only limited data is presented for Bioko and Pagalu, it appears that each island shows the same processes of magma formation from isotopically similar heterogeneous mantle sources. The similarity of mean Zr/Nb, K/Rb and La/Ce ratios (Table 4.4.1) of each island also gives strong support to this conclusion. Hence mantle models incorporating lateral inhomogeneities (Schilling, 1974, 1975; Sleep, 1974; Brooks et al., 1976b; Hanson, 1977) existing on the tens to hundreds of kilometre scale (Duncan and Compston, 1976; Davies, 1981) are invalid for the oceanic sector of the Cameroon Line (and elsewhere: Hofmann et al., 1978) since some 700 km separates the extremes of the region under discussion. Similar mantle to that supplying Pagalu, Principe and São Tomé must continue under the West African continental

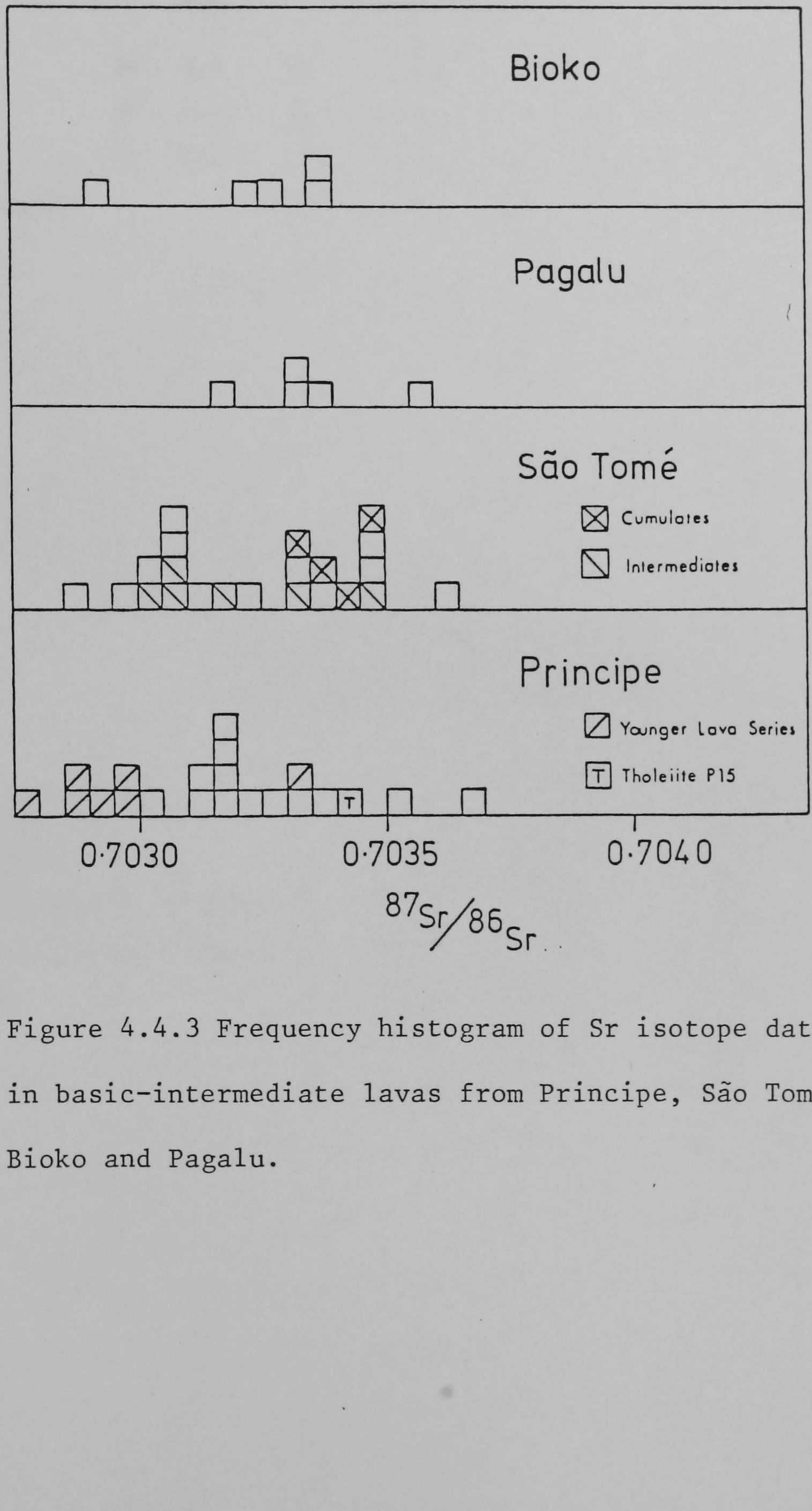


Figure 4.4.3 Frequency histogram of Sr isotope data in basic-intermediate lavas from Principe, São Tomé, Bioko and Pagalu.

TABLE 4.4.1

Mean selected Major and Trace Element Abundances and Ratios of Rocks with > 4% MgO

Suite		MgO (Wt%)	Mg Number	Ni (ppm)	Cr (ppm)	K/Rb	La/Ce	La/Y	P_2O_5/Ce	Zr/Nb
Principe	28	8.2	62	138	223	375	0.48	1.60	77	4.8
São Tomé	77	8.2	62	146	247	306	0.50	2.12	67	4.4
Bioko	23	8.5	62	171	302	332	0.48	1.94	54	4.3
"Primitive Magma"*			>64	>>100	>250				75 ± 15	

*Sun and Hanson (1975a); Frey et al. (1978)

TABLE 4.4.2

Mean Rb/Sr and $K_2O/(K_2O+Na_2O)$ Ratios; Mean Sr Isotopic Compositions of Mafic Rocks Selected for Isotopic Analysis

Suite-Location		Rb/Sr	$^{87}Rb/^{86}Sr$	$^{87}Sr/^{86}Sr_o$	$K_2O/(K_2O+Na_2O)$
Ol tholeiite - Principe	1	0.030	0.088	0.70342	0.164
Older Lava Series - Principe	13	0.032	0.092	0.70326	0.302
Younger Lava Series - Principe	7	0.044	0.128	0.70297	0.326
São Tomé	10	0.035	0.103	0.70320	0.309
Bioko	5	0.040	0.116	0.70322	0.310
Pagalu	5	0.043	0.124	0.70335	0.323

shelf, on which Bioko is situated.

If $^{87}Sr/^{86}Sr$ data is compared to the degree of silica saturation (Figure 4.4.4) it is evident that the lowest ratios are associated with strongly nepheline normative basanites and nephelinites whereas high ratios correspond to more transitional, hypersthene normative basalts. As with all the data employed in this discussion only mafic samples (>4% MgO) are under consideration to remove any effects of crystal fractionation (especially that of plagioclase) which may change incompatible element contents and ratios. These sample populations hence have high mean MgO, Ni, Cr contents and high Mg numbers (Table 4.4.1) which are parameters normally taken to indicate primitive if not primary liquids (Gast, 1968; Schilling, 1975; Sun and Hanson, 1975a; Frey et al, 1978). In addition Principe, Pagalu and São Tomé have P_2O_5/Ce ratios typical of liquids unmodified during magma ascent (Frey et al., 1978). In particular strongly magnesian rocks from Pagalu and São Tomé contain ultramafic xenoliths indicating a rapid ascent to the surface (in a matter of hours, Spera, 1980). Bioko however shows lower P_2O_3/Ce ratios and consequently its high MgO content may reflect cumulus enrichment. Incidentally, similar characteristics are to be noted for neighbouring Mt. Cameroon and Etinde. Although there is considerable scatter in the zone 5% normative ne to 2% "q" on Figure 4.4.4 this correlation is considered to be significant. All but Bioko show the same pattern individually. These patterns have already been demonstrated for Principe, São Tomé and Pagalu on diagrams of $^{87}Sr/^{86}Sr$ versus $^{87}Rb/^{86}Sr$ (Figures 4.1.8, 4.2.4, 4.3.4). On Principe, where the separation between earlier transitional and later alkalic lavas is also geologically and chemically evident (Fitton and Hughes, 1977) one sees a correlation between La/Y and $^{87}Sr/^{86}Sr$ (Figure

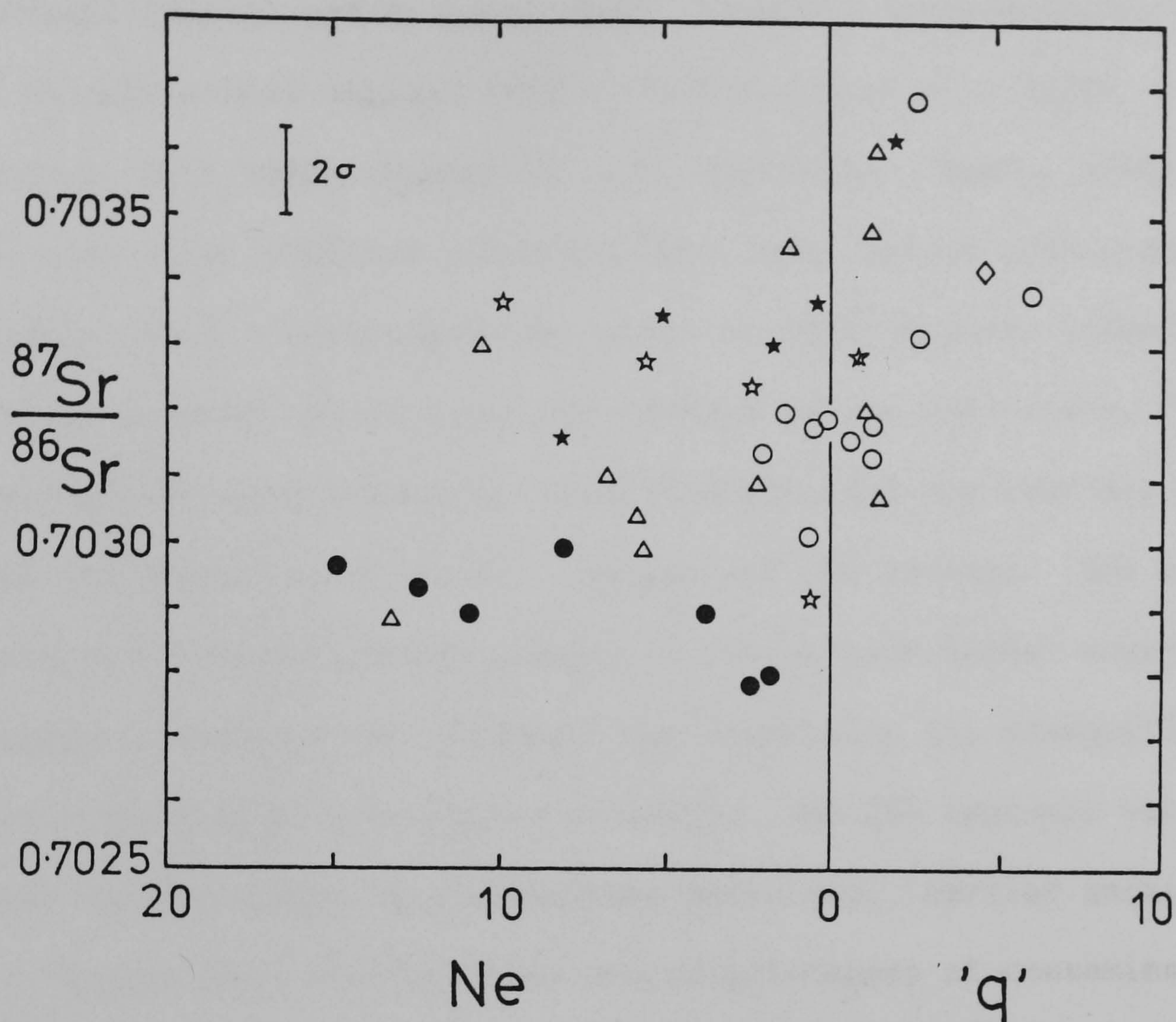


Figure 4.4.4 Initial strontium isotope ratios plotted against degree of silica over- and under-saturation for lavas with >4 % MgO on islands in the Gulf of Guinea.

○ Principe O.L.S.
● Principe Y.L.S.
◇ Principe tholeiite (P15)
✶ Pagalu
☆ Bioko
△ São Tomé

4.1.7, Dunlop and Fitton, 1979) whereby the more alkaline volcanics have lower $^{87}Sr/^{86}Sr$ ratios. Similar relationships have also been reported in Hawaii (Powell and De Long, 1966; Lanphere and Dalrymple, 1980) and in continental regions (Mull: Beckinsale et al., 1978; Biu Plateau: this work, Chapter 6; S.E. Australia: Ewart, 1982). In each case later alkaline volcanics have lower ratios than transitional basalts. Such a correlation may exist on other oceanic islands but although a wealth of isotopic data exists in the literature, few investigators have presented integrated chemical and isotopic studies (with the exception of Hawaii, Iceland and the Azores). The data on Figure 4.4.4 implies heterogeneity of the oceanic sector source (Chapter 2 outlines the arguments for dismissing (a) disequilibrium partial melting of a homogeneous source; and (b) isotopic variations caused by fractional crystallization processes; earlier sections of this Chapter have discussed the inappropriateness of contamination by seawater/altered basalts/oceanic sediments). While it is now universally accepted that the mantle is heterogeneous on the trace element and isotopic (Sr-Nd-Pb-O-He) level, the geochemical structure of the mantle, the nature and origin of heterogeneities is a subject currently under intense debate in the literature. Of the numerous proposed models hypotheses of large - scale vertical stratification are considered to be the most appropriate for the Gulf of Guinea volcanoes. In such models a large, broadly homogeneous (i.e. well mixed) reservoir characterized by depleted incompatible concentrations (1-2 x chondrite), high K/Rb (800-1500) and Zr/Nb (30) and usually by low $^{87}Sr/^{86}Sr$ ratios (<0.7030) is recognised as being the

source of N type MORB tholeiites (Kay et al., 1970; Hart, 1971; 1976; Schilling, 1971; Erlank and Kable, 1976; Kay and Hubbard, 1978) whereas alkalic island basalts are derived from enriched sources (incompatible 2-5 x chondrite) with low K/Rb (<300) and Zr/Nb ratios (<10) and with more variable $^{87}Sr/^{86}Sr$ ratios. This chemical structure is required since tholeiites and alkali basalts often occur in very close proximity (e.g. Principe, Galapagos, Hawaii, Iceland, Azores, Samoa, Kergulen). Such contrasting rock types cannot be derived from one N type MORB source by variations in partial melting or crystal fractionation processes (Kay and Hubbard, 1978). Some investigators have appealed to a thin, enriched heterogeneous layer occurring above the homogeneous MORB source (Kay and Gast, 1973; Green and Lieberman, 1976; Allegre and Bottinga, 1977; Ito, 1977; Anderson, 1981, 1982). While at first sight this model may seem logical since upward migration of incompatibles and volatiles would enrich this zone, it is difficult to reconcile with the observation that hotspots remain stationary with respect to the lithosphere (Jackson et al., 1972), that such hotspots are common on ridge crests and triple junctions and that they often tend to be long-lived (Morgan, 1971, 1972). On the other hand if the source of MORB was the uppermost mantle and the more isotopically heterogeneous, geochemically enriched zone is situated at a deeper level ("plume" model, Wilson, 1963; Morgan, 1971; Schilling, 1973; Schilling et al., 1982; Sun and Hanson, 1975a, Duncan and Compston, 1976; White and Schilling, 1978; Brooks, 1976a; Hofmann and Hart, 1978; Wasserburg and De Paolo, 1979; De Paolo, 1980; 1981; O'Nions et al, 1979; Zindler et al., 1979; Fitton, 1980; B.V.S.P., 1981; Turcotte, 1982; Allegre, 1982) the objections to the former model are obviated. This

model is also more in accord with the probable derivation of incompatible element enriched alkalic basalts, basanites and nephelinites from deeper levels than MORB by small degrees of partial melting of garnet lherzolite as constrained by phase equilibria studies (Green and Ringwood, 1967; Kushiro, 1968; Green, 1969; Jackson and Wright, 1970, Sun and Hanson, 1975a). The origin of this chemically enriched zone (e.g. by recycled subducted oceanic crust, Hofmann and White, 1982) is discussed in Chapter 7. Overall, the lower mantle may have $^{87}Sr/^{86}Sr$ ratios tending to slightly higher values than the MORB reservoir because Rb/Sr ratios are higher in the former and long term separation (1-2 Ga) of the two (Brooks et al., 1976a; Tatsumoto, 1978; B.V.S.P., 1981) will give rise to higher $^{87}Sr/^{86}Sr$ ratios. However the only way one can explain the fact that strongly alkaline lavas have lower ratios is by postulating that the source of ocean island basalts is itself isotopically heterogeneous (as indicated above) and by the occurrence of magma mixing during the melts' migration to the surface. Magmas derived from the lower part of the mantle must ascend through the depleted MORB source which is also partially molten, hence some degree of mixing or isotopic re-equilibration will be inevitable (Tatsumoto, 1978; Wasserburg and De Paolo, 1979; Zindler et al., 1979; Sun, 1980; Dupre et al, 1982; Anderson, 1982). This could be a viable mechanism for explaining the MORB type $^{87}Sr/^{86}Sr$ ratios of the geochemically enriched alkaline lavas such as the Principe Y.L.S. and would explain the higher ratios of the Pagalu nodule bearing lavas which probably ascended more rapidly to the surface, undergoing little interaction with the MORB reservoir.

Figure 4.4.5 shows the position of average $^{87}Sr/^{86}Sr$ ratios of Pagalu, Principe, São Tomé and Bioko on Brook's et al. (1976a) plot

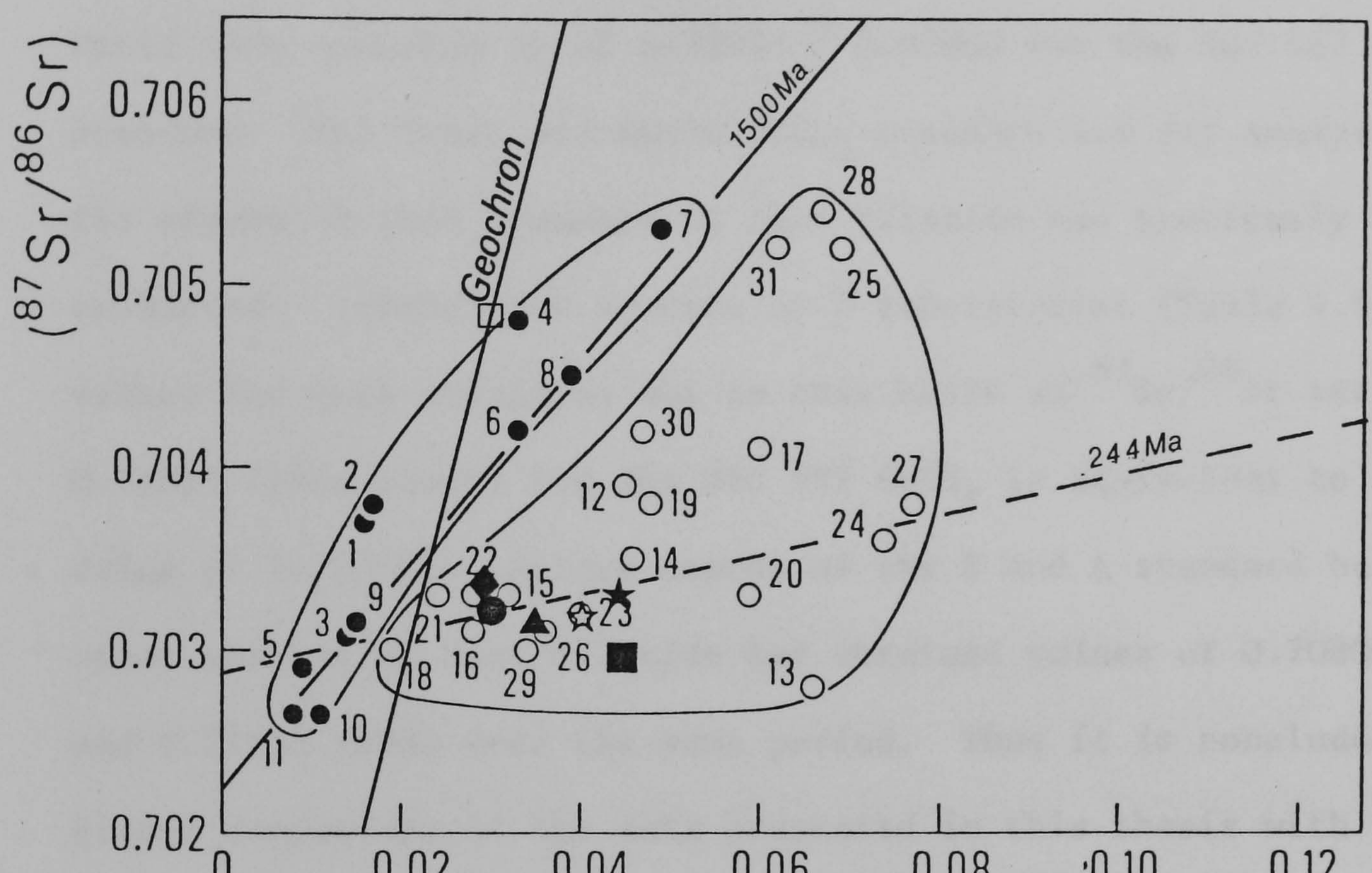


Figure 4.4.5 Initial strontium isotope ratios for all oceanic islands and MORB. Each point represents an average of available data on individual samples from a given island or island group. Filled circles are tholeiites and open circles are alkali basalts. Numbers refer to the data index in table 1, Brooks et al. (1976a). Also marked are the Geochron, 1500 Ma and 244 Ma isochrons, and averaged data of islands in the Gulf of Guinea.

□ Bulk Earth derived from Nd-Sr systematics

◆ Principe tholeiite P15

● Principe O.L.S.

■ Principe Y.L.S.

★ Pagalu

☆ Bioko

▲ São Tomé

of mean oceanic basalt data. Brooks et al (op. cit.) corrected all the data relative to a uniform value of 0.70800 for the Eimer and Amend $SrCO_3$ standard. The ratios presented in this thesis have been analysed under machine conditions which gave rise to an $^{87}Sr/^{86}Sr$ ratio (see Appendix A) of 0.71023 $\pm$ 0.00003 for the NBS 987 $SrCO_3$ standard. The Eimer and Amend $SrCO_3$ standard was not analysed since the stocks of this standard at East Kilbride had previously been exhausted. Independant workers of 3 laboratories (Table 4.4.3) quote values for both standards and on this basis an $^{87}Sr/^{86}Sr$ ratio of 0.71023 (this study) for the NBS 987 $SrCO_3$ is equivalent to an E and A value of 0.707993. Before stocks of the E and A standard had expired, other workers at East Kilbride had obtained values of 0.70800 (E and A) and 0.71023 (NBS) over the same period. Thus it is concluded that direct comparison of the data presented in this thesis with that of previous workers is valid. All the Gulf of Guinea Province data fall within the area of alkali basalts defined by Brooks et al (1976a) (Figure 4.4.5). P15 plots next to Hawaii; whilst the Principe O.L.S., Sao Tome and Bioko all plot in the same region as the Canaries, Cape Verde Islands, Madeira, Iceland and St. Helena. The Principe Y.L.S. and Pagalu data are displaced slightly further towards higher Rb/Sr ratios and fill an unoccupied space within the field of alkali basalts.

That all these samples come from a geochemically recently enriched mantle is evident since they all plot to the right of the geochron on Figure 4.4.5. If these samples had evolved by a single-stage process then they would have a measured ratio of 0.7055 now, not

the 0.7032 observed. The data thus represents recent incompatible enrichment accompanied by long term isotopic depletion. The timing of such enrichment events has been suggested to be given by mantle isochrons (Brooks et al., 1976a, 1976b; Duncan and Compston, 1976; Carlson et al, 1978; Mertzman, 1979; Dunlop and Fitton, 1979; Hofmann and White, 1982) although many workers currently doubt the significance of ages so derived (e.g. Pankhurst, 1977; Allegre, 1982). In addition good correlations only exist for MORB and island tholeiites and no such trend is observed between the islands in the Gulf of Guinea (Figure 4.4.5); only an internal isochron exists for the Principe O.L.S..

The Gulf of Guinea islands have Sr isotope compositions comparable to other islands in the central-south Atlantic Ocean (Figure 4.4.6) and to 'plume' type MORB (e.g: Azores platform, White and Schilling, 1978) Tristan da Cunha has distinctly elevated ratios however, perhaps reflecting subducted crustal material which has retained its identity in the upper mantle (Hawkesworth et al., 1979). Recent data from St. Helena and Ascension (Cohen and O'Nions, 1982; Harris et al., 1982) fall within the depicted fields of these islands.

Other workers (Peterman and Hedge, 1971; Faure and Powell, 1972; Klerkx et al., 1974; Gale, 1975; Lanphere and Dalrymple, 1980) have employed the geochemical ratio $K_2O/(K_2O+Na_2O)$ to compare $^{87}Sr/^{86}Sr$ ratios between oceanic basaltic rocks. Average data (Table 4.4.2) indicate that the oceanic sector of the Cameroon Line is potassic relative to many other Atlantic Ocean islands (for which there is data) with the spread of all the Gulf of Guinea data (0.14 to 0.43) being essentially identical to that of Cape Verdes (Figure 4.4.7). The

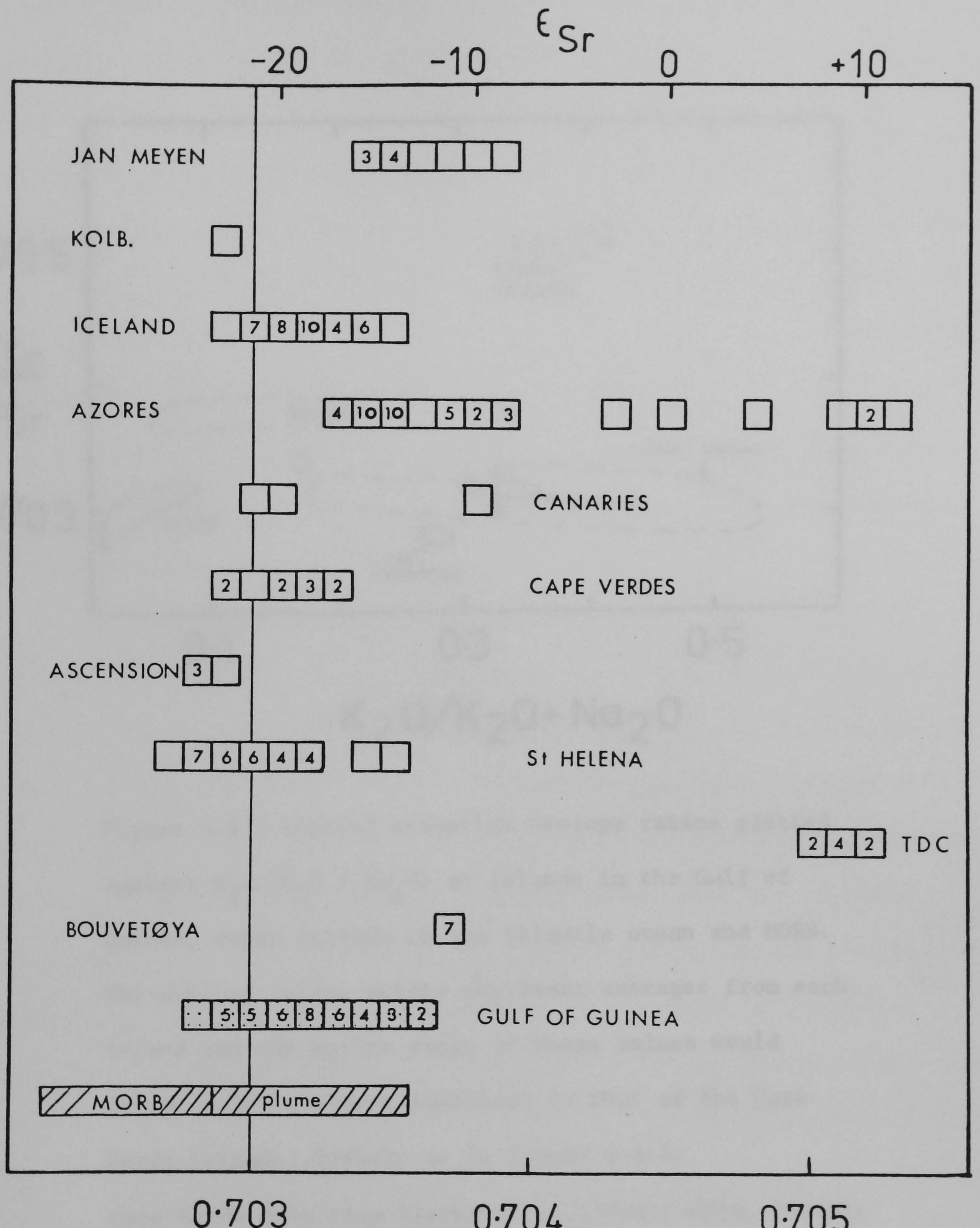


Figure 4.4.6 Initial Sr isotope data from islands in the Atlantic ocean and MORB. All oceanic island and MORB (N type) data except for the Gulf of Guinea are as reviewed by Hofmann and Hart (1978). "Plume" (or E type MORB) is from White and Schilling (1978). Numbers refer to number of analyses, a blank square represents one analysis.

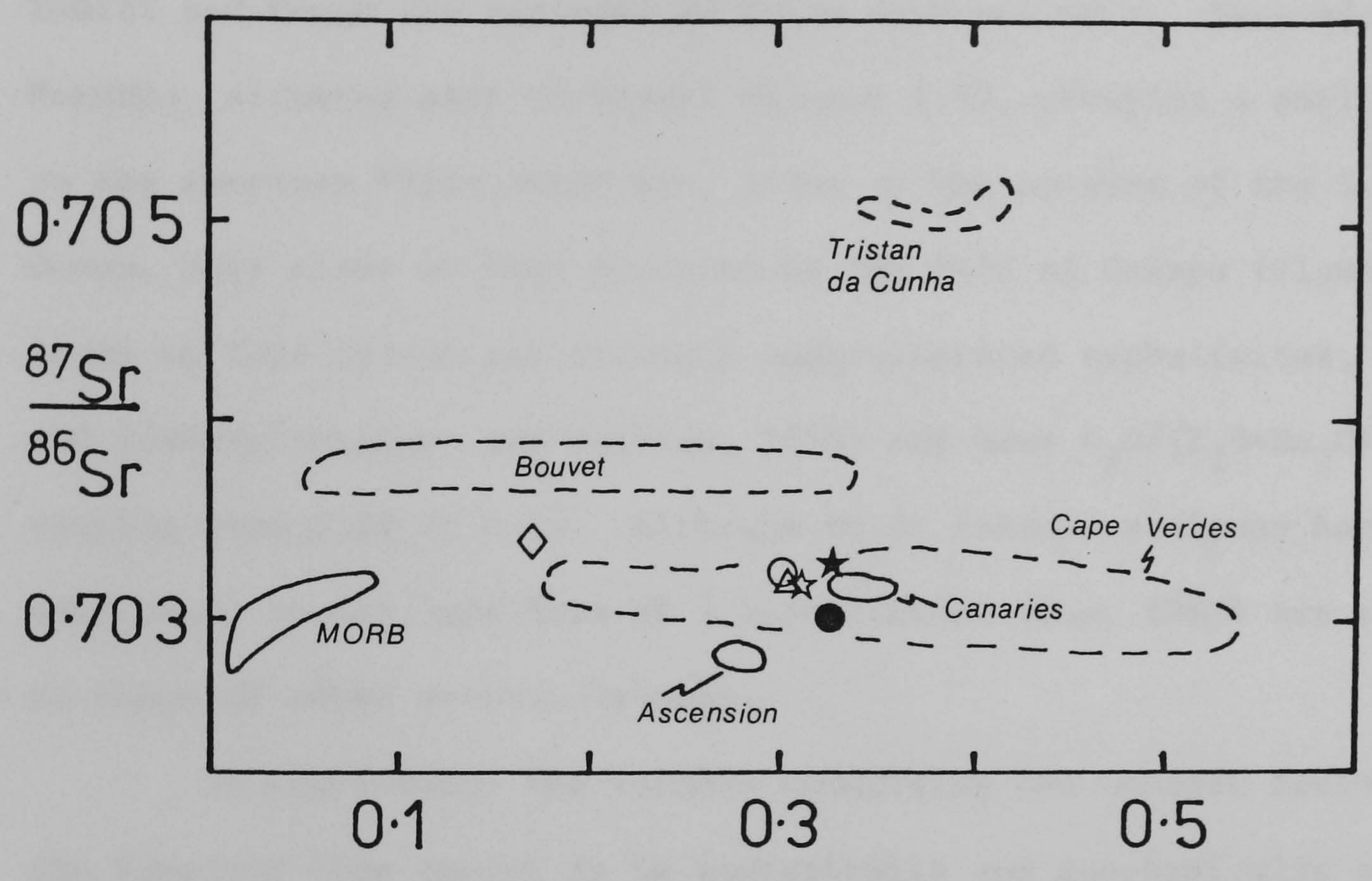


Figure 4.4.7 Initial strontium isotope ratios plotted against $K_2O/(K_2O + Na_2O)$ of islands in the Gulf of Guinea, other islands in the Atlantic ocean and MORB. The Gulf of Guinea points represent averages from each island and the entire range of these values would occupy a field almost identical to that of the Cape Verde islands. Symbols as in figure 4.4.4.

Cape Verde data from Klerkx et al.(1974); MORB, Bouvet, Ascension, Canaries and Tristan from O'Nions and Pankhurst (1974).

Honolulu alkaline volcanic rocks, Oahu (Lanphere and Dalrymple, op. cit.) have a similar range of $^{87}Sr/^{86}Sr$ ratios but range only from 0.16 to 0.27 in $K_2O/(K_2O+Na_2O)$ ratios. Worldwide, only Samoa, Tahiti and Gough are recorded as being more potassic. Fernando de Noronha, situated east of Brazil (Figure 1.3), occupies a position on the American Plate which was, prior to the opening of the S. Atlantic Ocean, very close to that occupied by the Gulf of Guinea islands. Lavas on this island are strongly undersaturated nephelinites, basanites and limburgites (Gunn and Watkins, 1976) and have $K_2O/(K_2O+Na_2O)$ ratios varying from 0.28 to 0.33. Although no Sr isotope analyses have been published, common lead data of 2 nephelinites (Sun, 1980) are similar to those of other oceanic islands.

In conclusion, the islands comprising the oceanic sector of the Cameroon Line appear to be isotopically and geochemically similar to other islands in the South Atlantic with the exception of Tristan da Cunha. Significant small-scale differences have been identified within the province indicating that their source region is heterogeneous (not laterally) and implying that this zone lies below the depleted MORB reservoir. The relations of the Gulf of Guinea islands to the remainder of the Cameroon Line and with other volcanic centres to which they may be associated are further discussed in Chapters 5-7.

CHAPTER 5

GEOCHEMISTRY OF VOLCANIC ROCKS FROM CAMEROON

Strontium isotope ratio analyses from Etinde, Mt. Cameroon Manengouba, Bambouto, Oku and Mandara are described and considered with chemical data (J.G.Fitton,unpublished) and isotope data in the literature on other continental intraplate volcanic provinces. Published isotope studies on the Tertiary ring complexes are also discussed. The geology and sample locations are described in chapter 3 (figures 3.2.1 and 3.2.2) and samples are listed in appendix D.

5.1 South Cameroon

5.1.1 Mt. Cameroon

Geochemistry The majority of lavas observed on Mt. Cameroon are alkali olivine basalts and hawaiites (often bearing titaniferous augite) with lesser volumes of basanite, nephelinitic basanite and nephelinite. These rocks are predominantly alkaline with all but one of the 27 samples chemically analysed (by J.G. Fitton, unpublished data) being ne-normative (Figure 5.1.1). The most alkalic rocks (15% ne) approach the strongly alkaline field of Etinde. No evolved rocks have been observed and none was reported by earlier researchers. The highest D.I. of this suite is 48.5 and MgO content ranges from 3.5 wt% to 9 wt% with two oceanites having high (12.5 and 14.2%)

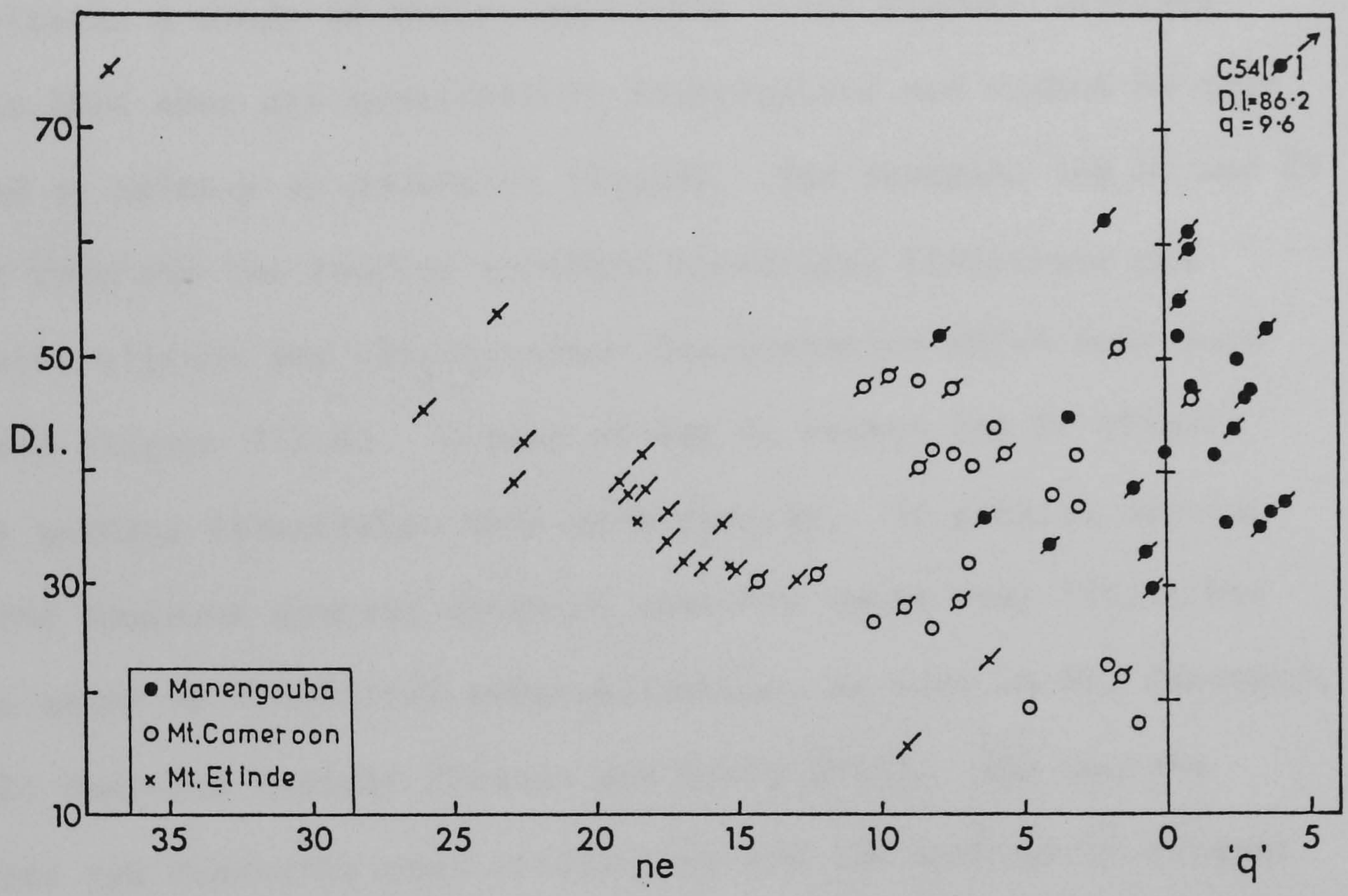


Figure 5.1.1 Differentiation index plotted against degree of silica over- and under-saturation for the S. Cameroon volcanoes. Chemical data from J.G.Fitton (unpublished). / : analysed for $^{87}Sr/^{86}Sr$ ratios.

MgO contents due to the presence of cumulus olivine. Likewise SiO_2 only varies from 43 to 51%. These features are shown in the major element variation diagrams (Figure 5.1.2) and their alkaline nature (as expressed by Na_2O and K_2O contents) is also illustrated in Figure 5.1.3.

Although these rocks are relatively uniform in major element compositions a study of their compatible trace element contents reveals that they are considerably fractionated and cannot be considered as primary or primitive liquids. For example, low Ni and Cr (apart from the two cumulus enriched oceanites) illustrate the extensive olivine and clinopyroxene fractionation which must have occurred (Figure 5.1.4). A plot of log Cr versus log Zr (Figure 5.1.5) perhaps illustrates this more clearly. If partial melting were the dominant process chromium contents would vary little but in the event of fractional crystallization, as seen on Mt. Cameroon, Cr will decrease rapidly (Pearce and Norry 1979). The vectors indicate cpx dominates over olivine but the low average Ni content of these rocks (71 ppm, excluding oceanites) show that significant olivine fractionation must have also occurred.

With regard to incompatible elements Mt. Cameroon shows the strong LREE enrichment typical of within-plate alkali basalts. The mean La content is 200 times that present in chondrites and the La/Y ratio of 2.5 (Table 5.1.1) indicates steep REE profiles. Other incompatible elements (e.g. Rb, Ba, Th, K, Nb, La, Ce, Sr, Nd, P, Zr, Ti, Y) are also enriched relative to the average oceanic alkali basalt of Sun (1980) (Figure 5.1.6). Mt. Cameroon would plot close of Wood's (1979, Figure 1) mean basanite from E. Australia

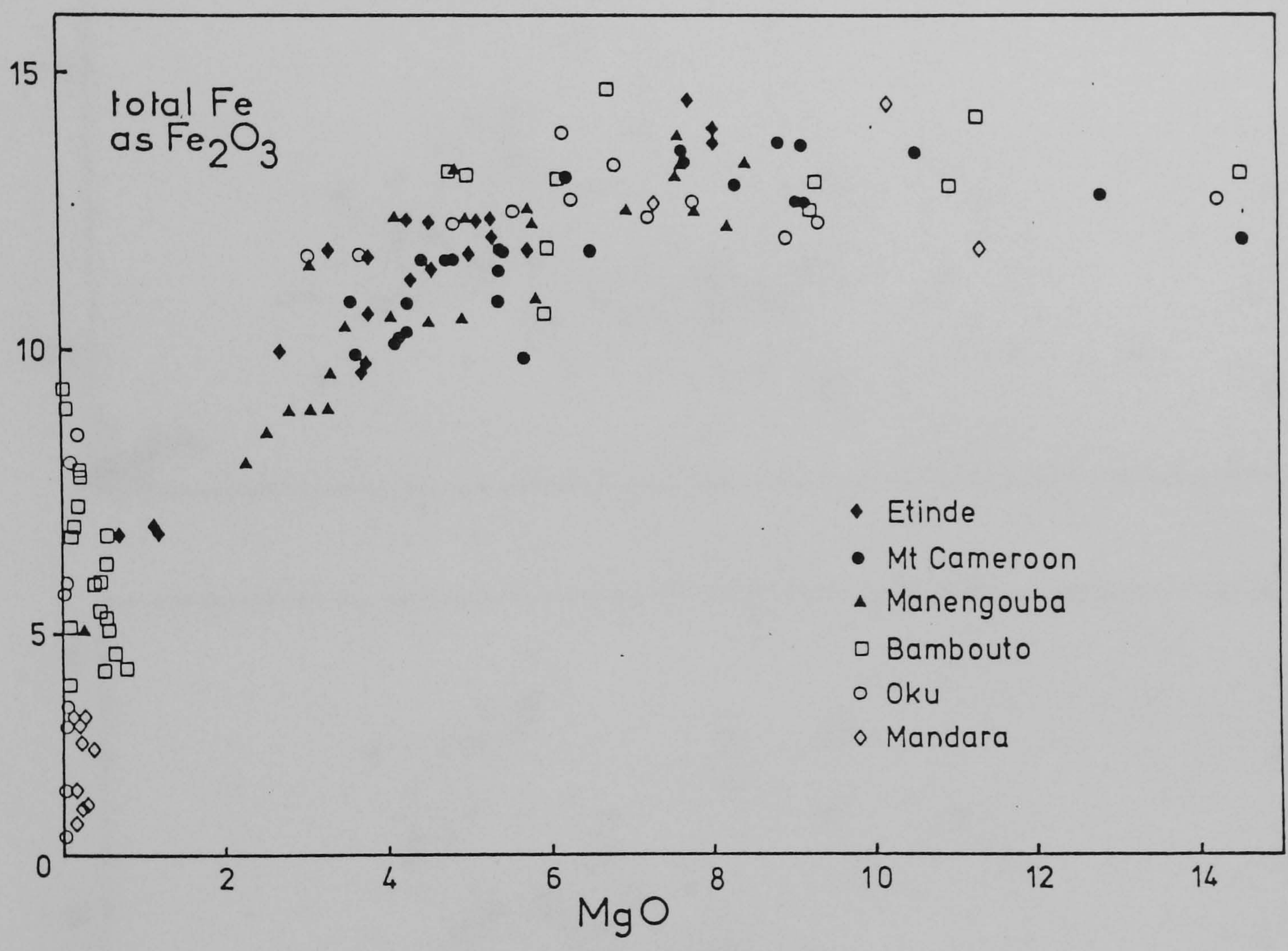


Figure 5.1.2 Major element variation in rocks from the continental sector of the Cameroon line. Analyst : J.G. Fitton. All concentrations in wt.% .

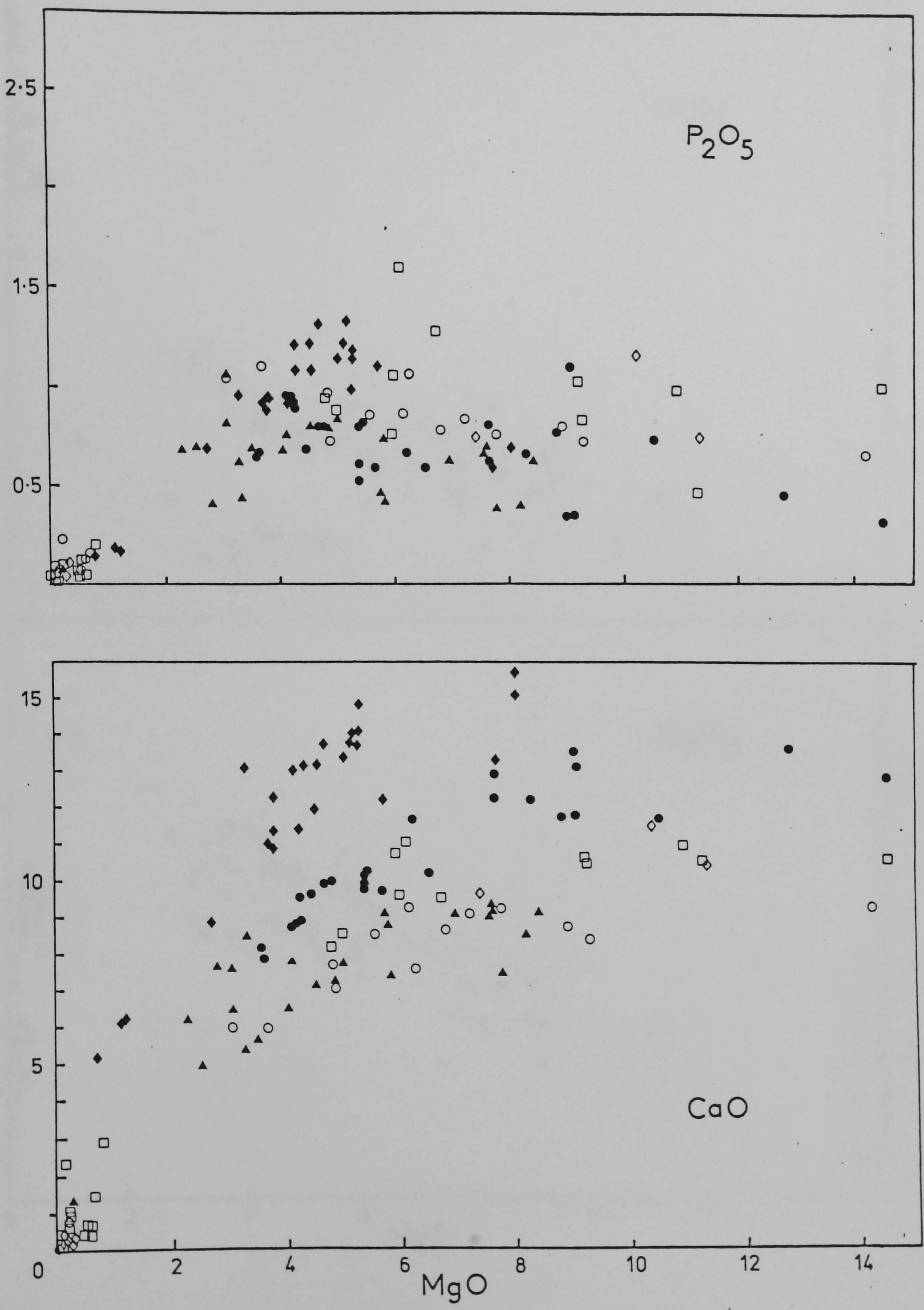


Figure 5.1.2 continued

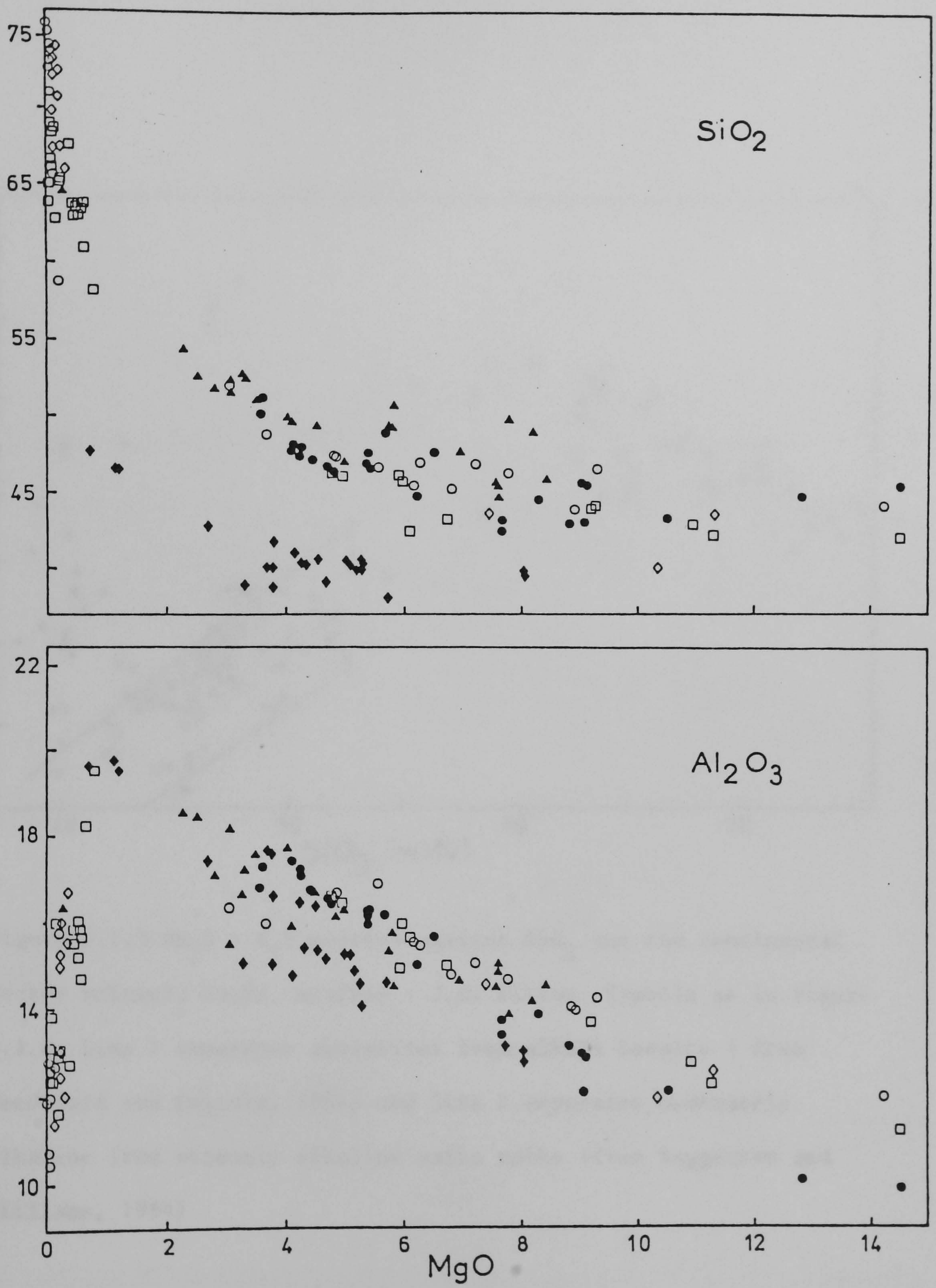


Figure 5.1.2 continued

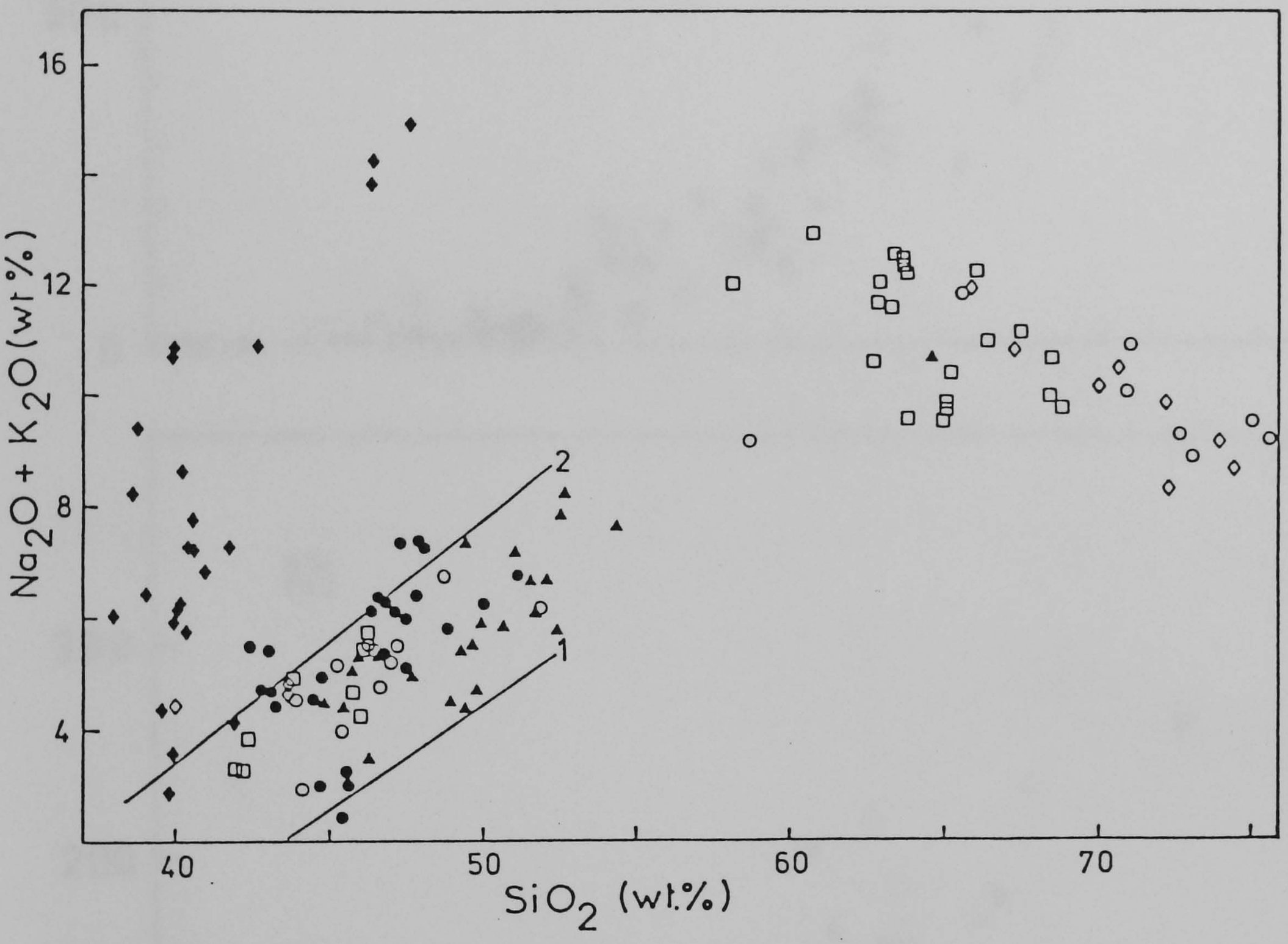


Figure 5.1.3 $Na_2O + K_2O$ plotted against SiO_2 for the continental sector volcanic rocks. Analyst : J.G. Fitton. Symbols as in figure 5.1.2. Line 1 separates tholeiites from alkali basalts (from MacDonald and Katsura, 1964) and line 2 separates moderately alkaline from strongly alkaline mafic rocks (from Saggerson and Williams, 1964)

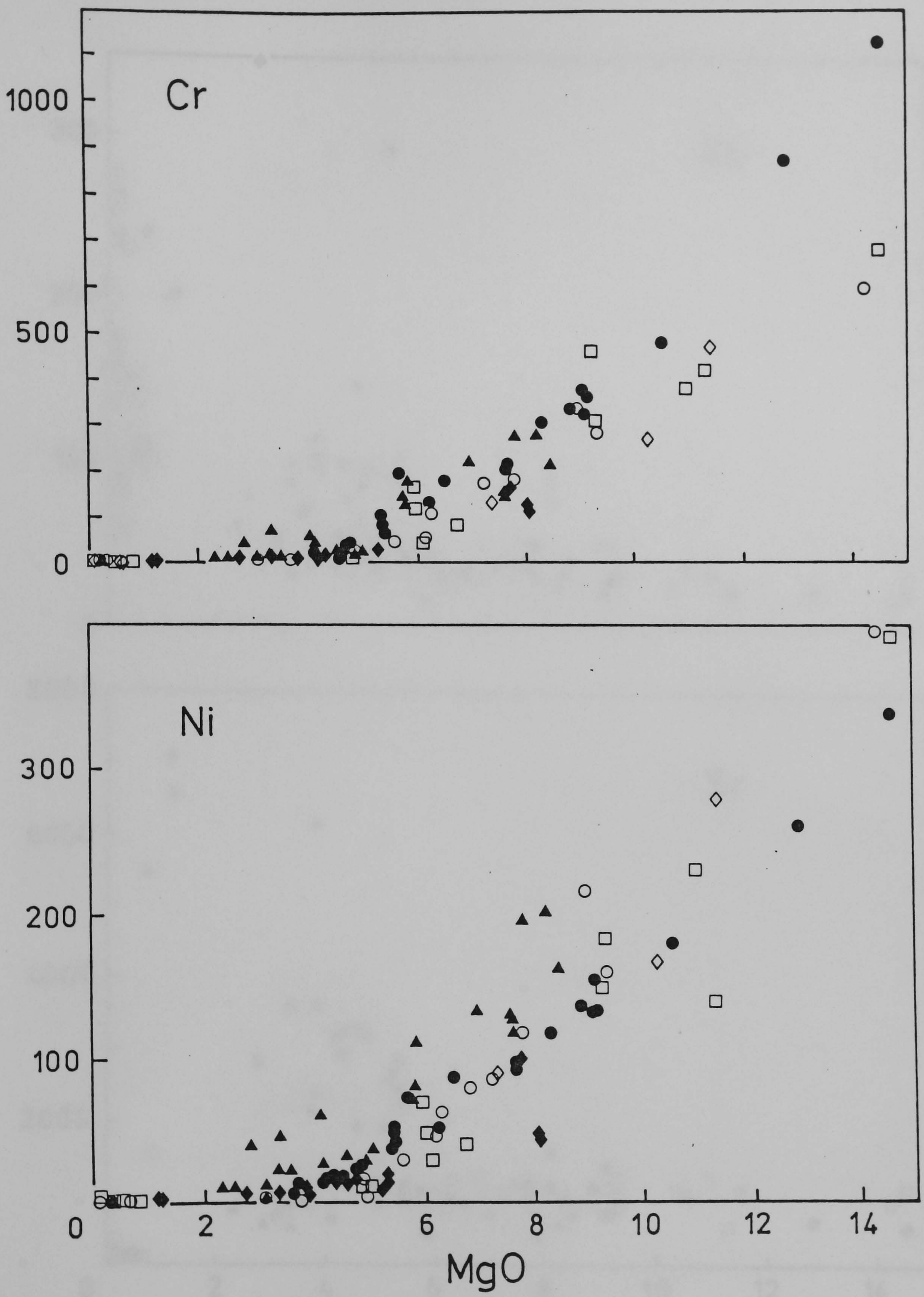


Figure 5.1.4 Trace element variation in rocks from the continental sector of the Cameroon line. Analyst : J.G. Fitton. Symbols as in figure 5.1.2. MgO concentrations in wt.% and all traces in P.P.M.

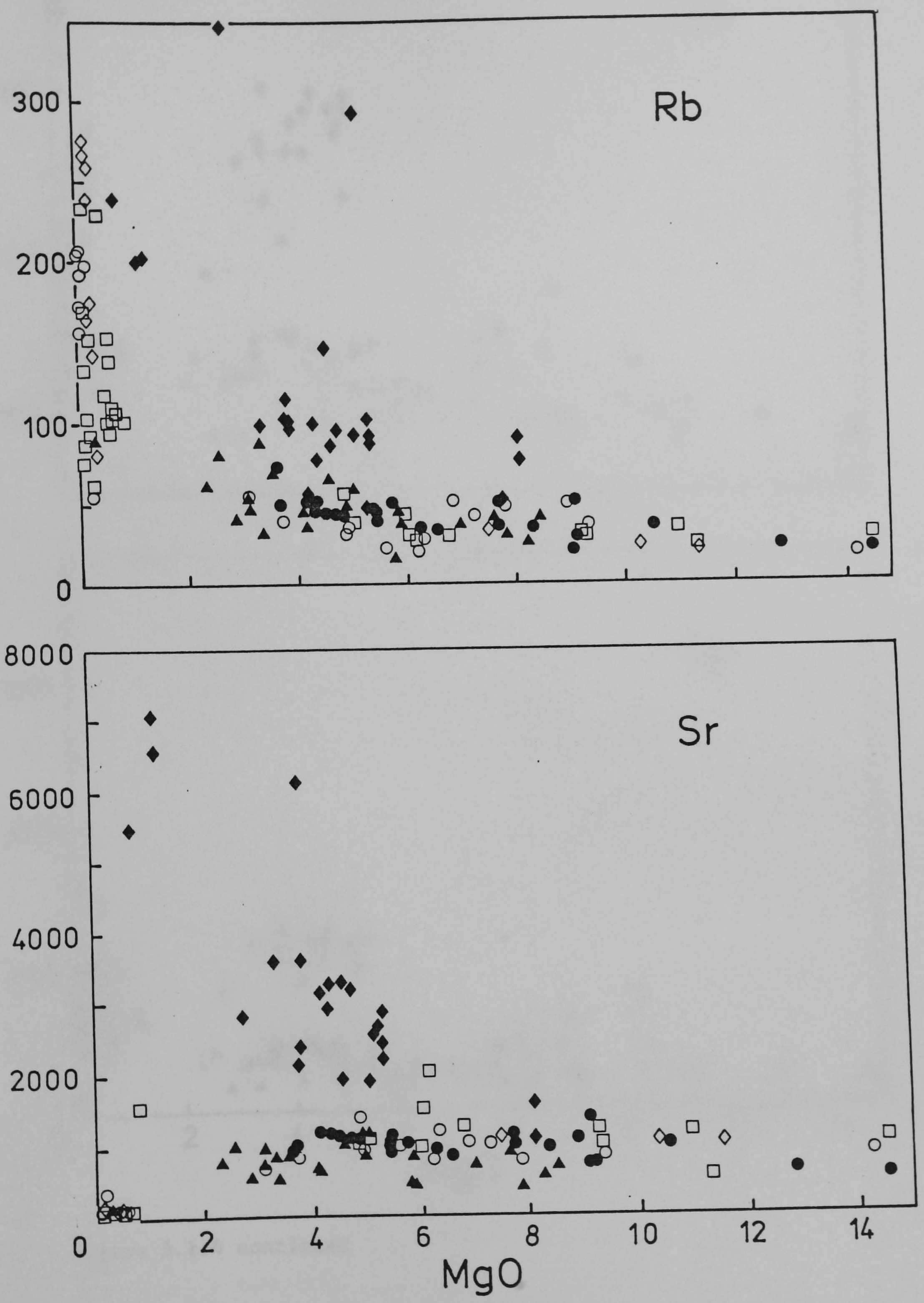


Figure 5.1.4 continued

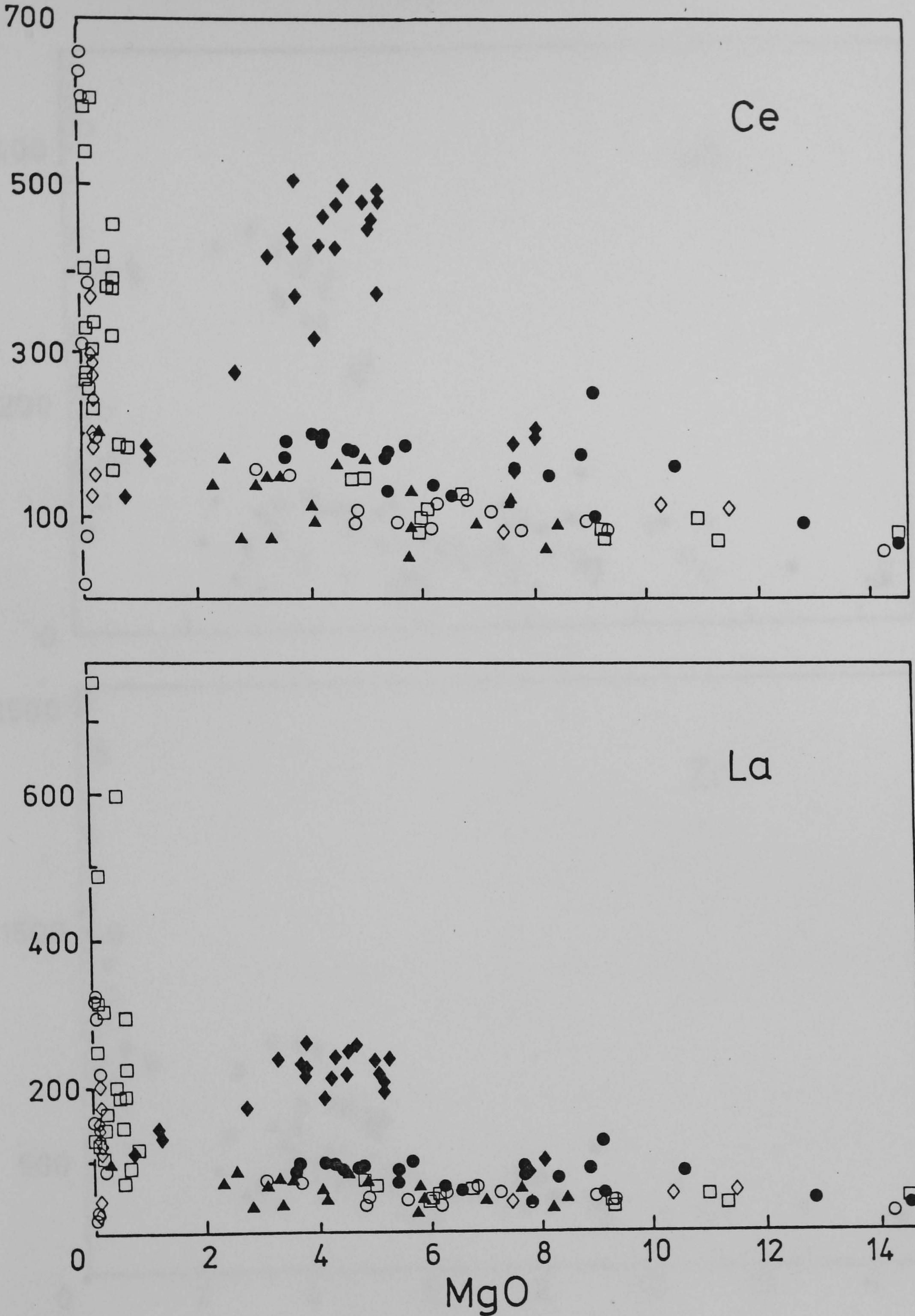


Figure 5.1.4 continued

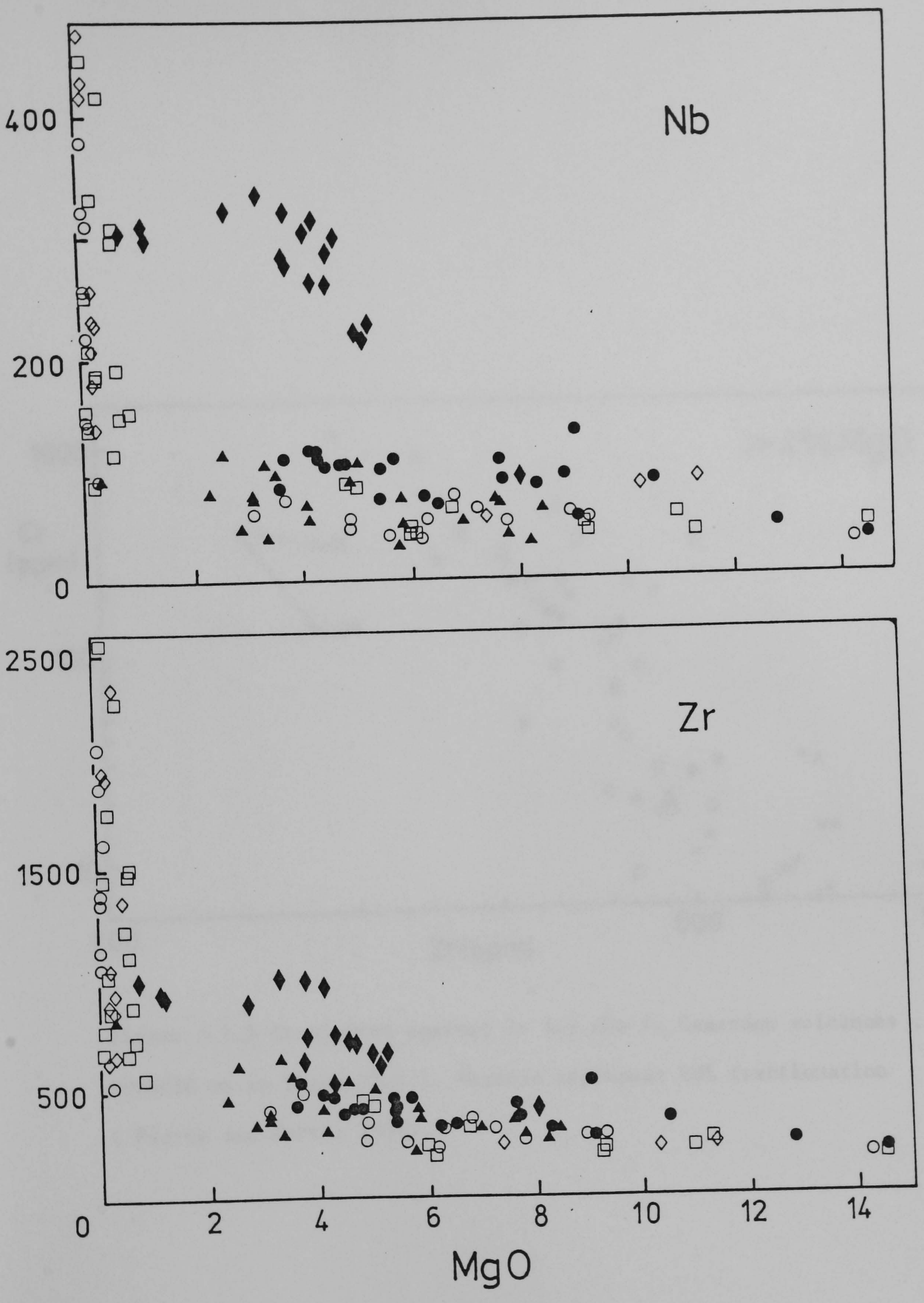


Figure 5.1.4 continued

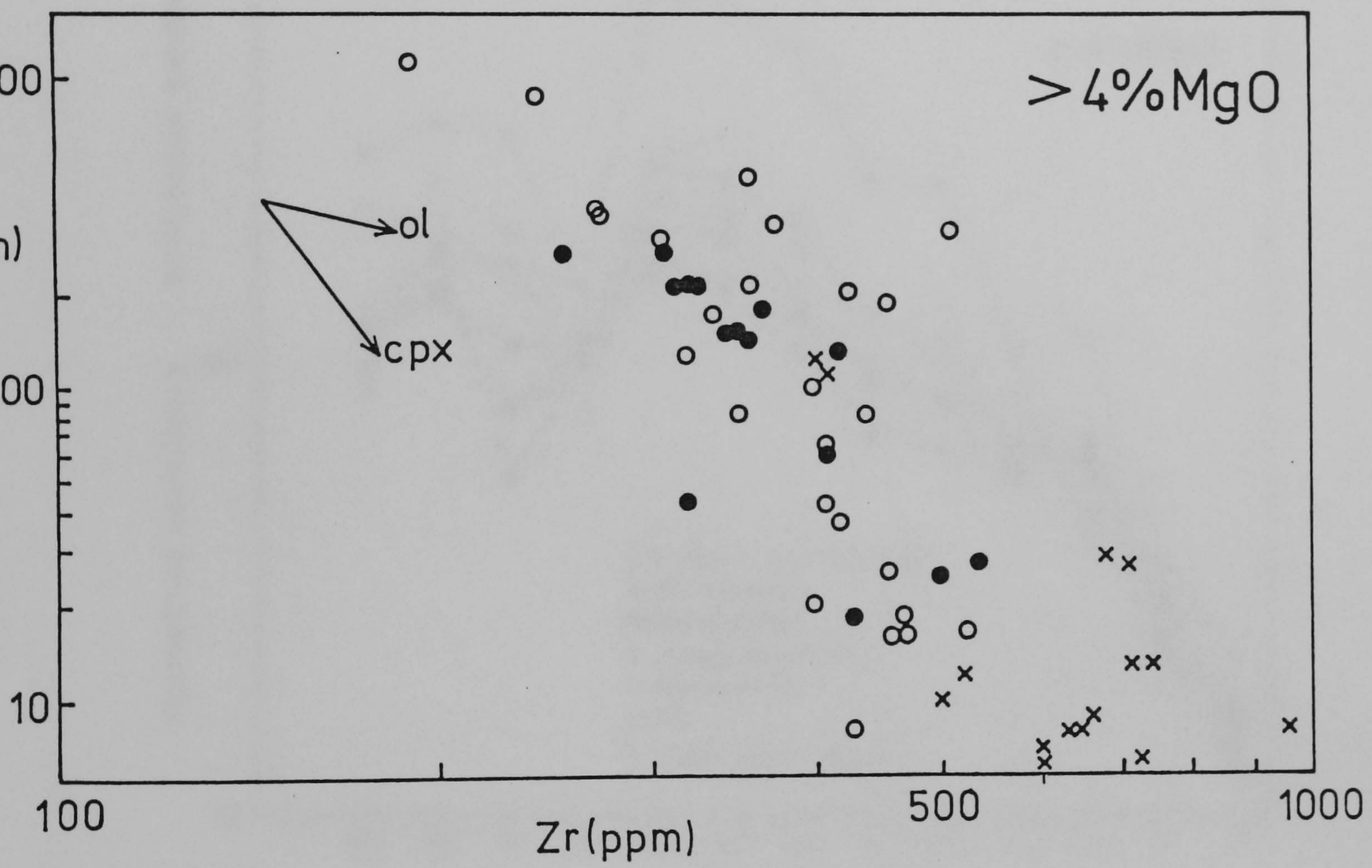


Figure 5.1.5 Cr plotted against Zr for the S. Cameroon volcanoes . Symbols as in figure 5.1.1. Vectors represent 20% fractionation (Pearce and Norry, 1979).

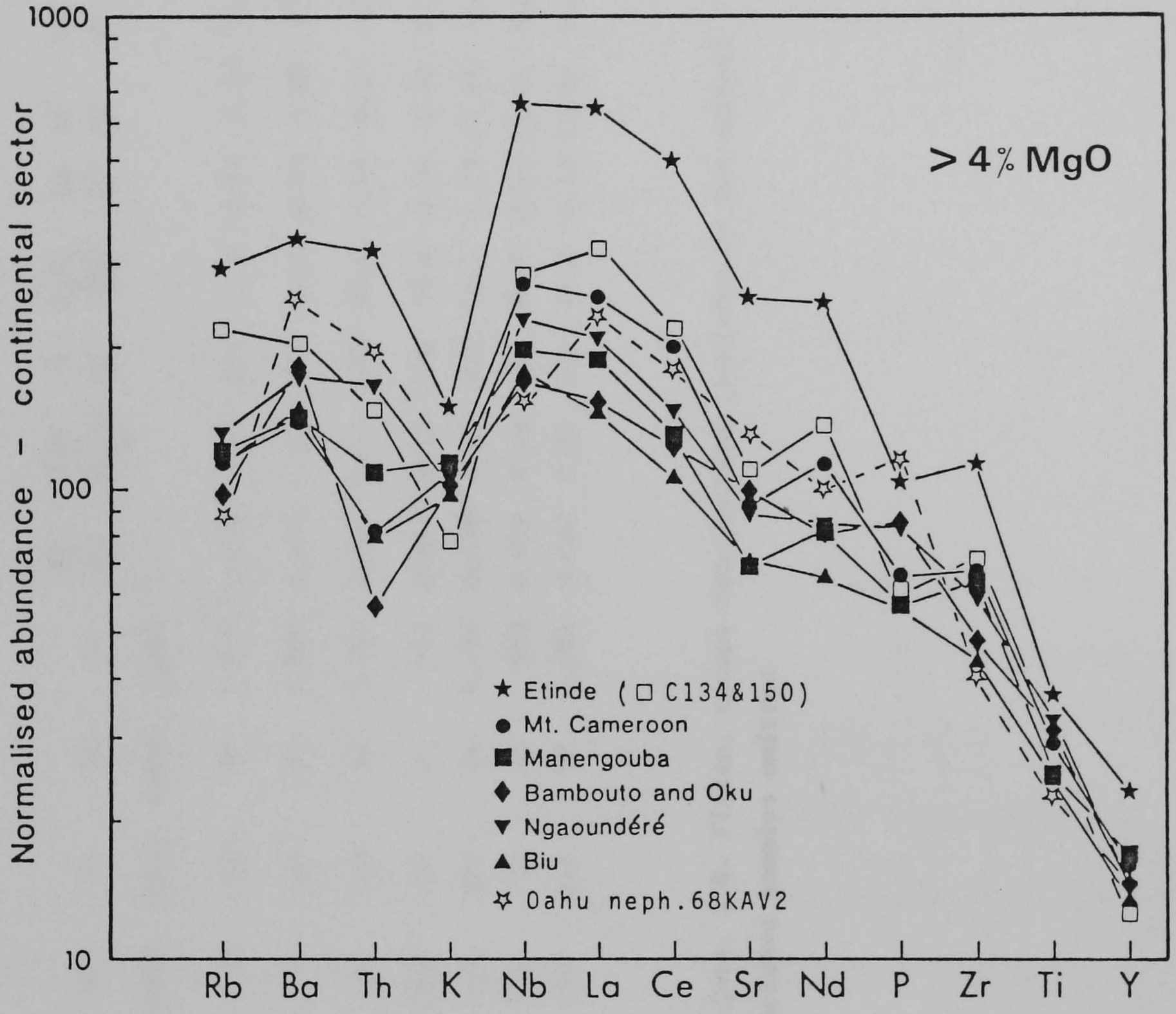


Figure 5.1.6 Normalized mean trace element abundances of lavas from Etinde, Mt. Cameroon, Manengouba, Bambouto, Oku, Ngaoundéré,(all analysed by J.G.Fitton) and the Biu plateau. Also shown is Oahu nephelinite 68KAV2 (Clague and Frey,1982). Normalizing values as in figure 4.4.2 .

TABLE 5.1.1

Mean element abundances and ratios of samples with >4% MgO[a] from Cameroon

Location	N	SiO_2 (Wt%)	MgO (Wt%)	MgN	$Na_2O + K_2O$ (Wt%)	Ni (ppm)	Cr (ppm)	Rb (ppm)	Sr (ppm)	$\frac{Rb}{Sr}$	$\frac{K_2O}{Na_2O}$	$\frac{K}{Rb}$	$\frac{P_2O_5}{Ce}$	$\frac{La}{Ce}$	$\frac{Sr}{Ce}$	$\frac{La}{Y}$	$\frac{Zr}{Y}$	$\frac{Nb}{Y}$	$\frac{Zr}{Nb}$
Mt. Cameroon	24	45.8	7.0	60.1	5.3	71*	162*	40	1,017	0.038	0.41	324	42.6	0.49	6.23	2.51	11.8	3.0	4.0
Etinde	15	40.0	5.3	52.6	6.1	17	26	104	2,801	0.037	0.55	173	26.6	0.50	6.89	4.43	13.8	5.0	2.8
C134+C150 (Etinde)	2	39.7	8.0	59.9	3.6	44	119	82	1,314	0.063	0.41	106	33.8	0.49	6.53	3.42	14.1	3.4	4.2
Manengouba	15	48.0	6.3	56.5	5.3	102	137	41	791	0.051	0.47	346	58.2	0.51	7.20	1.78	11.4	2.3	5.1
Bambouto	11	44.0	8.2	61.8	4.4	118	242	34	1,189	0.028	0.45	340	94.7	0.48	11.50	1.69	8.7	2.1	4.3
Oku	11	46.0	7.5	60.1	4.9	111	172	35	988	0.035	0.46	373	84.7	0.48	10.22	1.61	9.6	2.0	4.8
Mandara	3	42.4	9.7	65.8	4.7	180	295	27	1,096	0.024	0.35	375	81.0	0.52	10.24	1.97	9.7	2.9	3.4

a: Unpublished data, J.G. Fitton, except from Mandara (analysed by the author)

*: 2 cumulus enriched samples omitted

in terms of incompatible element compositions. High immobile element ratios such as Zr/Y (12) and Nb/Y (3) are typical of within-plate basalts (Pearce and Norry, 1979; Pearce, 1982) and are enriched relative to primordial mantle values. Other parameters, usually employed to establish whether a basalt is primary or not (e.g. Frey et al., 1978) such as high Mg numbers (>64), and P_2O_5/Ce ratios of 75 $\pm$ 15 (Sun and Hanson, 1975a) further illustrates the fractionated nature of these lavas where the mean Mg number = 60 and P_2O_5/Ce = 43 (Figure 5.1.12, Table 5.1.1). K/Rb ratios (mean = 324) are fairly typical of alkali basalts, albeit a little lower than the value proposed by Sun and Hanson (1975b), and Hanson (1977). A lack of ultramafic nodules also shows a period of residence in a magma chamber since alkaline volcanics such as these often carry such xenoliths. The fractionation is limited to olivine and clinopyroxene as is evident from the variation diagrams. An inspection of Rb and Sr contents (Figure 5.1.7) illustrates the lack of plagioclase fractionation since there is no horizontal trend of rapidly decreasing strontium contents relative to constant or slightly increasing Rb contents, typical of such crystallization. Mean Rb and Sr concentrations are 40 ppm and 1017 ppm respectively.

Strontium Isotope Studies Unspiked $^{87}Sr/^{86}Sr$ ratios were determined on representative samples (12) from the volcanic suite described above. These samples are marked on Figure 5.1.1. Eleven of the 12 samples studied show a very small range of $^{87}Sr/^{86}Sr$ from 0.70326 to 0.70339 with a mean of 0.70333 (Table 5.1.2). Similarly a very small range in $^{87}Rb/^{86}Sr$ gives rise to a tight clustering of points on the conventional isotope plot (Figure 5.1.8). Since this

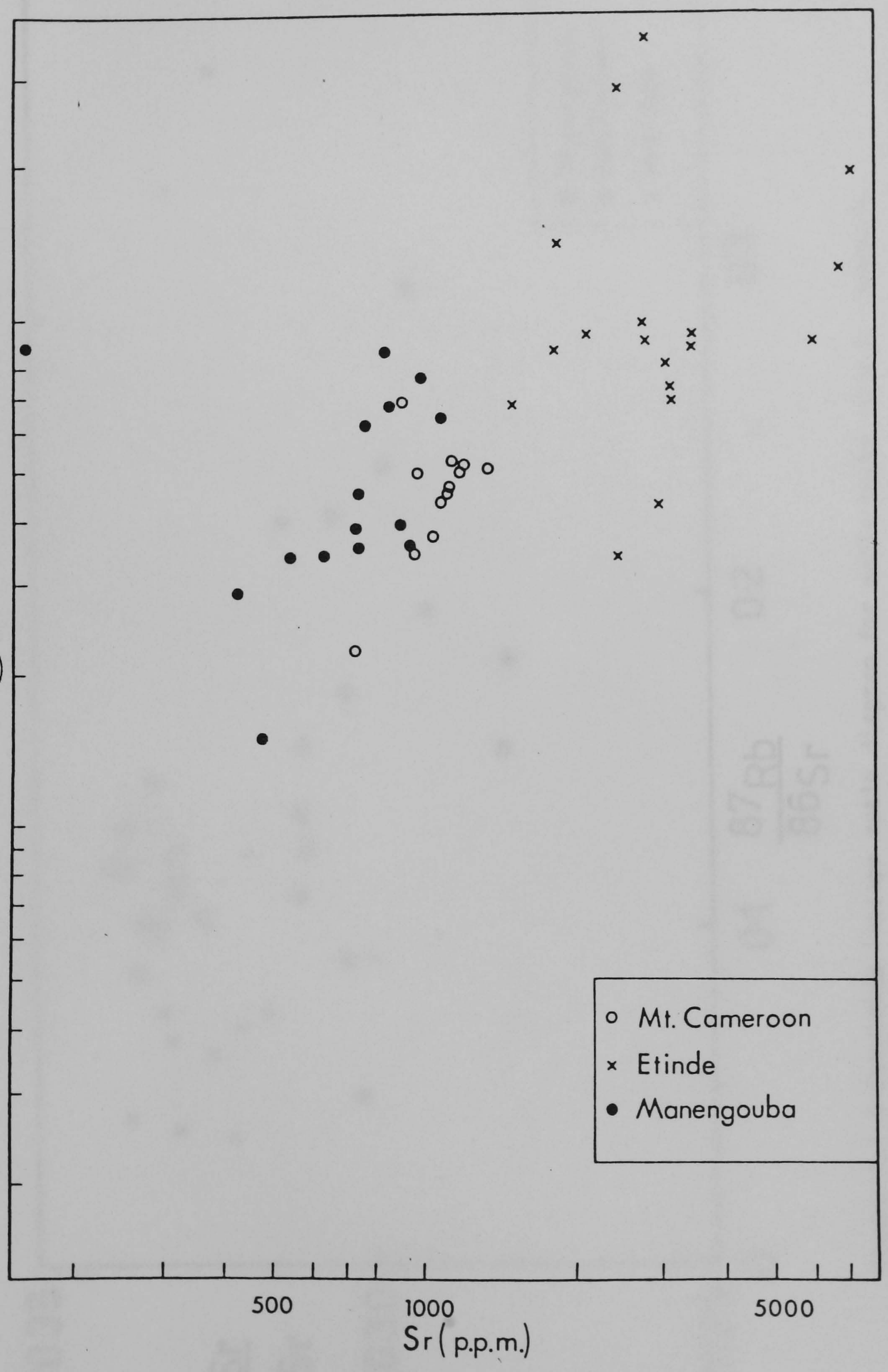


Figure 5.1.7 Rb versus Sr diagram for the S. Cameroon volcanoes

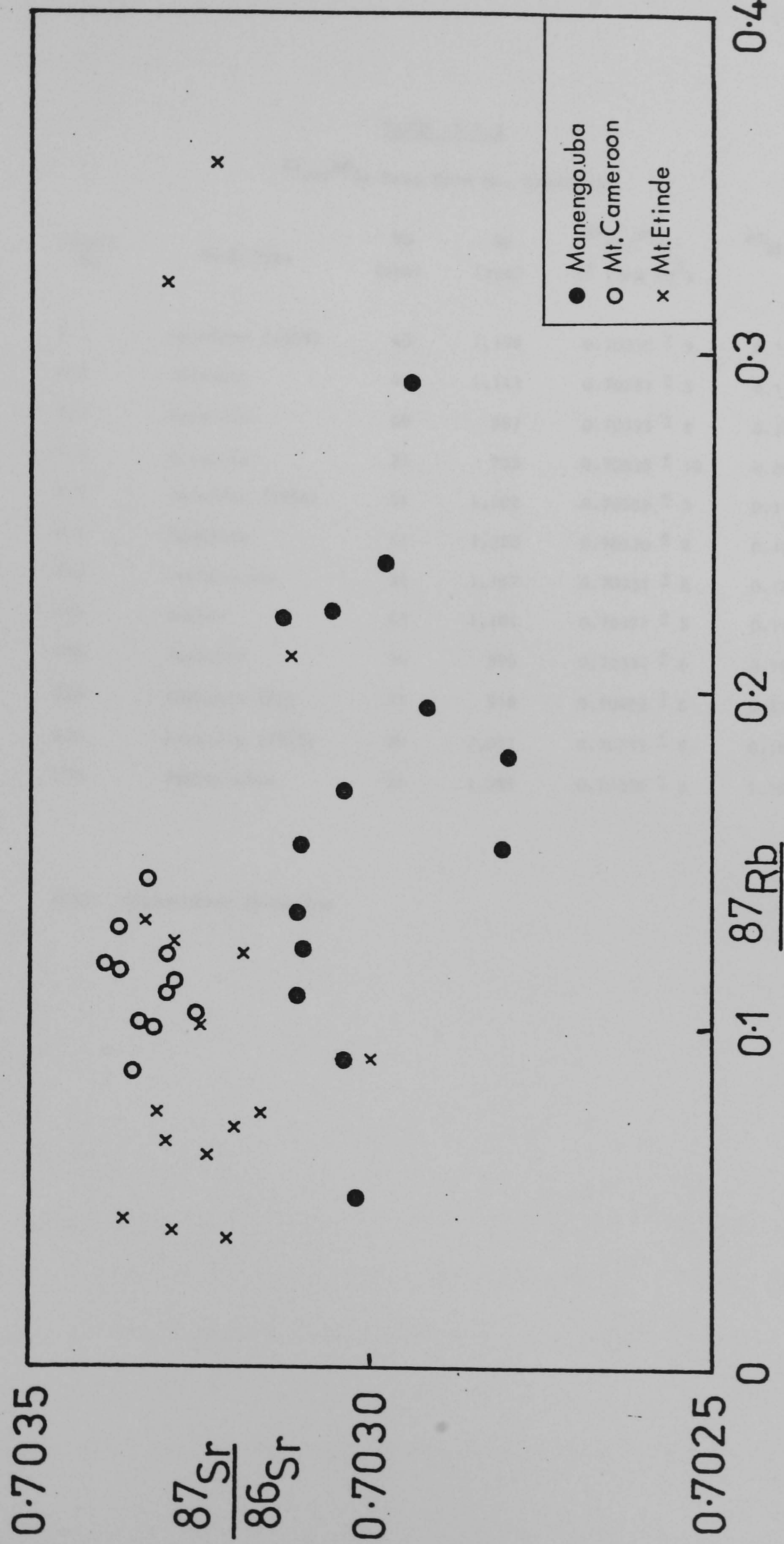


Figure 5.1.8 Strontium isotope ratio diagram for mafic rocks from S. Cameroon.

TABLE 5.1.2

$^{87}Sr/^{86}Sr$ Data from Mt. Cameroon

Sample No	Rock Type	Rb (ppm)	Sr (ppm)	$^{87}Sr/^{86}Sr$ ($\pm 2\sigma \times 10^5$)	$^{87}Rb/^{86}Sr$
C 1	Hawaiite (1959)	43	1,136	0.70330 ± 9	0.1096
C 2	Hawaiite	44	1,143	0.70337 ± 5	0.1166
C 3	Hawaiite	49	987	0.70333 ± 8	0.1435
C 4	Oceanite	21	735	0.70335 ± 10	0.0864
C 5	Hawaiite (1954)	51	1,202	0.70339 ± 5	0.1181
C 6	Hawaiite	51	1,220	0.70330 ± 8	0.1210
C12	Nephelinite	51	1,167	0.70337 ± 8	0.1294
C14	Basalt	43	1,101	0.70327 ± 5	0.1132
C16	Basanite	34	976	0.70334 ± 6	0.1006
C18	Hawaiite (hy)	71	918	0.70402 ± 6	0.2143
C26	Basanite (1922)	39	1,071	0.70332 ± 8	0.1002
C28	Nephelinite	51	1,369	0.70326 ± 5	0.1078

(hy): Hypersthene Normative

volcano is thought to be very recent (3 samples analysed were erupted this centure), age corrections on the observed $^{87}Sr/^{86}Sr$ ratios were considered unnecessary. These values show no correlation with chemical contents, e.g. SiO_2 (Figure 5.1.9). However, the twelfth analysed, C18, gave an elevated initial ratio of 0.70402 (Figure 5.2.4). This sample is the only hypersthene normative (3.54%) hawaiite in the collection. It is possible that its $^{87}Sr/^{86}Sr$ ratio has been disturbed by the assimilation of radiogenic material although no crustal fragments have been observed in this rock. Samples from Bambouto (C74) and Manengouba (C57) show similar isotopic and chemical characteristics and further discussion of these 3 samples is made in Section 5.2.1). Figure 5.1.10 shows that the other rocks display the pattern typical of fresh, uncontaminated oceanic island basalts and therefore, although chemically fractionated the strontium isotopes are largely undisturbed by post-partial melting events such as bulk assimilation, wall-rock interaction, or re-equilibration with the host country rock during residence in a sub-shield volcano magma chamber. These samples are not fractionated enough with regard to their Rb/Sr ratio to be able to observe effects due to protracted magma chamber residence periods.

5.1.2 Etinde

Geochemistry Etinde is a small nephelinite volcano located on the S.S.W. side of Mount Cameroon and predates the voluminous recent activity of the larger volcano (Chapter 3). Lavas show continuous chemical variation from olivine mela-nephelinite (>70% modal mafic minerals) to a nosean-leucite leuco-nephelinite (<40% modal mafic

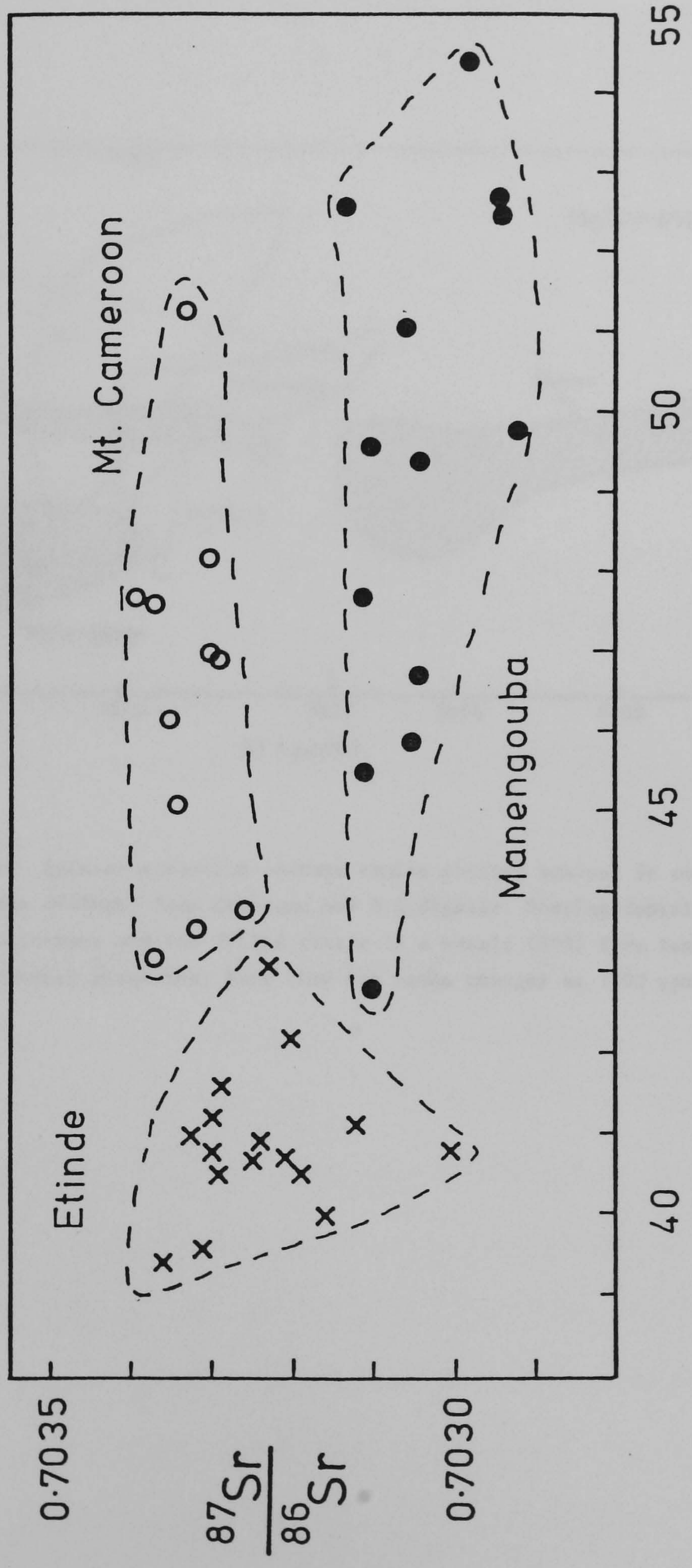


Figure 5.1.9 Initial strontium isotope ratios plotted against SiO_2 contents in mafic lavas from Etinde, Mt Cameroon and Manengouba.

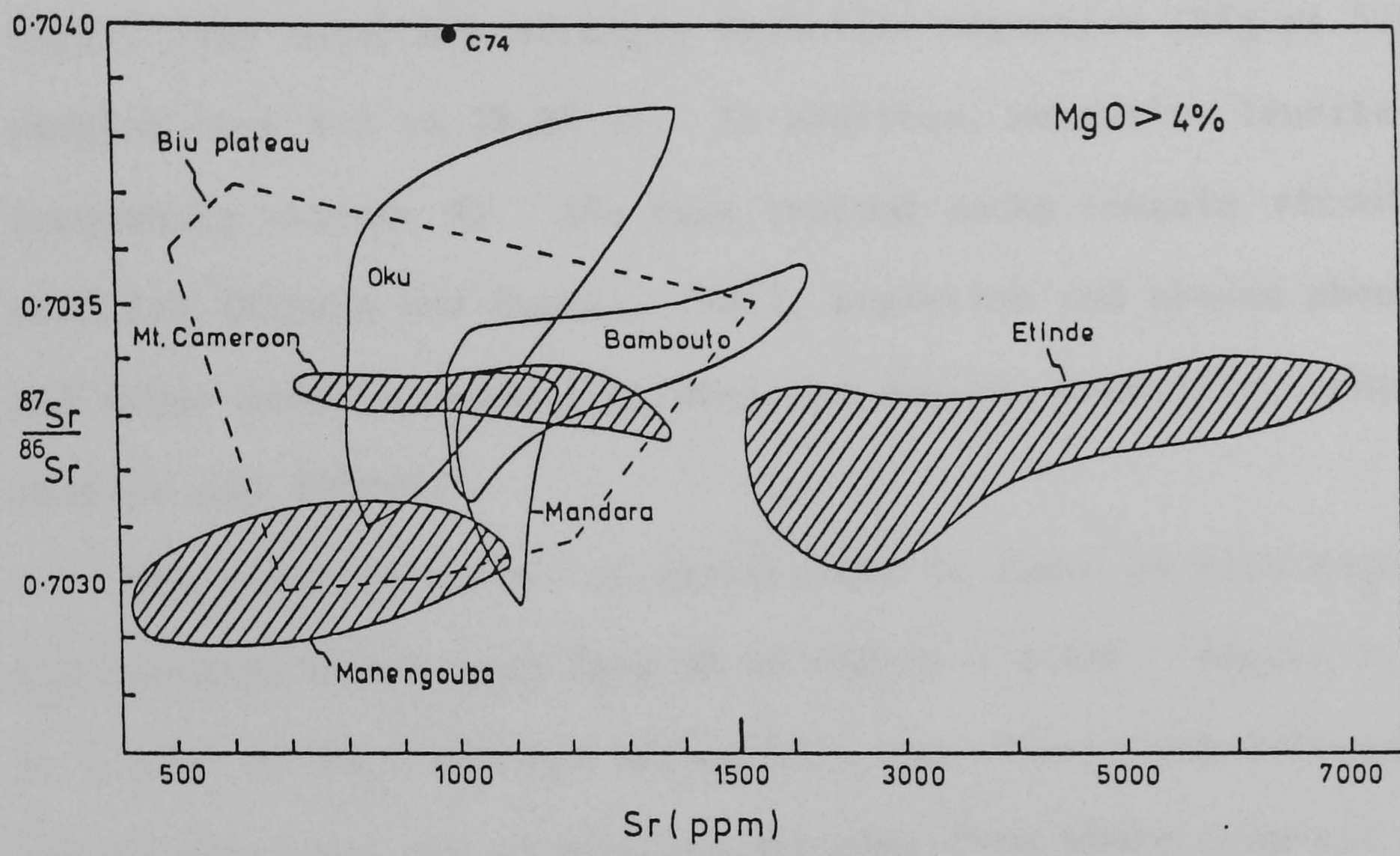


Figure 5.1.10 Initial strontium isotope ratios plotted against Sr contents in mafic lavas (>4%MgO) from Cameroon and N.E.Nigeria. Shading depicts the S.Cameroon volcanoes and the filled circle is a basalt (C74) from Bambouto containing crustal xenoliths. Note that the scale changes at 1500 ppm Sr.

minerals; nomenclature after Streckeisen, 1967). All the lavas contain abundant low pressure aluminous titanaugite phenocrysts; and magnetite, nepheline, apatite, hauyne and perovskite occur in most samples. Resorbed olivine crystals are rare being only present in the most basic samples. Feldspar-bearing lavas have not been reported. All of the samples chemically analysed (J.G. Fitton, unpublished data) are strongly nepheline-normative (Figure 5.1.1) ranging from 6.2 to 39.9% ne. In addition, normative leucite frequently exceeds 5%. The most evolved rocks contain strontian melilite (Fitton and Hughes, 1981), nepheline and nosean phenocrysts and minor leucite, sodalite, aegirine-augite, magnetite, schorlomite, apatite and sphene.

The alkaline nature of these rocks is shown by high Na_2O and K_2O contents which vary from 3% to 15% ($\bar{x}$ = 6.1%). Figure 5.1.3 is a plot of Na_2O and K_2O versus SiO_2 and clearly demonstrates that the Etinde lavas are chemically distinct from those from all other centres within the continental sector of the Cameroon Line. Etinde lavas may also be considered as being "K-rich" since K_2O/Na_2O is 0.5 (Wass, 1980 nomenclature). Although SiO_2 contents are low ($\bar{x}$ = 40%, Table 5.1.1) the entire suite is extensively fractionated as evidenced by low MgO (Figure 5.1.2, $\bar{x}$ = 5.3%), very low Ni and Cr contents ($\bar{x}$ = 17 and 26 ppm respectively, Figure 5.1.4) and a low mean Mg number of 52.6 (Table 5.1.1). In particular the low chromium contents (Figure 5.1.5) suggest a dominance of cpx in the fractionation sequence (as does low Sc). Cognate xenoliths of aluminous pyroxene similar in composition to the phenocrysts (plus nepheline, titanomagnetite and apatite) certainly suggest low pressure clinopyroxene fractionation had occurred. Low Ni contents indicate early olivine extraction

from the liquid. Using the approach of Hart and Davis (1978) and Hart and Allegre (1980), 15-20% olivine fractionation would be necessary to account for the observed Ni levels if 5% partial melting (giving a MgO content of 12%) of pyrolite occurred. A high mean CaO content of 13.5% (Figure 5.1.2) requires the fractionation of a Ca-depleted aluminous pyroxene under polybaric conditions, perhaps continuously from 40 Kb to the surface since low pressure fractionation alone cannot explain this calcium concentration (Fitton and Hughes, in prep.). A similar process has been proposed by Green (1973). Cundari and O'Hara (1976) found cpx to be the only liquidus phase of a potassic magma from 20 to 40 Kb.

The dominance of cpx fractionation over olivine, low MgO and Mg number, high K_2O ($\bar{x}$ = 2.2), very high CaO, high TiO_2, presence of abundant low pressure cpx, lack of ultra-mafic nodules, rare resorbed olivines (present only in the most mafic members of the suite) and volcano type all indicate that Etinde belongs to the Group 2, nephelinite-carbonatite association of Le Bas (1978). Le Bas has described the Principe nephelinites (Chapter 4) as belonging to Group 1 (olivine nephelinites). Another example of the Group 2 association is the Lake Victoria Province of East Africa.

Trace element contents and ratios indicate the very unusual nature of these rocks when compared to the rest of the Cameroon Line. LREE enrichment is extreme with La approximately 650 x chondrite in the more mafic rocks (Figure 5.1.4) as compared to 250 for Mt. Cameroon and 186 for the continental sector average (Cameroon Line rocks with MgO >4%, excluding Etinde). This would suggest magma generation by small degrees of partial melting at deeper mantle levels than the source of alkali olivine basalts (Green and Ringwood, 1967; Green, 1973; Kay and Gast, 1973; Sun and Hanson, 1975b; Frey et al,

1978) perhaps at pressures >20 Kb where garnet is in equilibrium with the melt (Gast, 1968; Basaltic Volcanism Study Project, 1981; Hughes, 1982). Steep LREE enriched patterns are often attributed to residual garnet (and to a lesser extent Ca poor pyroxene) remaining in the source (e.g: Gast, 1968; Kay and Gast, 1973; Sun and Hanson, 1975b; Frey et al, 1978; Yoder, 1976) after partial melting since garnet preferentially retains the HREE (Schnetzler and Philpotts, 1970; Helmke and Haskin, 1973; Shimizu and Kushiro, 1975). However, the presence of garnet is not universally thought to be the explanation for high LREE contents because it would have to be very effective in fractionating the REE which is unlikely since the near constancy of Yb and Lu contents in alkalic rocks worldwide would require extremely uniform garnet abundances and Kds (Wood, 1979; Campbell and Gorton, 1980). Similar extreme enrichments are apparent for the other incompatible elements (Figures 5.1.4, 5.1.6, 5.1.7). In particular the mean value of one of the most incompatible LIL elements, Rb ($\bar{x}$ = 103 ppm) is 2.6 x that of the continental sector average. Wood (1979) and Clague and Frey (1982) showed that high Rb contents are strong indicators of low degrees of partial melting since Rb concentrations are largely unaffected by later fractionation processes (other than those involving K-feldspars). Figure 5.1.6 and Table 5.1.3 show that K, also normally a strongly incompatible element, and P are significantly less enriched than Rb, Ba, Th, Nb, La, Ce, Nd and Sr which are all enriched to the same degree in Etinde lavas. K/Rb ratios are also very low (Table 5.1.1). Relatively depleted K contents may be explained by the presence of a hydrous K-bearing residual phase in the mantle source region. It has been shown experimentally (Green, 1970) that nephelinite can be generated by <15% partial melting at 18-37 Kb of hydrous peridotite. Although phlogopite is usually considered as the

TABLE 5.1.3

Enrichments of some incompatible elements in Etinde Lavas relative to (a) other Cameroon Line continental sector volcanoes and (b) Mt. Cameroon

	Samples with 4 Wt% MgO	Rb	Ba	Th	K	Nb	La	Ce	Nd	Sr	P
(a)	Etinde/Cont. Sector	2.7	2.2	3.5	1.5	3.2	3.6	3.6	3.0	3.1	1.5
(b)	Etinde/Mt. Cameroon	2.6	2.5	4.0	1.4	2.4	2.6	2.6	2.2	2.8	1.6

probable container of alkalies and H_2O in the mantle (Carmichael et al, 1974; Powell and Bell, 1974; Beswick, 1976; Smith et al, 1979; Boettcher et al., 1979; Dawson and Smith, 1982) K-richterite is the most likely residual hydrous phase for Etinde magmas, since the K/Rb ratio would be higher than that observed if phlogopite were to be the residual phase (Sun and Hanson, 1975b). Experimental evidence (Mysen and Boettcher, 1975 ; Wendlandt and Eggler, 1980b) shows amphibole to be a far stronger buffer of vapour compositions than phlogopite, especially at intermediate pressures of about 20 Kb. K-richterite bearing peridotites have been described in the literature by Aoki (1975) and Erlank and Ricard (1977). The presence of amphibole in the source limits the depth of the magma melt zone to 120 km (Aoki, op. cit.). Nephelinites described from the Cape Verde Islands (Klerkx et. al., 1974), Madeira (Hughes and Brown, 1972) and the Roman Province (e.g: Cox et al., 1976) also have low K/Rb ratios. Such a hydrous phase would buffer the K contents but not rubidium (or other LIL elements) which would remain incompatible. As with the pattern observed by Sun and Hanson (1975a), Etinde shows no correlation between K_2O and Ce contents (Figure 5.1.11). In marked contrast basalts from Mount Cameroon show a very strong positive correlation on this diagram indicating an absence of potassic minerals in the source. The Etinde nephelinite data is more scattered probably because of the presence of such a potassic hydrous phase in the residue at smaller degrees of partial melting and also because of perovskite fractionation (see below). Oxburgh (1964) originally suggested the presence of amphibole in the upper mantle and more recently Wood (1979) described negative K patterns (on plots of similar construction to Figure 5.1.6) as being due to refractory minor K-phases during small degrees of anatexis.

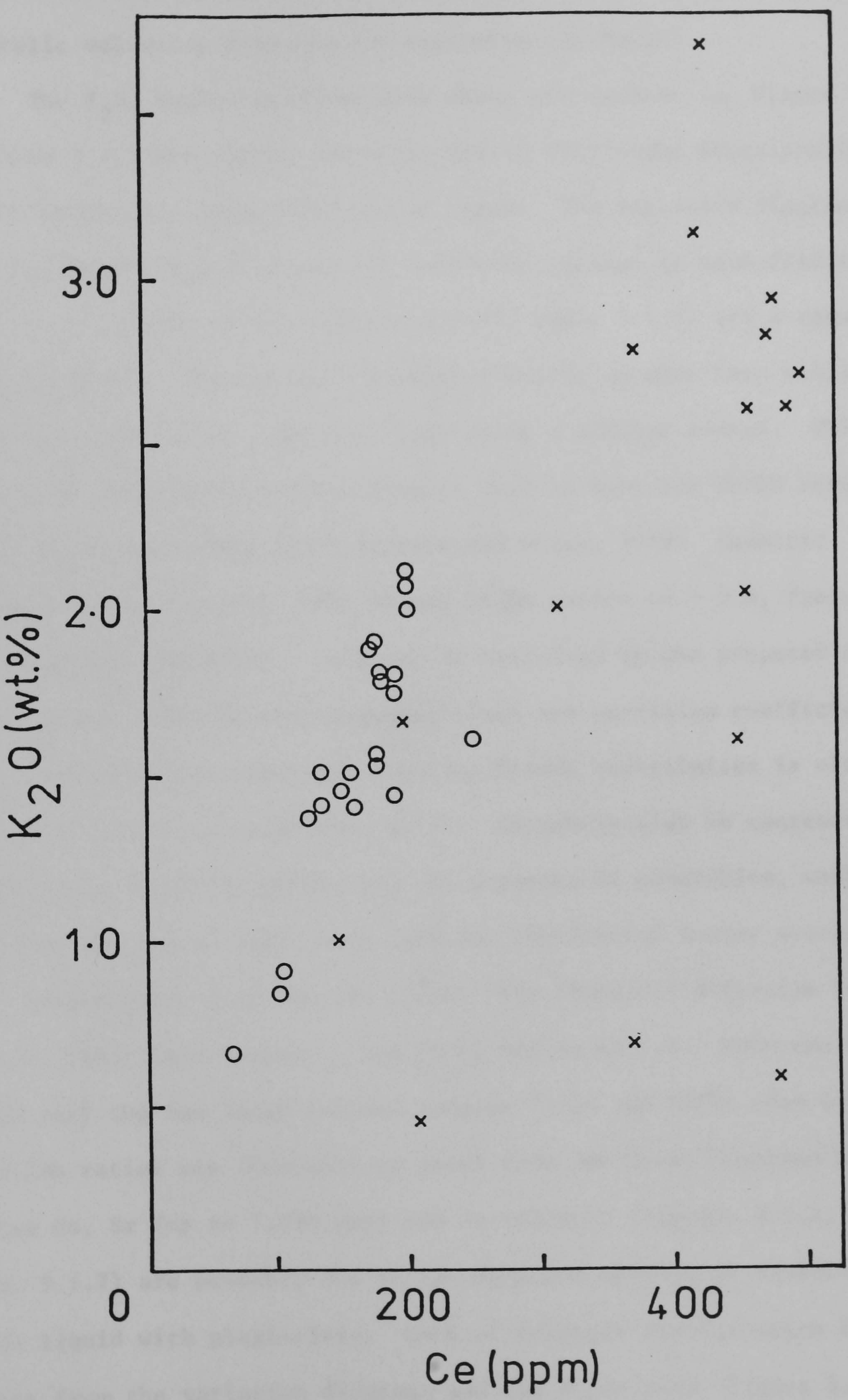


Figure 5.1.11 K_2O plotted against Ce for Mt Cameroon (O) and Etinde (X) lavas.

Wass (1980), Wass and Rogers (1980) and Clague and Frey (1982) also employed residual hydrous phases to account for trace element patterns in alkalic volcanics from Eastern Australia and Hawaii.

The P_2O_5 depletions mentioned above and evident on Figure 5.1.6 and Table 5.1.3 are almost certainly due to continuous fractionation of apatite which is a common phenocryst phase. The variation diagram MgO-P_2O_5 (Figure 5.1.2) shows the inflexion typical of such fractionation. Low P_2O_5/Ce ratios (Figure 5.1.12, Table 5.1.1) are a result of this process. The two most primitive Etinde samples have similar values to those of Mt. Cameroon, indicating a similar source. Whilst alkalic and other within-plate basalts tend to have low Zr/Nb ratios (6-10) relative to MORB (>30) (Pearce and Norry, 1979; Basaltic Volcanism Study Project, 1981) Etinde Zr/Nb ratios ($\bar{x}$ = 2.8, Table 5.1.1) are extremely low. This can be explained by the proposed dominance of cpx in the fractionation sequence since the partition coefficient for Zr in clinopyroxenes separated from the Etinde nephelinites is close to unity (J.G. Fitton, unpublished data). Extremely high Nb contents in Etinde lavas, probably reflecting the presence of perovskite, would also give rise to a lower ratio than the continental sector average of 4.2. Nephelinites from the Rio Grande rift (Basaltic Volcanism Study Project, 1981) have similarly low Zr/Nb ratios of 2.6. When one considers only the two least evolved samples (C134 and C150) from Etinde, the Zr/Nb ratios are identical to those from the Mount Cameroon Lavas.

Extreme Ca, Sr (up to 7,050 ppm) and Ba contents (Figures 5.1.2, 5.1.4, 5.1.6, 5.1.7) are probably due to the complete absence of equilibration of the liquid with plagioclase. Lack of feldspar fractionation is evident from the variation diagrams and the Rb-Sr plot (Figure 5.1.7). The extreme strontium enrichment explains the presence of low pressure

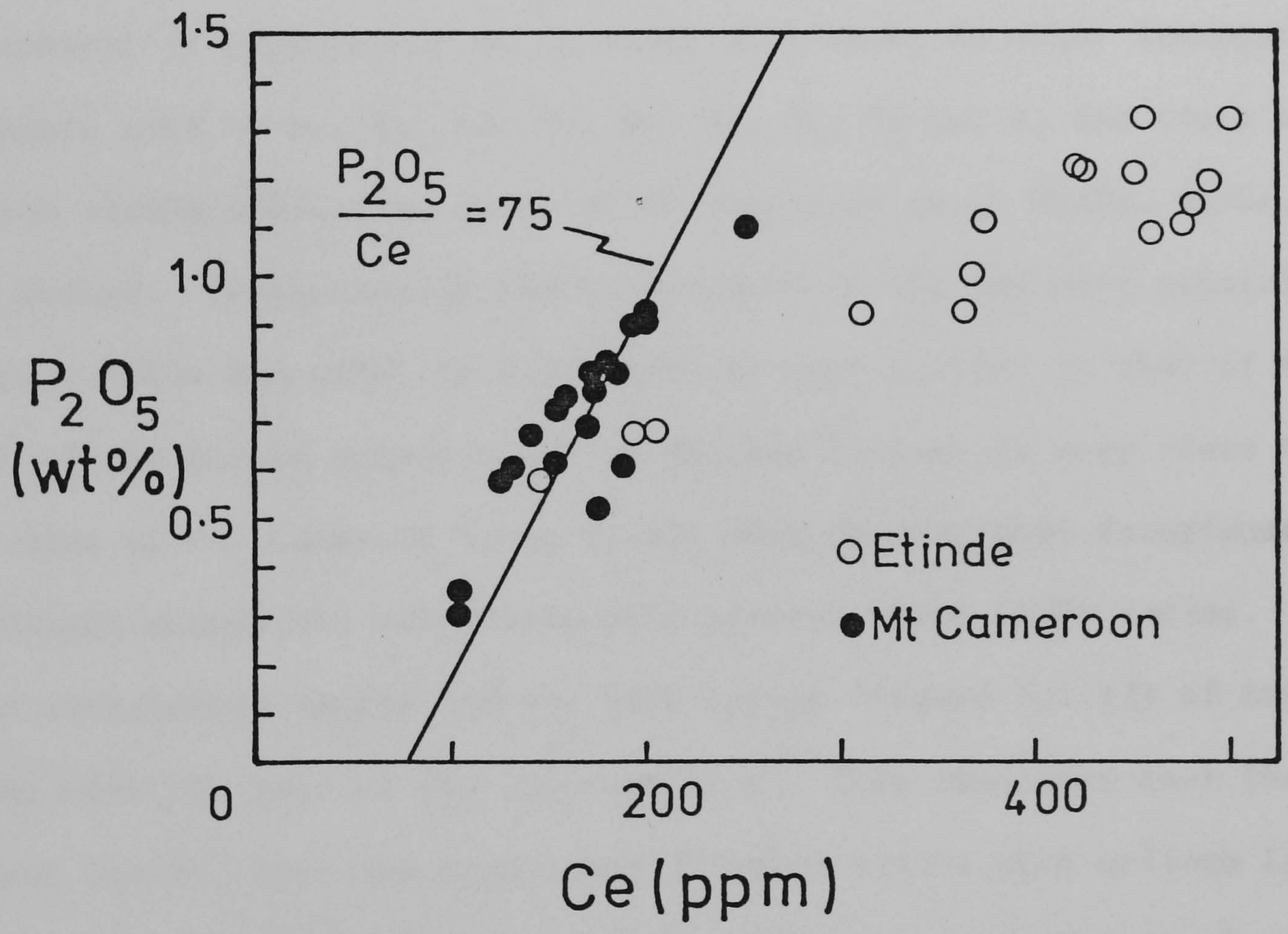


Figure 5.1.12 P_2O_5 plotted against Ce for Mt Cameroon and Etinde lavas.

strontian melilite containing up to 16% SrO (Fitton and Hughes, 1981). This phase must also be present in the groundmass since melilite phenocrysts alone are not abundant enough to account for the whole rock strontium contents. Although Alibert et al. (1981) have described melilites as being of deep seated origin, this mineral is usually considered as only equilibrating at low pressure under conditions of extreme fractionation (O'Hara and Biggar, 1969; Yagi and Onuma, 1978). In Etinde lavas it is only observed in the more fractionated leucocratic nephelinites. A consideration of trace element contents and ratios (Tables 5.1.1 and 5.1.3, and Figure 5.1.6) indicates that the strontium enrichment is accompanied by an equal enrichment in other incompatible elements such as Rb, Ba, La, Ce, Nb, Nd, Zr, Ti and Y, and trace element ratios remain similar to those of Mt. Cameroon (e.g. Rb/Sr, Ba/Ce, La/Ce and Nb/La). In particular the Sr/Ce ratio of the two most primitive samples (C134 and C150) is 6.53 which is very similar to that of the rest of the Etinde nephelinites (6.89) and in turn is very close to the mean of Mt. Cameroon lavas (6.23) thus showing that fractionation of Etinde magmas has not drastically altered their La/Ce ratios. A good correlation exists for the LREE ratios (Figure 5.1.13) of Etinde lavas with the rest of the Cameroon Line. This indicates that the Etinde and Mt. Cameroon magmas had a common source with uniform La/Ce and Nd/Ce ratios and that the data are largely controlled by the extent of either partial melting or zone refining (Sun and Hanson, 1975b). However, the slight deviation of the more fractionated Etinde rocks away from the general Nd-Ce correlation probably reflects clinopyroxene fractionation since diopside is enriched in Nd relative to Ce (Hanson, 1980). Scatter on trace element diagrams such as Figures 5.1.6 and 5.1.13 is probably also controlled by minor phases such as perovskite

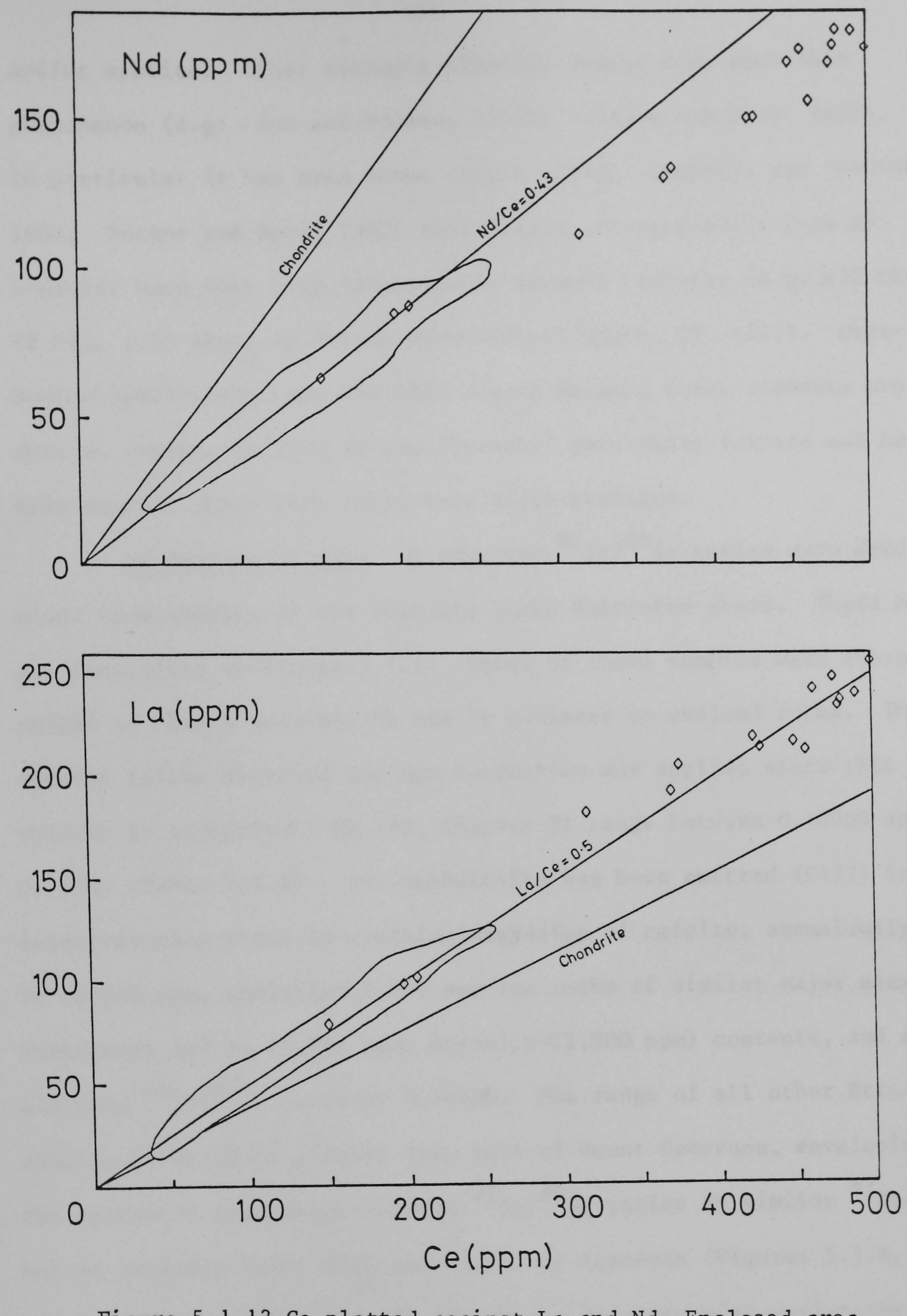


Figure 5.1.13 Ce plotted against La and Nd. Enclosed area is the total range described by Pagalu, Sao Tome, Principe, Bioko, Mt Cameroon, Manengouba, Bambouto, Oku, Mandara and Biu. ◇ = Etinde. All samples MgO >4%.

and/or apatite. Other strongly alkaline magmas also show this phenomenon (e.g: Sun and Hanson, 1975b; Clague and Frey, 1982). In particular it has been shown (Smith, 1970; Campbell and Gorton 1980; Boctor and Boyd, 1982) that species of perovskite such as loparite have very high incompatible element contents (e.g: >7% LREE, 1% SrO, 1.5% Nb_2O_5 in Etinde perovskites, Smith, op. cit.). Distribution coefficients for the LREE are >2 because these elements are able to replace calcium in the distorted perovskite lattice and hence this mineral shows very steep rare earth profiles.

Sr Isotope Studies 18 unspiked $^{87}Sr/^{86}Sr$ ratios were determined from samples of the volcanic rocks described above. These samples are identified on Figure 5.1.1. Three of these samples were subsequently spiked to obtain accurate Rb and Sr contents on evolved rocks. The isotope ratios observed (no age correction was applied since this volcano is probably<1 Ma old, Chapter 3) range between 0.70300 and 0.70336 (Table 5.1.4). One nephelinite has been omitted (C127) from interpretation since it contains amygdales of calcite, anomalously high Sr (6,935 ppm, normally<3,000 ppm for rocks of similar major element chemistry) and Ba (3,617 ppm, normally<1,000 ppm) contents, and an elevated $^{87}Sr/^{86}Sr$ ratio of 0.70346. The range of all other Etinde samples is slightly greater than that of Mount Cameroon, enveloping the spread of the larger volcano $^{87}Sr/^{86}Sr$ ratios at similar $^{87}Rb/^{86}Sr$ but at markedly lower SiO_2 and higher Sr contents (Figures 5.1.8, 5.1.9, and 5.1.10 respectively). No trends are observed with variations in Rb/Sr ratios or with chemistry; not even with the two extremely fractionated lavas (C36, C131) which contain 202 and 349 ppm Rb respectively. The extremely high Sr contents would preclude the possibility of these rocks being contaminated (Alibert et al., 1981), thus Etinde strontium isotope ratios can be confidently taken to represent the value of the

TABLE 5.1.4

Etinde $^{87}Sr/^{86}Sr$ Data

Sample	Rock Type	K-Ar Age (Ma)	Rb (ppm)	Sr (ppm)	$^{87}Sr/^{86}Sr$ ($\pm 2\sigma \times 10^5$)	$^{87}Rb/^{86}Sr$
Mafic Rocks						
C 20	Nephelinite	85(84.2)[a]	3,272(3,267)[a]		0.70330 ± 10	0.0752
C 21	Nephelinite	55	3,141		0.70329 ± 4	0.0507
C 23	Nephelinite	291	2,570		0.70330 ± 10	0.3276
C 31	Nephelinite	94	3,218		0.70316 ± 6	0.0845
C 32	Nephelinite	76	3,272		0.70324 ± 7	0.0672
C 33	Nephelinite	145	1,949		0.70312 ± 8	0.2153
C 34	Nephelinite	100	2,910		0.70325 ± 10	0.0994
C 35	Nephelinite	46	2,684		0.70321 ± 8	0.0496
C126	Nephelinite	101	6,147		0.70336 ± 3	0.0475
C127	Nephelinite	129	6,935		0.70346 ± 6	0.0538
C128	Nephelinite	96	3,606		0.70320 ± 5	0.0770
C129	Nephelinite	91	1,887		0.70333 ± 6	0.1395
C130	Nephelinite	99	3,599		0.70331 ± 7	0.0796
C132	Nephelinite	102	2,147		0.70319 ± 7	0.1375
C133	Nephelinite	99	2,939		0.70300 ± 8	0.0975
C134	Nephelinite	76	1,574		0.70329 ± 8	0.1397
Evolved Rocks						
C 36	Leuconephelinite	0.07	200(202)[a]	7,053(7,055)[a]	(0.70333 ± 6) (0.70333 ± 8)	0.0829[a]
C131	Leuconephelinite	349(349)[a]	2,825(2,818)[a]		0.70323 ± 8	0.3584

a : Isotope Dilution Analyses

underlying mantle source region. High strontium contents indicate a mantle origin at depths where plagioclase is not a stable residual phase (Alibert et al., 1981) and probably at depths where garnet is stable considering the extreme LREE enrichment. The idential $^{87}Sr/^{86}Sr$ ratios obtained from the leuconephelinites and their mafic counterparts illustrates convincingly that extreme low-pressure fractionation, resulting in low Ni, Cr, MgO contents and Mg numbers has imposed no effects on the Sr isotope ratios.

Discussion Over the past 20 years a vast amount of literature has accumulated concerning the genesis of alkalic volcanic rocks but to date their origin remains highly controversial. Although the generation of hyperalkaline nephelinites and carbonatites was originally attributed to limestone assimilation (Daly, 1910; Rittmann, 1933) it is now generally accepted on geological grounds (Holmes, 1950; Prider, 1960; Borley, 1967), experimental data (e.g: Wyllie, 1974) and Sr and O isotopes (Hoefs and Wedepohl, 1968; Powell and Bell, 1974; Turi and Taylor, 1976) that such a process is inapplicable. The only points on which all workers in this field agree is that nephelinites are derived by lower levels of melting at greater depths than that of transitional-mildly alkaline basalts (e.g: Green and Ringwood, 1967; Green, 1973). Otherwise, the origin of alkalic magmas has been attributed to a variety of mechanisms. (1) Various processes of assimilation of continental crust (e.g: Barbieri et al., 1975; Turi and Taylor, 1976; Taylor and Turi, 1976), in particular where $^{87}Sr/^{86}Sr$ ratios are elevated (Bell and Powell, 1969, 1970; Faure and Powell, 1972; Faure et al., 1974; Cox et al., 1979). (2) High pressure fractionation of picritic or alkali ultrabasic magma (Borley 1967; O'Hara,

1965, 1968; O'Hara and Yoder, 1967; Ferguson and Cundari, 1975). (3) Small degrees (<3%) of partial melting at deep levels (>15 Kb) of hydrous peridotite perhaps containing phlogopite and/or amphibole but having not more than 2 x REE of chondrites (Gast, 1968; Kay and Gast, 1973; Carmichael et al, 1974; Klerkx et al., 1974). (4) Disequilibrium partial melting (either on the isotopic or trace element level) of relatively homogeneous mantle containing phlogopite, apatite or other LREE rich accessory phases (Powell and Bell, 1974; James, 1975; Beswick, 1976; Beswick and Carmichael, 1978; Campbell and Gorton, 1980). (5) Larger degrees of partial melting (>3%<15%) of a heterogeneous upper mantle, again probably containing phlogopite and/or amphibole but anomalously enriched in K and incompatible elements (e.g. 5-10 x chondrites for the LREE) perhaps via alkali metasomatic processes either precursary to, or concomitant with, partial melting (Lloyd and Bailey, 1975; Aoki, 1975; Frey and Green, 1974; Harte and Gurney, 1975; Cox et al., 1976; Boettcher et al., 1975, 1979; Mysen and Holloway, 1977; Hanson, 1977; Pankhurst, 1977a; Sun and Hanson, 1975a, 1975b; Le Bas, 1977; Erlank and Richard, 1977; Hertogen et al., 1978; Frey et al., 1978; Duda and Schminke, 1978; Hawkesworth and Vollmer, 1979; Wood, 1979; Boettcher and O'Neil, 1980; Menzies and Murthy, 1980a, 1980b; Wendlandt and Eggler, 1980a, 1980b; Wass and Rogers, 1980; Clague and Frey, 1982; Barton and Hamilton, 1982; Boctor and Boyd, 1982). (6) Zone refining in the mantle (Harris, 1957; Kushiro, 1968; Harris and Middlemost, 1969; Harris, 1974; Kay, 1975; Green and Leiberman, 1976).

With regards to Etinde, the first two of the above hypotheses can be immediately ruled out. Low $^{87}Sr/^{86}Sr$ ratios (0.70300 - 0.70336) when considered alone cannot catagorically dismiss crustal contamination or extensive crustal wall-rock reaction because their extreme Sr contents

would mask any such effects. However, when taken together with the lack of correlation of $^{87}Sr/^{86}Sr$ with Rb/Sr, Sr or other elements (as observed by Hurley et al., 1966; Bell and Powell, 1969, 1970; Powell and Bell, 1970, 1974; Faure et al., 1974; Vollmer, 1975, 1976, 1977; Cox et al., 1976; Barbieri et al., 1975; Hawkesworth and Vollmer, 1979; Turi and Taylor, 1976) and the lack of crustal xenoliths all strongly suggest contamination of Etinde magmas by continental crustal material did not occur. The lack of cognate xenoliths or xenocrysts of high pressure origin does not support the second hypothesis. Recent experimental work (e.g. Wendlandt and Eggler, 1980a) suggests that strongly alkalic magmas cannot be generated by crystal fractionation processes operating on ultrabasic magmas.

At first sight hypothesis three is very appealing since virtually all mafic magmas from the Cameroon Line and similarly from other magmatic provinces (e.g: E. Australia, Frey et al., 1978) could be derived from one source having no more than 2 x chondritic REE abundances simply by varying the degree of partial melting and the depth. However, it is very hard to envisage such small melt fractions (sometimes $< 1\%$ as in the case of some nephelinites) rising to the surface (O'Hara, 1968; Harris, 1974; Sleep, 1974; Yoder, 1976; Arndt, 1977) or to near surface magma chambers. Furthermore O'Hara (1968) showed that at such very limited degrees of partial fusion residual phases (such phases are postulated by many workers as being necessary for the production of alkalic magmas) exercise only limited control over major element compositions in the melt. It is still possible however, that the rarity of alkalic rocks indicates that special tectonic conditions, rarely attained, are necessary to bring about segregation of such melts and to allow their passage to the surface.

If we now consider hypotheses 4 and 5, it is generally accepted that phlogopite and/or amphibole or other accessory phases (e.g. apatite or perovskite) is a geochemical necessity in the source mantle peridotite of these rocks (see references cited above under hypotheses 4 and 5 and Dawson and Smith, 1982 for review). Their presence has been shown petrographically (Dawson et al., 1970; Jackson and Wright, 1970; Aoki, 1975; Carswell, 1975; Dawson and Smith, 1975); discussed in experimental works (Yoder and Kushiro, 1969; Flower, 1971; Modreski and Boettcher, 1973; Carswell, 1975; Edgar et al., 1976; Eggler, 1976, 1978; Holloway and Eggler, 1976; Eggler and Holloway, 1977; Mysen and Holloway, 1977; Wendlandt and Eggler, 1980b); and considered to be in isotopic equilibrium with other mantle phases on the basis of their strontium isotopes (Menzies and Murthy, 1980a, b) and $\delta^{18}O$ ratios (Kurodo et al., 1975, 1977). δD is much more variable however (Boettcher et al., 1979; Boettcher and O'Neil, 1980) with micas having typical mantle values between -58 and -79‰ whereas amphiboles have highly variable values ranging from -113 to +8.2‰ indicating complicated shallower processes involving discrete aqueous fluid. Disequilibrium partial melting (hypothesis 4) has been discounted as a mechanism on isotopic grounds and mantle diffusion rates (Hofmann and Hart, 1978). However, Campbell and Gorton (1980) showed, on the basis of LREE distributions in several possible mantle accessory phases that disequilibrium partial melting could still occur, at the trace element level.

Recently, hypotheses 5, that of larger degree of melting (>3%) of an enriched mantle has received much attention and support in the literature; particularly in models where the mantle has suffered recent enrichment by metasomatism resulting in the influx of K, LILE, etc., either preceding or during magmatic activity (see references cited above). Such an enrichment event must have been geologically recent

since Sm-Nd isotope studies (e.g: De Paolo and Wasserburg, 1976b) preclude source regions from being LREE enriched for a very long time (100 - 1,000 Ma). Returning to the Cameroon Line, if metasomatism had occurred during or before the genesis of the Etinde magmas one would have expected to see more varied and probably elevated $^{87}Sr/^{86}Sr$ ratios since, by definition metasomatism involves the non-isochemical introduction of elements from an external source. Some workers (Boettcher and O'Neil, 1980; Menzies and Murthy, 1980b) suggest that hydrous minerals form during such metasomatism and certainly such minerals as pargasite, phlogopite and kaersutite can show elevated $^{87}Sr/^{86}Sr$ values (e.g: Basu, 1978) and highly variable δD ratios (as outlined above). Etinde data are similar to, but very slightly lower than, those from less alkalic rocks from neighbouring Mt. Cameroon (Etinde $\bar{x}$ = 0.70324; Mt. Cameroon $\bar{x}$ = 0.70333, Figures 5.1.9, 5.1.10) . Melting of a metasomatically veined mantle would produce magmas with anomalous isotopic compositions and a recent integrated Pb-Sr-Nd isotopic study of basalts from various environments (Zindler et al., 1982) suggest metasomatic processes, which fractionate parent/daughter and daughter/daughter ratios, do not have an important role in determining the chemistry of the mantle. Thus the kind of metasomatism described above is considered inappropriate for Etinde (and also for the remainder of the Cameroon line volcanoes) although it is acknowledged that the degree of partial melting cannot be the only controlling factor and that the presence of volatiles is a necessary requisite for the formation of alkalic basalts (as shown by Mysen and Holloway, 1977).

The last hypothesis mentioned above (6), that of zone refining, has been largely rejected in most discussions concerning the generation of strongly alkalic magmas. The original concept (Harris, 1957) involved a mechanism whereby as the first melt advances it simultaneously

assimilates material above it. Initially this is material which has not previously undergone melting. Hence equilibration of a small amount of melt with a very large volume of rock of similar composition was postulated as resulting in strong enrichment in the incompatible elements with little change in the major element chemistry (Harris and Middlemost, 1969; Harris, 1974; Kay, 1975; Green and Lieberman, 1976). Thus magmas derived by such a process would be indistinguishable from those resulting from very small degrees of partial melting (Harris, 1974; Sun and Hanson, 1975b). In most discussions concerning alkalic magma petrogenesis this hypothesis has been rejected because it would require a continual supply of superheat to enable assimilation to occur and subsequent heat loss would prohibit the advance of the molten layer and result in crystallization (Yoder, 1976; Pankhurst, 1977a; Cox et al., 1979). In addition the process would be terminated if a refractory layer was encountered. Bailey (1974a) made the important point that this process is also inadequate because the magma at higher levels would have to correspond to the appropriate melt-product for the lower-pressure environment and would therefore not be nephelinitic. Hanson (1977) postulated, on the basis of the constancy of LREE ratios regardless of concentration, that zone refining (as described by Kay, 1975; Green and Lieberman, 1976) was untenable. He showed on a diagram of La versus Ce that a curve would be expected rather than the straight line actually observed. However, the slight curve and the straight line are very close to one another (Figure 6 in Hanson, 1977). Powell and Bell (1974) argued that if a melt undergoes zone refining it should equilibrate isotopically with the vertical section of the upper mantle through which it passes and therefore such melts should have $^{87}Sr/^{86}Sr$ ratios similar to the upper mantle average.

They concluded zone refining was therefore not capable of producing "the wide range of $^{87}Sr/^{86}Sr$ ratios observed even within a single area like the Birunga Province", and hence accounted for the observed strontium isotope ratios by invoking crustal contamination. As I stated earlier, Etinde strontium ratios (and nephelinites from some other provinces) do in fact show typical mantle values and therefore zone refining could be a viable mechanism for the Etinde magmas but for the problem of the quantities of thermal energy required.

If one then considers a mechanism similar to the above but without assimilation, in which a diffusion of incompatible elements occurs into a magma from the walls of the conduits through which it ascends (e.g. Green and Ringwood, 1967), a similar effect would arise. Such a process would achieve an enrichment in incompatible elements without resorting to whole-rock assimilation. Watson (1982) showed the viability of such a mechanism by invoking an infiltration-precipitation process he termed "chemical stoping." This process would be effective if the melt existed as intergranular films (e.g. Kramers et al., 1981). Cox et al. (1979) were opposed to this process because although zone refining could satisfactorily explain observed volatile element (such as K, Rb) concentrations, they considered that this mechanism would not account for REE contents since diffusion rates for the REE are not high enough. Wendlandt and Harrison, (1979) on the other hand give convincing experimental and petrographical evidence showing that REE *are* mobile under CO_2 rich volatile conditions at upper mantle pressures. In addition it has been shown that grain boundaries are often enriched in REE and incompatible elements (e.g. Suzuki, 1981; Stosch, 1982). The ubiquitous presence of small (<30μm) biphase fluid inclusions in mantle minerals such as opx, cpx,

olivine, and chrome spinel (Roedder, 1965, 1976, 1979; Funkhauser and Naughton, 1968; Green and Radcliffe, 1975; Murck et al., 1978; Kirby and Green, 1980; Johan and Le Bel, 1980; Dunlop, 1982; Kyser and Rison, 1982) have been shown to be enriched in REE and alkalies (Green, 1979; Stosch, 1982) and of mantle origin since they have δD values between -60 and -85 (Kuroda et al., 1977; Dunlop and Fouillac, in prep).

There is therefore, evidence that REE and incompatible elements are concentrated on grain boundaries and within fluid inclusions in the upper mantle. Hence the process proposed is a mechanism whereby as the melt advances it becomes enriched in these elements without changing the major element chemistry.

When one considers the two least fractionated Etinde samples (C134, C150; Table 5.1.1) it is apparent that they overlap the Mt. Cameroon (and other S. Cameroon centres, Figure 5.1.6) field on major and trace element variation diagrams (Figures 5.1.2, 5.1.4), in $^{87}Sr/^{86}Sr$ values (Table 5.1.4), and have similar trace element abundances and ratios (Tables 5.1.1 and 5.1.3), being only slightly enriched in incompatible elements. Exceptions to this are that the most incompatible element, Rb, is present in double the concentration observed in Mt. Cameroon. Likewise Ba and LREE values are also higher. As with the rest of the Etinde nephelinites, K contents are depleted in C134 and C150 relative to other incompatible element concentrations when compared to the Mt. Cameroon basalts. These two samples are also very similar to a typical nephelinite from Oahu (data from Clague and Frey, 1982), which has also been plotted on Figure 5.1.6, except that the Etinde nephelinites are significantly enriched in Rb, Nb, Zr and Ti.

To conclude this section, strontium isotope data and incompatible element concentration and ratios suggest Etinde shares the same source with Mt. Cameroon and that the chemical differences may be explained by smaller degrees of anatexis in the case of Etinde (3-7%, c.f. Sun and Hanson, 1975a) at deeper levels of a peridotite mantle containing amphibole or phlogopite and perhaps with relatively high CO_2/H_2O ratios (e.g: Brey and Green, 1977; Duda and Schminke, 1978; Wendlandt and Eggler, 1980a). Fluid inclusions in mantle minerals and glass frequently have high CO_2/H_2O ratios indicating that CO_2 is the predominant volatile component in the environment of phenocryst formation (Roedder, 1965; Murck et al., 1978). Paucicity of olivine may also be evidence for $fCO_2 > H_2O$ (Bailey, 1974a) which would enhance the migration of alkalies. After segregation the melt advances through the upper mantle by a diffusive zone refining process as described above. Subsequent extensive, intermediate to low pressure evolution (as evidenced by low MgO, Ni, Cr, lack of ultramafic xenoliths and presence of low pressure minerals such as leucite) produced the rocks sampled. Although evidence in the literature (cited above) for the occurrence of metasomatism before or during magma generation is very strong, particularly with regard to kimberlites, the data presented here and in Chapters 4, 6 and 7 (derived from a very comprehensive suite of samples) covering a province over 1,600 km long, can be accounted for without resorting to mantle metasomatism.

5.1.3 Manengouba

The Manengouba volcanic massif (Figure 3.2.1) consists of two calderas, Elengoum and Eboga. Elengoum is considered as having been active in the period 1.5 Ma to 0.5 Ma ago and is composed mainly of

quartz normative trachytes with lesser volumes of both hypersthene and nepheline normative basalts, and intermediates. Eboga probably started< 0.8 Ma ago and was active until recent times. The younger centre shows a complete spectrum of volcanic rocks from basalt through hawaiite and mugearite to quartz-normative trachyte. However the most recent lavas, small cones and explosion pits, occurring after caldera collapse, appear to be restricted in composition to basalt and mugearite.

Figure 5.1.1 shows the distinctly transitional character of the Manengouba mafic and intermediate rocks, ranging continuously from 8% normative ne to 0.8% normative qz and a D.I. varying between 30 and 61. Figure 5.1.3 illustrates that these rocks do not enter the strongly alkaline field and that they contain higher SiO_2 concentrations than either Mt. Cameroon or Etinde for a given $Na_2O + K_2O$ content. Very primitive rocks have not been recovered, the most basic sample having a MgO content of 8.4%. Since most of these samples come from Eboga and mafic-intermediate rocks from the two calderas have similar chemistry the data have been grouped together under the same symbol in all the diagrams. Further geochemical analyses (particularly on samples from Elengoum) have however shown that the later Eboga activity is more alkaline than Elengoum (C.A. Hirst, pers. comm. 1982). The major element variation diagrams (Figures 5.1.2) show a pattern of continual fractionation from 2.3 to 8.4 wt% MgO. With respect to Mt. Cameroon and Etinde, Manengouba samples are distinctly enriched in SiO_2 and depleted in P_2O_5 and CaO. MgO versus CaO shows best the distinction between Etinde, Mt. Cameroon and Manengouba.

The trends shown on the major element variation diagrams may be entirely explained by low pressure fractionation of the observed equilibrium phenocryst phases in the sequence olivine + clinopyroxene, plagioclase, hornblende, K-feldspar, with apatite and opaques occurring throughout. Elengoum and the lower slopes of the massif consist of salic quartz normative trachytes and one sample (C54) was collected from this region by J.G. Fitton and D.J. Hughes. Although this sample is indicated on Figure 5.1.1 and is the single highly fractionated sample (0.28% MgO) having the Manengouba symbol on Figures 5.1.2, 5.1.3, 5.1.4 and 5.1.7, it has a K-Ar age of 11.8 Ma (Chapter 3) and an anomalous $^{87}Sr/^{86}Sr$ ratio (see below). This sample is therefore considered to be unrelated to the Elengoum activity and its major and trace element geochemistry is more similar to trachytes from Bambouto (Rb-Sr contents for example, Figure 5.2.2).

Trace element variation diagrams (Figure 5.1.4) show Manengouba falling in the general field of the other continental centres except Etinde but with higher Ni and lower LREE and Sr contents (Table 5.1.1). Chromium and zirconium contents are similar to those of Mt. Cameroon (Figure 5.1.5) and show the dominance of olivine and cpx fractionation during low pressure evolution since Cr decreases rapidly with increasing Zr. Trace element profiles (normalized to "primitive mantle", following Sun, 1980) occupy a position within the spread of most of the other continental centres except Etinde on Figure 5.1.6 and has slightly lower Nb, La, Ce, Sr and Nd concentrations than Mt. Cameroon. Manengouba falls within the main field outlined on Figure 5.1.13 indicating similar La/Ce and Nd/Ce ratios to the other volcanoes, albeit with lower concentrations. Immobile element ratios (Zr/Y = 11, Nb/Y = 2.3) are

similar to Mount Cameroon and other within-plate basalts (Pearce and Norry, 1979). Also, like Mt. Cameroon and Etinde, a complete lack of ultramafic nodules, a low mean Mg number of 57, a low mean MgO content of 6.3 wt%, and a low average P_2O_5/Ce ratio of 58 (Table 5.1.1, analyses with MgO 4%) all indicate that even the most primitive Manengouba rocks have resided and fractionated in a high level magma chamber. Limited early plagioclase fractionation is indicated by the relatively low strontium contents (Figures 5.1.4, 5.1.7; $\bar{x}$ = 790 ppm Sr) compared to the Cameroon Line average of 920 ppm. Rb contents ($\bar{x}$ = 41) are however similar to Mt. Cameroon and Rb/Sr ratios are consequently higher ($\bar{x}$ = 0.51) than mafic rocks from other centres.

Strontium Isotope Results 7 basalts, 2 hawaiites, 1 gabbro, 3 mugearites, 1 quartz normative trachybasalt and 1 quartz trachyte were selected for unspiked $^{87}Sr/^{86}Sr$ ratio analysis from the suite described above (Table 5.1.5). These samples are marked on Figure 5.1.1. The mafic-intermediate rocks have measured $^{87}Sr/^{86}Sr$ ratios ranging from 0.70292 to 0.70313 (no age correction has been applied since Rb/Sr ratios are low and none of the mafic-intermediate rocks analysed is more than 1.5 Ma old). Manengouba thus occupies a distinct area, lying below the fields of Mt. Cameroon and Etinde on a plot of $^{87}Sr/^{86}Sr$ versus $^{87}Rb/^{86}Sr$ (Figure 5.1.8). This distinction is also clearly visible when the strontium isotope data are plotted against SiO_2 and Sr contents (Figures 5.1.9 and 5.1.10 respectively). The data spread on these diagrams is horizontal indicating that no difference exists in the isotopic compositions between the Manengouba basalts and intermediate rocks. Consequently the mugearites and hawaiites are considered to be cogenetic with the more mafic rocks

TABLE 5.1.5

$^{87}Sr/^{86}Sr$ Data from Manengouba

Sample No	Rock Type	K-Ar Age (Ma)	Rb (ppm)	Sr (ppm)	$^{87}Sr/^{86}Sr$ ($\pm 2\sigma \times 10^5$)	$^{87}Rb/^{86}Sr$	$(^{87}Sr/^{86}Sr)_o$	Location
Mafic-Intermediate Rocks								
C48	Basanite		39	915	0.70310 ± 5	0.1233		Eboga
C49	Hawaiite		67	866	0.70306 ± 3	0.2239		Eboga
C51	Basalt(ne)		35	755	0.70311 ± 5	0.1341		Recent cone
C52	Hawaiite		64	1,091	0.70304 ± 5	0.1697		Eboga
C55	Basalt(hy)		34	638	0.70310 ± 7	0.1542		Elengoum
C56	Basalt(hy)		15	481	0.70304 ± 7	0.0902		Elengoum
C59	Basalt(ne)		36	951	0.70311 ± 5	0.1095		Eboga
C62	Mugearite		77	1,006	0.70313 ± 8	0.2215		Eboga
C63	Mugearite		86	854	0.70294 ± 6	0.2914		Eboga (PC)
C65	Basalt(hy)		29	430	0.70292 ± 10	0.1951		Recent cone
C67	Gabbro		34	547	0.70294 ± 4	0.1798		Eboga (PC)
C69	Mugearite		62	784	0.70298 ± 7	0.2288		Eboga (PC)
C70	Basalt(ne)		39	736	0.70305 ± 8	0.1533		Recent cone
Fractionated Rocks								
C54	Qz. trachyte	11.82	89, 87.1[a]	162, 161[a]	0.70578 ± 8 0.70579 ± 6	1.5901[a]	0.70552	Dome, N.W. Manengouba
C57	Trachybasalt	0.60	45, 45.1[a]	755, 766[a]	0.70394 ± 5	0.1725[a]	0.70394	Elengoum

a: Determined by isotope dilution PC: Post Eboga Caldera Collapse (ne): Nepheline or Hypersthene Normative

sampled (as has already been indicated by their major and trace element geochemistry) and no crustal contamination is evident. However, distinctions may be made between the strontium isotopic compositions of mafic-intermediate rocks from the three main phases of volcanic activity (viz: Elengoum lavas; Eboga main building phase lavas; post Eboga caldera collapse lavas, cones and a gabbro from the caldera floor). Table 5.1.6 shows that the most recent, slightly more alkaline, activity appears to have $^{87}Sr/^{86}Sr$ ratios 0.0001 lower than the two other phases of activity although there is considerable overlap. Such a distinction has also been observed elsewhere in the Cameroon Line (e.g: Principe, Biu Plateau), and in other intraplate volcanoes (e.g: Honolulu Series, Oahu; Clague and Frey, 1982). This is substantiated by further isotopic work

TABLE 5.1.6

	$\bar{x}$ $^{87}Sr/^{86}Sr$		n	$\bar{x}$ Sr (ppm)
Elengoum	0.70307	4	2	560
Eboga	0.70309	4	5	966
Post Caldera Collapse	0.70299	7	6	684

carried out on new samples by C.A. Hirst (Ph.D. thesis, in prep.) where the post caldera collapse ($\bar{x}$ = 0.70303 $\pm$ 4, 3 samples) and earlier Eboga activity (0.70309 $\pm$ 7, 11 samples) averages are virtually identical to the data presented above. However, the Elengoum samples analysed by Hirst have an average $^{87}Sr/^{86}Sr$ ratio of 0.70329 $\pm$ 16 (7 samples) where the maximum value for these mafic-intermediate rocks is 0.70344 and the minimum is 0.70302. Convincing

further evidence for the lack of crustal contamination of the Manengouba mafic-intermediate rocks is furnished by Pb isotopic compositions (C.A. Hirst, Ph.D. thesis, in prep.) which plot within the oceanic island array as defined by Tatsumoto (1978) and Sun (1980).

A quartz-normative trachyte and a quartz-normative trachybasalt from the Manengouba massif gave elevated measured $^{87}Sr/^{86}Sr$ ratios of 0.70578 (C54) and 0.70394 (C57) respectively. Corrections for radiogenic growth may be applied on these samples since K-Ar age determinations have also been carried out (Chapter 3) and they result in initial ratios of 0.70552 and 0.70394 respectively (Table 5.1.6). C54 is much older than the rest of the samples and is not considered to be part of the Manengouba volcano. The initial $^{87}Sr/^{86}Sr$ ratios of C54 and C57 are higher than those from the less evolved rocks of Manengouba (0.70292-0.70313) and are within the range of ratios obtained from fractionated rocks from Bambouto, Oku, Mandara, and volcanic remnants associated with the lower Tertiary intrusives, all of which are considered to have suffered contamination (see following sections). Sr isotopic analyses of highly fractionated rocks (10 ppm Sr) sampled from Elengoum also give high ratios (C.A. Hirst, Ph.D. thesis, in prep.) similar to Bambouto, Oku and Mandara.

In summary, the Manengouba mafic-intermediate rocks are cogenetic (with one exception, C57) but also show fine scale isotopic heterogeneities between the different stages of activity and lower $^{87}Sr/^{86}Sr$ ratios than either Mt. Cameroon or Etinde. Late stage, more alkaline rocks have slightly lower ratios as is also seen on the islands of Principe and São Tomé, and on the Biu Plateau. Only very limited study has been made of highly fractionated lavas from Manengouba by

the author but crustal contamination is manifest in these rocks, as seen elsewhere in the continental sector of the Cameroon Line.

5.2 North Cameroon

5.2.1 Bambouto and Oku

Geochemistry These volcanoes (Figure 3.2.1) are mainly composed of silica saturated to oversaturated peralkaline trachytes and rhyolites with lesser quantities of nepheline normative trachytes and phonolites occurring on Bambouto and rhyolitic ignimbrites on Oku. Moderately alkaline to transitional mafic extrusives (basanites and basalts) having up to 14% MgO are present on both volcanoes, with those from Bambouto tending to be slightly more alkaline than Oku (Figure 5.2.1). Both centres exhibit a pronounced "Daly gap" in their major element chemistry between 1 and 4% MgO and between a D.I. of 50 and 75 (Figures 5.2.1, 5.1.2). Major and trace element diagrams show that the mafic rocks have a very similar character to those from Manengouba and Mt. Cameroon (Figures 5.1.2, 5.1.3, 5.1.4, 5.1.6, 5.1.13). In addition for samples with MgO >4%, mean MgO contents, Mg numbers, K/Rb, La/Ce and Zr/Nb ratios are directly comparable to Mt. Cameroon and Manengouba (Table 5.1.1). In marked contrast, the highly fractionated rocks range up to 76% SiO_2. These are rock types absent from Mt. Cameroon, Etinde and the oceanic islands. The extremely evolved rocks are high-K rhyolites according to the classification of Ewart (1979) and are typical of anorogenic salic continental rocks. Their trace element contents (Figure 5.1.4) approach zero for Cr, Ni and Sr and extend to extremely elevated values for Zr (250 ppm), La (760 ppm), Ce (660 ppm), Nb (470 ppm) and Rb (240 ppm). The nature of this enrichment of incompatible elements (as depicted by Rb during

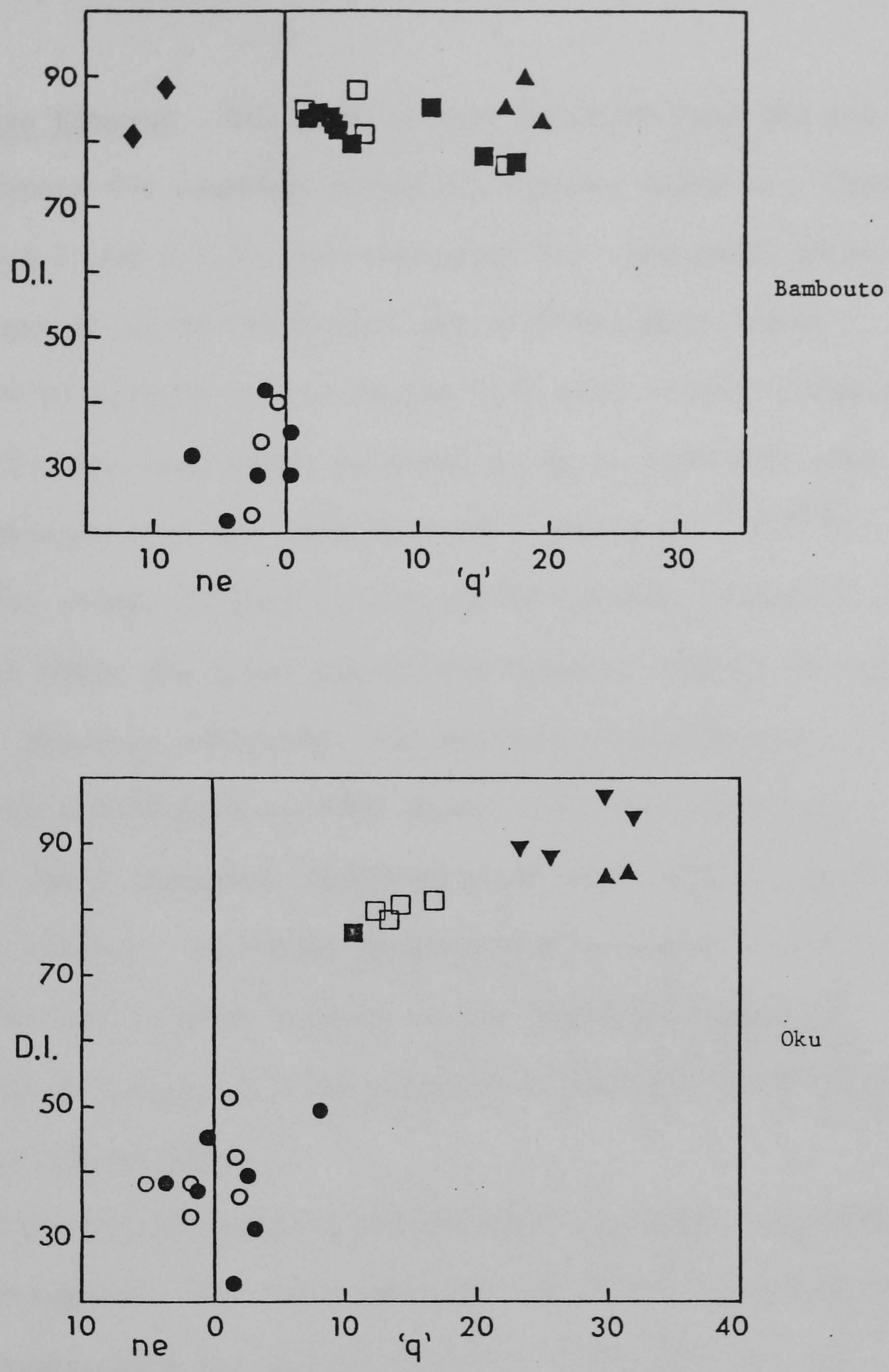


Figure 5.2.1 Differentiation Index plotted against over- and under-saturation for Bambouto and Oku
Chemical data from J. G. Fitton (unpublished).
Filled symbols ; analysed for strontium isotope ratios.

▲ rhyolite
▼ ignimbrite
■ trachyte
● basalt
◆ phonolite

fractional crystallization of feldspar is clearly illustrated in a plot of Rb versus Sr (Figure 5.2.2).

Sr Isotope Results Six basalts were selected from Oku and seven from Bambouto for unspiked strontium isotope analysis. These data (Tables 5.2.1 and 5.2.2) were corrected for radiogenic growth by employing ages of 14 Ma (Bambouto) and 17.5 Ma (Oku), dates determined by K-Ar methods on one basalt from each volcano (Chapter 3). Rb/Sr ratios are low, hence an error of up to 5 Ma will make very little difference to the initial ratio. Plots of $^{87}Sr/^{86}Sr$ versus $^{87}Rb/^{86}Sr$ atomic (Figure 5.2.3) and Sr content (Figure 5.1.10) illustrate that while the lower end of the range (0.70314) overlaps that of the S. Cameroon volcanoes, the maximum ratios observed for Bambouto and Oku extend up to 0.0006 higher than the upper limit identified for the S. Cameroon uncontaminated mafic rocks. Similar to the oceanic islands, the hypersthene-normative basalts tend to higher $^{87}Sr/^{86}Sr$ ratios with respect to the nepheline-normative samples (Figures 5.2.3 and 5.2.10) although a hawaiite (C91) from Oku is an exception to this.

Basalt C74 contains crustal charnockitic granulite xenoliths (C74C, C74F) which have also been analysed for $^{87}Sr/^{86}Sr$ ratios and Rb and Sr concentrations by isotope dilution (Table 5.2.3). By considering two end-members: uncontaminated basalt ($^{87}Sr/^{86}Sr$ = 0.70325, Sr = 1,000 ppm) and crustal contaminant (C74F, $^{87}Sr/^{86}Sr_{14}$ = 0.72088, Sr = 378 ppm); and by employing the mixing equation discussed in Section 4.2.2, the elevated ratio of the host basalt C74 (0.70403) can be explained by 11.5% contamination by the crustal

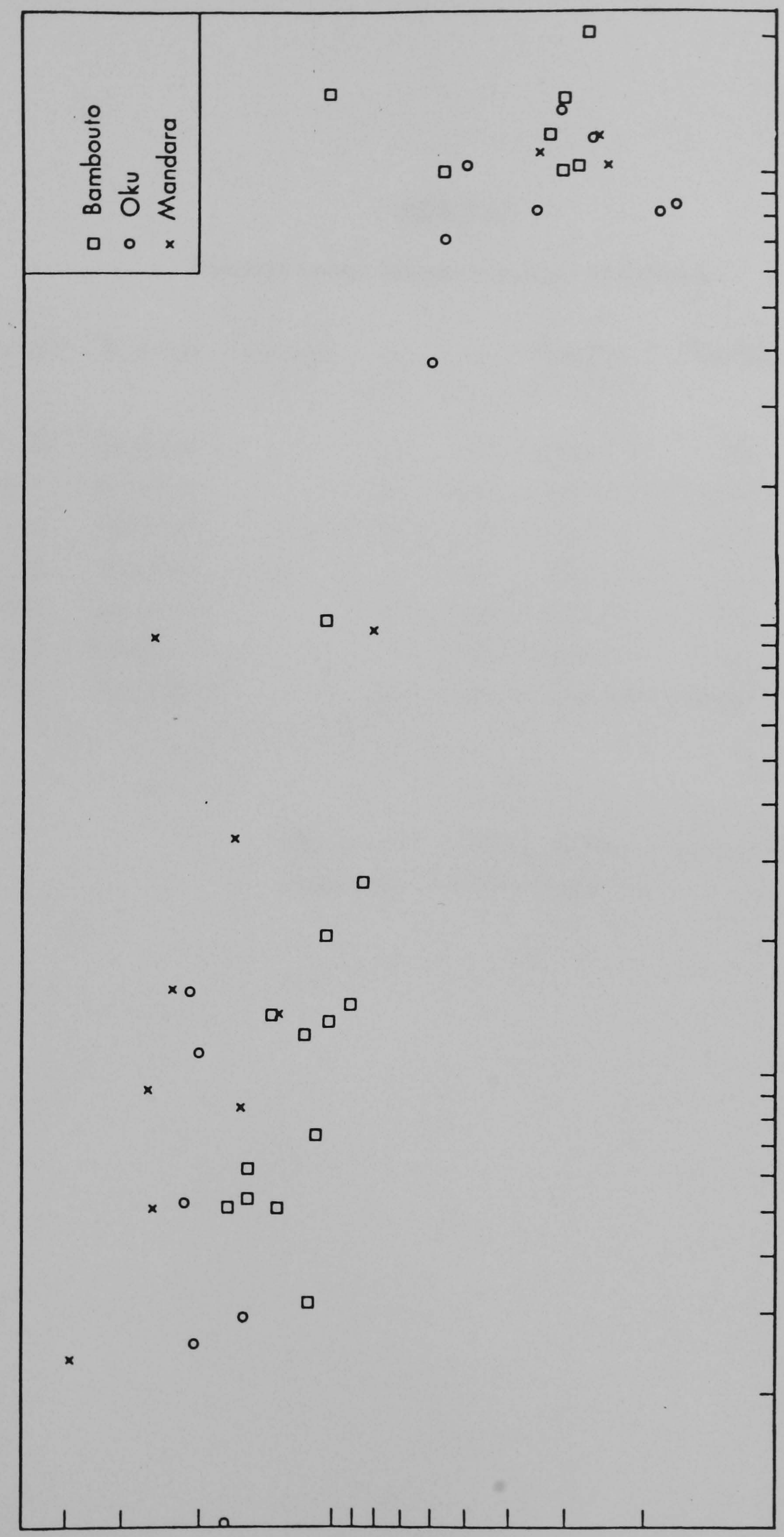


Figure 5.2.2 Rb-Sr diagram for the N.Cameroon volcanoes

TABLE 5.2.1

Strontium Isotope Data of Mafic Rocks from Bambouto

Sample	Rock Type	K-Ar Age (Ma)	Rb (ppm)	Sr (ppm)	$^{87}Sr/^{86}Sr$ ($\pm 2\sigma \times 10^5$)	$^{87}Rb/^{86}Sr$	$^{87}Sr/^{86}Sr_o$ [a]
C 74	Basalt(hy) [b]		43	994	0.70406 ± 3	0.1250	0.70403
C 99	Basalt(ne)		28	1,064	0.70343 ± 6	0.0760	0.70342
C102	Basalt(hy)		30	1,536	0.70342 ± 6	0.0573	0.70341
C108	Basalt(ne)	14.1	56	1,016	0.70317 ± 10	0.1590	0.70314
C110	Basalt(ne)		30	1,032	0.70346 ± 8	0.0845	0.70344
C112	Basanite		32	1,242	0.70333 ± 6	0.0750	0.70332
C121	Basalt(hy)		26	2,039	0.70357 ± 8	0.0363	0.70356

a Initial ratio calculated assuming an age of 14 Ma

b Hypersthene or nepheline normative

TABLE 5.2.2

Strontium Isotope Data of Mafic Rocks from Oku

Sample	Rock Type	K-Ar Age (Ma)	Rb (ppm)	Sr (ppm)	$^{87}Sr/^{86}Sr$ ($\pm 2\sigma \times 10^5$)	$^{87}Rb/^{86}Sr$	$^{87}Sr/^{86}Sr_o$[a]
C 78	Basalt(ne)[b]		51	1,065	0.70329 ± 10	0.1353	0.70326
C 90	Basalt(hy)		17	870	0.70366 ± 6	0.0567	0.70365
C 91	Hawaiite(ne)	17.5	31	1,410	0.70386 ± 12	0.0634	0.70384
C 94	Basalt(ne)		36	847	0.70309 ± 8	0.1203	0.70306
C 96	Basalt(hy)		28	1,216	0.70349 ± 12	0.0618	0.70348
C 97	Basalt(hy)		20	806	0.70337 ± 8	0.0639	0.70335

a Initial ratio calculated assuming an age of 17.5 Ma

b Hypersthene or nepheline normative

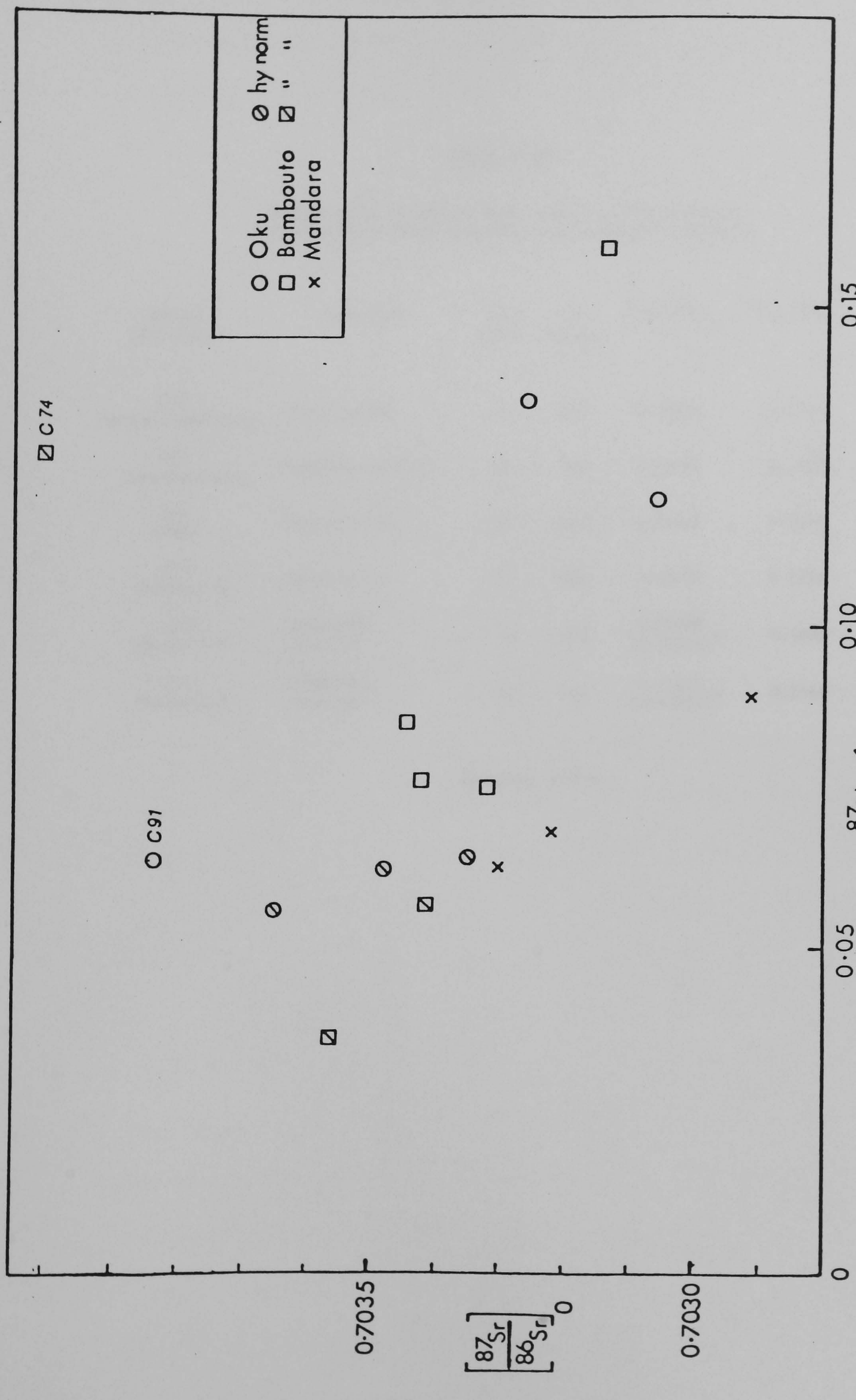


Figure 5.2.3 Initial strontium isotope ratios plotted against Rb/Sr atomic in mafic rocks
(> 4%MgO) from Bambouto, Oku and Mandara

TABLE 5.2.3

Isotope data of Contaminated Mafic and Intermediate Volcanic Rocks from Cameroon, and Granulite Xenoliths

Sample (Location)	Rock Type	Rb (ppm)	Sr (ppm)	$^{87}Sr/^{86}Sr_o$	$^{87}Rb/^{86}Sr$	Assumed Age (Ma)
C18 (Mount Cameroon)	Hawaiite(hy)	71	918	0.70402	0.2142	0
C57 (Manengouba)	Trachybasalt(hy)	45	755	0.70394	0.1725	0
C93 (Oku)	Hawaiite(qz)	54	692	0.70466	0.2242	24
C74 (Bambouto)	Basalt(hy)	43	994	0.70403	0.1250	14
C74F (Bambouto)	Granulite xenolith	13	378	0.72088 (0.72090)[a]	0.1000	14
C74C (Bambouto)	Granulite xenolith	39	442	0.71021 (0.71027)[a]	0.2560	14

a Measured ratios

end member. This is depicted on Figure 5.2.4. Likewise the elevated initial ratios of mafic-intermediate hypersthene or quartz-normative samples from Mt. Cameroon (C18), Manengouba (C57), and Oku (C93) could be generated by similar levels of contamination (11.4%, 7.6%, and 19.3% respectively). The isotopic data of all these samples is summarized in Table 5.2.3. Such initial ratios could not be explained by prolonged magma residence times (which is not, in any case, indicated by their chemistry) since 470 Ma would be required to account for C74 by radiogenic growth. The isotopic composition of C74F is probably a near approximation to crustal rocks in this region since Pan-African granite-gneisses in Cameroon and Nigeria have very similar $^{87}Sr/^{86}Sr$ ratios and Sr contents (Lasserre and Soba, 1976; Van Breemen et al., 1977). Crustal contamination of volcanic rocks is similarly manifest in Sr isotopic data from many continental volcanic provinces such as Eastern Australia (Ewart, 1982), Skye (Moorbath and Thompson, 1980; Thompson et al., 1982), East Africa (Bell and Powell, 1969), the Tuscan Province, Italy (Vollmer, 1977), and the Transantarctic Mts., (Faure et al., 1974; Hoefs et al., 1980). Recent Nd and $\delta^{18}O$ studies confirm the conclusions of the aforementioned investigators (e.g: Carter et al., 1978a; Carlson et al., 1981; Taylor, 1980; De Paolo, 1981), and a tracer Nd isotopic study carried out by the author on basalt C74 and granulite xenolith C74C supports the contamination hypothesis since the $^{143}Nd/^{144}Nd$ ratio of C74 (0.51263 $\pm$ 2) is distinctly lower than that typical of uncontaminated within-plate basalts (0.5128 - 0.5130 for basalts having an $^{87}Sr/^{86}Sr$ ratio of 0.703). Likewise, C74C has an enriched $^{143}Nd/^{144}Nd$ ratio of 0.51209 $\pm$ 6, typical of radiogenic continental crust (e.g: Carlson et al., op cit.).

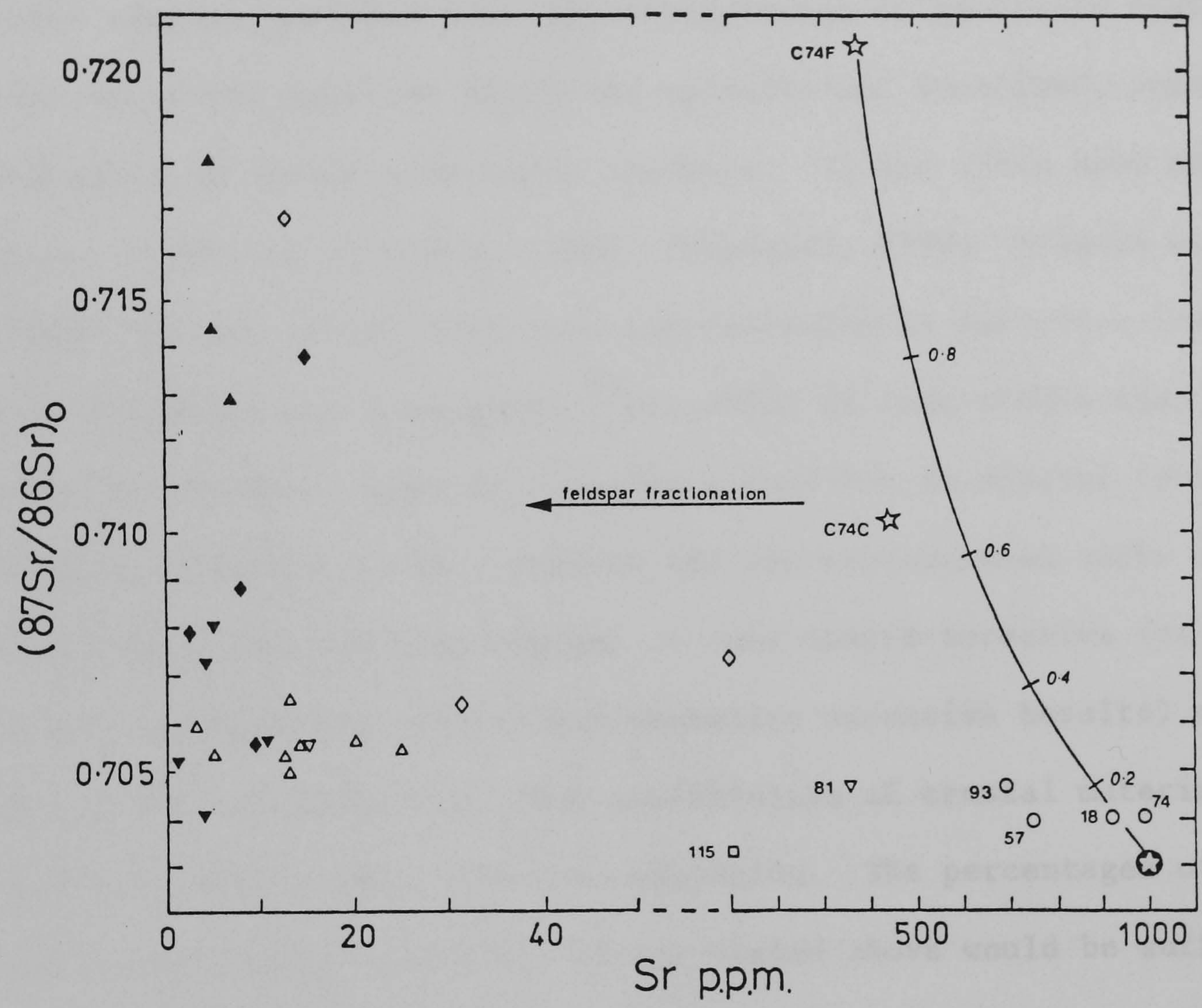


Figure 5.2.4 Initial strontium isotope ratios versus Sr contents for fractionated rocks from Bambouto, Oku and Mandara. The curve represents a simple mixing relationship (see text for explanation) between basalt (Sr=1000ppm, $^{87}Sr/^{86}Sr$=0.70325) and granulite xenolith C74F. Proportions of C74F in the resultant hybrid are indicated.

○ basalts and intermediates from Bambouto (C74), Oku (C93), Manengouba (C57), Mt. Cameroon (C18).
☆ Bambouto granulite xenoliths
✪ Basalt endmember
▲ Bambouto rhyolites
△ Bambouto qz-trachytes
□ Bambouto trachy-phonolite (C115)
▼ Oku rhyolites and ignimbrites
▽ Oku qz-trachytes
◆ Mandara rhyolites
◇ Mandara qz-trachytes

Post-consolidation interaction with meteoric water is not responsible for most of the variability in Sr and Pb isotope ratios of basic continental volcanics (Moorbath and Thompson, 1980; references cited therein), although $\delta^{18}O$ analyses would be necessary to prove this in the case of these samples. Since only a few of the many Cameroon mafic samples analysed have disturbed ratios it is likely that contamination of the basaltic magma was sporadic and localized, perhaps at the walls of conduits or magma chambers. It has often been suggested (e.g: Green and Ringwood, 1967; Pankhurst, 1969; Francis et al., 1980; Watson, 1982a) that such contamination is selective involving only volatiles and radiogenic ^{87}Sr, which is less stable than the other Sr isotopes since it occupies a position in mineral lattices formerly occupied by Rb. However all the contaminated rocks under discussion here are hypersthene- or even quartz-normative (as opposed to the isotopically undisturbed nepheline normative basalts) which may well be an indication that assimilation of crustal material has occurred, rather than selective migration. The percentages of contamination by crustal granulite as calculated above would be sufficient to change liquids with 4% ne in the norm to being just hypersthene-normative (J.G. Fitton, pers. comm. 1983). It should be pointed out however that a similar correlation between the degree of silica saturation and initial strontium isotopic ratios has already been demonstrated on the oceanic sector, a region devoid of radiogenic (crustal) contaminants, and that the correlation there was attributed to a heterogeneous source and magma mixing in the upper mantle. Thus the isotopic and geochemical data from these rocks may reflect the superposition of crustal contamination on mantle derived heterogeneities. A recent experimental study (Watson, 1982a) has shown that trace element

and isotope data alone cannot define the "specific physicochemical nature of the assimilation process" and that such mechanisms are not simple, two-end-member processes. Hence all that may be concluded here is that some form of contamination (at least with respect to the $^{87}Sr/^{86}Sr$ ratios, perhaps the chemistry) of some of the basaltic and intermediate rocktypes from Mt. Cameroon, Manengouba, Bambouto and Oku by highly radiogenic crustal material has occurred during the liquid's ascent through the crust to high level magma chambers.

$^{87}Sr/^{86}Sr$ ratios of two nepheline-normative phonolites (C115, C116, Table 5.2.4) from Bambouto are typical of those obtained from oceanic sector phonolites (Principe, São Tomé) indicating that they are comagmatic with the mafic rocks. This is supported by the lack of correlation between SiO_2 content and strontium initial ratios (Figure 5.2.10). In addition the measured ratios of C115 is consistent with an age of between 15 Ma (equivalent to 0.70340) and 18 Ma (0.70325) which is within the range obtained by K-Ar dating of two Bambouto trachytes (Chapter 3).

On the contrary, eight quartz-normative trachytes and three peralkaline rhyolites (Table 5.2.4) from Bambouto have extremely high measured $^{87}Sr/^{86}Sr$ ratios, partially as a consequence of their high Rb (up to 168 ppm) and low Sr (down to 3.12 ppm) contents (Figure 5.2.2). The trachyte data form an isochron (Figure 5.2.5a) with large scatter and the best obtainable fit by regression analysis (after York, 1969) gives an age of 16.6 Ma and an intercept of 0.70547 (Figure 5.2.5b). However the peralkaline rhyolite data plot well above this line and if individual sample initial ratios are calculated by assuming the age derived above, then the trachytes range from 0.70497 to 0.70640 whereas the rhyolites range from 0.71275 to 0.71804.

TABLE 5.2.4

Strontium Isotope Data of Fractionated Rocks from Bambouto

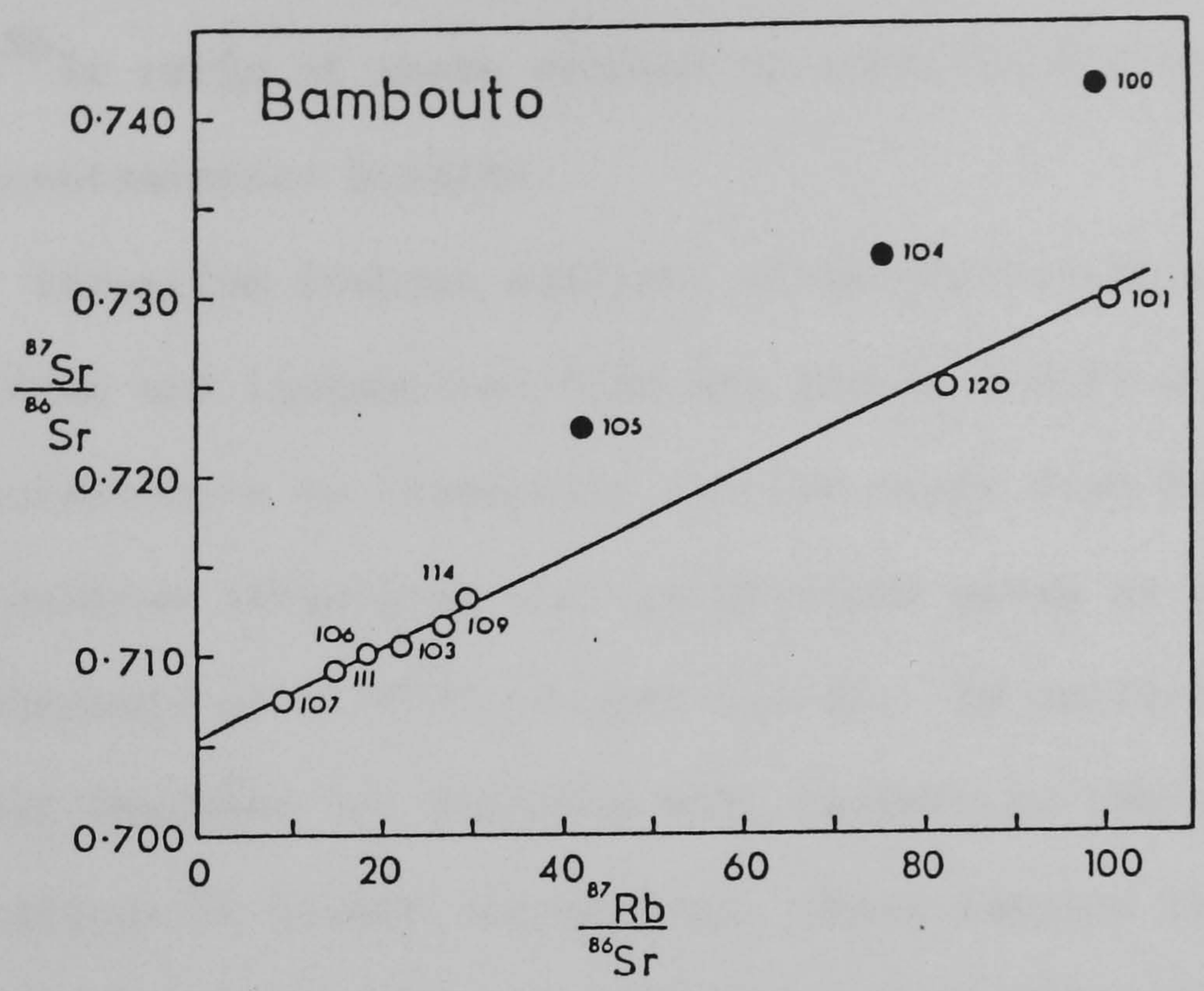
Sample	Rock Type	K-Ar Age (Ma)	Rb^a (ppm)	Sr^a (ppm)	$^{87}Sr/^{86}Sr^a$ ($\pm 2\sigma \times 10^5$)	$^{87}Rb/^{86}Sr^a$	$^{87}Sr/^{86}Sr_o^c$	$^{87}Sr/^{86}Sr_o^d$
C100	Rhyolite	18.5	168	4.91	0.74128 ± 10	98.59	0.71804	0.71538
C101	Qz-trachyte		109	3.12	0.72964 ± 21	100.67	0.70591	
C103	Qz-trachyte		99.0	12.74	0.71060 ± 20	22.488	0.70530	
C104	Rhyolite		132	5.04	0.73221 ± 18	75.800	0.71434	
C105	Rhyolite		106	7.23	0.72278 ± 19	42.539	0.71275	
C106	Qz-trachyte		88.1	13.79	0.70989 ± 10	18.468	0.70554	
C107	Qz-trachyte	22.7	83.3	25.52	0.70768 ± 18	9.441	0.70545	0.70464
C109	Qz-trachyte		118	12.73	0.71128 ± 12	26.774	0.70497	
C111	Qz-trachyte	15.8	101	19.69	0.70907 ± 18	14.889	0.70556	0.70573
C114	Qz-trachyte		134	13.25	0.71331 ± 16	29.314	0.70640	
C115	Trachyphonolite		101[b]	101[b]	0.70402 ± 3[b]	2.894	0.70334	
C116	Phonolite		100[b]	1524[b]	0.70344 ± 6[b]	0.1891	0.70339	
C120	Qz-trachyte		150	5.24	0.72483 ± 16	82.886	0.70529	

a By isotope dilution, several are means of duplicates (see Appendix Tables A2, A5)

b Unspiked determination (Rb, Sr concentrations by XRF)

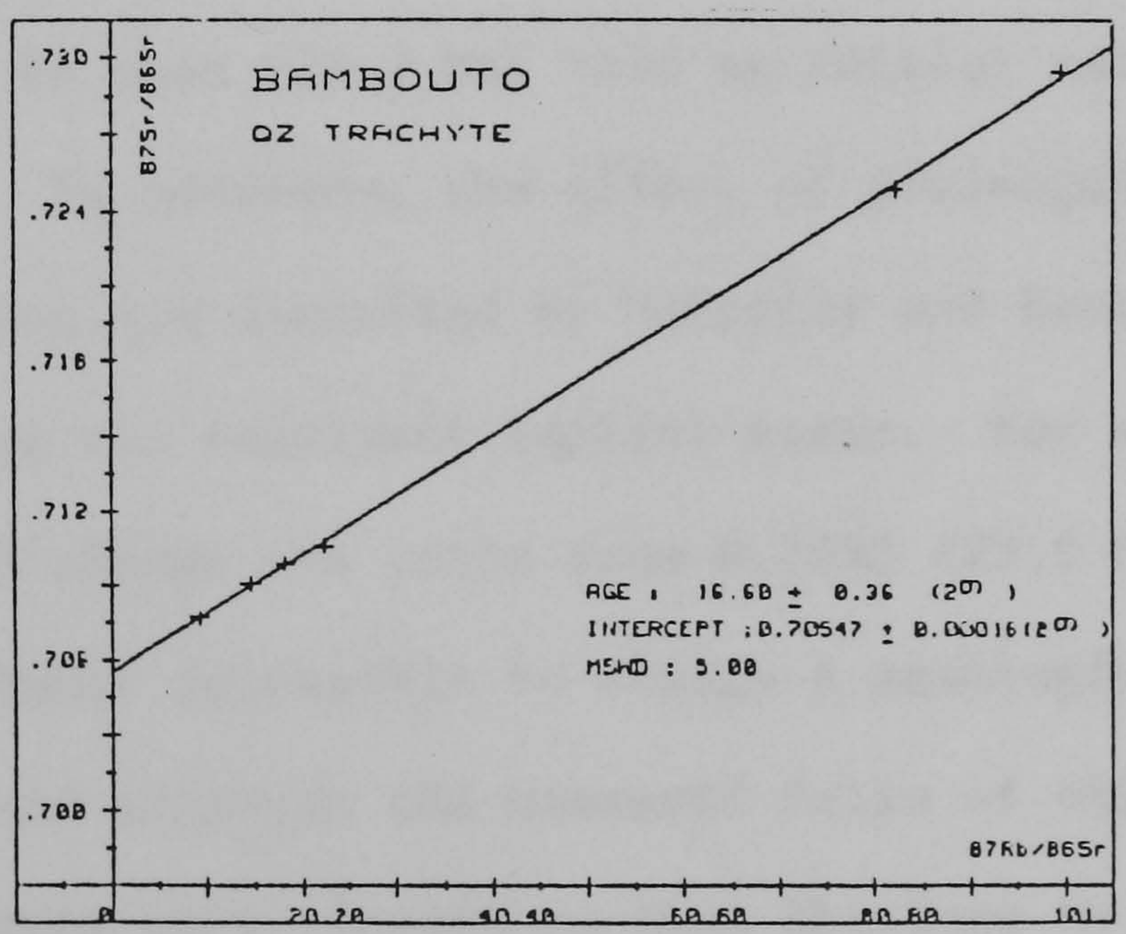
c Calculated using an age of 16.6 Ma (Rb-Sr isochron)

d Calculated using K-Ar ages



A

Figure 5.2.5A Strontium isotope ratios of Bambouto trachytes(o) and rhyolites (●) plotted against Rb/Sr atomic. Line is that derived from B.



B

Figure 5.2.5B Best fit isochron through 6 trachytes (C101,C103,C106,C107,C111, and C120).

To make better comparisons K-Ar dates would be required on all fractionated samples but calculated initial ratios of the three rocks analysed by K-Ar methods (C100, C107, C109) indicate that the $^{87}Sr/^{86}Sr$ ratio of these samples is consistently elevated relative to uncontaminated basalts.

Strontium isotope analyses of quartz-trachytes, peralkaline rhyolites and ignimbrites from Oku (Table 5.2.5) show almost identical characteristics to chemically similar rocks from Bambouto. The best fit isochron (rhyolites and ignimbrites) gives an age of 24.1 Ma having an intercept of 0.70535 (Figure 5.2.6). By utilizing the same approach to that employed for Bambouto with respect to the assignment of ages for radiogenic growth corrections, these samples range in initial ratios from 0.70462 (quartz-trachyte) to 0.70816 (rhyolite). One extremely fractionated rhyolite (C85), has a measured ratio of 0.9323 and a Rb/Sr atomic ratio of 683, and would therefore have an initial ratio of 0.6986 if the isochron age (24 Ma) was assumed. If however, its K-Ar age is used (22.7 Ma) then an initial ratio of 0.71699 is obtained. In addition, the effect of prolonged magma chamber residence times (as described by McCarthy and Cawthorn, 1980) could greatly change the resultant initial ratio. For example a difference of 1 Ma would change its ratio from 0.7035 (23.6 Ma) to 0.7132 (22.6 Ma). It is thus almost impossible to assign a meaningful initial ratio to this sample and although the measured ratio of this rock indicates an age which agrees very closely to that obtained by K-Ar methods it is not considered in the discussion in Section 5.2.3.

5.2.2 Mandara Mountains

Geochemistry This region consists of Pan-African basement cut by numerous deeply eroded trachyte and rhyolite plugs with minor

TABLE 5.2.5

Strontium Isotope Data of Intermediate and Fractionated Rocks from Oku

Sample	Rock Type	K-Ar Age (Ma)	Rb^b (ppm)	Sr^b (ppm)	$^{87}Sr/^{86}Sr^b$ ($\pm 2\sigma \times 10^5$)	$^{87}Rb/^{86}Sr^b$	$^{87}Sr/^{86}Sr_o^c$	$^{87}Sr/^{86}Sr_o^e$
C76	Rhyolitic ignimbrite		200	2.46	0.78590 ± 24	236.18	0.70521	
C81	Qz-trachyte		58.0	369	0.70477 ± 14	0.4544	0.70462	
C84	Rhyolite		209	5.24	0.74793 ± 14	116.19	0.70816	
C85	Rhyolite	22.2	170	0.81	0.93234 ± 20[d]	683.13	0.69856	0.71699
C87	Rhyolitic ignimbrite		205	15.03	0.71876 ± 16	39.510	0.70524	
C92	Rhyolitic ignimbrite		192	11.00	0.72238 ± 18	50.600	0.70506	
C93	Hawaiite(qz)[a]		54.4	702	0.70474 ± 8	0.2242	0.70466	
C95	Rhyolitic ignimbrite	23.2	156	4.3	0.75771 ± 12	156.671	0.70409	0.70610

a Quartz normative

b By isotope dilution, several are means of duplicates (see Appendix Tables A2, A5)

c Calculated assuming an age of 24 Ma (from Rb/Sr isochron)

d Blank corrected

e Calculated assuming K-Ar ages

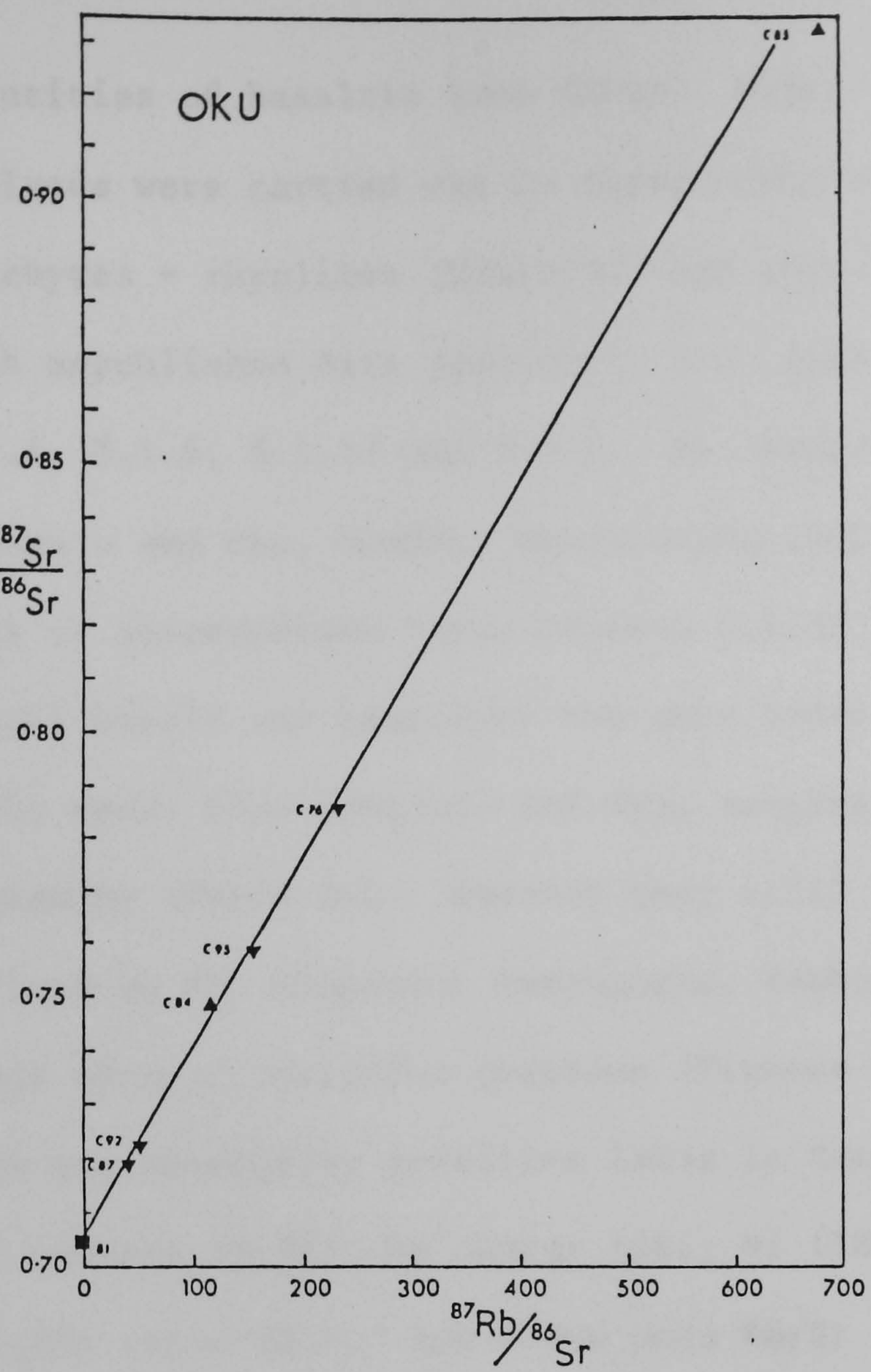


Figure 5.2.6A Sr isotope ratios of Oku trachyte (■), rhyolites(▲) and ignimbrites (▼) plotted against Rb/Sr atomic. Line is derived from figure 5.2.6B

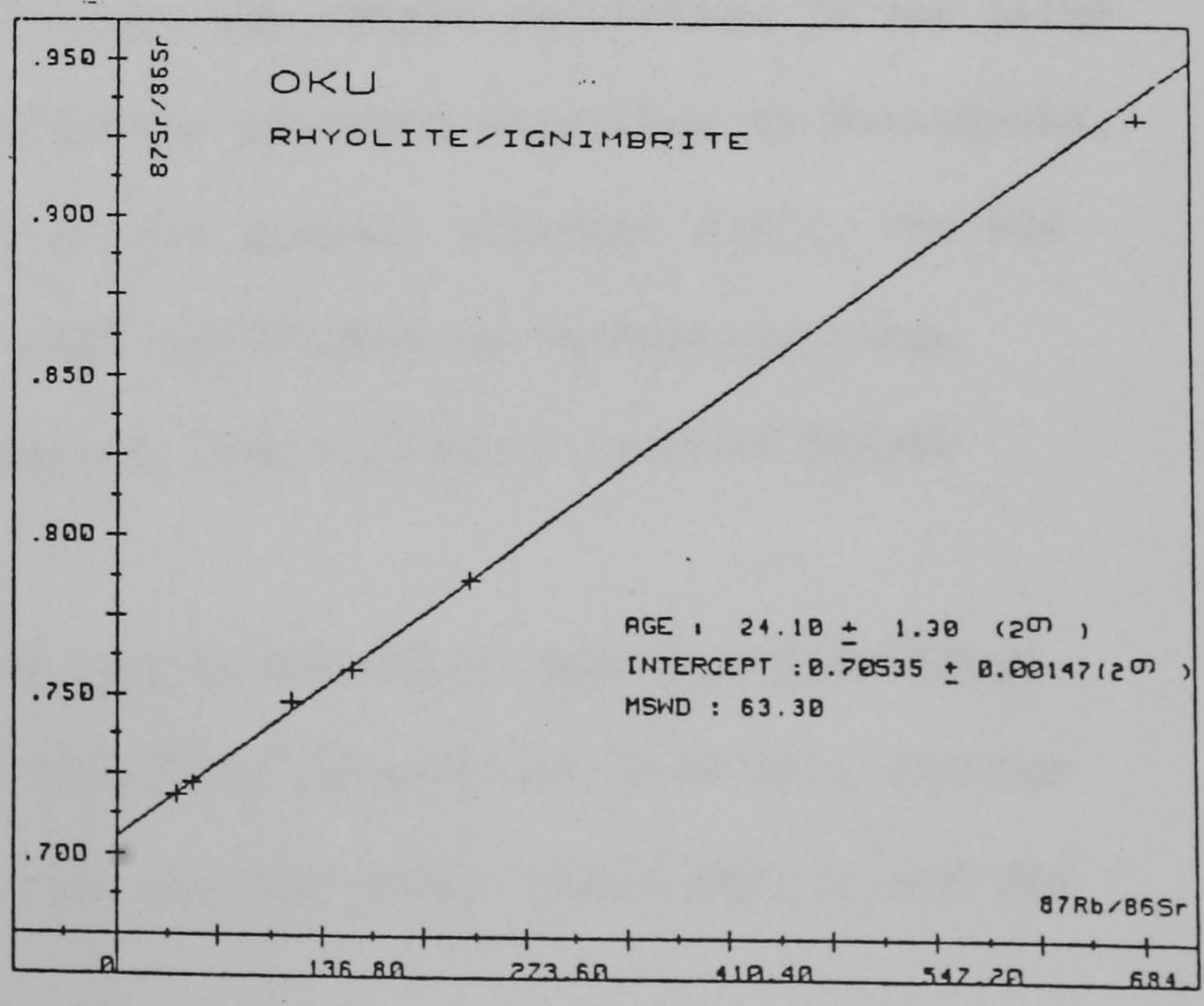


Figure 5.2.6B Best fit isochron through these samples (except for trachyte C81).

quantities of basaltic lava flows. Major- and trace-element geochemical analyses were carried out on three mafic rocks and ten highly fractionated trachytes - rhyolites (Table B2) and this data is plotted together with unpublished data (analyst: J.G. Fitton) on Figures 5.1.2 to 5.1.4, 5.1.6, 5.1.13 and 5.2.2. As observed in rocks sampled from Bambouto and Oku, Mandara shows a distinct bimodality with a complete lack of intermediate lavas between D.I.32 and 85 (Figure 5.2.7). The alkali basalt and basanites are more undersaturated than most of the mafic rocks from Bambouto and Oku, ranging from 5.7% to 14.1% normative nepheline (Table B4). However they still plot within the fields defined by Mt. Cameroon, Manengouba, Bambouto and Oku on major and trace element variation diagrams (Figures 5.1.2, 5.1.3, 5.1.4). That they are relatively primitive lavas is demonstrated by: high mean MgO content (9.7%), Mg number (66), Ni (180 ppm), Cr (295 ppm) and P_2O_5/Ce ratio (81); and a low mean Rb/Sr ratio of 0.024 (Table 5.1.1). Mean K/Rb ratios (375) and Zr/Nb ratios (3.4) are likewise very similar to ratios from all the other volcanoes, barring Etinde. The Mandara mafic rocks have not been plotted on the normalized incompatible trace element diagram (Figure 5.1.6) since the sample population is not large enough but they would fall within the spectrum described by Manengouba, Bambouto and Oku and also that of the nearest volcanic suite, the Biu Plateau. Hence the degree of LREE enrichment is within the range observed for all the other Cameroon Line volcanoes, except Etinde (Figure 5.1.13).

The highly fractionated quartz-trachytes and rhyolites range up to very high SiO_2 contents (74.5% by weight) and show very similar major element geochemistry to the evolved rocks from Bambouto and Oku

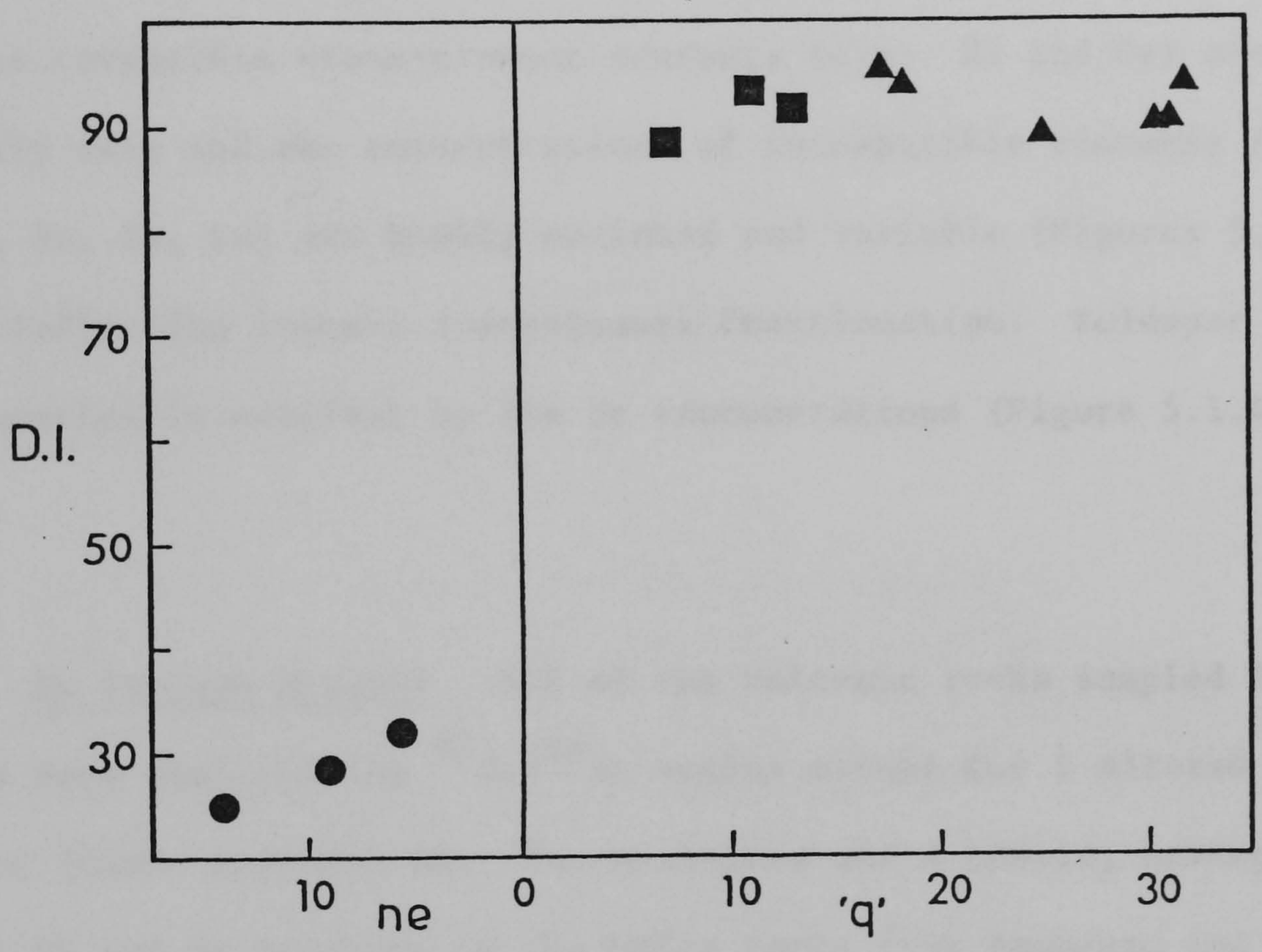


Figure 5.2.7 Differentiation Index plotted against degree of silica over- and under- saturation for Mandara volcanic rocks. All samples were analysed for $^{87}Sr/^{86}Sr$ ratios.

● basalts and basanites

■ qz-normative trachytes

▲ rhyolites

(Figures 5.1.2, 5.1.3). However, while the rhyolites are also all high-K varieties (following the classification of Ewart, 1979), only three rhyolites (C136, C142, C144) and one of the quartz-trachytes (C145) are peralkaline (employing the terminology of Shand, 1951). The remainder are all marginally peraluminous. Figure 5.2.8 shows that the normative compositions of three of the rhyolites (C137, C140, C144) plot near the thermal minimum in the Ab-Or-Q system (Tuttle and Bowen, 1958) and that the other rhyolites and trachytes lie close to the projection of the two-feldspar boundary curve. Trachyte and rhyolite compatible trace-element contents (e.g: Ni and Cr) are virtually zero and the concentrations of incompatible elements (e.g: Rb, Nb, Zr, Ce, La) are highly enriched and variable (Figures 5.1.4, 5.2.3) indicating intense low-pressure fractionation. Feldspar fractionation is manifest by low Sr concentrations (Figure 5.1.4, 5.2.2).

Sr Isotope Results All of the volcanic rocks sampled from Mandara were analysed for $^{87}Sr/^{86}Sr$ ratios except for 1 altered rhyolite (C139, Appendix B). Two basanites and a basalt, having similar Rb and Sr contents to the mafic rocks from Bambouto and Oku (Figure 5.2.2), show a variation in initial ratios from 0.70291 to 0.70330 (Table 5.2.6, Figure 5.2.3) and plot in the field of uncontaminated rocks from S. Cameroon (Figure 5.1.10). Hence the data does not extend to the higher values exhibited by basalts and intermediate lavas which have suffered contamination by continental crust. In addition, unlike most of the other centres, higher $^{87}Sr/^{86}Sr$ ratios do not equate to hypersthene- or quartz-normative lavas and in fact the most strongly nepheline-normative sample (C146) has the highest ratio.

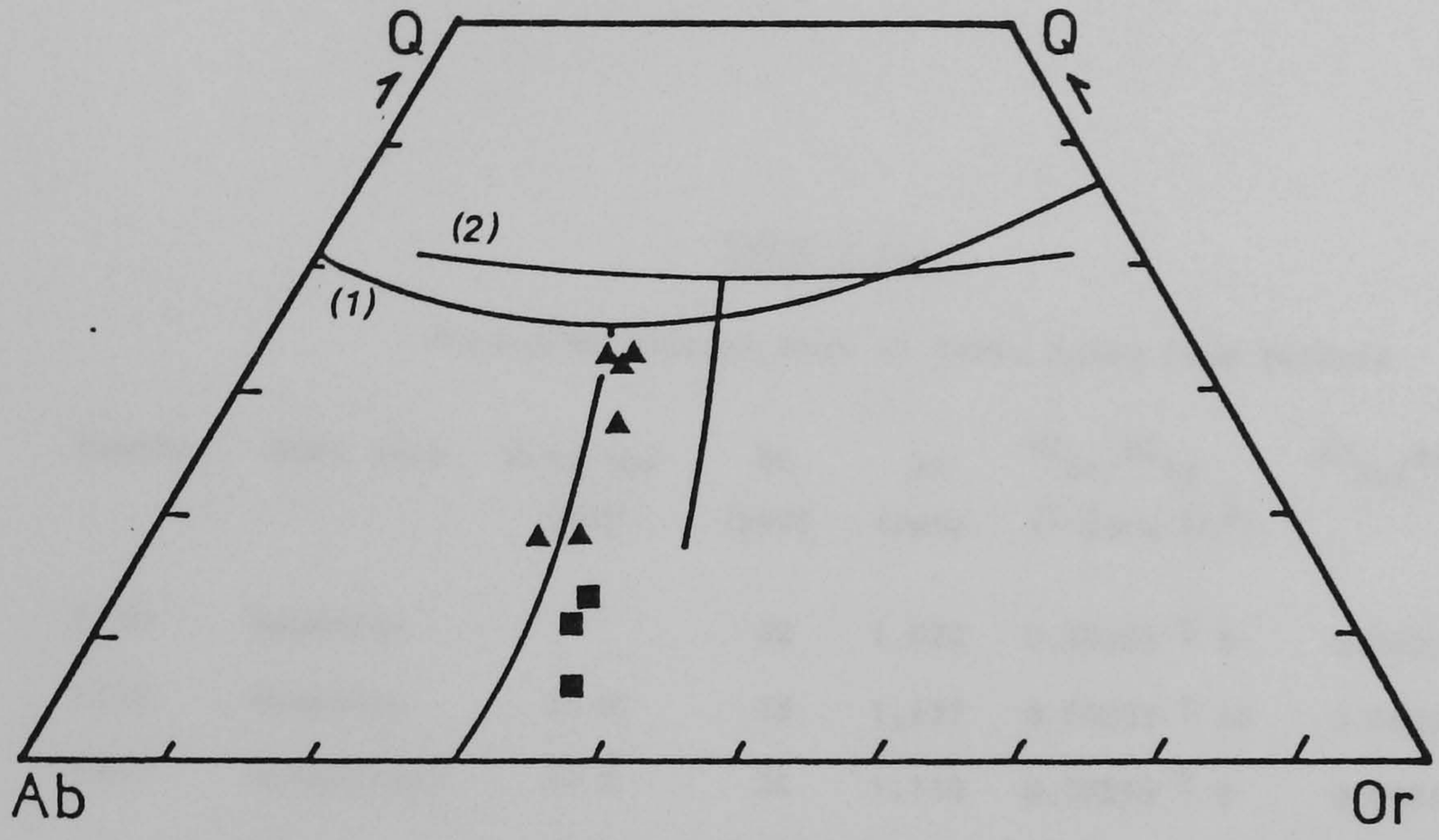


Figure 5.2.8 Normative quartz and feldspar compositions of Mandara trachytes (■) and rhyolites (▲) plotted in the quartz-feldspar ternary system. Curve (2) represents the quartz-feldspar and two feldspar boundary curves for compositions $(Ab\text{-}Or\text{-}Q)_{97}An_3$ (at 1Kb water vapour pressure) after James and Hamilton (1969). Curve(1), also at 1Kb is after Tuttle and Bowen (1958).

TABLE 5.2.6

Strontium Isotope Data of Mafic Rocks from Mandara

Sample	Rock Type	K-Ar Age (Ma)	Rb (ppm)	Sr (ppm)	$^{87}Sr/^{86}Sr$ ($\pm 2\sigma \times 10^5$)	$^{87}Rb/^{86}Sr$	$^{87}Sr/^{86}Sr_o^a$
C135	Basanite		22	1,022	0.70325 ± 8	0.0623	0.70322
C146	Basanite	33.2	25	1,157	0.70333 ± 16	0.0625	0.70330
C147	Basalt(ne)	30.4	34	1,110	0.70295 ± 8	0.0886	0.70291

a Initial ratio calculated assuming an age of 32 Ma

The qz-trachyte and rhyolite strontium isotope data (Table 5.2.7) plot about an errorchron (Figure 5.2.9a) with a great deal of scatter and regression calculations (on 6 points) give an age of 32.1 Ma and an intercept of 0.7073 (Figure 5.2.9b). Similar to the Bambouto-Oku trachytes and rhyolites these samples show extreme measured $^{87}Sr/^{86}Sr$ ratios with one rhyolite (C144) having a Rb/Sr atomic ratio of 493 and a measured strontium isotopic ratio of 0.9149. Since there is large error associated with this analysis and (as was observed for C85 from Oku) because of its extreme Rb/Sr ratio, it would be impossible to calculate its initial ratio with any certainty. The measured ratio does however indicate that its age is probably unlikely to be younger than 28.5 Ma (equivalent to an initial ratio of 0.716) or older than 29.5 (0.7086) when one considers what its initial ratio is likely to be in comparison to other samples of similar chemistry. By utilizing the Rb-Sr errorchron age of 32 Ma, initial ratios of the remaining highly evolved samples vary from 0.7056 to 0.7168.

5.2.3 Discussion on the Genesis of the Bambouto, Oku and Mandara Salic Rocks

Two important conclusions may be drawn from the above data: (1) that they have initial ratios markedly higher than associated basaltic rocks; and (2) that the data from each volcano plot on errorchrons, having ages approximately the same as those derived by K-Ar methods. Field relations and major- and trace-element geochemistry (Figures 5.1.2, 5.1.3, 5.1.4, 5.2.2) indicate that the Bambouto, Oku and Mandara salic rocks are associated with mafic counterparts by low-pressure fractionation. However, Figure 5.2.4, a plot of Sr initial ratios versus Sr content,

TABLE 5.2.7

Strontium Isotope Data of Trachytes and Rhyolites from Mandara

Sample	Rock Type	K-Ar Age	Rb^a (ppm)	Sr^a (ppm)	$^{87}Sr/^{86}Sr^a$ ($\pm 2\sigma \times 10^5$)	$^{87}Rb/^{86}Sr^a$	$^{87}Sr/^{86}Sr_o^b$	$^{87}Sr/^{86}Sr_o^c$
C136	Rhyolite		265	9.23	0.74342 ± 10	83.244	0.70559	
C137	Rhyolite		256	91.8	0.71148 ± 20	8.058	0.70782	
C138	Rhyolite		162	8.44	0.73420 ± 20	55.711	0.70888	
C140	Rhyolite		228	15.39	0.73338 ± 10	43.011	0.71384	
C141	Qz trachyte		166	33.1	0.71304 ± 26	14.520	0.70644	
C142	Rhyolite		255	4.89	0.77684 ± 14	151.76	0.70788	
C143	Qz trachyte		81.3	95.2	0.70843 ± 16	2.473	0.70731	
C144	Rhyolite		392	2.35	0.91494 ± 120[d]	492.5	-	
C145	Qz trachyte	35.3	133	13.5	0.72978 ± 14	28,54	0.71681	0.71549

a Analysed by isotope dilution

b Calculated assuming an age of 32 Ma (from Rb-Sr isochron)

c Calculated assuming the K-Ar age

d Blank corrected

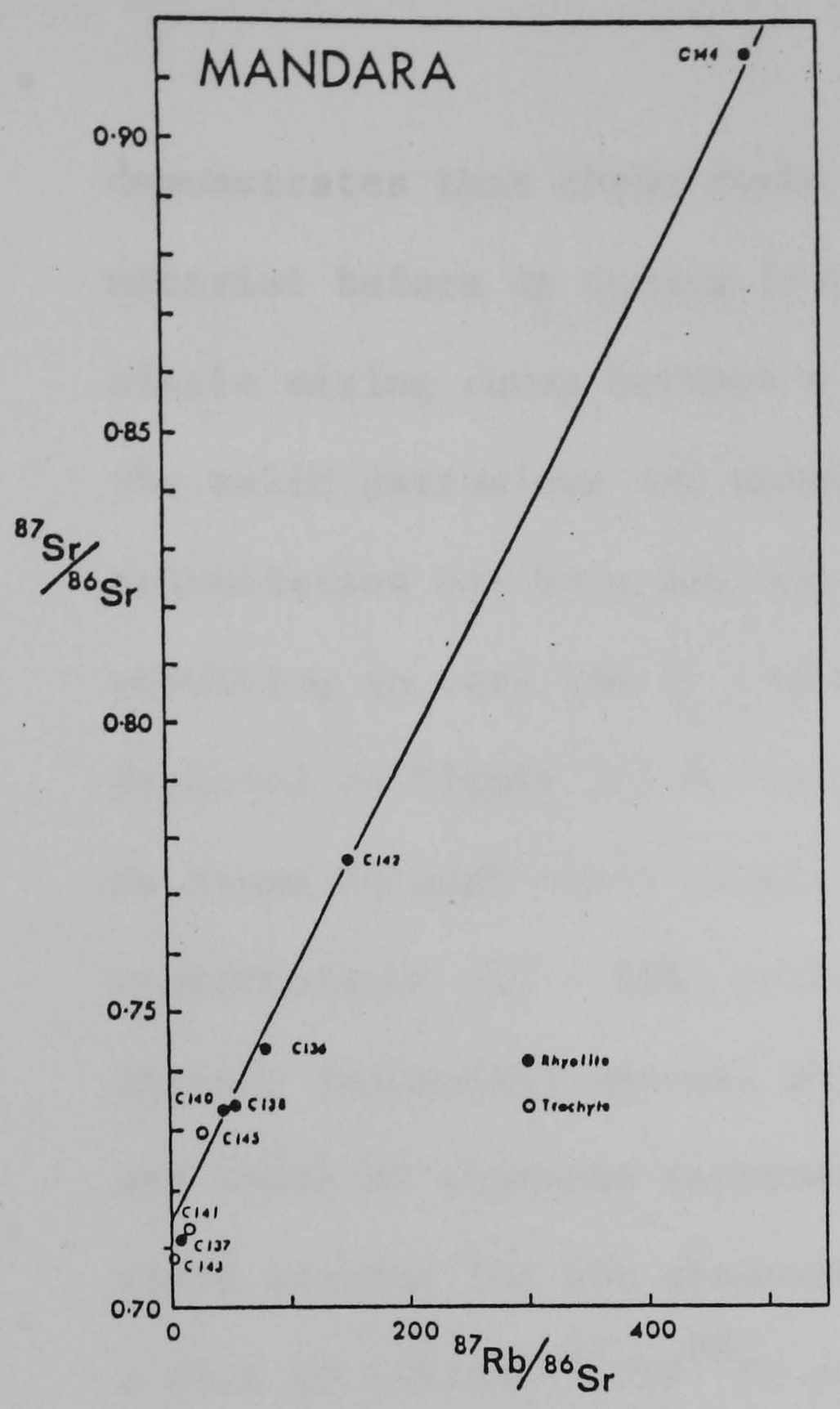
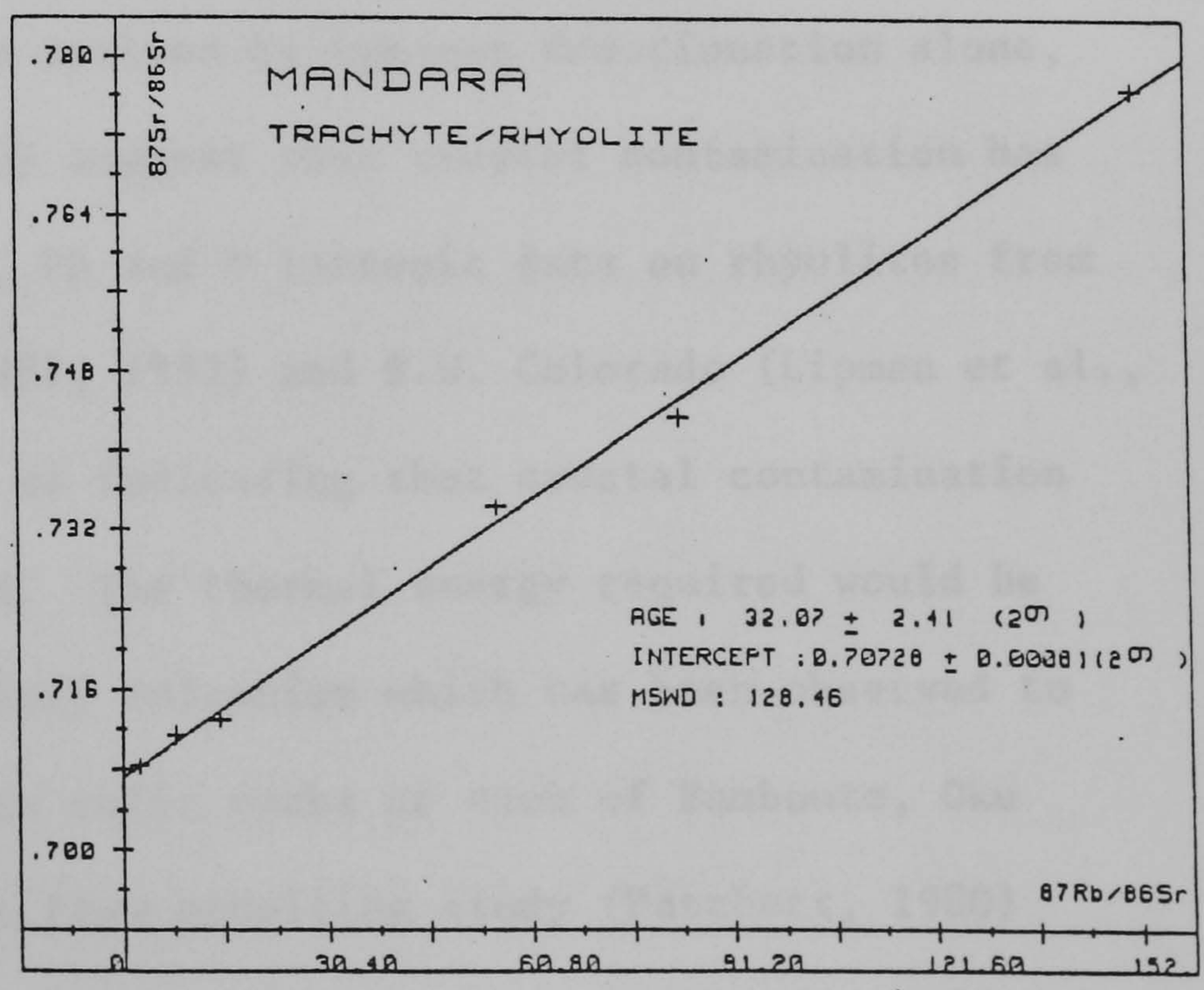


Figure 5.2.9A Sr isotope ratios of Mandara highly fractionated rocks plotted against Rb/Sr atomic. Line is that derived from B.

Figure 5.2.9B Best fit isochron through 6 of these samples (C136, C137,C138,C141,C142, C143).



demonstrates that these rocks were contaminated by radiogenic crustal material before or during fractionation in crustal magma chambers. A simple mixing curve between a likely contaminant (e.g. granulite (74F), the salic extrusives and uncontaminated basalt is not observed because assimilation has been accompanied by intense feldspar fractionation, resulting in very low Sr contents. A curve of similar form to that depicted on Figure 5.2.4, displaced to lower Sr contents could thus be drawn through these rocks. Hence variable degrees of crustal contamination (10 - 50%) probably produced the majority of the samples (mainly trachytes) whereas rhyolites having very high initial ratios and lower Sr contents represent 70 - 95% crustal melts. This mechanism would account for the observed hyperbolic pattern of Bambouto data on a plot of initial $^{87}Sr/^{86}Sr$ ratio versus SiO_2 (Figure 5.2.10) where the rhyolites have SiO_2 contents similar to those observed in the crustal xenoliths (J.G. Fitton, unpublished data). Likewise high and very variable Rb contents for a given Sr content (Rb concentrations are more constant in salic rocks derived by igneous fractionation alone, e.g: São Tomé, Figure 4.2.3) suggest that crustal contamination has occurred (Ewart, 1982). Sr, Pb and O isotopic data on rhyolites from eastern Australia (Ewart, 1981, 1982) and S.W. Colorado (Lipman et al., 1978) were also interpreted as indicating that crustal contamination and/or anatexis had occurred. The thermal energy required would be provided by concurrent basaltic volcanism which has been observed to occur in association with the salic rocks at each of Bambouto, Oku and Mandara. A recent heat flow modelling study (Patchett, 1980) indicated that such basaltic liquid emplacement would lead to wide zones of partial fusion and aqueous fluid circulation at most crustal levels.

Crustal assimilation must have occurred during the final stages of fractional crystallization (such assimilation probably accelerated

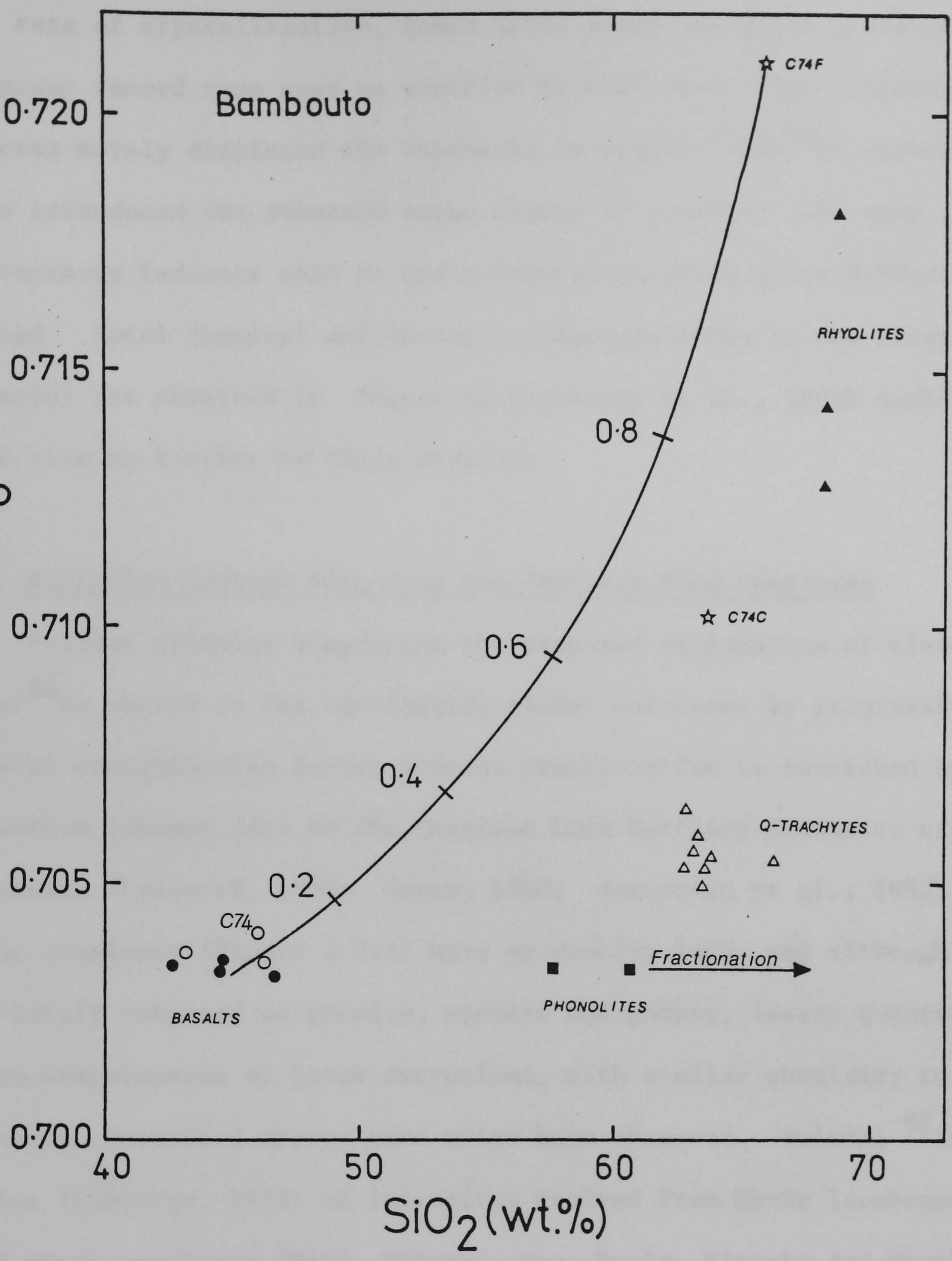


Figure 5.2.10 Initial Sr isotope ratios versus SiO_2 contents for Bambouto volcanic rocks and crustal xenoliths. Curve represents simple mixing of basalt (87Sr/86Sr=0.70325, SiO_2 =45%) and granulite C74F. The proportion of C74F in hybrids is indicated. Filled circles are nepheline-normative basalts and open circles are hypersthene- or quartz-normative basalts (including C74). Stars are granulite xenoliths enclosed in basalt C74.

the rate of crystallization, Bowen 1928) since the Rb-Sr isochron diagrams record true ages as verified by K-Ar data. The contamination process merely displaced the isochrons to higher $^{87}Sr/^{86}Sr$ values and also introduced the observed large degree of scatter. The very low Sr contents indicate that no contamination occurred after differentiation ceased. Local chemical and isotopic inhomogeneities in the crustal material (as observed in Hoggar by Leyreloup et al., 1982) would also give rise to scatter on these diagrams

5.3 Strontium Isotope Data from the Tertiary Ring Complexes

Further evidence supporting the proposed explanation of elevated $^{87}Sr/^{86}Sr$ ratios in the continental sector volcanoes by progressive crustal contamination during igneous fractionation is furnished by strontium isotope data on the Cameroon Line Tertiary intrusive ring complexes (Lasserre, 1978; Okeke, 1980; Jacquemin et al., 1982). These complexes (Figure 3.3.1) have an annular form, and although they are mainly composed of granite, syenite and gabbro, lesser quantities of contemporaneous or later extrusives, with similar chemistry to the volcanoes described above, have often been observed. Initial $^{87}Sr/^{86}Sr$ ratios (Lasserre, 1978) of intrusives derived from Rb-Sr isochrons of 5 of these complexes (Poli, Tchegui, Mayo Darle, Nlonako and Koupé) range from 0.7027 to 0.7068 (Table 5.3.1) and the average would be 0.7049. However there is considerable scatter of the data on the isochrons (MSWDs were not quoted) and there is also considerable disagreement between K-Ar ages (Cantagrel et al., 1978) and Rb-Sr ages derived from these isochrons (Lasserre, op. cit.), particularly for Mayo Darle. In this intrusion (initial strontium ratio = 0.7027) K-Ar ages are considerably lower (49 Ma) than that derived by Rb-Sr methods

TABLE 5.3.1

Published Initial Strontium Isotope Data from Tertiary Ring Complexes

Centre	Rock Types	Number of Samples	$^{87}Sr/^{86}Sr_o$ ($\pm 2\sigma$ on last digits)	Sr (ppm)	Reference	Comments
Poli	Granite	8	0.7042 ± 19		1	Isochron
Tchégui	Syenite, gabbro, trachyte	10	0.7046 ± 3		1	Isochron
Mayo Darle) Mbu Namboe)	Granite	6	0.7027 ± 11		1	Isochron
Nlonako	Syenite, microgabbro, granite	6	0.7055 ± 1		1	Isochron
Koupé	Syenite	5	0.7068 ± 12		1	Isochron
Golda Zuelva	Riebeckite granite	7	0.7020 ± 12		2	Isochron
"	Olivine gabbro		0.70349	706	2	Calculated assuming an age of 66 Ma
"	Microgabbro		0.70306	697	2	"
"	Riebeckite-diorite		0.70357	800	2	"
"	K benmoreite 177M		0.70413	1,083	2	"
"	K benmoreite G68-80		0.70451	381	2	"
"	Rhyolite 32GZ		0.70395	218	2	"
"	Rhyolite 4GZ		0.70370	932	2	"
Mboutou N. centre	Gabbro		0.70375	954	2	Calculated assuming an age of 60 Ma
"	Noritic leucogabbro		0.70401	1,014	2	"
"	Monzodiorite		0.70398	600	2	"
"	Syenite		0.70353	299	2	"
"	Syenite		0.70362	523	2	"
Mboutou S centre	Gabbro		0.70534	976	2	"
"	Gabbro		0.70517	820	2	"
"	Gabbro		0.70505	1,292	2	"
"	Monzonite		0.70540	60	2	"
"	Qz monzodiorite		0.70598	839	2	"
"	Granite		0.70454	67.6	2	"
"	Granite		0.70495	109	2	"

References: 1 Lasserre et al. (1978)

2 Jacquemin et al. (1982)

(63.3 Ma). The K-Ar dates are almost certain to be the more reliable since they were performed on K-feldspar or biotite separates (Table 3.3.3) whereas the Rb-Sr data were obtained from a whole-rock isochron. Hence the initial ratio of the Mayo Darle granite is probably higher than that proposed by Lasserre (op. cit.). For example the sample with the lowest Rb/Sr ratio (Sample RT 5360) would have an initial ratio of 0.7128 if the K-Ar ages were correct as opposed to 0.7029 if the Rb/Sr age is assumed. Where K-Ar and Rb-Sr age agreement is acceptable (Nlonako) the initial ratio is higher (0.7055). It is therefore concluded that many of the initial ratios of these complexes are probably higher than that indicated by Lasserre and are likely to range from greater than 0.704 to at least 0.713.

Jacquemin et al. (1982) have recently studied two of these complexes, Golda Zuelva and Mboutou in more detail. Data from Golda Zuelva (Table 5.3.1) indicate that volcanism (hawaiites, K-benmoreites and rhyolites) was essentially contemporaneous with alkaline plutonism (riebeckite-arfvedsonite granites, olivine gabbros) and that Pb and Sr isotopes of these rocks attest to a mantle origin. However, the oxygen isotope data these authors also presented indicate that at least the granitic endmembers have suffered some crustal contamination. In fact all the data on the extrusives are elevated with respect to uncontaminated Cameroon basalts (0.7029 to 0.7037) since they range from 0.70370 to 0.70451. For example the K-benmoreite G68-80 would plot very close to C81 on figure 5.2.4 and K-benmoreite 177M would likewise plot very close to C74. Both C81 and C74 have been demonstrated as having undergone small degrees of crustal contamination. Hence, in the light of the present work, most of the strontium isotope ratios on Golda Zuelva

extrusives reflect small amounts of crustal involvement during their evolution if the assumed age of 66Ma for this complex is correct. In addition such small levels of contamination may not necessarily be reflected in the Pb isotopic data since the crust and mantle have fairly similar U/Pb ratios (Hart and Allegre, 1980). If a much younger K-Ar age of the Golda Zuelva extrusives, obtained by Cantagrel et al. (1978) had been employed for radiogenic growth corrections then even higher initial ratios would result. As with Mayo Darle, the age of this complex is thus not sufficiently well known to enable further, more detailed discussion.

On the other hand, the K-Ar and Rb-Sr ages from Mboutou are in close agreement (Tables 3.3.2 and 3.3.3) at 56.5 and 60 Ma respectively. No extrusives were reported but plutonic rocks (gabbros, monzodiorities, syenites, monzonites and granites) have initial ratios ranging from 0.70353 to 0.70598 (Table 5.3.1). Pb and O isotopic data were also taken to indicate that the Mboutou magmas underwent magma-crust interactions at high crustal levels and the authors concluded that the evolution of this complex was dominated by fractional crystallization and progressive crustal contamination processes.

Sr isotopic data from the Kirawa rhyolite dome (Tables 3.3.1; this study, Chapter 3; Okeke, 1980) indicate that these rocks also underwent considerable contamination since a 6 point Rb-Sr isochron has an initial ratio of 0.7124, equivalent to approximately 70% crustal assimilation according to the curve on Figure 5.2.4.

5.4 Summary of the Sr-Isotope Data on the Mafic Volcanic Rocks from Cameroon

The above sections have demonstrated that the Etinde and Mt. Cameroon lavas have very similar isotopic ratios (Figure 5.4.1) and were probably

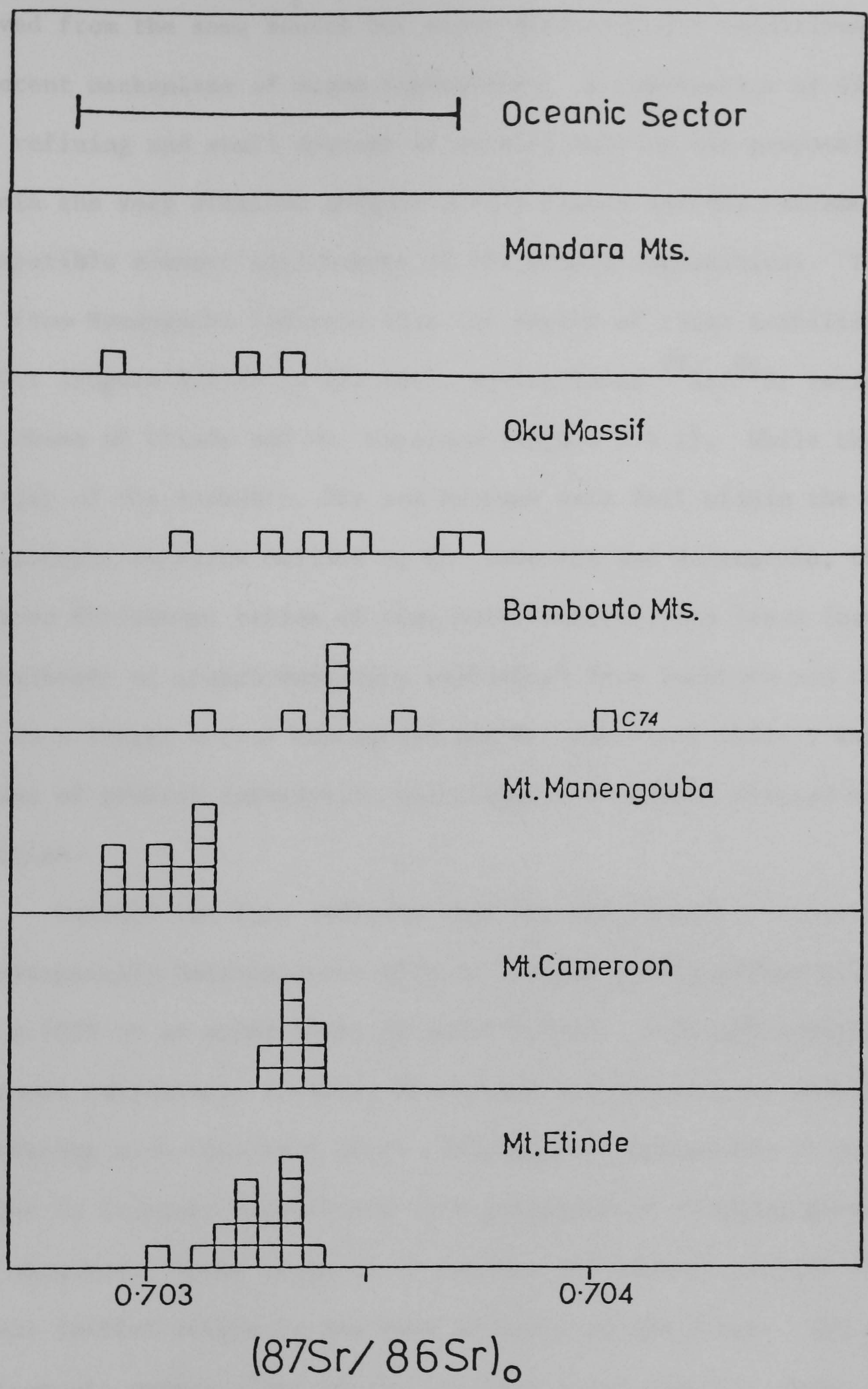


Figure 5.4.1 Frequency histogram of Sr isotope data in basic lavas from the Cameroon volcanoes. The range of values from the islands in the Gulf of Guinea (from figure 4.4.3) is also indicated.

derived from the same source but under different P-T conditions and different mechanisms of magma segregation. A combination of diffusive zone refining and small degrees of partial melting was proposed to explain the very alkaline (Figure 5.4.2) nature and the extreme incompatible element enrichments of the Etinde nephelinites. Isotope data from Manengouba indicate that the source of these transitional basalts (Figure 5.4.2) is distinct, having lower $^{87}Sr/^{86}Sr$ ratios than those of Etinde and Mt. Cameroon (Figure 5.4.1). While the majority of the Bambouto, Oku and Mandara data fall within the chemical and isotopic spectrum defined by Mt. Cameroon and Manengouba, the elevated Sr-isotope ratios of some mafic-intermediate lavas (usually hypersthene- or quartz-normative varieties) from Bambouto and Oku (and to a lesser extent Manengouba and Mt. Cameroon) reflect small degrees of crustal interaction superimposed on mantle derived heterogeneities.

Overall the data indicate that the sub-Cameroon source region is isotopically heterogeneous with Sr-isotope ratios probably ranging from 0.7029 to an upper limit of about 0.7037. Although several volcanoes demonstrate internal fine-scale inhomogeneities sometimes correlating with chemistry (e.g: Manengouba), systematic or progressive changes in isotopic composition with geographical location have not been observed. Hence there is no correlation between crustal thickness and the initial ratios in the vast majority of the lavas. The chemical and isotopic compositions of the uncontaminated basaltic rocks are virtually identical to those observed in the oceanic sector volcanoes where the data were interpreted as being indicative of a vertically heterogeneous mantle (Figures 5.4.1, 5.4.2). It can be concluded that the Cameroon volcanoes and the islands in the Gulf of Guinea constitute

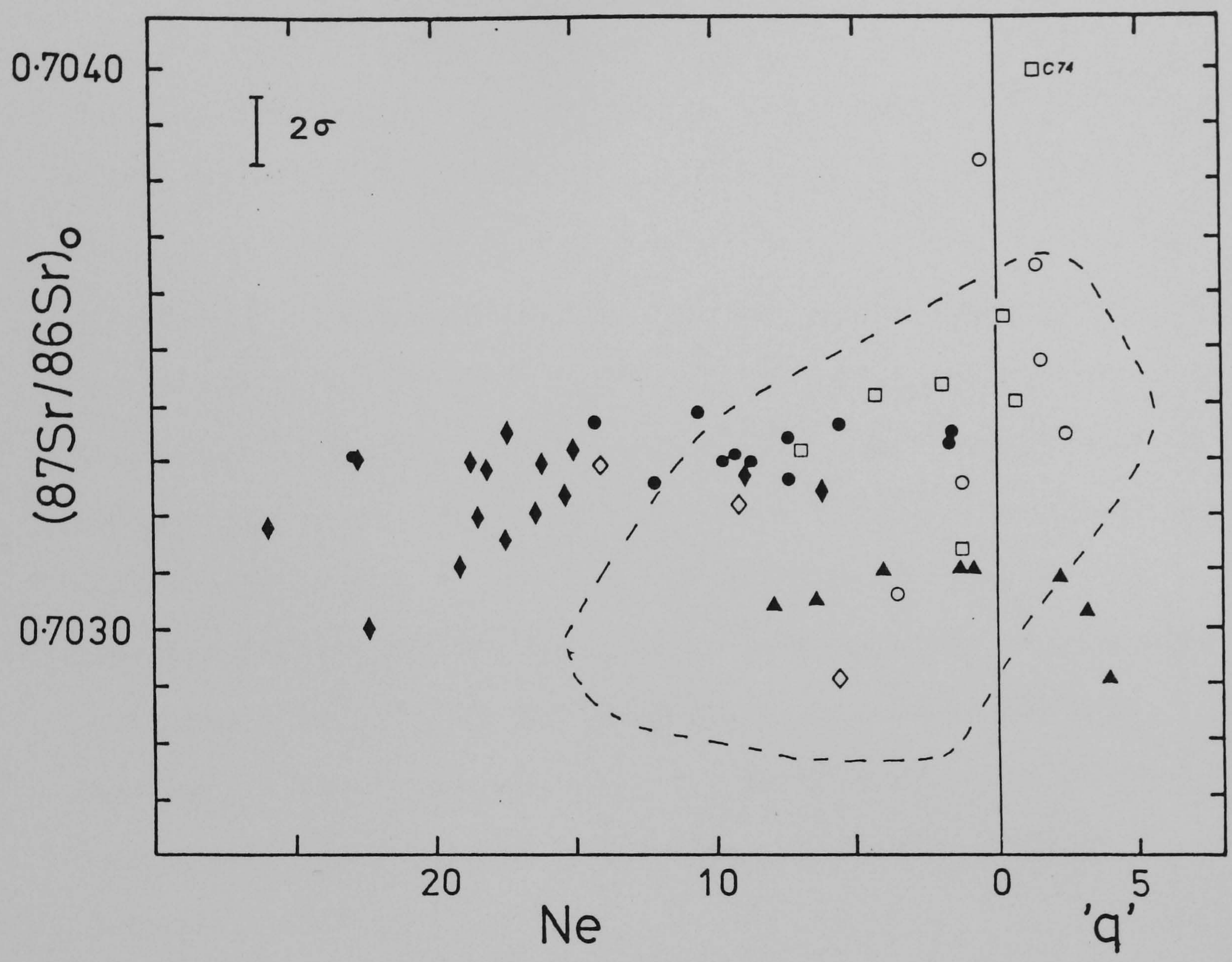


Figure 5.4.2 Initial strontium isotope ratios plotted against degree of silica over- and under- saturation for lavas with >4%MgO from the Cameroon volcanoes. Symbols as in figure 5.1.2 . The field of the islands in the Gulf of Guinea is also shown, as a dotted line (from figure 4.4.4).

one magmatic province. The implications of these findings are discussed in Chapter 7 and data from Cameroon are compared to the neighbouring Biu plateau in Chapter 6.

CHAPTER 6

GEOCHEMISTRY OF VOLCANIC ROCKS FROM N.E. NIGERIA

It is probable that the Biu, Song and Longuda plateaux (Figures 1.1, 1.2, 3.2.2) represent the northward continuation of the Cameroon Line volcanoes since: (a) cinder cones trend N-S; (b) the outline of the Cameroon Line volcanoes, with these plateaux, has a form identical to that of the Benue Trough (Fitton, 1980); and (c) the volcanism is of similar character to, and contemporaneous with centres in the Gulf of Guinea and Cameroon. The nature of the association of this region to the remainder of the Cameroon Line is critical to the understanding of the entire Tertiary-recent volcanic province and to the evolution of the West African rift-system. Consequently, comprehensive chemical (by XRF methods) and Sr-isotope analyses have been carried out in order that comparisons may be made with the Cameroon volcanoes, islands in the Gulf of Guinea and with other intercratonic Cenozoic igneous activity in west and northwest Africa.

6.1 Major and Trace Element Geochemistry

Whole-rock XRF analyses and normative calculations on lavas from Biu and Song (Tables B1 and B3) indicate that these plateaux are composed entirely of transitional to moderately alkaline basalts, basanites and rare hawaiites. There is a notable absence of highly fractionated salic rocktypes. A plot of Differentiation Index versus degree of silica over- and under-saturation (Figure 6.1.1) shows that the Biu basal lavas (resting on basement), other Biu and Song lavas, and lavas from recent cones plot within a restricted range of D.I. from

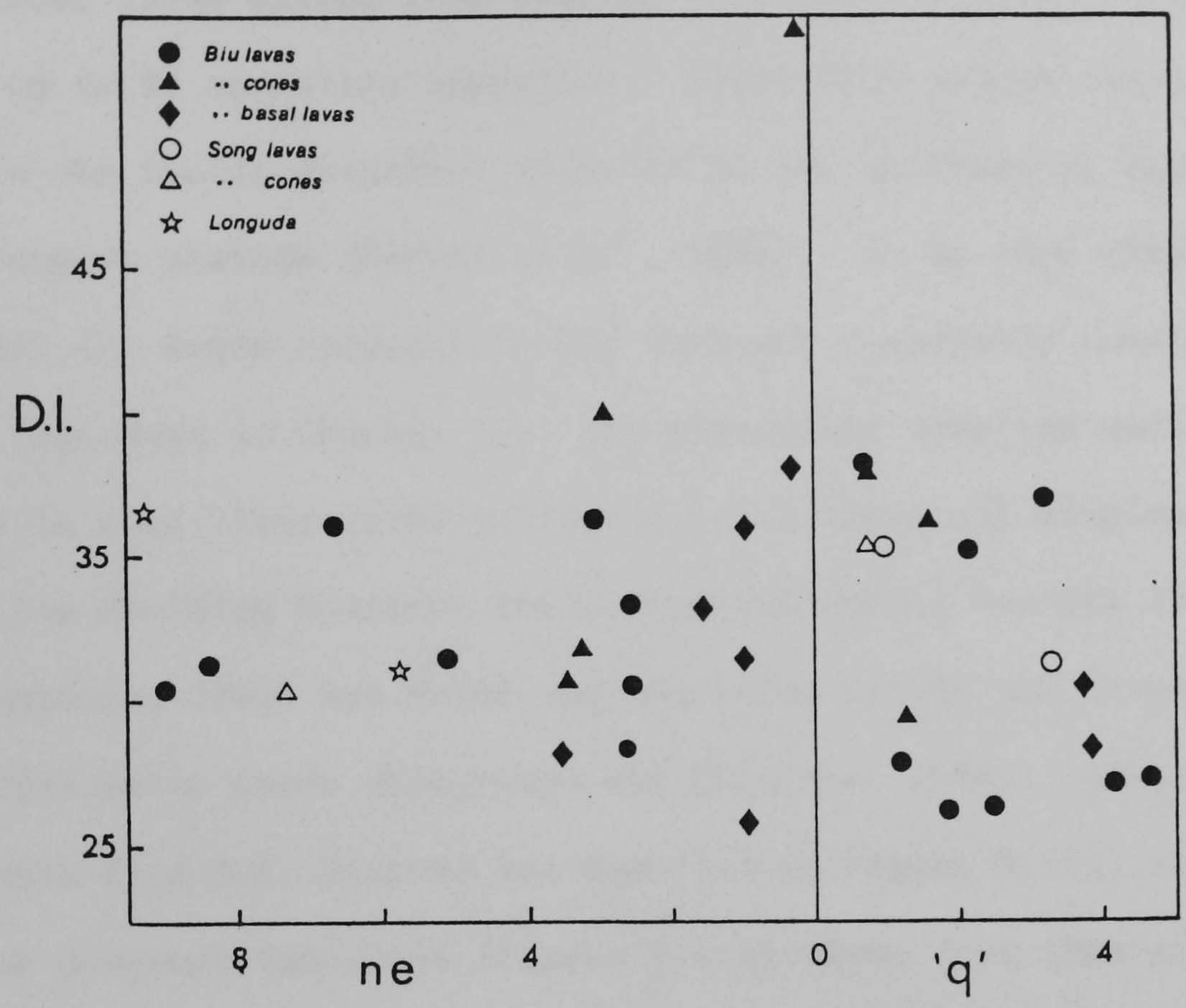


Figure 6.1.1 Differentiation Index plotted against degree of silica over- and under-saturation for lavas from the Biu, Song and Longuda plateaux. Longuda data from Carter et al. (1963).

25 to 40. The one hawaiite recovered (N29) is the sole exception to this, having a D.I. of 53. The basal lavas are transitional, ranging from 3.8% normative nepheline to 13.7% normative hypersthene whereas the later lavas extend from similar transitional basalts to basanites with up to 9% normative nepheline. Lavas from recent cones fall within the fields described above as do two analyses of basalts from the Longuda plateau (Carter et al., 1963). It is then clear that overall the magma composition has remained remarkably constant over 5 Ma (age data in Chapter 3). The moderately alkaline nature of these lavas is also illustrated on Figure 6.1.2 where all samples plot above the line dividing Hawaiian tholeiites and alkali basalts (MacDonald and Katsura, 1964) but below that dividing mildly and strongly alkaline mafic rocks (Saggerson and Williams, 1964). Comparison of the data from N.E. Nigeria (as depicted on Figure 6.1.2) with those of the Cameroon volcanoes (Figure 5.1.3) shows that they plot in a field defined by relatively primitive lavas from Mt. Cameroon, Manengouba, Bambouto, Oku and Mandara.

The relatively primitive nature of these rocks is demonstrated on Figures 6.1.3 and 6.1.4 where the total MgO variation is from 4% to 11.5% or 7.1% to 11.5% if the single hawaiite is omitted. Indeed, 10 lavas (N1, N2, N9, N10, N14, N18, N19, N22, N25, N36) may be described as picritic since they have MgO contents greater than 10%. These diagrams show the chemical similarity of the Biu and Song lavas to basaltic rocks from the other volcanoes forming the Cameroon Line (except Etinde) and are typical of within plate basalts such as Hawaii (Figure 6.1.5 and B.V.S.P., 1981). The compatible trace elements Ni and Cr reflect very slight degrees of olivine and clinopyroxene fractionation with all but hawaiite N29 suffering less than 5% olivine fractionation

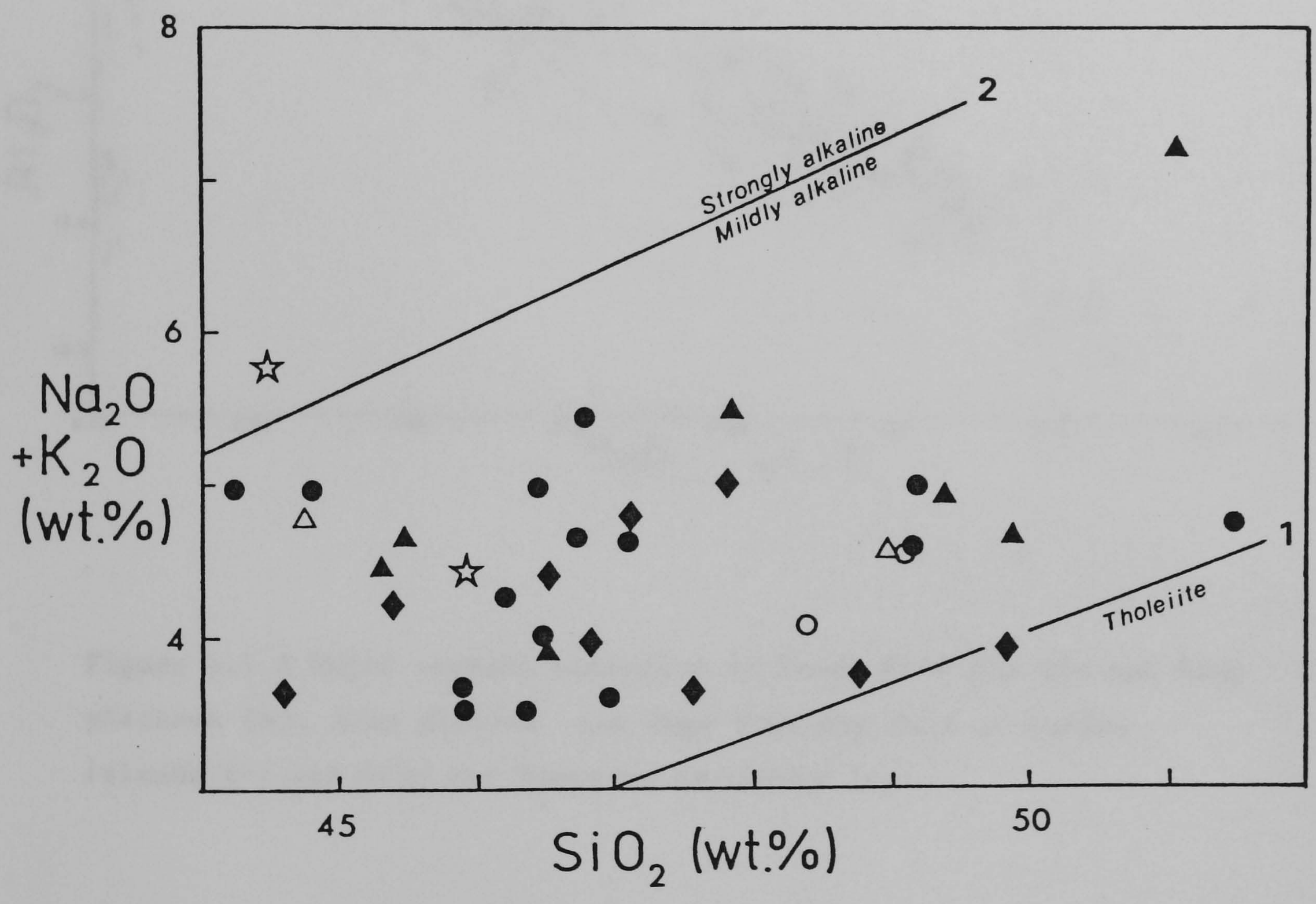


Figure 6.1.2 Na_2O + K_2O plotted against SiO_2 for lavas from the Biu, Song and Longuda plateaux. Symbols as in figure 6.1.1 and the Longudá data data is from Carter et al. (1963). Curves 1 and 2 as in figure 5·1·3.

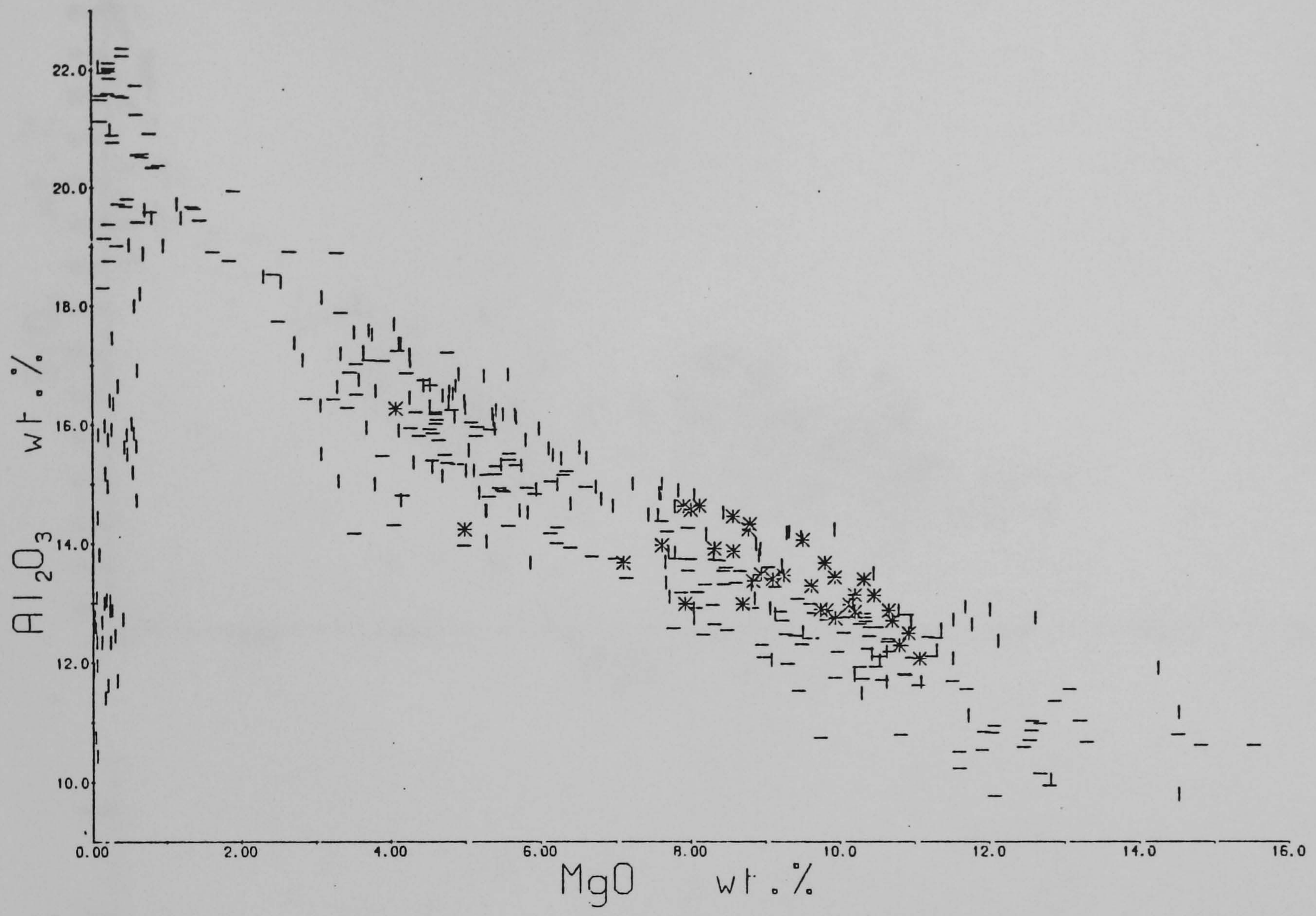


Figure 6.1.3 Major element variation in lavas from the Biu and Song plateaux (*). Also plotted are data from the Gulf of Guinea islands (-) and from the Cameroon volcanoes (ı).

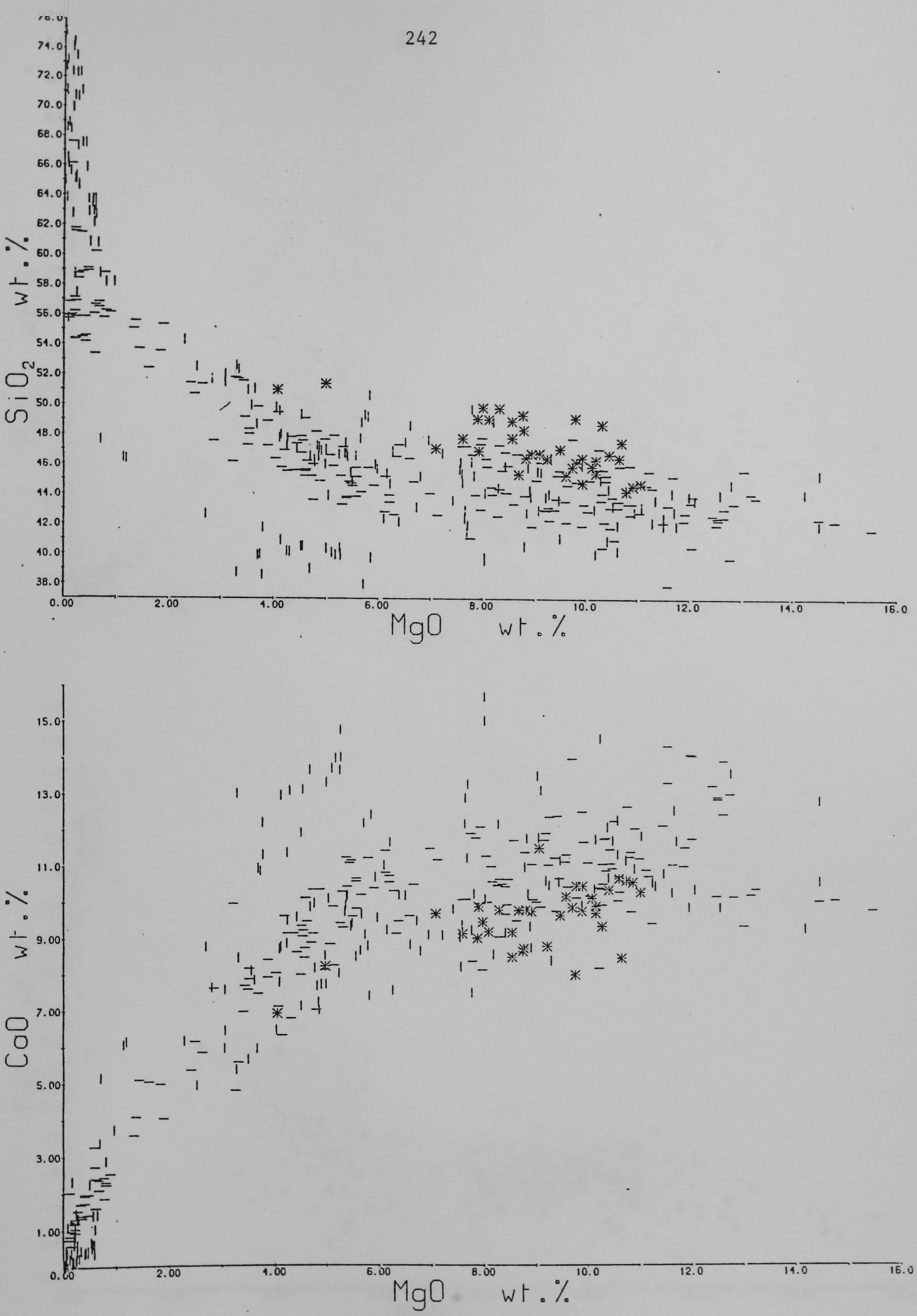


Figure 6.1.3 continued.

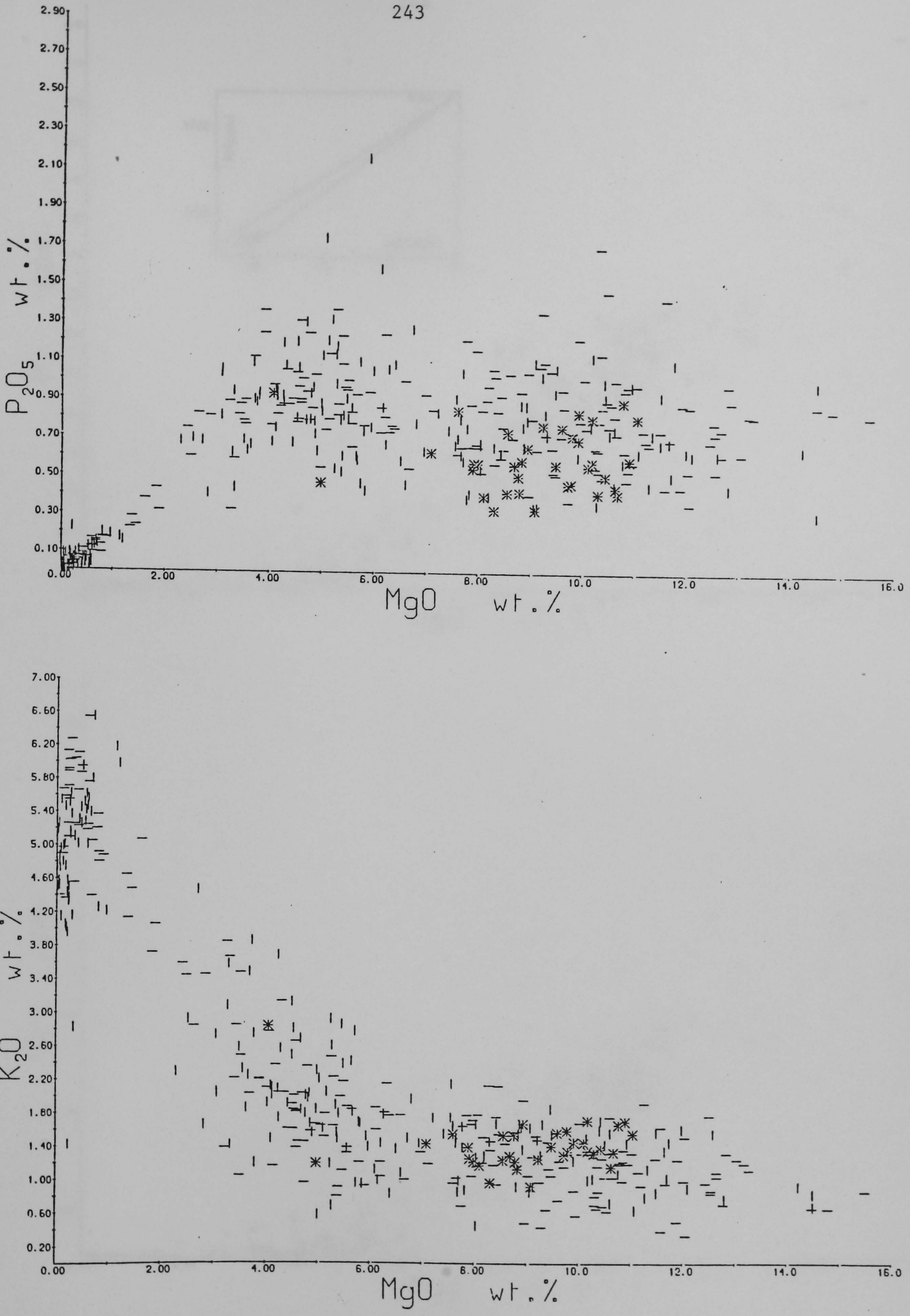


Figure 6.1.3 continued.

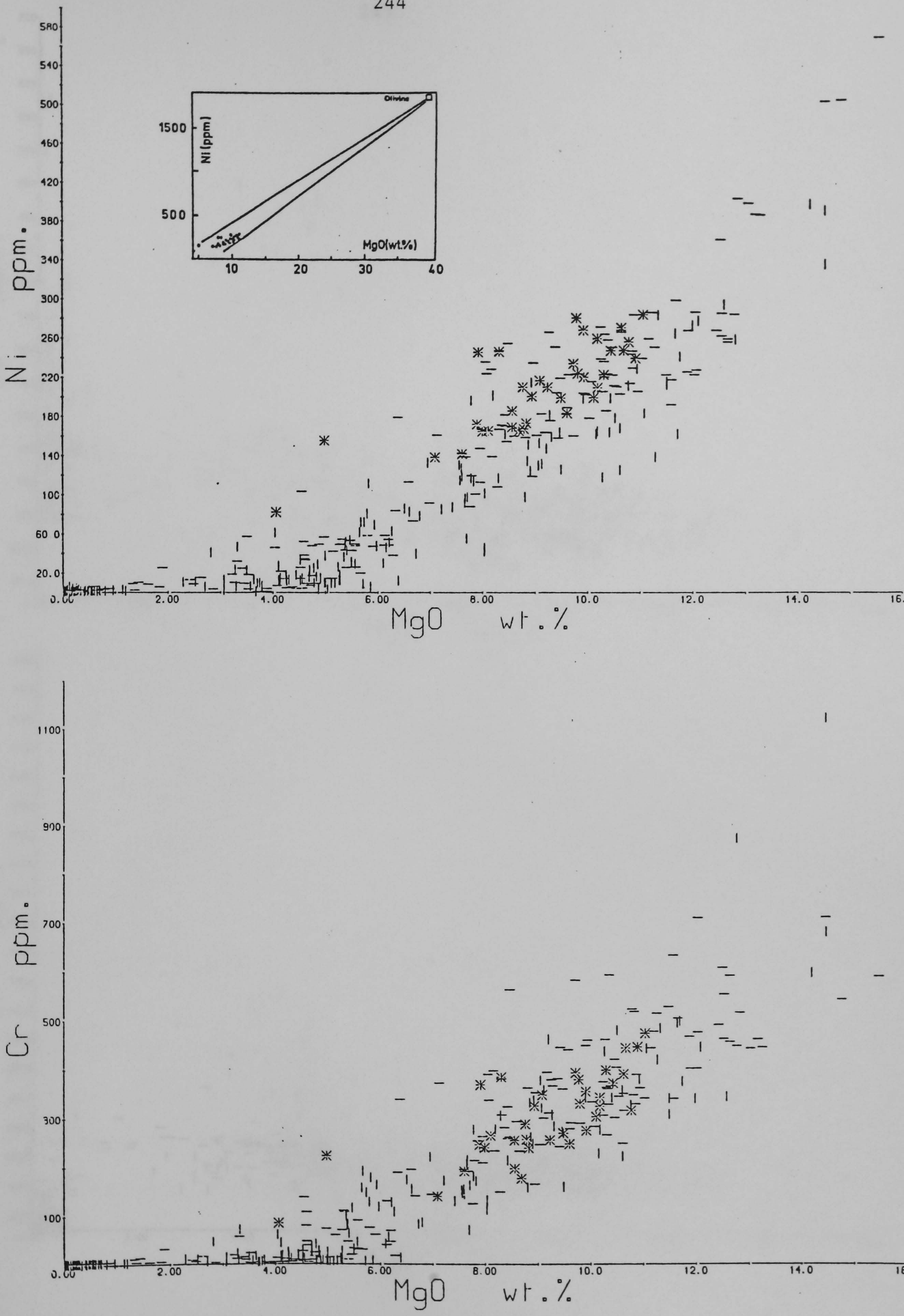


Figure 6.1.4 Trace element variation in lavas from the Biu and Song plateaux. Symbols as in figure 6.1.3. Inset in the MgO-Ni plot shows the limited olivine control of the Biu lavas; olivine

71).

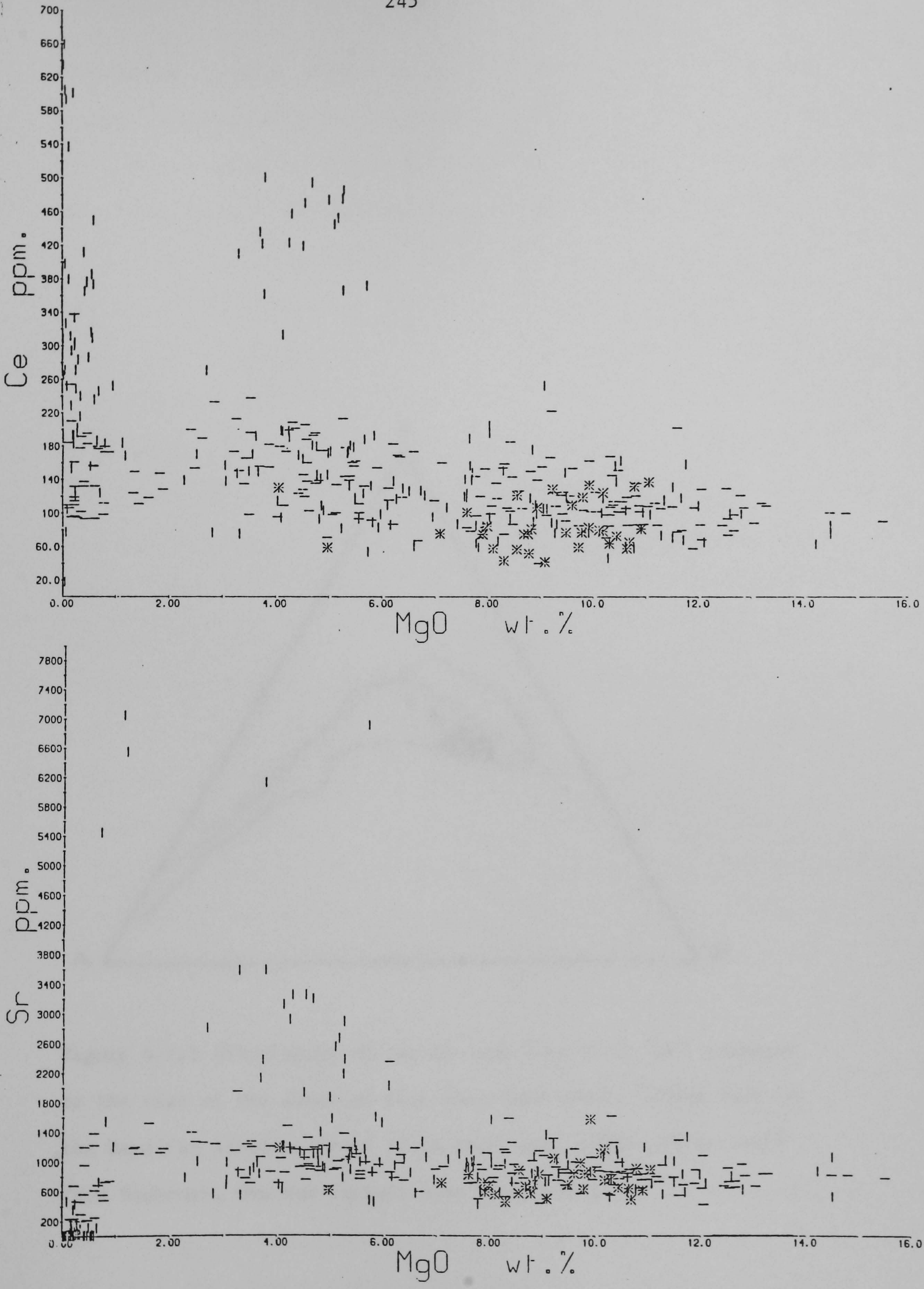


Figure 6.1.4 continued.

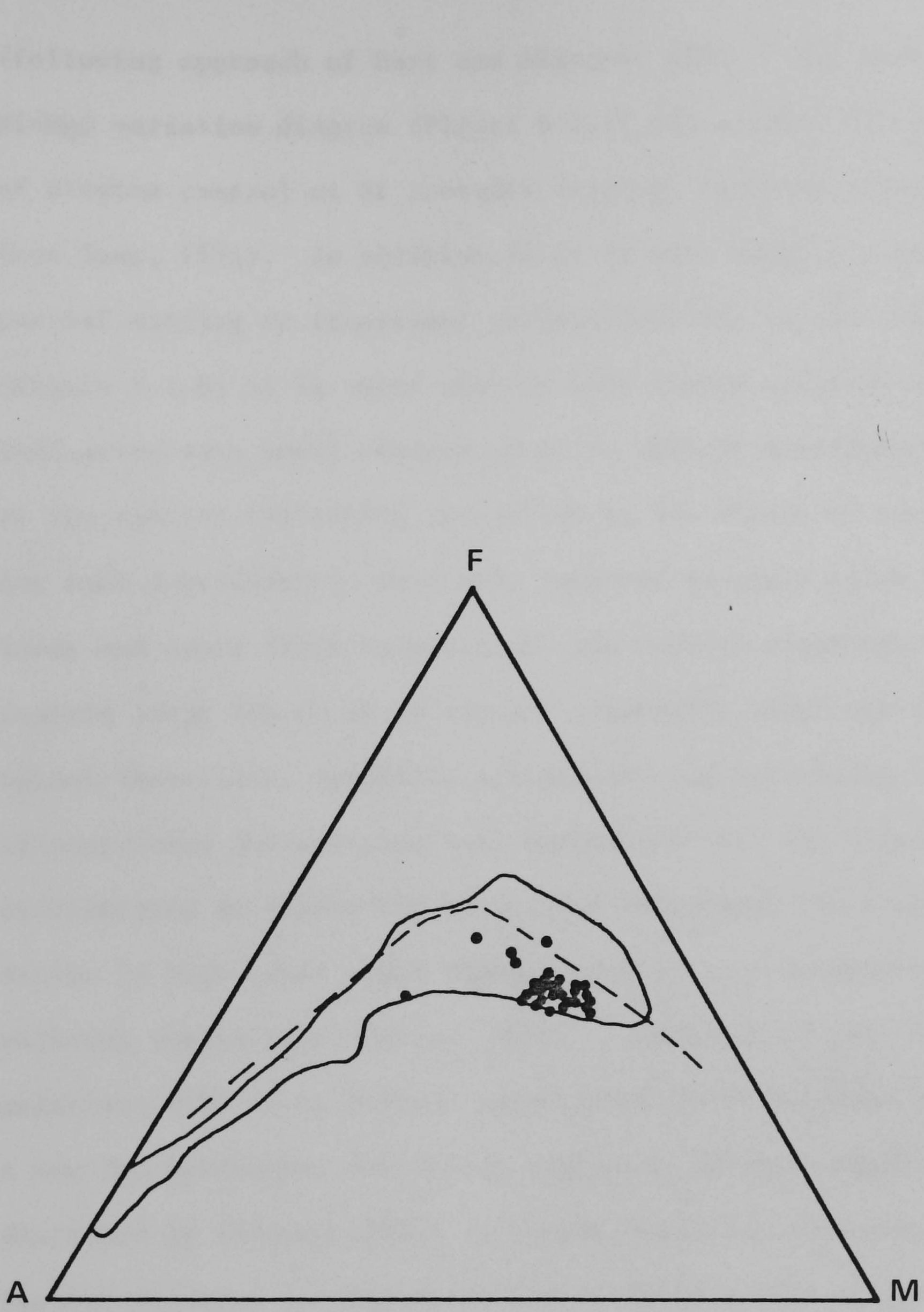


Figure 6.1.5 AFM diagram of the Biu and Song lavas (●) compared to the rest of the Cameroon line (enclosed area). Dotted line is the Hawaiian alkaline trend after Macdonald (1968). Salic rocks from Bambouto, Oku and Mandara have been omitted.

(following approach of Hart and Allegre, 1980). The inset in the Ni-MgO variation diagram (Figure 6.1.4) illustrates the slight degree of olivine control on Ni contents (typical Hawaiian olivine composition from Gunn, 1971). In addition if Zr (a very sensitive indicator of partial melting or fractional crystallization) is plotted against Cr (Figure 6.1.6) it is noted that Cr only varies slightly with Zr indicating very small degrees of mafic mineral fractionation with most of the scatter reflecting variations in the degree of partial melting. Any such fractionation must have happened at depth since many of the lavas and cones (both hypersthene- and nepheline-normative varieties) contain large (up to 20 cm across) ultramafic xenoliths (dunite, spinel-lherzolite, wehrlite, pyroxenite) and megacrysts of garnet, clinopyroxene and anorthoclase, indicating that the liquids last equilibrated at depths >30 km without subsequent fractional crystallization in high level magma chambers and without undergoing magma-wallrock interaction (Spera, 1980). Analyses of the clinopyroxene megacryst N12C (J.G. Fitton, unpublished data) indicate that it is a low Ti, aluminous, sub-calcic augite of similar composition to those described by Chapman (1976) as having formed at pressures >25 kb. Further evidence for fractionation at these depths is given by the fact that the hawaiite (which has undergone perhaps 10-20% olivine fractionation also contains spinel-lherzolite nodules. The possibility that such hawaiites may be generated at depth by fractional crystallization, perhaps within the mantle, was also demonstrated by Green et al. (1974).

The primitive nature of lavas from N.E. Nigeria is also evident from a high mean Mg number of 67, high mean MgO content of 9.1% and high mean Ni content of 208 ppm (Table 6.1.1). These are all values

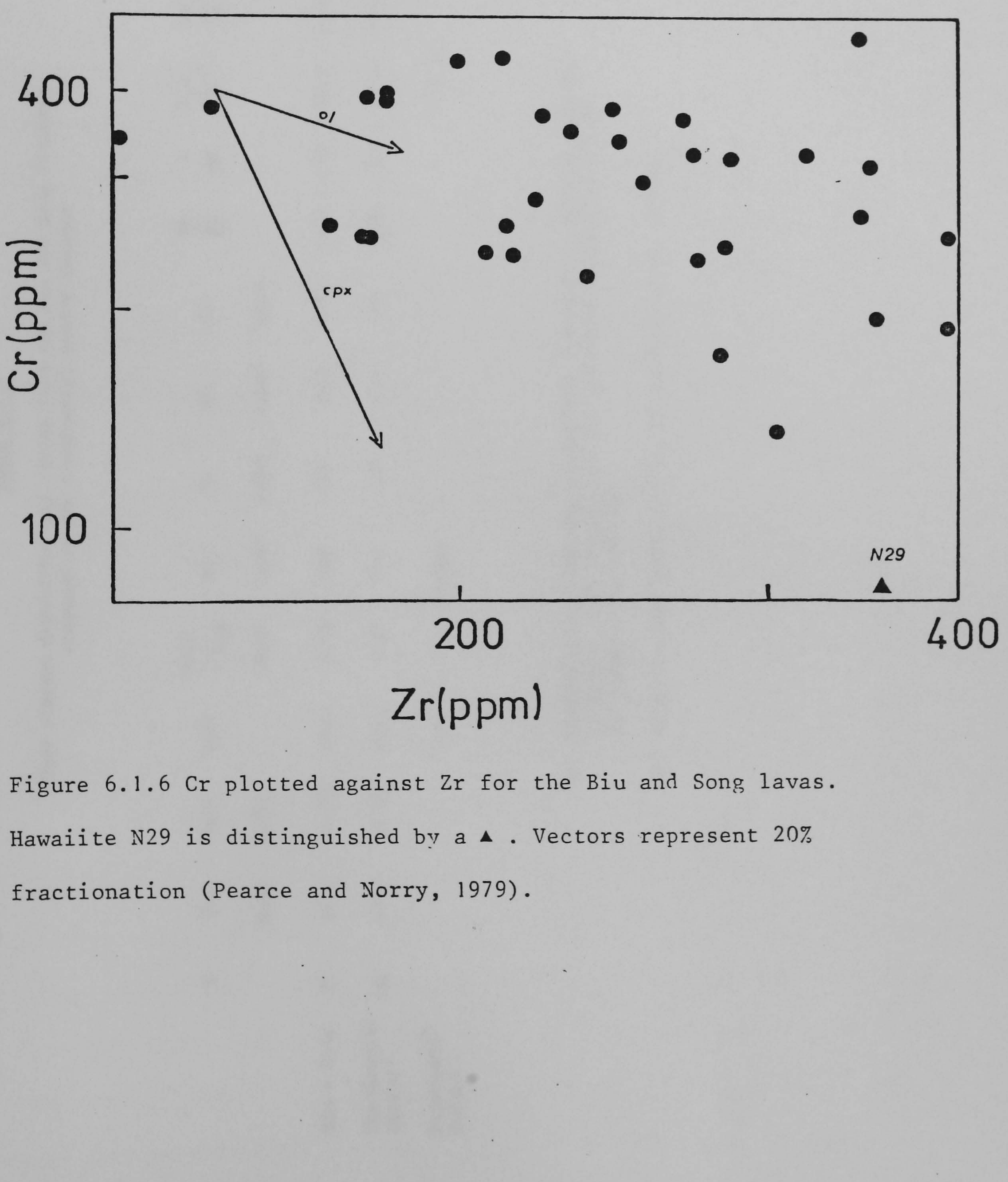


Figure 6.1.6 Cr plotted against Zr for the Biu and Song lavas. Hawaiite N29 is distinguished by a ▲ . Vectors represent 20% fractionation (Pearce and Norry, 1979).

TABLE 6.1.1

Mean element abundances and ratios from the Biu and Song Plateaux compared to the continental sector average

	N	SiO_2 (Wt%)	MgO (Wt%)	MgN	$Na_2O + K_2O$ (Wt%)	Ni (ppm)	Cr (ppm)	Rb (ppm)	Sr (ppm)	$\frac{Rb}{Sr}$	$\frac{K}{Rb}$	$\frac{P_2O_5}{Ce}$	$\frac{La}{Ce}$	$\frac{Sr}{Ce}$	$\frac{La}{Y}$	$\frac{Zr}{Nb}$
Biu + Song	35	47.4	9.06	67.1	4.48	208	299	39.6	778	0.05	293	69.4	0.53	9.09	1.7	4.0
Continental Sector[a]	134	45.7	8.18	62.9	4.82	141	237	39.0	919	0.04	312	65.3	0.52	8.24	2.0	4.2
Primitive[b] Values				>64			>>100					75 ± 15				

a: Comprises Mt. Cameroon, Manengouba, Ngaoundere, Bambouto and Oku (analyst: J.G. Fitton) and Biu and Mandara (analyst: H.M.D). All samples with >4% MgO

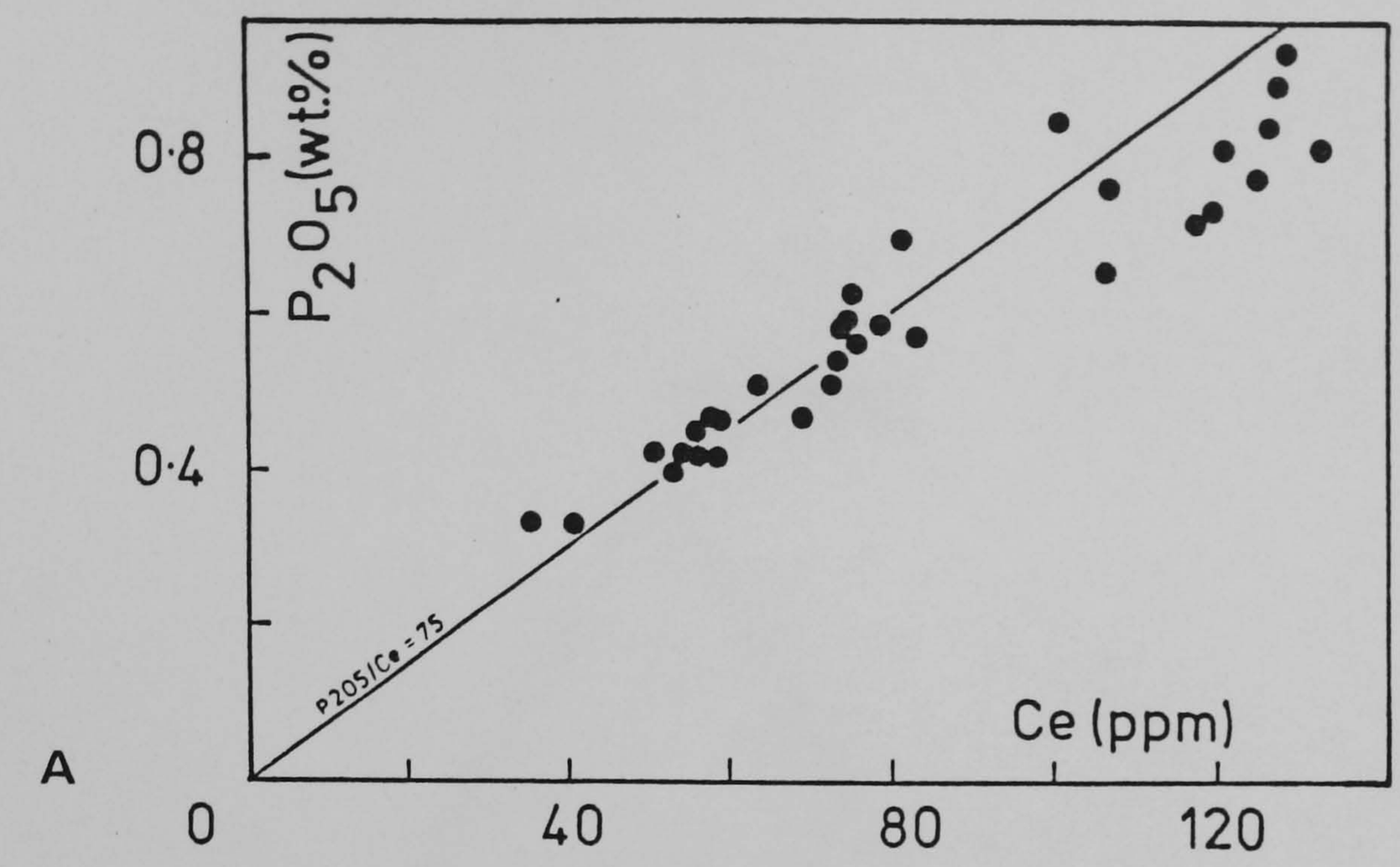
b: After Sun and Hanson (1975a, b) and Frey et al. (1978).

typical of primitive (or primary in many workers' terminology, e.g: Sun and Hanson, 1975b; Frey et al., 1978) compositions. In addition P_2O_5 demonstrates a very good correlation with Ce concentration (Figure 6.1.7a) with P_2O_5/Ce ratios typical of compositions having undergone no modification subsequent to mantle segregation.

The degree of incompatible element enrichment is depicted on Figure 5.1.6, where the Biu and Song plateaux show very similar patterns of normalized element concentrations to those from Manengouba, Bambouto and Oku mafic rocks. Consequently K/Rb, Zr/Nb, Sr/Ce, La/Ce, and La/Y incompatible element ratios (Table 6.1.1 and Figure 6.1.7b) are virtually identical to the other volcanoes constituting the Cameroon Line and Biu high field strength element concentrations (Ti, Zr, Y, Figure 6.1.8) are typical of within-plate basalts (following the terminology of Pearce and Cann, 1973).

6.2 Strontium Isotope Results and Discussion

$^{87}Sr/^{86}Sr$ ratios (unspiked determinations) of 20 basalts, 4 basanites and 1 hawaiite (Table 6.2.1) from the Biu and Song plateaux have a total range of values from 0.70298 to 0.70373. This is essentially the range exhibited by uncontaminated basalts both from islands in the Gulf of Guinea and from the Cameroon volcanoes (Figures 6.2.1, 5.1.10). There is no distinction to be made between samples containing or lacking ultramafic nodules (respective ranges are 0.70306 to 0.70372, and 0.70298 to 0.70368) and likewise the basal lavas have similar isotopic compositions to the later lavas and cones. Although these samples all have very similar Rb/Sr ratios (and Rb, Sr contents, Figure 6.2.2) it is immediately apparent from Figure 6.2.3 that the ne-normative basalts and basanites have lower strontium



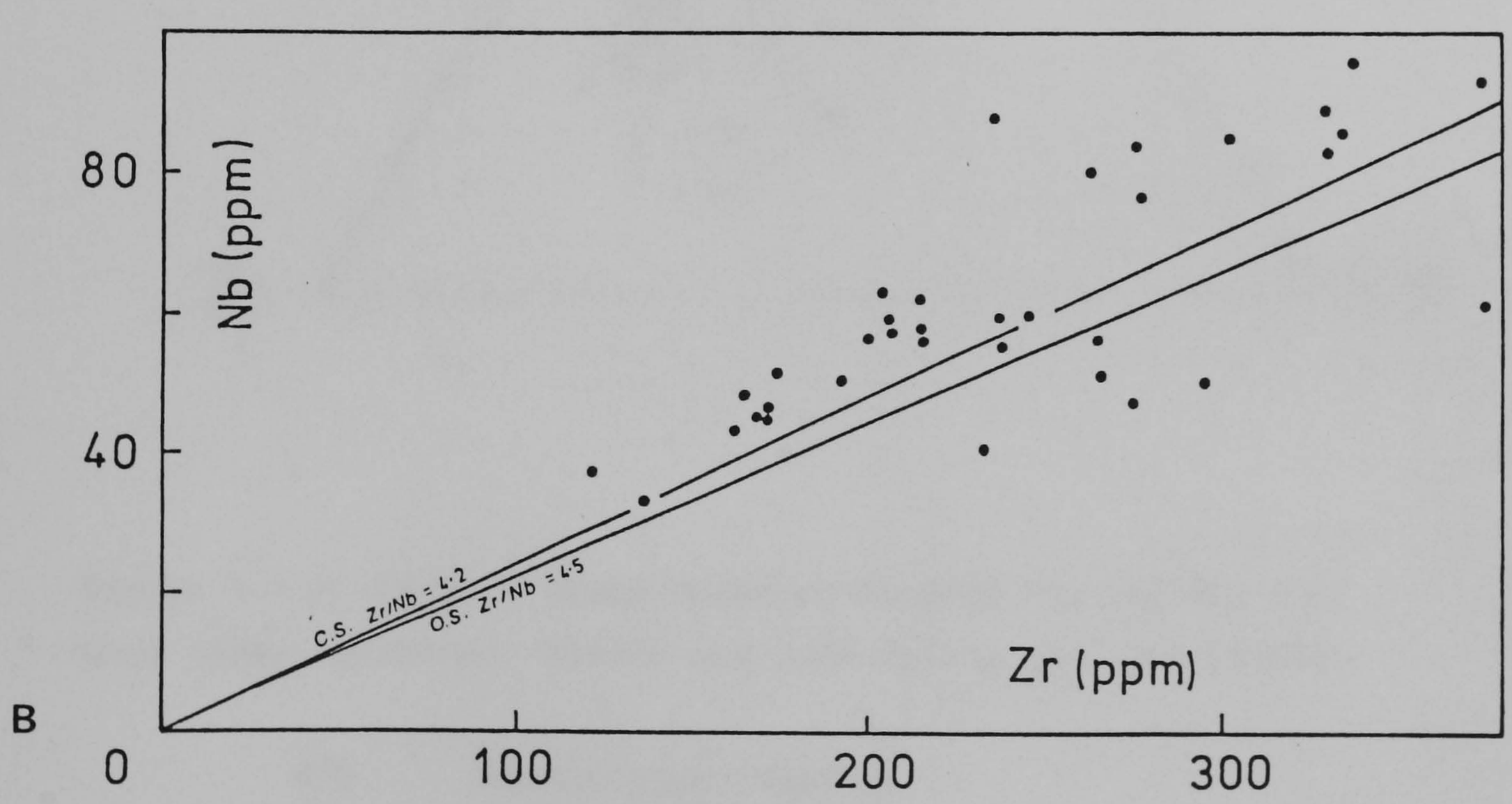


Figure 6.1.7A P_2O_5 - Ce correlation of the Biu and Song lavas. The primitive mantle P_2O_5/Ce ratio is indicated (Sun & Hanson,1975a).

Figure 6.1.7B Zr-Nb correlation of the Biu and Song lavas. The continental (excluding Etinde) and oceanic sector average Zr/Nb ratios (c.s. and o.s. respectively) are also shown.

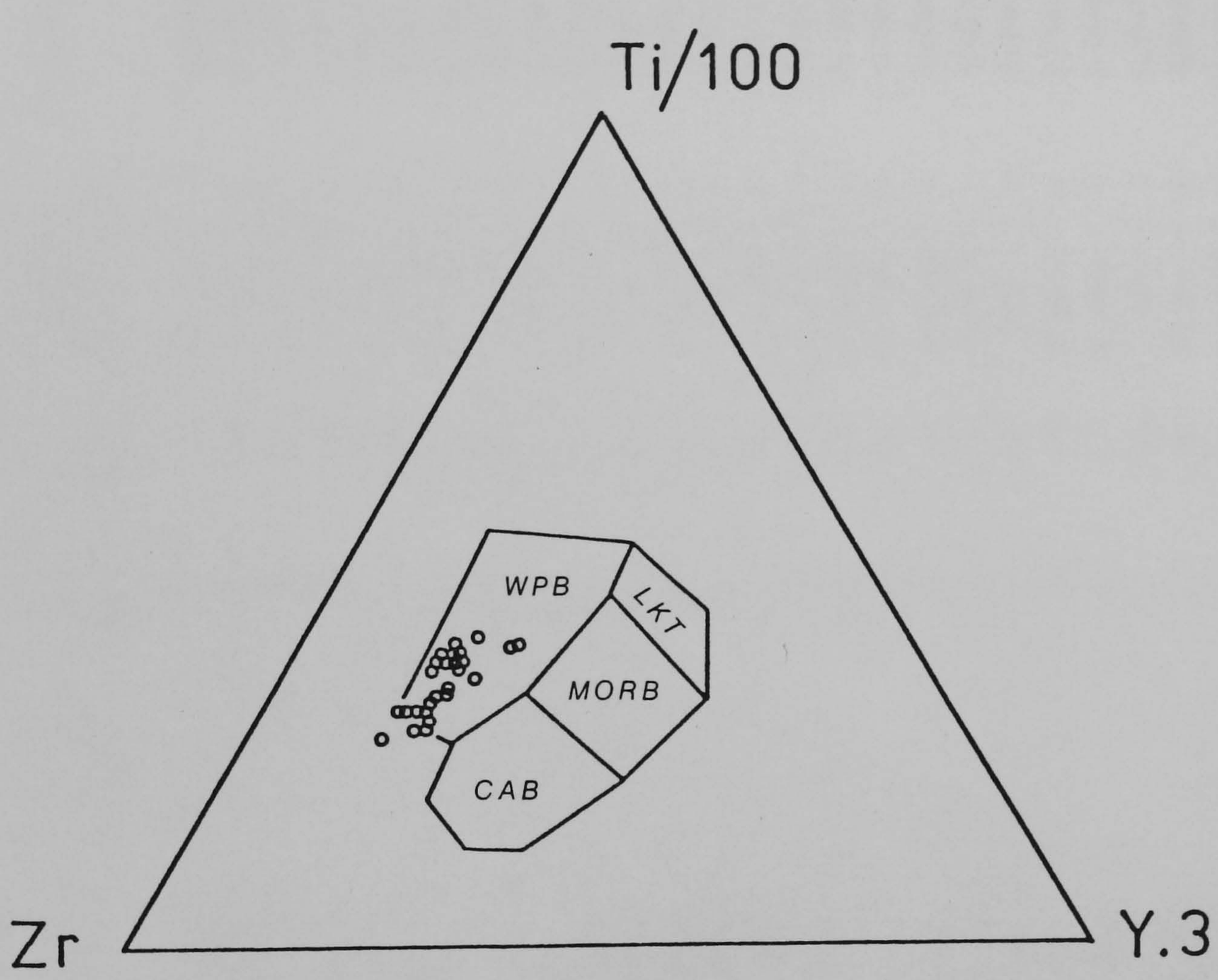


Figure 6.1.8 Ti-Zr-Y discrimination diagram for the Biu and Song lavas (circles). Fields are from Pearce and Cann (1973).

WPB	within plate basalts
LKT	low-K tholeiites
MORB	mid-ocean ridge basalt
CAB	calc-alkali basalts

TABLE 6.2.1

Strontium isotope data from N.E. Nigeria

Plateau	Sample	Rock Type	K-Ar Age (Ma)	Rb (ppm)	Sr (ppm)	$^{87}Sr/^{86}Sr$ ($\pm 2\sigma \times 10^5$)	$^{87}Rb/^{86}Sr$
Biu	N 2	Basalt(hy)	5.3	32	768	0.70368 ± 6	0.1206
Biu	N 3	Basalt(ne)		30	715	0.70298 ± 4	0.1214
Biu	N 4	Basalt(ne)		28	667	0.70312 ± 6	0.1215
Biu	N 5	Basalt(ne)		46	695	0.70317 ± 7	0.1915
Biu	N 9	Basalt(ne)		27	637	0.70311 ± 6	0.1227
Biu	N10*	Basanite		33	652	0.70311 ± 8	0.1465
Biu	N11*	Basalt(ne)		57	841	0.70306 ± 10	0.1755
Biu	N13*	Basalt(ne)		140	885	0.70323 ± 12	0.4578
Biu	N14	Basanite		44	910	0.70298 ± 8	0.1399
Biu	N15*	Basalt(ne)		36	690	0.70308 ± 4	0.1510
Biu	N16*	Basalt(ne)		66	1,051	0.70312 ± 7	0.1817
Biu	N18	Basalt(hy)		33	1,115	0.70310 ± 4	0.0856
Biu	N19	Basalt(hy)		40	751	0.70316 ± 8	0.1541
Song	N20	Basalt(hy)		30	560	0.70338 ± 6	0.1550
Song	N21	Basalt(hy)		27	574	0.70332 ± 8	0.1361
Song	N23	Basalt(hy)		30	576	0.70335 ± 6	0.1507
Biu	N25	Basalt(hy)		32	491	0.70357 ± 11	0.1886
Biu	N27	Basalt(hy)		29	685	0.70318 ± 2	0.1225
Biu	N29*	Hawaiite(ne)		75	1,192	0.70316 ± 7	0.1821
Biu	N31*	Basalt(hy)		35	632	0.70373 ± 8	0.1603
Biu	N33*	Basanite		43	829	0.70314 ± 6	0.1501
Biu	N34	Basalt(hy)		31	719	0.70336 ± 6	0.1248
Biu	N35*	Basalt(hy)		35	654	0.70333 ± 6	0.1549
Biu	N37*	Basalt(hy)		32	1,522	0.70357 ± 11	0.0608
Biu	N38	Basanite	0.84	41	859	0.70304 ± 8	0.1381

*: Bearing ultramafic xenoliths

( ): Hypersthene or nepheline normative

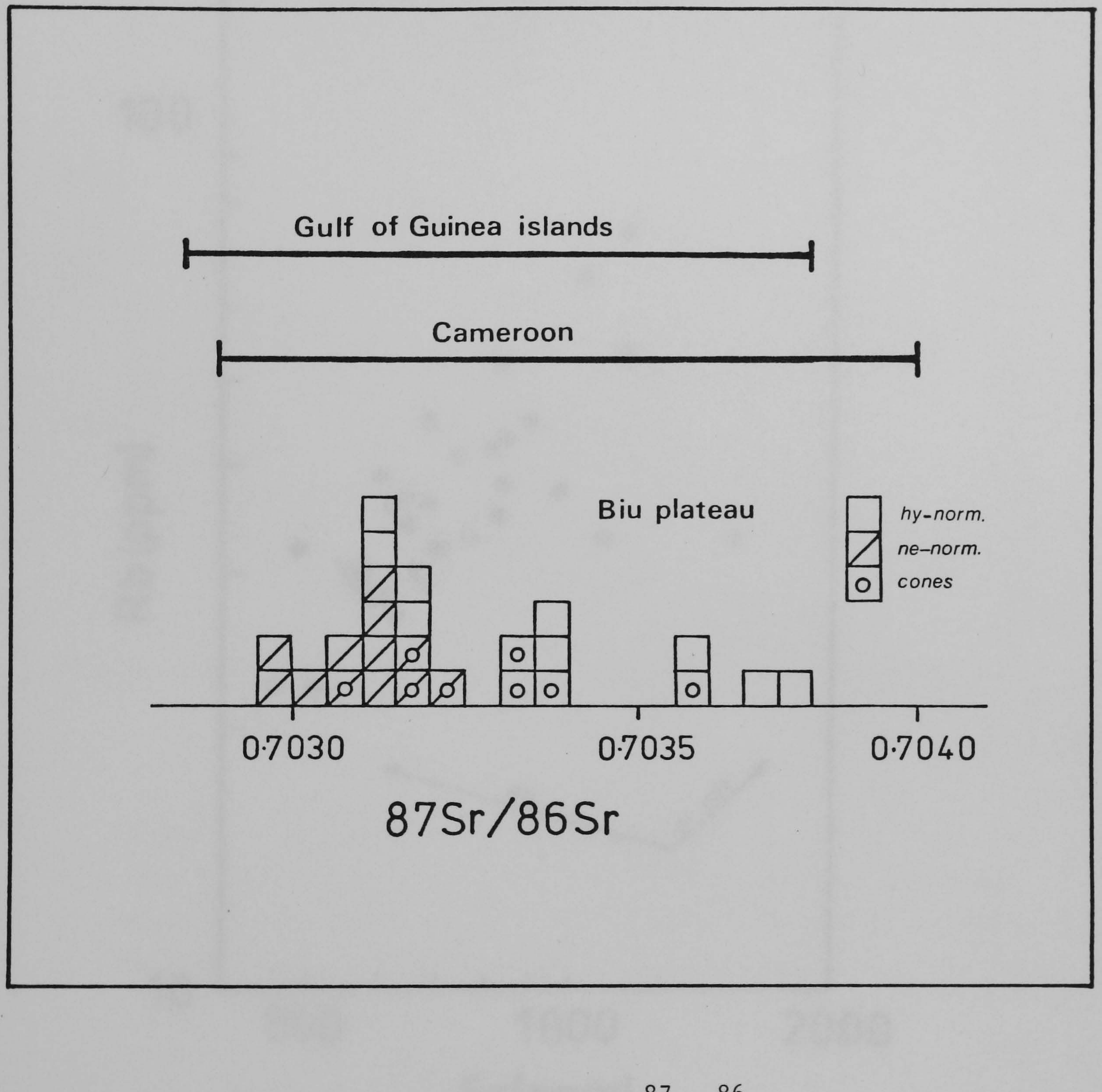


Figure 6.2.1 Frequency histogram of intial $^{87}Sr/^{86}Sr$ ratios in Biu and Song lavas compared to basic rocks from the Gulf of Guinea islands (49 samples) and from the Cameroon volcanoes (56 samples). A square represents one sample.

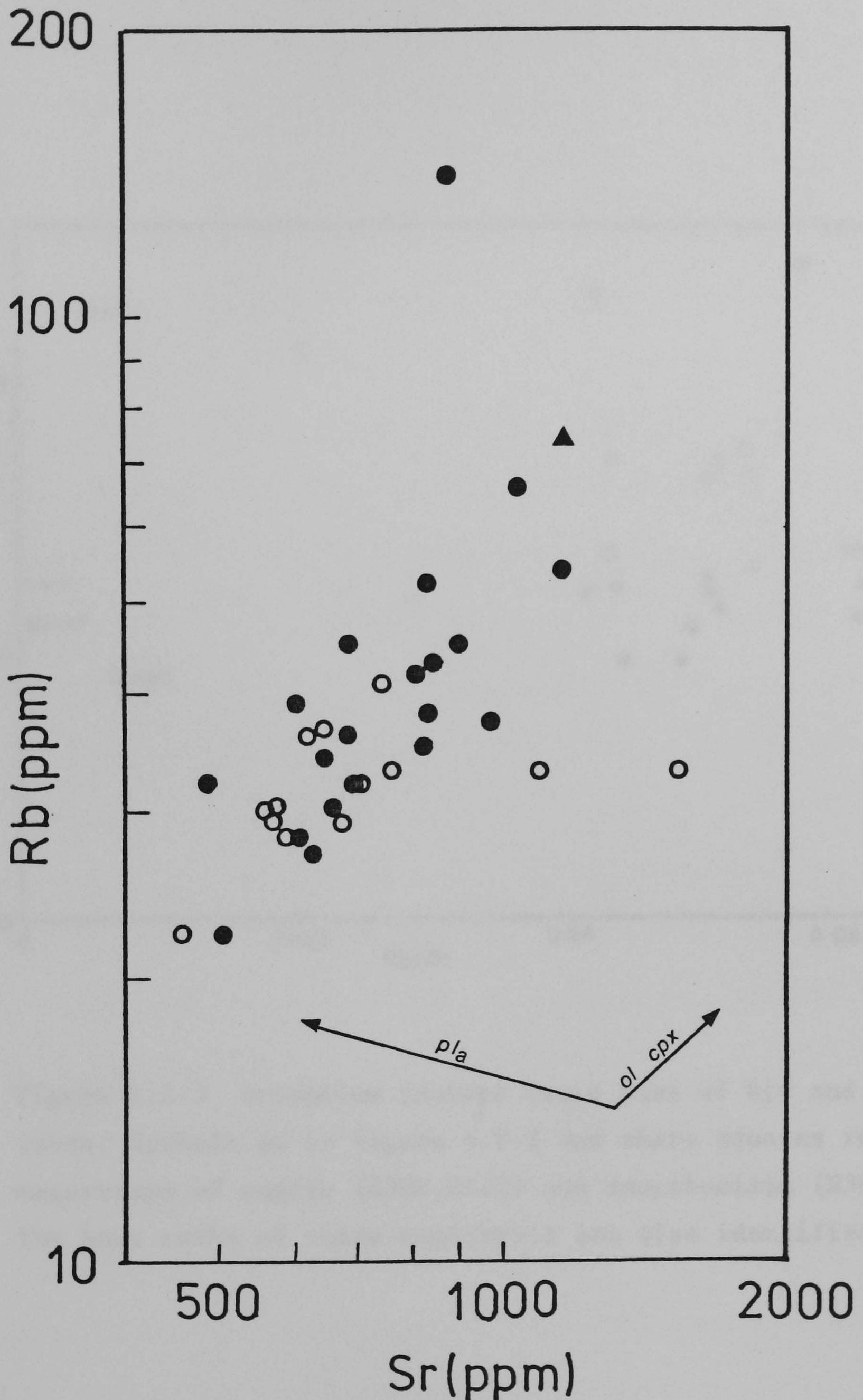


Figure 6.2.2 Rb-Sr diagram of Biu and Song lavas. Filled and open circles are nepheline and hypersthene normative basalts respectively. The triangle represents hawaiite N29. Vectors show 20% fractionation plagioclase from an acidic melt (pl_a), of olivine (ol) and clinopyroxene (cpx) from basic melts.

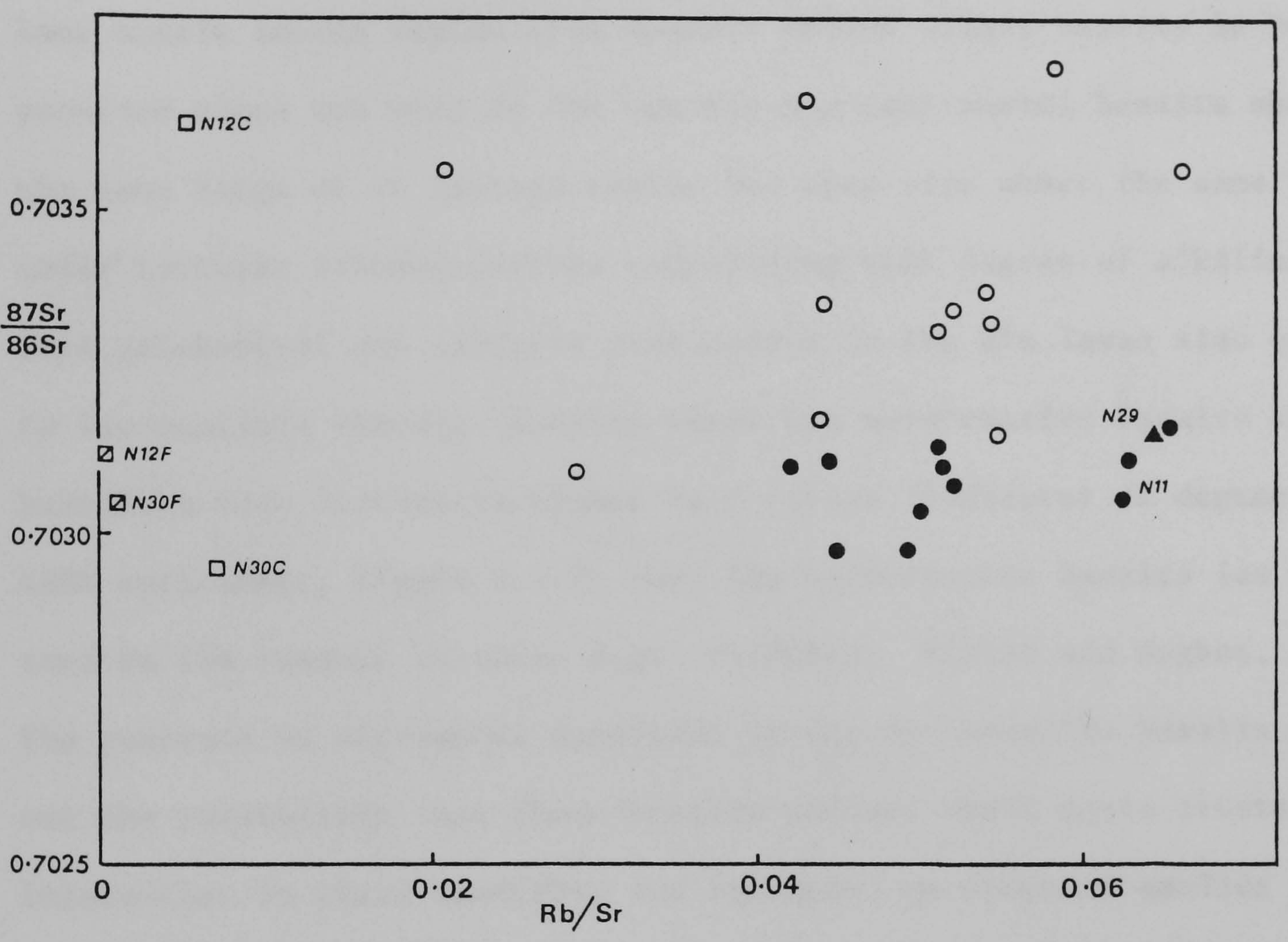


Figure 6.2.3 Strontium isotope ratio plot of Biu and Song lavas. Symbols as in figure 6.2.2 and where squares represent megacrysts of augite (N30C,N12C) and anorthoclase (N30F,N12F). The host rocks of these megacrysts are also identified (N29,N11).

isotope ratios (0.70298 to 0.70323, $\bar{x}$ = 0.70310) relative to hypersthene normative basalts (0.70310 - 0.70373, $\bar{x}$ = 0.70339). This is perhaps better demonstrated on Figure 6.2.4 where the Biu and Song data fall within the field defined by the oceanic island sector. Strong additional support to the hypothesis that continental alkali basalts share the same mantle source region with oceanic island alkali basalts is hence provided since not only do the oceanic and continental basalts share the same range of Sr isotope ratios but they also share the same fine scale isotopic inhomogeneities correlating with degree of alkalinity. This geochemical and isotopic distinction in the Biu lavas also extends to incompatible element contents where the ne-normative basalts and basanites have distinctly higher La/Y ratios (indicator of degree of LREE enrichment, Figure 6.2.5) than the hy-normative basalts (as is seen in the oceanic sectors, e.g: Principe; Fitton and Hughes, 1977). The presence of ultramafic xenoliths in the hy-normative basalts rules out the possibility that these basalts reflect small scale crustal interaction in their chemistry and isotopes, as proposed earlier for some mafic lavas from Mt. Cameroon, Manengouba, Bambouto and Oku (Section 5.2.1).

That the small variations in chemistry are due to fractionation at depth rather than in high-level crustal magma chambers is also shown by isotopic data on megacrysts. Anorthoclases and aluminous subcalcic augites enclosed in two lavas (N11 and N29) were analysed for $^{87}Sr/^{86}Sr$ ratios and Rb, Sr concentrations (by isotope dilution, Table 6.2.2). Figure 6.2.3 shows that 3 of the 4 megacrysts analysed fall within a very restricted range of $^{87}Sr/^{86}Sr$ ratios from 0.70295 to 0.70313 indicating that they are in isotopic equilibrium with their host lavas (also marked on Figure 6.2.3). The fourth megacryst, N12C, gave a

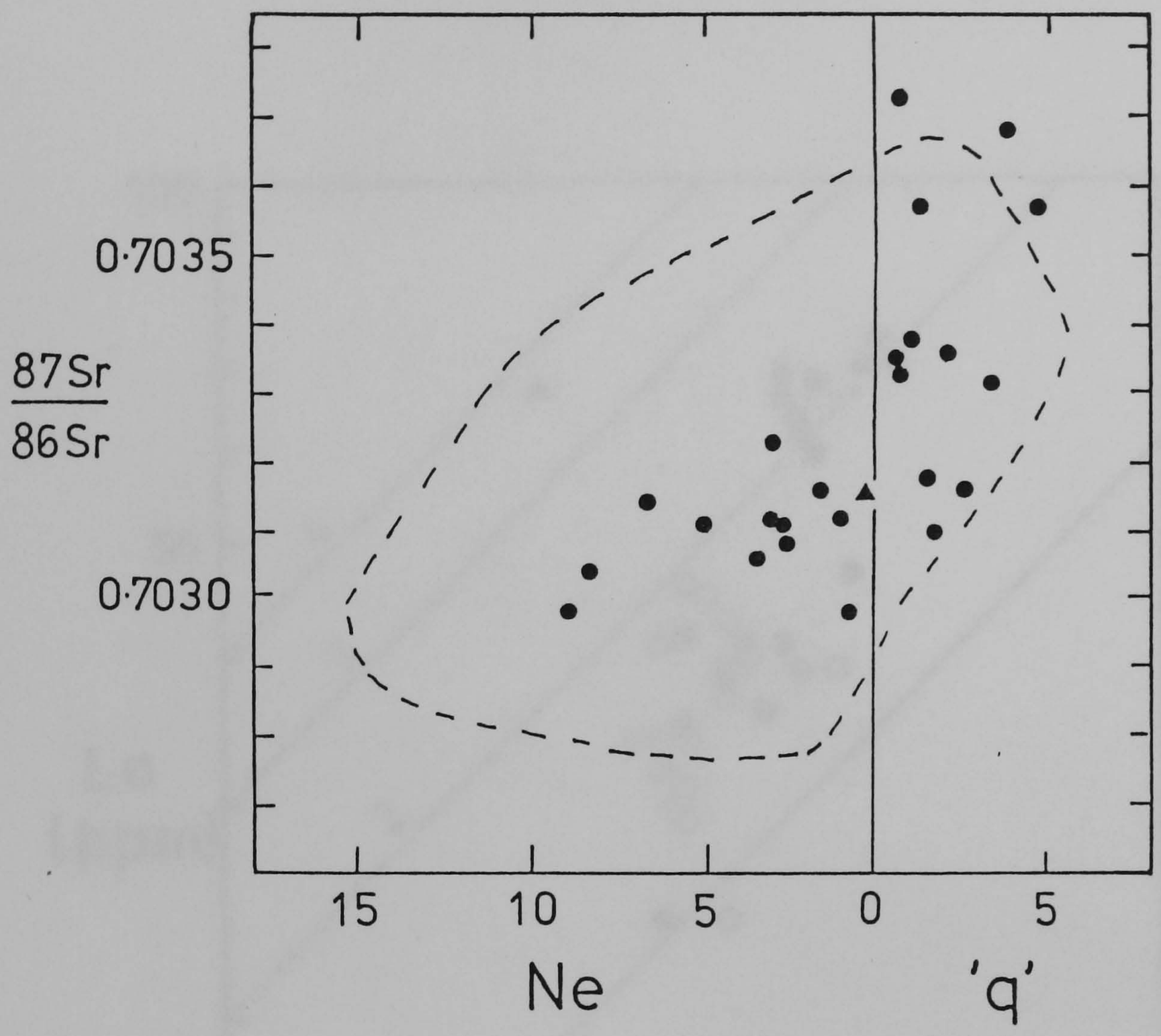


Figure 6.2.4 Initial strontium isotope ratios plotted against degree of silica over- and under- saturation for the Biu and Song lavas. Symbols as in figure 6.1.6 . The field of the Gulf of Guinea islands is also shown (dotted line).

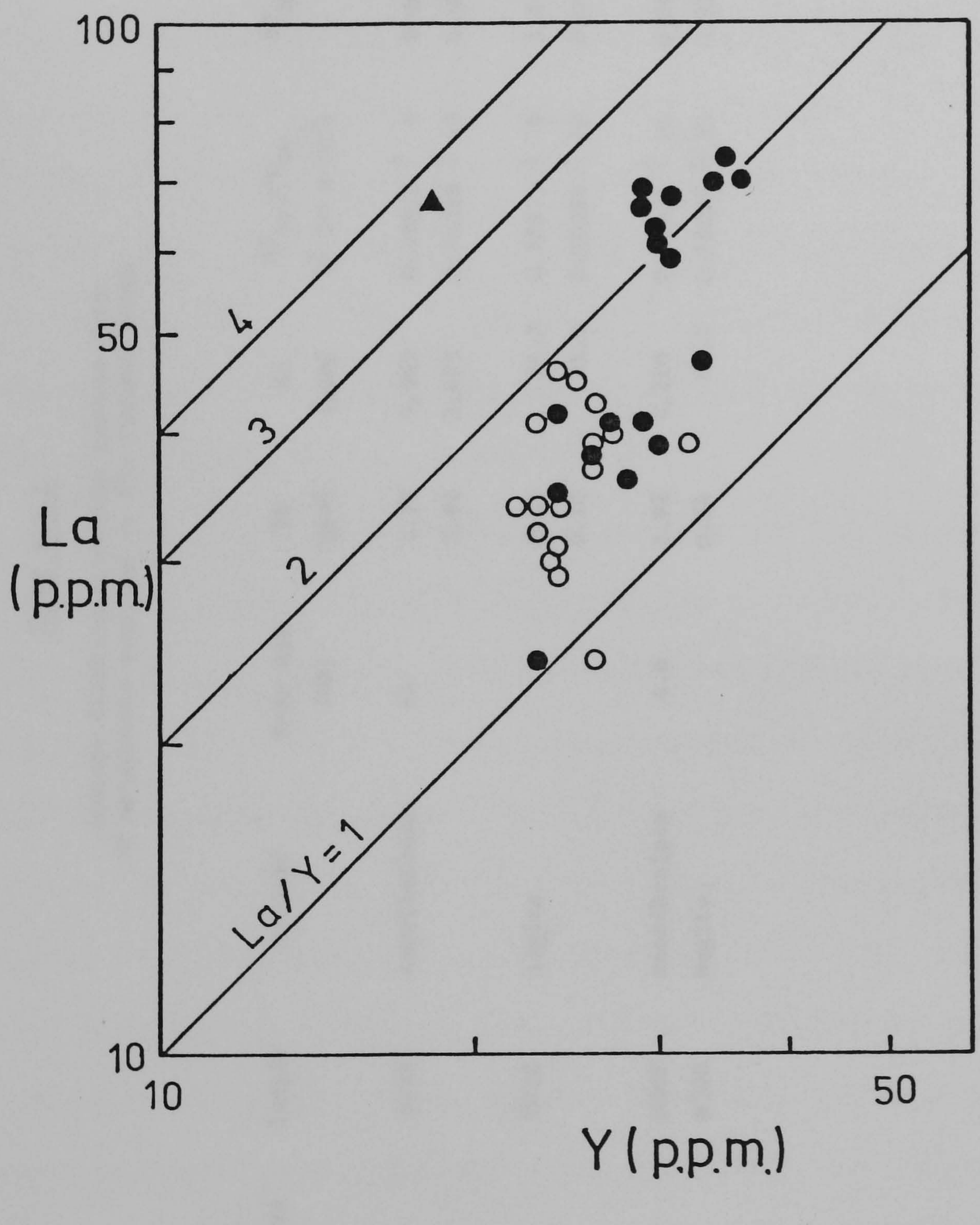


Figure 6.2.5 Lanthanum-yttrium variation in Biu and Song lavas. Symbols as in figure 6.2.2 .

TABLE 6.2.2

Isotope dilution strontium isotope data
of megacrysts enclosed in Biu Plateau lavas

Host Lava	Sample	Mineral	K-Ar Age (Ma)	Rb (ppm)	Sr (ppm)	$^{87}Sr/^{86}Sr$ ($\pm 2\sigma \times 10^{5}$)	$^{87}Rb/^{86}Sr$
N11	N12F	Anorthoclase	12	2.79	3,962	0.70313 ± 8	0.0020
				2.86	3,975	0.70313 ± 18	0.0021
N11	N12C	Augite		0.21	36.3	0.70375 ± 8	0.0165
				0.20	35.9	0.70353 ± 10	0.0158
N29	N30F	Anorthoclase	4.6	5.92	4,210	0.70305 ± 16	0.0041
	N30C	Augite		0.54	69.7	0.70295 ± 30	0.0222

value somewhat higher at 0.70364, falling within the range of hypersthene normative basalts. In addition, N12F has already been shown to be in equilibrium with its host from K-Ar studies (Chapter 3). Experimental and geochemical studies on similar augites (Chapman, 1976) to N12C and N30C indicated that they could precipitate from an alkali basaltic magma at about 25 kb whereas anorthoclase is only stable in a basanitic liquid below 9 kb. Hence it is likely that limited medium-high pressure fractionation occurred either in the upper mantle or in the lower continental crust. This would explain variations in the Ni and Cr concentrations although it should be emphasised that most of the incompatible trace element variation and the correlation observed on Figure 6.2.4 must be a result of varying degrees of partial melting of a heterogeneous mantle.

Figure 1.2 shows that the Biu plateau and the Cameroon volcanoes from only a small part of a larger region of Cenozoic volcanic activity comprising many volcanic fields in west and central north Africa. Allegre et al. (1981) recently analysed similar unmodified, ultramafic xenolith-bearing alkali basalts and nephelinites from Hoggar for Pb-Sr-Nd isotope ratios and their Sr isotope data, varying from 0.70310 to 0.70345, is very similar to that obtained during the course of this work from the Cameroon Line volcanoes. This would indicate that identical heterogeneous mantle source regions exist under islands in the central-south Atlantic Ocean and under much of, if not the entire African continent. This is also supported by the Pb-Nd isotope data of Allegre et al. (op. cit.) where the Hoggar lavas have values typical of oceanic islands.

CHAPTER 7

PETROGENESIS OF THE CAMEROON LINE VOLCANOES

A summary of the isotopic and chemical data presented in earlier chapters is integrated with a discussion on the similarity of oceanic and continental mid-plate activity and on the chemical and isotopic nature of the mantle source regions of olivine tholeiite - nephelinite magmas. Previous research concerning the plate tectonic history of the West African Rift System is briefly reviewed and models concerning the origin of the Cameroon line volcanoes are discussed in the light of new isotopic evidence.

7.1 Anorogenic Intraplate Volcanism on the Oceanic and Continental Sectors of the Cameroon Line

Comprehensive K-Ar age determinations of these volcanoes (Figure 3.3.3) together with published Rb-Sr and K-Ar ages of the ring complexes have shown that activity has been continuous over the past 66Ma, that there is no consistent migration with time and that Oligocene - Recent magmatism on the oceanic and continental sectors has been essentially contemporaneous. Overall, the range of geochemical character of basaltic lavas from all the volcanoes (except hyper-alkaline lavas from Etinde) are very similar (Figure 7.1.1). This alkali basalt - basanite - nephelinite association is typical of oceanic islands (e.g.: Hawaii, Clague and Frey, 1982), continental rift systems (e.g.: Kenya rift, Williams, 1972; Rhine Graben, Duda and Schminke, 1978) and other continental intraplate activity (e.g.: S.E. Australia, Frey et al., 1978). Trace element concentrations in mafic rocks from each sector of the Cameroon line are virtually identical (Figure 7.1.2) with incompatible element contents showing the enrichment typical of within-plate basalts (other than continental

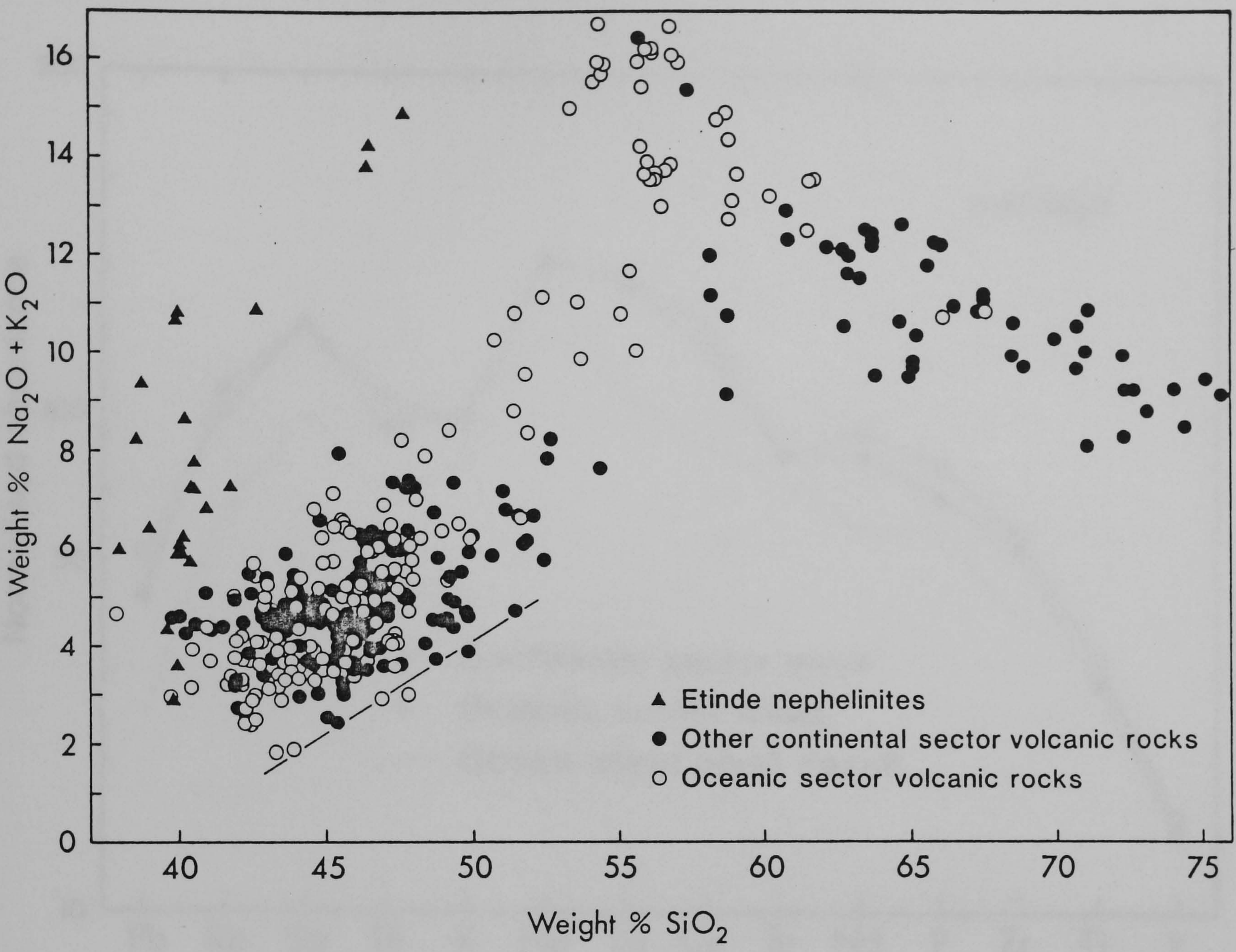


Figure 7.1.1 Alkali - silica diagram for the Cameroon line volcanic rocks. The line separating Hawaiian alkaline and tholeiitic rocks (MacDonald and Katsura, 1964) is shown for reference. From Fitton (1983).

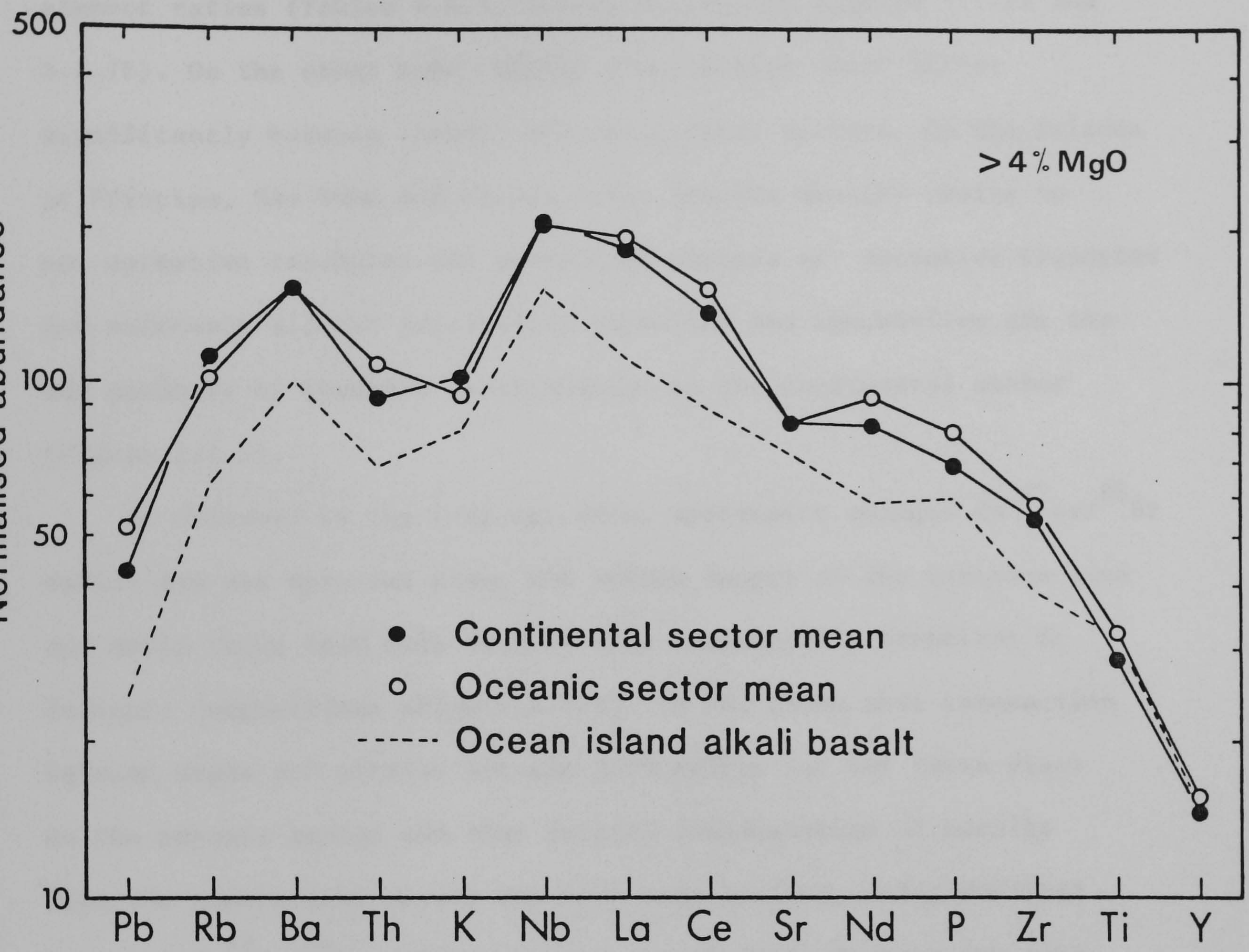


Figure 7.1.2 Normalised mean trace element abundances in mafic lavas from the Cameroon line (J.G.Fitton, unpublished). Normalising factors as in figure 4.4.2 . Oceanic island basalt average from Sun (1980).

tholeiites). The nature or thickness of the earth's crust (oceanic lithosphere or continental crust) has not affected incompatible element ratios (Tables 4.4.1, 5.1.1, 6.1.1; and Figures 5.1.13 and 6.1.7b). On the other hand, highly fractionated rocks differ significantly between oceanic and continental sectors. On the islands of Principe, São Tomé and Pagalu mafic liquids usually evolve to ne- normative trachytes and phonolites whereas qz- normative trachytes and extremely silicic peralkaline rhyolites and ignimbrites are the end products of magmatic fractionation on the continental sector (Figure 7.1.1).

As observed in the K-Ar age data, systematic changes in $^{87}Sr/^{86}Sr$ ratios are not apparent along the 1600Km length of the Cameroon line and mafic rocks from both sectors have essentially identical Sr isotopic compositions (Figure 7.1.3). It was shown that interaction between magma and altered oceanic lithosphere has not taken place on the oceanic sector and that crustal contamination of basalts from the continental sector has been very limited, being manifest by initial $^{87}Sr/^{86}Sr$ ratios greater than 0.7037. Perhaps the most convincing evidence attesting to the relative lack of continental crust - basaltic magma interaction has come from the Biu Plateau data (Figure 7.1.3). These primitive lavas are the only rocks from the continental sector containing large ultramafic xenoliths and are therefore the least likely lavas to have undergone isotopic (or chemical) re-equilibration with radiogenic crust. Their range of $^{87}Sr/^{86}Sr$ ratios is identical to that of mafic lavas from islands in the Gulf of Guinea and to that displayed by the Cameroon volcanoes. Further, lavas from individual volcanic centres located on both sides of the continental margin, have the same fine scale isotopic heterogeneities (particularly Principe, São Tomé and the Biu Plateau)

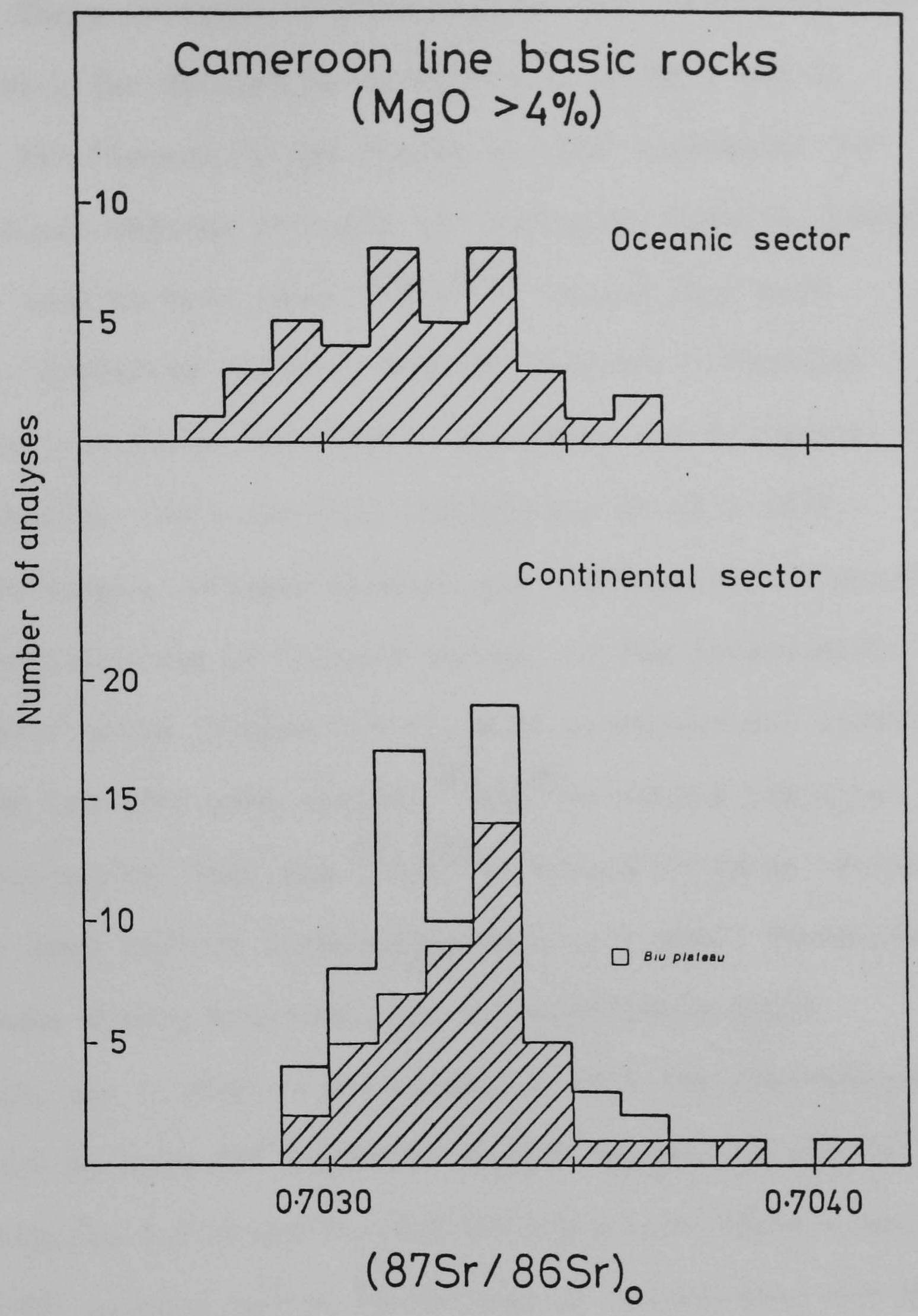


Figure 7.1.3 Histogram of 87Sr/86Sr ratios in mafic rocks from the Cameroon line volcanoes.

as illustrated on Figures 4.1.7, 4.1.8, 4.4.4, 5.4.2 and 6.2.4, and in Table 7.1.1 . These isotopic heterogeneities are correlated with degree of alkalinity (as defined by normative ne or hy), and in Principe and the Biu Plateau by the degree of LREE enrichment (as shown by La/Y ratios) whereby strongly ne- normative basalts, basanites and nephelinites tend to have lower $^{87}Sr/^{86}Sr$ ratios than more transitional, hy- normative basalts. Similar isotopic - chemical relationships exist in lavas from Hawaii (Lanphere and Dalrymple, 1980), S.E. Australia (Ewart, 1982) and Mull (Beckinsale et al., 1978).

The major difference between oceanic and continental volcanism occurs in the chemistry and Sr isotope ratios of the intermediate-highly fractionated rocks (Figure 7.1.4). Most trachytes and phonolites from Principe and São Tomé have initial $^{87}Sr/^{86}Sr$ ratios identical to their mafic counterparts. Only the $^{87}Sr/^{86}Sr$ ratios of three evolved samples from São Tomé reflect interaction with very small quantities of oceanic sediment during fractionation in subvolcanic magma chambers. However, qz- trachytes and rhyolites from the continental sector (Figure 7.1.4) have all suffered varying degrees of crustal contamination (Figures 5.2.4 and 5.2.10) with the most salic rocks representing 80-90% crustal melts. Where crustal interaction has not occurred during fractionation then liquids evolve to uncontaminated phonolites (Bambouto, Figure 5.2.10) by very similar processes to those occuring on oceanic islands. Published isotopic and chemical data on the Cameroon Lower Tertiary ring - complexes (Figure 7.1.4; section 5.3 and references therein) likewise reflect a similar interplay between crustal interaction and low - pressure fractionation during the evolution of salic rocktypes.

It may be concluded that all the mafic rocks have sampled a similar mantle source and that the continental crust has imposed

Table 7.1.1

Mean initial 87Sr/86Sr ratios of nepheline and hypersthene-normative mafic lavas (MgO>4%) from Principe, São Tomé and the Biu plateau

Volcanic centre	Lava suite	87Sr/86Sr mean	n	$\left[\frac{87Sr}{86Sr}_{hy} - \frac{87Sr}{86Sr}_{ne}\right].10^5$	
Principe	O.L.S. *(hy norm)*	0.70326	13		29
Principe	Y.L.S. *(ne norm)*	0.70297	7		
São Tomé	*hy norm*	0.70334	4		23
São Tomé	*ne norm*	0.70311	7		
Biu	*hy norm*	0.70339	12		29
Biu	*ne norm*	0.70310	13		

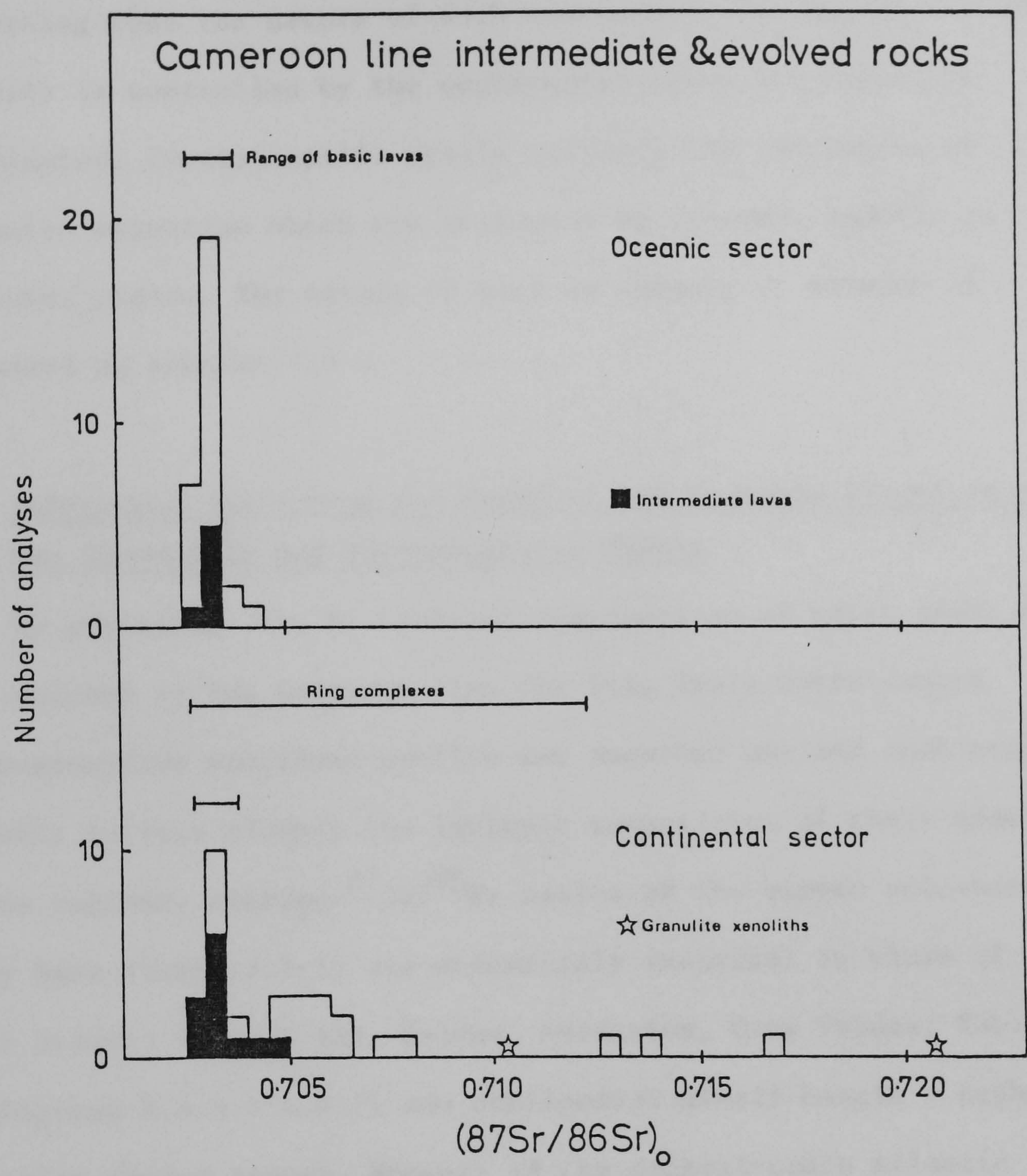


Figure 7.1.4 Histogram of initial 87Sr/86Sr ratios in intermediate and evolved rocks (87Rb/86Sr < 50) from the Cameroon line volcanoes.

very little effect on the chemical and isotopic character of the vast bulk of the mafic lavas. Theories (cited in section 1.2) suggesting that the nature of such continental intraplate volcanic activity is controlled by the continental crust are therefore invalidated. Crustal uplift merely reflects the initiation of extensive magmatism which was activated by a thermal anomaly in the lower mantle. The nature of such an anomaly or hotzone is discussed in section 7.3 .

7.2 Inferences Concerning the Chemical and Isotopic Structure of the Suboceanic and Subcontinental Mantle

By averaging the Sr isotopic compositions of basic lavas from each volcano in the Cameroon line the fine scale intra-centre inhomogeneities mentioned earlier are smoothed out and such means will probably reflect closely the isotopic composition of their mantle source regions. Average $^{87}Sr/^{86}Sr$ ratios of the eleven volcanoes under study here (Table 7.2.1) are essentially identical to those of most other oceanic islands (St. Helena, Ascension, Cape Verdes; Table 7.2.2 and Figures 4.4.5 - 4.4.7) and continental alkali basalt - nephelinite volcanism (Benue trough, Hoggar) in the central-south Atlantic Ocean and on the West African continent. Hence the same isotopically heterogeneous mantle must be present under this entire region and it is quite likely that such a portion of the mantle exists on the global scale since similar Sr isotopic compositions have been recorded in volcanic rocks from Hawaii (Lanphere and Dalrymple, 1980), S.E. Australia (Ewart, 1982), Kenya (Norry et al., 1980), and the Rhine Graben (Calvez and Lippolt, 1980). However, anomalous mantle may exist under Tristan da Cunha, Gough and the Walvis Ridge since $^{87}Sr/^{86}Sr$ ratios are elevated in this region ($\geq$0.705, O'Nions et al., 1977; White and Hofmann, 1982; Richardson et al.,1982).

Table 7.2.1

Mean initial 87Sr/86Sr ratios in mafic lavas from the Cameroon volcanoes

Volcanic centre	$(87Sr/86Sr)_0$	n
Principe	0.70316	21
São Tomé	0.70320	10
Pagalu	0.70335	5
Bioko	0.70322	5
Mt. Cameroon	0.70333	11
Etinde	0.70325	16
Manengouba	0.70304	13
Bambouto	0.70338	6
Oku	0.70344	6
Mandara	0.70314	3
Biu	0.70324	25

Table 7.2.2

Mean initial 87Sr/86Sr ratios of mafic lavas from Atlantic Ocean islands and from West African volcanic fields

Volcanic centre	$(87Sr/86Sr)_0$	n	reference
St. Helena	0.70290	6	1
"	0.70291	1	2
"	0.70301	13	3
Ascension	0.70276	3	2
"	0.70282	4	4
"	0.70296	7	5
Cape Verdes	0.70313	7	6
Canaries	0.70307	5	7
Benue trough	0.70300	5	8
Hoggar	0.70327	6	9

1 : White and Hofmann, 1982

2 : Cohen and O'Nions, 1982

3 : Grant et al., 1976

4 : O'Nions et al., 1977

5 : Harris et al., 1982

6 : Klerkx et al., 1974

7 : Zindler et al., 1982

8 : Grant et al., 1972a

9 : Allègre et al., 1981

Note: oceanic island data plotted in figure 4.4.6 did not include data from references 1,2,5 & 7, but the fields depicted therein would be virtually unaffected by the inclusion of these new analyses.

This research has shown that the presence of thick continental crust imposes very little effect on the chemistry and strontium isotope ratios of the vast majority of alkali basalts, basanites and nephelinites, and comprehensive integrated chemical-isotopic studies indicate an upper limit of approximately 0.7037 for the initial $^{87}Sr/^{86}Sr$ composition of both the suboceanic and subcontinental mantle source regions. Theories appealing to an extensive enriched continental mantle (relative to that underlying the oceans) to explain elevated $^{87}Sr/^{86}Sr$ ratios in such anorogenic provinces (e.g.: Brooks et al.,1976b; Sun and Hanson, 1975b) can be dismissed since ratios higher than 0.7037 are most likely a consequence of varying degrees of crustal interaction. Strong support for this conclusion has come from Nd isotopic studies of continental volcanics (e.g.: De Paolo, 1981).

It has been considered that theories involving: disequilibrium partial melting; fractionation of Sr isotopes during fractional crystallization; and interaction with seawater-contaminated lithosphere are all inapplicable (Chapters 1,2, and 4) as explanations of the isotopic and chemical characteristics of these lavas. Likewise lateral inhomogeneities in the mantle cannot explain the Cameroon line data (although Tristan da Cunha and the Walvis Ridge may reflect an anomalously enriched zone under the Atlantic Ocean) and general models involving mantle metasomatism (although they may be relevant to the generation of kimberlites) are not considered necessary to account for the Cameroon line magmas, not even for the exceedingly alkaline Etinde lavas (Section 5.1.2).

As discussed in chapter 4 the preferred mantle structure is one consisting of a depleted, relatively homogeneous, convecting upper zone (source of N-type MORB) and a lower, heterogeneous,

less differentiated, more primitive zone (source of oceanic island and continental alkaline volcanic rocks). The interface between these zones may well be the 670Km seismic discontinuity (e.g.: Richter and MacKenzie, 1978; De Paolo, 1980; Allègre, 1982; Turcotte, 1982). The depleted upper mantle and the continental crust are broadly isotopically and chemically complementary and the creation of this mantle structure is probably a result of crustal extraction from a primordial mantle. Mass balance calculations (O'Nions et al., 1979, 1980; Jacobsen and Wasserburg, 1979, 1981; De Paolo, 1980) have shown that 10-50% of the original well mixed undifferentiated mantle was involved in crustal extraction since about 3.6Ga ago. Pb and Sr isotope systematics (B.V.S.P., 1981,and references therein) indicate that these reservoirs have been separated for at least 1500Ma. $^{18}O/^{16}O$ ratios also indicate that MORB has a source distinct from that of alkali basalts (Kyser et al., 1982) since $\delta^{18}O$ is consistently lower in ridge tholeiites with respect to oceanic island basalts. Figure 4.4.5 indicates that the lower mantle (as recorded by the alkali lavas erupting on the surface) has apparently undergone recent incompatible enrichment (<< 1000Ma ago) since these rocks all plot to the right of the Geochron. A process of diffusive zone refining is proposed to occur (as described in Section 5.1.2) whereby as the melt, derived from the lower mantle, migrates upward it becomes enriched in incompatible elements.

Although a two-reservoir mantle can satisfactorily explain the Sr isotope data of the Cameroon line mafic rocks and most other intra-plate activity the Pb, Sr and Nd isotopes of some regions (e.g.: St. Helena and Tristan da Cunha, White and Hofmann, 1982) require a third , enriched component to complement the depleted and the undifferentiated reservoirs (Zindler et al., 1982) if ad hoc models

incorporating the transport of lead to the core throughout geologic time are not to be employed (e.g.: Dupré and Allègre, 1980). Zindler et al. (op.cit.) suggest that the coherence of Nd-Sr-Pb isotope systematics requires the presence of 3 components and that magmas reflect variable linear combinations of these endmembers. It is possible that the third component is subducted oceanic crust (Chase, 1981; Hofmann and White, 1982; White and Hofmann, 1982; Zindler et al., op.cit.) although a careful appraisal of this suggestion (Cohen and O'Nions, 1982) has indicated that such material would have to reside in the mantle for $>10^9$ years to explain observed isotope (particularly Pb) systematics and it is therefore unlikely to be the cause or source of within-plate alkali basalts. However, it may well represent the source of island arc or back-arc volcanism.

In conclusion, the data presented here gives strong support to the hypothesis that the earth's mantle comprises at least two components (a well-mixed, depleted, convecting, upper mantle; and a heterogeneous, less differentiated, lower mantle) which extend under continents as well as underlying oceanic regions. Magmas derived by small, variable degrees of partial melting (but >3-5%) of the lower mantle migrate upwards undergoing diffusive zone refining . Magma mixing with the upper mantle may subsequently occur, depending on the speed of magma ascent. Such a process could explain the observed fine scale heterogeneities, including the 'mantle isochron' in the Principe O.L.S. Limited olivine and cpx fractionation may occur at depth (at a pressure of ≥20Kb, e.g. the Biu Plateau), and if liquids later reside in high level magma chambers they will evolve towards phonolitic endmembers or to peralkaline rhyolite, if interaction with radiogenic crust takes place.

7.3 Tectonic Models Concerning the Origin of the Cameroon Line Volcanoes and its Association with the Nearby Benue Trough

That there is no correlation between age of volcanism and geographic position on the Cameroon line (Chapter 3) clearly demonstrates that this chain of magmatism cannot simply represent the surface expression of the African plate moving over a stationary hotspot in the asthenosphere. This is in accord with the overwhelming evidence (Burke and Wilson, 1972; McElhinny, 1973; Piper and Richardson, 1972; Oxburgh and Turcotte, 1974; Briden and Gass, 1974; Thorpe and Wright, 1979) that this plate has been more or less stationary since about 45Ma ago. Hence membrane tectonic models (Freeth, 1978a,b, 1979) explaining the genesis of this feature by requiring the rapid northward movement of the African plate since 20Ma ago are not applicable. It is unlikely that the Cameroon line volcanoes are associated with the Ascension fracture zone or other oceanic transforms (as has been suggested by Hedberg, 1968; Burke, 1969; LePichon and Hayes, 1971; Gorini and Bryan, 1976; Wright, 1976a; Mascle, 1975; Sibuet and Mascle, 1978) because although such transforms have been noted to continue into continental crust in N.E. Brazil (Gorini and Bryan, op. cit.) and in W. and S.W. Africa (Sibuet and Mascle, op. cit.; Marsh, 1973; Blundell, 1976) the trend of the Cameroon volcanoes is about 15-25° more northerly than the strike of transform directions (Sykes, 1978). Hence there is no structural - tectonic link with Ascension although they do share similar mantle source regions. In addition it should be made clear that the emplacement of the continental sector magmatism has almost certainly not been controlled by pre-existing lineaments or fractures (as postulated by Gorini and Bryan, op. cit.; Gass et al., 1978; Hughes, 1982) since the eastern branch (Ngaoundéré) runs

obliquely through a series of regional faults and mylonite zones. In particular, volcanic fissures in this region cut across the lines of weakness in the basement (Fitton, 1980,1983). Likewise the northern branch (towards the Biu Plateau) cuts the eastern limb of the Benue trough. The geochemistry and isotopic characteristics of the Cameroon line mafic rocks remain remarkably constant on traversing the continental margin, hence it is concluded that the structure or the isotopic - chemical composition of the crust has not controlled the spatial location or the nature of the mafic volcanic activity. While the Cameroon line volcanic rocks are typical of those from continental rift valleys (e.g. the East African rift system) and although there has been uplift of the Precambrian basement of about 1Km (Black and Girod, 1970) there is no evidence of rift faulting, extension or graben formation (Fitton, 1980). However, unsupported statements to the contrary still pervade the literature (from Gèze, 1943; to Machens, 1973; and Freeth, 1978b, 1979).

A more likely explanation for the origin of the Cameroon line volcanoes may lie in its relationship with the nearby Benue trough rather than with the models outlined above. Recent reviews of the geology of the Benue trough have been given by Fitton (1980) and Wright (1981). This structure is a linear depression filled with up to 6000m of Cretaceous, mainly marine sediments (Burke et al., 1972). A positive Bouguer anomaly (Cratchley and Jones, 1965; Ajakaiye and Burke, 1973; Adighije, 1979) coincident with the axis of the trough, and closely associated belts of brine springs, Pb-Zn and barytes mineralization (Olade, 1976) support the interpretation of the Benue trough as a rift valley. Many authors (e.g. Burke and Wilson, 1976; B.V.S.P., 1981) describe the Benue trough as one of the best examples

of a failed arm of a r-r-r triple junction. This feature appears to have originated as a tensional graben from about 125-80Ma ago (Burke et al., 1971) and the other two rifts continued to develop as the Atlantic Ocean opened. Burke et al (op. cit.) suggested that the Benue trough underwent seafloor spreading during the early Cretaceous and that the new oceanic crust was subsequently consumed by subduction. However, Thorpe and Wright (1979) contended that there was no evidence for either seafloor spreading or subduction and in fact the earliest described volcanics (Albian) in the area are alkaline, having within-plate affinities (Olade, 1978). Further support for this contention comes from Sykes (1978): "since large distortions on the ocean floor in the Gulf of Guinea do not appear to be present, it seems reasonable to conclude that large amounts of oceanic crust were not consumed in the Benue trough at the end of the Cretaceous". Olade (1975) and Wright (1981) have also demonstrated the purely ensialic and tensional nature of this rift structure and they drew analogies with the Afar depression and the Midland Valley of Scotland.

Fitton (1980,1983) has recently presented a model for the combined origin of the Cameroon line and the Benue trough which is considered to best fit the data presented here. It was shown that the form of the Benue trough and the Cameroon line (Figure 1.1) may be superimposed by rotating one relative to the other by 7° about a pole in Sudan. The fit of extensive Oligocene - Recent volcanism on the outline of the limit of Benue trough Cretaceous sediments is very good but if the earlier ring complexes (Figure 3.3.1) and minor contemporaneous and isotopically similar (Grant et al., 1972a) volcanics on the Jos Plateau and overlying the Benue trough sediments

are included then the entire volcanic zone becomes slightly more diffuse. By suggesting that the African lithosphere has been displaced by such a rotation the area occupied by the Cameroon line now overlies a thermal anomaly or hotzone (probably Y shaped) in the mantle which was originally under the Benue trough. Fitton (1980) presented compelling evidence for such a required movement of the otherwise anticlockwise rotation of the African plate during the short period between the end of tectonic activity in the Benue trough (80Ma) and earliest magmatism in the Cameroon line (66Ma). Hence a branch of the same hotzone which initiated the opening of the S. Atlantic Ocean is considered to be the source of these magmas. It was discussed earlier that such a plume-type source within the lower mantle is indicated by the Sr isotope systematics of these lavas. In such a model the continental crust would not control the site of volcanicity and in the West African rift system the only significant effect the Pan-African continental crust has imposed on volcanism, as reflected by Sr isotope compositions and geochemistry, has been the formation of salic peralkaline trachytes and rhyolites by a combination of extreme fractionation and variable degrees of crustal contamination.

APPENDIX A

ANALYTICAL TECHNIQUES

A1 Rb-Sr Techniques

A1.1 Sample Preparation

It was ensured that all the samples analysed were free of visible signs of alteration in thin section. In addition, access to major element X.R.F. data (analysed by J.G. Fitton) of all samples from Principe, São Tomé, Mt. Cameroon, Mt. Etinde, Mt. Manengouba, Bambouto and Oku Mts; and from the Biu Plateau and Mandara Mts. (analysed by the author), has enabled the iron oxidation ratio and the volatile content of the rocks to be considered when selecting material for Rb-Sr isotopic analysis. Only samples showing no change in these parameters and having low volatile contents were analysed. After analysis there was no correlation observed between $^{87}Sr/^{86}Sr$ and the iron oxidation ratio.

Samples were ground to a fine powder (<100 mesh) by using a steel Sturtevant jaw-crusher, a Cutrock Engineering hydraulic splitter and a tungsten carbide Tema mill. Chips showing alteration were discarded before the mill stage. These instruments were washed and dried with 'Analar' acetone between samples to prevent cross-contamination. Inhomogeneous and porphyritic samples were coned and quartered. Samples analysed for $^{87}Sr/^{86}Sr$ were taken from the same powder as that prepared for major and trace element X-ray fluorescence work. Almost all analyses employed whole-rock methods and where mineral determinations are discussed these were separated by hand-picking since they are megacrysts of clinopyroxene, garnet and feldspar.

A1.2 Chemical Procedures

All laboratory ware are subject to ultra-high cleaning procedures before their use in sample, standard, spike or blank preparation. This involved overnight heating in 'Analar' reagent grade HNO_3 followed by overnight heating in reagent grade HCl and then rinsing in twice distilled H_2O. When not in use, ware was wrapped in cling-film and stored in clean drawers. HCl reagents were calibrated with reagent grade anhydrous Na_2CO_3. Acids were distilled at sub-boiling temperatures in a quartz still.

For unspiked strontium analysis a 0.1 g split of powdered sample was weighed into a Teflon beaker having a neutral static charge (static was removed using an anti-static pistol). Approximately 15 mls of Merck Suprapur HF (48%) was added, the beaker covered with a Teflon lid and left overnight at a temperature of 200°C. After drying down the sample has to be oxidised since fluorides are insoluble in HCl and this was achieved by dissolving the residue with approximately 3 ml of twice distilled HNO_3 and 15 ml of twice distilled water. This is left to reflux for 1 hour and then evaporated to dryness. The sample was then dissolved in 5 - 10 mls of twice distilled 2.5N HCl and evaporated down to a 2 ml solution, which was diluted by 50% with H_2O. If any suspension was present the sample was centrifuged. The sample is eluted through a cation-exchange column of Biorad AG 50W - X8 (200 - 400 mesh) resin supported on a porous glass sinter disc set into the column. The ion-exchange column was calibrated by using a SrCa standard which was cut at 5 ml intervals. The cuts were analysed by atomic absorption spectrometry to determine the strontium and rubidium peaks. The strontium cut was collected in a Teflon beaker and evaporated to dryness. Columns are cleaned between samples by passing through HCl and H_2O in the following fashion:

40 ml of 6NHCl, 20 ml of H_2O, 40 ml of 6NHCl and finally 80 ml of 2.5N HCl to reconstitute the resin.

Samples were spiked for evolved rocks showing elevated $^{87}Sr/^{86}Sr$ ratios. For isotope dilution analysis 0.1 g of powder was weighed (to 0.01 mg) into a Teflon beaker and suitable aliquots of ^{87}Rb and ^{84}Sr enriched (spike) solutions were added; ideally so that the $^{86}Sr/^{84}Sr$ and the $^{87}Rb/^{85}Rb$ ratios are close to unity. Spikes used were 99.2% ^{87}Rb (Harwell) and 99.78% ^{84}Sr (N.B.S.) and were calibrated for concentration and composition against U.S. National Bureau of Standards Stoichiometric RbCl (S.R.M. 984) and $SrCO_3$ (S.R.M. 987). Stock spike solutions were stored in 500 ml polythene bottles with clingfilm and parafilm coverings to minimise evaporation. Working spike solutions were kept in 50 ml polythene drip bottles and again clingfilm was used to minimise evaporation. The remaining chemical procedure for isotope dilution work is the same as that for unspiked samples except that a rubidium cut was taken from the ion-exchange columns and evaporated to dryness as well as the strontium cut.

A1.3 Analytical Blanks

Overall total process blanks were analysed for Rb and Sr concentrations to ensure that the chemical procedures were free of possible contamination. Two analyses were done by the author and gave 1.5 ng and 0.7 ng of Rb, and 7 ng and 8 ng Sr for the period of data collection. Similar values were obtained by other workers at the East Kilbride laboratory. Only two samples (C85 and C144) needed blank strontium correction since they have very high $^{87}Sr/^{86}Sr$ ratios and very low strontium contents.

A1.4 Mass-Spectrometry

Isotopic analysis at East Kilbride employs the use of a modified A.E.I.-G.E.C. MS12 solid-source mass spectrometer with a 12" radius and 90° sector. The collector system comprises a Faraday Cup and a

Cary 401 vibrating reed electrometer with a 10^{11} ohm resistor. Data is input directly to the on-line computer which is linked to a teletype. Programs for the continuous treatment of the data were written by J. Hutchinson.

Strontium was loaded, in the form of a phosphate onto a single, tantalum filamented bead. The strontium was taken up in a small drop of a solution containing 1% H_3PO_4 in 6NHCl using a fine glass capillary tube, placed on the filament and dried on by means of an electric current. Rubidium was loaded as the chloride onto a side filament of a triple-filament assembly. These beads are cleaned in dilute HNO_3 and are then filamented, and outgassed in high vacuum at a current of 4.2 amps; at least 1 amp higher than the operating current.

Strontium runs were performed at an H.T. voltage of 8 Kv after an outgassing period of 15 min. at a filament current of 2.5 A. For unspiked strontium analyses, 4 peaks (85, 86, 87, 88) and an in-run zero were measured using an automatic peak switcher (Ross, 1973) with a 2 second count and integration time. The computer calculates (taking into account the decay characteristics of the vibrating reed electrometer) the mean 88/86, and 87/86 ratios together with standard deviation, standard error and percentage error after every set of 10 peak height scans. Each mass is checked manually for centring after every set of data. Sets having percentage errors in excess of 0.02 were discarded. Typically 12 sets of 10 scans are taken from each sample load (to give a 2σ error on the $^{87}Sr/^{86}Sr$ of <0.00012) although this may be increased to 16 sets if the run is not very stable. Samples very rich in strontium (in excess of 1000 ppm Sr) often take 4 or 5 sets to settle down. At the end of the run the computer summarizes the data, correcting for mass-spectrometer fractionation due to the lighter isotopes boiling off preferentially. Mass 85 is monitored continuously

to enable correction to the ^{87}Sr peak for any ^{87}Rb present (which is usually zero). A separate source block was used for the unspiked samples of this study to avoid any contamination from highly radiogenic samples run by other workers. The block is cleaned regularly, after every 20 samples. The sample source chamber is kept at high vacuum ($<5 \times 10^{-7}$ torr) with the aid of a liquid N_2 finger as well as an ion pump.

Spiked samples were run for strontium isotopic compositions as above, but in addition a rubidium run was also necessary for every sample. Masses 85 and 87 were monitored and care was taken to ensure minimum mass fractionation (since it is not possible to correct for such fractionation when there are only two isotopes) by keeping the running filament temperature as low as possible. Three sets of ten scans were usually sufficient.

Ten basalts from Bioko and Pagalu were analysed on the recently installed VGMM30B semi-automatic mass-spectrometer by J. Hutchinson. NBS987 standard determinations are identical to that obtained from the AE1 MS12.

The granulite xenoliths and its host basalt (C74) described in Chapter 5 were analysed for $^{87}Sr/^{86}Sr$ ratios at the Open University using an automated VG Isomass 54E. The NBS 987 $SrCO_3$ standard gave 0.71014 during the analysis period.

A1.5 Data Treatment

Strontium data are corrected for mass spectrometer fractionation effects by assuming an internationally accepted value of 8.37521 for the $^{88}Sr/^{86}Sr$ ratio ($^{87}Sr/^{86}Sr$ ratios are corrected by half the difference between the $^{88}Sr/^{86}Sr$ ratios). In this study, where the material is very young, mafic rocks having a $^{87}Rb/^{86}Sr$ ratio of 0.3 or less do not require an age correction for the measured $^{87}Sr/^{86}Sr$

ratios to be considered initial ratios. Where the rocks are evolved and have elevated measured $^{87}Sr/^{86}Sr$ ratios the initial ratios were calculated using an assumed age, according to the equation:

$$\Delta^{87}Sr/^{86}Sr = {}^{87}Rb/^{86}Sr \times 1.42.10^{-11} \times \text{age (in Ma)}$$

where $\Delta^{87}Sr/^{86}Sr$ is the age related increment to be subtracted from the measured $^{87}Sr/^{86}Sr$ ratio to arrive at the initial ratio.

$^{87}Rb/^{86}Sr$ was calculated from X.R.F. values of Rb and Sr concentrations for unspiked data according to the following equation:

$$\frac{Rb}{Sr} \cdot \frac{\left(\frac{^{87}Sr}{^{86}Sr} \times A_{87}\right) + A_{86} + \frac{A_{84}}{17.6071} + (A_{88} \times 8.37521)}{A_{87} + (A_{85} \times 2.59)}$$

where A = atomic wt. in A.M.U.

$17.6071 = {}^{86}Sr/^{84}Sr$ ratio

$8.37521 = {}^{88}Sr/^{86}Sr$ ratio

$2.59 = {}^{85}Rb/^{87}Rb$ ratio

For spiked data Rb and Sr concentrations and $^{87}Rb/^{86}Sr$ ratios are calculated from an isotope dilution program which takes into acount the spike concentrations, the sample and spike weights, and the mean measured $^{85}Rb/^{87}Rb$, $^{86}Sr/^{84}Sr$, $^{88}Sr/^{86}Sr$, and $^{87}Sr/^{86}Sr$ ratios of the sample in question. For $^{87}Rb/^{86}Sr$ ratios determined by isotope dilution a 1σ error of 0.4% is assumed (based on replicate analyses of other workers at East Kilbride). The measured $^{87}Sr/^{86}Sr$ ratios of unspiked determinations usually have a 1σ error better than 0.01% (as determined during the mass-spectrometer run). This is supported by duplicate analyses in Table A1.

For isochrons and pseudoisochrons a regression program following that of York (1969) was employed for calculating the best estimate of the slope, the intercept and associated analytical and geological scatter.

TABLE A1

Replicate* $^{87}Sr/^{86}Sr$ Analyses

Sample	$^{87}Sr/^{86}Sr$	$^{87}Sr/^{86}Sr$	$^{87}Sr/^{86}Sr$	% Difference
P12	0.70334±10	0.70325± 4		0.01
P13	0.70302± 7	0.70297± 7		0.007
P15	0.70344±12	0.70348±12		0.006
P16	0.71102±30	0.71099±10		0.004
P20	0.70294±10	0.70294±10		0.00
P35	0.70310±12	0.70307± 7		0.004
P51	0.70299±12	0.70298± 5	0.70302 ± 6	0.001, 0.006
C121	0.70354±10	0.70359± 8		0.007
C36	0.70333± 6	0.70333± 8		0.00
ST110	0.70296± 9	0.70306± 6		0.01
ST13A	0.70343±13	0.70343± 8		0.00
ST3	0.70332± 8	0.70333± 8		0.001
ST39	0.70324±12	0.70329± 5		0.007
ST84	0.70805± 9	0.70804± 6		0.001
ST57	0.70386± 8	0.70400± 7		0.02
ST58	0.70405± 8	0.70386±10		0.02
			$\bar{X}$	0.007

*different sample, dissolutions, beads and runs

TABLE A2

Duplicate * Rb-Sr Isotope Dilution Analyses

Sample	Rb		Sr	
	1	2	1	2
C76	200	198	2.46	2.46
C85	170	169	0.82	0.79
C87	206	205	15.09	14.97
C92	198	191	11.11	11.18
C95	154	154	2.87	2.85
C100	167	169	4.93	4.88
C101	109	109	3.12	3.12
C105	106	106	7.20	7.26

*different dissolutions, beads and runs

A1.6 Replicate and Standard Analyses

Table A1 is a list of duplicate unspiked $^{87}Sr/^{86}Sr$ determinations and Table A2 is a list of duplicate isotope dilution concentration analyses. These data show very good reproduceability and fall within the 1σ limits of 0.4% for $^{87}Rb/^{86}Sr$ and 0.01% for $^{87}Sr/^{86}Sr$ ratios used for regression calculations.

The internationally accepted strontium standard for inter-laboratory comparison, N.B.S.987, was analysed by the author at regular intervals and gave a mean of 0.71023 ± 0.00006 (2σ error of the mean) over the analysis period. This value compares well with other laboratories, other workers in this laboratory (0.71020 $\pm$ 10 2σ) and the "standard value" of 0.71014. The 2σ error on each determination was 0.00008 or better; this was achieved by taking a minimum of 10 sets of 10 scans.

A2 K-Ar Techniques

Holocrystalline samples free of glass, secondary minerals and visible alteration in thin section were selected for K-Ar studies. Whole rock samples were crushed and -1.4 mm + 20 B.S. mesh or -20 + 30 B.S. mesh chips were used for argon analysis. Representative portions of the size fraction used for argon analysis were ground to a powder (<100 μm) for potassium analysis.

Potassium was determined by flame photometry on a Corning EEL 450 photometer using sodium buffering and a lithium internal standard and burning a mixture of air and propane. A known weight of the sample powder is dissolved in "Aristar" HF (48%) and concentrated H_2SO_4 and evaporated to dryness overnight. The residue was redissolved in HNO_3 and H_2O. Lithium internal standard and a sodium buffer were added and the solution was made up to standard volume and measured against

potassium standard solutions made up from potassium salts. Analyses were done in duplicate and agreed to 1% (Table A3).

Argon analyses were performed in duplicate (within 6 weeks of crushing) by isotope dilution using 99.99% pure ^{38}Ar as a spike, and isotopic ratios were measured statically on an A.E.1.MS10 gas source mass-spectromter. The weighed sample chips (0.4 to 0.9 grams) were encased in copper phials and loaded in a 10 sample loader onto the machine. The extraction system was baked overnight (120°C) and the molybdenum crucible outgassed prior to use to reduce any atmospheric contamination. The sample was heated with a radio-frequency induction coil in the molybdenum crucible to about 1500°C for 20 minutes. The gases were trapped in a zeolite molecular sieve and activated charcoal finger, both cooled with liquid N_2. The spike ^{38}Ar was pipetted into the line (a fixed volume is allowed in by means of 2 valves) and allowed to mix with the sample gas. The gases were cleaned using a titanium sublimation pump. The sample and spike was moved along the extraction line to the mass-spectrometer by way of activated charcoal fingers. The isotopic composition of argon was determined by measuring mass peaks at 40, 38 and 36 as measured on a chart recorder and scanned in the sequence 40, 38, 36, 38, 40, 38, 36, 38, 40, 38, 36, 38, 40. The measured $^{40}Ar/^{38}Ar$ and $^{36}Ar/^{38}Ar$ ratios were corrected for mass-fractionation resulting from leaking the gas into the mass-spectrometer. The volume of the spike reservoir is monitored by periodic calibrations (after every 9 samples) against a mineral of known radiogenic argon content, BS 133 biotite (Newcastle). The amount of radiogenic ^{40}Ar present in the sample is calculated by taking into account the following considerations. The argon analysed is made up of three components: radiogenic, spike

TABLE A3

Replicate Flame Photometric Potassium Analyses
Compared with X.R.F. Data

	Flame Photometric			X.R.F.
K%	K%	Mean	K%
P15	0.449	0.446	0.45	0.40
25	1.184	1.173	1.18	1.15
28	1.080	1.086	1.08	1.10
18	1.331	1.347	1.34	1.34
20	1.895	1.858	1.88	1.76
5	4.256	4.285	4.27	4.23
12	3.540	3.530	3.54	3.72
16	4.000	4.040	4.02	4.12
11	5.114	5.131	5.12	5.07
ST60	0.790	0.784	0.79	0.79
96	2.296	2.323	2.31	2.31
44	1.303	1.331	1.32	1.24
43	3.798	3.841	3.82	3.78
84	4.658	4.677	4.67	4.60
90	4.797	4.805	4.80	4.73
C55	1.253	1.250	1.25	1.24
57	1.681	1.676	1.68	1.70
52	2.104	2.137	2.12	2.11
54	4.516	4.523	4.52	4.45
100	3.418	3.454	3.44	3.44
107	3.900	3.909	3.90	3.93
85	3.744	3.745	3.74	3.78
95	4.328	4.367	4.35	4.29
108	1.678	1.707	1.69	1.69
111	4.171	4.198	4.18	4.17
91	1.655	1.664	1.66	1.66
145	4.401	4.449	4.43	4.40
146	0.841	0.827	0.83	0.81
147	1.322	1.273	1.30	1.28
N 2	1.053	1.071	1.06	1.08
38	1.185	1.185	1.19	1.19
12F	0.815	0.815	0.82	0.78
30F	0.945	0.897	0.92	
C36		5.13		5.23

and atmospheric. The argon spike contains small amounts of ^{36}Ar and ^{40}Ar which have already been determined when the spike was calibrated. The atmospheric contribution has contents of ^{40}Ar, ^{38}Ar and ^{36}Ar in fixed proportions to one another. The equation for calculating the amount of radiogenic argon is:

$$^{40}Ar^{*} = {}^{38}Ar_s\left\{\left(\frac{^{40}Ar}{^{38}Ar}\right)_m - \left(\frac{^{40}Ar}{^{38}Ar}\right)_s - \left[\frac{1-(^{38}Ar/^{36}Ar)_m(^{36}Ar/^{38}Ar)_s}{(^{38}Ar/^{36}Ar)_m(^{36}Ar/^{38}Ar)_a - 1}\right]\left[\left(\frac{^{40}Ar}{^{38}Ar}\right)_a - \left(\frac{^{40}Ar}{^{36}Ar}\right)_m\right]\right\}$$

where subscripts: s = spike, m = measured mixture, a = atmospheric

Errors are controlled largely by atmospheric Ar contamination since the volumes of Ar are very low in these samples. Errors in the calculated ages have been computed assuming 1σ errors of 1%, 0.5%, 0.5% and 1.5% on the ^{36}Ar, ^{38}Ar, ^{40}Ar peak heights and potassium determination respectively by using the following formula:

$$\left[E_k^{\,2} + (1 + A/R)^2 E_{40}^{\,2} + E_{38}^{\,2} + (A/R)^2 E_{36}\right]^{\frac{1}{2}}$$

where R = % radiogenic ^{40}Ar

A = % atmospheric ^{40}Ar

E = % errors of the various peak heights

E_k = % error of the potassium determination.

Calculation of ages and associated errors from peak height data were done by computer; as were the potassium contents of samples, from count data recorded from the flame photometer.

A3 X-Ray Fluorescence Methods

Major element and trace element (Ni, Cr, V, Sc, Cu, Zn, Sr, Rb, Zr, Nb, Ba, Th, La, Ce, Nd, and Y) concentration data were available for all the samples analysed for strontium isotopic compositions and for K-Ar ages. This data was obtained by J.G. Fitton except for the Biu Plateau and Mandara Mountains which were analysed by the author.

All concentrations were determined using a Philips PW 1450/20 fully automatic spectrometer. Analytical techniques are summarized below; for full details see Thirlwall (1980). Major element compositions were determined using a chromium-anode X-ray tube under vacuum. Samples were analysed in the form of fused glass discs. The discs were prepared (following a method similar to that of Norrish and Hutton, 1969) by fusing dried sample powder with Johnson Matthey Spectroflux 105 (made up of lithium tetraborate, lithium oxide and lanthanum oxide, as a heavy absorber) in Pt - 5% Au crucibles. Calibrations were based on international USGS and CRPG standards. Trace elements were measured on pressed powder discs using tungsten - and chromium - anode tubes in an evacuated X-ray path. Analyses were corrected for mass absorption using coefficients calculated from the major element compositions of the samples. Pressed powder discs were made up of approximately 7 g of sample powder with a backing of boric acid. This weight was calculated by J.G. Fitton (personal communication) to give absorption of 99% of NbK radiation in a matrix of very low absorption. Discs were compressed in tungsten carbide pressing apparatus to 10 t in^{-2} using a Research and Industrial Instruments press. Elements obtained using the Cr tube are Sc-V-Cu-Ba and La; and from the W tube are Rb-Sr-Y-Nb-Nd-Zr-Ce-Ni-Zn-Th-Cr. In addition Ti was determined together with each group of traces and agreement of TiO_2 values was acceptable. Accuracy and precision are believed to be better than ± 1% for both Rb and Sr in concentrations higher than 40 p.p.m and less than 2500 p.p.m. Four U.S.G.S. standards (BCR1, AGU1, GSP1, G2) are compared in Table A4 with isotope dilution determinations (Pankhurst and O'Nions 1973). 63 samples were also analysed for Rb and Sr content by isotope

dilution at East Kilbride and these are compared with X.R.F. values in Table A5. These tables illustrate that the X.R.F. rubidium and strontium data are well within the limits required for isotopic geochemical studies of basaltic material. For consistency, X.R.F. values were used in this study except where concentrations fall below 40 p.p.m or above 2500 p.p.m. (especially Sr) in evolved rocks.

The author has had access to normative data calculated for samples analysed by J.G. Fitton. In addition, norms have been calculated on samples which the author analysed by X-ray fluorescence. All norms were calculated using a $Fe_2O_3/(FeO + Fe_2O_3)$ ratio of 0.3. This value is close to that measured wet chemically on samples from Principe (Fitton and Hughes, 1977) and reduction of all analyses to this ratio enables normative comparisons to be made without effects of subsequent oxidation.

TABLE A4

U.S.G.S. Standards Duplicate X.R.F. Analyses

	Rubidium (p.p.m.)					Strontium (p.p.m.)				
Standard	ID*	X.R.F.			$\bar{x}$	ID*	X.R.F.			$\bar{x}$
BCR1	47.3	48.4	46.7	47.9	47.5	332.1	334.4	332.4	332.1	332.5
AGU1	67.1	68.1	67.3	68.0	66.7	662.0	661.1	659.4	657.6	663.3
GSP1	254.7	255.3	256.1	254.9	255.5	233.1	235.3	237.2	233.3	231.5
G2	169.3	170.2	169.5	169.0	168.1	476.3	476.4	476.9	474.7	474.8

* Pankhurst and O'Nions, 1973

TABLE A5

Comparison of Edinburgh X.R.F. and S.U.R.R.C. Isotope Dilution (ID) Analyses of Samples for Rubidium and Strontium

	Rubidium		Strontium	
Sample	I.D.	X.R.F.	I.D.	X.R.F.
P2	235	244	41.0	42
P5	382	393	85.8	86
P11	129	133	961	959
P16	301	314	9.37	11
P35	288	297	298	295
P39	261	271	78.3	79
P51	21.5	22	674	658
ST3	157	160	221	221
ST5	16.0	20	985	974
ST39	170	178	243	248
ST56	157	164	1383	1387
ST57	120	124	226	231
ST58	119	124	219	225
ST84	192	200	16.6	19
ST90	231	239	33.4	36
C18	68.2	71	944	918
C20	84.2	85	3267	3272
C36	202	200	7055	7053
C54	87.1	89	161	163
C57	45.1	46	766	753
C91	29.3	31	1413	1410
C108	54.3	56	1031	1016
C110	29.0	30	1049	1032
C115	103	107	103	106
C116	98.3	101	1549	1532
C131	349	349	2818	2825
C135	23.2	22	1043	1022
C136	265	275	9.23	10
C137	256	266	91.8	94
C138	162	167	8.44	11
C139	55.6	58	58.2	63
C140	228	238	15.4	16
C141	166	172	33.1	35
C142	255	259	4.89	6
C143	81.3	84	95.2	98
C144	392	402	2.35	4
C145	133	138	13.5	16
C146	24.8	25	1182	1157
C147	32.3	34	1139	1110
C76	200) 198)	205	2.46) 2.46)	5
C81	58.0	55	369	358
C84	209	206	5.24	7
C85	170) 169)	172	0.82) 0.79)	4
C87	205) 204)	207	15.09) 14.97)	15
C92	197) 191)	192	11.11) 11.18)	11
C93	54.4	54	702	692
C95	154) 153)	156	2.87) 2.85)	4
C97	18.0	20	814	806
C121	25.7	26	2053	2039
C100	167) 169)	169	4.93) 4.88)	4
C101	109	110	3.12	5
C103	99.0	101	12.74	14
C104	132	133	5.04	6
C105	106	103	7.20) 7.26)	6
C106	88.1	88	13.79	15
C107	83.3	84	25.52	27
C109	118	118	12.73	13
C111	101	102	19.69	20
C114	134	138	13.25	15
C118	154	152	6.10	7
C120	150	153	5.24	7
N11	51.7	51	877	841
N29	73.3	75	1208	1192

APPENDIX B

WHOLE ROCK X-RAY FLUORESCENCE ANALYSES

Analyses determined by the author of samples from the Biu Plateau, N. Nigeria, and the Mandara Mountains, Cameroon are listed in Tables B1 and B2 respectively. The concentrations of major and minor elements are given in weight % and trace elements in p.p.m. Total iron content is as Fe_2O_3. An asterix indicates that the concentration level was not detectable. Table B2 contains C139, which was omitted from all diagrams since it is badly altered, as indicated by a very low majors total, loss of alkalies and trace elements. Tables B3 and B4 contain the CIPW norms derived from the analyses contained in Tables B1 and B2.

Table B1 XRF analyses of Biu Plateau lavas

	N1@8	N2@8	N3@8	N4@8	N5@8	N6@8	N7@8	N8@8	N9@8
SIO2	44.59	48.75	47.12	45.40	46.51	46.80	49.84	47.81	46.48
AL2O3	12.50	13.41	13.69	12.99	13.39	13.42	13.93	13.99	12.89
FE2O3	11.52	10.80	12.33	11.97	11.97	11.60	11.29	12.39	11.51
MGO	10.91	10.31	7.09	8.69	8.83	9.09	8.31	7.60	10.64
CAO	10.48	9.27	9.65	9.72	9.74	11.44	9.74	9.09	10.59
NA2O	1.96	2.44	3.36	2.93	3.29	3.06	2.95	3 46	2.85
K2O	1.68	1.30	1.42	1.27	1.11	0.91	0.95	1.54	1.13
TIO2	2.64	2.12	3.32	3 37	3.32	1.84	2.03	3.16	2.33
MNO	0.16	0.15	0.13	0.15	0.15	0.15	0.16	0.16	0.16
P2O5	0.59	0.42	0.62	0.56	0.59	0.33	0.33	0.85	0.44
TOTAL	97.03	98.98	98.75	97.05	98.89	98.63	99.52	100.05	99.04
NI	241	224	139	166	174	218	247	142	272
CR	443	396	138	174	237	345	382	190	388
V	356	305	389	394	391	294	287	341	337
SC	21	21	20	22	23	22	24	19	24
CU	20	56	51	43	41	70	51	39	62
ZN	89	90	103	99	98	82	90	118	89
SR	614	768	715	667	695	501	456	828	637
RB	38	32	30	28	46	22	22	33	27
ZR	204	171	296	274	266	121	136	377	174
NB	63	44	49	47	56	37	33	61	51
BA	542	504	560	415	454	471	390	470	661
PB	4	5	5	9	3	6	5	6	4
TH	3	3	2	3	2	2	3	4	2
LA	42	34	39	36	41	24	24	47	35
CE	81	64	76	75	81	42	43	101	58
ND	37	29	40	39	40	20	21	52	28
Y	23	22	29	29	29	23	25	31	24

Table B1 continued

	N10@8	N11@8	N13@8	N14@8	N15@8	N16@8	N17@8	N18@8	N19@8	N20@8	N21@8	N22@8
SIO2	46.72	45.32	47.84	44.24	47.10	46.45	45.89	45.91	46.36	49.09	48.38	44.75
AL2O3	13.14	13.30	13.89	12.30	14.08	13.48	12.90	12.98	13.15	14.65	14.34	12.07
FE2O3	11.64	11.66	11.17	12.38	11.83	11.30	11.31	11.48	11.68	11.17	11.04	12.29
MGO	10.44	9.60	8.56	10.78	9.49	9.23	9.73	10.11	10.19	8.11	8.78	11.05
CAO	10.27	10.10	8.43	10.53	9.57	8.73	9.80	10.05	9.83	9.14	8.67	10.21
NA2O	3.30	2.90	3.96	3.32	3.24	3.74	2.40	2.10	2.18	3.38	2.87	3.25
K2O	1.35	1.55	1.52	1.64	1.39	1.23	1.28	1.43	1.33	1.16	1.20	1.53
TIO2	2.70	2.49	2.81	2.97	2.43	2.67	2.38	2.81	2.90	1.87	1.93	2.64
MNO	0.17	0.18	0.16	0.20	0.16	0.17	0.15	0.16	0.15	0.15	0.15	0.19
P2O5	0.51	0.76	0.73	0.89	0.57	0.77	0.46	0.56	0.58	0.40	0.42	0.81
TOTAL	100.24	97.86	99.06	99.25	99.85	97.77	96.30	97.59	98.35	99.11	97.80	98.80
NI	248	184	186	257	200	211	235	200	210	166	168	285
CR	369	245	195	313	267	253	390	300	340	262	254	471
V	364	343	369	398	330	334	308	364	373	269	296	391
SC	24	20	20	23	25	18	23	24	23	24	23	25
CU	50	44	35	47	58	37	46	50	45	53	55	51
ZN	90	110	111	112	95	120	89	98	95	90	93	122
SR	652	841	885	910	690	1051	983	1115	751	560	574	893
RB	33	51	140	44	36	66	36	33	40	30	29	46
ZR	216	277	337	336	206	374	165	246	238	162	169	330
NB	56	84	86	88	59	93	48	60	59	43	45	89
BA	459	663	655	842	497	741	509	559	461	420	431	642
PB	4	5	7	5	4	5	7	5	4	7	7	*
TH	3	5	8	6	4	8	1	3	2	4	1	9
LA	38	61	66	70	41	69	32	39	40	31	31	74
CE	73	110	122	132	77	129	60	80	78	58	52	138
ND	32	47	51	57	35	55	29	38	37	25	25	59
Y	25	39	29	33	27	30	22	27	27	23	24	34

Table B1 continued

	N23@8	N24@8	N25@8	N26@8	N27@8	N29@8	N31@8	N32@8	N33@8	N34@8	N35@8	N36@8
SIO2	48.97	46.21	47.55	51.48	49.87	51.07	49.18	46.96	46.77	49.12	49.37	45.48
AL2O3	14.47	12.88	12.71	14.25	14.58	16.28	13.69	13.00	13.50	14.64	14.26	12.86
FE2O3	11.15	11.53	10.74	10.90	10.41	9.22	10.94	12.69	11.79	10.76	10.66	11.40
MGO	8.56	9.80	10.69	4.98	7.99	4.06	9.78	7.92	8.94	7.89	8.76	10.18
CAO	9.12	10.39	8.40	8.23	9.41	6.93	7.94	9.83	9.69	8.97	8.60	9.64
NA2O	3.34	2.94	2.33	3.54	3.44	4.32	3.42	2.35	3.78	3.20	3.42	2.92
K2O	1.32	1.32	1.31	1.19	1.21	2.85	1.57	1.24	1.65	1.38	1.52	1.69
TIO2	1.94	2.26	2.35	2.70	2.07	2.23	2.17	3.30	2.65	2.08	2.07	2.67
MNO	0.15	0.18	0.15	0.17	0.14	0.09	0.15	0.15	0.18	0.15	0.14	0.16
P2O5	0.42	0.72	0.41	0.46	0.57	0.93	0.47	0.57	0.65	0.54	0.50	0.81
TOTAL	99.34	98.24	96.64	97.91	99.71	97.98	97.31	98.01	99.60	98.73	99.30	97.83
NI	170	225	249	156	165	82	282	247	201	173	211	261
CR	252	327	441	222	238	84	376	367	323	244	286	322
V	293	343	322	312	292	240	295	443	357	292	300	372
SC	25	24	19	17	21	5	24	27	23	23	22	22
CU	55	56	40	40	45	16	44	47	51	53	48	45
ZN	95	111	95	124	91	133	96	103	104	89	95	114
SR	576	837	491	616	685	1192	632	593	829	719	654	1175
RB	30	38	32	27	29	75	35	27	43	31	35	53
ZR	171	264	193	233	207	338	239	267	278	201	215	303
NB	46	79	48	40	57	96	55	51	77	56	57	85
BA	457	740	453	481	457	1021	527	424	686	513	526	588
PB	5	4	6	4	5	6	8	8	4	6	6	5
TH	3	6	3	3	4	8	4	4	5	5	3	6
LA	34	68	34	29	46	66	37	39	59	45	41	63
CE	57	119	66	59	85	130	77	75	107	75	76	125
ND	25	48	31	33	36	57	33	39	47	34	32	53
Y	24	32	23	24	23	18	27	32	31	25	23	30

Table B1 continued

	N37@8	N38@8
SIO2	46. 50	44. 80
AL2O3	13. 45	12 76
FE2O3	11. 34	13. 05
MGO	9. 92	9. 92
CAO	9. 69	10. 38
NA2O	2. 47	3. 53
K2O	1. 44	1. 43
TIO2	2. 60	2 65
MNO	0. 14	0. 20
P2O5	0. 69	0. 84
TOTAL	58. 24	99. 57
NI	269	221
CR	352	272
V	365	373
SC	21	24
CU	53	52
ZN	97	118
SR	1577	859
RB	32	41
ZR	215	331
NB	64	83
BA	534	693
PB	5	4
TH	4	7
LA	43	70
CE	83	134
ND	37	57
Y	26	35

TableB2 XRF analyses ofvolcanic rocks from Mandara

	C135@9	C136@9	C137@9	C138@9	C139@9	C140@9	C141@9
SIO2	43. 66	70. 73	74. 44	69. 95	73. 49	72. 35	67. 32
AL2O3	12. 56	14. 96	13. 04	15. 17	16. 41	12. 44	15. 91
FE2O3	11. 78	1. 44	1. 69	2. 10	0. 46	3. 51	3. 05
MGO	11. 34	0. 20	0. 18	0. 17	0. 23	0. 30	0. 25
CAO	10. 39	0. 13	0. 18	0. 16	0. 14	0. 25	0. 19
NA2O	3. 50	6. 17	4. 52	5. 60	1. 28	4. 17	5. 75
K2O	1. 11	4. 44	4. 02	4. 75	1. 42	4. 16	5. 16
TIO2	3. 15	0. 14	0. 12	0. 20	0. 22	0. 31	0. 49
MNO	0. 18	0. 00	*	*	*	0. 00	0. 07
P2O5	0. 73	0. 02	0. 07	0. 04	0. 06	0. 06	0. 06
TOTAL	98. 41	98. 23	98. 26	98. 14	93. 71	97. 55	98. 25
NI	285	2	4	1	1	3	4
CR	482	3	3	3	2	2	2
V	454	8	6	11	11	24	38
SC	25	*	*	0	1	0	2
CU	70	*	*	*	*	*	*
ZN	99	39	43	80	7	165	123
SR	1022	10	94	11	63	16	35
RB	22	275	266	167	59	238	172
ZR	299	1073	893	632	660	2355	860
NB	92	472	208	225	257	418	226
BA	559	6	23	7	38	12	134
PB	4	19	20	11	13	15	15
TH	3	81	62	39	42	52	31
LA	61	115	101	174	171	122	143
CE	116	183	193	294	303	283	271
ND	49	66	72	87	97	105	86
Y	27	67	73	45	54	100	55

Table B2 continued

	C142@9	C143@9	C144@9	C145@9	C146@9	C147@9
SIO2	72.31	67.53	74.03	65.87	40.04	43.60
AL2O3	12.33	16.64	11.40	15.62	11.80	14.50
FE2O3	3.35	1.59	3.49	2.93	14.19	12.66
MGO	0.24	0.34	0.17	0.43	10.19	7.42
CAO	0.18	0.44	0.09	0.41	11.68	9.78
NA2O	5.63	6.15	5.26	7.02	3.62	3.32
K2O	4.37	5.10	4.05	5.31	0.98	1.54
TIO2	0.28	0.47	0.12	0.43	3 71	3.91
MNO	0.16	0.01	0.10	0.32	0.21	0.16
P2O5	0.01	0.10	0.01	0.07	1.13	0.74
TOTAL	98.87	98.38	98.78	98.39	97.54	97.63
NI	1	2	1	2	166	88
CR	3	2	3	2	274	129
V	20	35	7	27	535	503
SC	0	4	*	5	26	19
CU	*	*	*	*	48	43
ZN	282	31	307	162	108	90
SR	6	98	4	16	1157	1110
RB	259	84	402	138	25	34
ZR	1925	918	1938	1365	264	250
NB	430	136	576	178	89	62
BA	35	376	9	50	609	485
PB	30	9	37	14	4	6
TH	49	13	81	24	*	*
LA	25	137	41	198	62	45
CE	126	240	153	365	118	87
ND	37	83	29	109	53	44
Y	94	45	78	53	32	25

TABLE B3

BIU PLATEAU

C.I.P.W. Norms

	N1	N2	N3	N4	N5	N6	N7	N8	N9	N10	N11	N13	N14	N15	N16	N17	N18	N19
qz	-	-	-	-	-	-	-	-	-	-	-	-	-	-	-	-	-	-
or	9.92	7.68	8.41	7.52	6.56	5.37	5.64	9.09	6.70	7.98	9.13	8.96	9.69	8.18	7.30	7.56	8.43	7.86
ab	14.92	20.67	26.67	22.95	24.98	19.31	24.96	28.73	19.28	18.50	18.11	28.00	11.53	22.63	25.93	20.28	17.76	18.48
an	20.33	21.80	18.05	18.54	18.45	20.33	21.95	18.08	19.01	17.04	18.73	15.66	13.79	19.78	16.35	20.67	21.79	22.14
ne	0.92	-	0.98	1.00	1.57	3.54	-	0.32	2.64	5.12	3.47	2.97	9.00	2.59	3.09	-	-	-
di	22.18	17.16	20.68	20.78	20.79	27.60	19.46	17.28	24.46	24.43	21.11	17.11	26.02	19.24	17.52	19.91	19.47	18.21
hy	-	13.69	-	-	-	-	13.34	-	-	-	-	-	-	-	-	4.11	6.55	9.72
ol	16.91	7.86	10.35	12.87	13.17	12.81	4.19	12.70	16.02	15.53	15.27	14.02	15.67	15.88	15.35	12.79	11.49	10.53
mt	4.65	4.36	4.98	4.83	4.83	4.69	4.56	5.00	4.65	4.70	4.71	4.51	5.00	4.78	4.56	4.56	4.63	4.71
il	5.01	4.03	6.30	6.40	6.31	3.50	3.85	6.01	4.43	5.13	4.73	5.34	5.64	4.62	5.07	4.32	5.34	5.52
ap	1.37	0.96	1.45	1.30	1.36	0.76	0.76	1.96	1.03	1.17	1.76	1.70	2.07	1.31	1.78	1.07	1.29	1.34

Abbreviations

qz	quartz	hy	hypersthene
or	orthoclase	ol	olivine
ab	albite	mt	magnetite
an	anorthite	il	ilmenite
ne	nepheline	ap	apatite
di	diopside	na-m	Na-metasilicate

TABLE B3 (continued)

	N20	N21	N22	N23	N24	N25	N26	N27	N29	N31	N32	N33	N34	N35	N36	N37	N38
qz	-	-	-	-	-	-	3.63	-	-	-	-	-	-	-	-	-	-
or	6.87	7.12	9.04	7.23	7.82	7.76	7.04	7.13	16.81	9.27	7.36	9.78	8.15	8.96	9.99	8.49	8.45
ab	28.62	24.25	13.95	28.23	20.19	19.68	29.98	29.13	36.19	28.96	19.88	19.62	27.08	28.91	18.73	20.91	14.48
an	21.36	22.72	13.86	20.91	18.04	20.36	19.45	20.78	16.62	17.36	21.24	14.99	21.52	19.09	16.97	21.36	14.71
ne	-	-	7.32	-	2.55	-	-	-	0.22	-	-	6.68	-	-	3.26	-	8.36
di	17.19	14.08	25.15	17.34	23.06	14.81	14.86	17.78	9.48	15.16	19.09	23.08	15.60	16.24	20.39	17.71	25.12
hy	3.47	11.76	-	2.53	-	16.46	11.55	5.55	-	2.42	14.79	-	7.56	2.63	-	4.43	-
ol	11.82	7.98	16.74	13.14	15.15	7.03	-	9.13	7.90	15.74	2.04	13.29	8.50	13.31	16.12	13.41	15.26
mt	4.51	4.46	4.96	4.50	4.65	4.33	4.40	4.20	3.72	4.42	5.12	4.76	4.34	4.30	4.60	4.58	5.27
il	3.54	3.67	5.01	3.69	4.29	4.47	5.14	3.98	4.23	4.12	6.26	5.04	3.95	3.93	5.08	4.94	5.04
ap	0.92	0.98	1.88	0.97	1.66	0.96	1.08	1.32	2.16	1.08	1.33	1.52	1.26	1.17	1.87	1.61	1.94

TABLE B4 Mandara Mts. C.I.P.W. Norms

	C135	C136	C137	C138	C140	C141	C142	C143	C144	C145	C146	C147
qz	-	16.91	31.70	17.97	30.07	12.53	24.39	10.74	29.48	6.22	-	-
or	6.56	26.21	23.74	28.06	24.56	30.48	25.85	30.17	23.94	31.35	5.79	9.11
ab	12.83	52.23	38.26	47.40	35.27	48.62	39.08	52.00	36.08	50.79	4.54	17.55
an	15.27	0.01	0.38	0.49	0.84	0.52	-	1.52	-	-	13.06	20.10
ne	9.11	-	-	-	-	-	-	-	-	-	14.14	5.72
di	25.08	0.47	-	-	-	-	0.71	-	0.35	1.38	30.01	18.87
hy	-	1.42	1.85	2.10	3.61	2.88	4.06	1.62	4.39	3.75	-	-
ol	16.28	-	-	-	-	-	-	-	-	-	13.59	11.12
mt	4.75	0.58	0.68	0.85	1.42	1.23	-	0.64	-	-	5.72	5.11
il	5.99	0.27	0.24	0.38	0.60	0.93	0.53	0.90	0.23	0.81	7.05	7.42
ap	1.68	0.04	0.17	0.10	0.14	0.15	0.03	0.24	0.03	0.16	2.62	1.72
na-m	-	-	-	-	-	-	1.28	-	1.22	1.38	-	-

abbreviations as for Table B3

APPENDIX C

CLASSIFICATION SCHEME EMPLOYED

The samples studied in this thesis have been named according to variation in SiO_2 content with respect to total alkalis as described by Cox et al. (1979) in their Figure 2.2. The fields on this diagram were essentially derived from the very comprehensive paper of Le Maitre (1976). Porphyritic picritic basalts have been termed oceanite or ankaramite following the traditional terminology as found in texts on igneous petrology such as Turner and Verhoogen (1960). For the hyperalkaline rocks of Etinde the classification scheme of Streckeisen (1967) was adopted.

APPENDIX D List of Samples Studied

PRINCIPE ISLAND (Figure 3.1.1)

Sample No.	Description	Rock Type	Grid Ref.
P 2	Block from Pico Papagaio	Phonolite	1°37'30"N 7°23'30"E
P 3	Dyke, Praia Caixão	Hawaiite	1°37'N 7°22'E
P 5	Block from Caixão peak	Phonolite	1°37'15"N 7°22'15"E
P 6	Flow, ¾ km S.W. of Ponta Chindela	Hawaiite	1°37'30"N 7°27'30"E
P 8	Block in agglomerate, below P6	Hawaiite	" "
P11	Block, Ribeira Fria	Phonolite	1°35'30"N 7°25'30"E
P12	Block from Os Dois Irmãos	Tristanite	1°35'N 7°25'45"E
P13	Outcrop in Rio Chivala	Tristanite	1°34'30"N 7°25'15"E
P15	Outcrop from Rio Cambumgo	Olivine tholeiite	1°34'15"N 7°25'15"E
P16	" " " "	Trachyphonolite	" "
P17	Outcrop, 1 km S.E. of San Antonio	Basanite	1°38'N 7°25'45"E
P18	" " " " "	Nephelinite	1°38'15"N 7°25'45"E
P19	Flow, 1 km S.W. of Belo-Monte	Basanite	1°40'45"N 7°26'30"E
P20	Flow, Precipicio, Praia Banana	Basanite	1°41'15"N 7°26'45"E
P21	Flow, W. side of Ponta Banana	Hawaiite	1°41'30"N 7°26'30"E
P22	Block, S.W. of Conceicão	Phonolite	1°39'0"N 7°24'15"E
P25	Flow, Ponta Candumbo	Hawaiite	1°41'N 7°22'45"E
P26	Flow, Ponta Marmita	Hawaiite	1°41'15"N 7°22'30"E
P27	Flow, 1 km N.W. of Santa Rita	Hawaiite	1°41'15"N 7°24'15"E
P28	Flow, headland S. of Llhéu Bom-Ban	Basalt	1°41'45"N 7°24'15"E
P29	Dyke, " " " " "	Hawaiite	" "

Sample No.	Description	Rock Type	Grid Ref.	
P31	Dyke, Praia de Santa Riba	Basalt	1°41'30"N	7°24'30"E
P32	" " " " "	Basalt	"	"
P33	" " " " "	Hawaiite	1°41'45"N	7°24'45"E
P34	Flow, 300 m W. of San Joaquim	Nephelinite	1°37'30"N	7°22'30"E
P35	Block, from Caixão, Praia da Lopa	Phonolite	1°38'45"N	7°22'E
P38	Block, Ribeira Das Agulhas, probably from Pico Agulhas	Phonolite	1°36'N	7°22'E
P39	Block, 300 m S.W. of Francisco Mantero, from A Mesa	Phonolite	1°36'N	7°21'15"E
P40	Block, foot of Focinho do Cão	Phonolite	1°36'N	7°20'30"E
P41	Block, Morro Mabemba	Trachyte	1°36'30"N	7°22'E
P45	Flow, 500 m N. of Oquê-Daniel trig. point	Basanite	1°40'N	7°22'30"E
P50	Flow, Ponta Santana	Basalt	1°40'N	7°27'E
P51	Flow, 500 m W. of Ponta Santana	Basanite	1°39'45"N	7°26'45"E
BIOKO (Figure 3.1.5)				
FP1	See Piper and Richardson (1972)	Basalt	3°43'N	8°57'E
FP23	"	Basalt	3°23.5'N	8°46'E
FP32	"	Hawaiite	3°26'N	8°38.5'E
FP38	"	Basalt	3°42'N	8°48.5'E
FP44	"	Basalt	3°44'N	8°37'E

PAGALU (Figure 3.1.6)

Sample No.	Description	Rock Type	Grid Ref.	
AN3	See Piper and Richardson (1972)	Basalt	1°24'S	5°36'E
AN8	"	Basalt	"	"
AN12	"	Basalt	"	"
AN13	"	Basanite	"	"
AN20	"	Basalt	"	"

SÃO TOMÉ (Figure 3.1.3)

ST3	Block from Pico Fraternidade	Phonolite	0°6'45"N	6°39'15"E
ST5	Flow, Dova Augusta	Basalt	0°6'45"N	6°37'45"E
ST10	Block from Cão Grande	Phonolite	0°7'00"N	6°34'15"E
ST12	Block from M. Sinai?	Phonolitic Tephrite	0°4'45"N	6°34'30"E
ST13	Flow, small bay N. of Mesquita	Basalt	0°4'30"N	6°34'15"E
ST13A	Nodules in flow, small bay N. of Mesquita	Hornblendite	0°4'30"N	6°34'15"E
ST14	Nodule in agglomerate, small bay N. of Mesquita	Hornblendite	"	"
ST16	Flow, small bay N. of Mesquita	Mugearite	"	"
ST16A	Nodules in flow, small bay N. of Mesquita	Hornblendite	"	"
ST19	Flow, Morro Corregado (cinder cone)	Basanite	0°25'30"N	6°37'00"E
ST35	Block, Praia Moça	Benmoreite	0°18'30"N	6°30'00"E
ST39	Block, Santa Catarina	Phonolite	0°16'30"N	6°29'00"E
ST43	Block, from São José (Monte Cafe)	Trachyte	0°18'45"N	6°38'45"E
ST44	Flow, Palmar	Basanite	0°21'00"N	6°43'00"E
ST54	Blocks, from Cão Pequeno	Phonolite	0°6'30"N	6°32'15"E

Sample No.	Description	Rock Type	Grid Ref.	
ST56	Block, 1.5 km E. of San Antonio	Phonolite	0°6'30"N	6°32'00"E
ST57	Flow, N.E. peak of Ilhéu das Cabras	Trachyte	0°25'00"N	6°43'15"E
ST58	Flow, S.W. " " " " "	Trachyte	"	"
ST60	Flow, Agua Izé (Ilheu das Rolas)	Basalt	0°13'30"N	6°44'15"E
ST69	Flow, E. side of Ponta de Santo Antonio	Basanite	0°0'15"N	6°32'00"E
ST80	Nodules in boulder, Rio M. Luisa	Hornblendite	0°20'00"N	6°31'30"E
ST84	Block, from S. side of Mizambu	Trachyphonolite	0°13'45"N	6°41'30"E
ST90	Block, from Agua João, N.E. of Maria Fernandes	Phonolite	0°10'45"N	6°39'30"E
ST92	Flow, 1 km. N.E. of Ribeira Afonso	Basalt	0°12'15"N	6°42'30"E
ST96	Dyke, Praia Capitango	Hawaiite	0°5'30"N	6°36'45"E
ST98	Flow, " "	Hawaiite	0°5'15"N	6°37'00"E
ST100	Block, João Paulo, from Calvario area	Benmoreite	0°17'45"N	6°35'00"E
ST107	Flow, 1 km S.W. of Milagrosa	Hawaiite	0°17'00"N	6°39'45"E
ST109	Flow, Zampalura	Basanite	0°16'30"N	6°36'45"E
ST110	Flow, bridge over Rio Manuel Jorge	Phonolitic Tephrite	0°17'00"N	6°39'30"E
ST115	Block, Santa Cruz	Ankaramite (picrite)	0°8'15"N	6°39'15"E
ST117	Blocks, 1 km S. of Rebordelo, from Morro Vilela?	Phonolitic Tephrite	0°18'00"N	6°34'30"E
ST117A	Nodules, " " " " " " "	Hornblendite	"	"
ST117B	Nodules, " " " " " " "	Feldspar	"	"
UBF	Blocks, Rio Maria Luisa	Sandstone	0°15'15"N	6°41'00"E

MT. CAMEROON (Figure 3.2.1)

Sample No.	Description	Rock Type	Grid Ref.	
C 1	Flow, nose of 1959 flow	Hawaiite	4°14'N	9°19'E
C 2	Flow, stream bed 1 km S.E. of hut 1	Hawaiite	4°11'N	9°13'E
C 3	Flow, Gaskin's grotto	Hawaiite	4°12'N	9°12'E
C 4	Flow, ½ km N.E. of hut 2	Basalt (Oceanite)	"	"
C 5	Flow, 1954 eruption, summit	Hawaiite	4°13'N	9°11'E
C 6	Flow, N. side Battle peak (summit)	Hawaiite	"	"
C12	Flow, below Upper Farm, Buea	Nephelinite	4°09'N	9°14'E
C14	Flow, 50 m N. of school at Bova II	Basalt	4°12'N	9°16'E
C16	Flow, N.E. of Ewonda	Basanite	4°11'N	9°15'E
C18	Block, same site as C12	Hawaiite	4°09'N	9°14'E
C26	Flow, 1922, 4 km S.E. of Bibundi Camp	Basanite	4°11'N	9°00'E
C28	Flow, 750 m S. of Debundsha	Nephelinite	4°6'N	8°59'E

MT. ETINDE (Figure 3.2.1)

C20	Block from stream, 500 m E. of Elonge	Mela Nephelinite	4°03'N	9°05'E
C21	" " " " " "	Mela Nephelinite	"	"
C23	" " " " " "	Mela Nephelinite	"	"
C31	Block in river by bridge at Batoke I Camp	Mela Nephelinite	4°02'N	9°06'E
C32	" " " " " " "	Mela Nephelinite	"	"
C33	" " " " " " "	Mela Nephelinite	"	"
C34	" " " " " " "	Mela Nephelinite	"	"
C35	" " " " " " "	Mela Nephelinite	"	"
C36	" " " " " " "	Leuco Nephelinite	"	"
C126	" " " " " " "	Mela Nephelinite	"	"
C127	" " " " " " "	Mela Nephelinite	"	"

Sample No.	Description	Rock Type	Grid Ref	
C128	Block in river by bridge at Batoke I Camp	Mela Nephelinite	4°02'N	9°06'E
C129	" " " " " " " " "	Mela Nephelinite	"	"
C130	" " " " " " " " "	Mela Nephelinite	"	"
C131	" " " " " " " " "	Leuco Nephelinite	"	"
C132	" " " " " " " " "	Mela Nephelinite	"	"
C133	" " " " " " " " "	Mela Nephelinite	"	"
C134	" " " " " " " " "	Mela Nephelinite	"	"
MT. MANENGOUBA (Figure 3.2.1)				
C48	Flow, 2.5 km N.W. of Bareko	Basalt	5°07'N	9°57'E
C49	Flow, by roadside, junction with road to Nyabang plantation	Hawaiite	5°03'N	9°55'E
C51	Flow, small cone, Melong	Basalt	5°07'N	9°57'E
C52	Flow, between river and junction, Wot Njinjo	Hawaiite	5°07'N	9°53'E
C54	Block, 4 km N of Bangem	Trachyte	5°06'N	9°47'E
C55	Block, Ndoungue	Basalt	4°55'N	9°54'E
C56	Flow, 1 km S.E. of Manengouba village	Basalt	4°57'N	9°53'E
C57	Block, in stream by C56	Trachy Basalt	4°57'N	9°53'E
C59	Flow, 1 km E. of Ekoh	Basalt	5°02'N	9°56'E
C61	Xenolith, from Ndom cone (Basalt)	Gabbro	5°04'N	9°56'E
C62	Flow, 300 m N.W. of Mbouroukou	Mugearite	5°04'N	9°53'E
C63	Block, N.W. rim of Manengouba caldera	Mugearite	5°03'N	9°49'E
C65	Flow, S. wall of Lac de la Femme	Basalt	5°02'N	9°50'E
C67	Intrusion, base of S. side of peak on N. side of caldera (Haw.)	Gabbro	5°02'N	9°50'E
C69	Block, from S.W. rim of caldera	Mugearite	5°02'N	9°49'E
C70	Block, cinder cone on N.W. rim of caldera	Basalt	5°03'N	9°49'E

BAMBOUTO MTS. (Figure 3.2.1)

Sample No.	Description	Rock Type	Grid Ref.	
C99	Block, 3 km S.E. of Guzang	Basalt	5°49'N	9°57'E
C100	Flow, Ashong	Rhyolite	5°47'N	9°59'E
C101	Flow, 2 km E. of Ashong	Trachyte	"	"
C102	Block, 4 km N.E. of Ashong	Basalt	5°47'N	10°00'E
C103	Outcrop, Wontoko	Trachyte	5°47'N	10°01'E
C104	Outcrop, 200 m S.E. of Pinyin Crop Farm	Rhyolite	5°47'N	10°05'E
C105	Flow, cutting, 500 m N. of Santa	Rhyolite	5°48'N	10°10'E
C106	Outcrop, 2 km W. of Santa Coffee Factory	Trachyte	"	"
C107	Flow, 2 km E. of Santa	Trachyte	"	"
C108	Quarry, 3 km N.E. of Dschang	Basalt	5°28'N	10°03'E
C109	Scarp, 2 km N.E. of Metsi	Trachyte	5°32'N	10°05'E
C110	Flow, just N. of Ndo	Basalt	5°34'N	10°04'E
C111	Flow, 2.5 km S.E. of Lekwué Leloé	Trachyte	5°35'N	10°02'E
C112	Flow, W.S.W. of Lekwué Leloé	Basanite	5°36'N	10°02'E
C114	Flow, rim of Bambouto caldera, overlooking Baranka	Trachyte	5°38'N	10°01'E
C115 C116	Flow, S. rim of caldera, 1 km W. of summit	Phonolite	5°38'N	10°04'E
C118	Cliff, above Fongo Tongo	Trachyte	5°30'N	10°00'E
C120	Flow, midway between Djeuand Ndo	Trachyte	5°33'N	10°02'E
C121	Quarry, 1 km N.W. of Djutitsa	Basalt	5°35'N	10°05'E

OKU MTS. (Figure 3.2.1)

Sample No.	Description	Rock Type	Grid Ref.	
C76	Cliff, E. of Bamenda	Rhyolitic ignimbrite	5°57'N	10°10'E
C78	Flow, 5 km N. of Bafut	Basalt	6°08'N	10°07'E
C81	Cliff, overlooking Bamenda	Trachyte	5°56'N	10°10'E
C84	Flow, N. of Sabga Pass	Rhyolite	6°01'N	10°18'E
C85	Flow, 2 km W. of Sabga	Rhyolite	"	"
C87	Cliff, 6 km S.W. of Jakim	Rhyolitic ignimbrite	6°03'N	10°36'E
C90	Block, 8 km S.W. of Kumbo	(picrite) Basalt	6°10'N	10°39'E
C91	Quarry, 9 km S.W. of Kumbo	Hawaiite	6°09'N	10°39'E
C92	Ignimbrite, 1 km N.E. of Sop	Rhyolitic ignimbrite	6°09'N	10°38'E
C93	Flow, 5 km S.W. of Jakim (above C87)	Hawaiite	6°03'N	10°37'E
C94	Flow, 10 km N. of Bambui	Basalt	6°06'N	10°13'E
C95	Ignimbrite, Mbingo	Rhyolitic ignimbrite	6°10'N	10°18'E
C96	Flow, by road to Belo Water Project	Basalt	6°12'N	10°22'E
C97	Flow, hill above Fanantui	Basalt	6°14'N	10°22'E

BIU PLATEAU (Figure 3.2.2)

N 1	Flow, overlying basement, 300 m S. of Kuvai	Basalt	10°23'30"N	12°10'30"E
N 2	Flow, 1 km N.E. of Kuvai	Basalt	10°24'00"N	12°10'45"E
N 3	Flow, 1 km S.E. of Pirkisu	Basalt	10°24'15"N	12°10'45"E
N 4	Flow, 1 km N.W. of N3	Basalt	10°24'30"N	12°10'30"E
N 5	Flow, Humisi	Basalt	10°24'30"N	12°09'45"E
N 6	Flow, 1 km W. of N5	Basalt	10°24'30"N	12°09'30"E
N 7	Block, 300 m S. of Targasi	Basalt	10°25'00"N	12°09'15"E

Sample No.	Description	Rock Type	Grid Ref.
N 8	Flow, Lema	Basalt	10°25'15"N 12°09'15"E
N 9	Block, 500 m N. of Leuburdugu	Basalt	10°29'30"N 12°10'15"E
N10	Block, Kirm Bote	Basanite	10°30'30"N 12°12'15"E
N11	Flow, Miringa Cone	Basalt	10°44'30"N 12°7'00"E
N12	Nodules, " "	Nodules	10°44'15"N 12°7'00"E
N13	Bomb, Dutsi Gidi Cone	Basalt	10°43'15"N 12°7'30"E
N14	Flow, 500 m S. of Miringa	Basanite	10°43'15"N 12°9'00"E
N15	Flow, 3 km S. of Miringa	Basalt	10°42'00"N 12°9'15"E
N16	Flow, near Tangurimi	Basalt	10°41'30"N 12°9'15"E
N17	Flow, 750 m S. of Yam Kuri	Basalt	10°39'00"N 12°10'00"E
N18	Flow, new road cutting, 3 km N.W. of Biu	Basalt	10°38'30"N 12°10'30"E
N19	Flow, " " " 2 " " " "	Basalt	10°38'00"N 12°11'00"E
N20	Flow, Mayo Song riverbed, Song Plateau	Basalt	9°51'15"N 12°37'00"E
N21	" " " " " "	Basalt	" "
N22	Bomb, in quarry 1 km S.E. of Song	Basanite	9°49'20"N 12°38'00"E
N23	Block, Mugaba, 2 km N. of Song	Basalt	9°51'00"N 12°37'05"E
N24	Flow, Hawal River, 4 km S.W. of Garkida	Basalt	10°23'30"N 12°32'20"E
N25	Flow, 2 km W. of Tashon Alade	Basalt	10°29'00"N 12°24'15"E
N26	Flow, Tirkalon	Basalt	10°29'30"N 12°23'30"E
N27	Block, Tila Lake	Basalt	10°32'30"N 12°8'00"E
N29	Flow, N. side of Tila Lake	Hawaiite	10°33'00"N 12°7'45°E
N30	Megacryst suite, N. side of Tila Lake	Megacrysts	" "

Sample No.	Description	Rock Type	Grid Ref.
N31	Flow, 1.5 km S.E. of Gombe Road	Basalt	10°35'30"N 12°6'30"E
N32	Flow, new cutting, 5 km W. of Biu	Basalt	10°37'00"N 12°8'30"E
N33	Block, immed. S. of Biu Rest House	Basanite	10°35'45"N 12°12'45"E
N34	Flow, 300 m N. of Wuro Malum Jubro	Basalt	10°49'45"N 12°7'30"E
N35	Blocks, base of cone, 500 m N. of N34	Basalt	10°50'15"N 12°7'00"E
N36	Bomb, cone, 500 m N. of N34	Basalt	10°50'00"N 12°7'00"E
N37	Flow, Zagu cone	Basalt	10°56'45"N 12°4'45"E
N38	Flow,	Basanite	11°04"N 12°03'E

MANDARA MOUNTAINS (Figure 3.2.2)

C135	Flow, resting on basement, immed. N.E. of Roumsiki	Basanite	10°31'N	13°35'E
C136	Block, Kama, 4 km N. of Roumsiki	Rhyolite	10°32'N	13°35'E
C137	Dyke, 6 km N. of Roumsiki	Rhyolite	10°33'N	13°35'E
C138	Block, from Zevou Spine, 1.5 km N. of Roumsiki	Rhyolite	10°32'N	13°35'E
C139	Dyke, N. of Zevou Spine	Rhyolite	10°32'N	13°35'E
C140	Block, by Gado Mayo	Rhyolite	10°36'N	10°35'E
C141	Block, hill E. of Mogode	Trachyte	10°37'N	13°34'E
C142	Spine, Roumkou, 3 km N.E. of Mogode	Rhyolite	10°38'N	13°35'E
C143	Dyke, E. of Moguemchil	Trachyte	10°35'N	13°35'E
C144	Spine, Aiguille Mchingui	Rhyolite	10°38'N	13°34'E
C145	Block, from Omtemale spine	Trachyte	10°38'N	13°34'E
C146	Flow, midway between Jiri and Kila	Basanite	10°27'N	13°36'E
C147	Flow, Kila	Basalt	10°27'N	13°38'E

APPENDIX E

"A K-Ar and Sr-Isotopic Study of the Volcanic Rocks of the Island of Principe, West Africa - Evidence for Mantle Heterogeneity Beneath the Gulf of Guinea"

by H.M. Dunlop and J.G. Fitton

Published by Springer Verlag (1979) in Contributions to Mineralogy and Petrology.

Contrib. Mineral. Petrol. 71, 125–131 (1979)

Contributions to Mineralogy and Petrology
© by Springer-Verlag 1979

A K–Ar and Sr-Isotopic Study of the Volcanic Rocks of the Island of Principe, West Africa – Evidence for Mantle Heterogeneity Beneath the Gulf of Guinea

H.M. Dunlop[1] and J.G. Fitton[2]

[1] Scottish Universities Research and Reactor Centre, East Kilbride, Scotland
[2] Grant Institute of Geology, University of Edinburgh, Scotland

Abstract. K–Ar dating on a suite of volcanic rocks from the island of Principe gives the following chronology.

1. Basal palagonite breccia (30.6 ± 2.1 Ma).
2. Older Lava Series (OLS) basalt (23.6 ± 0.7 Ma) and hawaiite (19.1 ± 0.5 Ma).
3. Younger Lava Series (YLS) nephelinite (5.60 ± 0.32 Ma) and basanite (3.51 ± 0.15).
4. Intrusive phonolite (5.32 ± 0.17 Ma, 5.48 ± 0.19 Ma), tristanite (4.89 ± 0.15 Ma) and trachyphonolite (6.93 ± 0.68 Ma) plugs.

Phonolites and YLS samples plot on a 5.9 ± 0.3 Ma Rb–Sr isochron. The tristanite-trachyphonolite suite samples also lie on this isochron. This lends support to the suggestion that the YLS basanite magmas were parental to the phonolites but rules out a similar relationship between the OLS magmas and the tristanite-trachyphonolite suite. The mean initial $^{87}Sr/^{86}Sr$ ratio for the YLS nephelinites and basanites is 0.70297.

The basalts and hawaiites of the OLS show a positive $^{87}Sr/^{86}Sr$ vs. Rb/Sr correlation which may be interpreted as a 244 ± 43 Ma pseudoisochron. This could be the result of a large-scale heterogeneity generated in the mantle during the early stages in the break-up of Gondwanaland. The mean initial $^{87}Sr/^{86}Sr$ ratio (at 21 Ma) for the OLS (0.70326) is significantly higher than that for the YLS and implies an isotopically distinct mantle source.

Introduction

The island of Principe lies off the west coast of Africa in the Gulf of Guinea and forms part of the oceanic sector of the volcanic Cameroun Line (Fig. 1). The structure and volcanic stratigraphy of the island have been described by Fitton and Hughes (1977).

The oldest rocks on Principe are small inliers of palagonite breccia representing a submarine phase in the evolution of the island. These breccias contain blocks of fresh tholeiitic basalt. The oldest subaerial volcanic rocks comprise a sequence of transitional basalt and hawaiite flows intruded by compositionally similar dykes and other minor intrusions. Together the lavas and intrusions form the Older Lava Series (OLS).

The Older Lava Series is overlain with slight unconformity by a distinctive suite of basanite and nephelinite flows of the Younger Lava Series (YLS). Field evidence suggests that a long period of erosion separated the eruption of the two units. The YLS rocks are

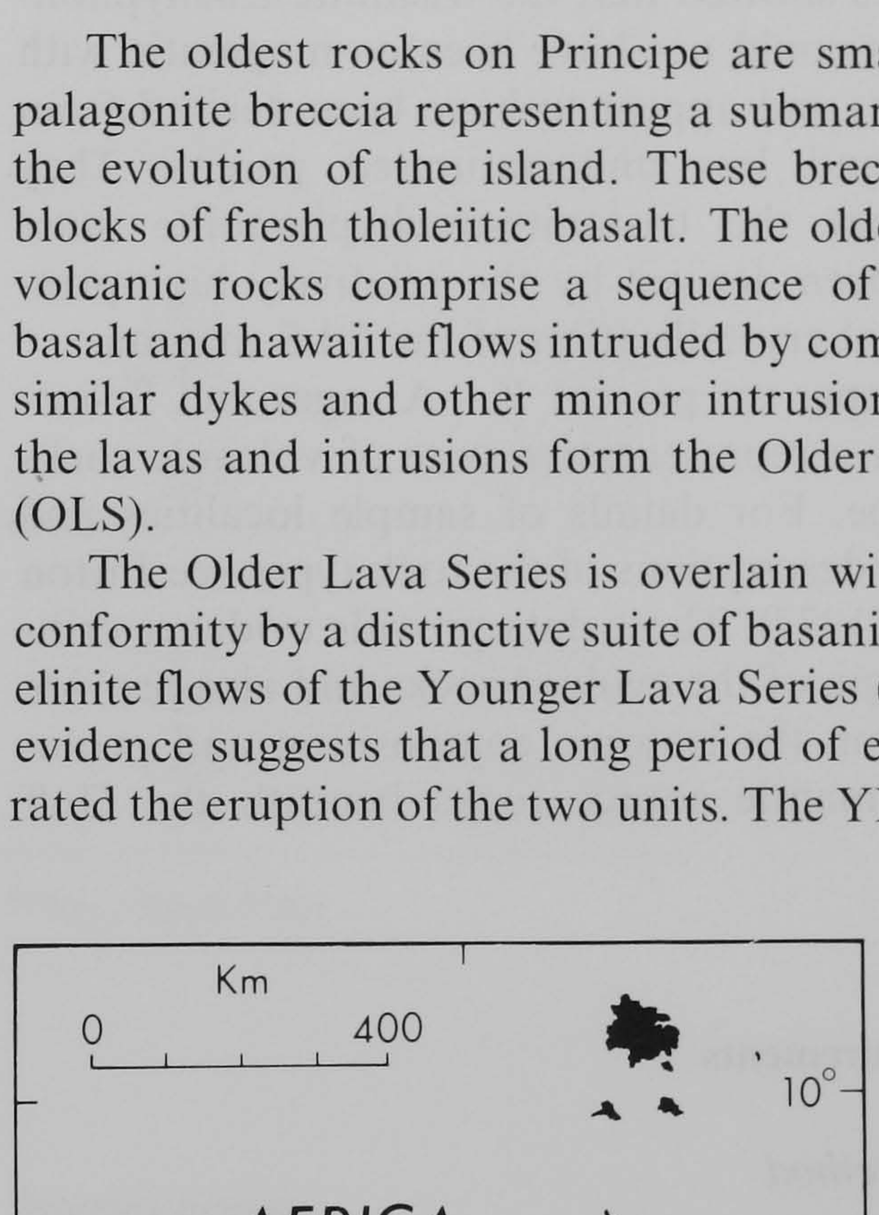


Fig. 1. Location map showing the distribution of the Cameroun Line volcanic rocks *(black)*

0010-7999/79/0071/0125/$01.40

generally fresher than are those from the OLS and are not seen to be intruded by dykes. The pre-YLS topography of Principe must have been very subdued as the base of this series occurs at about the same height above the present sea level wherever it is seen. There is no evidence of recent volcanic activity on the island.

Phonolite lavas overlie the basic lavas of the YLS and the lava pile is intruded, in the southern part of Principe, by plugs ranging in composition from tristanite to phonolite. These evolved rocks form two suites: tristanite to trachyphonolite and phonolite. Mineralogical evidence suggests that the phonolites were derived by low-pressure crystal fractionation of YLS basanite magma (Fitton and Hughes, 1977). These authors showed that the tristanite-trachyphonolite magmas could not have been co-magmatic with the phonolites and appear to have been derived from a separate and less undersaturated parent. They suggested that the tristanite-trachyphonolite suite could have been derived by the relatively high-pressure fractional crystallisation of the OLS magma.

In this paper we present K–Ar ages and Sr-isotope data for a representative suite of volcanic rocks from Principe. For details of sample localities and petrographic descriptions of the rock types see Fitton and Hughes (1977). These data provide evidence critical to the origin of the evolved rocks and also provide information on the isotopic composition and evolution of the mantle source rocks beneath the Gulf of Guinea.

K–Ar Measurements

Analytical Method

Nine samples, free of glass, secondary minerals, and visible alteration in thin section, were selected for K–Ar studies. Whole rock samples were crushed and −1.4 mm+20 B.S. mesh chips were used for argon analysis. Representative portions were ground in a Tema mill for potassium analysis. Potassium was determined in replicate with a precision of 1.5% on a Corning EEL 450 flame photometer employing sodium buffering and a lithium internal standard.

Argon analyses were performed in duplicate by isotope dilution using a ^{38}Ar spike and isotopic ratios were measured statically on an A.E.I. M.S. 10 mass-spectrometer. Samples were run within 1 month of crushing. Errors are controlled largely by the atmospheric Ar contamination since the volumes of Ar are very low. Errors in the calculated ages have been computed assuming errors of 1%, 0.5%, and 0.5% on the ^{36}Ar, ^{38}Ar, and ^{40}Ar peak heights respectively. K–Ar data for a basal tholeiite, 2 O.L.S. samples, 2 Y.L.S. samples, 2 phonolites, a tristanite, and a trachyphonolite are presented in Table 1.

Results. The K–Ar age data (Table 1) of representative samples from all the volcanic units exposed on Principe give an indication of the history of volcanism and assist in the interpretation of the measured $^{87}Sr/^{86}Sr$ ratios, particularly of the evolved rocks. A block of tholeiitic basalt within an inlier of basal palagonite breccia gives a mean age of 30.6 ± 2.1 Ma and probably represents the period of initial submarine activity on the island.

The data presented here substantiate Fitton and Hughes' (1977) division of the subaerial volcanic rocks into two lava series. The OLS is of Lower Miocene age since a hawaiite and a basalt give ages of 19.1 ± 0.5 Ma and 23.6 ± 0.7 Ma respectively. Hedberg (1968) reported a single K–Ar date of 24 Ma from the same lava series. Field evidence suggests that a long period of erosion separated the OLS from the YLS basanites and nephelinites. This is supported by K–Ar dating on a nephelinite and a basanite of the YLS which give ages of 5.60 ± 0.32 Ma and 3.51 ± 0.15 Ma respectively.

The evolved rocks analysed all fall within the Pliocene eruption period of the YLS. This is consistent with the derivation of the phonolites by low pressure fractionation of the YLS basanitic magma. However it is clear that the other evolved rocks are not of the same age as the OLS, thus apparently ruling out any direct genetic link between the two.

Rb–Sr Isotopic Studies

Analytical Methods

All the samples analysed were free from visible signs of alteration. In the field, the OLS rocks are generally more altered than are those from the YLS. Since this could bias the analytical data only the freshest material was collected from the OLS and this material was further selected before analysis. There are, therefore, no significant differences in degree of alteration, iron oxidation ratio and volatile content between the OLS and YLS samples used in this study.

$^{87}Sr/^{86}Sr$ ratios of all samples were measured by the precise unspiked whole-rock method on an A.E.I. M.S.12, 12 in. rad., 90° sector solid source mass-spectrometer at S.U.R.R.C. East Kilbride. At least 12 sets of 10 scans were taken per sample to obtain a precision of $\leqq \pm 0.00012 (2\sigma)$ and several samples were analysed in replicate. An in-run zero and mass 85 were monitored as well as 86, 87, and 88 peaks. Fractionation during analysis was corrected by normalizing $^{88}Sr/^{86}Sr$ ratios to a standard value of 8.37521. Preparation of sample powders for mass-spectrometry followed standard HF-HNO_3 dissolution plus HCl cation exchange separation procedures. All errors quoted on $^{87}Sr/^{86}Sr$ ratios are at 2σ level and an ^{87}Rb decay constant of 1.42×10^{-11} (Steiger and Jäger, 1977) was used in all calculations. The measured mean $^{87}Sr/^{86}Sr$ value for the NBS 987 strontium standard over the analysis period was $0.71023 \pm 0.00003 (2\sigma)$. Isochron regressions were calculated using the methods of York (1969).

Rb and Sr concentrations were determined by X-ray fluorescence analysis at Edinburgh using a Philips PW1450/20 spectrometer. Mass absorbtion corrections were made by applying coefficients calculated from the major-element compositions of the sam-

Table 1. K–Ar data from Principe

Sample no.	Rock type	*K* (%)	$^{40}Ar^*/^{40}Ar_T$	$^{40}Ar^*$ ($\times 10^{-6}$ scc/g)	Age (ma)
Lava from palagonite breccia					
*P*15	tholeiite	0.445	0.166	0.537	30.79 ± 2.3
			0.194	0.530	30.37 ± 1.9
Older Lava Series					
*P*25	hawaiite	1.175	0.687	0.873	19.01 ± 0.44
			0.474	0.884	19.25 ± 0.56
*P*28	basalt	1.085	0.570	0.983	23.15 ± 0.60
			0.389	1.021	24.05 ± 0.81
Younger Lava Series					
*P*18	nephelinite	1.340	0.251	0.296	5.68 ± 0.28
			0.181	0.288	5.52 ± 0.37
*P*20	basanite	1.875	0.377	0.258	3.54 ± 0.12
			0.251	0.254	3.48 ± 0.17
Phonolites					
*P*5	phonolite	4.270	0.447	0.903	5.43 ± 0.16
			0.346	0.863	5.22 ± 0.19
*P*11	phonolite	5.120	0.459	1.113	5.60 ± 0.16
			0.310	1.067	5.37 ± 0.22
Tristanite-trachyphonolite suite					
*P*12	tristanite	3.535	0.430	0.672	4.88 ± 0.15
			0.411	0.675	4.91 ± 0.16
*P*16	trachyphonolite	4.020	0.153	1.057	6.96 ± 0.55
			0.108	1.049	6.91 ± 0.80

λ_e: 0.581×10^{-10} y^{-1}. λ_β: 4.962×10^{-10} y^{-1}. $^{40}Ar^*$: Radiogenic ^{40}Ar. $^{40}Ar_T$: Total ^{40}Ar

ples. Accuracy and precision are believed to be better than ±1% for both Rb and Sr in concentrations higher than 40 ppm. Four U.S.G.S. standards were analysed at the same time as the Principe samples and the results, together with isotope dilution determinations for comparision (from Pankhurst and O'Nions, 1973), are given below.

	ppm Rb (XRF)	Rb (ID)	ppm Sr (XRF)	Sr (ID)
BCR-1	47.5	47.3	332.5	332.1
AGV-1	66.7	67.1	663.3	662.0
GSP-1	255.5	254.7	231.5	233.1
G-2	168.1	169.3	474.8	476.3

The whole-rock Rb–Sr isotopic data are presented in Table 2. Initial ratios have been calculated using ages of 21 Ma for the OLS and 6 Ma for the YLS and evolved samples. Varying these ages within the range of the K–Ar data makes a significant difference only in the case of sample P16. The use of the measured age for this sample (6.93 Ma) gives an unreasonably low initial ratio (0.70143).

Interpretation

The transitional basalt-hawaiite Older Lava Series shows a positive correlation of measured $^{87}Sr/^{86}Sr$ ratios versus Rb/Sr (Fig. 2). These samples range in $^{87}Sr/^{86}Sr$ from 0.70302 to 0.70373 and regression calculations give an 'age' of 244 ± 43 Ma with an intercept of 0.70293 ± 14 (Pearson correlation coefficient = 0.86). This age is in gross excess of the eruption age (~21 Ma). With the exception of sample *P*18 the YLS basanites and nephelinites have a range in measured $^{87}Sr/^{86}Sr$ of 0.70279 to 0.70300 thus occupying a distinct part of the $^{87}Sr/^{86}Sr$ field from the OLS and do not show any pre-eruption correlations. The YLS do however plot on a true isochron along with the phonolite flows and plugs. This isochron gives an age of 5.9 ± 0.3 Ma with an initial ratio of 0.70295 ± 6 (Pearson correlation coefficient = 0.98) and supports the conclusion, based on geochemical

Table 2. Rb, Sr and $^{87}Sr/^{86}Sr$ data from Principe

Sample no.	Rock type	*K*–Ar age (Ma)	Rb (ppm)	Sr (ppm)	$^{87}Sr/^{86}Sr$ ($\pm 2\sigma \times 10^5$)	$(^{87}Sr/^{86}Sr)_0$[a]
Lava from palagonite breccia						
*P*15	tholeiite	30.6	13.4	443	0.70344 ± 12 0.70348 ± 12	0.70342
Older Lava Series						
*P*3	hawaiite		13.3	712	0.70330 ± 12	0.70328
*P*6	hawaiite		17.5	936	0.70320 ± 12	0.70318
*P*8	hawaiite		23.1	792	0.70321 ± 8	0.70318
*P*21	hawaiite		20.3	596	0.70322 ± 9	0.70319
*P*25	hawaiite	19.1	29.2	871	0.70323 ± 8	0.70320
*P*26	hawaiite		27.9	919	0.70317 ± 6	0.70314
*P*27	hawaiite		24.8	896	0.70315 ± 8	0.70313
*P*28	basalt	23.6	27.8	567	0.70336 ± 10	0.70332
*P*29	hawaiite		45.4	772	0.70355 ± 11	0.70350
*P*31	basalt		37.5	620	0.70373 ± 12	0.70368
*P*32	basalt		29.2	553	0.70343 ± 8	0.70338
*P*33	hawaiite		36.2	943	0.70320 ± 6	0.70316
*P*50	basalt		5.7	708	0.70302 ± 8	0.70301
Younger Lava Series						
*P*17	basanite		29.6	762	0.70279 ± 9	0.70278
*P*18	nephelinite	5.60	38.8	1,295	0.70335 ± 8	0.70334
*P*19	basanite		41.2	1,158	0.70290 ± 10	0.70289
*P*20	basanite	3.51	40.4	1,180	0.70294 ± 10 0.70294 ± 10	0.70293
*P*34	nephelinite		59.5	844	0.70297 ± 8	0.70296
*P*45	basanite		19.5	676	0.70290 ± 9	0.70289
*P*51	basanite		23.0	660	0.70299 ± 12 0.70298 ± 5 0.70302 ± 6	0.70299
Phonolites						
*P*2	phonolite		243	39.6	0.70433 ± 6	0.70282
*P*5	phonolite	5.32	392	84.5	0.70411 ± 11	0.70296
*P*11	phonolite	5.48	133	955	0.70310 ± 5	0.70307
*P*22	phonolite		177	1,230	0.70298 ± 6	0.70294
*P*35	phonolite		296	295	0.70310 ± 12 0.70307 ± 7	0.70283
*P*38	phonolite		192	1,205	0.70311 ± 7	0.70307
*P*39	phonolite		272	78.8	0.70391 ± 3	0.70306
*P*40	phonolite		218	236	0.70322 ± 6	0.70299
Tristanite-trachyphonolite suite						
*P*12	tristanite	4.89	181	1,117	0.70334 ± 10 0.70325 ± 4	0.70326
*P*13	tristanite		187	1,192	0.70302 ± 7 0.70297 ± 7	0.70295
*P*16	trachyphonolite	6.93	315	9.37[b]	0.71102 ± 30 0.71099 ± 10	0.70271
*P*41	trachyte		175	481	0.70311 ± 8	0.70302

[a] Initial $^{87}Sr/^{86}Sr$ ratio calculated assuming the following ages: palagonite breccia, 31 Ma; OLS, 21 Ma; YLS and evolved samples, 6 Ma

[b] Determined by isotope dilution (XRF gave 8.6 ppm)

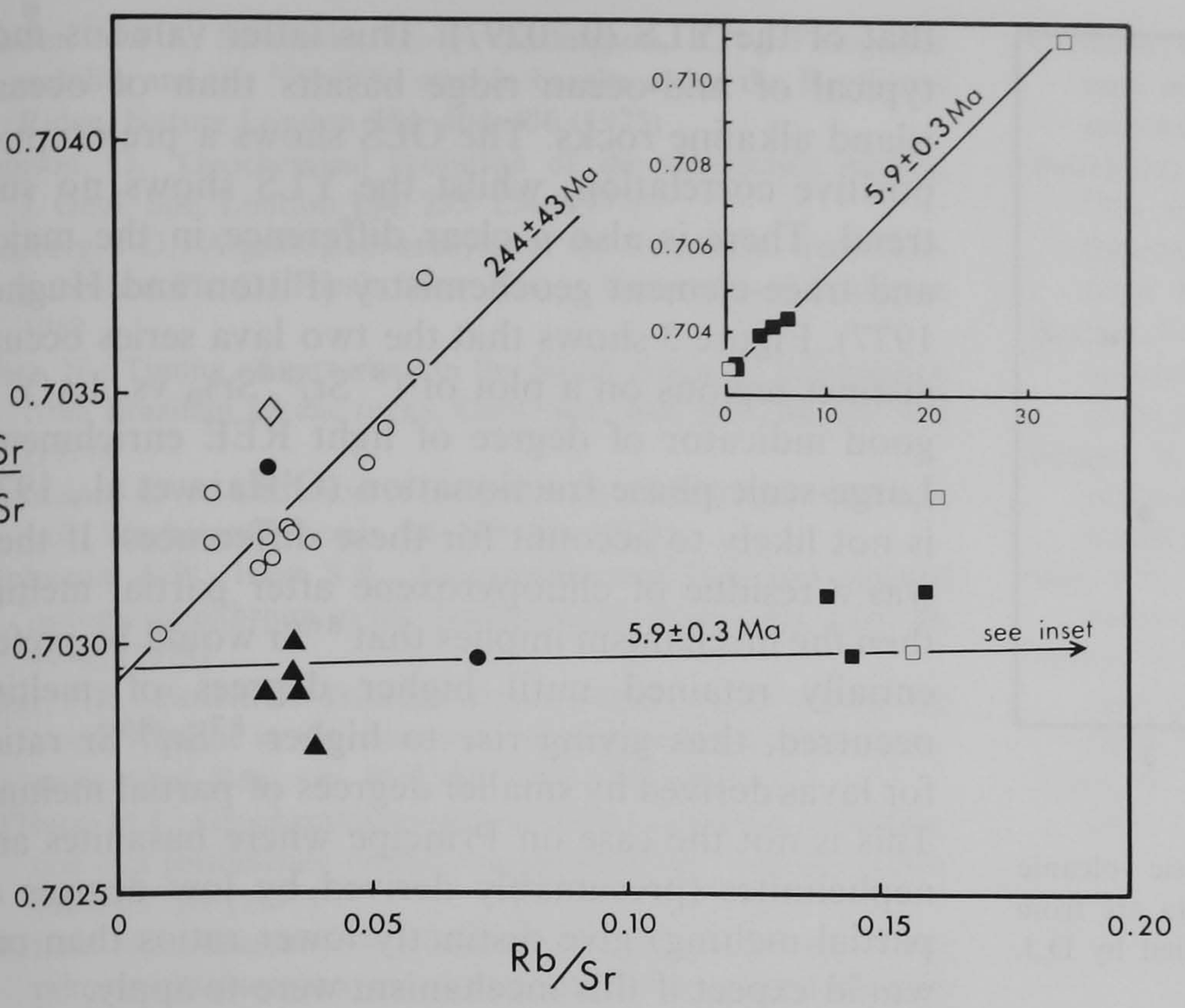


Fig. 2. Rb – Sr whole-rock isochron diagram for the volcanic rocks of Principe. ◇ Olivine tholeiite from palagonite breccia. ○ Older Lava Series (transitional basalts and hawaiites). ▲ Younger Lava Series basanites. ● Younger Lava Series nephelinites. ■ Phonolites. □ Tristanite-trachyphonolite suite. The 5.9 Ma isochron has been calculated using the YLS (excluding sample *P*18) and phonolite data; the tristanite-trachyphonolite suite samples were not included in the regression calculation. The 244 Ma isochron is derived from the OLS data only

evidence, that the YLS magmas were parental to the phonolites.

Samples from the tristanite-trachyphonolite suite plot close to the YLS-phonolite isochron and its extrapolation (Fig. 2) although data from these samples were not included in the regression. This suite, therefore, appears to be in isotopic equilibrium with the phonolites. The samples were excluded from the regression because geochemical data (Fitton and Hughes, 1977) shows that the tristanite-trachyphonolite suite cannot lie on the same liquid line of descent as the phonolites but may have evolved from the OLS magma. However, the similarity in K – Ar ages and the apparent isotopic equilibrium shown by the two suites of evolved rocks suggests that they had a common parent. It now seems likely that *both* suites evolved from the YLS magma, possibly under different *P-T* conditions. Alternatively, the tristanite-trachyphonolite suite could have evolved from a basic magma, not represented by the samples collected, which had a common mantle source with the YLS.

Discussion

That the correlation of $^{87}Sr/^{86}Sr$ with Rb/Sr of the OLS and the difference in Sr isotopic ratios between the two lava series are a function of processes operating in the source region is indicated by several considerations. Firstly, no visible signs of hydrothermal alteration or secondary minerals are apparent in thin section and there is no correlation of $^{87}Sr/^{86}Sr$ with iron oxidation ratio to suggest possible ground-water or sea-water effects. Secondly, the fact that the Pb isotope regression line for oceanic basalts (Sun and Hanson, 1975) is distinctly different from the regression line for oceanic sediment and sea-water argues against the involvement of sea-water in the evolution of oceanic island magmas, as suggested by O'Hara (1977). Thirdly, these variations are unlikely to be due to linear isotopic fractionation since all such isotopic fractionation is corrected for by normalizing to a standard $^{88}Sr/^{86}Sr$ value. Any non-linear fractionation of heavy isotopes such as strontium (where the mass difference is very slight) which may occur will be insignificant. Fourthly, there is no observed correlation between $^{87}Sr/^{86}Sr$ and 1/Sr in the Principe samples, thereby ruling out contamination by material with substantially higher or lower ratios than the lavas. Finally the incompatible behaviour of Sr in the OLS magmas (Fitton and Hughes, 1977; Fig. 5) suggests that the variation in Rb/Sr is due to differences in the mantle source rather than to plagioclase fractionation.

Many instances of pseudoisochrons, mantle isochrons, positive correlations, and erupted isochrons have been cited by other workers (e.g., Brooks et al., 1976; Carter and Norry, 1976; Faure, 1977; Dosso and Vidal, 1978; White et al., 1978). Of the two likely processes postulated as operating in the source region, namely disequilibrium partial melting of a homogeneous mantle (O'Nions and Pankhurst, 1974; Flower et al., 1975; O'Hara et al., 1975) and equilibrium partial melting of a vertically or horizontally heterogeneous mantle (Brooks et al., 1976; Hanson, 1977; Hofmann and Hart, 1978) likely to give rise to these observed patterns, the latter is generally favoured. Hofmann (1975) has shown that at mantle tempera-

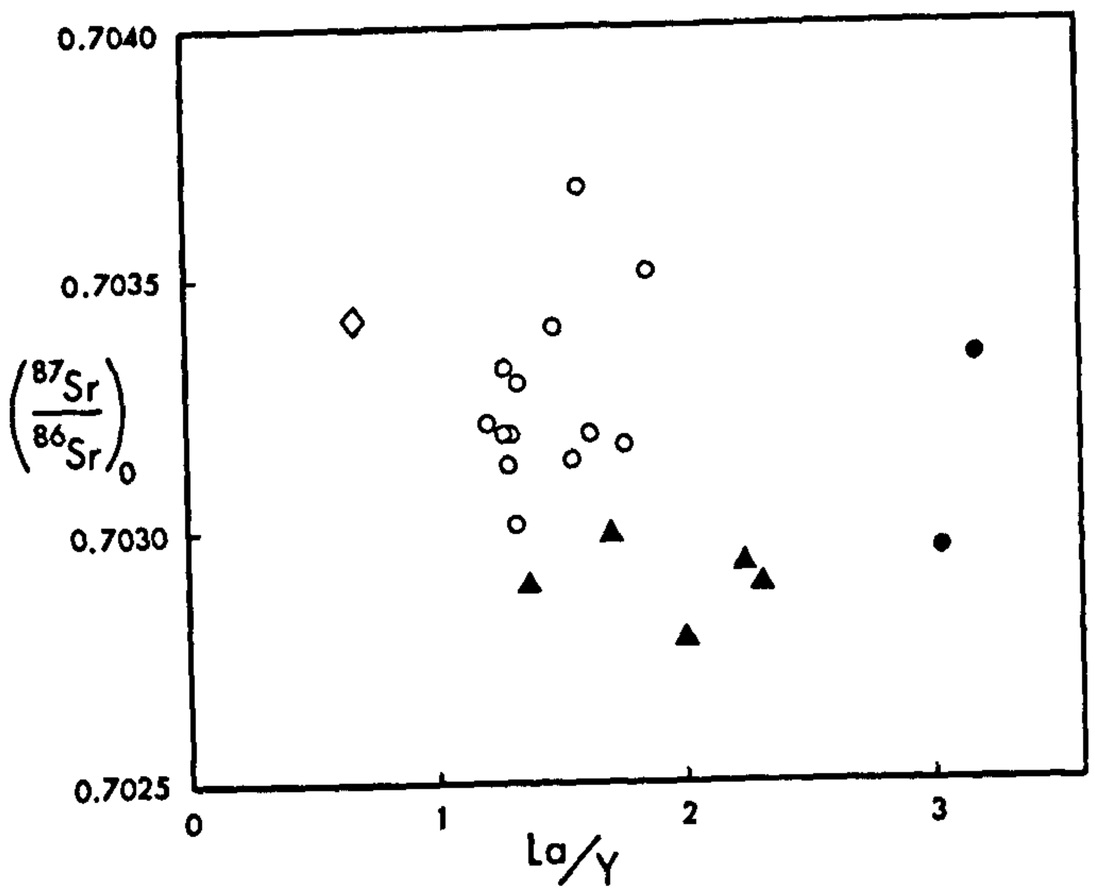


Fig. 3. Initial $^{87}Sr/^{86}Sr$ plotted against La/Y for the basic volcanic rocks of Principe. Symbols as in Fig. 2. La and Y data are from Fitton and Hughes (1977) with additional data supplied by D.J. Hughes

tures diffusion rates are sufficiently rapid for it to be unlikely that minerals will retain isotopically separate identities for long periods of time as would be required for disequilibrium partial melting to be effective. The OLS correlation is therefore considered primary.

If the $^{87}Sr/^{86}Sr$ vs. Rb/Sr correlation shown by the OLS samples has any age significance then this age of ~240 Ma must reflect some event occurring at about that time which caused large-scale heterogeneity in the mantle source rocks. The period from 200 to 100 Ma was one of intense magmatic activity in southern and western Africa and eastern South and North America. The Karoo (Cox, 1972), Kaoko (Siedner and Mitchell, 1976), and Parana Basin (Herz, 1977; Siedner and Mitchell, 1976) volcanics and intrusives all belong to this period. In West Africa an extensive suite of post-Visean, pre-Jurassic tholeiitic dolerite sills and dykes (Black and Girod, 1970) may have been emplaced during this period. The Triassic dolerite intrusives of eastern North America give K–Ar ages clustering around 200 Ma but with a group of ages from 220 to 244 Ma (Armstrong and Besancon, 1970). This magmatic activity accompanied the break-up of Gondwanaland (Cox, 1972) and the initiation of Atlantic sea-floor spreading (May, 1971) and may well have left its mark on large areas of the sub-African mantle. We suggest that the apparent isochron shown by the OLS rocks is an expression of this important magmatic event.

Several lines of evidence suggest that the differences between the OLS and YLS lavas indicate a vertically heterogeneous mantle. The mean $(^{87}Sr/^{86}Sr)_0$ of the OLS (0.70326) is quite distinct from that of the YLS (0.70297). This latter value is more typical of mid-ocean ridge basalts than of oceanic island alkaline rocks. The OLS shows a pre-eruption positive correlation, whilst the YLS shows no such trend. There is also a clear difference in the major- and trace-element geochemistry (Fitton and Hughes, 1977). Figure 3 shows that the two lava series occupy distinct regions on a plot of $(^{87}Sr/^{86}Sr)_0$ vs. La/Y (a good indicator of degree of light REE enrichment). Large-scale phase fractionation (O'Hara et al., 1975) is not likely to account for these differences. If there was a residue of clinopyroxene after partial melting then the mechanism implies that ^{86}Sr would be preferentially retained until higher degrees of melting occurred, thus giving rise to higher $^{87}Sr/^{86}Sr$ ratios for lavas derived by smaller degrees of partial melting. This is not the case on Principe where basanites and nephelinites (presumably derived by low degrees of partial melting) give distinctly lower ratios than one would expect if this mechanism were to apply.

Acknowledgements. The samples used in this study were collected by one of the authors (J.G.F.) and Dr. D.J. Hughes as part of a research programme on the Cameroun Line volcanoes, funded by a grant from the U.K. Natural Environment Research Council. We are indebted to Senhor Leopoldo do Vale, Chief Engineer on the island of São Tomé, for his assistance with the organisation of the field work on Principe. The Isotope Geology Unit at S.U.R.R.C. is also supported by N.E.R.C. and the analytical work was carried out during the tenure of an N.E.R.C. Research Studentship (H.M.D.). The assistance of J. Hutchinson and T. McMenamin is gratefully acknowledged.

References

Armstrong, R.L., Besancon, J.: A Triassic time scale dilemma: K–Ar dating of Upper Triassic mafic igneous rocks, eastern U.S.A. and Canada, and post-Upper Triassic plutons, western Idaho, U.S.A. Eclogae Geol. Helv. **63**, 15–28 (1970)

Black, R., Girod, M.: Late Palaeozoic to Recent igneous activity in West Africa and its relation to basement structure. In: African Magmatism and Tectonics (T.N. Clifford, I.G. Gass, eds.), pp. 185–210. Edinburgh: Oliver and Boyd 1970

Brooks, C., Hart, S.R., Hofmann, A., James, D.E.: Rb–Sr mantle isochrons from oceanic regions. Earth Planet. Sci. Lett. **32**, 51–61 (1976)

Carter, S.R., Norry, M.J.: Genetic implications of Sr isotopic data from the Aden volcano, South Arabia. Earth Planet. Sci. Lett. **31**, 161–166 (1976)

Cox, K.G.: The Karroo volcanic cycle. J. Geol. Soc. London **128**, 311–336 (1972)

Dosso, L., Vidal, P.: The isotopic geochemistry of Pb and Sr of rocks from the Kerguelen Islands. U.S. Geol. Surv. Open File Report **78–701**, 96–98 (1978)

Faure, G.: Principles of Isotope Geology. 464 pp. New York: Wiley 1977

Fitton, J.G., Hughes, D.J.: Petrochemistry of the volcanic rocks of the island of Principe, Gulf of Guinea. Contrib. Mineral. Petrol. **64**, 257–272 (1977)

Flower, M.F.J., Schminke, H.-U., Thompson, R.N.: Phlogopite stability and the $^{87}Sr/^{86}Sr$ step in basalts along the Reykjanes Ridge, Nature London **254**, 404–406 (1975)

Hanson, G.: Geochemical evolution of the suboceanic mantle. J. Geol. Soc. London **134**, 235–254 (1977)

Hedberg, J.D.: A geological analysis of the Cameroun trend. Unpublished Ph. D. Thesis. New Jersey: University of Princeton 1968

Herz, N.: Timing of spreading in the South Atlantic: Information from Brazilian alkalic rocks, Geol. Soc. Am. Bull. **88**, 101–112 (1977)

Hofmann, A.W.: Diffusion of Ca and Sr in a basalt melt. Carnegie Inst. Washington Yearb. **74**, 183–189 (1975)

Hofmann, A.W., Hart, S.R.: An assessment of local and regional isotopic equilibrium in the mantle. Earth Planet. Sci. Lett. **38**, 44–62 (1978)

May, P.R.: Pattern of Triassic-Jurassic diabase dykes around the North Atlantic in the context of predrift position of the continents. Geol. Soc. Am. Bull. **82**, 1285–1292 (1971)

O'Hara, M.J.: Geochemical evolution during fractional crystallisation of a periodically refilled magma chamber. Nature London **266**, 503–507 (1977)

O'Hara, M.J., Saunders, M.J., Mercy, E.L.P.: Garnet-peridotite, primary ultrabasic magma and eclogite: interpretation of upper mantle processes in kimberlite. Phys. Chem. Earth. **9**, 571–604 (1975)

O'Nions, R.K., Pankhurst, R.J.: Petrogenetic significance of isotope and trace element variations in volcanic rocks from the mid-Atlantic. J. Petrol. **15**, 603–634 (1974)

Pankhurst, R.J., O'Nions, R.K.: Determination of Rb/Sr and $^{87}Sr/^{86}Sr$ ratios of some standard rocks and evaluation of X-ray fluorescence spectrometry in Rb–Sr geochemistry. Chem. Geol. **12**, 127–136 (1973)

Siedner, G., Mitchell, J.G.: Episodic Mesozoic volcanism of Namibia and Brazil: A K–Ar isochron study bearing on the opening of the south Atlantic. Earth Planet. Sci. Lett. **30**, 292–302 (1976)

Steiger, R.H., Jäger, E.: Subcommission on geochronology: convention on use of decay constants in geochronology and cosmochronology. Earth Planet. Sci. Lett. **36**, 359–362 (1977)

Sun, S.S., Hanson, G.: Evolution of the mantle: geochemical evidence from alkali basalt. Geology **3**, 297–302 (1975)

White, W.M., Hofmann, A.W., Bow, C.S.: Isotope and LIL element geochemistry of the Galapagos Islands. U.S. Geol. Surv. Open File Report **78–701**, 449–451 (1978)

York, D.: Least squares fitting of a straight line with correlated errors. Earth Planet. Sci. Lett. **5**, 320–324 (1969)

Received May 30, 1979; Accepted September 17, 1979

ABBREVIATIONS

Å	Ångström unit
B.V.S.P.	Basaltic Volcanism Study Project (1981)
cpx	clinopyroxene
D.I.	Thornton and Tuttle (1960) Differentiation Index
$^{40}Ar^{*}$	radiogenic ^{40}Ar
$^{40}Ar^{t}$	total ^{40}Ar
Ga	10^{9} years
HREE	heavy rare-earth elements
hy	normative hypersthene in wt.%
Kd	partition coefficient
LILE	large-ion lithophile element
LREE	light rare-earth elements
Ma	10^{6} years
Mg number	$100Mg/(Mg+Fe^{++})$
E-MORB	enriched mid-ocean ridge basalt
N-MORB	normal mid-ocean ridge basalt
M.S.W.D.	mean square of weighted deviates
ne	normative nepheline in wt.%
ol	olivine
O.L.S.	Principe Older Lava Series
'q'	wt.% SiO_2 equivalent to normative hypersthene
opx	orthopyroxene
REE	rare-earth elements
r-r-r	rift - rift - rift triple junction
$sccg^{-1}$	standard cm^3 per gram
$(87Sr/86Sr)_0$	initial strontium isotopic composition
σ	1 standard deviation
S.U.R.R.C.	Scottish Universities Research and Reactor Centre
$\bar{x}$	mean
XRF	X-ray fluorescence
Y.L.S.	Principe Younger Lava Series
λ	decay constant

REFERENCES

ADIGHIJE, C. 1979. Gravity field of the Benue trough, Nigeria. Nature 282, 199-201.

AJAKAIYE, D.E. & BURKE, K. 1973. A bouguer gravity map of Nigeria. Tectonophysics 16, 103-115.

ALIBERT, C., MICHARD-VITRAC, A. & ALBAREDE, F. 1981. Sr,Nd, isotope and REE geochemistry of European melilitites: inferences for a LIL element depleted sub-continental mantle. E.O.S., Trans. Am. Geophys. Union 62, 1078.

ALLEGRE, C.J. 1982. Chemical geodynamics. Tectonophysics 81, 109-132.

_____ & BOTTINGA, Y. 1977. The rising deep crust: an alternative to the hotspot model. E.O.S., Trans. Am. Geophys. Union 58, 535-536.

_____, DUPRE, B., LAMBRET, B. & RICHARD, P. 1981. Subcontinental versus suboceanic debate, I. Lead-neodymium-strontium isotopes in primary alkali basalts from a shield area: the Ahaggar volcanic suite. Earth Planet. Sci. Lett. 52, 85-92.

_____, _____, RICHARD, P., ROUSSEAU, D. & BROOKS, C. 1982. Subcontinental versus suboceanic mantle, II. Nd-Sr-Pb isotopic comparison of continental tholeiites with mid-ocean ridge tholeiites, and the structure of the continental lithosphere. Earth Planet. Sci. Lett. 57, 25-34.

ANDERSON, D.L. 1975. Chemical plumes in the mantle. Geol. Soc. Am. Bull. 86, 1593-1600.

_____ 1981. Hotspots, basalts and the evolution of the mantle. Science 213, 82-89.

_____ 1982. Isotopic evolution of the mantle: the role of magma mixing. Earth Planet. Sci. Lett. 57, 1-12.

AOKI, K. 1975. Origin of phlogopite and potassic richterite bearing peridotite xenoliths from S.Africa. Contrib. Mineral. Petrol. 53, 145-156.

ARMSTRONG, R.L. & BESANCON, J. 1970. A Triassic time scale dilemma: K-Ar dating of Upper Triassic mafic igneous rocks, eastern U.S.A. and Canada, and post Upper Triassic plutons, western Idaho, U.S.A. Eclogae Geol. Helv. 63, 15-28.

_____, LEEMAN, W.P. & MALDE, H.E. 1975. K-Ar dating, Quaternary and Neogene volcanic rocks of Snake River Plain, Idaho. Am. J. Sci. 275, 225-251.

ARNDT, N.T. 1977. The separation of magmas from partially molten peridotite. Carnegie Inst. Washington Yearb. 76, 424-428.

ASSUNCAO, C.F.T. 1956. Lavas feldspatoidicas de São Tomé. 6th. sess. Conf. Intern. Africa Occid. 2, 11-17. Lisbon.

_____ 1957. Algunas aspectos de petrografia da Ilha de São Tomé. Garcia de Orta 5, 497-515.

BAILEY, D.K. 1974. Continental rifting and alkaline magmatism. In Sørensen, H. (ed.): The Alkaline Rocks. J. Wiley & Sons, New York, 148-159.

_____ 1974a. Nephelinites and ijolites. Ibid, 53-66.

_____ 1977. Lithosphere control of continental fift magmatism. J.Geol. Soc. London 133, 103-106.

BAKER, M.C.W. & FRANCIS, P.W. 1978. Upper Cenozoic volcanism in the central Andes - ages and volumes. Earth Planet.Sci.Lett. 41, 175-187.

BAKSI, A.K. 1973. K-Ar dating- loading techniques in argon extraction work and sources of air argon contamination. Can. J. Earth Sci. 10, 1678-1684.

BARBIERI, M., PENTA, A. & TURI, B. 1975. Oxygen and Sr isotope ratios in some ejecta from Alban Hills volcanic area, Roman comagmatic region. Contrib. Mineral. Petrol. 51, 127-133.

BARROS, L.A. 1960. A ilha do Principe e a "Linha dos Camaroes". Mem. Junta. Investig. do Ultramar no.17, Lisbon.

BARTON, M. & HAMILTON, D.L. 1982. Water-undersaturated melting experiments bearing on the origin of potassium-rich magmas. Mineral. Mag. 45, 267-278.

BASALTIC VOLCANISM STUDY PROJECT (B.V.S.P.), 1981. Basaltic Volcanism on the Terrestrial Planets. Pergamon Press Inc. New York, 1286pp.

BASU, A.R. 1978. Trace elements and Sr-isotopes in some mantle derived hydrous minerals and their significance. Geochim.Cosmochim.Acta. 42, 659-668.

_____ & TATSUMOTO, M. 1980. Nd-isotopes in selected mantle derived rocks and minerals and their implications for mantle evolution. Contrib. Mineral. Petrol. 75, 43-54.

BECKINSALE, R.D. & GALE, N.H. 1969. A reappraisal of the decay constants and branching ratio of ^{40}K. Earth Planet. Sci. Lett. 6, 289-294.

_____, PANKHURST, R.J., SKELHORN, R.R. & WALSH, J.N. 1978. Geochemistry and petrogenesis of the early Tertiary lava pile of the isle of Mull, Scotland. Contrib. Mineral. Petrol. 66, 415-428.

BELL, K. & POWELL, J.L. 1969. Sr isotope studies of alkalic rocks: the potassium-rich lavas of the Birunga and Toro-Ankole regions, E. and central equatorial Africa. J. Petrol. 10, 536-572.

_____, & _____ 1970. Sr isotope studies of alkalic rocks: the alkalic complexes of E. Uganda. Geol. Soc. Am. Bull. 81, 3481

_____, BLENKINSOP, J., COLE, T.J.S. & MENAGH, D.P. 1982. Evidence from Sr isotopes for long-lived heterogeneities in the upper mantle. Nature 298, 251-253.

BESWICK, A.E. 1976. K and Rb relations in basalts and other mantle derived minerals : is phlogopite the key? Geochim. Cosmochim. Acta 40, 1167-1183.

_____ 1978. Author's reply to critical comments of Menzies. Ibid 42, 149.

_____ & CARMICHAEL, I.S.E. 1977. Nd isotope variations in basic magmas: a disequilibrium melting model. Geol. Soc. Am. Abstacts 9, 896.

_____ & _____ 1978. Constraints on mantle source compositions imposed by phosphorus and the rare-earth elements. Contrib. Mineral. Petrol. 67, 317-330.

BLACK, R. & GIROD, M. 1970. Late Palaeozoic to Recent igneous activity in West Africa and its relationship to basement structure. In Clifford, T.N. & Gass, I.G.(eds.): African Magmatism and Tectonics. Oliver & Boyd, Edinburgh, 185-210.

BLUNDELL, D.J. 1976. Active faults in West Africa. Earth Planet. Sci. Lett. 31, 287-290.

BOCTOR, N.Z. & BOYD, F.R. 1982. Petrology of kimberlite from the De Bruyn and Martin mine Bellsbank, South Africa. Am. Mineral. 67, 917-925.

BOESE, W. 1912. Petrographische untersuchungen an jungvulkanischen ergussgesteine von São Thomé und Fernando Poo. Neues Jahrb. Geologie u. Palaontologie Abh., B.B. 34, 255-320.

BOETTCHER, A.L. & O'NEIL, J.R. 1980. Stable isotope, chemical and petrographic studies of high pressure amphiboles and micas: evidence for metasomatism in the mantle source regions of alkali basalts and kimberlites. Am. J. Sci. 280A, 594-621.

_____, MYSEN, B.O. & MODRESKI, P.J. 1975. Melting in the mantle: phase relationships in natural and synthetic peridotite - H_2O and peridotite-H_2O-CO_2 with application to kimberlites. Phys. Chem. Earth. 9, 855-867.

_____, O'NEIL, J.R., WINDOM,K.E., STEWART,D.G. & WILSHIRE, H.G. 1979. Metasomatism of the upper mantle and the genesis of kimberlites and alkali basalts. In Boyd,F.R. & Meyer,H.O.(eds.): Mantle Sample: Inclusions in Kimberlites and other volcanics. Am. Geophys. Union. 173

BORLEY, G.D. 1967. Potassium rich volcanic rocks from southern Spain. Mineral. Mag. 36, 364-379.

BOWEN, N.L. 1928. The Evolution of the Igneous Rocks. Princeton Univ. Press, Princeton New Jersey. 332pp.

BREY, G. & GREEN, D.H. 1977. Systematic study of liquidus phase relations in olivine melilitite + H_2O + CO_2 at high pressures and petrogenesis of an olivine tholeiite magma. Contrib. Mineral. Petrol. 61, 141-162.

BRIDEN, J.C. & GASS, I.G. 1974. Plate movement and continental magmatism. Nature 248, 650-653.

BROOKS, C. & HART, S.R. 1978. Rb-Sr mantle isochrons and variations in the chemistry of Gondwanaland's lithosphere. Nature 271, 220-223.

_____, _____, HOFMANN,A. & JAMES, D.E. 1976a. Rb-Sr mantle isochrons from oceanic regions. Earth Planet. Sci. Lett. 32, 51-61.

_____, JAMES, D.E. & HART, S.R. 1976b. Ancient lithosphere: its role in young continental volcanism. Science 193, 1086-1094.

_____, _____, _____ & HOFMANN, A. 1976c. Rb-Sr mantle isochrons. Carnegie Inst. Washington Yearb. 75, 176-207.

BURKE, K. 1969. Seismic areas of the Guinea coast where Atlantic fracture zones reach Africa. Nature 222, 655-657.

_____ & WILSON, J.T. 1972. Is the African plate stationary? Nature 239, 387-390.

_____ &_____ 1976. Hotspots on the earth's surface. Sci. Am. 235, 46-57.

_____, DESSAUVAGIE, T.F.J. & WHITEMAN, A.J. 1971. Opening of the Gulf of Guinea and geological history of the Benue depression and Niger Delta. Nature Phys. Sci. 233, 51-55.

_____, _____ & _____ 1972. Geological history of the Benue valley and adjacent areas. In Dessauvagie, T.F.J. & Whiteman, A.J.(eds.) : African Geology. Ibaden, 187-205.

BURKE, W.H., OTTO, J.B. & DENISON, R.E. 1969. Potassium-argon dating of basaltic rocks. J. Geophys. Res. 74, 1082-1086.

CALVEZ, J-Y. & LIPPOLT,H.J. 1980. Strontium isotope constraints to the Rhine graben volcanism. Neues Jahrb. Miner. Abh. 139, 59-81.

CAMPBELL, I.H. & GORTON, M.P. 1980. Accessory phases and the generation of LREE enriched basalts- a test for disequilibrium melting. Contrib. Mineral. Petrol. 72, 157-163.

CANTAGREL, J-M. JAMOND, C. & LASSERRE, M. 1978. Le magmatisme alcalin de la ligne du Cameroun au Tertiare inférieur: données géochronologiques K/Ar. C.R.Somm. Soc. Geol. Fr. 6, 300-303.

CARLSON, R.W., MACDOUGALL, J.D. & LUGMAIR, G.W. 1978. Differential Sm/Nd evolution in oceanic basalts. Geophys. Res. Lett. 5, 229-232.

_____, LUGMAIR, G.W., MACDOUGALL, J.D. 1981. Columbia River volcanism: the question of mantle heterogeneity or crustal contamination. Geochim. Cosmochim. Acta 45, 2483-2499.

CARMICHAEL, I.S.E., TURNER, F.J. & VERHOOGEN, J. 1974. Igneous Petrology. McGraw-Hill, New York, 739pp.

CARSWELL, D.A. 1975. Primary and secondary phlogopites and clinopyroxenes in garnet lherzolite xenoliths. Phys. Chem. Earth 9, 417-429.

CARTER, J.D., BARBER, W. & TAIT, E.A. 1963. The geology of parts of Adamawa, Bauchi, and Bornu provinces in N.E.Nigeria. Bull. Geol. Surv. Nigeria 30.

CARTER, S.R. & NORRY, M.J. 1976. Genetic implications of Sr isotope data from Aden volcano, S.Arabia. Earth Planet. Sci. Lett. 31, 161-166.

_____, EVENSEN, N.M., HAMILTON,P.J. & O'NIONS, R.K. 1978. Continental volcanics derived from enriched and depleted source regions : Nd and Sr isotope evidence. Earth Planet. Sci. Lett. 37, 401-408.

_____, _____, _____ & _____ 1978a. Neodymium and strontium isotope evidence for crustal contamination of continental volcanics. Science 202, 743-747.

_____, _____, _____ & _____ 1979. Basalt magma sources during the opening of the N.Atlantic. Nature 281, 28-30.

CATANZARO, E.J., MURPHY, T.J., GARNER, E.L. & SHIELDS, W.R. 1969. Absolute abundance ratio and atomic weight of terrestrial rubidium. J. Res. Nat. Bur. Std. Phys. and Chem. 73A, 511-516.

CHAPMAN, N.A. 1976. Inclusions and megacrysts from undersaturated tuffs and basanites, East Fife Scotland. J. Petrol. 17, 472-498.

CHARLTON, S.R. & MUSSETT, A.E. 1973. Crucible contribution to atmospheric contamination in connection with K-Ar dating. Chem Geol. 11, 237-241.

CHASE, C.G. 1981. Ocean island Pb: two-stage histories and mantle evolution. Earth Planet. Sci. Lett. 52, 277-284.

CLAGUE, D.A. & FREY, F.A. 1982. Petrology and trace element geochemistry of the Honolulu volcanics, Oahu: implications for the oceanic mantle below Hawaii. J.Petrol. 23, 447-504.

CLIFFORD, T.N. 1967. The Damaran episode in the Upper - Proterozoic-Lower Palaeozoic structural history of southern Africa. Geol. Soc. Am. Special paper 92.

COHEN, R.S. & O'NIONS, R.K. 1982. Identification of recycled continental material in the mantle from Sr, Nd and Pb isotope investigations. Earth Planet. Sci. Lett. 61, 73-84.

CORNEN, G. & MAURY, R.C. 1980. Petrology of the volcanic island of Annobon, Gulf of Guinea. Marine Geol. 36, 253-267.

COX, K.G., HAWKESWORTH, C.J., O'NIONS, R.K. & APPLETON, J.D. 1976. Isotopic evidence for the derivation of some Roman region volcanics from anomalously enriched mantle. Contrib. Mineral. Petrol. 56, 173-180.

_____, BELL, J.D. & PANKHURST, R.J. 1979. The Interpretation of Igneous Rocks. George Allen & Unwin,London, 450pp.

CRATCHLEY, C.R. & JONES, G.P. 1965. An interpretation of the geology and gravity anomalies of the Benue valley, Nigeria. Overseas Geol. Surv. of U.K. Geophys. paper no.1, 26pp.

CUNDARI, A. & O'HARA, M.J. 1976. Experimental study of atmospheric and high pressures of a mafic leucitite from New South Wales, Austalia. Prog. Exp. Petrol. 3rd report, NERC,London p 260.

DALRYMPLE, G.B. & LANPHERE, M.A. 1969 Potassium-Argon Dating. W.H. Freeman and Co., San Francisco, 258pp.

_____, JARRARD, R.D. & CLAGUE, D.A. 1975. K-Ar ages of some volcanic rocks from the Cook and Astral islands. Geol. Soc. Am. Bull. 86, 1463.

_____, CLAGUE, D.A. & LANPHERE, M.A. 1977. Revised age for Midway volcano, Hawaiian volcanic chain. Earth Planet. Sci. Lett. 37, 107-116.

DALY, R.A. 1910. Origin of alkaline rocks. Geol. Soc. Am. Bull. 21, 87-118.

_____ 1925. The geology of Ascension island. Proc. Am. Acad. Arts Sci. 60, 1-80.

DASCH, E.J. 1969. Strontium isotopes in weathering profiles, deep sea sediments, and sedimentary rocks. Geochim. Cosmochim. Acta 33, 1521-1552.

_____, HEDGE, C.E. & DYMOND, J. 1973. Effect of seawater interaction on strontium isotope composition of deep sea basalts. Earth Planet. Sci. Lett. 19, 177-183.

DA SILVA, H.G. 1958. Nota sobra a microfaune du Miocenico marinho da ilha do Principe. Mem. Not. Publ. Mus. Lab. Miner. Geol. Univ. Coimbra 45, 56.

DAVIES, G.F. 1981. Earth's neodymium budget and structure and evolution of the mantle. Nature 290, 208-213.

DAVIS, D.W., GRAY, J., CUMMING, G.L. & BAADSGAARD, H. 1977. Determination of the ^{87}Rb decay constant. Geochim. Cosmochim. Acta 41, 1745-1749.

DAWSON, J.B., POWELL, D.G. & REID, A.M. 1970. Ultrabasic xenoliths and lavas from the Lashaine volcano, northern Tanzania. J. Petrol. 11, 519-548.

_____ & SMITH, J.V. 1975. Chemistry and origin of phlogopite megacrysts in kimberlites. Nature 253, 336-338.

_____ & _____ 1982. Upper - mantle amphiboles: a review. Mineral. mag. 45, 35-46.

DEPAOLO, D.J. 1978. Nd and Sr isotope systematics of young continental igneous rocks. U.S. Geol. Surv. Open - File Rep. 78-701, 91-93.

_____ 1979. Implications of correlated Nd and Sr isotopic variations for the evolution of the crust and mantle. Earth Planet. Sci. Lett. 43, 201-211.

_____ 1980. Crustal growth and mantle evolution: inferences from models of element transport and Nd and Sr isotopes. Geochim. Cosmochim. Acta 44, 1185-1196.

_____ 1981. Trace element and isotopic effects of combined wallrock assimilation and fractional crystallization. Earth Planet. Sci. Lett. 53, 189-202.

_____ & WASSERBURG, G.J. 1976a. Nd isotope variations and petrogenetic models. Geophys. Res. Lett. 3, 249-252.

_____ & _____ 1976b. Inferences about magma sources and mantle structure from variations of $^{143}Nd/^{144}Nd$. Ibid.3, 743-746.

_____ & _____ 1977. The sources of island arcs as indicated by Nd and Sr isotope studies. Ibid.4, 465-468.

_____ & _____ 1979. Petrogenetic mixing models and Nd-Sr isotopic patterns. Geochim. Cosmochim. Acta 43, 615-627.

DE SOUZA, H.A.F. 1974. Potassium-argon ages of Carboniferous igneous rocks from East Lothian and the south of Scotland. Univ. Leeds, MSc. thesis (unpubl.).

_____ 1979. The geochronology of Scottish Carboniferous volcanism. Univ. Edinburgh, PhD. thesis (unpubl.).

DESSAUVAGIE, T.F.J. 1975. A geological map of Nigeria. Scale 1:1000000. Nigeria Mining, Geological and Metallurgical Society.

DE SWARDT, A.M.J. 1954. The 1954 eruption of Cameroon Mountain. Records of the Geol. Surv. Nigeria, 1954, 35-40.

DICKINSON, D.R., DODSON, M.H., GASS, I.G. & REX, D.C. 1969. Correlation of initial $^{87}Sr/^{86}Sr$ with Rb/Sr in some late Tertiary volcanic rocks of South Arabia. Earth Planet. Sci. Lett. 6, 84-90.

DRESCH, J. 1952. Observations dans la région de Mokolo, Nord Cameroun. C.R. Soc. Géol. Fr., p88-90.

DUDA, A. & SCHMINKE, H-Ü. 1978. Quaternary basanites, melilite nephelinites and tephrites from the Laacher See area (Germany). Neues Jahrb. Miner. Abh. 132, 1-33.

DUMORT, J.C. 1967. Caractères chimiques de trois volcanismes du Cameroun. Bull. de B.R.G.M. 3, 22-75.

_____ & PERRONE, Y. 1966. Notice explicative de la feuille de Maroua. Dir. Mines Géol. Cam., no. 62, 49pp.

DUNCAN, R. A. & COMPSTON, W. 1976. Sr isotopic evidence for an old mantle source region for French Polynesian volcanism. Geology 4, 728.

DUNLOP, H.M. 1982. Geochimie isotopique des chromites, de leurs inclusions fluides et des roches mafique - ultramafiques associees du cortège ophiolitique D'Oman. Rapport d'activité 1981-1982, CNRS/CRSCM Orléans.

_____ & FITTON, J.G. 1979. A K-Ar and Sr- isotopic study of the volcanic rocks of the island of Principe, West Africa - evidence for mantle heterogeneity beneath the Gulf of Guinea. Contrib. Mineral. Petrol. 71,125-131.

_____ & _____ 1981. Strontium isotope and K-Ar studies of volcanic rocks of the Cameroon Line, West Africa. 11th Colloq. African Geol. abstsracts, Open Univ. Milton Keynes, U.K. p46.

DUPRE, B. & ALLEGRE, C.J. 1980. Pb-Sr-Nd isotopic correlations and the chemistry of the Norh Atlantic mantle. Nature 286, 17-22.

_____, LAMBRET, B. & ALLEGRE, C.J. 1982. Isotopic variations within a single oceanic island: the Terciera case. Nature 299, 620-622.

DU PREEZ, J.W. 1949. The geology and hydrology of Biu division. Geol. Surv. Nigeria. Unpubl. report no.751.

EDGAR, A.D., GREEN, D.H. & HIBBERSON, W.O. 1976. Experimental petrology of a highly potassic magma. J. Petrol. 17, 339-356.

EGGLER, D.H. 1976. Composition of the partial melt of carbonated peridotite in the system $CaO-MgO-SiO_2-CO_2$. Carnegie Inst. Washington Yearb. 75, 623-626.

_____ 1978. The effect of CO_2 upon partial melting of peridotite in the system $Na_2O-CaO-Al_2O_3-MgO-SiO_2-CO_2$ to 35Kb, with an analysis of melting in a peridotite-H_2O-CO_2 system. Am. J. Sci. 278, 305-343.

EGGLER, D.H. & HOLLOWAY, J.R. 1977. Partial melting of peridotite in the presence of H_2O and CO_2: principles and review. In Dick, H.J.B. (ed.): Proceedings of Chapman conference on partial melting in the upper mantle. Oregon Dept. Geology Mineral Industries Bull. 96, 15-36.

ENO, B.S.M. & OSSCH, N.H. 1974. Etude géologique de la région de Bamenda; premiers résultats petrographiques. Rapport Polycop. Dépt. Sci. Terre, Yaoundé,14pp.

ERLANK, A.J. & KABLE, E.J.D. 1976. The significance of incompatible elements in Mid-Atlantic ridge basalts from 45°N with particular reference to Zr/Nb. Contrib. Mineral. Petrol. 54, 281-291.

_____ & RICKARD, R.S. 1977. Abstract, 2nd Int. Conf. Kimberlites, Santa Fe.

ESCH, E. 1901. Der vulcan Etinde in Kamerun und seine Gesteine. Sitzung--sberichte der König. preuss. Akad. der Wissenschaften. 1, 277-299 & 400-417.

EWART, A. 1979. A review of the mineralogy and chemistry of Tertiary -Recent dacitic, latitic, rhyolitic and related salic volcanic rocks. In Barker,F. (ed.) : Trondhjemites, Dacites and Related rocks, Elsevier, Amsterdam, 13-21.

_____ 1981. The mineralogy and chemistry of the anorogenic Teriary silicic volcanics of S.E. Queensland and N.E. New South Wales, Australia. J. Geophys. Res. 86, 10242-10256.

_____ 1982. Petrogenesis of the Tertiary anorogenic volcanic series of Southern Queensland, Australia, in the light of trace element geochemistry and O,Sr and Pb isotopes. J. Petrol. 23, 344-382.

_____ & STIPP, J.J. 1968. Petrogenesis of the volcanic rocks of central North Island, New Zealand, as indicated by a study of $^{87}Sr/^{86}Sr$ ratios, and Sr,Rb,K,U,Th, abundances. Geochim. Cosmochim. Acta 32, 699-736.

FALCONER, J.D. 1911. The Geology and Geography of Northern Nigeria. MacMillan & Co. Ltd. London. 295pp.

FAURE, G. 1977. Principles of Isotope Geology. J. Wiley & Sons, New York, 464pp.

_____ & HURLEY, P.M. 1963. Isotopic composition of strontium in oceanic and continental basalts: application to the origin of igneous rocks. J. Petrol. 4, 31-50.

_____ & POWELL, J.L. 1972. Strontium Isotope Geology. Springer-Verlag New York, 188pp.

_____, CROCKET, J.H. & HURLEY, P.M. 1967. Some aspects of the geochem--istry of Sr and Ca in the Hudson Bay and the Great Lakes. Geochim. Cosmochim. Acta 31, 451-461.

FAURE, G., BOWMAN, J.R., ELLIOT, D.H. & JONES, L.M. 1974. Sr isotopic composition and petrogenesis of the Kirkpatrick basalt, Queen Alexandria range, Antarctica. Contrib. Mineral. Petrol.48, 153-169.

FERGUSON, A.K. & CUNDARI, A. 1975. Petrological aspects and evolution of the leucite bearing lavas from Bufumbira, southwest Uganda. Contrib. Mineral. Petrol. 50, 25-46.

FISHER, D.E. 1971. Excess rare gases in a subaerial basalt from Nigeria. Nature Phys. Sci. 232, 60-61.

FITCH, F.J., MILLER, J.A. & HOOKER, P.J. 1976. Single whole-rock K-Ar isochrons. Geol. Mag. 113, 1-10.

FITTON, J.G. 1980. The Benue trough and Cameroon line - a migrating rift system in West Africa. Earth Planet. Sci. Lett. 51, 132-138.

_____ 1983. Active versus passive continental rifting: evidence from the West African rift system. Tectonophysics, in press.

_____ & HUGHES, D.J. 1977. Petrochemistry of the volcanic rocks of the island of Principe, Gulf of Guinea. Contrib. Mineral. Petrol. 64, 257-272.

_____ & _____ 1981. Strontian melilite in a nephelinite lava from Etinde,Cameroon. Mineral. Mag. 44, 261-264.

FLOWER, M.J. 1971. Evidence for role of phlogopite in genesis of alkali basalt. Contrib. Mineral. Petrol. 32, 126-137.

_____, SCHMINKE, H-U. & THOMPSON, R.N. 1975. Phlogopite stability and the $^{87}Sr/^{86}Sr$ step in basalts along the Reykjanes Ridge. Nature 254, 404.

FRANCIS, P.W., THORPE, R.S.,MOORBATH, S., KRETZSCHMAR, G.A. & HAMMILL, M. 1980. Strontium isotope evidence for crustal contamination of calc-alkaline volcanic rocks from Cerro Galan, Northwest Argentina. Earth Planet. Sci. Lett. 48, 257-267.

FREETH, S. 1978a. Tectonic activity in West Africa and Gulf of Guinea since Jurassic Times: an explanation based on membrane tectonics. Earth Planet. Sci. Lett. 38, 298-300.

_____ 1978b. A model for tectonic activity in West Africa and the Gulf of Guinea during the last 90Ma based on membrane tectonics. Geol. Rundsch. 67, 675-688.

_____ 1979. Deformation of the African plate as a consequence of membrane stress domains generated by Post-Jurassic drift. Earth Planet. Sci. Lett. 45, 93-104.

FREY, F.A. & GREEN, D.H. 1974. The mineralogy, geochemistry and origin of lherzolite inclusions in Victorian basanites. Geochim. Cosmochim. Acta 38, 1023-1059.

_____, _____ & ROY, S.D. 1978. Integrated models of basalt petro-genesis: a study of quartz tholeiites to olivine melilitites from Southeastern Australia utilizing geochemical and experimental petrological data. J. Petrol. 19, 463-513.

FUNKHOUSER, J.G. & NAUGHTON, J.J. 1968. Radiogenic helium and argon in ultramafic inclusions from Hawaii. J. Geophys. Res. 73, 4601-4607.

FUSTER-CASAS, J.M. 1950. Las rocas ultra-basicas de Annobon y su relacion con los magmas basalticos de otras islas del Golfo de Guinea. Arch. Inst. Estud. Africa 4, 37-54.

_____ 1954. Estudio petrogenetico de los volcanes del Golfo de Guinea. Inst. Estud. Africa. Madrid, 155pp.

_____ 1956. Vulcanologia de la isla de Fernando Poo. Conf. Int. Africa Occid. sess. 6 Sao Tomé 2, p77.

GALE, N.H. 1975. The contribution of trace element and isotope geochemistry to the petrogenesis of oceanic basalts and the composition of the upper mantle. Soc. Ital. Mineral. e Petrol. 31, 99-123.

GASS, I.G., CHAPMAN, D.S., : POLLACK, H.N. & THORPE, R.S. 1978. Geological and geophysical parameters of mid-plate volcanism. Phil. Trans. R. Soc. A288, 581-597.

GAST, P.W. 1968. Trace element fractionation and origin of tholeiitic and alkali magma types. Geochim. Cosmochim. Acta 32, 1057-1086.

_____, TILTON, G.R. & HEDGE, C. 1964. Isotopic composition of Pb and Sr from Ascension and Gough islands. Science 145, 1181-1185.

GEZE, B. 1943. Géographie physique et géologie du Cameroun occidental. Mus. Nat. Hist. Nat. Mem. 17, 1-271.

_____ 1953. Les volcans du Cameroun occidental. Bull. Volcanol. 13, 63-92.

GILLETTI, B.J. 1974. Diffusion related to geochronology. In Hofmann,A.W., Gilletti, B.J., Yoder, H.S. & Yund, R.A. (eds.) : Geochemical Transport and Kinetics. Carnegie Inst. Washington Publ. 634, 61-76.

GORINI, M.A. & BRYAN, G.M. 1976. Tectonic fabric of the equatorial Atlantic and adjoining continental margins: Gulf of Guinea to northeastern Brazil.An. Acad. Brasil. Cienc. 48, 101-119.

GOUHIER, J., NOUGIER, J. & NOUGIER, D. 1974. Contribution à l'etude volcanologique du Cameroun ("Ligne du Cameroun" - Adamaoua). Ann. Fac. Sci. Cameroun 17, 3-48.

GRAHAM, A.L. & RINGWOOD, A.E. 1971. Lunar basalt genesis: the origin of the europium anomaly. Earth Planet. Sci. Lett. 13, 105-115.

GRANT, N.K. 1970. Geochronology of Precambrian basement rocks from Ibaden, S.W. Nigeria. Earth Planet. Sci. Lett. 10, 29-38.

_____, REX, D.C. & FREETH, S.J. 1972a. Potassium - argon ages and strontium isotope ratio measurements from volcanic rocks in N.E. Nigeria. Contrib. Mineral. Petrol. 35, 277-292.

_____, FREETH, S.J. & REX, D.C. 1972b. K/Ar data and the origin of feldspar megacrysts in basalt: rejoinder to J.B.Wright. Nature Phys. Sci. 238, 42-43.

_____, POWELL, J.L., BURKHOLDER, F.R., WALTHER, J.V. & COLEMAN, M.L. 1976. The isotopic composition of Sr and O in lavas from St. Helena, S. Atlantic. Earth Planet. Sci. Lett. 31, 209-223.

GREEN, D.H. 1969. The origin of basaltic and nephelinitic magmas in the earth's mantle. Tectonophysics 7, 409-422.

_____ 1970. A review of experimental evidence on the origin of basaltic and nephelinitic magmas. Phys. Earth Planet. Int. 3, 221-235.

_____ 1973. Experimental melting studies on a model upper mantle composition at high pressure under water saturated and water undersaturated conditions. Earth Planet. Sci. Lett. 17, 456-465.

_____ & RINGWOOD, A.E. 1967. The genesis of basaltic magmas. Contrib. Mineral. Petrol. 15, 103-190.

_____ & LIEBERMAN, R.C. 1976.Phase equilibria and elastic properties of a pyrolite model for the oceanic upper mantle. Tectonophysics 32,61-92.

_____, EDGAR, A.D., BEASLEY, P., KISS, E. & WARE, N.G. 1974. Upper mantle source of some hawaiites, mugearites and benmoreites. Contrib. Mineral. Petrol. 48, 33-43.

GREEN, H.W. 1979. Trace elements in the fluid phase of the earth's mantle. Nature 277, 465-467.

_____ & RADCLIFFE, S.V. 1975. Fluid precipitates in rocks from the earth's mantle. Geol. Soc. Am. Bull. 86, 846-852.

GRUNAU, H.R., LEHNER, P., CLEINTUAR, M.R., ALLENBACH, P. & BAKKER, G. 1975. New radiometric ages and seismic data from Fuerteventura (Canary islands), Maio (Cape Verde islands) and São Tomé (Gulf of Guinea).In Borradaile,G.J.,Ritsema,A.R.,Rondiel,H.E.&Simon,O.J.(eds.) :Progress in Geodynamics. R.Neth.Acad. Arts Sci. Amsterdam, 90-118.

GUILLAUME, G.M.D. 1966. Notes on the Cameroon Mountain. Ministry of Agric. Buéa, 16pp.

GUILLEMAIN, C. 1909. Profil der Kreideschichten am Mungo. Beiträge zur geologie von Kamerun, no.17 Abh. d.k. preuss geol. Landesanst., N.F. no. 62, 405-432.

GUNN, B.M. 1971. Trace element partitioning during olivine fractionation of Hawaiian basalts. Chem. Geol. 8, 1-13.

_____ & WATKINS, N.D. 1976. Geochemistry of the Cape Verde Islands and Fernando de Noronha. Geol. Soc. Am. Bull. 87, 1089-1100.

HANSON, G.N. 1977. Geochemical evolution of the suboceanic mantle. J. Geol. Soc.London 134, 235-254.

_____ 1980. REE in petrogenetic studies of igneous systems. Ann. Rev. Earth Planet. Sci. 8, 371-406.

HARRIS, C., BELL, J.D. & ATKINS, F.B. 1982. Isotopic composition of lead and strontium in lavas and coarse grained blocks from Ascension Island, S. Atlantic. Earth Planet. Sci. Lett. 60, 79-85.

HARRIS, P.G. 1957. Zone refining and the origin of potassic melts. Geochim. Cosmochim. Acta 12, 195-208.

_____ 1974. Origin of alkaline magmas as a result of anatexis. In Sørensen, H.(ed.): The Alkaline Rocks. J. Wiley & Sons, 427-436.

_____ & MIDDLEMOST, E.A.K. 1969. The evolution of kimberlites. Lithos. 3, 77-88.

HART, S.R. 1971. K,Rb,Cs,Sr, and Ba contents and Sr isotope ratios of ocean floor basalts. Phil. Trans. R. Soc. London A268, 573-587.

_____ 1976. LIL- element geochemistry, Leg 34 basalts. Init. Rep. Deep Sea Drilling Project 34, 283-288.

_____ & ALLEGRE, C.J. 1980. Trace element constraints on magma genesis. In Hargreaves,R.B.(ed.): Physics of Magma Processes. Princeton University Press, Princeton,N.J.,121-159.

_____ & DAVIS, K.E. 1978. Ni partitioning between olivine and silicate melt. Earth Planet. Sci. Lett. 40, 203-219.

_____, ERLANK, A.J. & KABLE, E.J.D. 1974. Seafloor basalt alteration; some chemical and Sr isotopic effects. Contrib. Mineral. Petrol. 44, 219-230.

HARTE, B. & GURNEY, J.J. 1975. Ore mineral and phlogopite mineralization within ultramafic nodules from the Matsoku kimberlite pipe, Lesotho. Carnegie Inst. Washington Yearb. 74, 528-536.

HAWKESWORTH, C.J. & VOLLMER, R. 1979. Crustal contamination versus enriched mantle: $^{143}Nd/^{144}Nd$ and $^{87}Sr/^{86}Sr$ evidence from the Italian volcanics. Contrib. Mineral. Petrol. 69, 151-165.

_____, NORRY, M.J., RODDICK, J.C. & VOLLMER, R. 1979. $^{143}Nd/^{144}Nd$ and $^{87}Sr/^{86}Sr$ ratios from the Azores and their significance in LIL-element enriched mantle. Nature 280, 28-31.

HAYATSU, A. & CARMICHAEL, C.M. 1970. K-Ar isochron method and initial argon ratios. Earth Planet. Sci. Lett. 8, 71-76.

_____ & _____ 1977. Removal of atmospheric argon contamination and the use and misuse of the K-Ar isochron method. Can. J.Earth Sci. 14, 337-345.

HEDBERG, J.D. 1968. A geological analysis of the Cameroun trend. Univ. Princeton, PhD. thesis (unpubl.).

HEDGE, C. & PETERMAN, Z.E. 1970. The strontium isotopic composition of basalts from the Gordo and Juan de Fuca Rises, N.E.Pacific Ocean. Contrib. Mineral. Petrol. 27, 114-120.

HELMKE, P.A. & HASKIN, L.A. 1973. Rare-earth elements,Co,Sc,Hf, in the Steens Mountain basalts. Geochim. Cosmochim. Acta 37, 1513-1530.

HERTOGEN, J., DEUTSCH, S., DEPAEPE, P. & KLERKX, J. 1978. Petrogenetic implications of Sr- isotope and trace- element data in alkaline lavas from the Cape Verde Islands and Canary Islands. U.S. Geol. Surv. Open File Rep. 78-701, 176.

HOEFS, J. & WEDEPOHL, K.H. 1968. Sr isotope studies on young volcanic rocks from Germany and Italy. Contrib. Mineral. Petrol. 19, 328-338.

_____, FAURE, G. & ELLIOT, D.H. 1980. Correlation of $\delta^{18}O$ and initial $^{87}Sr/^{86}Sr$ ratios in Kirkpatrick basalt on Mt. Falla, Transantarctic Mountains. Contrib. Mineral. Petrol. 75, 199-203.

HOFMANN, A.W. & HART, S.R. 1978. An assessment of local and regional isotopic equilibrium in the mantle. Earth Planet. Sci. Lett. 38, 44-62.

_____ & WHITE, W.M. 1982. Mantle plumes from ancient oceanic crust. Earth Planet. Sci. Lett. 57, 421-436.

_____, _____ & WHITEFORD, D.J. 1978. Geochemical constraints on mantle models: the case for a layered mantle. Carnegie Inst. Washington Yearb. 77, 548-562.

HOLLOWAY, J.R. & EGGLER, D.H. 1976. Fluid - absent melting of peridotite containing phlogopite and dolomite. Ibid. 75, 636-639.

HOLMES, A. 1950. Petrogenesis of katungite and its associates. Am. Mineral. 35, 772-792.

HUGHES, C.J. 1982. Igneous Petrology. Elsevier, Amsterdam & New York, 557pp.

HUGHES, D.J. & BROWN, G.C. 1972. Basalts from Madeira: A petrochemical contribution to the genesis of oceanic alkali rock series. Contrib. Mineral. Petrol. 37, 91-109.

HURLEY, P.M., FAIRBAIRN, H.W. & PINSON, W.H. 1966. Rb-Sr isotopic evidence in origin of potash-rich lavas of W. Italy. Earth Planet. Sci. Lett. 1, 301-306.

ITO, L. 1977. Magma genesis in a dynamic mantle. In Imai, H. (ed.) : Genesis of Metalliferous Ore Deposits in Japan and East Asia. Tokyo Univ. Press.

JACKSON, E.D. & WRIGHT, T.L. 1970. Xenoliths in the Honolulu Volcanic Series, Hawaii. J. Petrol. 11, 405-430.

_____, SILVER, E.A. & DALRYMPLE, G.B. 1972. Hawaiian-Emperor chain and its relation to Cenozoic circum-Pacific tectonics. Geol. Soc. Am. Bull. 83, 601-618.

JACOBSEN, S.B. & WASSERBURG, G.J. 1979. The mean age of crustal and mantle reservoirs. J, Geophys. Res. 84, 7411-7427.

_____ & _____ 1981. Transport models for crust and mantle evolution. Tectonophysics 75, 163-179.

JACQUEMIN, H. 1981. Contribution de l'étude géochimique des élements en traces à la pétrogenèse des complexes anorogéniques. Exemple des massifs de Mboutou et de Golda Zuelva (Nord Cameroun). Univ. Nancy, Thèse 3e cycle (unpubl.).

_____, SHEPPARD, S.M.F. & VIDAL, P. 1982. Isotopic geochemistry (O,Sr,Pb) of the Golda Zuelva and Mboutou anorogenic complexes, North Cameroun: mantle origin with evidence for crustal contamination. Earth Planet. Sci. Lett. 61, 97-111.

JAMES, D.E. 1975. Sr isotopic composition of late Cenozoic central Andean volcanic rocks: a disequilibrium melting model. Carnegie Inst. Washington Yearb. 74, 250.

JAMES, R.S. & HAMILTON, D.L. 1969. Phase relations in the system $NaAlSi_3O_8$-$KAlSi_3O_8$-$CaAl_2Si_2O_8$ at 1 kilobar water vapour pressure. Contrib. Mineral. Petrol. 21, 111-141.

JENNINGS, J.H. 1959. The eruption of Mt. Cameroon, Febuary-March 1959. Geography 44, 207-208.

JEREMINE, E. 1941. Sur les laves des massifs volcaniques du Cameroun occidental. C.R. Acad. Sci. 212, 495-497.

JEREMINE, E. 1943. Contribution à l'étude pétrographique du Cameroun occidental. Mém. Mus. Nat. Hist. Nat. 17, 273-320.

JOHAN, Z. & LE BEL, L. 1980. Genèse des couches et podes de chromitite dans les complexes ophiolitic. Abstracts 26th Int. Geol. Cong. Paris 3, 950.

KAY, R.W. 1975. Chemical zonation of the oceanic mantle. EOS. Trans. Am. Geophys. Union 56, 1077.

_____ & GAST, P.W. 1973. The rare earth content and origin of alkali-rich basalts. J. Geol. 81, 653-681.

_____ & HUBBARD, N.J. 1978. Trace elements in ocean ridge basalts. Earth Planet. Sci. Lett. 38, 95-116.

_____, _____ & GAST, P.W. 1970. Chemical characteristics and origin of oceanic ridge volcanic rocks. J. Geophys. Res. 75, 1585-1613.

KEELING, D.L. & NAUGHTON, J.J. 1974. K-Ar dating: addition of atmospheric argon on rock surfaces from crushing. Geophys. Res. Lett. 1, 43-46.

KIRBY, S.H. & GREEN, H.W. 1980. Dunite xenoliths from Hualalai volcano: evidence for mantle diapiric flow beneath the island of Hawaii. Am. J. Sci. 280A, 550-575.

KLERKX, J., DEUTSCH, S. & DE PAEPE, P. 1974. Rubidium, strontium content and strontium isotopic composition of strongly alkalic basaltic rocks from the Cape Verde islands. Contrib. Mineral. Petrol. 45, 107-118.

KORNPROBST, J., OHNENSTETTER, D. & OHNENSTETTER, M. 1981. Na and Cr contents in clinopyroxenes from peridotites: a possible discrimin--ant between "subcontinental"and "suboceanic" mantle. Earth Planet. Sci. Lett. 53, 241-254.

KRAMERS, J.D., SMITH, C.B., LOCK, N.P., HARMON, R.S. & BOYD, F.R. 1981. Can kimberlites be generated from ordinary mantle? Nature 291, 53-56.

KURODA, Y., SUZUOKI, T. & MATSUO, S. 1975. D/H ratios of the co--existing phlogopite and richterite from mica nodules and a peridotite in S. African kimberlites. Contrib. Mineral. Petrol. 52, 315-318.

_____, _____ & _____ 1977. Hydrogen isotope composition of deep-seated water. Contrib. Mineral. Petrol. 60, 311-315.

KUSHIRO, I. 1968. Compositions of magmas formed by partial zone melting of the earth's upper mantle. J. Geophys. Res. 73, 619-634.

KYSER, T.K. & RISON, W. 1982. Systematics of rare gas isotopes in basic lavas and ultramafic xenoliths. J. Geophys. Res. 87, 5611-5630.

KYSER, T.K., O'NEIL, J.R. & CARMICHAEL, I.S.E. 1982. Genetic relations among basic lavas and ultramafic nodules: evidence from oxygen isotope compositions. Contrib. Mineral. Petrol. 81,88-102.

LACROIX, A 1923. Min. Madagascar Paris, iii, 65.

LANPHERE, M.A. & DALRYMPLE,G.B. 1980. Age and strontium isotopic composition of the Honolulu volcanic series, Oahu, Hawaii. Am. J. Sci. 280A, 736-751.

LASSERRE, M. 1966. Confirmation de l'existence de granites Tertiares du Cameroun: gisement, pétrographie et géochronologie. Bull. B.R.G.M. 2e sér. sect.IV, 143-159.

_____ 1967. Données géochronologiques nouvelles acquis au 1er janvier 1967 par la méthode au strontium appliquée aux formations crystallines et cristallophylliennes du Cameroun. Ann. Fac. Sci. Clermont Ferrand, no. 36, Geol. Min. Fasc. 16.

_____ 1978. Mise au point sur les granitöides dits 'ultimes' du Cameroun: gisement, petrographie et géochronologie. Bull. B.R.G.M. 2e sér. sect,IV, 143-159.

_____ & SOBA, D. 1976. Ages cambriens des granites de Nyîbi et de Kongolo (centre-est Cameroun). C.R.Acad. Sci. Paris 283, 1695-1698.

LE BAS, M.J. 1971. Peralkaline volcanism, crustal swelling and rifting. Nature Phys. Sci. 230, 85-87.

_____ 1977. Carbonatite - Nephelinite Volcanism. J. Wiley & Sons, London, 347pp.

_____ 1978. Nephelinite volcanism at plate interiors. Bull. Volcanol. 41, 459-462.

LEEMAN, W.P. 1975. Radiogenic tracers applied to basalt genesis in the Snake River Plain - Yellowstone National Park region - evidence for a 2.7b.y.- old upper mantle keel. Geol. Soc. Am. Abs. 7, 1165.

_____ 1977. Comparison of Rb/Sr, U/Pb and rare earth characteristics of sub-continental and sub-oceanic mantle regions. In Dick, H.J.B. (ed.) : Proceedings of Chapman Conference on Partial melting in the upper mantle. Oregon Dept. Geology Mineral Industries Bull. 96, 149-167.

_____ 1982. Tectonic and magmatic significance of strontium isotopic variations in Cenozoic volcanic rocks from the western United States. Geol. Soc. Am. Bull. 93, 487-503.

LE MAITRE, R.W. 1976. The chemical variability of some common igneous rocks. J. Petrol. 17, 589-637.

LE PICHON, X. & HAYES, D.E. 1971. Marginal offsets, fracture zones and the early opening of the S. Atlantic. J. Geophys. Res. 76, 6283-6293.

LEYRELOUP, A., BODINIER, J.L., DUPUY, C. & DOSTAL, J. 1982. Petrology and geochemistry of granulite xenoliths from central Hoggar (Algeria) - implications for the lower crust. Contrib. Mineral. Petrol. 79, 68-75.

LIPMAN, P.W., DOE, B.R., HEDGE, C.E. & STEVEN, T.A. 1978. Petrologic evolution of the San Juan volcanic field, south-western Colorado: Pb and Sr isotope evidence. Geol. Soc. Am. Bull. 89, 59-82.

LLOYD, F.E. & BAILEY, D.K. 1975. Light element metasomatism of the continental mantle: the evidence and the consequences. Phys. Chem. Earth 9, 389-416.

LOUBET, M. 1981. Trace element geochemistry of peridotite nodules : evidence for a residual nature of the upper mantle. Terra Cognita spec. issue Spring 1981, 82.

McCARTHY, T.S. & CAWTHORN, R.G. 1980. Changes in initial 87Sr/86Sr during protracted fractionation in igneous complexes. J. Petrol. 21, 245-264.

MACDONALD, G.A. 1968. Composition and origin of Hawaiian lavas. Geol. Soc. Am. Mem. 116, 477-522.

_____ & KATSURA, T. 1964. Chemical composition of Hawaiian lavas. J. Petrol. 5, 82-133.

McDOUGALL, I. & SCHMINKE, H-U. 1977. Geochronology of Gran Canaria, Canary Islands: age of shield building volcanism and other magmatic phases. Bull. Volcanol. 40, 57-77.

McELHINNY, M.W. 1973. Palaeomagnetism and Plate Tectonics. Cambridge Univ. Press, Cambridge, 358pp.

MACEDO, C.R., FERREIRA, M.P. & FERREIRA, J.T. 1977. K-Ar ages on Eastern Atlanic islands.E.C.O.G. conf. abstracts, Pisa, Italy.

MACHENS, E. 1973. Geological history of the marginal basins along the north shore of the Gulf of Guinea. In Nairn,A.E.M. & Stehli, F.G. (eds.): The Ocean Basins and Margins 1, 351-390. Plenum publ. co. New York.

MANKINEN, E.A. & DALRYMPLE, G.B. 1972. Electron microprobe evaluation of terrestrial basalts for whole-rock K-Ar dating. Earth Planet. Sci. Lett. 17, 89-94.

MARECHAL, A. 1977. Geologie et géochimie des sources thermominérales du Cameroun. Travaux et Doc. de l'O.R.S.T.O.M. no. 59.

MARSH, J.S. 1973. Relationships between transform directions and alkaline igneous rock lineaments in Africa and S.America. Earth Planet. Sci. Lett. 18, 317-323.

MASCLE, J. 1975. Géologie sous-marine du golfe de Guinée. Univ. P. et M. Curie, Thèse d'Etat (unpubl.).

MENDELSOHN, A.C. 1942. Geological report on the investigation for oil and gas in the islands of Principe and Sao Tomé. Junta Invest. do Ultramar. Report, Lisbon.

MENZIES, M.A. 1978. Comment on "is phlogopite the key?" by A.E.Beswick Geochim. Cosmochim. Acta 42, 146-150.

_____ & MURTHY, V.R. 1978. Sr isotope geochemistry of alpine tectonite lherzolites: data compatible with a mantle origin. Earth Planet. Sci. Lett. 38, 346-354.

_____ & _____ 1980a. Enriched mantle: Nd and Sr isotopes in diopsides from kimberlite nodules. Nature 283, 634-636.

_____ & _____ 1980b. Mantle metasomatism as a precursor to the genesis of alkaline magmas - isotopic evidence. Am. J. Sci. 280A, 622-638.

_____ & _____ 1980c. Nd and Sr isotope geochemistry of hydrous mantle nodules and their host alkali basalts: implications for local heterogeneities in metasomatically veined mantle. Earth Planet. Sci. Lett. 46, 323-334.

_____ & SEYFRIED, W.E. 1979. Basalt- seawater interaction: trace element and strontium isotope variations in experimentally altered glassy basalt. Earth Planet. Sci. Lett. 44, 463-472.

MERTZMAN, S.A. 1979. Strontium isotope geochemistry of a low potassium olivine tholeiite and two basalt- pyroxene andesite magma series from the Medicine Lake Highland, California. Contrib. Mineral. Petrol. 70, 81-88.

MESCH, D. 1916. Die basalte des Kamerungebirges und des Gebietes zwischen Kamerungebirge und Elefantensee. Neues Jahrb. Miner. B-B 40, 457-532.

MITCHELL-THOME, R.C. 1970. Geology of the South Atlantic Islands. Gerbruder Borntraeger, Berlin - Stuttgart.

MODRESKI, P.J. & BOETTCHER, A.L. 1973. Phase relationship of phlogopite in the system K_2O-MgO-CaO-Al_2O_3-SiO_2-H_2O to 35 kilobars: a better model for micas in the interior of the earth. Am. J. Sci. 273, 385-414.

MOORBATH, S. & THOMPSON, R.N. 1980. Strontium isotope geochemistry and the petrogenesis of the Early Tertiary lava pile of the Isle of Skye, Scotland, and other basic rocks of the British Tertiary province: an example of magma-crust interaction. J. Petrol. 21,295-321.

_____, TAYLOR, P.N. & GOODWIN, R. 1981. Origin of granitic magma by crustal remobilization: Rb-Sr and Pb-Pb geochronology and isotope geochemistry of the late Archaean Qorqut Granite Complex of southern West Greenland. Geochim. Cosmochim. Acta 45, 1051-1060.

MORGAN, W.J. 1971. Convection plumes in the lower mantle. Nature 230, 42-43.

_____ 1972. Plate motions and deep mantle convection. Geol. Soc. Am. Mem. 132, 7-22.

MURCK, B.W., BURRUSS, R.C. & HOLLISTER, L.S. 1978. Phase equilibria in fluid inclusions in ultramafic xenoliths. Am. Mineral. 63, 40-46.

MYSEN, B.O. & BOETTCHER, A.L. 1975. Melting of hydrous mantle: II geochemistry of crystals and liquids formed by anatexis of mantle peridotite at high temperatures and high pressures as a function of controlled activities of water, hydrogen and carbon dioxide. J. Petrol. 16, 520-548.

_____ & HOLLOWAY, J.R. 1977. Experimental determinations of rare earth fractionation patterns in partial melts of peridotite in the upper mantle. Earth Planet. Sci. Lett. 34, 231-237.

NEIR, A.O. 1950. A redetermination of the relative abundances of the isotopes of carbon, nitrogen, oxygen, argon and potassium. Phys. Rev. 77, 789-793.

NEIVA, J.M.C. 1954a. Chimisme des roches éruptives des îles de S. Thomé et Prince. Proc. 19th Geol. Congr. 21, 321-333.

_____ 1954b. Quelques laves vacaolaires de l'ile de St. Tomé et de l'ilot de Rolas. Garcia de Orta (Rev. Junta Miss. Geofr. Invest. Ultram.) Lisbon, 2, 53-59.

_____ 1956a. Contribução para a geologia e geomorfologia de Ilha do Principe. Conf. Int. Africa Occid. Lisbon. 2, 157-162.

NEIVA, J.M.C. 1956b. Contribuição paraoestudo geologico e geomorfologico da ilha de S. Tomé e dor ilheus das Rolas e das Cabras. Conf. Int. Africa Occid. Lisbon. 2, 147-153.

_____ & ALBUQUERQUE, C.R. 1962. Geologia e petrografia do ilheu das Rolas. Mem. Mus. Lab. Miner. Geol. 53, 3-19. Univ. Coimbra.

NORRISH, K. & HUTTON, J.T. 1969. An accurate X-ray spectrometric method for the analysis of a wide range of a geological samples. Geochim. Cosmochim. Acta 33, 431-453.

NORRY, M.J., TRUCKLE, P.H., LIPPARD, S.J., HAWKESWORTH, C.J., WEAVER, S.D. & MARRINER, G.F. 1980. Isotopic and trace element evidence from lavas, bearing on mantle heterogeneity beneath Kenya. Phil. Trans. R. Soc. London A297, 259-271.

O'HARA, M.J. 1965. Primary magmas and the origin of basalts. Scot. J.Geol. 1, 19-40.

_____ 1968. The bearing of phase equilibria studies in synthetic and natural systems on the origin and evolution of basic and ultrabasic rocks. Earth Sci. Rev. 4, 69-133.

_____ 1977. Geochemical evolution during fractional crystallisation of a periodically refilled magma chamber. Nature 266, 503-507.

_____ 1980. Nonlinear nature of the unavoidable long-lived isotopic , trace and major element contamination of a developing magma chamber. Phil. Trans. R. Soc. London A297, 215-227.

_____ & BIGGAR, G.M. 1969. Diopside and spinel equilibria, anorthite and forsterite reaction relationships in silica poor liquids in the system $CaO-MgO-Al_2O_3-SiO_2$ at atmospheric pressure and the bearing on the origin of melilitites and nephelinites. Am. J. Sci. 267A, 364-390.

_____ & MATHEWS, R.E. 1981. Geochemical evolution in an advancing, periodically tapped, continuously fractionated magma chamber. J. Geol. Soc. London 138, 237-277.

_____ & YODER, H.S. Jr. 1967. Formation and fractionation of basic magmas at high pressures. Scot. J. Geol. 3, 67-117.

_____, SAUNDERS, M.J. & MERCY, E.L.P. 1975. Garnet- peridotite, primary ultrabasic magma and eclogite; interpretation of upper mantle processes in kimberlite. Phys. Chem. Earth 9, 571-604.

OKEKE, P. 1980. Petrology of igneous and metamorphic rocks in the area around Gwoza, Northeast Nigeria. Univ. Edinburgh, MPhil. thesis (unpubl).

OLADE, M.A. 1975. Evolution of Nigeria's Benue trough(aulacogen): a tectonic model. Geol. Mag. 112, 575-583.

_____ 1976. On the genesis of lead-zinc deposits in Nigeria's Benue rift(aulacogen): a re-interpretation. J. Mining and Geol. Nigeria 13, 20-27.

_____ 1978. Early Cretaceous basalt volcanism and initial continental rifting in the Benue trough, Nigeria. Nature 273, 458-459.

O'NIONS, R.K. & CLARKE, D.B. 1972. Comparative trace element geochemistry of Tertiary basalts from Baffin Bay. Earth Planet. Sci. Lett. 15, 436-446.

_____ & PANKHURST, R.J. 1974. Petrogenetic significance of isotope and trace element variation in volcanic rocks from the mid-Atlantic. J. Petrol. 15, 603-634.

_____, _____ & GRONVOLD, K. 1976. Nature and development of basalt magma sources beneath Iceland and Reykjanes Ridge. J. Petrol. 17, 315-338.

_____, HAMILTON, P.J. & EVENSON, N.M. 1977. Variations in $^{143}Nd/^{144}Nd$ and $^{87}Sr/^{86}Sr$ ratios in oceanic basalts. Earth Planet. Sci. Lett. 34, 13-22.

_____, EVENSON, N.M. & HAMILTON, P.J. 1979. Geochemical modeling of mantle differentiation and crustal growth. J. Geophys. Res. 84, 6091-6101.

_____, _____, _____ & CARTER, S.R. 1980. Melting in the mantle past and present: isotopic and trace element evidence. Phil. Trans. R. Soc. London A288, 547-559.

OXBURGH, E.R. 1964. Petrological evidence for the presence of amphibole in the upper mantle and its petrogenetic and geophysical implications. Geol. Mag. 101, 1-19.

_____ & TURCOTTE, D.L. 1974. Membrane tectonics and the East African rift. Earth Planet. Sci. Lett. 22, 133-140.

PANKHURST, R.J. 1969. Strontium isotope studies related to petrogenesis in the Caledonian basic igneous province of N.E. Scotland. J. Petrol. 10, 115-143.

_____ 1977. Strontium isotope evidence for mantle events in the continental lithosphere. J. Geol. Soc. London 134, 255-268.

_____ 1977a. Open system crystal fractionation and incompatible element variations in basalts. Nature 268, 36-38.

PANKHURST, R.J. & O'NIONS, R.K. 1973. Determination of Rb/Sr and $^{87}Sr/^{86}Sr$ ratios of some standard rocks and the evaluation of X-ray fluorescence spectrometry in Rb-Sr geochemistry. Chem. Geol. 12, 127-136.

PATCHETT, P.J. 1980. Thermal effects of basalt on continental crust and crustal contamination of magmas. Nature 283, 559-561.

PEARCE, J.A. 1982. Trace element characteristics of lavas from destructive plate boundaries. In Thorpe, R.S. (ed.): Andesites. J. Wiley & Sons, 525-548.

_____ & CANN, J.R. 1973. Tectonic setting of basic volcanic rocks determined using trace element analysis. Earth Planet. Sci. Lett. 19, 290-300.

_____ & NORRY, M.J. 1979. Petrogenetic implications of Ti, Zr, Y and Nb variations in volcanic rocks. Contrib. Mineral. Petrol. 69, 33-47.

PERRONE, Y. 1969. Notice explicative de la feuille de Wum-Banyo au 1/500000. Dir. Mines Géol. Cameroun. no. 40, 49pp.

PETERMAN, Z.E., HEDGE, C.E. & TOURTELOT, H.A. 1970. Isotopic composition of strontium in seawater throughout Phanerozoic time.Geochim. Cosmochim. Acta. 34, 105-120.

_____ & _____ 1971. Related strontium isotopic and chemical variations in oceanic basalts. Geol. Soc. Am. Bull. 82, 493-500.

PIPER, J.D.A. & RICHARDSON, A. 1972. Palaeomagnetism of Gulf of Guinea volcanic province. West Africa. Geophys. J.R. Astro. Soc. 29, 147-171.

POLLACK, H.N. & CHAPMAN, D.S. 1977. On the regional variation of heatflow, geotherms and lithospheric thickness. Tectonophysics 38, 279-296.

POWELL, J.L. & BELL, K. 1970. Strontium isotopic studies of alkalic rocks - localities from Australia, Spain and W. U.S.A. Contrib. Mineral. Petrol. 27, 1-10.

_____ & _____ 1974. Isotopic composition of strontium in alkalic rocks. In Sorensen, H. (ed.): The Alkaline Rocks. J.Wiley & Sons New York, 412-421.

_____ & DE LONG, S.E. 1966. Isotopic composition of strontium in volcanic rocks from Oahu, Hawaii. Science, 153, 1239-1242.

PRIDER, R.T. 1960. The leucite lamproites of Fitzroy basin, Western Australia. J. Geol. Soc. Aust. 6, 71-118.

RICHARDSON, S.H., ERLANK, A.J., DUNCAN, A.R. & REID, D.L. 1982. Correlated Nd,Sr and Pb isotope variations in Walvis Ridge basalts and implications for the evolution of their mantle source. Earth Planet. Sci. Lett. 59, 327-342.

RICHTER, F. & McKENZIE, D.P. 1978. Simple plate models of mantle convection . J. Geophys. 44, 441-471.

RITTMANN, A. 1933. Die geologisch bedingte Evolution und differentiation des Somma-Vesuvius magma. Z. Vulkanol. 5, 8-94.

ROEDDER, E. 1965. Liquid CO_2 inclusions in olivine bearing nodules and phenocrysts from basalts. Am. Mineral. 50, 1746-1782.

_____ 1976. Petrologic data from experimental studies on crystallized silicate melt and other inclusions in Lunar and Hawaiian olivine. Am. Mineral. 61, 684-690.

_____ 1979. Origin and significance of magmatic inclusions. Bull. Mineral. 102, 487-510.

ROSS, W.G. 1973. A simple device for magnetic field control. Int. J. Mass Spec. Ion Phys. 11, 393-398.

SAGGERSON, E.P. & WILLIAMS, L.A.V. 1964. Ngurumanite from southern Kenya and its bearing on the origin of rocks in the northern Tanganyika alkaline district. J. Petrol. 5, 40-81.

SARCIA, J. & SARCIA, J.A. 1952. Volcanisme et tectonique dans le nord-est Adamaoua (Cameroun français). Bull. Volcanol. 12, 129-143.

SAVIN, S.M. & EPSTEIN, S. 1970. The oxygen and hydrogen isotope geochemistry of ocean sediments and shales. Geochim. Cosmochim. Acta. 34, 43-64.

SCHILLING, J-G. 1971. Sea-floor evolution: rare earth evidence. Phil. Trans. R. Soc. London A268, 663-706.

_____ 1973. Iceland mantle plume : geochemical study of Reykjanes Ridge. Nature 242, 565.

_____ 1974. Faeroe -Iceland plume: rare earth evidence. Earth Planet. Sci. Lett. 24, 1-14.

_____ 1975. Azores mantle blob: rare earth evidence. Earth Planet. Sci. Lett. 25, 103-115.

_____, MEYER, P.S.& KINGSLEY, R.H. 1982. Evolution of the Iceland hotspot. Nature 296, 313-320.

SCHNETZLER, C.C. & PHILPOTTS, J.A. 1970. Partition coefficients of rare - earth elements between igneous matrix material and rock-forming mineral phenocrysts- II. Geochim. Cosmochim. Acta 34, 331-340.

SCHULTZE, A. 1913. Die inseln Annobon. Peterm. Mitt. 59, 131-133.

SCHUSTER, N. 1887. Petrographische untersuchungen der von Oskar mitgebrachten Gesteine - baumann aus Fernando Poo. Peterm. Mitt. , 268-269.

SCHWARZER, R.R. & ROGERS, J.J.W. 1974. A worldwide comparison of alkali olivine basalts and their differentiation trends. Earth Planet. Sci. Lett. 23, 286-296.

SHAFIQULLAH, M. & DAMON, P.E. 1974. Evaluation of K-Ar isochron methods. Geochim. Cosmochim. Acta 38, 1341-1358.

SHAND, S.J. 1951. Eruptive Rocks. J. Wiley & Sons , New York, 488pp.

SHEPPARD, S.M.F. 1981. Stable isotope chemistry of fluids. Chemistry and geochemistry of solutions at high temperatures and pressures. Phys. Chem. Earth 13-14, 419-445.

SHIMIZU, N. & KUSHIRO, I. 1975. The partitioning of rare earth elements between garnet and liquid at high pressures : preliminary experiments. Geophys. Res. Lett. 2, 413-416.

SIBUET, J-C. & MASCLE, J. 1978. Plate kinematic implications of Atlantic equatorial fracture zone trends. J. Geophys. Res. 83, 3401-3421.

SLEEP, N.H. 1974. Segregation of magma from a mostly crystalline mush. Geol. Soc. Am. Bull. 85, 1225-1232.

SMITH, A.L. 1970. Sphene, perovskite, and coexisting Fe-Ti oxide minerals. Am. Mineral. 55, 264-269.

SMITH, J.V., HERVIG, R.L., ACKERMAND, D., & DAWSON, J.B. 1979. K, Rb and Ba in micas from kimberlite and peridotitic xenoliths and implications for origins of basaltic rocks. In Boyd, F.R. & Meyer, H.O.A. (eds.): Kimberlites, Diatremes and Diamonds: Their Geology, Petrology and Geochemistry. Am. Geophys. Union,241-251

SPERA, F.J. 1980. Aspects of magma transport. In Hargreaves, R. (ed.) : Physics of Magmatic Processes. Princeton Univ. Press, 265-323.

SPOONER, E.T.C. 1976. Sr isotopic composition of seawater and the seawater-crust interaction. Earth Planet. Sci. Lett. 31, 167- 174.

STACEY, J.S. & KRAMERS, J.D. 1975. Approximation of terrestrial lead isotope evolution by a two stage model. Earth Planet. Sci. Lett. 26, 207-221.

STEIGER, R.H. & JAGER, E. 1977. Subcommission on geochronology: convention on the use of decay constants in geo- and cosmochron--ology. Earth Planet. Sci. Lett. 36, 359-362.

STOSCH, H-G. 1982. Rare earth element partitioning between minerals from anhydrous spinel peridotite xenoliths. Geochim. Cosmochim. Acta 46, 793-811.

STRECKEISEN, A.L. 1967. Classification and nomenclature of igneous rocks. Neues. Jarhb. Miner. Abh. 107, 144-240.

SUN, S-S. 1980. Lead isotopic study of young volcanic rocks from mid-ocean ridges, ocean islands and island arcs. Phil. Trans.R. Soc. London A297, 409-445.

_____ & HANSON, G.N. 1975a. Evolution of the mantle - geochemical evidence from alkali basalts. Geology 3, 297-302.

_____ & _____ 1975b. Origin of Ross Island basanitoids and limitations upon the heterogeneity of mantle sources for alkali basalts and nephelinites. Contrib. Mineral. Petrol. 52, 77-106.

_____ & _____ 1976. Evolution of the mantle : geochemical evidence from alkali basalt: reply. Geology 4, 626-631.

_____, NESBITT, R.W. & SHARASKIN, A.Y. 1979. Geochemical character--istics of mid-ocean ridge basalts. Earth Planet. Sci. Lett. 44, 119-138.

SUZUKI, K. 1981. Grain boundary concentration of rare earth elements in a hornblende cumulate. Geochem. J.Japan 15, 295-303.

SYKES, L.R. 1978. Intraplate seismicity, reactivation of pre--existing zones of weakness, alkaline magmatism and other tectonism postdating continental fragmentation. Rev. Geophys. Space Phys. 16, 621-688.

TATSUMOTO, M. 1978. Isotopic composition of lead in oceanic basalts and its implication to mantle evolution. Earth Planet. Sci. Lett. 38, 63-87.

TAYLOR, H.P. 1980. The effects of assimilation of country rocks by magmas on $^{18}O/^{16}O$ and $^{87}Sr/^{86}Sr$ systematics in igneous rocks. Earth Planet. Sci. Lett. 47, 243-254.

_____ & TURI, B. 1976. High - ^{18}O igneous rocks from the Tuscan magmatic province, Italy. Contrib. Mineral. Petrol. 55, 33-54.

TCHOUA, F. 1972. Sur la formation des calderas des Monts Bambouto (Cameroun). C.R.Acad.Sci. 274D, 799-801.

_____ 1973. Sur l'existence d'une phase initiale ignimbritique dans le volcanisme des Monts Bambouto (Cameroun) Ibid. 276D, 2863-2866.

_____ 1974. Contribution à l'étude géologique et pétrologique de quelques volcans de la ligne du Cameroun (Monts Manengouba et Bambouto). Univ. Clermont Ferrand, Thèse d'Etat (unpubl.).

TEIXEIRA, C. 1949. Geologia das ilhas de Sao Tomé e do Principe e do territorio de S. Joao Baptista de Ajuda. Anab. Junta. Invest. Colon. 2, 5-20.

THIRLWALL, M.F. 1980. The petrochemistry of the British Old Red Sandstone volcanic province. Univ. Edinburgh, PhD. thesis (unpubl.).

THOMPSON, R.N. 1972. Evidence for a chemical discontinuity near the basalt -"andesite" transition in many anorogenic volcanic suites. Nature 236, 106-110.

_____, DICKIN, A.P., GIBSON, I.L. & MORRISON, M.A. 1982. Elemental fingerprints of isotopic contamination of Hebridean Palaeocene mantle - derived magmas by Archaean sial. Contrib. Mineral. Petrol. 79, 159-168.

THORNTON, C.P. & TUTTLE, O.F. 1960. Chemistry of igneous rocks: part 1, Differentiation Index. Am. J. Sci. 258, 664-684.

THORPE, R.S. & SMITH, K. 1974. Distribution of Cenozoic volcanism in Africa. Earth Planet. Sci. Lett. 22, 91-95.

_____ & WRIGHT, J.B. 1979. Discussion of "Tectonic activity in West Africa and the Gulf of Guinea since Jurassic times- an explanation based on membrane tectonics" by S.J.Freeth. Earth Planet. Sci. Lett. 42, 327-328.

TILLEY, C.E. 1953. The nephelinite of Etinde, Cameroons, West Africa. Geol. Mag. 90, 145-151.

TURCOTTE, D.L. 1982. Geochemical light on mantle convection. Nature 296, 487-488.

TUREKIAN, K.K. 1964. the marine geochemistry of strontium. Geochim. Cosmochim. Acta 28, 1479-1496.

TURI, B. & TAYLOR, H.P. 1976. Oxygen isotope studies of potassic volcanic rocks of the Roman province, central Italy. Contrib. Mineral. Petrol. 55, 1- 31.

TURNER, F.J. & VERHOOGEN, J. 1960. Igneous and Metamorphic Petrology. McGraw- Hill, New York, 694pp.

TUTTLE, O.F. & BOWEN, N.L. 1958. Origin of granite in the light of experimental studies in the system $NaAlSi_3O_8$-$KAlSi_3O_8$-SiO_2-H_2O. Geol. Soc. Am. Mem. 74, 1-153.

TYRRELL, G.W. 1934. Petrographical notes on rocks from the Gulf of Guinea. Geol. Mag. 71, 16-23.

VAN BREEMEN, O., PIDGEON, R.T. & BOWDEN, P. 1977. Age and isotopic studies of some Pan-African granites from north-central Nigeria. Precambrian Res. 4, 307-319.

VEIZER, J. & COMPSTON, W. 1974. Composition of seawater during the Phanerozoic. Geochim. Cosmochim. Acta 38, 1468-1484.

VINCENT, P.M. 1971. Données nouvelles sur le volcan du Mont Cameroun. 6th Colloq. African Geol. Leicester, abstract.

_____ & ARMSTRONG, R.L. 1973. Le volcanisme du plateau Kapsiki (nord Cameroun) et les formations sédimentaires sous-jacentes. 7th Colloq. African Geol. Firenze, abstract.

VOLLMER, R. 1975. Origin of alkaline rocks. Nature 257, 116-117.

_____ 1976. Rb-Sr and U-Pb-Th systematics of alkaline rocks: the alkaline rocks of Italy. Geochim. Cosmochim. Acta 40, 283-295.

_____ 1977. Isotopic evidence for genetic relations between acid and alkaline rocks in Italy. Contrib. Mineral. Petrol. 60, 109-118.

WASS, S.Y. 1980. Geochemistry and origin of xenolith bearing and related alkali basaltic rocks from the southern highlands, New South Wales, Australia. Am. J. Sci. 280A, 639-666.

_____ & ROGERS, N.W. 1980. Mantle metasomatism - precursor to continental alkaline volcanism. Geochim. Cosmochim. Acta 44, 1811-1823.

WASSERBURG, G.J. & DEPAOLO, D.J. 1979. Models of earth structure inferred from neodymium and strontium isotopic abundances. Proc. Nat. Acad. Sci. U.S.A. 76, 3594-3598.

WATSON, E.B. 1982. Melt infiltration and magma evolution. Geology 10, 236-240.

_____ 1982a. Basalt contamination by continental crust: some experiments and models. Contrib. Mineral. Petrol. 80, 73-87.

WEBB, A.W. & McDOUGALL, I. 1967. A comparision of mineral and whole-rock potassium-argon ages of Tertiary volcanics from central Queensland, Australia. Earth Planet. Sci. Lett. 3, 41-47.

WENDLANDT, R.F. & EGGLER, D.H. 1980a. The origins of potassic magmas :I. melting relations in the systems $KAlSiO_4$-Mg_2SiO_4-SiO_2 and $KAlSiO_4$-MgO-SiO_2-CO_2 to 30 kilobars. Am. J. Sci. 280, 385-420.

_____ & _____ 1980b. The origin of potassic magmas: II. Stability of phlogopite in natural spinel lherzolite and in the system $KAlSiO_4$-MgO-SiO_2-CO_2 at high temperatures and pressures. Am. J. Sci. 280, 421-437.

_____ & HARRISON, W.J. 1979. Rare earth partitioning between immiscible carbonate and silicate liquids and CO_2 vapor: results and implications for the formation of light rare earth enriched rocks. Contrib. Mineral. Petrol. 69, 409-419.

WETHERILL, G.W. 1966. Radioactive decay constants and energies. In Clark, S. (ed.): Handbook of Physical Constants. Geol. Soc. Am. Mem. 97, 513-519.

WHITE, W.M. & HOFMANN, A.W. 1982. Sr and Nd isotope geochemistry of oceanic basalts and mantle evolution. Nature 296, 821-825.

_____ & SCHILLING, J-G. 1978. The nature and origin of geochemical variation in mid-Atlantic ridge basalts from the central North Atlantic. Geochim. Cosmochim. Acta 42, 1501-1516.

WILSON, J.T. 1963. Evidence from islands on the spreading of ocean floors. Nature 197, 536-538.

WILLIAMS, L.A.J. 1972. The Kenya rift volcanics: a note on volumes and chemical composition. Tectonophysics. 15, 83-96.

WOOD, D.A. 1979. A variably veined suboceanic upper mantle- genetic significance for mid-ocean ridge basalts from geochemical evidence. Geology 7, 499-503.

_____, GIBSON, I.L. & THOMPSON, R.N. 1976. Element mobility during zeolite facies metamorphism of Tertiary basalts of East Iceland. Contrib. Mineral. Petrol. 56, 241-254.

WRIGHT, J.B. 1972. K-Ar dating and the origin of feldspar megacrysts in alkali basalts. Nature Phys. Sci. 236, 89.

_____ 1976. Volcanic rocks of Nigeria. In Kogbe, C.A. : Geology of Nigeria. Elizabethan Pub. Co., Lagos, 93-142.

_____ 1976a. Fracture systems in Nigeria and initiation of fracture zones in the South Atlantic. Tectonophysics. 34, T34-T47.

_____ 1981. Review of the origin and evolution of the Benue trough in Nigeria. Earth Evolution Sci. 2, 98-103.

WYLLIE, P.J. 1974. Limestone assimilation. In Sørensen, H. (ed.): The Alkaline Rocks. J. Wiley & Sons, London, New York, 459-474.

YAGI, K. & ONUMA, K. 1978. Genesis and differentiation of nephelinitic magma. Bull. Volcanol. 41, 467-472.

YODER, H.S.Jr. 1976. Generation of Basaltic Magma. Nat. Acad. Sci. Washington D.C., 265pp.

_____ & KUSHIRO, I. 1969. Melting of hydrous phase phlogopite. Am. J. Sci. 267, 558-582.

YORK, D. 1969. Least squares fitting of a straight line with correlated errors. Earth Planet. Sci. Lett. 5, 320-324.

ZINDLER, A., HART, S.R., FREY, F.A. & JAKOBSSON, 1979. Nd and Sr isotope ratios and rare earth element abundances in Reykjanes peninsula basalts: evidence for mantle heterogeneity beneath Iceland. Earth Planet. Sci. Lett. 45, 249-262.

_____, JAGOUTZ, E. & GOLDSTEIN, S. 1982. Nd, Sr and Pb isotopic systematics in a three - component mantle: a new perspective. Nature 298, 519-523.